Design, synthesis, and characterisation of small molecule inhibitors of the coagulation factor XIIa (FXIIa)

Ali Hasson Hussein (M.Sc.)

Thesis submitted to the University of Nottingham for the degree of Doctor of Philosophy

April 2018

Declaration

The work presented in this thesis is submitted to the University of Nottingham in support of my application for the degree of Doctor of Philosophy. No part has been submitted for any other degree at The University of Nottingham or any other institution. The work presented in this thesis has been carried out by myself, except for:

- Setting the protocol for the *in vitro* assay of FXIIa and FXa activity and pharmacologically testing 20 out of 131 of the synthesised compounds in this project was carried out by Dr James Awford of the University of Nottingham.
- Homology model FXIIa-H was built in collaboration with Dr James Anthony Wilson of the University of Nottingham.

Ali Hasson Hussein

Abstract

Thromboembolic disorders are the major cause of death and disability worldwide. Anticoagulants are the mainstay in the prevention and treatment of thromboembolic diseases. However, almost all the currently available anticoagulants cause therapy-related haemorrhages as a side effect. In the recent years, FXIIa was highlighted as an attractive target for the development of new anticoagulant drugs with low rates of therapy-related haemorrhages. In this work, the development of a new class of chemical inhibitors as potent and selective nonpeptidic inhibitors of FXIIa has been described.

The structural information of FXIIa is not as prevalent as that of FXa and thrombin. Therefore, the 3D-structure of FXIIa in the active conformation was elaborated by homology studies. Given the structural and functional similarities between FXIIa and FXa, rivaroxaban, a known FXa inhibitor, was used as a starting point for this project.

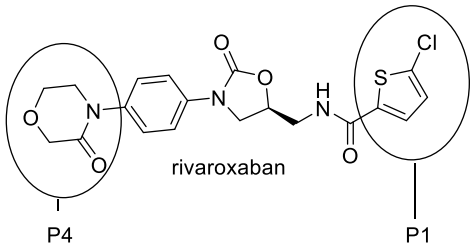

Substituted with morpholine, benzene, pyridine, fluoropyridine, piperazine, methylpiperazine, piperazinone, methylpiperazinone, methoxybenzene, or dimethoxybenzene

(Substituted with thiophene, *tert*-butylbenzene, aniline, cyclohexylmethylamine, cyclohexylamine, benzylamine, benzamidine, benzamide or benzenesulphonamide)

Using a combination of medicinal chemistry and computational chemistry strategies, rivaroxaban analogues with acceptable inhibitory activity against FXIIa were readily identified. However, these early analogues showed poor selectivity profiles.

Two important structural features of FXIIa inhibitors have been extracted from iterative make-test cycles, an amine derivative at the P1-position and piperazine derivative at the P4-position. Compound 4-(aminomethyl)-*N*-({(5S)-2-oxo-3-[4-(piperazin-1-yl)phenyl]-1,3-oxazolidin-5-yl}methyl)benzamide **(v8)** was synthesised with piperazine at the P4-position and 4-(aminomethyl)benzoyl at the P1-position. It was found that compound

v8 inhibited FXIIa activity in a chromogenic biochemical assay with an IC_{50} value of 0.18 ± 0.1 μM. Interestingly, this compound was found to be 72-fold more potent against FXIIa than FXa. In another set of compounds, compound 4-carbamimidoyl-*N*-({(5*S*)-2-oxo-3-[4-(piperazin-1-yl)phenyl]-1,3-oxazolidin-5-yl}methyl)benzamide **(z8)** was synthesised with a 4-carbamimidoylbenzoyl group at the p1-position and piperazine at the P4-position. This compound was 14-fold more potent against FXIIa than FXa. Also, this compound was 1.5-fold more potent against FXIIa than compound **v8,** but it was less selective to FXIIa. In a further structural refinement, 4-(aminomethyl)benzoyl was replaced with a 4-carbamoylbenzoyl at the P1-position. This afforded compound N^1-({(5*S*)-2-oxo-3-[4-(piperazin-1-yl)phenyl]-1,3-oxazolidin-5-yl}methyl)benzene-1,4-dicarboxamide **(w8)** with an IC_{50} against FXIIa of 0.16 ± 0.05 μM, but with significant improvement in the selectivity factor to FXIIa (selectivity factor = 206) compared to compounds **z8** and **v8**.

Docking studies showed that FXa inhibitory activity depends mainly on hydrophobic interactions at the S1- and S4-subpockets. Compounds deprived of the Cl-π interactions at the S1-pocket and/or π-π stacking at the S4-pocket were almost always less potent against FXa than compounds that can make such interactions. However, the inhibitory potency against FXIIa depends mainly on electrostatic interaction in the S1- and S4-pockets especially with Asp189 residue at the bottom of the S1-pocket.

Acknowledgements

I would like to thank Prof. Fischer and Dr Dekker, my project supervisors, for their time, help, teaching, guidance and advice given throughout my time as a PhD student. I would like to thank Prof. Fischer's and Dr Dekker's research groups for their practical advice and guidance given in the lab during my time at the University of Nottingham. Also, I would like to thank my fellow research colleagues in the University of Nottingham, Centre of Biomolecular Sciences, C floor labs, Dr James Anthony Wilson, Dr Christopher Fromont, Akeel Abo Alarad, and Xi Chen, for their help during my PhD journey. In addition, this work would not be possible without the technical support provided by Lee Hibbett.

The last four years would not have been possible without my close friends: Muhammed Al-Ameedee and Wathiq Al-Hachami for their continuous support during hard times.

Finally, my grateful thanks to my parents and my brothers and sisters for their constant help in all the times and for my wife Zainab for her encouragement all the time.

Many thanks to the government of Iraq/ Prime Minister Office/ the Higher Committee for Education Development in Iraq (HCED) for sponsoring me to complete a PhD degree in pharmacy and funding this project.

Abbreviations

AD	Alzheimer’s disease
aPTT	Activated partial thromboplastin time
ATIII	Antithrombin III
BK	Bradykinin
Boc	Tert-butyloxycarbonyl protecting group
CDI	N,N-carbonyldiimidazole
CIT	Corn trypsin inhibitor
DCM	Dichloromethane
DIPEA	Diisopropylethylamine
DMAP	Dimethylaminopyridine
DMF	Dimethylformamide
DVT	Deep venous thrombosis
ECMO	extracorporeal membrane oxygenation
EGF	Epidermal growth factor
FII	Prothrombin
FIIa	Thrombin
FIX	Factor 9 zymogen
FIXa	Activated factor 9
flash-LC	Flash liquid chromatography
FV	Factor 5 zymogen
FVa	Activated factor 5
FVII	Factor 7 zymogen
FVIIa	Activated factor
FVIII	Factor 8 zymogen
FVIIIa	Activated factor 8
FX	Factor 10 zymogen
FXa	Activated factor 10
FXI	Factor 11 zymogen
FXIa	Activated factor 11
FXII−/−	Factor 12 null
FXII	Factor 12 zymogen
FXIIa	Activated factor 12

FXIII	Factor 13 zymogen
FXIIIa	Activated factor 13
HAE	Hereditary angioedema
HBTU	2-(1H-benzotriazol-1-yl)-1,1,3,3-tetramethyluronium hexafluorophosphate
HF	Hagman factor
HGFA	Hepatocyte growth factor activator
HIT	heparin-induced thrombocytopenia
HK	High molecular weight kininogen
HPLC	High-performance liquid chromatography
IC_{50}	Half-maximal inhibitory concentration
PK	Kallikrein
Ki	Inhibitory constant
LC/MS	Liquid chromatography/Mass spectrometry
LMWH	Low molecular weight heparin
MRI	Magnetic resonance image
NMR	Nuclear magnetic resonance
PPK	PreKallikrein
PL	Phospholipids
PPACK	H-D-Pro-Phe-Arg-chloromethylketone
PRR	Proline-Rich Region
PT	Prothrombin time
rHA	Recombinant Human Albumin
rt	Room temperature
SEMCl	2-(Trimethylsilyl)ethoxymethyl chloride
TEA	Triethylamine
TF	Tissue factor
THF	Tetrahydrofuran
THRB	Thrombin
TLC	Thin layer chromatography
tMCAO	transient middle cerebral artery occlusion
tPA	tissue-type Plasminogen activator
uPA	Urokinase-type plasminogen activator

αFXIIa	Alpha factor 12
βFXIIa	Beta factor 12

Table of contents

List of Figures

List of Schemes

List of Tables

Chapter one: Background and Introduction

1.1. Background

The process of blood coagulation has been described as proceeding in cascading steps. This process is initiated by either the intrinsic or the extrinsic pathways (Figure 1).

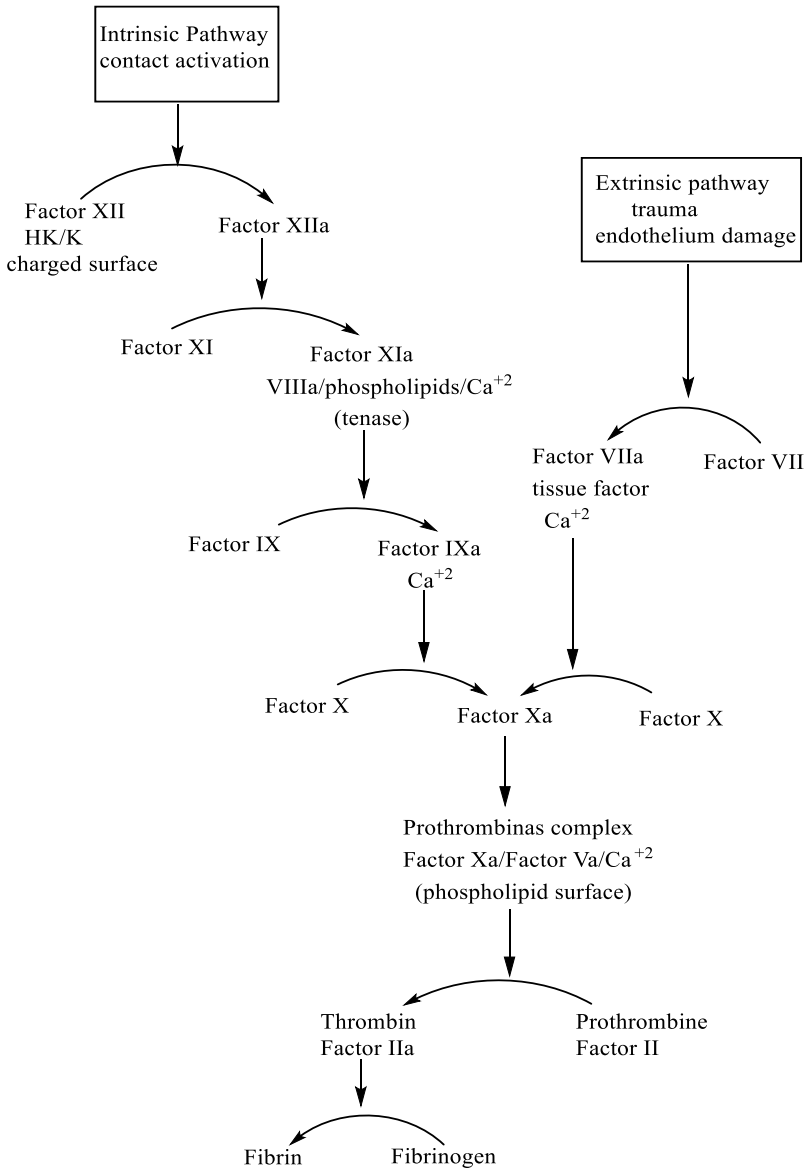

Figure 1: The blood coagulation cascade.[1] Roman numerals indicate inactivated coagulation factors, and activated factors are indicated by a lower case “a”.

Ratnoff and Colopy first described the role of factor XII (FXII) in haemostasis in 1955. They noticed that plasma from some patients lacked a certain

component that can accelerate clot formation.[2] They reported that this unknown factor plays a role at the early stages of the blood coagulation process and that its deficiency was not associated with any bleeding disorders. They referred to this fraction as the 'Hagman factor', named after the first patient who was reported to have a deficiency in this factor. Then in 1958, Ratnoff and Rosenblum described the necessity of 'Hagman factor' (HF), which was later called FXII, for the clotting of blood upon contact with glass or other adsorbent surfaces.[3] This test was then called activated Partial Thromboplastin Time (aPTT) test, which is used in combination with other tests for detecting the efficacy of the blood coagulation process until the present day.[4]

It has been thought that a glass surface might remove an inhibitor of HF upon contact with plasma, and this would lead to freeing of HF to initiate blood coagulation,[3] but the nature of this inhibitor or the mechanism of its removal has never been described. By contrast, another study dismissed this theory and suggested that HF itself is activated when adsorbed on a glass surface and that leads to its contribution to clot formation via activation of FXI (previously known as Plasma Thromboplastin Antecedent PTA).[5]

Although the mechanism of FXII activation and its contribution to blood coagulation *in vitro* is well characterised, the mechanism of its activation *in vivo* remains uncertain. This issue in addition to the observation that FXII deficient patients do not suffer from any haemorrhagic disorders,[2] lead to the dismissal of a role of FXII in haemostasis for many decades. In contrast, the role of FXII in inflammation is well documented.[6] However, the current experiments on FXII genetic mouse knock-out models highlights the importance of FXII in pathological clot formation.[7-10] The results of these experiments have shown that FXII contributes mainly to the pathological clot formation, with a minor contribution to haemostasis. Therefore, they present FXII as a possible target for anticoagulant drugs that will diminish pathological clot formation with minimum bleeding side effects.[11,12]

This study aims to design a selective, small-molecule FXII inhibitor that can be used for the prevention or treatment of thrombotic disorders such as stroke

and myocardial infarction. Such an inhibitor, if invented, would have an advantage over currently available anticoagulants, since it would likely be devoid of the bleeding side effect associated with almost all currently available antithrombotic drugs. Furthermore, as a tool, such compounds would enable scientists to understand better the exact role of FXII in physiological and pathological coagulation.

1.2. Introduction

Blood coagulation can be a physiological or pathological process. Physiological blood coagulation, which is called haemostasis, is an essential activity that prevents excessive blood loss following vascular injury. Haemostasis is a highly-balanced process that involves the participation of many cellular and noncellular components. An imbalance in this process can lead to pathological clot formation or uncontrolled bleeding. The pathological clot formation, which is also called thrombosis, can cause life-threatening diseases such as myocardial infarction or stroke.[13] The main cellular components of clot formation are platelets, whereas the noncellular components include many enzymatic and nonenzymatic substances that aid in this process such as clotting factors, calcium, tissue factor, and vitamin K.

The clotting factors that play an essential role in haemostasis and thrombosis are mainly protease zymogens that need activation. These zymogens are activated through a cascade of proteolysis reactions (Figure 1). There are two ways for initiating the coagulation cascade: the intrinsic and extrinsic pathways. The two pathways converge in the activation of FX (the zymogen form of factor X) to form FXa (activated factor X), which in turn activates prothrombin to thrombin. Thrombin, in turn, converts fibrinogen to fibrin leading to the formation of fibrin meshwork that strengthens the preliminary clot formed by the action of activated platelets at the site of injury.[14]

1.3. Role of platelets in haemostasis and thrombosis

Platelets play an important role in the blood coagulation process. Under normal conditions, inactivated platelets circulate in the blood without adhering to each other or to the endothelial lining of the blood vessel. In addition to the absence of activating factors, three thromboregulatory systems prevent platelet

aggregation under normal conditions. These systems include expression of ecto-ADPase enzyme and production of prostacyclin (prostaglandin 12) and Nitric oxide (NO) by the healthy endothelium. However, in case of blood flow disruption, such as in case of blood vessel injury or ruptured atherosclerotic plaques, platelets will be activated and aggregates to form the preliminary haemostatic plugs or thrombi which then stabilised by fibrin meshwork.[15,16]

Several factors are involved in the platelets activation, among these are the glycoprotein (GP) Ib/IX/V receptor complex on the platelet surface and von Willebrand factor in the subendothelium and plasma.[17,18] Fibronectin, present on the vessel wall, is also involved in platelet adhesion to the subendothelium where the interaction between platelets integrins (transmembrane cell adhesion proteins) and fibronectin provides stable adhesion.[19]

In case of blood vessel injury, the underlying collagen will be exposed to circulating platelets. Von Willebrand factor binds to the exposed collagen and undergoes conformational changes that help it to bind tightly to the abundant platelet receptor glycoprotein Ib. This localisation of platelets to the extracellular matrix promotes collagen interaction with platelet glycoprotein VI. Binding of collagen to glycoprotein VI triggers a signalling cascade that results in activation of platelet integrins. Activated integrins mediate tight binding of platelets to the extracellular matrix. This process adheres platelets to the site of injury.[16]

The adherent platelets are stimulated to form thromboxane A2 and release the contents of their storage granules, including ADP and serotonin, which in turn cause more platelets aggregation.[15] The process of platelet aggregation helps in the formation of a weak clot that then will be strengthened by the action of fibrin fibrils generated through the extrinsic or the intrinsic pathways of blood coagulation.

1.4. The extrinsic pathway

The extrinsic pathway, which is sometimes referred to as the tissue factor pathway, starts when the tissue factor, which is not normally found at high concentrations in blood but is present on cell membranes in subendothelial layers of blood vessels, is exposed to factor VIIa (FVIIa) when the

endothelium is injured (Figure 2).[20] The exposure of blood to cells expressing tissue factor (TF or tissue thromboplastin) such as the cells of vascular adventitia,[21] leads to the formation of a complex between TF and FVII or FVIIa. After complexion with TF, FVII will be activated, and its catalytic activity will be increased enormously.[22]

The TF/FVIIa complex activates both FX and FIX zymogens to their serine protease counterparts FXa and FIXa, respectively.[23,24] Although the quantity of FXa generated by this route is small, it is sufficient to convert small quantities of prothrombin to thrombin. The traces of thrombin produced in this way are enough to activate FVIII and FV to their activated counterparts FVIIIa and FVa, respectively.[25]

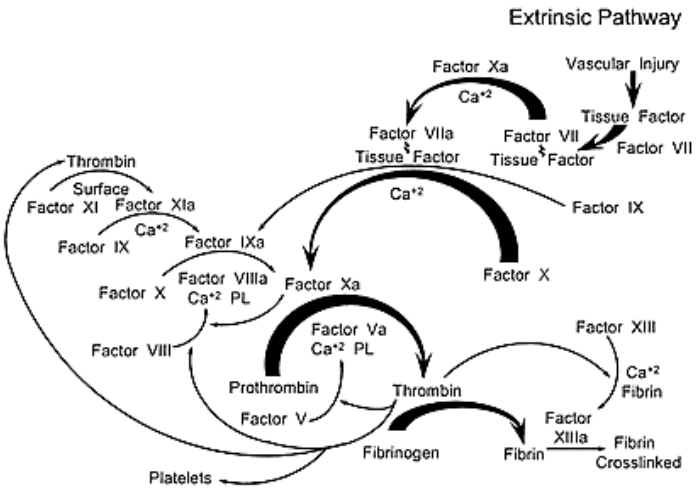

Figure 2: The extrinsic pathway of the coagulation cascade.[26]

After activation by TF/FVIIa complex, Factor IX forms the tenase complex with Factor VIIIa (Factor IXa/FVIIIa complex). This complex causes an amplification of FX activation that eventually leads to binding of FXa to FVa to form the prothrombinase complex (FXa/FVa complex) in the presence of calcium ions and phospholipids.[27] Prothrombin will then be converted to thrombin, by activation via the prothrombinase complex, in quantities that are sufficient to perform its pivotal roles in haemostasis. Although the conversion of fibrinogen to fibrin fibrils is the primary role of thrombin, it also plays many other functions in haemostasis. Thrombin functions include activation of FVIII and FV that leads to the amplification of both FXa and thrombin

formation; activation of FXIII that facilitate the formation of covalent cross-links between fibrin fibrils; platelets activation; and activation of FXI to its serine protease form, FXIa.[28]

The formation of fibrin from fibrinogen leads to its polymerisation to form fibrin fibrils that are cross-linked covalently with the aid of Factor XIIIa, forming a stable meshwork that strengthens the preliminary clot and blocks blood leakage from the site of injury.[29]

1.5. The intrinsic pathway

Many components play a role in the intrinsic (contact) pathway of blood coagulation. These components, which are collectively called the plasma contact system, includes FXIIa, FXIa, FIXa, prekallikrein (PPK), kallikrein (PK), and high molecular weight kininogen (HK).[30]

Many studies reported that the intrinsic pathway of blood coagulation is initiated *in vitro* when FXII is activated to αFXIIa when it encounters negatively charged surfaces.[31-33] However, the precise mechanism for FXII's *in vivo* activation has not yet been determined. Formation of αFXIIa leads to the conversion of PPK to PK that in turn converts αFXIIa to βFXIIa (Hagman factor fragment) and liberates bradykinin (BK) from HK.[34]

Alpha FXIIa activates FXI to FXIa by proteolytic activity.[35] When formed, FXIa activates FIX to FIXa.[36] FIXa complexes with FVIIIa forming a tenase complex that in turn activate FX to FXa.[37] At this step, the intrinsic and extrinsic pathways converge (Figure 3).

It was thought that plasma elements contributing to thrombosis are primarily those involved in haemostasis. Therefore, it was believed that the thrombosis is "the haemostasis in the wrong place".[38,39] this means that the major processes leading to thrombin generation during pathologic coagulation are similar to those involved in haemostasis, perhaps differing only in intensity or location. However, recent studies raise questions about this notion.[40-42] Deficiency of FIX or its cofactor, FVIII, causes a severe form of bleeding disorders called haemophilia A and haemophilia B, respectively.[43] In contrast, deficiency of FXI causes a milder form of bleeding disorders (sometimes

called haemophilia C),[44] whereas FXII-deficient patients do not exhibit an abnormal bleeding tendency, even with surgery, despite having markedly prolonged PTT clotting times.[45,46] These observations contrast the premise that haemostasis and thrombosis represent “two sides of the same coin”.[40]

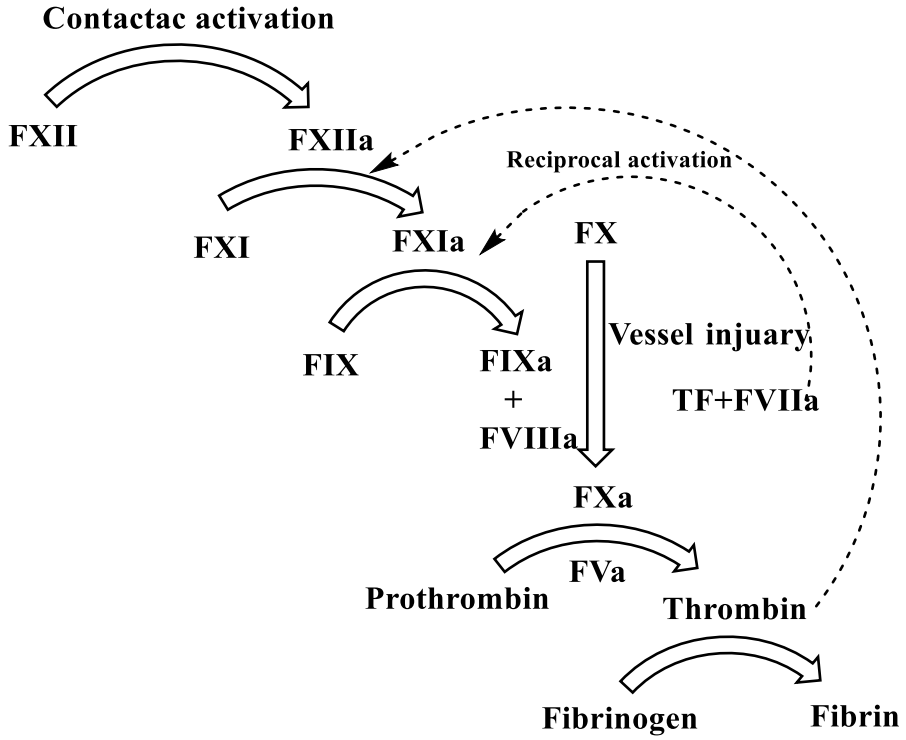

Figure 3: The intrinsic pathway of the blood coagulation cascade.[47]

Recent models of haemostasis lessen the importance of FXII for the generation of fibrin at the wound site, and they give this role primarily, if not exclusively, to TF/FVIIa complex.[48,49] This idea is supported by the finding that FXI, the substrate of FXIIa, can also be activated by thrombin, independently of FXIIa (Figure 3, dotted line).[50] Moreover, the absence of the FXII-gene in inframammalian vertebrates, such as birds and fish, suggest that FXII is a modern protein in term of evolution and hence it is not essential for sealing blood vessels during injuries.[51,52] However FXII has a vital role in thrombosis and inflammation, which will be discussed later in this chapter.

1.6. Factor XII

FXII is a zymogen form of a trypsin-like serine protease enzyme FXIIa.[52] It is synthesised in the liver from a gene that maps to chromosome 5. This gene is 12 kb long and is composed of 13 introns and 14 exons. Human Factor XII is

596 amino acids long and consists of several structural domains. Starting from the N-terminus, the domains are a leader peptide, a fibronectin domain type II, an epidermal-growth-factor-like (EGF-like)domain, a fibronectin domain type I, a second EGF-like domain, a kringle domain, a proline-rich region and the catalytic domain (Figure 4).[53,54]

FXII circulates in the plasma as a single chain zymogen (80 kDa) at a concentration of 15 to 47 µg/ml.[55] By contact with the negatively charged surfaces (autoactivation) and also by the proteolytic activity of PK, FXII will be converted into the two-chain serine protease αFXIIa by the hydrolysis of its Arg353-Val354 peptide bond. Further proteolytic cleavage of αFXIIa converts it into βFXIIa.[56] Alpha FXIIa consists of a heavy chain of 353 amino acids (residues 1-353), and a light chain of 243 amino acids (residues 354-596).[57] On the other hand, βFXIIa consists of the light chain (2800 kDa) in addition to peptide chain of 2000 kDa linked together by disulphide bond.[58]

FXIIa has procoagulant, proinflammatory, mitogenic, and neurodegenerative activities as they will be discussed in the next sections.

1.6.1. Factor XII structure

1.6.1.1. Fibronectin domains

Fibronectin is a glycoprotein secreted by the liver with a molecular weight of approximately 450 kDa.[59] Fibronectin play an important role in cell surface binding through interaction with a group of cell surface receptors called integrins.[60] In addition, fibronectin can bind other biologically important substances such as heparin, collagen, and fibrin.[61] Furthermore, it has been postulated that fibronectin plays a vital role in thrombus formation because it can be detected on the surface of activated but not on non-activated platelets.[62,63] Many studies also reported that fibronectin could polymerise in the same way as fibrin upon contact with specific molecules on cell surfaces.[64,65] Additionally fibronectin may cross-link with fibrin fibrils, thereby strengthening and stabilising the already formed fibrin clot.[66]

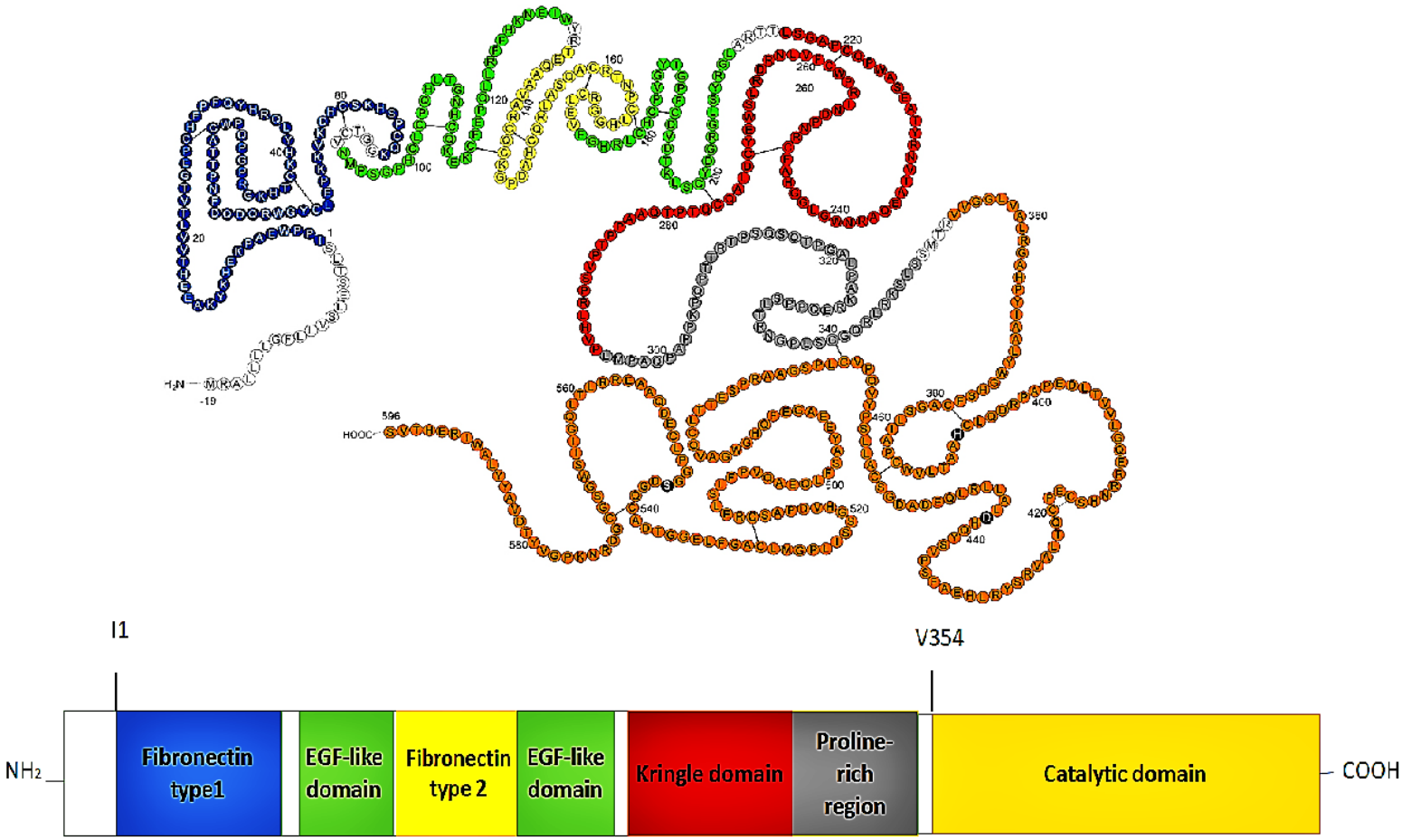

Figure 4: Structure of FXII.FXII is divided into several domains. Top: amino acid sequence; bottom: linear diagram. Colour coding each of the regions of the protein. Amino acids -19-1: leader peptide, 1-88: fibronectin type II domain, 94-131: EGF-like domain, 133-173: fibronectin type I domain, 174-210: EGF-like domain, 215-295: kringle domain, 296-349: proline-rich region, 354-596: catalytic domain or light chain. Amino acids 1-353 are the so-called heavy chain. Each of these areas is highlighted in the same colour as the linear cartoon below it. This figure is adapted from Stavrou E. and Schmaier A. H..[67]

FXII contains two fibronectin-like domains. The N-terminus region of FXII (residues 1-88) shares strong sequence homology with type II fibronectin. Also, residues 133-173 of FXII share limited sequence homology with type I fibronectin.[67] The surface binding properties of FXII may be attributed to these fibronectin-like domains, where many studies assigned surface binding sites on either fibronectin type II or fibronectin type I of the heavy chain of FXII. Residues 134-153 have been designated as a putative surface-binding site of FXII by some studies,[68] also other studies reported that FXII has a surface-binding region at residues 1-28.[69,70] Consistent with these observations, Citarella *et al*. have generated two recombinant FXII proteins missing the fibronectin type II and type I domains and they found that the surface binding ability of these recombinant proteins had decreased significantly. Therefore, they concluded that the N-terminal end of FXII plays a crucial role in its binding to negatively charged surfaces.[71] Nonetheless, Citarella *et al*. in another study found that this region (residues 3-19) may constitute the FXI binding site and it has a minor role in binding to negatively charged surfaces.[72]

The type II fibronectin domain may also be involved in the mitogenic activity of FXII (angiogenesis) through interaction with urokinase-type plasminogen activator receptors (uPAR), which are multidomain cell membrane-linked glycoprotein receptors participate in angiogenesis and cell proliferation. It has been found that interaction between FXII through its type II fibronectin domain and these receptors leads to the activation of kinase activity of extracellular regulated kinases (ERK) that eventually leads to the stimulation of mitosis.[73]

In addition to FXII, the fibronectin type I domain also found in tissue-type Plasminogen activator (tPA), hepatocyte growth factor activator, and extracellular matrix protein fibronectin. It was found that fibronectin type 1 domain in these proteins to be involved in binding to amyloid and misfolded proteins.[74] Therefore, it was thought that there is an essential link between fibronectin-containing proteins and the neurodegenerative diseases. In a recent study, it was found that depletion of FXII in Alzheimer's disease (AD) mice improved the cognitive function in these mice.[75] The result of this study showed that there is a mechanistic link between the Amyloid beta (Aβ), which

is generally recognized as a primary driver of the AD,[76,77] and FXII. Therefore, FXII was suggested as a possible target for the treatment of AD.

The Fibronectin domains of FXII and αFXIIa may also be responsible for the ability of these proteins to bind fibrinogen and/or fibrin. A recent study has demonstrated that FXII and αFXIIa (containing fibronectin domains), but not βFXIIa (lacking fibronectin domains), can bind directly to fibrinogen or fibrin and thereby increase the density and stiffness of formed clots.[78] Moreover, the ability of FXII and αFXIIa to bind to collagen,[33] activated platelets,[79] endothelial cells,[80] and neutrophils[81] may be attributed to its fibronectin domains.

It has been reported that zinc ions play an important role in the activation of FXII.[82] The fibronectin type II domain of FXII and αFXIIa contains two zinc-binding regions, which are residues 40-44 and residues 78-82, whereas βFXIIa does not contain any zinc-binding region.[83]

The presence of zinc ions and surface binding regions on fibronectin domains of FXII and αFXIIa may demonstrate the importance of fibronectin domains in the activation of factor XII through binding to negatively charged surfaces in the presence of zinc ion. βFXII, which lacks the fibronectin domains, also lacks its ability to bind to negatively charged surfaces.[84]

1.6.1.2. Epidermal Growth Factor (EGF) like domains

Growth factors are a group of unclassical hormones that modulate different aspects of cell growth such as proliferation and differentiation.[85] They also play an important role in various physiological and pathological conditions such as infection, wound healing, and tumorigenesis.[86] Epidermal Growth Factor (EGF) is a prototype of a family of growth factors, which called EGF-like molecules, that bind to epidermal growth factor receptors (EGFR).[87] This family also include Transforming Growth Factor-α (TGF-α), the poxvirus growth factors, and amphiregulin. The members of this family share many functional and structural characteristics, and they all can induce mitogenesis (triggering of mitosis) in sensitive cells by interaction with specific cell surface EGF receptors.[87]

Epidermal growth factor-like domains are found in many proteins that mainly involve in adhesion, coagulation, and receptor-ligand interactions.[88,89] Almost all vitamin K-dependent factors involved in blood coagulation or fibrinolysis contain EGF-like domains such as Factor VII, FIX, FX, protein C, and protein S. Additionally, some non-vitamin K-dependent factors also contain EGF-like domains such as urokinase-type plasminogen activator (uPA), tissue Plasminogen Activator (tPA), and FXII. [90]

EGF-like domains in non-vitamin K-dependent factors such as tPA and uPA are involved in binding of these factors to their receptors.[91] EGF-like domains also found in complement system subcomponents (parts of the immune system). In these proteins, the EGF-like domains play a role in Ca^{2+} ion binding and formation of Ca^{2+}-dependent oligomers that are essential for the activation of these factors upon contact with an appropriate activator.[92] Additionally EGF- like domains are involved in the interaction between FIXa and FVIIa, and between FXa and FVa,[93,94] also they play an important role in the binding of FIXa to platelets.[95]

Factor XII contains two EGF-like domains, one at sequence position 94-131 and the other at sequence position 174-210.[67] The exact function of these domains in FXII has not yet been determined, however, it is postulated that the EGF-like domains in FXII contain sites for the binding of this enzyme with negatively charged surfaces. Two sites for this binding are already assigned to the N-terminal region of FXII.[69,70] The other site is postulated to be located on the second EGF-like domain,[71] where this domain contains the histidine residues (166, 176, 180) that may be involved in this interaction.[70] The first EGF-like domain may participate in the binding of FXII to PPK and/or FXI, where FXII missing this domain has diminished ability to activate PPK or FXI.[71]

The mitogenic effect of FXII [96] may be attributed to the interaction between one of its EGF-like domains and EGFR.[97,98] In contrast, recently solved crystal structure of the first EGF-like domain of FXII in combination with fibronectin type I domain (FXII-FnIE) shows that it is unlikely for either EGF-like domains to interact with EGFR because they both lack the arginine residue

necessary for this interaction.[99] The EGF-like domains of FXII and αFXIIa may also be involved in Zn^{2+} ion binding, which plays an important role in the binding of FXII and αFXIIa to negatively charged surfaces, and in the enzymatic activation of FXII.[82,83,100,101]

1.6.1.3. Kringle domain

Kringle domain is an independent module that exists in approximately 31 human proteins.[102] It is typically composed of 80 amino acid residues that form a strong triple- loop tertiary structure connected by three disulphide bonds.[103] It is found mainly in growth factors, proteases, transmembrane receptors, and in blood factors that participate in coagulation or fibrinolysis.[102] For example, it is found in plasminogen,[104] tPA,[105,106] urokinase,[107] and prothrombin.[108]

The exact function of kringle domains is not known, but it may be involved in protein-protein or protein-receptor binding.[109] In plasminogen and plasmin, which contain five kringle domains in their heavy chain, two of these kringle domains contain a site for binding lysine. These lysine-binding sites are found to be important for fibrin binding.[109,110] Therefore, the antifibrinolytic drugs, such as aprotinin and tranexamic acid, inhibit fibrinolysis by competitively binding to these sites on plasminogen and plasmin.[111] Furthermore, the kringle domain in Urokinase mediates the binding of this enzyme with heparin and dextran sulphate.[112]

FXII contains one kringle domain at residues 215-295. The exact function of this domain in FXII has not been elucidated yet. However, certain studies assigned the binding region to negatively charged surfaces at the kringle domain.[71] Another study found that FXII might participate in clot formation through direct deposition on fibrin fibrils.[78] This interaction between FXII and fibrin may occur through this domain, especially since the kringle domains in FXII and tPA share 41 % sequence identity,[67] and the kringle domain in plasminogen play a role in its binding to fibrin.[109,110] Furthermore, the kringle domain may play a role in the activation of FXII by PK.[113]

1.6.1.4. Proline-Rich domain

Near its C-terminus, Factor XII contains a unique region that does not share sequence homology with any other coagulation factor. This region comprised of 33% proline residues (17 out of 52 residues).[114] The exact function of Proline-Rich Region (PRR) in FXII has not been known yet. However, it is generally accepted that PRRs play mainly a structural role in the proteins they are found in. In addition, they may participate in the binding of these proteins to their substrates or receptors.[115]

This region may be responsible for FXII substrate specificity. For instance, FXII shares a significant homology with tPA, which promote fibrinolysis by activating plasminogen. The arrangement of FXII domains at its C-terminus is similar to that of tPA except that one of the kringle domains of tPA is replaced by the PRR.[114] Therefore, the presence of this domain in FXII may lead to that FXII has more procoagulant than fibrinolytic activity.

1.6.1.5. The Catalytic domain

The catalytic domain of FXII (residues 354-596), or also called the light chain, contains the catalytic triad of the active site: His57, Asp102, and Ser195.[54] The catalytic domain of FXII shows substantial homology to the catalytic domains of HGFA, pancreatic serine proteases, trypsin, chymotrypsin, and elastases. For example, it shares 35% sequence identity with the three pancreatic serine proteases. Remarkably, this percentage is close to one between pancreatic serine proteases themselves (they share 41% sequence intra-family homology).[114] By using this strong homology between the catalytic domain of FXII and pancreatic serine proteases, trypsin, chymotrypsin and elastases, Cool *et al*. use computer-modelling to build a three-dimensional model of βFXIIa to predict its tertiary structure.[114] This model shows that the catalytic triad His57–Asp102–Ser195 of trypsin can be aligned with the corresponding residues of βFXIIa, His393, Asp442, and Ser544. Moreover, this model shows that alanine in FXIIa has replaced the serine residue at the position 190 in trypsin (Figure 5). Therefore, they suggested that the absence of the serine residue at this site might be responsible for the preference of FXIIa to cleave the peptide bond where the carboxyl side of the amide bond is arginine rather than lysine. The hydroxyl group of the Ser190 residue of trypsin form

hydrogen bond with the positively charged amino end of the lysyl-side chain of trypsin substrate. This hydrogen bond restricts the positioning of the lysyl-side chain at the bottom of the binding site allowing for the catalytic triad to cleave the peptide bond. Therefore, the absence of this hydrogen bond interaction in FXIIa due to the replacement of serine with alanine results in a lower affinity for lysyl side chains, and increased volume at the bottom of the primary binding subsite that could more easily accommodate the larger and more rigid side chain of arginine.[114] Factor XIIa in this matter similar to thrombin, FXa, tPA, and activated protein C that all prefer cleavage at arginine rather than lysine residues, and all have alanine residue at position 190.[116]

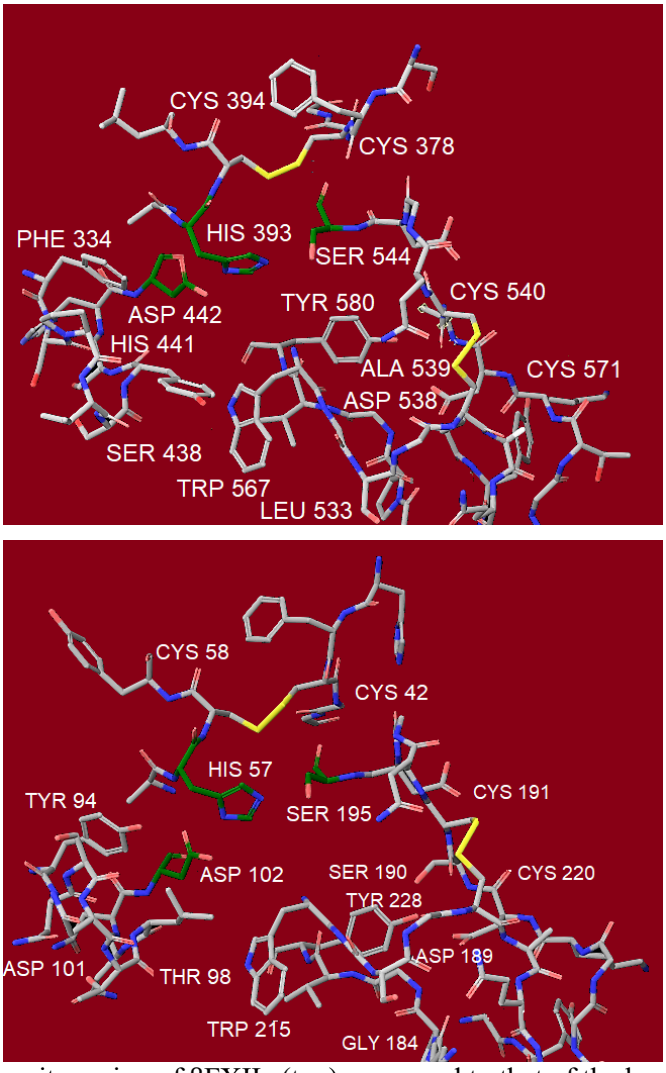

Figure 5: Active site region of βFXIIa (top) compared to that of the bovine trypsin (bottom) according the three-dimensional model that was built by Cool *et al* in 1985. The backbone of the catalytic triad was coloured green; the backbone of the rest residues was coloured gray; blue: nitrogen; red: oxygen. In both drawings the direction of view presented is the same. Adapted from Cool et al.[117]

Additionally, the catalytic domain of FXII also shows strong homology with fibrinolytic agents such as plasmin, urokinase, and tPA.[118] In fact, the homology between the catalytic domain of FXII and those fibrinolytic agents is even higher than that present between FXII and the coagulation factors such as FX and FXI.[119] This has led to the thought that FXII may play a more significant physiological role in fibrinolysis than in the coagulation.[118] However this notion has been opposed by the findings that FXIIa has a role in pathological thrombosis and the suggestions that FXIIa inhibition may protect from thromboembolic diseases.[10,41,120-129]

1.6.2. Factor XII activation

Factor XII undergoes two phases of activation, which are termed 'the solid phase' and 'the fluid phase', respectively.[84] They are called so because in the first phase FXII undergoes activation by contact with negatively charged surfaces while in the second step FXII is activated by enzymatic action (Figure 6).

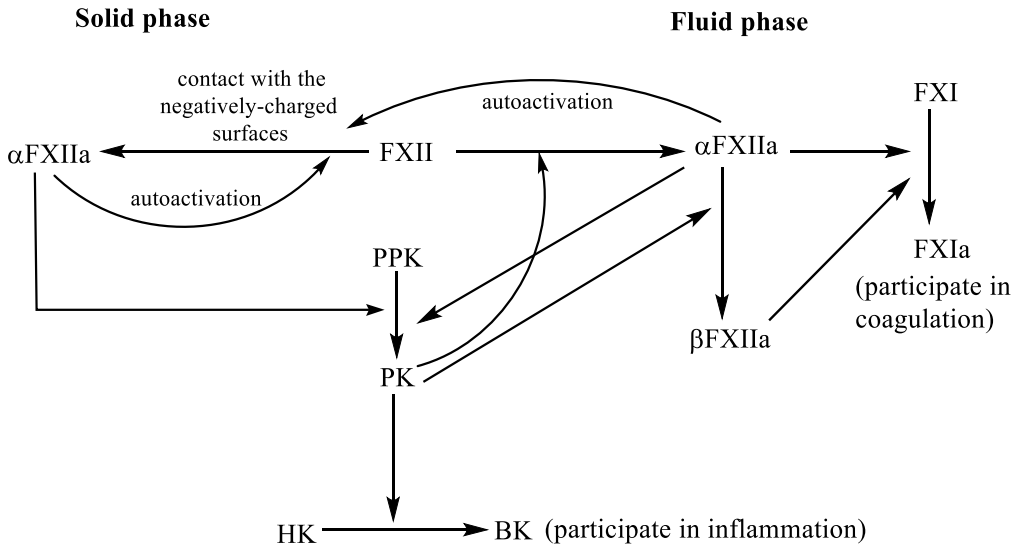

Figure 6: Overview of the mechanism of activation of FXII. FXII: Factor XII zymogen; FXIIa: Activated factor XII; FXI: Factor XI zymogen; FXIa: Activated FXI; PPK: prekallikrein; PK: Kallikrein; HK: High molecular weight kininogen.

In the solid phase, FXII undergoes conformational changes upon contact with the negatively charges surfaces.[130] These conformational changes lead to the formation of a small amount of FXIIa that in turn can activate FXII reciprocally (autoactivation) and to convert PPK to PK in the presence of the

surface-bound high molecular weight Kininogen (HK). The conformational changes that occur in FXII upon contact with negatively charged surfaces make it more susceptible to the second phase of activation.[131]

In the fluid phase, the PK formed during the solid phase causes activation of FXII by proteolytic cleavage of the peptide bond between Arg353 and Val354 leading to the formation of a significant amount of αFXIIa. Alpha FXIIa, in turn, autoactivates FXII, converts PPK to PK, and converts FXI to FXIa.[84,130,132] The activation of FXI by αFXIIa leads to the initiation of the intrinsic pathway of blood coagulation *in vitro*.[133] moreover, PK can generate bradykinin, which is a primary inflammatory mediator, from HK.[134,135]

Alpha FXIIa (80 kDa) is still composed of the original domains of its zymogen (FXII), but instead of the single chain that comprised the zymogen, αFXIIa consist of two chains (heavy and light chains) connected by a single disulphide bond [130]. Further proteolytic cleavage of αFXIIa by PK,[136] trypsin,[118] or plasmin[137] between the residues Arg334 and Asn335 and between Arg343 and Leu344 converts it to βFXIIa or Hageman Factor fragment.[138] βFXIIa itself is also composed of two chains linked together by a single disulphide bond, which are a light chain (28 kDa) and a peptide chain (2 kDa).[139] Although βFXIIa has lost its ability to bind the negatively charged surfaces, it still retains the ability to activate FXI or to convert PPK to PK.[136]

Several physiological and non-physiological surfaces have been found to activate FXII *in vitro*, such as kaolin,[140] ellagic acid-metal complex,[141,142] sulfatides,[142] endotoxins,[143] dextran sulphate,[144] glass,[145] ion-exchange resins,[146] collagen,[33] polyphosphates,[147] and many others (for a review see reference [133]).

Many physiological materials have been suggested to be involved in FXII activation *in vivo* despite the exact activation mechanism not yet being solved. Platelets have been found to be participating in the activation of FXII by providing a surface for the assembly of FXII and its physiological activators,[79,147] or by providing the polyphosphates necessary for this activation.[148-150]

For a long time, it was believed that platelets contribute to contact system activation, but the exact mechanism of this contribution was unknown.[151] However the findings that polyphosphate stored in platelets' dense granules and secreted during platelet activation, and that the synthetic polyphosphates can trigger the contact system of the blood coagulation has led to the idea that polyphosphate is one of the physiological activators of FXII. [152-154]

Many studies have elucidated the way by which polyphosphates contribute to coagulation. In one study, an *in vitro* model of clotting and fibrinolysis has been used to assess the idea that polyphosphates can activate FXII, and it was found that polyphosphates can trigger clotting only in the presence of FXII.[155] In another study, it was seen that polyphosphates increase vascular permeability and induce fluid extravasation in skin microvessels of mice. However, mice deficient in FXII or bradykinin receptors were found to be resistant to polyphosphate-induced leakage. Furthermore, it was found that the removal of intrinsic coagulation pathway proteases FXII and FXI, or targeting polyphosphate with phosphatases protected mice from a polyphosphate-triggered lethal pulmonary embolism. In contrast, Addition of polyphosphates restored defective plasma clotting of Hermansky-Pudlak Syndrome patients, who lack platelet polyphosphates. Therefore, it was concluded that procoagulant and proinflammatory roles of polyphosphates are mediated through the activation of the contact pathway of the blood coagulation.[148] In contrast, other studies dismissed this idea completely, where it was found that the procoagulant activity of activated platelets does not depend on FXII.[156] However, in a recent study, the inhibition of polyphosphates by specific inhibitors (Recombinant Escherichia coli exopolyphosphatase) was found to abolish the platelet's procoagulant activity in FXII-dependent manner.[157]

Misfolded proteins such as those accumulated in patients with systematic amyloidosis are also suggested as a possible *in vivo* activator of FXII.[158] Another study reported that the neutrophils trapped in the preliminarily formed clot might bind FXII and support its activation through the production of neutrophil extracellular traps (NETs) that provide the negatively charged surface necessary for this activation.[159,160] Fibrinogen and fibrin are also found to be involved in the activation of FXII.[161] This is consistent with the

recent finding that FXII modulates clot density and strength through direct binding with fibrin.[78] Another study reported that collagen might play a significant role in thrombus formation through two possible mechanisms. Collagen could activates FXII directly, or it activates platelets that may lead to FXII activation.[33] However, regardless of the mechanism of FXII activation, the consequences of this activation seem to be different for *in vivo* from that for *in vitro* activation. *In vitro*, FXIIa has a crucial role in the blood coagulation, whereas, *in vivo*, FXIIa has a minor role in the physiological blood coagulation (haemostasis), though it has an essential role in pathological clot formation (thrombosis), as we will see in the next section.

1.6.3. The role of FXII in haemostasis and thrombosis

The role of FXII in haemostasis and thrombosis has drawn a significant debate since Ratnoff and Colopy discovered the Hageman factor in 1955.[2] The finding that FXII deficient patients do not suffer from any bleeding disorders has led to the thought that FXII contribution to haemostasis is dispensable, though it is essential for aPTT test *in vitro*.[48,162]

The breakthrough about the role of FXIIa in haemostasis and thrombosis began when FXII knock-out mouse model was created in 2004.[163] The study of these animals showed that they are normally viable and have normal bleeding time after a vessel injury, though they have significantly elongated aPTT. Renné *et al*. used the same model to examine the contribution of FXII to thrombus formation.[164] They induced thrombosis by various techniques and in different *loci*. They found that these FXII-null mice are protected from death after a lethal collagen/epinephrine-induced pulmonary embolism compared to wild-type mice. Similarly, they found that FXII knock-out caused defective arterial thrombus formation induced by $FeCl_3$-oxidative injury, mechanical injury, or by ligation of the carotid artery. Furthermore, when human FXII was infused into FXII-null mice, the injury-induced thrombus formation was restored. Similarly, FXI-deficient mice show resistant to ferric chloride-induced thrombosis with mild bleeding diathesis. In contrast, FIX-deficient mice show similar resistant to $FeCl_3$-triggered arterial thrombosis but with severely prolonged bleeding time.[42] These results have led to the conclusion

that FXII may be of significant importance to pathological thrombus formation, but that it plays a minor role in haemostasis. It can be noticed in Figure 5 (A) that Initiation of thrombus formation at sites of vascular lesions is predominantly caused by TF and collagens exposed in the subendothelial matrix. TF in complex with FVII initiates thrombin formation, which promotes fibrin formation and platelet activation. The contribution of FXIIa in this early phase of thrombus formation is minor. In contrast, in the propagation phase (B) FXIIa activity on the exposed surface of the thrombus contributes to thrombin generation and additional platelet activation, propagating thrombus growth. Accordingly, FXII, as well as factor XI, deficiency severely impairs thrombus formation.

Inhibition of PPK in mice model has a similar effect to that of the inhibition of FXIIa in resistant to arterial and venous thrombosis.[10] However, given that FXII is a substrate to the activated PPK (reciprocal activation) so that depletion of PPK may lead to a diminution of FXII and vice versa. Therefore, the depletion of any member of the contact system may ultimately lead to induced-thrombosis resistant through the FXII-dependent pathway.

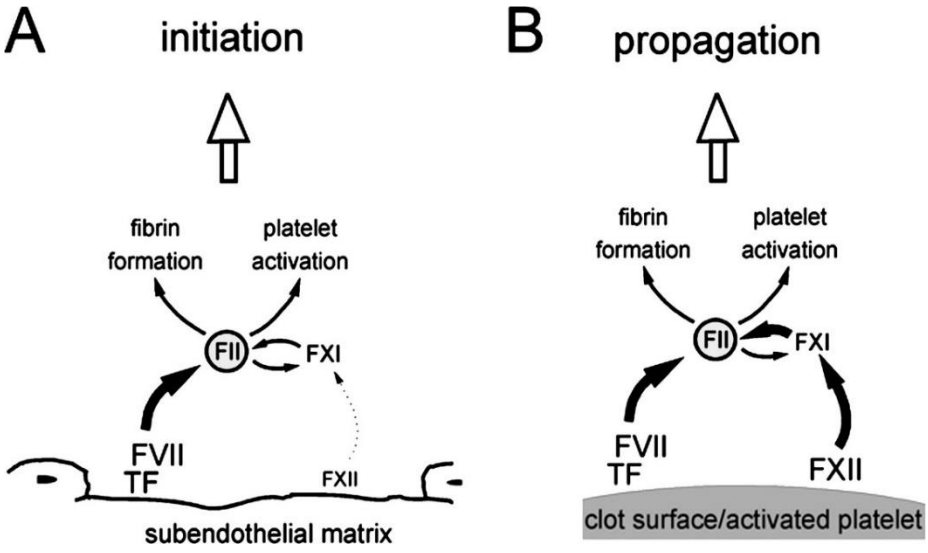

Figure 7: A model of arterial thrombus formation.[164]

Other studies have reinforced the previous findings. One of these studies demonstrated that FXII knock-out mice have normal haemostasis despite having significantly reduced infarct size and significantly better neurological, motor, and coordination functions (according to Bederson's score, and grip

test) compared to mice with normal FXII.[12] Similarly other study showed that the outcome of cerebral reperfusion after transient occlusion of a middle cerebral artery (*t*MCAO) was significantly improved in FXII knock-out mice compared to wild-type mice.[7] In the later study, stroke development *in vivo* in $FXII^{-/-}$ mice has been followed by multimodal high field MRI. The data suggested that the cerebral blood flow, as an indication to cerebral perfusion, is similarly reduced in $FXII^{-/-}$ and Wildtype (Wt) mice early after transient middle cerebral artery occlusion (*t*MCAO), but recovers in the cortex of $FXII^{-/-}$ animals at later time points leading to smaller infarctions. These findings indicate that FXII deficiency allows enhanced tissue reperfusion after transient ischemia compared to mice with a functional intrinsic coagulation system.

Other studies used antibodies against Factor XII to investigate its contribution to haemostasis and thrombosis. One of these studies used a 14E11 antibody to inhibit FXI activation in mice and baboons. They found that 14E11 prevented arterial occlusion induced by $FeCl_3$ in mice, and reduced platelet-rich thrombus growth in collagen-coated grafts inserted into an arteriovenous shunt in baboons to a similar degree to total FXI deficiency. Interestingly, FXII-deficient mice were more resistant to the development of thrombosis than both FXI- or FIX-deficient mice, thus suggesting that FXII may exert additional activities on thrombosis, independent from activation of FXI.[165] Similarly, other researchers used an antibody that inhibits FXII activation and tested it on mice and baboons. According to this study, it was found that the amount of fibrin formed after insertion of a collagen-coated vascular graft into arteriovenous in baboons was reduced significantly due to inhibition of FXII. This study has also shown that FXII-inhibited mice are resistant to $FeCl_3$-induced arterial thrombosis, and the antibodies against FXII caused compromised fibrin formation in human blood placed in collagen-coated tubes.[129] Furthermore, FXII(a)-inhibitor was developed from the tick *Ixodes ricinus*. This protein has been found to contribute to the compromised thrombosis induced in the arteries and veins of rats and mice without promoting bleeding.[166]

Larsson et al. have also recently developed an antibody against FXII and have tested it on mice and rabbits with the extracorporeal device (an apparatus that takes the blood outside the body before returning it to the circulation).[125] The results firstly reinforced the other studies' finding that shows that FXII-deficient mice are protected from induced thrombus formation without suffering from bleeding. Additionally, the study stated that this antibody is as effective as heparin in protecting rabbits from arteriovenous shunt-induced thrombosis without causing a bleeding side effect. Furthermore, it was also found that the antiFXII antibody was as capable as heparin in the protection of rabbits from thrombosis during the 6-hours period of using the extracorporeal device with having an advantage over heparin in that it does not have a bleeding side effect.

Many scenarios may be responsible for the minor contribution of FXIIa in haemostasis compared to its crucial role in thrombosis. The platelets may play a pivotal role in this issue. The binding of activated platelets to the endothelium via binding of their surface receptors glycoprotein Ibα to the Von Willebrand factor is well documented.[167] In addition, the nonactivated platelets can bind to the activated endothelium via interaction with P-selectin.[168] On the other hand FXII has been found to be activated by contact with platelets,[79,147] or the activated platelets may provide the materials necessary for the activation of FXII such as polyphosphates.[148,149] Hence, endothelium and/or platelets activation by thrombosis inducers (such as atherosclerotic plaques or hypoxia) may lead to binding of the platelets to the endothelium. This binding may provide the necessary surface for the activation of FXII, or leads to the formation of polyphosphates that activate FXII directly. Then, FXIIa contributes to the thrombosis through activation of other components of the contact activation system such as FXI and PK. This hypothesis can be supported by the finding that the inhibition of glycoprotein Ibα platelets receptors has a similar effect to that of the inhibition of FXII. For instance, it was found that the inhibition of glycoprotein Ibα receptors or FXII in mice model committed to the thrombosis by transient middle cerebral artery occlusion has led to the reduction of infarct size significantly.[169]

The other possible scenario for the mechanism of Factor XII contribution to thrombosis is through collagen. Collagen, which is the most abundant vascular protein, may play a role in this issue. It has been found that collagen secretion from endothelial cells intensified under conditions of increased shear stress such as atherosclerotic plaque or hypertension. [170] Collagen plays a double role in the activation of factor XII: It activates platelets that in turn activate FXII, and it activates FXII through direct binding. [33] So, the contribution of collagen to the thrombus formation[171] may be attributed eventually to the activation of FXII. However, the mechanism of FXII contribution to the thrombus formation needs more in-depth clinical studies.

1.6.4. The role of factor XII in thromboembolic diseases

Thrombosis refers to the disturbance occurs in the haemostasis process that leads to the formation of abnormal clots inside blood vessels. Thrombosis can occur in arteries (arterial thrombosis) or veins (venous thrombosis). The thrombus sometimes detaches from the wall of the blood vessel and migrates in the circulation potentially causing major harm to other organs. This migrating thrombus is called embolus, and the process is called embolism. Because thrombosis and embolism mainly occur together, they are often combined in the term thromboembolism.[172]

Venous thromboembolic diseases include Deep Venous Thrombosis (DVT), and pulmonary embolism. Arterial thromboembolic disorders include atrial fibrillation and cardiovascular diseases such as myocardial infarction and stroke.[173] Thromboembolic diseases are the major cause of morbidity and mortality worldwide. Ischaemic heart diseases and stroke have caused 13.2 million deaths worldwide in 2011, accounting for 21.8 % of deaths that year. Furthermore, they were the most common cause of death during the past decade (2000-2011).[174] On the other hand, it has been estimated that venous thromboembolism may cause 1 million adverse events such as disability or death annually in six European countries alone.[175]

Epidemiological studies show conflicting results on whether FXII is associated with a decreased or an increased risk of thromboembolic diseases. On one hand, many studies showed that FXII deficiency is associated with an

increased risk of thromboembolic disorders.[176-179] The finding that John Hageman, who is the first person to be described as having FXII deficiency, died from a pulmonary embolism may represent support for this idea.[180] However, it has been later found that in almost all cases of FXII deficiency suffering from the thromboembolic condition, there was an associated congenital or acquired risk factors such as hip fracture or trauma, pregnancy, postpartum period, or deficiency of antifibrinolytic agent such as antithrombin or the patient was heterogeneous for Factor V Leiden.[181] John Hageman, for example, had a hip fracture a few days before he passed away.[180]

On the other hand, other studies have also shown that either FXII deficiency has no correlation with or has a protective role in thromboembolic disorders. In a study of 21 patients with homozygous and 58 patients with heterozygous FXII deficiencies, none developed a thromboembolic disease during the whole period of the follow-up (16 years).[182] Another study reported that the incidence of FXII deficiency is not significantly increased in patients with thromboembolic disorders compared to a healthy control group.[183] In addition, it has been found that there is no significant difference in the prevalence of FXII deficiency in those patients with thromboembolic diseases compared to healthy people.[183,184] It has also been reported that Americans with Asian ethnicity have low levels of FXII compared to people with other ethnicities.[185] This ethnic group (Asian Americans) are known to have a low risk of thromboembolic diseases.[186]

Girolami *et al.* performed a comprehensive analysis of the literature that shows that there is an association between FXII-deficiency and thromboembolic disorders, and they concluded that one or more flaws might be found.[181] For example, although the Study of Myocardial Infarction Leiden (SMILE) has shown that decreased FXII levels are associated with an increased risk of myocardial infarction, it may be there is a bias in this study.[187] for instance, in this study, the consequence of severe FXII deficiency was not examined, instead only patients with mild FXII deficiency or patients having FXII levels at the borders of normal range were enrolled. Additionally, the study of Endler *et al*. showed that there is an association between decreased FXII levels and myocardial infarction.[188] Surprisingly, this study showed that patients with

mild FXII deficiency were associated with an increased risk of myocardial infarction whereas those with severe deficiency were not.

It seems that many studies support the notion that FXII deficiency plays a protective role in thromboembolic disorders. In one study, FXII has been found to be a risk factor for coronary artery disease.[189] In another study, αFXIIa predicted recurrent coronary events after acute myocardial infarction.[190] moreover, studies on FXI, which is the natural substrate of FXIIa, may also support this observation. The increased FXI level has been found to be associated with an increased risk of myocardial infarction by 2-fold, and it increases the risk of cerebrovascular diseases in patients over 50-year old.[47] However, there is a need for more clinical studies to reveal the contribution of Factor XII to thromboembolic disorders.

1.6.5. The role of FXII in inflammation

Inflammation is a complex body response to harmful stimuli or injury. It is of immense importance to protect the body and initiate tissue repair. However, continuous inflammation may lead to serious health problems such as chronic inflammatory diseases.[191] Therefore, inflammation is linked to the most virulent diseases such as atherosclerosis,[192] cancer,[193] metabolic disorders,[194] and diabetes.[195]

Bradykinin (BK) is one of the molecular mediators of inflammation. It is a peptide kinin formed from a plasma protein, HK by the action of PK; it is a potent vasodilator that increases capillary permeability and it also constricts smooth muscle and stimulates pain receptors.[196]

Bradykinin is the end-product of the contact activation system. The contact of FXII with the negatively charged surfaces induces intramolecular conformational changes that lead to the formation of minute amounts of FXIIa which in turn activates PPK to PK by limited proteolysis. Kallikrein then reciprocally activates further FXII and also cleaves HK to release BK.[131] Once formed BK activates endothelial cells and, as a consequence, lead to vasodilatation, increased vascular permeability, production of nitric oxide, and mobilisation of arachidonic acid.[197] Thus, excessive BK levels due to

increased FXII activity or due to decreased metabolism, such as in case of angiotensin-converting enzyme inhibitors therapy, can lead to serious medical conditions, such as Hereditary angioedema (HAE).[198] Additionally, there is a growing body of evidence that links FXII to the AD through neuroinflammation. Alzheimer's disease characterised by the accumulation of misfolded amyloid proteins which in turn can activate FXII. Therefore, FXIIa can enhance the production of BK in the brain tissue which ultimately leads to neuroinflammation.[76,158] Furthermore, FXII plasma levels increased in systemic amyloidosis and the mouse model and patients with AD.[199] Therefore, contact system may represent the interface between inflammation and coagulation and the targeting of FXII may be of a significant importance for the treatment of inflammatory, neurodegenerative, as well as thromboembolic diseases.

1.7. Anticoagulants

In addition to its vital role to transfer nutrient and oxygen to cells, blood acts as a natural defence system. There is a strict balance between blood flow and stasis inside the body.[200] However, several triggers can disturb this balance resulting in aberrant clotting. These result in the formation of a pathologic clot that can become life-threatening if not treated quickly. A pathologic clot, called thrombus, impairs normal blood flow, which manifests, depending on its location, in the form of, for example, myocardial infarction, stroke, or pulmonary embolism. Together these arterial and venous thrombotic diseases are the leading cause of death in the world recently.[201] Therefore, the discovery of anticoagulants was of interest to the researchers as early as 19th century.

Hirudin (a substance found in the saliva of leeches) was described to have an anticoagulant effect by Haycraft J. in 1884.[202] Hirudin extracts from the medicinal leech were first used for parenteral anticoagulation in the clinic in 1909, but their use was limited due to adverse effects and difficulties in achieving highly purified extracts. The anticoagulant effect of heparin was discovered by McLean in 1915. In the 1980s low molecular-weight heparins (LMWH) were developed. They are derived from heparin by enzymatic or

chemical depolymerisation and have better pharmacokinetic properties than heparin. In 1955 the first clinical use of warfarin, a vitamin K antagonist, was reported.[203]

Today, there are two major classes of anticoagulants in clinical use. These are the classical anticoagulants comprising of the vitamin-K antagonist, warfarin, and heparins; and the new anticoagulants, which include direct thrombin and FXa inhibitors.

Heparin and its most recent derivatives, Low Molecular-Weight Heparins (LMWH) and heparin-like pentasaccharide (fondaparinux), are the most widely used anticoagulant in the world.[204] Heparins are very efficient anticoagulants because they inhibit thrombin in extremely fast and quantitative way. However, heparin does have some distinct disadvantages. First, heparin is poorly absorbed from the gastrointestinal tract, requiring intravenous administration.[205] Heparin also undergoes substantial protein binding, mostly to low-density lipoproteins, globulins and fibrinogens, resulting in a variable dose-response curve.[206]

Heparins act by activating antithrombin III (ATIII) that in turn inactivates thrombin and FXa.[207] Heparin binds simultaneously to thrombin and ATIII, thereby promoting the formation of a thrombin/antithrombin complex.[208] The heparin/antithrombin complex is unable to bind its usual exosite in fibrin-bound thrombin.[209] Furthermore, FXa bound to the surface of activated platelets is also resistant to inactivation by the heparin/ antithrombin complex.[210,211] Therefore, bound thrombin and FXa continue to promote systemic thrombogenesis without inhibition from heparin, and that explains why heparin is relatively ineffective in the treatment of acute coronary syndromes..[212,213]

Furthermore, heparin is mainly of animal origin and has a high rate of contamination.[214] Lastly, heparin binds platelet factor 4, resulting in immune-mediated platelet activation and the well-known syndrome of heparin-induced thrombocytopenia (HIT), which can lead to fatal thrombosis.[215] Low-molecular-weight heparins (LMWH) were developed to address many of these

issues. However, LMWH is similarly unable to inactivate fibrin- or clot-bound thrombin, and it also can lead to the development of HIT.[216]

The other classical anticoagulant is warfarin. Warfarin inhibits the formation of γ-carboxyglutamic acid residues in thrombin and other enzymes of the coagulation cascade through the inhibition of vitamin-K epoxide reductase. Despite its effectiveness as an anticoagulant, its ease of production and its oral bioavailability, warfarin has many disadvantages. For example, polymorphism of the genes of the enzymes responsible for the metabolism of warfarin causes significant individual variation in the dose.[217] Moreover, warfarin has a high rate of food-drug and drug-drug interactions.[218] Therefore warfarin-treated patients required close monitoring due to the high possibility of bleeding complications and unpredictable pharmacokinetics.[219]

The past decade or so has seen several new anticoagulants reach the clinic. These include argatroban, melagatran (in the form of its prodrug ximelagatran) and dabigatran (in the form of its prodrug dabigatran etexilate), which target the active site of thrombin, and apixaban and rivaroxaban, which target the active site of FXa. Although ximelagatran was taken off the market soon after its introduction, these newer anticoagulants show good promise and have improved the safety profile of anticoagulant therapy. However, the common problem with these drugs is still bleeding complications.[220]

1.7.1. The development of oral direct thrombin or FXa inhibitors

The discovery and development of new medicines is a highly complex, time-consuming, and expensive endeavour that has faced many changes and challenges over the last two decades.[221] The process of drug discovery consists of a series of discrete steps starting with target identification and validation and end with lead optimisation. The target identification process includes identifying the potential linked-disease target(s). Then, compounds that can modulate the target(s) in a desirable way should be identified in what is called hit discovery. The methods that can be used for hit-discovery includes knowledge-based screening, virtual-screening (VS), high-throughput screening

(HTS), and fragment-based drug discovery. In knowledge-based screening, sufficient knowledge already exists (for example from literature, knowledge of receptor ligands or substrate catalysis mechanism of an enzyme) to design compounds for testing. On the other hand, VS involves using the computational technique to search libraries of small molecules to identify those structures which are most likely to bind to a drug target. However, HTS is most widely used methods for drug discovery in recent years. It involves the assaying of a large number of potential biological modulators against a chosen set of defined targets. Fragment-based drug discoversy based on identifying small chemical fragments, which may bind only weakly to the biological target, and then combine them to produce a lead with a higher affinity.[222]

Serine proteases have been shown to play a multifarious role in health and disease. As a result, there has been considerable interest in the design and development of synthetic inhibitors of these enzymes. the most widely studied group of serine proteases has been those involved in the coagulation cascade, complement system and fibrinolysis. Most clotting abnormalities and associated diseases are mediated by the inappropriate activity of these enzymes.[223]

The classic anticoagulants were discovered mainly in the late 19th and early 20th century and serendipity plays a major role in their discovery.[203] However, classic anticoagulants have several disadvantages, and their administration is inconvenient, especially for long-term therapy such as prevention of stroke in patients with atrial fibrillation. Therefore, there was a need for new anticoagulants that can produce a predictable anticoagulant activity, can be administered orally, with less bleeding side effect, and with less food-drug and drug-drug interaction. A wide range of new anticoagulants, both parenteral and oral, are in various stages of development. New anticoagulants targeted mainly one enzyme of the coagulation cascade, specifically thrombin or FXa.[224]

Thrombin was chosen as a target for anticoagulant drugs because it plays pivotal roles in the blood coagulation cascade. Early thrombin inhibitors were bivalent inhibitors in analogy to hirudin, such as hirulog, which is a synthetic analogue of hirudin with 20 amino acids.[225] In addition, basic arginine

derivatives, such as NAPAP[226] and argatroban[227] were also developed as the first direct thrombin inhibitors.

Ximelagatran was the first-orally available direct thrombin inhibitor. It was approved in many European and South American countries as an alternative to warfarin in the treatment of DVT and prevention of stroke in patients with atrial fibrillation.[228] However, it was withdrawn from the market because of possible hepatotoxic side effect.[228] Dabigatran is a synthetic benzamidine-derivative selective thrombin inhibitor.[229] It has only low oral bioavailability (3-7%).[230] Therefore a prodrug dabigatran etexilate has been synthesised to increase its oral bioavailability. Dabigatran etexilate is converted in the enterocyte to dabigatran by the action of esterases. It was approved in 2008 in Europe for the prevention of venous thromboembolism (VTE) in patients undergoing elective hip or knee surgery. In 2010, it was approved for the prevention of stroke and embolism in patients with nonvalvular atrial fibrillation.[231,232] In spite of the many advantages of direct thrombin inhibitors over heparin and warfarin, they still have many drawbacks such as narrow therapeutic window and bleeding side effects.[231]

Factor Xa inhibitors were also introduced. Rivaroxaban was licensed by the FDA in the USA and Canada for the prevention of DVR in patients undergoing hip or knee replacement surgery and for the prevention of stroke with nonvalvular atrial fibrillation.[233,234] In phase III clinical trials, it appeared to be more effective than enoxaparin (low molecular weight heparin) in the prevention VTE with a fewer bleeding side effect.[235] Apixaban is another orally available FXa inhibitor approved for the prevention of VTE after an orthopaedic surgery.[236] Factor Xa inhibitors are similar to thrombin inhibitors but with a less bleeding side effect. However, bleeding side effects were still present and were increased in a dose-dependent manner in phase II trials with both thrombin and FXa inhibitors. Nonetheless, these inhibitors seem safer so can be administered at fixed doses and require less monitoring.[237,238]

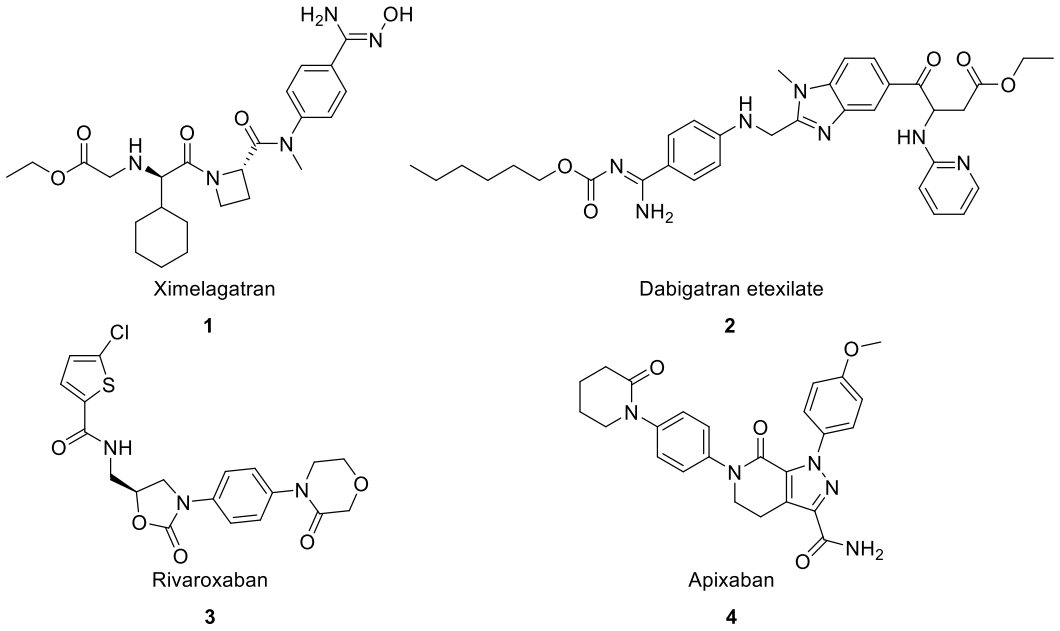

Figure 8: Examples of direct thrombin or FXa inhibitors.

The safety profile of these drugs was affected by the lack of antidotes. Additionally, recent studies have shown that rivaroxaban and apixaban discontinuation could result in thromboembolic events, and the use of rivaroxaban associated with warfarin increases the risk of major bleeding in nonvalvular atrial fibrillation patients.[239-241] Therefore, enthusiasm for their use among both patients and physicians has tempered because of the perception of better safety with warfarin as a result of the availability of effective reversal strategies. However, in the recent years, many studies were attempted to develop such antidotes. Two candidate reversal agents, andexanet alfa[242] and ciraparantag,[243] are in various stages of development, and recently, idarucizumab, a humanised monoclonal antibody antigen-binding fragment that binds to dabigatran, licensed by US, Canadian, and European drug regulators.[244] In addition, The manufacturer of andexanet alfa, Portola Pharmaceuticals, is currently seeking licensure in North America and Europe.[245]

1.7.2. Factor XII(a) inhibitors

Treatment of thromboembolic diseases is still challenging because of the above-listed drawbacks of both classic and new anticoagulants. Factor XIIa plays an important role in pathological thrombosis whereas it has a minor

contribution to haemostasis so that the development of drugs targeting FXIIa seems to be a promising approach. There is currently no factor FXIIa inhibitor in clinical use or advanced clinical trials. Several substances have been suggested as FXII(a) inhibitors such as antibodies,[125,129] recombinant proteins,[246,247] RNA-aptamers,[248] synthetic peptides,[249,250], antisense oligonucleotides (ASO),[126] and small molecule inhibitors.[251,252]

Monoclonal antibodies 9A2 and 15H8 were developed to inhibit activation of FXII.[129] They were tested in mice and baboon, and it was found that the antibody-treated animals are resistant to ferric chloride- and collagen-induced thrombosis. Interestingly, this resistance can be reversed by infusion of human FXII. Furthermore, both anti-FXII antibodies reduced fibrin formation in human blood perfused through collagen-coated tubes. Another antibody (3F7) against FXIIa has also been reported to protect mice and rabbits from pathological thrombosis. It was reported that this antibody inhibits FXIIa-driven coagulation *ex vivo*, inhibits experimental thrombosis in mice and rabbits, and prevents occlusive clot formation in extracorporeal membrane oxygenation (ECMO) cardiopulmonary bypass system without increasing bleeding. In ECMO treatment, a bypass tubing machine is used between lung and heart to assist blood oxygenation in patients with severe heart or lung failure. Therefore this treatment exposes blood to highly procoagulant conditions. The 3F7 antibody shows similar thromboprotection to that observed with heparin without increasing bleeding in ECMO treatment of rabbit model.[125] Moreover, 3F7 abolished bradykinin generation in hereditary angioedema type III (HAEIII) patient plasma and blunted oedema in HAEIII mice.[253] Although promising, these antibodies have common limitations related to high production cost especially they have to be injected in large amounts to achieve clinical efficacy, inadequate pharmacokinetics and tissue accessibility, and unpredictable mode of action once injected.[254,255]

In studies with animal models, a recombinant protein from the ticks *Ixodes ricinus* has been found to diminish pathological thrombosis without affecting haemostasis by inhibiting FXII/FXIIa. This protein, Ixodes ricinus contact phase inhibitor (Ir-CPI), was found to prolong activated partial thromboplastin

time (aPTT) and fibrinolysis time and interferes with thrombus formation in rats with minimal disturbances to haemostasis processes.[166]

Infestin-4 is a protein from the haematophagous insect Triatoma infestans.[256] Purified recombinant Human Albumin-tagged Infestin-4 (rHA-Infestin-4) is a recently described FXIIa inhibitor that displayed strong anticoagulant activity without compromising haemostasis in several animal models. Recombinant HA-Infestin-4 was found to be a competitive inhibitor of FXIIa that can block FXIIa activation of its physiological substrates (PK and FXI). Rats and rabbits treated with the rHA-Infestin-4 show a marked reduction in clot weight in the arteriovenous shunt thrombosis models accompanied with a minimal increase in cuticle bleeding times in either species.[246] Furthermore, it was found that rHA-Infestin-4 is a strong FXIIa inhibitor in human, mouse and rat plasma in vitro. Moreover, it was found that administration of rHA-Infestin-4 protects from arterial thrombosis and ischaemic stroke in rat and mice.[247] However, rHA-Infestin-4 has drawbacks in that it can modestly inhibit plasmin and FXa,[246] and the insect-derived protein has immunogenic properties.[198]

RNA aptamers, which are single-stranded, highly structured oligonucleotides, was also tested against FXII(a). Aptamer R4cXII-1 was reported to bind with high affinity and specificity to FXII(a). It was found that this aptamer functions as a potent anticoagulant *in vitro* by inhibiting the autoactivation of FXII as well as inhibiting intrinsic pathway activation (FXI activation). However, the aptamer does not affect the FXIIa-mediated activation of the proinflammatory kallikrein-kinin system.[248]

Synthetic peptides were also used for FXII(a) inhibition. the synthetic peptide H-D-Pro-Phe-Arg-chloromethylketone (PPACK) was known to irreversibly inhibit the amidolytic activity of FXIIa and plasma kallikrein-mediated activation of FXII.[257] When PPACK was added to the plasma from wild-type mice, the aPTT prolonged in a dose-dependent manner but it did not prolong the prothrombin time (PT). Additionally, mice pretreated with the inhibitor were resistant to cerebral infarction in the tMCAO model[249] and were protected from polyphosphate-induced oedema formation[258] and hypotension during acute episodes of anaphylaxis.[259]

A macrocyclic peptide was also developed and tested against FXIIa and other serine proteases. Although this peptide inhibits FXIIa with high selectivity over related proteases (>100 fold), but its potency was modest (Ki = 1.2 μM).[260] The same group of researchers developed FXIIa inhibitor (Figure 9) by generating and screening novel combinatorial libraries comprising of structurally diverse bicyclic peptides. This peptide macrocycle inhibits FXIIa with an inhibitory constant K_i of 22 nM and a selectivity of >2000-fold over other proteases.[250]

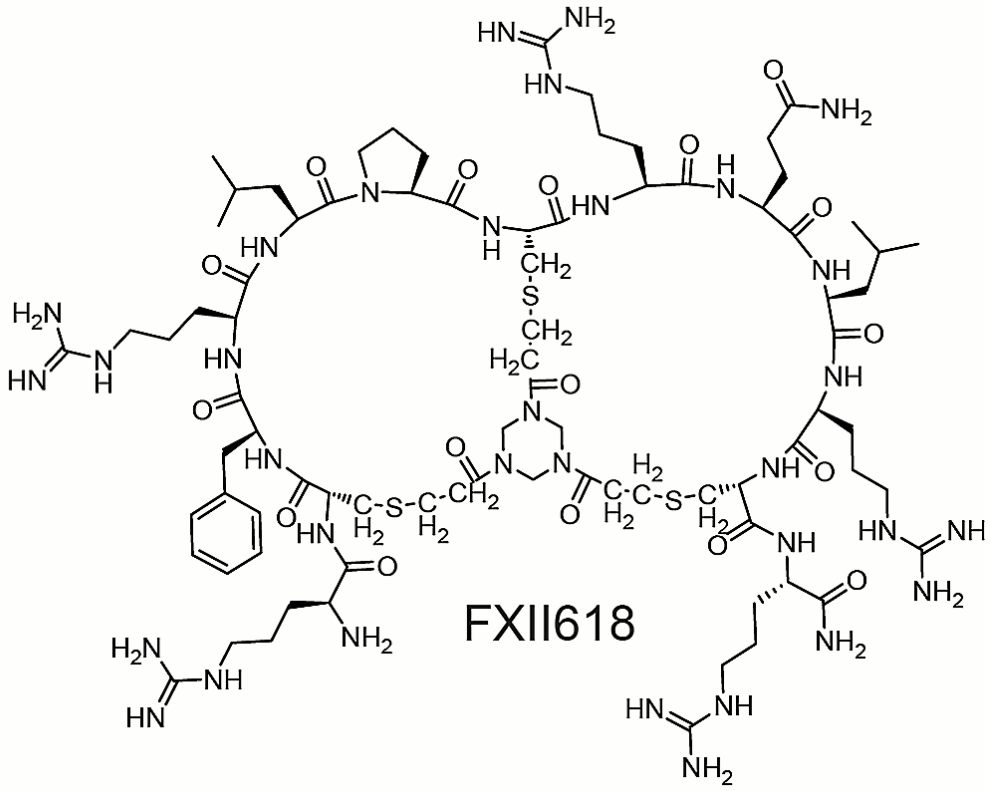

Figure 9: The structure of FXII618, a macrocyclic FXIIa inhibitor.

In addition, natural substances that bear FXIIa inhibitory activities were identified decades ago, and they include a reasonably selective corn trypsin inhibitor (CTI) (K_i for human FXIIa is 24 nM)[261] which has been used as an anticoagulant during blood sampling to eliminate *ex vivo* artefactual activation of the contact factors[262] and a less selective small peptide inhibitor from pumpkin seeds (Ki for human FXIIa is 41 nM) [263] However further studies are needed to evaluate the potential of these inhibitors *in vivo.*

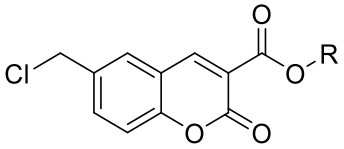

Figure 10: The general structure of coumarins as thrombin or FXa inhibitors.

Coumarin derivatives were proposed as the first small molecule and selective FXIIa inhibitors.[251] Coumarins were first synthesised as thrombin and FXa inhibitors (Figure 10). Two structural features were noticed to be important for the inhibition of these enzymes: the ester link between the coumarin ring and the side chain and the chloromethyl moiety in the 6-position of coumarin ring.[264] Therefore, synthesis of coumarins deprived of these structural features led to a drastic loss of inhibitory potency toward thrombin and FXa (Figure 11). The researchers first tested a series of N-substituted-6-methyl-2-oxo-2H-1-benzopyran-3-carboxamides. Among this series, the compounds bearing a small aliphatic side chain such as isopropyl (**5**) were inactive toward FXIIa. However, the presence of a bulky groups such as naphthalen-1-ylmethyl (**6**) or phenyl (**7**) led to active compounds. Second, the researchers introduced various modifications on the aromatic part of the coumarin ring keeping a 3-phenylcarboxamide side chain. It was observed that disubstitution in the 6 and 8 positions by halogens improved the inhibitory potency (**8**, **9** vs **7**). The best compound in this series was **COU254** (**9**) having an IC_{50} value for inhibition of FXIIa of 4.4 µM and it is selective to FXIIa over thrombin, FXa, TF/FVIIa, and PK in the *in vitro* enzymatic assays.[251]

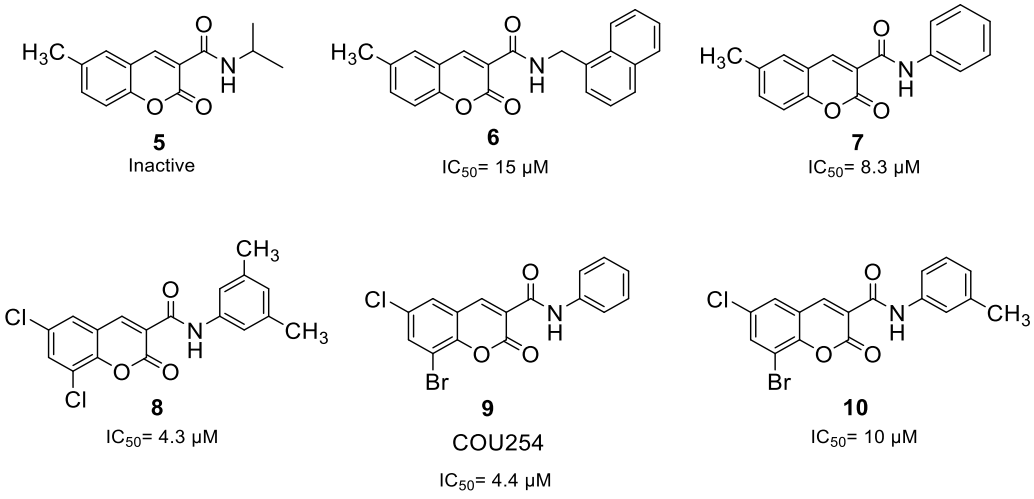

Figure 11: The most potent coumarin derivatives proposed as FXIIa inhibitors.

Mechanistically, the study shows that **9** inhibits FXIIa irreversibly through the formation of stable acyl-enzyme that could be formed by the reaction of the FXIIa active serine with the carbonyl group of the lactone ring or with the exocyclic amide function.[251] Despite that **9** given at a concentration of 40 mg/kg to mice-model failed to demonstrate efficacy in acute ischemic stroke after tMCAO, and **9** treatment did not prevent intracerebral fibrinogen formation.[265] However, the lack of effectiveness of **9** may be related to the low FXIIa inhibitory potency of this compound or some technical difficulties such as the lack of pharmacodynamics and pharmacokinetics information of this compound in animals. Therefore, further preclinical studies may be needed to assess the antithrombotic potentials of these compounds.

In summary, FXII(a) has emerged as a promising target for antithrombotic therapy in recent years. Many types of molecules have been tested as potential FXII(a) inhibitors with some showing thromboprotection properties in animal studies. However, there is a need for further efforts to develop low molecular weight inhibitors of FXIIa that would be a useful tools to assess its role in haemostasis, thrombosis, and inflammation.

1.8. The aim of this study

This study aims to design, synthesise, and pharmacologically test small molecules as selective FXIIa inhibitors that can be used as an anticoagulants for the treatment and prophylaxis of thromboembolic disorders. An important limitation of this study is the lack of structural data to help in the design of FXIIa inhibitors. However, the active site of FXIIa has been modelled using the crystal structure of FXII zymogen solved by Professor Jonas Emsley's group (PDB: 4XE4).[266]

In recent years, there have been extensive studies directed toward the synthesis of a new generation of anticoagulants. These new anticoagulants targeted mainly FXa and thrombin within the coagulation cascade. Therefore, the only coagulation factors that have potent small-molecule inhibitors in clinical use are FXa and thrombin. Accordingly, these enzymes were subjected to comprehensive studies that revealed the structural similarities and differences between them, and the binding modes of their inhibitors.[1] Therefore, to

explore the structure of the FXIIa binding pocket and relate it to the *in vitro* inhibitory activity of the known inhibitors, the preliminary homology and docking studies in this study were focused primarily on FXa and its inhibitors, rivaroxaban and apixaban, and thrombin and its inhibitor, dabigatran.

The literature reported that rivaroxaban with an *S*-configuration has an *in vitro* IC_{50} against FXa of 0.7 nM, whereas the *R*-configuration IC_{50} was 2300 nM.[267] The results of this study agree with these reports and show that rivaroxaban in an *S*-configuration has an *in vitro* IC_{50} against FXa of 0.6 nM whereas the *R*-configuration IC_{50} was 2100 nM. However, rivaroxaban in the *S*-configuration has an IC_{50} of 77µM against FXIIa whereas the *R*-configuration was inactive. Apixaban (a FXa inhibitor) and argatroban (a direct thrombin inhibitors) were also pharmacologically tested against FXIIa in vitro. Apixaban was 2-fold less active, and argatroban was 5-fold less active against FXIIa when compared to rivaroxaban.

According to the preliminary alignment and homology studies, which were carried out at the start of this work using the crystal structures of FXIIa and FXa, rivaroxaban was found to bind to similar pockets in FXIIa and FXa, respectively. Therefore, rivaroxaban was chosen for pharmacomodulation in this project. The main objective of this work is to design and synthesise low molecular weight compound that has an IC_{50} against FXIIa < 100 nM, and it is at least 100-fold more selective to FXIIa than other coagulation factors and related serine proteases.

In order to shift the activity of rivaroxaban toward FXIIa, it was planned to synthesise and test rivaroxaban analogues for their *in vitro* pharmacological activity toward FXIIa and FXa. Furthermore, it was planned to use docking experiments throughout this work to better understand the SAR of the synthesised compounds. For this purpose, a homology model of FXIIa will be built using the crystal structures of FXIIa's catalytic domain (PDB: 4XE4) and FXa in complex with rivaroxaban (PDB: 2w26).

1.9. Rationale of the study

There is a wide range of indications for anticoagulants from prophylaxis and treatment of thromboembolic disorders to the prevention of thrombosis during

certain surgical procedures such as the installation of prosthetic heart valves, dialysis, and vascular surgery (e.g. angioplasty and stent placement). There is an increasing demand for anticoagulants because of an increased number of the patients presenting with thromboembolic disorders, and an increased in the longevity that leads to an increase in the number of elderly people who need anticoagulant therapy. Hence, many anticoagulants have been invented with variable pharmacokinetics and pharmacodynamics properties for the different indications.

Almost all the currently available anticoagulants still have some problems. Classical anticoagulants (such as warfarin and heparin), although effective, require close monitoring and dose adjustment, and are inconvenient for long-term therapy (see previous section). Even the recently approved orally administered direct thrombin and FXa inhibitors such as dabigatran, apixaban, and rivaroxaban still causing bleeding side-effects.[236,237,268] Moreover, these agents have another drawback compared to warfarin and heparin which is the limited availability of their antidotes, whereas vitamin K and protamine sulphate can act as antidotes for warfarin and heparin, respectively.[190,269] Bleeding that occurs due to the administration of anticoagulants can be life-threatening and requires various preventive measures such as close monitoring and dose adjustment, especially in the elderly.[270,271] Additionally, the duration of treatment of thromboembolic disorders is mostly affected by the appearance of this bleeding disorder.[272] Hence, the need for orally administered anticoagulant with no bleeding side effect is of the utmost importance.

FXII has been identified as a new target for anticoagulant drug therapy for many reasons. Firstly, the demonstration that humans and animals deficient in FXII do not suffering from any bleeding disorders.[2,163,273] Secondly, many studies using animal models have shown that FXII deficiency has a protective effect in thrombotic diseases.[10,12,164] Thirdly, anti FXII antibodies demonstrated a protective role from thromboembolic disorders in animal models without causing bleeding side effects.[129,166,246,247] Fourthly, many epidemiological studies have shown that FXII deficiency could protect from thromboembolic diseases.[189,190] Therefore, many studies support the idea that

targeting FXII may provide a good alternative for the currently available anticoagulants.[52,67,134]

It can be expected that the development of a small molecule, orally administered, selective FXII inhibitor would have many advantages over the currently available anticoagulants. The treatment will be suitable for the long-term administration because it will have fewer bleeding side- effects than current therapies. In addition, patients taking such a drug would not require close monitoring or dose adjustment so that it will be suitable for in-hospital or out-patients. Hence, the development of such a drug will improve the efficacy and safety of anticoagulants or at least will provide a tool to understand the role of contact system in haemostasis and thrombosis.

Chapter two: Compounds design and rationale

2.1. Introduction

Rational drug design generally follows a three-step process. Initially, a target, such as a receptor or an enzyme has to be identified relating to a particular disease state. This target then has to be fully characterised and, finally, a molecule must be designed that binds to it. However, the process is not straightforward because even when the 3D-structure of the target molecule is identified (e.g. by X-ray crystallography), there is still the factor of the flexibility of the target and the ligand that can affect the whole process.[274] Proteins and ligands are in constant motion between different conformational states with similar energies. This flexibility is frequently essential for function.[275] Many structure-based or computational aided drug-discovery programs ignore the factor of flexibility od the targets and the ligand. However, the structural information of the targets and computational-aid drug design have been used for decades in the discovery of important drugs, such as FXa and thrombin inhibitors.[276]

In relation to this study, FXIIa was identified as a possible target for anticoagulation therapy, and therefore the identification of small-molecule FXIIa inhibitors is of the utmost importance in the field of antithrombosis therapy.

Usually, the existence of structurally characterised inhibitors, as well as the availability of protein-inhibitor co-crystal structure depicting the interactions between the inhibitor and the target, are precious assets in terms of the design of more potent and selective inhibitors. Regarding FXIIa, such information is limited. Indeed, only four studies are using FXIIa 3D models to propose structure-activity relationships of inhibitors.[250,252,277,278]

There are only few PDB files attributed to FXIIa deposited in the protein data bank (PDB) amongst them 4BDW, and 4XE4. The PDB file 4BDW attributed to the structure of the FnI-EGF tandem domain of coagulation factor XII[99] whereas 4XE4 is the X-ray crystal structure of FXII catalytic domain in the zymogen configuration.[266] Regarding the numbering of residues, it should be

mentioned that in the following sections, residues will be numbered according to the nomenclature of chymotrypsin. The main residues that will be encountered in this project were listed in Table 1.

Table 1: Residue correspondence between crystal structure (PDB:4XE4) and residues numbering in the chymotrypsin numbering system.

Crystal structure (PDB: 4XE4)	**Chymotrypsin**	**Subpocket**
Asp442	Asp102	catalytic triad
His393	His57	
Ser544	Ser195	
Ala539	Ala190	S1
Asp538	Aps189	
Asp543	Asp194	
Cys540	Cys191	
Gly542	Gly193	
Gln541	Gln192	
Tyr580	Tyr 228	
Val579	Val227	
Cys571	Cys223	S2
Gly567	Gly219	
Gly568	Gly220	
Ser569	Ser221	
Ser566	Ser214	
Trp567	Trp215	
Val565	Val213	
Glu437	Glu97	S3
Lys436	Pro96	
Thr438	Thr98	
Tyr439	Tyr99	S4
His519	His171	
Gly520	Gly172	
Ser521	Ser173	
Ser522	Ser174	
Ile523	Ser175	

According to the nomenclature of Schechter and Berger, the amino acids within the substrate from the N terminus to the cleavage site are termed P4-P3-P2-P1 and the corresponding binding pockets of the enzyme, S4-S3-S2-S1 (Figure 12).[279]

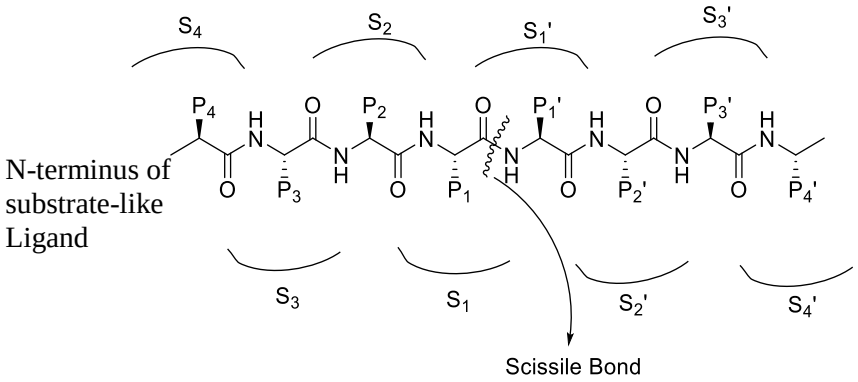

Figure 12: The nomenclature of proteases' binding site according to Schechter and Berger.

In the crystal structure 4XE4 (Figure 13a), the features that defined the protein as a zymogen-like structure are: the absence of an oxyanion hole between Gly193 and Ser195, the flipping of Asp189 from the so-called specificity S1 pocket and a buried zymogen-like conformation of the Asp194 side-chain. Therefore, to elaborate the 3D structure of FXIIa catalytic domain in the active conformation, it was necessary to create a homology model of FXIIa using the bulk of this crystal structure as a template, but taking the position of certain loops from X-ray structures of similar serine proteases (e.g. HGFA, uPA, thrombin, or FXa), which are known to be in active conformations.

FXa and thrombin are the only coagulation factors that have potent small-molecule inhibitors in clinical use. Moreover, these coagulation factors are extensively studied which has revealed the structural similarities and differences amongst them, and the binding modes of their inhibitors.[1] Therefore, in order to explore the 3D conformation of the FXIIa binding pocket and relate it to the *in vitro* inhibitory activity of the already known inhibitors, the preliminary homology and docking studies in this projects were focused primarily on FXa and its inhibitors, rivaroxaban and apixaban, and thrombin and its inhibitor, dabigatran.

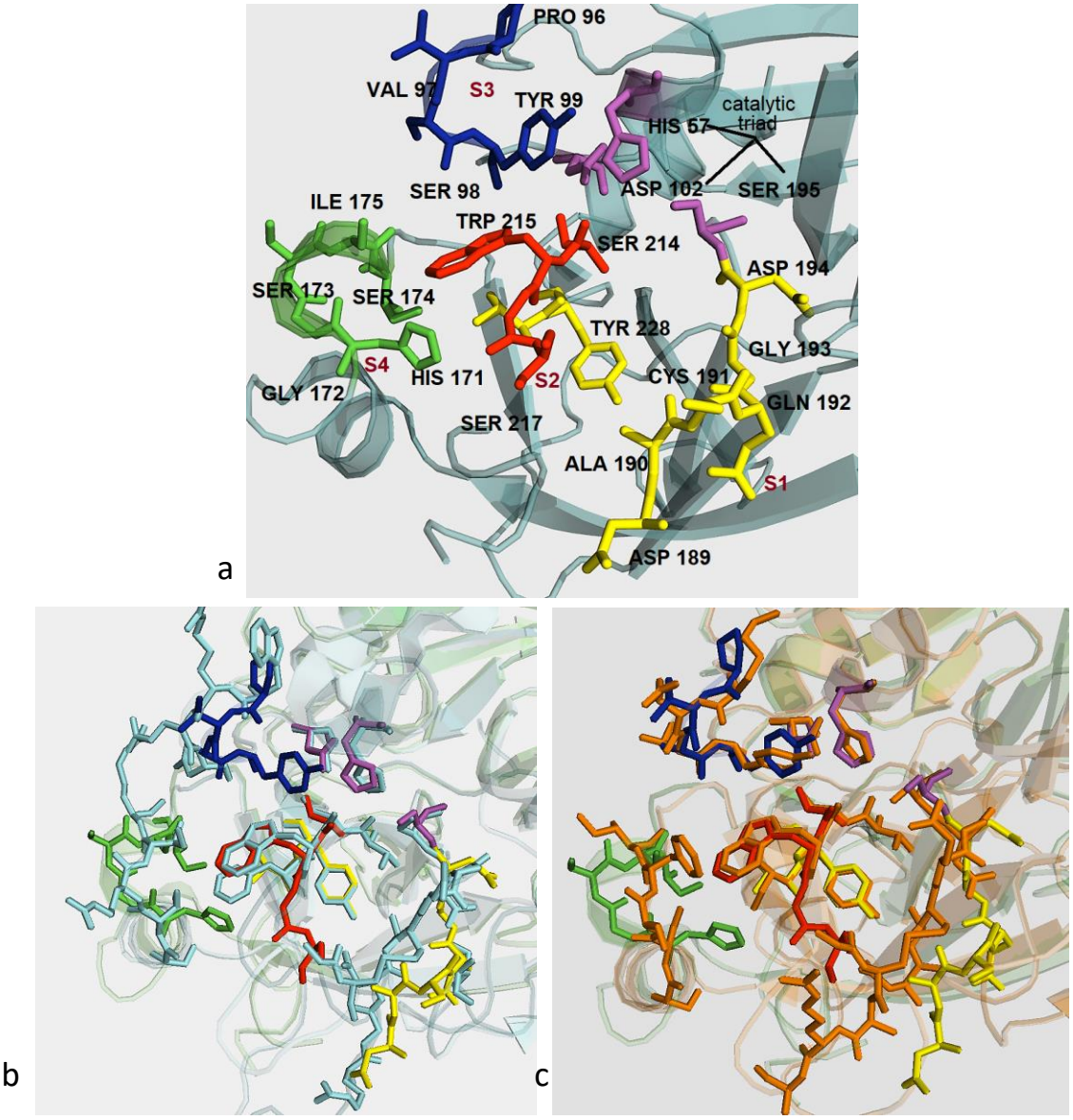

Figure 13: Comparison between the FXIIa (PDB: 4XE4), FXa (PDB: 2W26), and thrombin (PDB: 1KTS) crystal structures. a) FXIIa crystal structure (PDB: 4XE4). Colour code: yellow: S1-subpocket; red: S2-subpocket; blue: S3-subpocket; green: S4-pocket; magenta: catalytic triad. b) Alignment of FXIIa and thrombin crystal structures. FXIIa residues coloured as previous, and thrombin residues coloured as cyan. c) Alignment of FXIIa and FXa crystal structures. FXIIa residues coloured as previous and FXa residues as orange.

The *in vitro* inhibitory activity of rivaroxaban, apixaban, and dabigatran was assessed against FXIIa. It was found that rivaroxaban has an *in vitro* IC_{50} against FXIIa of 77 µM compared to apixaban and dabigatran which have IC_{50} values of 128 and 814 µM, respectively. The higher activity of FXa inhibitors against FXIIa compared to thrombin inhibitors would appear to be a result of more significant similarity in the binding pockets amongst FXIIa and FXa compared to thrombin.

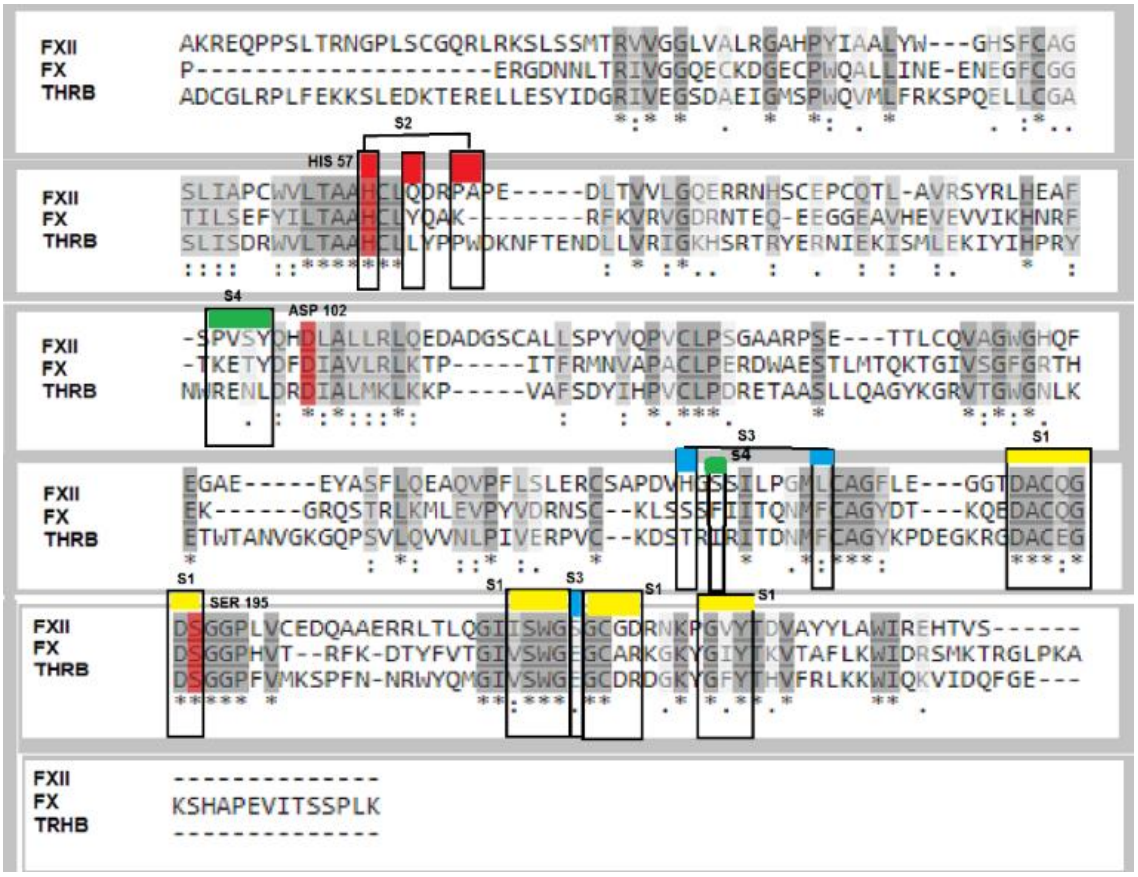

Figure 14: Sequence alignment of FXII, FX, and thrombin (THRB). (created using uniport alignment tool) http://www.uniprot.org/align/. Dark grey: identical amino acids; light grey: similar amino acids. The substrate binding pockets S1 (yellow), S2 (red), S3 (blue), and S4 (green), as well as the amino acids involved in the catalytic mechanism (His57, Asp102, Ser195), are highlighted.

The amino acid sequence alignment of FXII, FX, and thrombin shows that these enzymes share sequence similarity in the catalytic domains of more than 50% (Figure 14). However, the 3D structure alignment of FXIIa with FXa or thrombin shows that the similarities in the 3D structures of FXIIa and FXa are more prominent than that between FXIIa and thrombin (Figure 13b and c).

In the three enzymes, the catalytic centre is formed from the triad His57, Asp102 and Ser195. At the bottom of the S1-pocket of all enzymes, Asp189 is located. According to the sequence alignment, FXIIa, FXa and thrombin have the same amino acids in the S1-pocket (Figure 14). In contrast, the 3D structure alignment of FXIIa with FXa and Thrombin (Figure 13) shows that the differences in the S4-pockets between FXIIa and thrombin are more pronounced than between FXIIa and FXa. In thrombin, this pocket is formed by two aliphatic lipophilic amino acids (Leu99 and Ile174) and the aromatic residue Trp215 at the base of this subpocket. In FXa, through the lateral lining

of aromatic amino acids Tyr99 and Phe174, it is deep and hydrophobic. In FXIIa Tyr99 is located at the same position of that in FXa. Additionally, in the S4-pockets of FXIIa an FXa there is an ensemble of several carbonyl groups of the protein backbone, the so-called "cation hole".[1] Hence hydrophobic interactions, as well as electrostatic interactions with positively charge inhibitors, are possible. Accordingly, and because rivaroxaban was more potent against FXIIa than dabigatran, it was reasoned that a homology model of the crystal structure of FXIIa (PDB: 4XE4) based on the crystal structure of FXa in complex with rivaroxaban (PDB: 2W26) would be more suitable to elaborate the 3D active conformation of FXIIa than homology models based on other serine proteases. Moreover, at the start of this project, there were no reports describing the synthesis of small molecule inhibitors of FXIIa and information about the structural requirements of FXIIa inhibitors was scarce. Therefore, rivaroxaban was chosen for pharmacomodulation to shift its activity toward FXIIa instead of FXa.

2.2. Structural comparison of FXIIa and FXa

To generate a structure for the active conformation of the FXIIa protease a homology model of FXIIa was created. To create this homology model the bulk of the crystal structure 4XE4 (which is the crystal structure of FXII protease in a zymogen-like state) was used as a template except for those loops which were taken from the crystal structure of FXa (2w26): Val359-Ala364, His431-Asp442, Ser460-Gly471, Ser476-Leu480, Ile524-Gly526, Asp552-Arg558, Gly568-Ser569, Arg-lys576 (Figure 15) (the homology model was built with the aid of Dr James Anthony Wilson/ University of Nottingham). Hence forth, this homology model will be referred as FXIIa-H.

Glide program of Schrodinger suite (Schrödinger Release 2017-3: Glide, Schrödinger, LLC, New York, NY, 2017) was used for creating this homology model. The Van der Waals radii of protein atoms scaled by 1.00 and the charge cut-off for polarity scaled by 0.25. Energy minimisation follows the refinement of the initial model of FXIIa-H. The model FXIIa-H was prepared using the protein preparation wizard within the Schrödinger suite of the modelling software (Schrödinger Release 2017-3: Schrödinger Suite 2017-3

Protein Preparation Wizard; Epik, Schrödinger, LLC, New York, NY, 2016; Impact, Schrödinger, LLC, New York, NY, 2016; Prime, Schrödinger, LLC, New York, NY, 2017.). Using the protein preparation wizard, bond orders are assigned, hydrogens added, and any unwanted water molecules removed from the protein. Energy minimisation is carried out using the Impref module of the Schrödinger suite with the default cut-off root mean square deviation (RMSD) value set to 0.3 Å using Optimized Potentials for Liquid Simulations (OPLS) 2005 force field parameters.

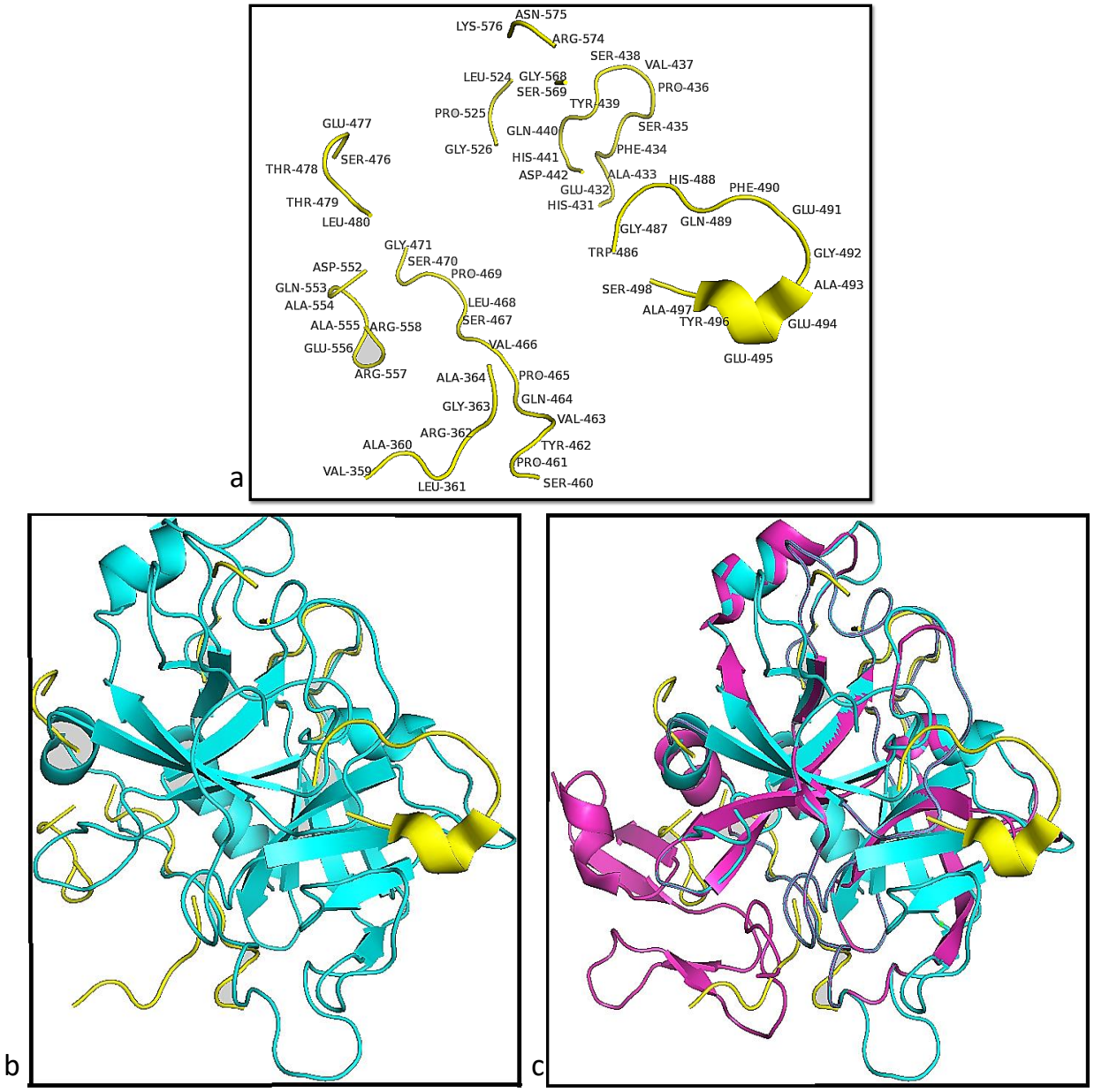

Figure 15: Homology model of FXIIa. a) The loops in 4XE4 which was changed based on the corresponding loops in 2W26, b) overlay of the changed loops in 4XE4 (yellow) and FXIIa-H (blue), c) overlay of the changed loops in 4XE4 (yellow), FXIIa-H (blue), and 2w26 (magenta).

Docking of rivaroxaban to the resulting FXII-H model showed the extent of similarities and differences in the 3D-structure FXa and that predicted for FXIIa. Rivaroxaban adopts an L-conformation binding mode in both enzymes with the chlorothiophene residue resides in the S1-pocket whereas the S4-pocket accommodates the morpholinone moiety (Figure 16).

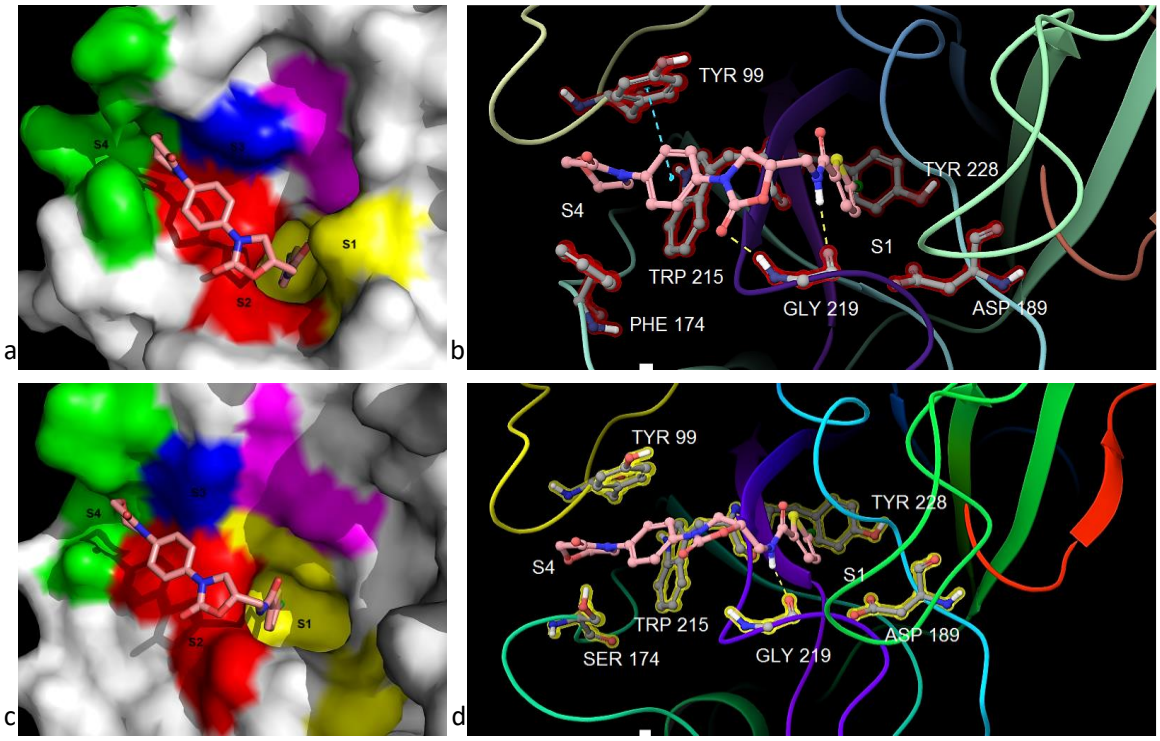

Figure 16: Comparison of the substrate binding sites of FXa and FXIIa-H. a) Surface representation of FXa with rivaroxaban (PDB: 2W26); b) The binding mode of rivaroxaban in FXa. The main residues in the S1 and S4 pockets were red highlighted; c) Surface representation of FXIIa-H model with rivaroxaban; d) The binding mode of rivaroxaban docked to FXIIa-H. The main residues in the S1 and S4 pockets were yellow highlighted. Colour code: The substrate binding pockets S1 (yellow), S2 (red), S3 (blue), S4 (green), catalytic triad (magenta), rivaroxaban (orange), nitrogen (blue), oxygen (red), hydrogen bond (yellow dotted line), π-π interaction (blue dotted line).

In FXa, the chlorine atom of the chlorothiophene group makes a critical Cl-π contact with the Tyr228 residues. In addition, rivaroxaban binding to FXa is mediated through two hydrogen bonds to the amino acid Gly219. These two hydrogen bonds serve an essential role directing the drug into the S1 and S4 subsites of FXa. The first hydrogen bond is a strong interaction which comes from the carbonyl oxygen of the oxazolidinone core of rivaroxaban. The second hydrogen bond is a weaker interaction and comes from the amino group of the chlorothiophene carboxamide moiety. These two hydrogen bonds result in the drug forming an L-shape and fit in the S1 and S4 pockets.

In FXa, the morpholinone group of rivaroxaban is sandwiched between the aryl rings of Tyr99 and Phe174. The carbonyl group of the morpholinone moiety affects the planarization of the morpholinone group and brings it into a perpendicular orientation to the aryl ring of rivaroxaban. This orientation allows the formation of the CH_2-π-interaction with Trp215 and π- π-stacking of the aryl ring with Tyr99.[1]

The top pose of rivaroxaban docked to FXIIa-H model predicts that rivaroxaban takes the L-shape binding mode in FXIIa as same in the FXa. However, the S4 pocket of FXIIa is shaped by different residues than those of FXa. The S4 pocket in FXa is deep and hydrophobic due to the presence of the aromatic rings of Tyr99, Phe174, and Trp215. However, FXIIa has the polar amino acid serine at position 174 instead of the nonpolar phenylalanine. Therefore the S4-pocket of FXIIa is more polar compared to that of FXa.

Despite the predicted similarities in the binding pockets of FXa and FXIIa, it seems that there are significant differences that are likely to account to the specificity of FXa and FXIIa to different substrates. The natural substrate of FXa is thrombin. FXa has a proteolytic activity on two sites in thrombin; Phe281-Asn282-Pro283-Arg284-//-Thr285-Phe286 and Tyr317-Asp318-Gly319-Arg320-//-Ile321-Val322. FXa cleaves between Arg284 and Thr285 and between Arg320 and Ile321 (P13/P1'), which leads to the separation of the light chain from the activation peptide 2 and the heavy chain and hence the activation of thrombin.[1] On the other hand, the natural substrate of FXIIa is FXI. FXIIa has a proteolytic activity on a site in FXI composed of Ile384-Lys385-Pro386-Arg387-//-Ile388-Val389-Gly390-Gly391 where FXIIa breaks the bond between Arg387 and Ile388.[280] Therefore both enzymes can accommodate proline at the S2 pocket. However, the S4-subpocket of FXa accommodates the aromatic amino acids phenylalanine or tyrosine whereas the S4-position of FXIIa accommodates the aliphatic side chain of isoleucine. Moreover, the S3-pocket of FXIIa accommodates the positively charged lysine wherase in FXa the S3-pocket accommodate the negatively charged aspartate or the uncharged asparagine. Therefore, the differences in the S3 and S4 pockets of the two enzymes could be responsible for the preference for different substrates.

The alignment and modelling studies showed that FXIIa and FXa are very similar in the amino acids sequence as well as in the 3D structure. In both enzymes, the catalytic centre is formed from the triad His57, Asp102, and Ser195. Both FXIIa and FXa have a very similar S1 pocket where aspartate residue is at the bottom of this pocket (Figure 16). In FXa, this residue (Asp189) participates in ionic and hydrogen-bond interactions with the positively charged P1 arginine of the substrate.[1]

The main focus of this project was on substituting different moieties at the P1- and P4-positions of rivaroxaban and measuring the effect of these substituents on the inhibitory activity against FXIIa and FXa, respectively. Although the structural information of FXIIa was obtained mainly from homology models rather than a high-resolution X-ray crystal structure of FXIIa in complex with a ligand, the docking studies were used throughout this project as a helping tool to design potent FXIIa inhibitors.

2.3. Discovery of rivaroxaban

Due to the drawbacks of the traditional anticoagulants, such as heparins and warfarin,[281,282] recent research has focused on the inhibition of a single enzyme in the coagulation cascade, particularly FXa and thrombin. Particular has been placed on the development of small-molecule, orally-available direct thrombin or FXa inhibitors.

Argatroban, melagatran (and its prodrug ximelagatran), and dabigatran (and its prodrug dabigatran etexilate), which target thrombin, and apixaban and rivaroxaban, which target FXa, are all small molecules anticoagulants which are in clinical use today except melagatran and its prodrug which were withdrawn from the clinic after reported side effects and death cases.[216,220]

The starting compound that led to the discovery of rivaroxaban was derived from High Throughput Screening (HTS), (Figure 17, compound **11**). The optimisation of this compound led to the discovery of isoindolinone **12** as potent FXa inhibitors with an IC_{50} value against FXa of 8 nM in the *in vitro* enzymatic activity assay.[283] Further optimisation of these compounds had been done to achieve the pharmacokinetic properties necessary for oral bioavailability. During these optimisations, the 5-chlorothiophene-2-

carboxamide moiety had been discovered as a necessary group for the activity against FXa.[267]

Reviewing the HTS's results led to the discovery of oxazolidinones as very weak FXa inhibitors (e.g. **13,** IC_{50} 20 μM). However, taking into account, the necessity of the 5-chlorothiophene-2-carboxamide moiety for activity against FXa led to the exchange of the thiophene moiety in **13** with 5-chlorothiophene, which resulted in the discovery of lead compound **14** with an IC_{50} against FXa of 90 nM.[284]

Further optimisation of **14** by fixing the chlorothiophene moiety and changing the thiomorpholine group with, for example, morpholine, morpholinone, pyrrolidine, pyrrolidinone, or piperazine, led to the discovery of compound **3** (rivaroxaban) with a morpholinone group at one end and chlorothiophene group at the other. Furthermore, it was discovered that FXa has preferences for the compounds with an (*S*)-configuration at the oxazolidinone core, where the (*R*)-enantiomer of rivaroxaban is 3286-times less potent than its (*S*)-enantiomer counterpart (IC_{50} value of 0.7 nM for (*S*)-enantiomer rivaroxaban vs 2.3 μM for (*R*)-enantiomer). In addition, fixing the morpholinone moiety of **14** and changing the chlorothiophene group with, for example, bromothiophene, methylthiophene, bromofuran, or chlorobenzenes was lead to rivaroxaban with a potent IC_{50} against FXa of 0.7 nM in *in vitro* enzymatic assay, and with pharmacokinetic properties necessary to achieve the required oral bioavailability.[267]

All in all, the SAR of rivaroxaban led to the discovery that there are three essential conditions for oxazolidinones to be highly potent against FXa; It should be in an (*S*)-configuration, with 5-chlorothiophene-2-carboxamide moiety at one side, and morpholinone moiety at the other side.

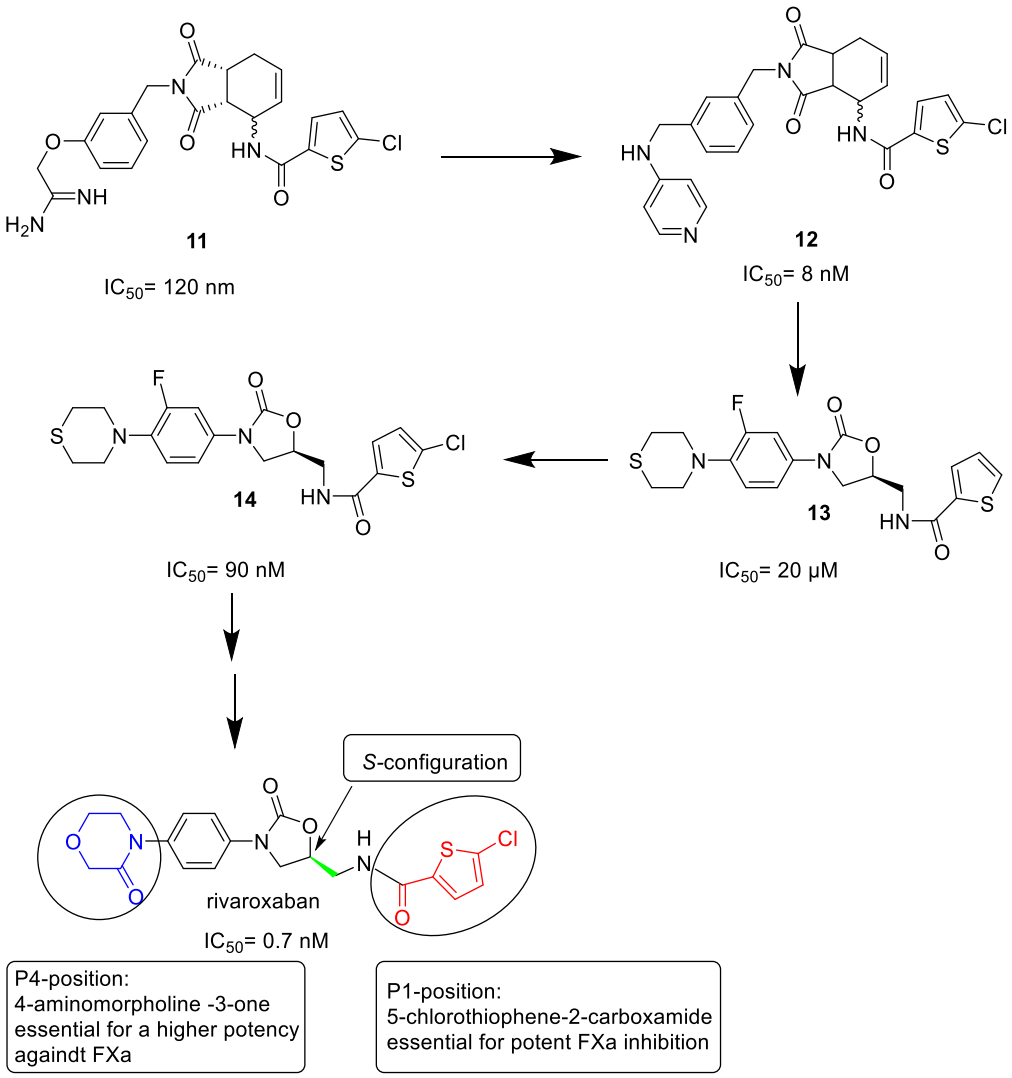

Figure 17: Optimisation to oxazolidinone FXa inhibitors that led to the discovery of rivaroxaban.

2.4. Design of rivaroxaban analogues

Rivaroxaban adopts an L-shape binding mode in FXa, and is predicted to take the same conformation in FXIIa according to our docking studies. The oxazolidinone ring participates in directing rivaroxaban into the S1 and S4 subsites through forming hydrogen bonds with the Gly219 residue (Figure 18). Therefore, the oxazolidinone core was preserved throughout this project, and the focus was on substituting different groups at the P1 and P4-positions and test the effect of this substitutions on the potency of the inhibitors against FXIIa and FXa.

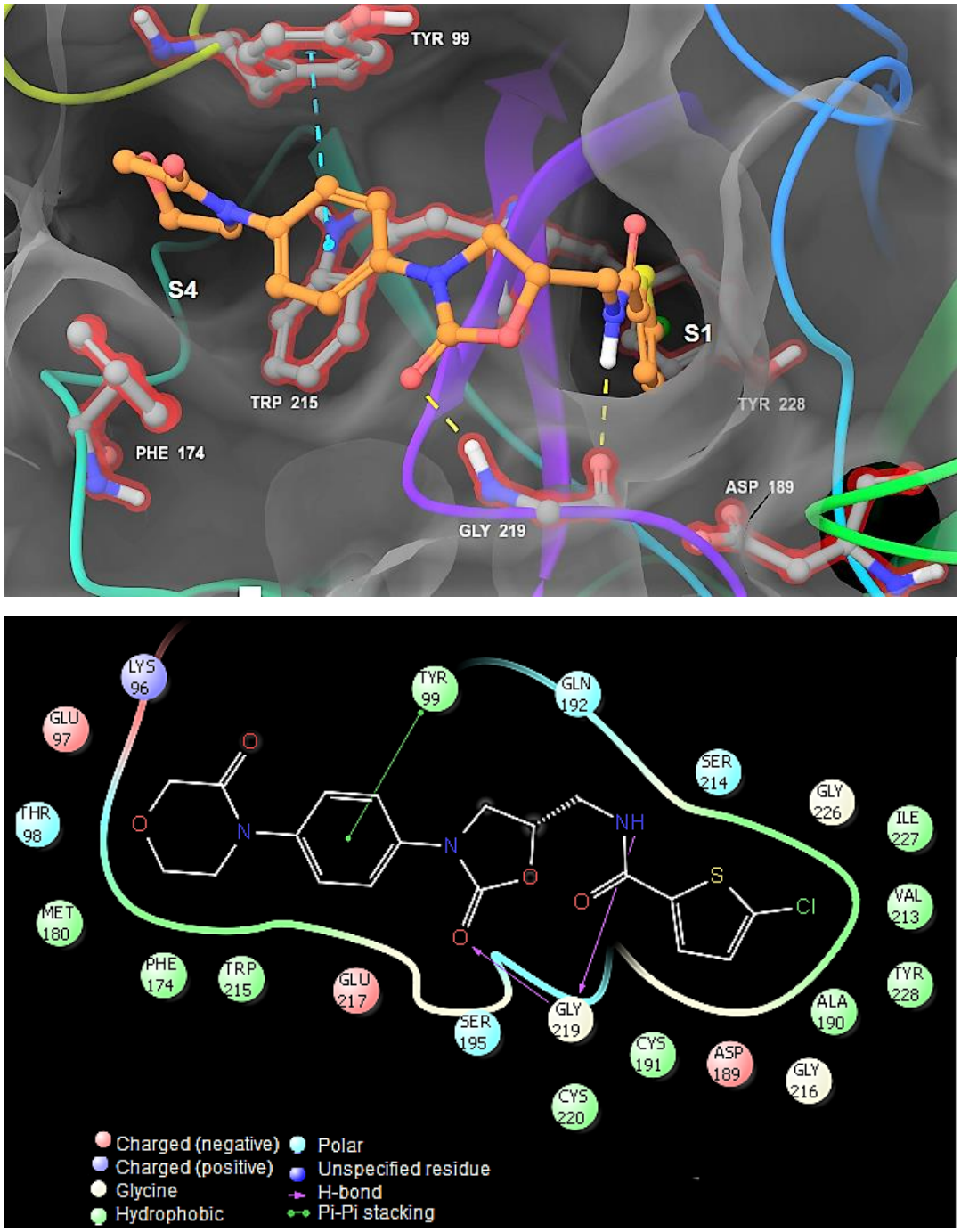

Figure 18: The binding mode of rivaroxaban in FXa (PDB: 2W26). (Above): Surface representation of rivaroxaban binding mode in FXa. Only important residues were shown. Carbon backbone colour: Orange: rivaroxaban; grey: enzyme residues. Blue dotted line: π-π interactions, yellow dotted line: H-bonds.; (bottom): 2D-schematic representation of rivaroxaban binding mode in FXa.

As discussed above, during the discovery of rivaroxaban, the chlorothiophene moiety was shown to be very important for its activity against FXa. Replacing the chlorine atom of the chlorothiophene group with a methyl as in, **16** led to a six-fold decrease in FXa inhibitory activity of **16** compared to rivaroxaban (Table 2). In addition, replacing the chlorothiophene group with 4-

chlorobenzene as in **18** or 3-chlorobenzene as in **19,** led to a drop in the inhibitory activity compared to rivaroxaban by 28- and 1671-fold, respectively.[267]

Table 2: Reported effect of changing the chlorothiophene moiety of rivaroxaban on the *in vitro* anti-FXa potency. [267]

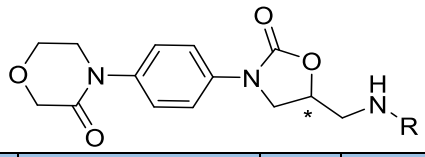

compd	R=	ent*	IC_{50} nM FXa
riv.	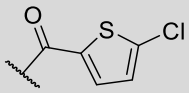	*S* *R*	0.7 2300
15	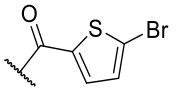	*S*	0.4
16	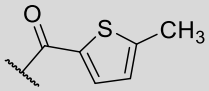	*S*	4.2
17	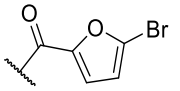	*S*	26
18	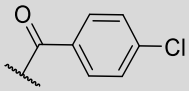	*S*	20
19	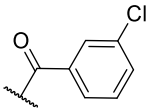	*S*	1170
20	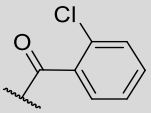	*S*	2000
21	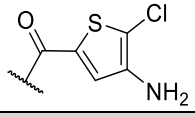	*S*	8.5
22	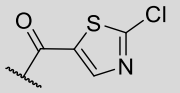	*S*	290
23	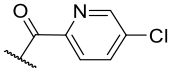	*S*	29
24	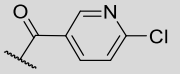	*S*	24
25	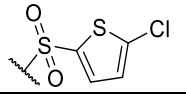	*S*	1200

FXa shows significant affinity for the *S*- compared to *R*-enantiomer of the rivaroxaban. In the current project, rivaroxaban was first synthesised in *S*- as well as in *R*-enantiomeric form and tested against FXIIa and FXa. The *S*-enantiomer of rivaroxaban was found to has an *in vitro* inhibitory activity against FXa with an IC_{50} value of 0.6 nM whereas the *R*-enantiomer IC_{50} was 2100 nM. Furthermore, the *S*-enantiomer of rivaroxaban inhibits FXIIa with an IC_{50} of 77 µM whereas the *R*-enantiomer was completely inactive against this enzyme. Therefore, it was hypothesised that the binding pocket of FXIIa has the same stereospecificity of that of FXa. Hence, the majority of the synthesised compounds in this project are in *S*-enantiomer.

As the ultimate goal of this project is to synthesis selective small-molecule inhibitors of FXIIa, the initial interest was to resynthesis compounds that show slight activity against FXa compared to that of rivaroxaban, for example, compounds **19**, **20**, and **25**. These compounds are much less active against FXa than rivaroxaban. For example, compound **19** is 1600-fold less active against FXa than rivaroxaban. Hence, if these compounds show an improved inhibitory activity toward FXIIa, then this will represent a shortcut toward improving the selectivity of the synthesised compounds. Furthermore, the chlorine atom of the 5-chlorothiophene group at the P1-position of rivaroxaban (see Figure 17) was omitted, or the whole group was replaced with benzene, 4-fluorobenzene, *tert*-butylbenzene, benzonitrile, aniline, cyclohexylmethylamine, cyclohexylamine, benzylamine. benzamidoxime, benzamidine, benzamide, or benzenesulphonamide.

For substituents at the P1-position of rivaroxaban, various groups were selected. Some of these groups were selected because it appears in other compounds that show activity against FXIIa. For example, Peter's Fischer group working with different pharmacophore as FXIIa inhibitor that suggested *tert*-butyl benzene as a potential P1-substituent (unpublished data). On the other hand, the benzamidine group was selected because benzamidine-containing compounds are the classic inhibitors of serine proteases, and the benzamidine fragment is a medium-potency inhibitor for all members of the trypsin family (K_i ~15 nM).[285]

The amidine group in these compounds mimics the guanidine or amine group of arginine or lysine, respectively, which found at the scissile bond of the common substrates of serine proteases.[286] However, the amidine groups are highly hydrophilic and strongly basic (pK_a ~12.5). These characteristics lead to poor or insufficient oral absorption of amidine-containing compounds. Moreover, these compounds are also characterised by very short half-life due to high clearance.[287] Therefore, replacement of the amidine group with derivatives of low basicity has studied, for example, benzamide, or benzenesulphonamide. Moreover, the choice of the amide group at the P1-position was supported by the fact that inhibitors of some coagulation factors contain an amide at the P1-position.[288]

2.5. Changes to the P4 position of rivaroxaban

The S4 pocket in FXa is a narrow hydrophobic "box" defined by the aromatic rings of Tyr99, Phe174 and Trp215. The non-polar aryl ring of rivaroxaban extends across the face of Trp215, and the morpholinone moiety is sandwiched between Tyr99 and Phe174, thus leading to hydrophobic interactions. The carbonyl group of the morpholinone does not interact directly with FXa but exerts its beneficial effect through polarisation of the ring CH_2 on top of Trp215 (C-Trp distance: 3.5 A˚), thereby increasing the CH_2... π interaction as well as through conformational preorganization of a perpendicular arrangement to the adjacent phenyl ring.[289] This effect is reflected by the 60-fold higher potency of rivaroxaban compared with the morpholine derivative of rivaroxaban **28** (Table 3). Other six-membered rings such as lactams **30** and **33**, were also introduced as a non-basic P4-residues of FXa inhibitors.[284] However, as explained earlier, according to our homology and docking studies, the major difference in the binding pocket of FXa and FXIIa was in the S4-pocket. Therefore, to test this hypothesis, the chlorothiophene group at the P1-position was kept unchanged and the morpholinone moiety at the P4-position was replaced with various groups.

The effect of deleting the carbonyl group of the morpholinone moiety on the inhibitory activity against FXIIa was first tried through resynthesise of compound **28**. Furthermore, various groups were also tried as a surrogate at

the P4-position such as benzene, pyridine, methoxybenzene, or dimethoxybenzene.

Table 3: Effect of changing the P4-moiety of rivaroxaban on the *in vitro* anti-FXa potency[284]

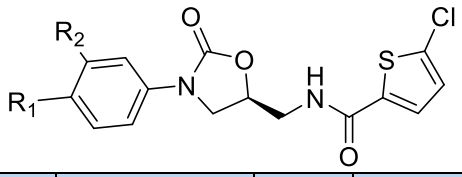

compd	R_1=	R_2=	IC_{50} nM FXa
26	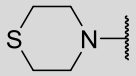	F	90
27	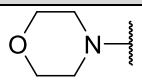	F	32
28	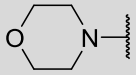	H	43
29	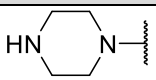	F	140
30	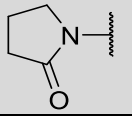	H	4
31	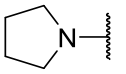	F	40
32	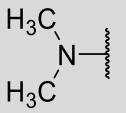	H	74
33	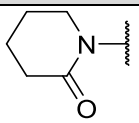	H	1
34	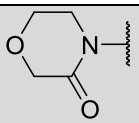	F	1.4

Given that the importance of the carbonyl group, it is expected that compounds with morpholinone at the P4-position (e.g. compound **34**) be more active against FXa than compounds with piperazine at this position (e.g. compound **29**). However, compounds with morpholine (e.g. compound **27**) are also reported to be more active against FXa than compounds with piperazine (e.g.

compound **29**). There are literature reports that piperazine group at the P4-position result in a drop in the activity against FXa by 100-fold (**29** vs **34**).[284] This means that piperazine at the P4-position was unattractive for the inhibition of FXa more than morpholine or morpholinone. Thus, piperazine and piperazine derivatives were also attempted as a surrogate at the P4-position.

2.6. Conclusion

The structural information of the FXIIa is much less than for FXa or thrombin. Therefore, in order to model the 3D structure of this enzyme, a homology models of FXIIa was made using the X-ray crystal structure of the catalytic domain of FXIIa in a zymogen-like state (PDB: 4XE4) as a template and taking the conformation of certain loops from the X-ray crystal structures of other serine proteases of a known active conformation (see Figure 15).

Thrombin and FXa were the only coagulation factors with selective-high affinity small-molecule inhibitors in clinical use today. Furthermore, these enzymes have been the subject of extensive research projects that revealed their 3D structural characteristics. For example, to date, more than 270 crystal structures of FXa are available in the protein data bank, of which 150 have co-crystallized small-molecule ligand.[290] Therefore, X-ray crystal structures of FXa and thrombin appeared to be more relevant for building a FXIIa homology model than other serine proteases. However, sequence and X-ray crystal structure alignment of FXIIa and FXa and thrombin revealed that all three enzymes bear a significant resemblance at the S1-pocket, but for FXIIa and thrombin the differences at the S4-pocket were more prominent than that between FXIIa and FXa. Besides that, rivaroxaban and apixaban (FXa inhibitors), and dabigatran (thrombin inhibitor) were tested for pharmacological activity against FXIIa. The results showed that rivaroxaban was the most active compounds against FXIIa amongst the three compounds. Therefore, I decided to amend the rivaroxaban structure to be more selective to FXIIa than FXa.

A homology model of FXIIa (FXIIa-H) was built based on the X-ray crystal structures of FXIIa (PDB: 4XE4) and FXa (PDB:2W26). The homology

studies showed that FXIIa and FXa share the same amino acid sequence and the same 3D-conformation at the S1-pocket. However, the S4-pockets of both enzymes were shaped by different residues. The S4-pocket of FXa was lined with aromatic amino acids whereas the FXIIa S4 pocket was less hydrophobic. Moreover, docking studies showed that rivaroxaban adopts the same L-shape binding modes in both enzymes.

During the discovery of rivaroxaban, the researchers noticed the importance of the chlorothiophene moiety at the P1-position and the morpholinone moiety at the P4-position for the inhibitory potency against FXa. The pattern of P1 and P4 residues present in rivaroxaban proved to be particularly efficient and was also adopted in other structures.[1] Therefore this model was utilised in this project to synthesise rivaroxaban analogues with high antiFXIIa activity.

Several groups will be evaluated at the P1-position among them chlorothiophene, thiophene, *tert*-butylbenzene, aniline, cyclohexylmethylamine, cyclohexylamine, benzylamine, benzamidine, benzamide or benzenesulphonamide. The groups considered for P4-position includes morpholinone, morpholine, benzene, pyridine, fluoropyridine, piperazine, methylpiperazine, piperazinone, methylpiperazinone, methoxybenzene, or dimethoxybenzene. Furthermore, various rivaroxaban analogues were synthesised. The groups at P1- and P4-position were selected mainly based on iterative make-test cycle.

Docking studies were also carried out in this project using the homology-model of FXIIa (FXIIa-H) in order to predict the binding-conformation of the synthesised compounds and better understand the structure-activity-relationships. in addition, the *in vitro* pharmacological activity of the synthesised compounds was assessed against FXIIa and FXa using biochemical enzymatic assays.

Chapter Three: Synthesis

The synthetic routes for target compounds in this project will be presented in this chapter. First, a short literature review of the reported methods used for the synthesis of rivaroxaban will be presented. After that, the synthesis of the rivaroxaban and rivaroxaban analogues with an altered P1- and/or P4-moieties will be illustrated in Scheme 4. Then, the synthesis of rivaroxaban analogues with an amidoxime or amidine group at the P1-position will be stated. The synthesis of rivaroxaban analogues by Suzuki reaction will be presented after that. Finally, synthesis of various rivaroxaban fragments will be shown.

The compounds will be labelled according to their P1- and P4- moieties. A number and a letter were assigned for each compound. The letter represents the P1-group of the compound whereas the number represents the P4-moiety. For example, whenever the letter **e** appears in the label of the compound, this means that the group at the P1-position is 5-chlorothiophene-2-carbonyl. Similarly, the letter **g** indicates that the P1-group of the compound is 4-*tert*-butylbenzene-1-carbonyl, and so on as shown in Scheme 4. On the other hand, whenever number one appears in the label of the compound, this means that the P4-group of the compound is morpholin-3-on-4yl. Similarly, number two in the label of the compound indicates that the P4-moiety is thiophene-5-yl, and so on. However, compounds which do not follow P1/P4 pattern were labelled sequentially starting from number one to eighty.

3.1. Literature reported methods for synthesis of rivaroxaban

Oxazolidinones are heterocyclic compounds, which contain oxygen and nitrogen in a five-membered ring. One of the first uses of these rings system was as a bacteriostatic antibiotic against methicillin-, penicillin-, or cephalosporin-resistant staphylococci and vancomycin-resistant enterococci.[291] Eperezolid and linezolid were the first members of this class of antibiotics that were discovered in the late 1980s. Linezolid was approved by the FDA for the treatment of infections caused by methicillin-resistant staphylococci or

vancomycin-resistant enterococci, such as skin infections and pneumonia. The emergence of bacterial resistance to this antibiotic has led to the discovery of other oxazolidinones as potent antibacterial agents.[292]

In the last decade, a range of oxazolidinone-containing compounds were discovered to have anticoagulant activity. One of these compounds was rivaroxaban, which was synthesised as the first orally available and selective FXa inhibitor.[267] Thereafter fluorinated oxazolidinone[293], tricyclic fused-oxazolidinone[294], and cyclic amidine-containing oxazolidinone[295] were synthesised for use in the prevention and treatment of thrombotic disorders.

In the literature, there are several reported methods for the synthesis of rivaroxaban,[296-302] One of these methods (Scheme 1), starts by the reaction of the commercially available epoxide **35** with aniline derivative **36**. The epoxide opened from the least substituted carbon to result in the formation of amino alcohol **37**. The second step in this process involves the cyclisation of **37** with carbonyldiimidazole and adding 4-(dimethylamino)pyridine in a catalytic amount results in the formation of **38**. The amine group of **38** is then deprotected by reaction with aqueous methylamine in ethanol. The resulting primary amine **39** is then dissolved in pyridine and reacted with 5-chlorothiophene-2-carbonyl chloride giving rivaroxaban **3**.[267]

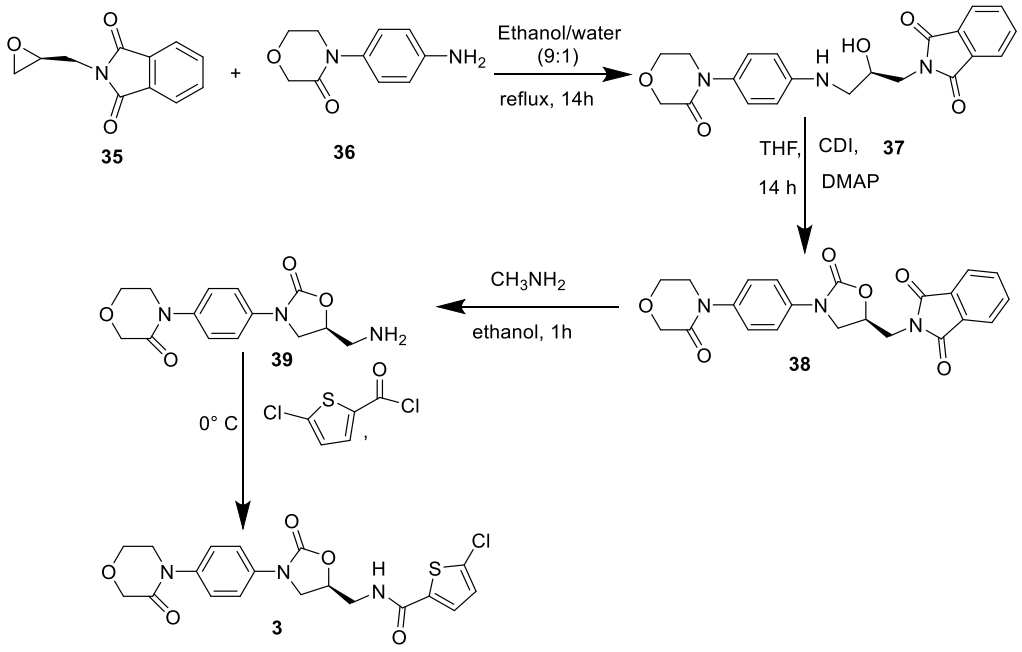

Scheme 1: The general method for the synthesis of rivaroxaban.[267]

One of the alternative procedures reported in the literature for the synthesis of rivaroxaban starts by the reaction of **36** with *(R)*-epichlorohydrine **40** to form compound **41** (Scheme 2). In the next step, **41** either cyclized with N,N-carbonyldiimidazole (CDI) and then reacted with potassium phthalimide or the other way around (reacted with potassium phthalimide and then cyclized with CDI) to result in the formation of **38**. The phthalimide group of **38** is then deprotected with hydrazine to result in the formation of **39**, which finally reacted with 5-chlorothiophene-2-carbonyl chloride in pyridine to form rivaroxaban.[300]

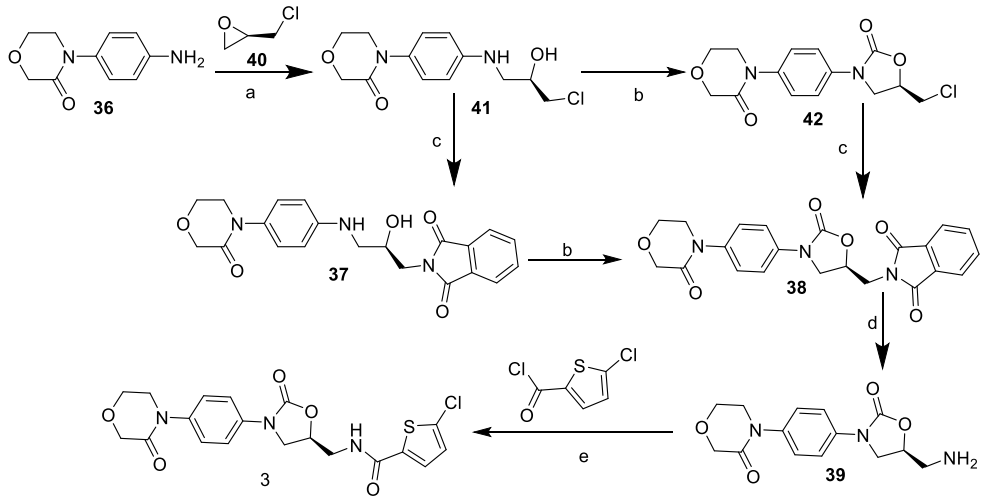

Scheme 2: Alternative method for the synthesis of rivaroxaban. Reagents and conditions: (a) MeOH, reflux, 16h; (b) N,N-carbonyldiimidazole (CDI), DCM, 30°C, 20h; (c) potassium phthalimide, DMF, reflux, 5h (f) MeOH, hydrazine hydrate, reflux, 1h-rt; (g) pyridine, 0° C to room temperature.[267,300]

An other literature-reported methods for the synthesis of rivaroxaban involves the reaction of (*R*)-epichlorohydrine **40** with sodium cyanate to produce (*R*)-5-(chloromethyl)oxazolidin-2-one intermediate **43**, which is then reacted with potassium phthalimide to form **44** (Scheme 3). Then compound **44** coupled with 4-(4-bromophenyl)morpholin-3-one **45** in an Ullmann type of reaction with copper iodide to result in the formation of **38**. The next step in this method involves deprotection of the amine of **38** with hydrazine hydrate in MeOH to result in the formation of **39**. In the last step, **39** reacted with 5-chlorothiophene-2-carboxylic acid to produce rivaroxaban.[302]

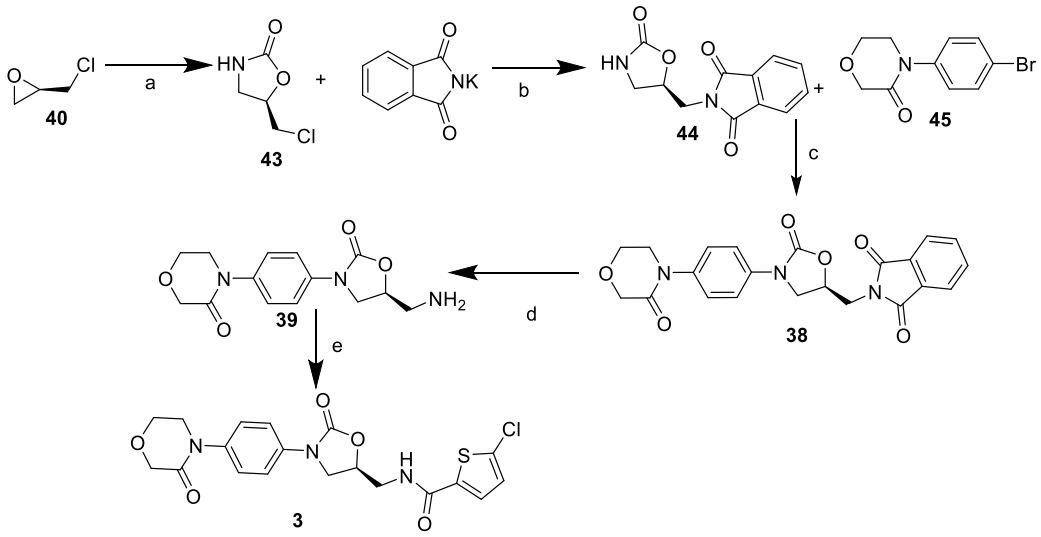

Scheme 3: Another example of a method for the synthesis of rivaroxaban. Reagents and conditions: (a) NaOCN, 60 °C; (b) potassium phthalimide, DMF, 80 °C; (c) CuI (5 mmol %), (Z)-1,2-diaminocyclohexane (10 mol %), dioxane, K_2CO_3, 110 °C; (d) hydrazine hydrate (80%), MeOH, reflux; (e) 5-chlorothiophene-2-carboxylic acid, thionyl chloride, TEA, DCM, r.t.[302]

For the purpose of this project, the general methodology described in Scheme 1 was adopted (with some modifications) as the general route for the preparation of rivaroxaban derivatives designed to be selective for FXIIa rather than FXa. The selection of this method was based on the availability of the starting material, high yield, and the ease of purification.

3.2. Synthesis of rivaroxaban analogues with an altered P1 and/or P4 moieties

In order to test the effect of changing the P1 and/or P4 positions of rivaroxaban on the activity toward FXIIa and FXa, the same oxazolidinone core used for the synthesis of rivaroxaban was adopted in this project (Figure 19).

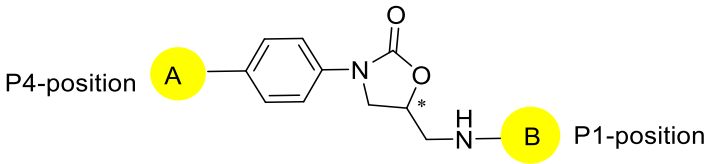

Figure 19: Oxazolidinone template used for the synthesis of rivaroxaban analogues.

The moieties for P4-position (ring A) was chosen from either morpholine, morpholin-3-one, bromine, 1-methylpiperazine, 4-methylpiperazin-2-one, -

piperazine, or 3-oxopiperazine. The carbonyl group of the morpholinone moiety at the P4-position of rivaroxaban is essential for the inhibitory activity against FXa. Omitting this group was responsible for the significant drop in inhibitory activity against FXa.[267] Therefore, to test the potential of this group on the inhibitory activity against FXIIa, a set of compounds with morpholinone or morpholine was synthesised. Furthermore, the homology and docking studies in this project (see chapter 2) showed that the major difference in the binding sites of FXIIa and FXa lies in the S4-subpocket. In addition, the literature reported that compounds with piperazine at the P4-position were 200-fold less potent against FXa than rivaroxaban.[267] Therefore, another set of compounds was synthesised to test the effect of putting piperazine or piperazine derivatives at the P4-position on the inhibitory activity against FXIIa and FXa.

On the other hand, moieties for P1-position (ring B) was chosen from either 2-chlorothiophene, thiophene, benzonitrile, benzene, 3-chlorobenzene, 2-chlorobenzene, 4-chlorobenzene, 4-fluorobenzene, 4-tert-butylbenzene, aniline, cyclohexylmethylamine, cyclohexylamine, benzylamine, benzamide, or benzenesulfonamide. The link between nitrogen and the P4-position was either carbonyl, sulfonyl, or $C(O)CH_2(O)$ group. Finally, the configuration of the chiral carbon * can only be *(S)* or *(R)*.

Scheme 4 describes the general route for the synthesis of rivaroxaban analogues with an altered P1 and/or P4 groups. The opening of the epoxide **35** with the desired substituted anilines **a1-7**[284] provided the amino alcohols **b1-7**, which was subsequently converted to the oxazolidinones **c1-7** via ring closure with CDI.[303] After deprotection of the phthalimide group with methylamine, hydrazine, or sodium borohydride, amines **d1-7** was acylated with either the desired acyl chloride or Boc-protected carboxylic acid.[304] The Boc-protected intermediates were then subjected to acidolysis to remove the Boc-group.

.

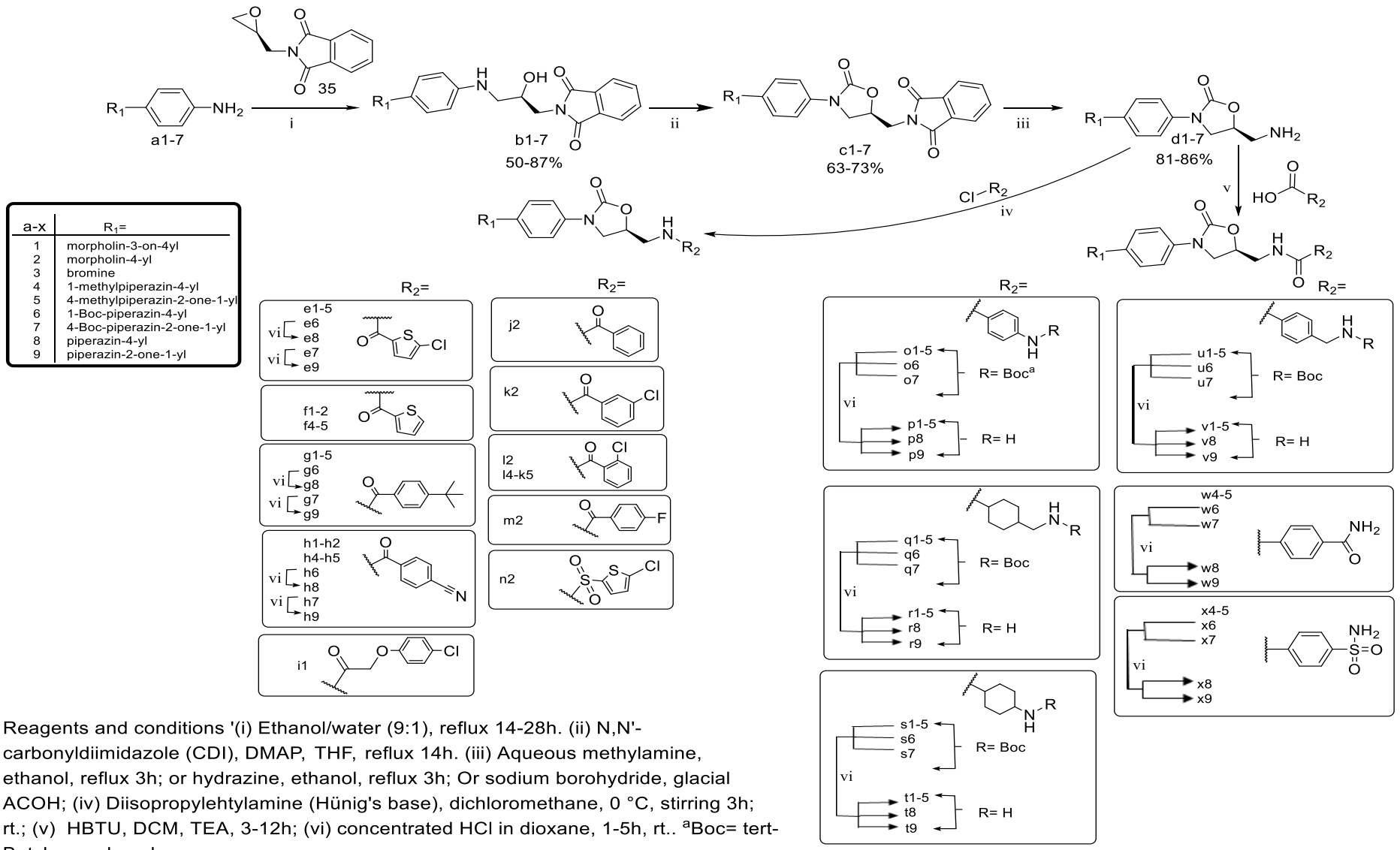

Reagents and conditions '(i) Ethanol/water (9:1), reflux 14-28h. (ii) N,N'-carbonyldiimidazole (CDI), DMAP, THF, reflux 14h. (iii) Aqueous methylamine, ethanol, reflux 3h; or hydrazine, ethanol, reflux 3h; Or sodium borohydride, glacial ACOH; (iv) Diisopropylehtylamine (Hünig's base), dichloromethane, 0 °C, stirring 3h; rt.; (v) HBTU, DCM, TEA, 3-12h; (vi) concentrated HCl in dioxane, 1-5h, rt.. [a]Boc= tert-Butyloxycarbonyl.

Scheme 4: The general route for the synthesis of rivaroxaban analogues with an altered P1 and/or P4 groups.

In the first step, substituted anilines **a1-7** was reacted with **35** to result in the formation of compounds **b1-7** in a yield of 50-87%. This reaction is described in the literature as to proceed in two stages.[266] in the first stage 1:1 amounts of aniline derivatives and epoxide **35** were used, and the reaction was refluxed overnight. The reaction mixture was then stopped, and the precipitate was filtered. In the second stage, the residue left after the filtration was concentrated in vacuo and re-reacted with another one equivalent of the epoxide **35**. However, in the current project, this reaction was done in one stage only by using 1:1.2 equivalents of aniline derivatives **a1-7**: epoxide **35**. The residue left after filtration was not reacted again despite it still contained unreacted starting material **a1-7** because it was uneconomical to use another equivalent of epoxide in the further stage.

The reaction between **a1-3** and **35** took 14 h until completion, whereas compounds **a4-7** took more time (28 h). Moreover, the yield of the former compounds was considerably higher than that of the latter compounds. Compounds **b1-3** were precipitated from the solution when the reaction mixture cooled to an ambient temperature, and diethyl ether was added, whereas compounds **b4-7** still in solution even after adding ether. Therefore, the purification of compounds **b1-3** was done by recrystallisation from diethyl ether, whereas compounds **b4-7** were purified by flash-LC using a gradient of DCM/MeOH solvent.

In the next step, intermediates **b1-7** were cyclized in the presence of carbonyldiimidazole (CDI). This reaction was attempted with and without base catalysis, and it was noticed that the yield had increased when a base was added in a catalytic amount. Two equivalents of CDI were used, and the reaction was refluxed for 14 hours. Compounds **c1-3** were recrystallised from MeOH, whereas compounds **c4-7** were purified by flash-LC. The purified yields of compounds **c1-3** were 70-73%, whereas the yields for compounds **c4-7** were 63-68%.

For deprotection of the amine derivatives **c1-7**, three methods were tested. The first method was carried out by using hydrazine hydrate (Ing-Manske procedure) as a deprotecting agent.[305] In another method, aqueous

methylamine (40%) was used for the deprotection.[306] The last route was comprised of two steps, which was performed in a one-pot reaction. In the first step, sodium borohydride was used as a reducing agent before adding glacial acetic acid to complete the reaction.[307] By comparison the yield and the ease of working-up for the three methods, it was found that methylamine method was the superior due to the high yield and the ease of purification.

Hydrazinolysis, although mild, the separation of the resulting phthalhydrazides was challenging. Phthalhydrazides precipitate out of the solution as a white solid. However, after several rounds of filtration, some of the phthalhydrazides remain in the solution, so the resulting residues need further purification via flash-LC. The repeated cycles of filtration, washing, and further purification by flash-LC have led to lower the yield of the desired compounds. The purified yield for this method was 43-56%. Direct purification via flash-LC was also tried using gradients of MeOH/DCM, EtOAc/DEE, or 1N NH_3 in MeOH/DCM. However, a large amount of solvent was needed for the purification of the crude compounds, and the yield was still low. By comparison, the methylamine method is mild, and it does not have the disadvantage of reducing carbonyl groups elsewhere in the reactant (which is the disadvantage of the sodium borohydride procedure), and the resultant side-products are easy to purify. The purified yield of this method was 81-86%. The reduction of phthalimide group by sodium borohydride leads to a reduction of the carbonyl group elsewhere in the reactants (i.e. the carbonyl group of morpholinone moiety).

To form an amide bond, the primary amine intermediates **d1-7** was reacted with an acid chloride in the presence of DIPEA as a base. The work-up for the final compounds includes filtration, crystallisation from a suitable solvent, extraction, and/or purification by flash-LC. The target compounds were obtained in 55-81% yield. The Boc-containing compounds **e6-7** and **g-h(6-7)** were then subjected to acidolysis and extracted into the organic layer from the saturated solution of $NaHCO_3$ or Na_2CO_3 to obtain compounds **e8-9** and **g-h(8-9)** in 73-80% yield.

Where the desired acyl chloride was commercially unavailable, or it was expensive, the amide bond was synthesised by reacting intermediates **d1-7** with the desired carboxylic acid in the presence of 2-(1*H*-benzotriazol-1-yl)-1,1,3,3-tetramethyluronium hexafluorophosphate (HBTU) as a coupling reagent, and triethylamine (TEA) as a base. The target compounds **o1-7, q1-7, s1-7, u1-7, w4-7, x4-7** were obtained in 50-56%. Then compounds **o6-7**, **q6-7**, **s6-7**, **u6-7**, **w6-7**, and **x6-7** were subjected to acidolysis to remove the Boc-group. The free base of these compounds was then obtained by either through aqueous extraction or by the use of the ion-exchange resin Amberlyst® A21. Compounds **o8-9**, **q8-9**, **s8-9**, **u8-9**, **w8-9**, and **x8-9** were obtained in 70-84% yield.

This method for the synthesis of rivaroxaban and rivaroxaban analogues was found to be efficient, economical and high yielding process. The developed process avoids the use of hazardous chemicals or unpleasant substances, and special purification techniques

3.2.1. Synthesis of amino alcohol intermediates (b1-7)

Optically active carbon is introduced into the molecule of rivaroxaban and its analogues by reaction of the aniline derivatives (**a1-7**) with the commercially available epoxide **35**. Compound **35** was purchased from Sigma Aldrich with an optical purity of ≥ 99%. According to the literature, rivaroxaban and its analogues synthesised by this route can be afforded with retaining the enantiomeric excess of 99%, introduced by the starting material **35**.[267, 301,308,309]

The solvent used in this step is a mixture of ethanol: water in 9:1 ratio. This mixture was found to be more basic media than pure water, and it can dissolve more compounds than pure solvents.[310] The epoxide undergoes reaction in basic media and ring-opening occurs by an S_N2 mechanism, and the less substituted carbon is the site of the nucleophilic attack. The postulated mechanism for this step is as described in Scheme 5.

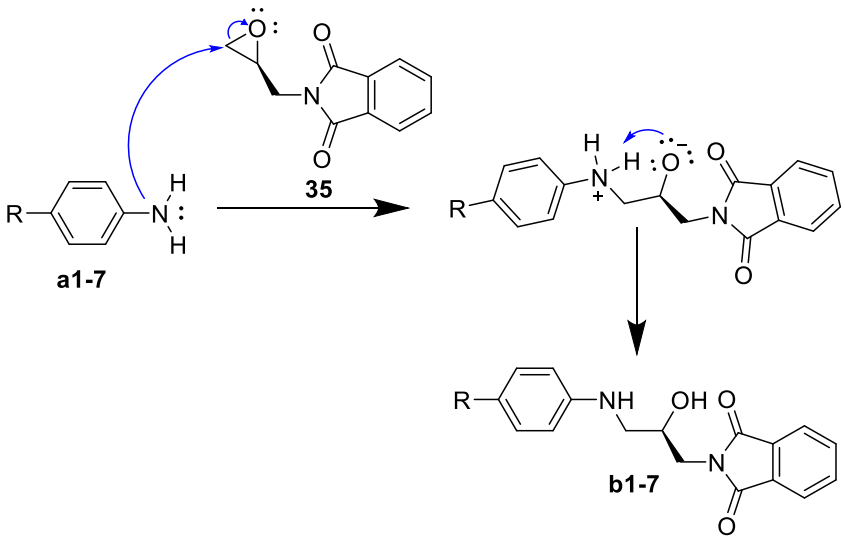

Scheme 5: The postulated mechanism for epoxide's ring opening.

Compounds **b1-2** and **b4-5** precipitated from the solution mixture when the reaction was stopped, allowed to cool to an ambient temperature and DEE was added. In contrast, compounds **b3** and **b6-7** were still in solution even after the addition of DEE.

The main impurity of this step includes the formation of a dimer (Figure 20). This impurity was formed because that the secondary amine group of the product (compounds **b1-7**) also can open the epoxide's ring. The addition of another equivalent of the epoxide **35** to the reaction mixture to reduce the formation of this impurity was uneconomical because the epoxide was pricy. This impurity was removed from compounds **2(a-b)** and **2(d-e)** by recrystallisation from MeOH, whereas it was removed from compounds **2c** and **2(f-g)** by purification via flash-LC using a gradient of MeOH/DCM solvent.

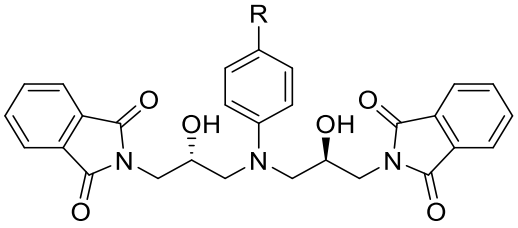

Figure 20: The dimer impurity.

3.2.2. Formation of the oxazolidinone ring (compounds c1-7)

Scheme 6 shows the postulated mechanism for the formation of the 2-oxo-1,3-oxazolidine ring in compounds **c1-7.** This cyclisation was achieved by using

N,N'-carbonyldiimidazole (CDI) in the presence of dimethylamino pyridine (DMAP) as a catalyst in tetrahydrofuran (THF) as a solvent.[267] In the first step, the carbonyl group of CDI is first activated by DMAP. In the next step, the secondary amine group of **b1-7** attacks the carbonyl group of CDI and forms a protonated tertiary amine transition state. The intramolecular electron transfer of this transition state leads to the formation of imidazole carboxamide intermediate. The carbonyl group of this intermediate is then attacked by the alcoholic hydroxyl group to form a second transition state. The transfer of the electron density of this transition state leads to the separation of imidazolide ion and completion of the cyclisation process.

Although the reaction mixture contains traces of (*S*)-enantiomer of **b1-7** because the starting material, (*S*)-2-(oxiran-2-ylmethyl)isoindoline-1,3-dione **35** is not 100% optically-pure, compounds **c1-7,** according to the experimental data by Urbasek *et al*., can be obtained in 96-99% optical purity since the (*R*)-enantiomer reacts considerably faster with CDI than the (*S*)-enantiomer.[301]

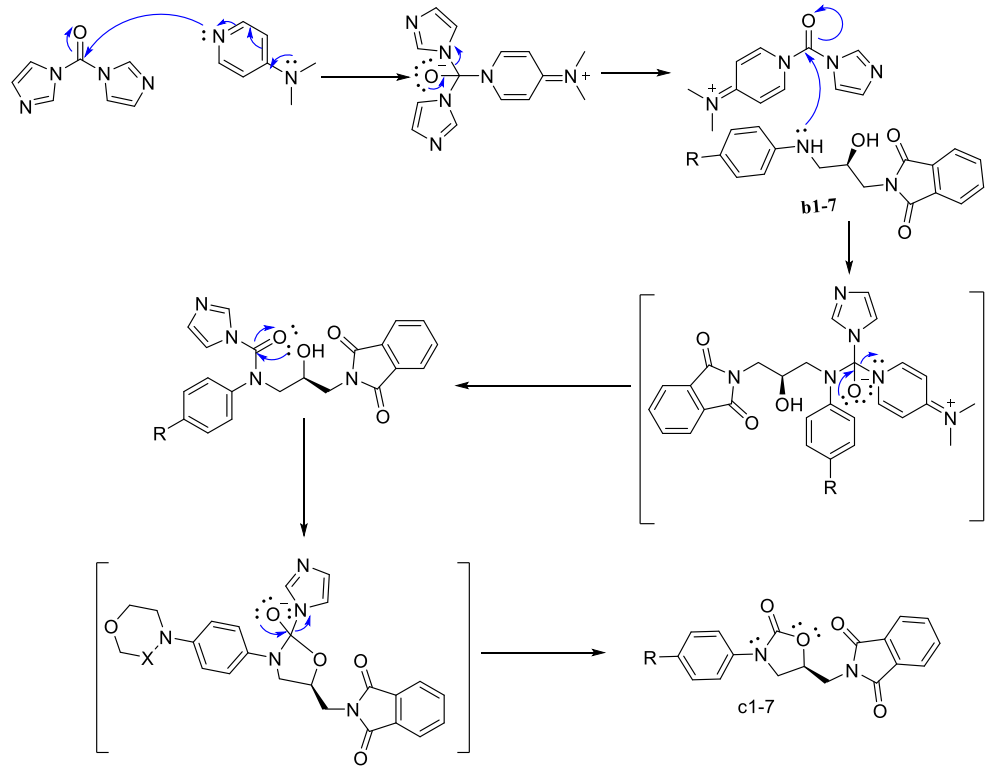

Scheme 6: The postulated mechanism of the formation of oxazolidinone ring.

Compounds **c1-2** and **c4-5** were purified by recrystallisation from a MeOH or DCM, whereas compounds **c3** and **c6-7** were purified via flash-LC using

gradients of MeOH/DCM in all cases except compound **c6**, which was purified via flash-LC using gradients of EtOAc/ether solvent.

3.2.3. Deprotection of amine

For removal of phthalimide group, three methods were evaluated. In the first method, aqueous methylamine was used as a deprotecting agent, as shown in Scheme 7.

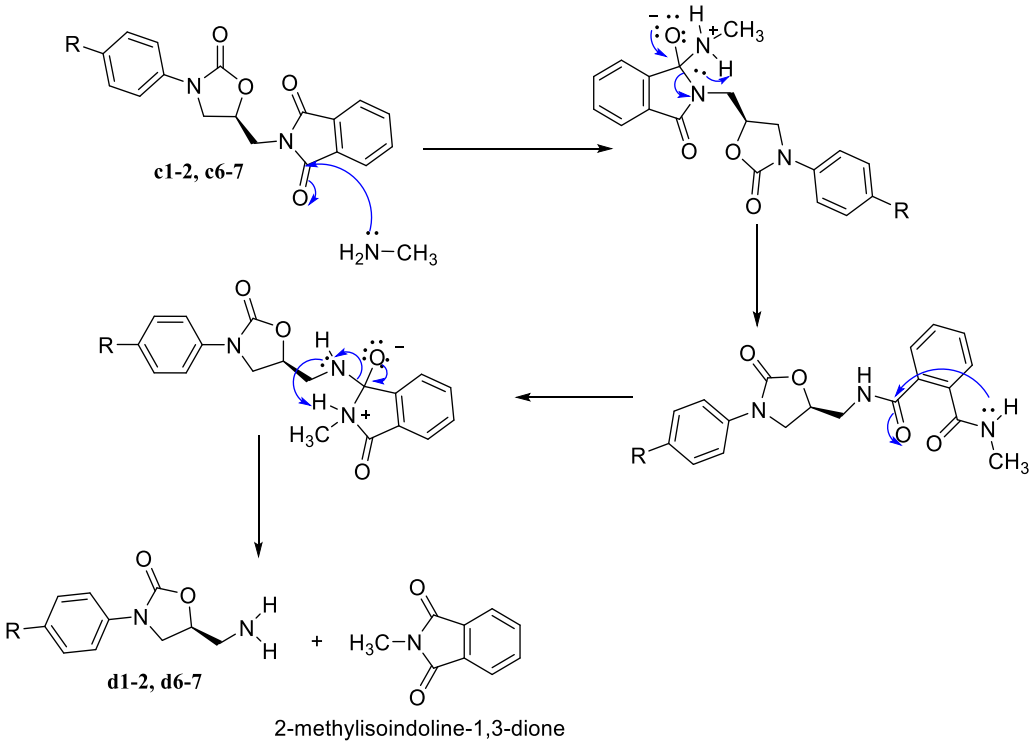

Scheme 7: The mechanism for phthalimide group deprotection using an aqueous methylamine.

Methylamine is a good nucleophile and a weak base (pK_a = 10.62).[311] Therefore, it can be used as a mild method to remove phthalimide. The impurity (2-methylisoindoline-1,3-dione) formed during the reaction was removed through acid-base extraction or by flash-LC. The target compounds can be obtained in 81-86% yield.

Another method that was experimented for the deprotection of phthalimide group involved using hydrazine hydrate. Hydrazine is traditionally used for deprotection of phthalimide group.[311,312] Hydrazine attacks the two carbonyl groups of phthalimide sequentially to form the primary amines with the formation of 2,3-dihydrophthalazine-1,4-dione as an impurity (Scheme 8).

Phthalhydrazide is generally less soluble than the target compounds in ethyl acetate. Therefore, it could be precipitated as a white solid from ethyl acetate solution. However, not all phthalhydrazide precipitated out of the solution. Hence, the resulting filtrate needs purification by Flash-LC using a suitable solvent(s). This process of repeat filtration and purification by flash-LC leads to lower the yield (43-56%). In this method, the target compound cannot be obtained through acid-base extraction.

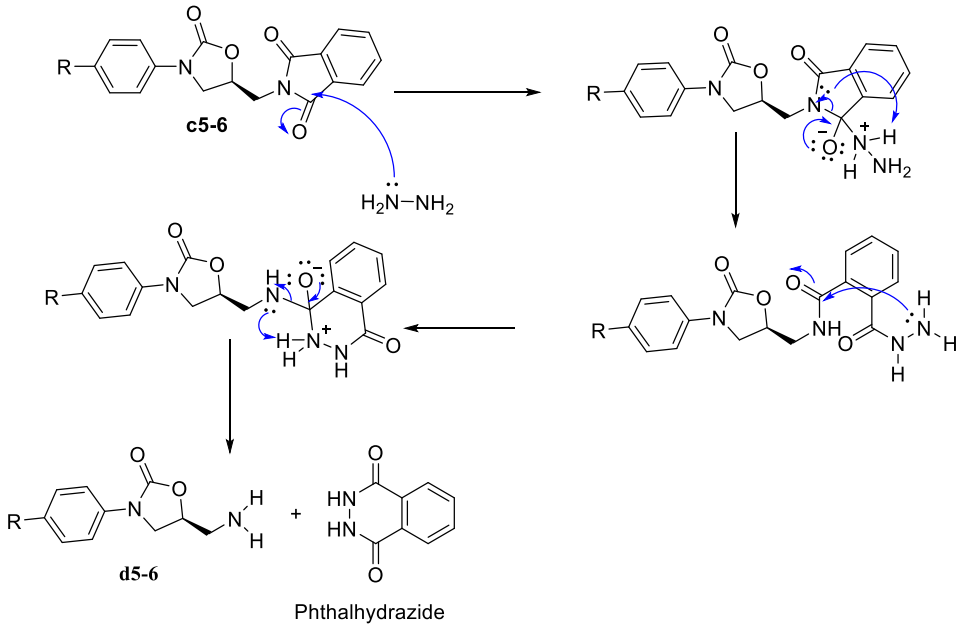

Scheme 8: Postulated mechanism for the deprotection of phthalimide group using hydrazine.

Another method was evaluated for removal of phthalimide group involves using sodium borohydride and glacial acetic acid in two stage, one-pot operation (Scheme 9).[307]

Compounds **c3-4** was dissolved in 2-propanol/water (6:1) solvent, then 5-equivalent of sodium borohydride was added with continuous stirring for 12-24 h at room temperature. If TLC indicates complete consumption of starting material, 18-equivalent of glacial acetic acid was added carefully. After that, the reaction flask stoppered, and the reaction mixture stirred at 80 °C for 2-6 h. Then water was added, and the crude mixture extracted with DCM and purified with flash-LC using a suitable solvent(s) if necessary. The target compounds were obtained in 86-90% yield. However, this method takes more

time compared to methylamine and hydrazine methods and it is unsuitable for compounds with another reduction-prone carbonyl group such as the carbonyl group of morpholinone moiety of rivaroxaban and other analogues with similar moiety.

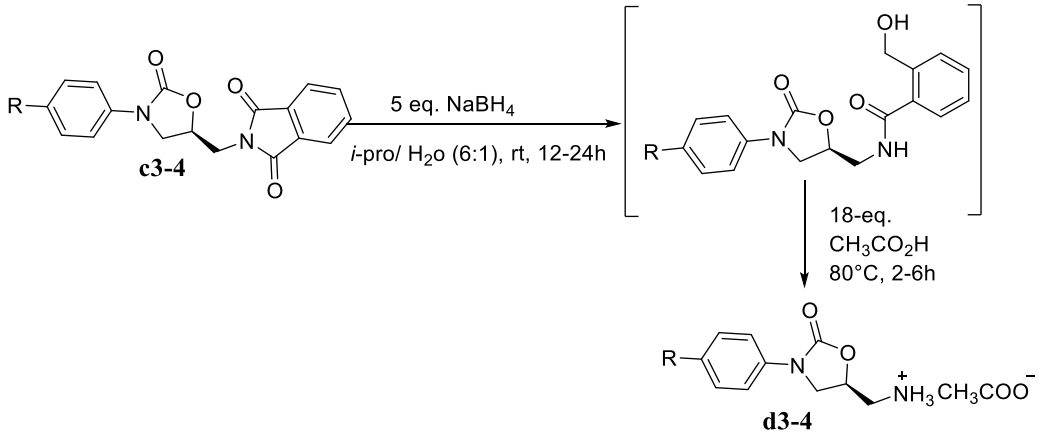

Scheme 9: Deprotection of phthalimide group with sodium borohydride and glacial acetic acid.[307]

3.2.4. Amide bond formation

Because of the importance of carboxamide group for medicinal chemists, a plethora of methods and strategies has been developed for the synthesis of an amide bond.[313] Two of these methods were tried in this project.

In the first method, amide bond was synthesised by reacting various commercially available acid chlorides with an amine (**d1-7**) in the presence of Hünig's base in DCM solvent. This reaction was carried out at 0 °C to room temperature, and the reaction mixture stirred for 1-3h. The crude compounds then extracted from DCM. The organic phase was washed with brine, dried over sodium sulphate, and then concentrated *in vacuo*, and purified by flash-LC using gradients of DCM/MeOH, 1N NH_3 in MeOH/DCM, or ethyl acetate/diethyl ether.

Where acid chloride is unavailable, another method for amide bond formation was tried. 2-(1H-Benzo[d][1,2,3]triazol-1-yl)-1,1,3,3-tetramethyluronium hexafluorophosphate(V) (HBTU) was used as a coupling agent for the reaction between the amine group of compounds **d1-7** and various carboxylic acids in the presence of an organic base (triethylamine) in DCM solvent. HBTU

activates carboxylic acids and yields a hydroxybenzotriazole ester, and the driving force for the reaction is the formation of the by-product tetramethylurea (Scheme 10).

Carboxylic acids were mixed with TEA in DCM solvent before adding HBTU, and the mixture was stirred for half an hour at room temperature, then amine was added with continuous stirring. The reaction mixture then stirred at room temperature for 12-24 h. After the reaction was stopped, water was added, and the crude product extracted from DCM. Then, the desired pure compounds were obtained by further purification with flash-LC.

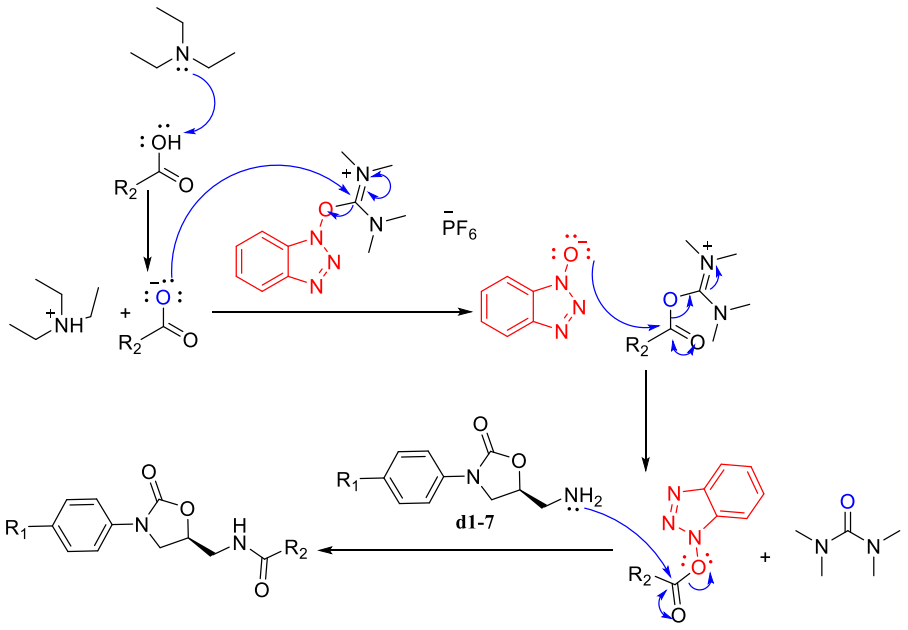

Scheme 10: The postulated mechanism for HTBU-coupling reaction.

3.2.5. Protection and deprotection of amines with Boc-group

Tert-butyloxycarbonyl (Boc-group) was used to protect amine groups. The amine was dissolved in a suitable solvent (DCM, THF, MeOH, etc.), then $(Boc)_2O$ was added, then, the reaction mixture was stirred for 3-12 h at room temperature to 80 °C.

For removal of Boc-group, a concentrated HCl acid solution in dioxane was used. The reaction mixture was stirred for 3-6 hour at room temperature (Scheme 11). The hydrochloric acid salt of the compounds was then obtained by recrystallisation from DCM.

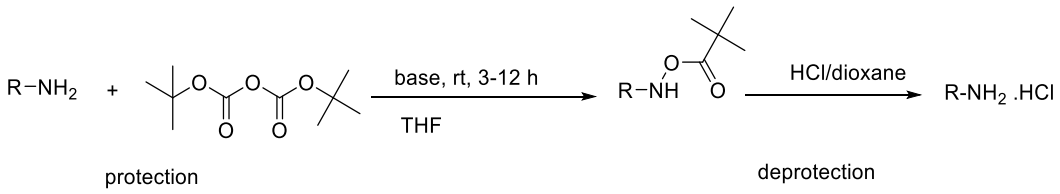

Scheme 11: Boc protection and deprotection of amine group containing compounds.

If the compounds were needed to test their pharmacological activity in *in vitro* assay, the free amine was then obtained by dissolving the hydrochloric acid salt in a saturated solution of Na_2CO_3 or $NaHCO_3$. Then an organic solvent was added, and the free base then extracted into the organic layer.

Compounds **p2, r2** and **v2** were slightly soluble in the aqueous solutions. Therefore amine salt of these compounds could not be partitioned between immiscible organic and aqueous phases. Therefore, the amine freed by using the commercially available Amberlyst® A21 free base (purchased from Sigma Aldrich).

Amberlyst® A21 is a bead form, weakly basic polymeric resin. First Amberlyst® A21 was first washed with THF to remove any moisture. Then the hydrochloric acid's salt was dissolved in DCM with continuous stirring at room temperature. After that Amberlyst® A21 was added, and the mixture was stirred for 3-6 h. The Amberlyst® A21 was then removed by filtration, and the filtrate was condensed under high vacuum to get the free amine compound.

3.2.6. Synthesis of the starting materials (Compounds a4-7)

Starting materials, **a1-3** were purchased from commercially available sources. Compound **a4** was synthesised in two steps. First methyl piperazine was reacted with 1-chloro-4-nitrobenzene to form 1-methyl-4-(4-nitrophenyl)piperazine .[314] Then the nitro group was reduced to an amine by using Pd/C catalyst under hydrogen gas (Scheme 12).

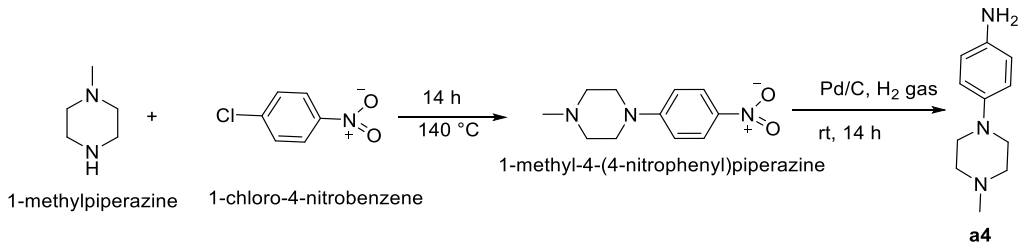

Scheme 12: Synthesis of starting material **a4**.

Compound **a5** was synthesised by reacting the commercially available 4-methylpiperazin-2-one with Iodoaniline in an improved Ullmann chemistry using K_2CO_3 as a base, CuI as a catalyst, and 10 mol% (1*R*,2*R*)-cyclohexane-1,2-diamine as a ligand (Scheme 13).[315,316]

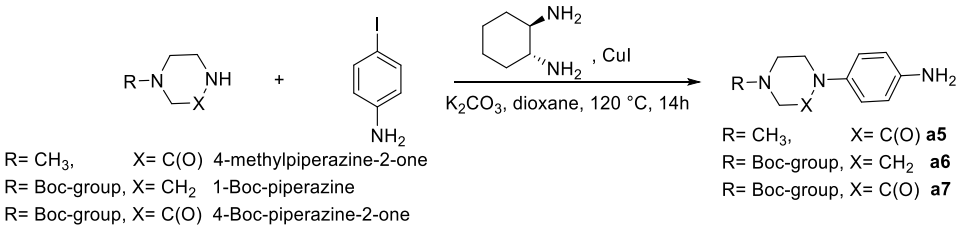

Scheme 13: Synthesis of starting material **a5**, **a6** and **a7**.

The reaction was achieved in an oxygen-free environment, and the targeted compound was obtained by purification of the crude product by flash-LC.

Compounds **a6** and **a7** were obtained by the same route described for compound **a4.** However, the commercially available piperazine or piperazine-2-one was first reacted with Boc_2O before coupled with iodoaniline

In this cross-coupling reaction, CuI was used as a catalyst and cyclohexane diamine as a ligand. Copper has four easy accessible oxidation states from 0 to +3. Therefore, it is more preferable than Ni or Pd for this type of reaction because most likely, the cross-coupling catalytic cycle with copper is serviced by +1/+3 oxidation states, whereas with Pd it serviced by 0/+2 oxidation states.[315]

3.3. Synthesis of amidine derivatives from substituted nitriles via amidoximes (compounds y1-9, z1-9)

Amidines are an important intermediate in the synthesis of heterocyclic compounds.[317] Therefore, synthesis of amidine containing compounds represents an important part of many drug discovery projects.

Unsubstituted amidines can be synthesised via amination of imidates (Pinner reaction),[318] from thioamides,[319] by amination of nitrile with alkali-metal amides, use of nitriles and ammonium chlorides, by ammonolysis of substituted amidines, from triazanes, from amides, by hydrolysis of amidic esters, amongst other methods.[320]

These procedures commonly include harsh reaction conditions, reagents that are difficult to handle, hydrogen gas, some are water-sensitive, the isolation is complicated, and the yields are variable.

In the current project, amidine derivatives were synthesised according to the procedure described in Scheme 14. This method was found to be efficient, involves mild reaction conditions, and gives yield in the range of 25-60%.[321]

Compounds **h1-2** and **h4-9**, which were synthesised according to the procedure described in Scheme 14, were used as starting material for the synthesis of amidine derivatives.

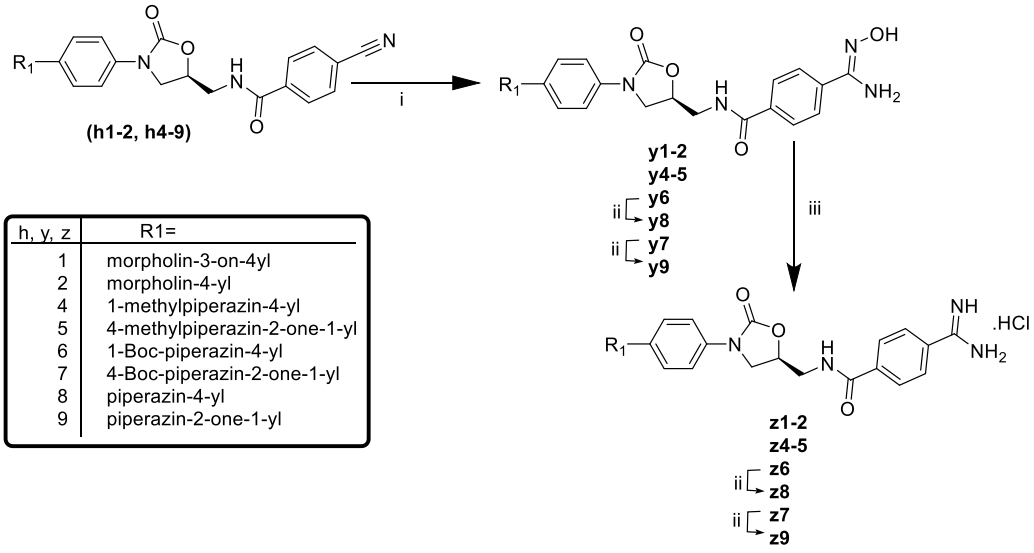

h, y, z	R1=
1	morpholin-3-on-4yl
2	morpholin-4-yl
4	1-methylpiperazin-4-yl
5	4-methylpiperazin-2-one-1-yl
6	1-Boc-piperazin-4-yl
7	4-Boc-piperazin-2-one-1-yl
8	piperazin-4-yl
9	piperazin-2-one-1-yl

Scheme 14: Synthesis of amidine derivatives from nitriles via amidoximes. (i) TEA, $NH_2OH.HCl$, ethanol, 14-24 h, 80°C; (ii) Concentrated HCl in dioxane, 1-5 h, rt; (iii) HCOOK/ ACOH, ethanol, 10% Pd/C, rt.

Firstly, amidoximes were synthesised by the action of hydroxylamine on nitriles in the presence of TEA base.[322] The required amount of hydroxylamine hydrochloride (1.5-2 eq.) was dissolved in ethanol, then TEA was added with vigorous stirring at 80 °C to liberate the hydroxylamine from the hydrochloride. After that, the starting material (one of the compounds **h1-2** and **h4-7**) was added, and the reaction mixture was stirred at 80 °C for 14-24 h. The solution was cooled, and the solvent was removed in *vacuo*, and the residue was suspended with water and extracted with DCM. The organic layer was then dried over sodium sulphate and evaporated in *vacuo*. After that, the residue was tested by TLC or LC-MS and purified by flash-LC to afford compounds **y1-2, y4-7** in 25-60% yield. The Boc-protected group in

compound **y6** and **y7** was deprotected by acidolysis to provide compounds **y8** and **y9**, respectively, as the hydrochloride salt. However, the yield for this reaction was low (20-35%) due to the hydrolysis of amidoximes in acidic media, even though the reaction was carried out at room temperature. Therefore, as an alternative approach, compound **h8** or **h9,** which has piperazine or piperazine-2-one group, respectively, was used as a starting material for the synthesis of compounds **y8** and **y9**, respectively, but again the yield was in the range 20-30%.

In the next step, the parent amidoxime was dissolved in a mixture of glacial AcOH and potassium formate solution in ethanol, followed by the addition of 10% Pd/C. The mixture was stirred at r.t. until the reaction was complete based on TLC and/or LC/MS (it completed in 24-48 h). The solids were filtered, washed with MeOH or EtOH, and the filtrate was evaporated. The residue was dissolved in anhydrous EtOH and 5 M HCl in anhydrous EtOH (12 eq.) was then added. The solids were filtered, washed with anhydrous EtOH and the filtrate was evaporated, and tested by TLC and/or LC/MS for impurities, and purified by flash-LC if necessary to obtain the target compounds **z1-7** in 45-55% yield.[321]

In case that compound **h6** and **h7** were used in the first reaction, then the Boc-protected group was removed by acidolysis to obtain compounds **z8** and **z9**, respectively.

3.4. Synthesis of rivaroxaban analogues e10-16 and g10-16 by Suzuki reaction

The Suzuki cross-coupling reaction is a palladium-catalysed carbon-carbon bond forming reaction.[323] Many important pharmaceutical products have been synthesised by using Suzuki reaction such as dragamacidin F (antiviral),[324] valsartan (antihypertension),[325] and boscalid (fungicide).[326]

The general mechanism for Suzuki reaction is illustrated in Figure 21. Firstly Pd(0) (the catalyst is tris(dibenzylideneacetone)dipalladium(0) in this project) is inserted through oxidative addition into the carbon-bromine bond of the aryl bromide, providing an aryl Pd(II) intermediate. In the next step, the ligand

substitution in the basic environment produces an aryl-hydroxypalladium complex. The hydroxyl group, now attached to the Palladium metal, can bind to the Lewis acidic aryl boronic acid to form an ate complex. This pre-coordination of the palladium hydroxide to the boronic acid facilitates the subsequent transfer of the aryl group to palladium (transmetallation). Finally, the palladium is extricated from between the two aromatics via reductive elimination, producing targeted compound and refreshing the palladium catalyst for another cycle.[323]

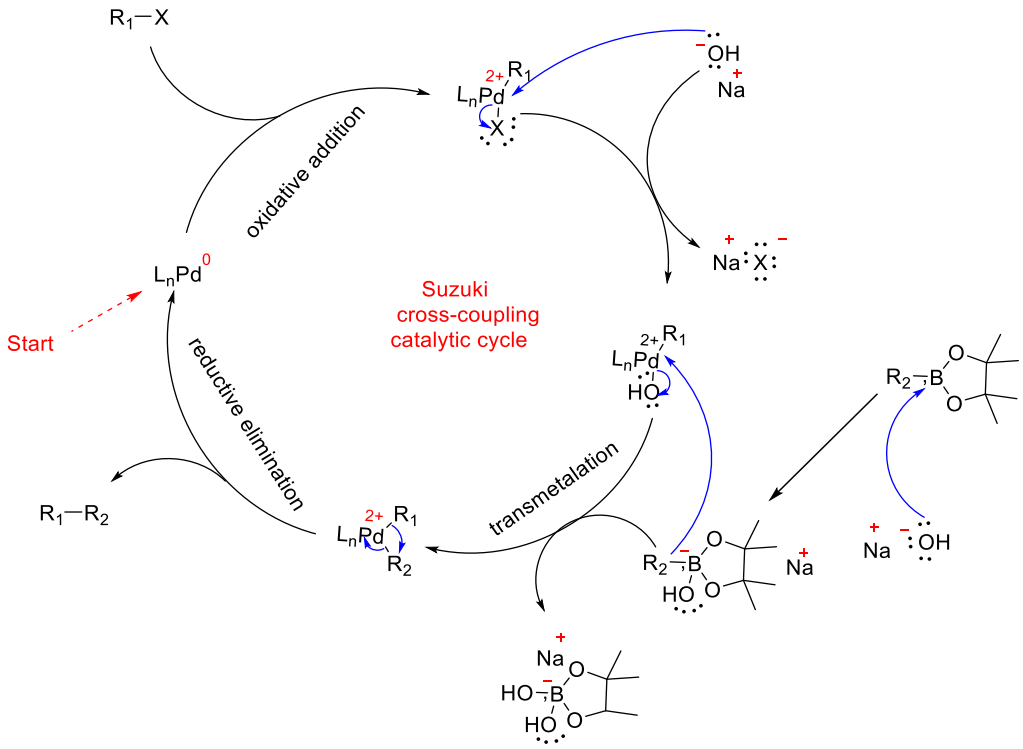

Figure 21: The general mechanism of Suzuki reaction. [327]

The general procedure for the synthesis of compounds **e10-16 and g10-16** (Scheme 15) involves using compounds **e3** or **g3** (see Scheme 4) as a starting material. Tris(dibenzylideneacetone)dipalladium(0) was used as a catalyst and Na_2CO_3 as a base. The dba ligands of the catalyst are easily displaced, so the complex is usually used as a source of soluble Pd in Suzuki reaction. Different solvents were tried in this reaction. However, it was found that Dioxane/water was the preferable solvent system for Suzuki reactions in this project.

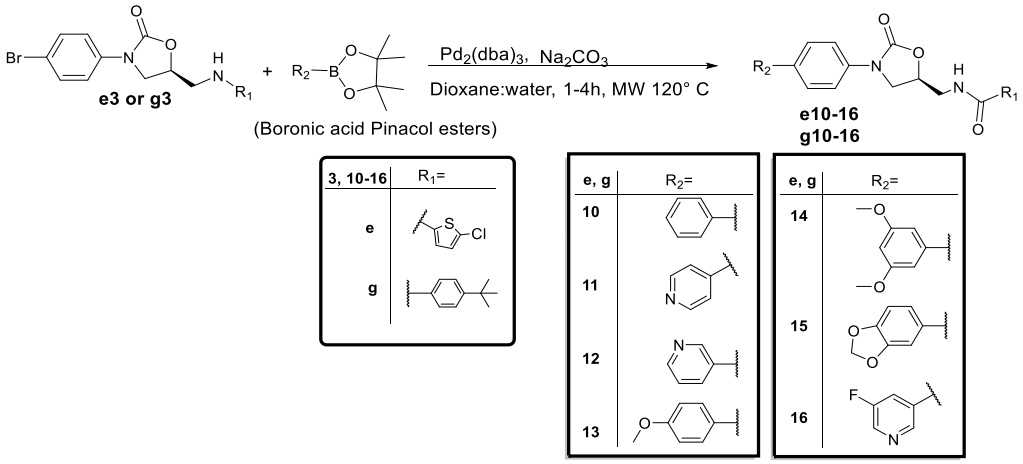

Scheme 15: The general procedure for the synthesis of compounds e10-16 and g10-16.

Different temperatures were tried. However, it was found that Suzuki reactions work optimally using microwave irradiation. Furthermore, it was found that using boronate pinacol esters instead of the boronic acids significantly improve the reaction's yield. This may be related to the improved stability of boronate pinacol esters over boronic acids.[328]

Boronic acids can form anhydrides or boroxines through dimerisation or trimerisation under anhydrous conditions.[329] Moreover, under normal laboratory conditions a mixture of monomer, dimer, and boroxine exist.[330] This disadvantage was overcome by using boronate pinacol esters, which are air- and water-stable and exist only in a monomeric form.[330,331] additionally, boronate pinacol esters are mostly more stable to purification using column chromatography, and this will aid in the purification process in the case that some residual boronic acid remain in the final crude product due to incomplete conversion.[328]

It is believed that the transmetallation step (see Figure 21) is facilitated by trace water, either from a hydrated base or through the addition of a small amount of water to the reaction mixture. This is because that water most likely hydrolyses the boronate ester either partially or fully to allow for transmetallation to occur efficiently.[330] Therefore 10% of water was added to the solvent system of the reactions in this projects.

Suzuki reactions were performed through conventional methods and under microwave conditions. It was found that the time and yield of the microwave-

assisted reactions were significantly improved. The Suzuki reaction, which was carried out under conventional conditions, took 14-24 h to complete. On the other hand, under the microwave, these reactions took only 1-4h.

After completion, the reaction mixture was cooled to ambient temperature, and the palladium catalyst and other insoluble substances were removed by filtration through celite and washed with ethyl acetate. The filtrate was then extracted and purified by flash-LC using suitable solvent(s).

3.5. Synthesis of compounds e17-31 and g17

Compound **e17** and **g17** (Scheme 16) were synthesised by starting from the commercially available compound methyl-5-amino-1H-1,2,4-triazole-3-carboxylate. In the first instance, this compound was reacted directly with **35**, but the reaction was very slow, and the yield was very low. Most of the starting materials remain unreacted after 48h, and the reaction yield was <5%. Therefore, methyl-5-amino-1*H*-1,2,4-triazole-3-carboxylate was first reacted with phthalic anhydride in dioxane and reflux for 48h to afford compound **46** in 65% yield.[332]

The secondary amine group of **46** was then protected with 2-(Trimethylsilyl)ethoxymethyl chloride (SEMCl) in the presence of 1.1 equivalent of NaH in DMF.[333] The reaction mixture was stirred at 50 °C for 12 h to obtain compound **47**. The next step involved the deprotection of the phthalimide group of **47** with methylamine, which has been explained earlier (Section 3.2.3). Methylamine was used to avoid using strongly acidic or basic environment, which may affect the ester group of the compound. The product (compound **48**) was then reacted with **35** to afford compound **49**. The aminoethanol group of **49** then cyclized using CDI to furnish compound **50**, and then the phthalimide group was deprotected by methylamine to obtain the primary amine derivative (compound **51**). The next step involves acylation of the primary amine product either with 5-chlorothiophene-2-carbonyl chloride or 4-(tert-butyl)benzoyl chloride. In the last step, Trimethylsilyl ethoxymethyl (SEM) protecting group was removed by acidolysis to result in the formation of compound **e17** or **g17**, respectively.

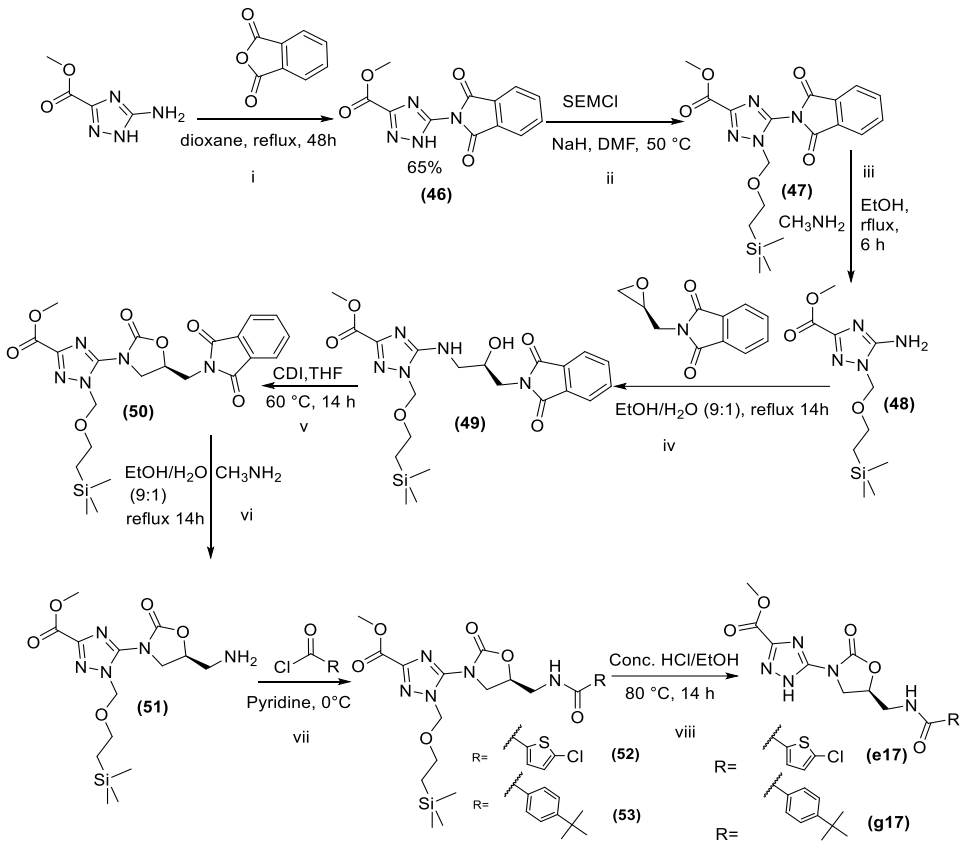

Scheme 16: The general method for the synthesis of compounds **e17** and **g17**.

Compounds **e18-31** were synthesised according to the procedure described in Scheme 17. Firstly, the target compound **43** was obtained in 63 % yield by reacting the commercially available (*R*)-epichlorohydrine **40** with sodium cyanate and magnesium sulphate in water at 60 °C. Then, compound **44** was obtained in 71 % yield by reacting compound **43** and potassium phthalimide in DMF. In the next step, compound **44** was coupled with various bromine or iodine derivatives. For bromine derivatives, an Ullmann-type coupling reaction was used as described earlier (see Section 3.2.6).

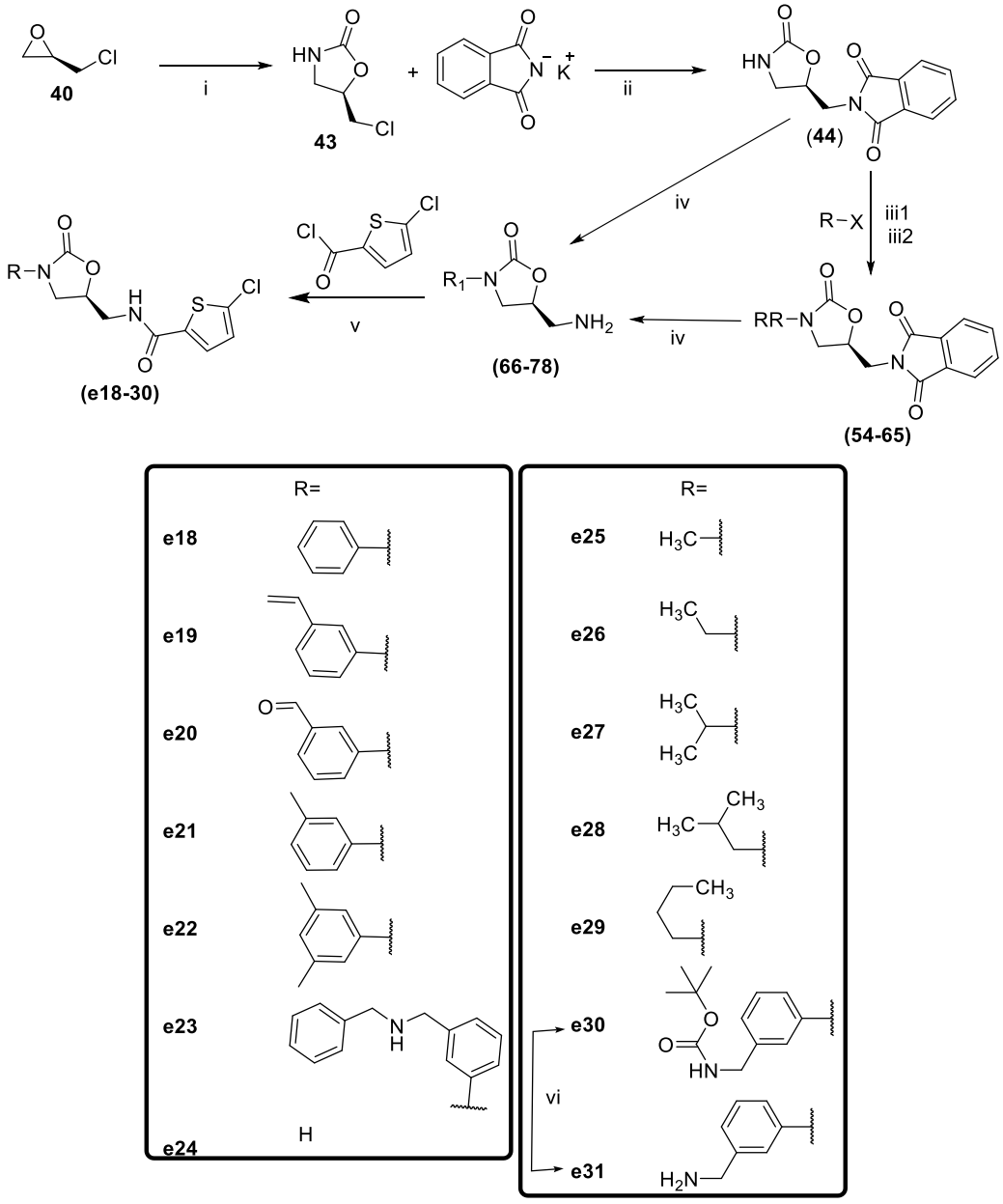

Scheme 17: Synthesis of compounds **e18-31**. Reagents and conditions: (i) NaOCN, $MgSO_4$, 60 °C, 5h; ii) potassium phthalimide, DMF, 80 °C, 14 h; iii1) R_1-X (bromine derivatives), CuI (5 mmol %), (Z)-1,2-diaminocyclohexane (10 mol %), dioxane, K_2CO_3, 120 °C, 14 h; iii2) R_1-X (iodine derivatives), NaH, DMF, 0 °C-rt, 6-14h; (iv) NH_3CH_3, EtOH, 80 °C, 5h; (v) DIPEA, DCM, 0 °C-rt, 3h; (vi) Concentrated HCl in dioxane, dioxane, 1-4 h, rt.

Alkylation of the secondary amine group of compound **44** by iodine derivatives was performed by dissolving it and iodo-compound in DMF, and sodium hydride as a base. The target compounds were obtained through purification by flash-LC using suitable solvent(s) if necessary to afford intermediates **54-65**.[334] The amine group of compounds **54-65** then deprotected using aqueous methylamine solution (40 %) to afford

intermediates **66-78.** Those intermediates then acylated with 5-chlorothiophene-2-carbonyl chloride in the presence of DIPEA to afford compounds **e18-e31** in 33-60% yield. The Boc-group of compound **e30** was removed by acidolysis in HCl/dioxane solution to afford compound **e31** as hydrochloric acid salt. The free amine compound was then obtained from organic layer after partitioning the hydrochloric acid salt compound between Na_2CO_3 and DCM.

3.6. Summary and Conclusion

Most of the compounds in this project were synthesised following the general route described in the literature for the synthesis of rivaroxaban[335] with some modifications. This route was found to be efficient, does not need special purification techniques, and result in the synthesis of compounds with high yields.

The key intermediates for the synthesis of rivaroxaban analogues were compounds **d1-7**. These compounds were successfully obtained through three steps starting with the reaction of substituted anilines (compounds **a1-7**) with epoxide **35** followed by cyclisation with CDI and deprotection of phthalimide with aqueous methylamine. Epoxide **35** was commercially available. Therefore, it was purchased from the commercial sources with an optical purity of 99%. However, compound **35** can be obtained by a reaction of (*S*)-epichlorohydrine and phthalimide as described in the literature.[335] Seven aniline derivatives were used as starting materials **(a1-7**) for the synthesis of the desired rivaroxaban analogues. Compounds **a1-3,** which contain morpholine, morpholinone or bromine, respectively, were purchased from commercial sources. On the other hands, compounds **a4-7**, which have methylpiperazine, methylpiperazinone, Boc-piperazine or Boc-piperazinone were synthesised in situ. Over 106 compounds were synthesised using these intermediates (compounds **d1-7**). Most of these compounds were novel final compounds which were biologically tested as potential inhibitors of FXIIa.

Rivaroxaban molecule has three main parts: The P1-group which is 5-chlorothiophene-2-carboxamide, P4-position which is 4-aminomorpholine-3-one, and the oxazolidinone core. The oxazolidinone core was kept unchanged

during this project. However, the P1- and P4-positions of the molecule were replaced by various groups.

Benzamidine group was introduced at the P1-position through the conversion of the compounds with benzonitrile (**h1-2, h4-9)** into amidoximes (**y1**-9) followed by reduction of these compounds into amidines (**z1-9**). The synthesis of the benzamidine derivatives in this project represents a challenge because of the sensitivity of amidine group to various conditions. However, the adopted method for the synthesis of these compounds was found to be efficient despite the low yield in some instances.

Compounds with bromine at the P4-position (**e3** and **g3**) were subjected to Suzuki type reaction to introduce various groups at the P4-position. By adopting Suzuki reaction, seven different groups were successfully introduced into the P4-position of the compounds **e3** and **g3**. Other groups could have been put in this place but the limited time prevented it. The advantages of Suzuki coupling over other similar reactions include the availability of common boronic acids, mild reaction conditions, and its less toxic nature. Further, this reaction is preferable because it uses relatively cheap reagents.

Compound with triazole carboxylate at the P4-position appears in one of the potential inhibitors of FXIIa worked by Peter Fischer's group (unpublished data). Therefore, synthesis were attempted for compounds **e17** and **g17** which has triazole carboxylate at the P4-position and 5-chlorothiophene-2-carbonyl or 4-*tert*-butylbenzene-1-carbonyl, respectively, at the P1-position. The method for the synthesis of these compounds was lengthy where it includes eight steps. However, the procedure was straightforward and includes mild conditions. Additionally, the copper-catalysed reaction was used for the synthesis of various rivaroxaban analogues (compounds **e18-31**).

All procedures used in this project were optimised for the use of mild conditions and nontoxic reagents and solvents. The common intermediate in each route was first synthesised on small scale. After optimisation of the reaction conditions (temperature, solvents, duration of reaction, catalysts) these intermediates were scaled up so that they can used for the synthesis of the desired final compounds.

Chapter four: Pharmacological activity and structure-activity relationships

4.1. *In vitro* FXa and FXIIa inhibitory activity

Inspired by the observation of the X-ray crystal structure of rivaroxaban in complex with human FXa in which the benzene ring and the oxazolidinone core are in coplanar conformation, compounds with this conformation was synthesised in this project and tested for FXIIa inhibitory activity. As an early exploration, rivaroxaban in both *S*- and *R*-configurations was prepared and tested against FXa and FXIIa inhibitory activity.

The literature reported that rivaroxaban with an *S*-configuration has an *in vitro* IC_{50} against FXa of 0.7 nM, whereas the *R*-configuration IC_{50} was 2300 nM.[267] The results of the *in vitro* enzymatic assay of this project showed that rivaroxaban in *S*-configuration (**e1**) has an *in vitro* IC_{50} against FXa of 0.6 nM whereas the *R*-configuration IC_{50} was 2100 nM. However, rivaroxaban in *S*-configuration has an IC_{50} of 77µM against FXIIa whereas the *R*-configuration was inactive. Apixaban (as FXa inhibitor) and argatroban (as direct thrombin inhibitors) were also pharmacologically tested against FXIIa *in vitro*. Apixaban was 2-fold, and argatroban was 5-fold less active against FXIIa than rivaroxaban.

Early docking studies in this project showed that the active site of both FXa and FXIIa adopt the same conformation and that rivaroxaban has almost the same binding mode in both enzymes (Figure 22). Furthermore, the fact that the *S*-enantiomer of rivaroxaban was more active against both FXa and FXIIa than its *R*-enantiomer means that both enzymes have the same stereospecificity. To confirm these results, several rivaroxaban analogues were synthesised with either the P1- or P4- position of rivaroxaban was fixed while changing the other side of the molecule. Other series of the compounds include changing of both the P1- and P4-positions according to iterative make-test cycles.

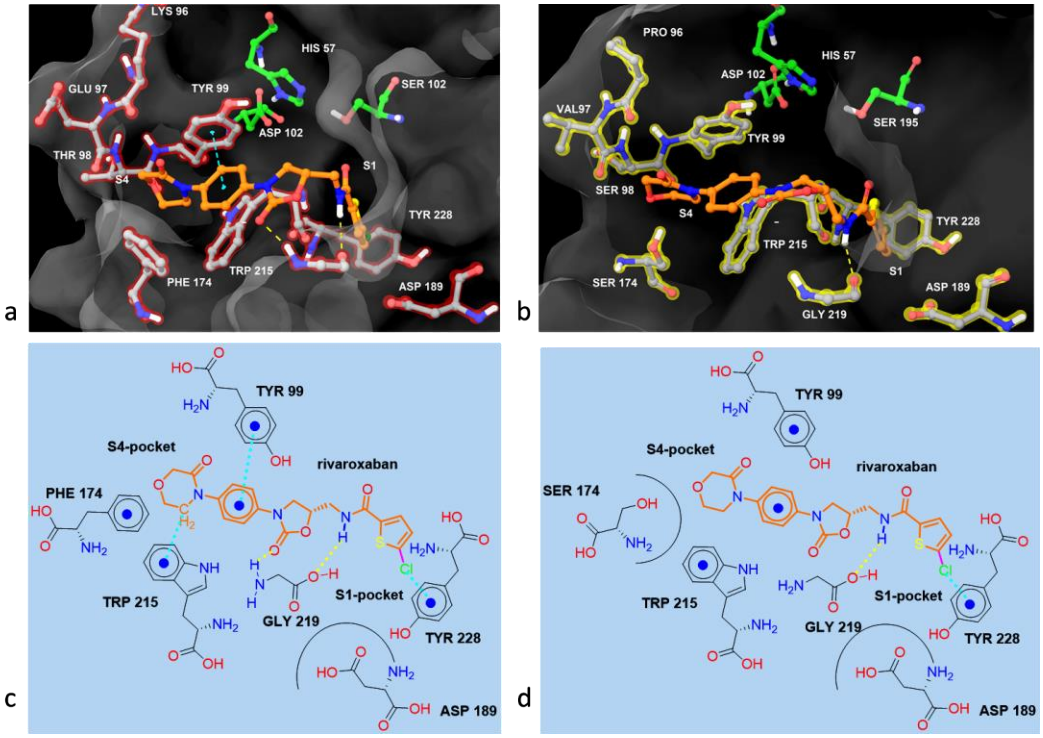

Figure 22: The binding mode of rivaroxaban in FXa and FXIIa. a) Surface representation of FXa complexed with rivaroxaban (PDB: 2W26). The main residues in the S1 and S4 pockets were red highlighted; b) rivaroxaban docked to FXIIa-H model; The main residues in the S1 and S4 pockets were yellow highlighted; c) 2D-schematic representation of rivaroxaban in FXa; d)2D-schematic representation of rivaroxaban in FXIIa. Colour code: Orange: rivaroxaban; green carbon backbone: catalytic triad; blue: nitrogen; red: oxygen; yellow: sulfur; green: chlorine; yellow dotted lines: hydrogen bonds; blue dotted line: hydrophobic- interaction. Rivaroxaban forms two hydrogen bonds with Gly219; the aromatic ring of rivaroxaban forms π-π-interaction with Trp215; the carbonyl group of morpholinone moiety increase the polarization of the underneath CH_2-group and this leads to formation of CH_2-π-interaction between this group and the aromatic ring of Trp215; in the S1-pocket, the chlorine atom of the thiophene residues forms Cl-π-interaction with Tyr228 residue; the distance between the chlorine atom and Tyr228 residue is 3.61 Å in FX and 3.57 Å in FXIIa.

To obtain information about target-inhibitor interactions that would beneficial to understand the structural requirements for FXIIa inhibition, a docking study using FXIIa-H model was performed. In addition, for comparison purposes, all synthesised compounds were also docked to FXa (PDB: 2w26). The docking studies were carried out using the automated Schrodinger suite (Schrödinger Release 2017-4: Glide, Schrödinger, LLC, New York, NY, 2017). For each compound, ten solutions were generated and ranked according to their docking score (Kcal mol^{-1}). For each compound, the top-pose that represents the prevalent overall binding mode of the ten solutions was retained. The interaction between the enzyme and inhibitor were visualised with Maestro

program (Schrödinger Release 2017-4: Maestro, Schrödinger, LLC, New York, NY, 2017).

For comparison purposes, the selectivity of the tested compounds towards FXIIa and FXa will be determined according to a parameter that will be called 'the selectivity factor (SF)'. The selectivity factor is the ratio of the IC_{50} of the tested compounds against FXa to that against FXIIa:

SF= IC_{50} value against FXa/ IC_{50} value against FXIIa

If the SF < 1, this means that the compound is more selective to FXa than FXIIa. In contrast, SF > 1 indicates that the compound is more selective to FXIIa than FXa. The bigger the selectivity factor, the more selective to FXIIa is. If the tested compound was inactive against one of the enzymes, the selectivity factor cannot be determined, so it will be indicated in the activity tables by the symbol na which means not applicable

4.2. Rivaroxaban analogues with a substituted P1-position

The early synthesised rivaroxaban-analogues were compounds that retain a morpholinone moiety at the P4-position with slight changes at the P1-position of the molecule. As shown in Table 4, the results showed the importance of the chlorine atom at the thiophene moiety for the activity against FXIIa as it is important for the activity against FXa. Compound **f1** which missing only this chlorine atom was inactive against FXIIa, and it was 13-fold less potent than rivaroxaban toward FXa. In the early docking studies, it was found that the chlorine atom at the thiophene moiety of rivaroxaban form Cl-π stacking with the aromatic ring of Tyr228 at the bottom of the S1-subpocket in both FXa and FXIIa (Figure 22). Substitution of the thiophene group with *tert*-butylbenzene (as in compound**g1**) further diminishes the activity towards both enzymes compared to that of rivaroxaban. However, putting an amine group at this position (as in compound **p1)** resulted in the improvement of the activity toward both enzymes compared to **g1**. Compound **p1** was 2-fold more active

than rivaroxaban against FXIIa, and it was 50-fold less active than rivaroxaban toward FXa.

Table 4: *In Vitro* FXIIa and FXa inhibitory activity of rivaroxaban and P1-substituted derivatives

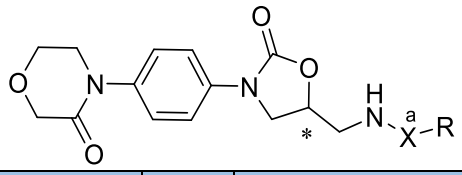

Compd	R=	ent*	IC_{50} µM ±SD		SF
			FXIIa	FXa	
e1	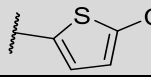	*S* *R*	77±6.0 ia[b]	0.0006±0.0 2.10±0.0	77×10^{-7} na[c]
f1	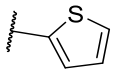	*S*	ia	0.0079±0.0	na
g1	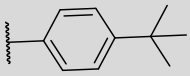	*S*	ia	122±6.0	na
i1	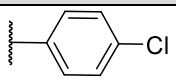	*S*	101±11	4.89±2.0	0.04
p1	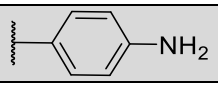	*S*	39±4.0	0.03±0.0	0.0007
r1	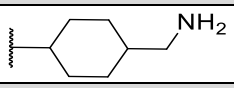	*S*	60±6.0	8.36±4.0	0.14
t1	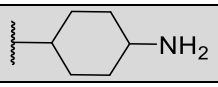	*S*	95±10	54±8.0	0.57
v1	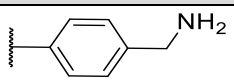	*S*	19±3.0	0.02±1.0	0.001

a: X= C(O) in all compounds except **i1** where it is $C(O)CH_2(O)$
b: ia= inactive; c: na= not applicable.

A cyclohexylmethylamine group at the P1-position **r1** caused a decrease in the inhibitory activity against both FXIIa and FXa compared to **p1**. Compound **r1** is almost as active as rivaroxaban toward FXIIa, and it was 278-fold less active than **p1** against FXa. However, the SF of **r1** was 0.14 which is 200-fold more than that of compound **p1**. This means that compound **r1** is more selective to FXIIa than compound **p1** though it was less potent. Moreover, cyclohexylamine substitution (as in compound **t1**) further decreased the activity towards both enzymes compared to **p1**. However, the selectivity for FXIIa improved compared to **p1** and **r1** (SF of t1 is 0.57). On the other hand, compound **v1** with benzylamine at the P1-position was the most active compound of this series against FXIIa (IC50 = 19 µM), and it was also more active against FXa (IC50 = 0.02 µM) than **p1**, **r1**, and **t1**. The SF of compound

v1 was 0.001. This indicates that **v1** was less selective to FXIIa than **t1** and **r1**. However, **v1** was more active against and more selective to FXIIa than **P1**.

These results confirmed the suggestion that both enzymes (FXa and FXIIa) have a very similar S1-subpockets. The chlorine atom of the thiophene moiety is very important for the inhibition of both enzymes. Furthermore, both enzymes tolerate the aromatic ring more than cyclohexane, and prefer longer arm to be extended from the aromatic ring at the P1-position toward the S1-subpocket of the enzyme binding site. This was confirmed by the comparison of compounds **p1**, **r1**, **t1** and **v1**. Compound **v1**, which has both the aromatic ring and an extended arm at the P1-position, was 2-fold, 3-fold, and 5-fold more active against FXIIa than **p1**, **r1**, and **t1** respectively. Similarly, compound **v1** was far more active against FXa than **p1**, **r1**, and **t1**. However, it appears that FXIIa strongly prefers the extended arm at the P1-position more than FXa. That can be observed by comparing compound **p1** vs **t1**, and **r1** vs **v1**. Substitution of the aromatic ring of compound **P1** by cyclohexane in compound **t1** decrease the activity against FXIIa while increase the selectivity. However, substitution of the cyclohexyl-group of compound **r1** with aromatic ring in **v1** significantly improve the activity and the selectivity for FXIIa.

Accordingly, it was thought that substituting chlorothiophene with chlorobenzene with an extended linker between the oxazolidinone core and the aromatic ring (compound **i1**) will further improve the activity. However, compound **i1** was much less potent against both enzymes than compound **f1** and has only an *in vitro* IC_{50} of 101 µM and 4.89µM against FXIIa and FXa, respectively. However, this compound (**i1**) was much more selective To FXIIa than **p1** and **v1.** This support the previously mentioned idea that FXIIa prefer the existence of an extended arm at the P1-position more than FXa.

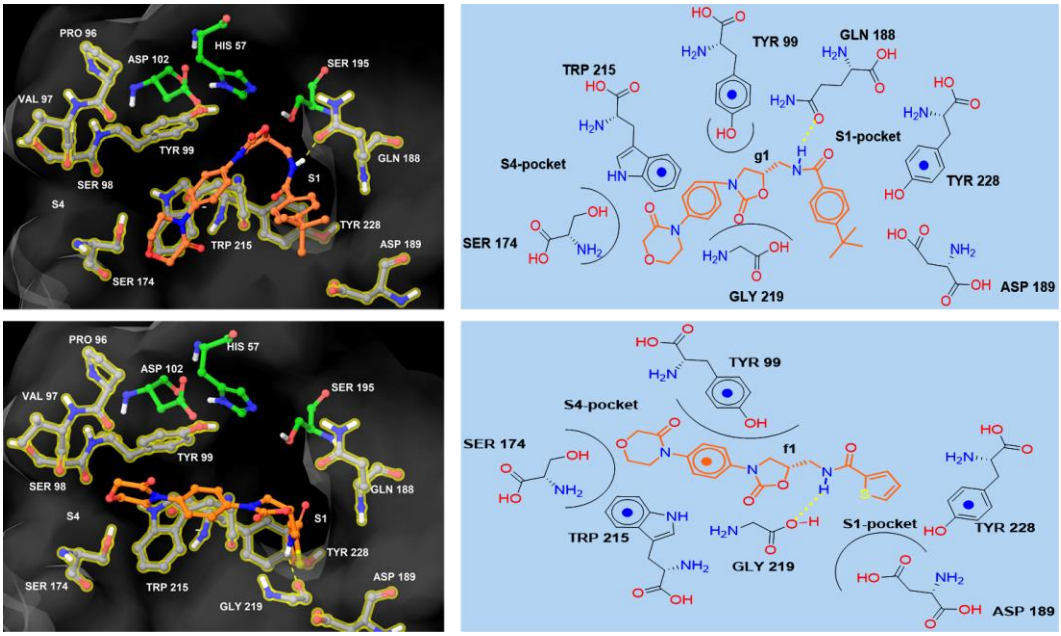

Figure 23: Compound **g1** (above) and **f1** (below) docked to FXIIa-H. The right side is the surface representation of the binding modes; left side is the 2D-schematic representation of the binding modes. Only important residues at the S1- and S4-pocket were shown (yellow silhouetted). orange: carbon backbone of the docked compound; grey: carbon backbone of the enzyme's residues; light green: carbon backbone of the catalytic triad; blue: nitrogen; red: oxygen; yellow: sulfur; white: hydrogen; yellow dotted lines: hydrogen bonds.

Docking to FXIIa-H-model showed that the *tert*-butylbenzene at the P1-position in compound **g1** was not tolerated by FXIIa (Figure 23). In contrast, the thiophene group of compound **f1** directed toward the Tyr228 residue at the bottom of the S1-subpocket and the oxygen of the amide bond forms hydrogen bond with Gly219 residue. Compound **r1**, on the other hand, adopts a reverse conformation where the amine group directed toward the S4-position whereas the morpholinone moiety tends to occupy the S1-pocket. Similarly, the amine group of compounds **t1** tends not to occupy the S1-position.

In contrast, the amine group of compounds **p1** and **v1** fit exactly in the S1-pocket (Figure 24). Docking studies also showed that compounds **p1**, **r1**, **t1**, and **v1** adopt the usual rivaroxaban binding mode in FXa where the morpholinone moiety occupies the S4-pocket while the group at the other end of the molecule resides in the S1-pocket.

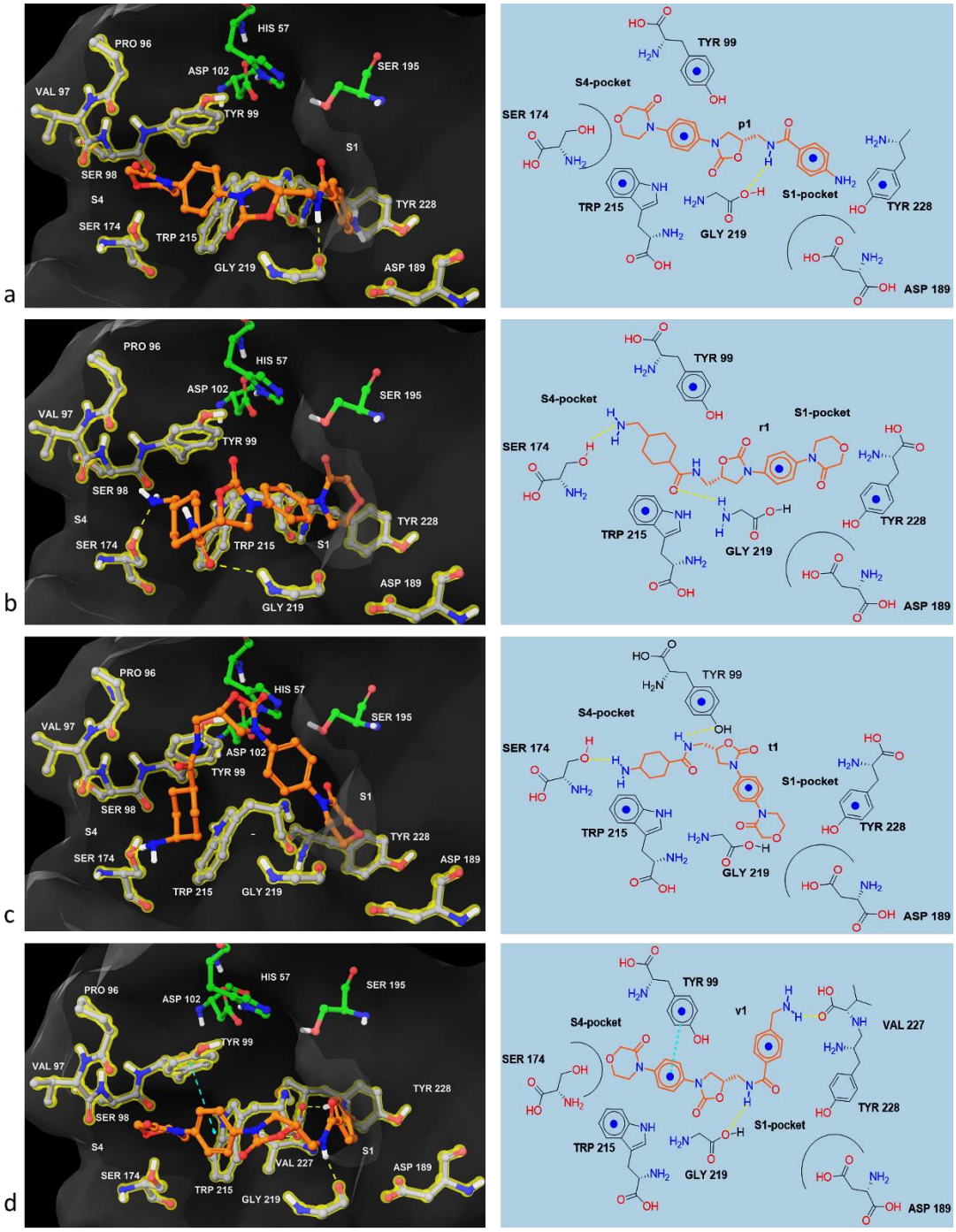

Figure 24: Compound **p1** (a), **r1** (b), **t1** (c), **v1** (d) docked to FXIIa-H. The right side is the surface representation of the binding modes; left side is the 2D-schematic representation of the binding modes. Only important residues at the S1- and S4-pocket were shown (yellow silhouetted). orange: carbon backbone of the docked compound; grey: carbon backbone of the enzyme's residues; light green: carbon backbone of the catalytic triad; blue: nitrogen; red: oxygen; yellow: sulfur; white: hydrogen; yellow dotted line: hydrogen bond; blue dotted line: π-π stacking.

Interestingly, the activity of compounds **p1**, **r1**, **t1**, and **v1** against both FXa and FXIIa decrease in this order **v1**>**p1**>**r1**>**t1**. This means that the S1-position of both enzymes prefer groups at the P1-position in this order: benzylamine>aniline>cyclohexylmethylamine>cyclohexylamine. Therefore, it

could be concluded that compounds with an aromatic amine substituent were more favourable as P1-surrogate for FXIIa inhibitors more than compounds with cyclic derivatives at this position. Also, these results suggest that the S4-pocket of FXIIa can accommodate basic groups more favourably than that of FXa. These results were consistent with the early homology and docking studies of this study that showed that the major structural difference between FXa and FXIIa binding lies in the S4-subpocket.

4.3. Rivaroxaban analogues with a substituted P4 position

During rivaroxaban discovery, the researchers found that the morpholinone group of rivaroxaban is sandwiched between the aryl rings of Tyr99 and Phe174 residues at the S4-subpocket. The carbonyl group of the morpholinone moiety affects the planarization of the morpholinone group and brings it into a perpendicular orientation to the aryl ring. This orientation allows the formation of the CH_2-π-interaction with The Trp215 and π- π-stacking of the aryl ring with Tyr99 (Figure 22 and Figure 25).[1]

Table 5: *In vitro* FXIIa and FXa inhibitory activity of P4-substituted rivaroxaban derivatives

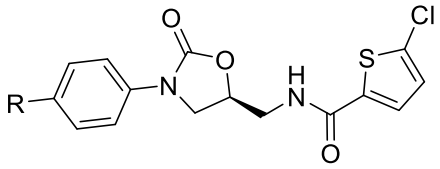

Compd	R=	IC_{50} µM ±SD		SF
		FXIIa	FXa	
e2	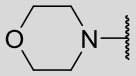	ia	0.07±0.03	na
e3	Br	ia	226±17	na
e4	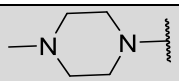	167±12	1.06±1.0	0.0063
e5	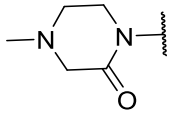	414±13	0.06±0.50	0.0001
e8	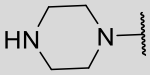	21±2.0	0.36±0.02	0.017
e9	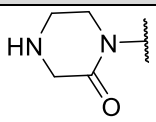	55±6	0.0006±0.0	1×10^{-5}

The results of the *in vitro* enzymatic assay of this project shows that omitting the carbonyl group from the morpholinone moiety of rivaroxaban (as in compound **e2**) decreases the inhibitory activity of this compound against FXa by 125-fold (Table 5). Furthermore, this slight change to rivaroxaban structure abolished its activity toward FXIIa completely. Docking studies showed that omitting the carbonyl group of morpholinone moiety disrupted the co-planner orientation of the morpholinone and the aryl ring and deprived the compound of important interactions at the S4-pockets (Figure 25).

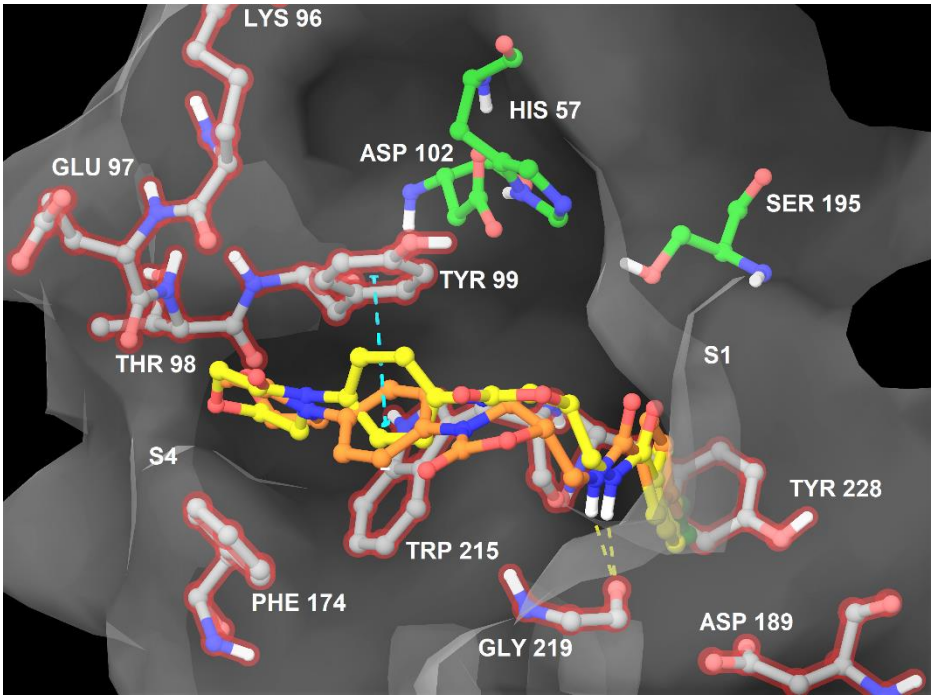

Figure 25: The top poses of rivaroxaban **e1** (orange) and compound **e2** (yellow) docked to FXa. Only important residues at the S1- and S4- pocket were shown (red silhouetted). Orange: carbon backbone of the docked compound; grey: carbon backbone of the enzyme's residues; light green: carbon backbone of the catalytic triad; Dark green: chlorine; blue: nitrogen; red: oxygen; yellow: sulfur; white: hydrogen; yellow dotted line: hydrogen bond; blue dotted line: π-π stacking.

Substitution of the morpholinone group with bromine **e3** further decreases the activity toward FXIIa. In contrast, the compound with methylpiperazine at the P4-position **e4** has slight inhibitory activity against FXIIa and an improved activity toward FXa albeit it was 15-fold less active compared to **e2**. Also, the selectivity of this compound to FXIIa was 818-fold more than that of rivaroxaban (**e1**). These results may confirm the idea that FXIIa tolerates more basic groups at the S4-subpocket than FXa. S4-subpocket of FXa is shaped by the aromatic rings of Tyr99, Phe174, and Trp215.[1] Therefore, FXa preferably

accommodate aromatic ligands by π-interactions. In contrast, the S4-pocket of FXIIa has more hydrogen bond donor/acceptor residues such as Ser174 residue which takes the place of the missing Phe174 residue.

Omitting the methyl group of methylpiperazine moiety of compound **e4** gives compound **e8** which was more active against both FXIIa and FXa. Compound **e8** has an IC_{50} of 21 µM and 0.36 µM against FXIIa and FXa, respectively. This means that **e8** is 3-fold as active as rivaroxaban against FXIIa. Furthermore, the selectivity of **e8** to FXIIa was improved by 2.7-fold compared to **e4**.

The top poses of **e1** and **e8** docked to FXIIa-H-model shows that both compounds adopt the same binding mode at the S1-subpocket, as expected. On the other hand, the piperazine and the aryl ring was at the same plane in compound **e8,** whereas the morpholinone ring is co-planar to the aryl ring in **e1** (Figure 26). This probably suggests that the co-planarity between the moiety at the P4-position and the aryl ring do not enforce the inhibitory activity of the compound toward FXIIa in contrary to that observed in FXa.

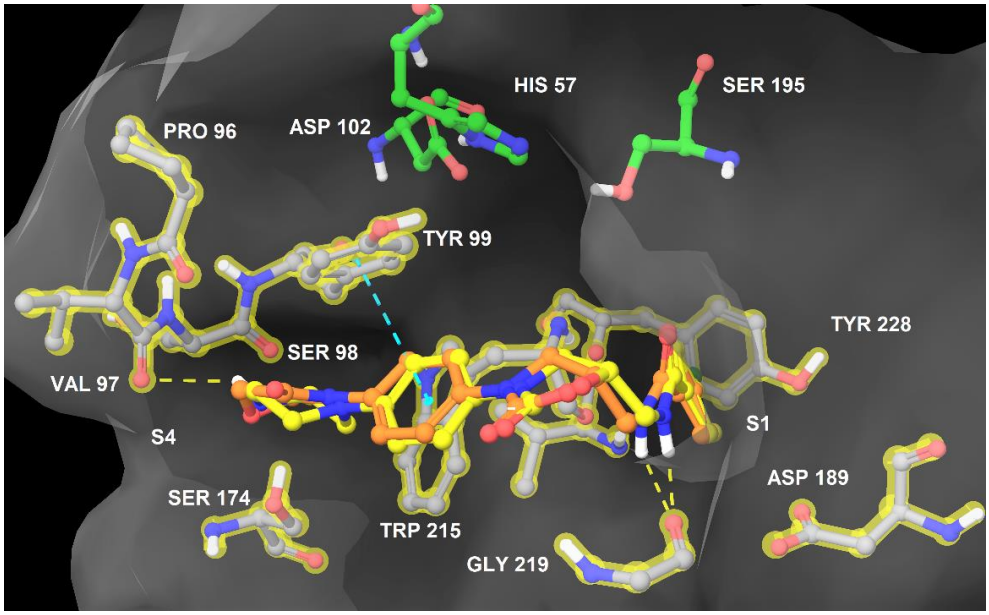

Figure 26: Comparison of binding modes **e8** (yellow) and **e1** (orange) docked to FXIIa-H. Only important residues at the S1- and S4- pocket were shown (yellow silhouetted). Grey: carbon backbone of the enzyme's residues; light green: carbon backbone of the catalytic triad; dark green: chlorine blue: nitrogen; red: oxygen; yellow: sulfur; white: hydrogen; yellow dotted line: hydrogen bond; blue dotted line: π-π stacking.

Comparison of compounds **e5** and **e4** confirmed this notion. The methylpiperazinone moiety of compound **e5** is co-planar with the aryl ring due to the presence of the carbonyl group at 2-position. This causes an improvement in the inhibitory activity toward FXa. On the other hand, despite retention of the co-planarity, the inhibitory activity of compound **e5** diminished toward FXIIa. Compound **e5** is 15-fold more active than **e4** against FXa whereas it was 3-fold less active against FXIIa. Furthermore, compound **e5** is 63-fold less selective to FXIIa than compound **e4**, and it was 170-fold less selective to FXIIa than **e8**.

Omitting the methyl group of the methylpiperazinone moiety of compound **e5** led to improving the activity of the compound towards both enzymes. Compound **e9** was as active as rivaroxaban toward FXa, and it has 55µM IC_{50} toward FXIIa. However, compound **e9** was more selective to FXIIa by 1.3-fold compared to rivaroxaban. In contrast, **e9** was 10-fold less selective to FXIIa than **e5**. Therefore, it was concluded that substitution of the nitrogen atom of the piperazine moiety at the P4-position with methyl group decreases the inhibitory activity of the compound toward FXIIa but increase the selectivity to this enzyme. However, the presence of the carbonyl group at the P4-position decreases both the activity of the compound against and the selectivity for FXIIa (**e5** vs **e4** and **e9**). On the other hand, omitting both, the carbonyl and the methyl groups from the P4-position significantly improves both the activity and the selectivity of the compound toward FXIIa (**e8** vs **e4** and **e9**)

Although these compounds have only modest inhibitory activity against FXIIa, comparison of compounds **e4**, **e5**, **e8**, and **e9** reveals an important difference between FXa and FXIIa. The trend of the reduction of inhibitory activity of these compounds toward FXIIa was **e8**>**e9**>**e4**>**e5** whereas the selectivity of the compound to FXIIa decrease in this order **e8**>**e4**>**e5**>**e9**. In contrast, the trend of the reduction of the inhibitory activity of these compounds toward FXa was: **e5**>**e9**>**e8**>**e4**. This may indicate that piperazine could be a favourable surrogate at the P4-position for FXIIa inhibitors. Compound with unsubstituted piperazine at the P4-position (**e8**) was a stronger inhibitor of FXIIa, and it was more selective to this enzyme than compounds with

substituted piperazine. However, the selectivity factors for all of these compounds were less than one, so this indicates that these compounds were more selective to FXa than FXIIa.

In summary, the substitution of the nitrogen of piperazine negatively affects the inhibitory activity of the compound towards both enzymes. Also, compounds with moieties at the P4-position on the same plane of the aryl ring were more tolerated by FXIIa than FXa.

4.4. Chlorothiophene *vs tert*-butylbenzene at the P1-position

Although compound with *tert*-butylbenzene **g1** shows no inhibitory activity toward FXIIa, Peter Fischer's group working with different pharmacophore as FXIIa inhibitor that suggested *tert*-butyl benzene as a potential P1-substituent (unpublished data). Therefore, to elaborate the potential of this group further, several compounds with chlorothiophene or tert-butylbenzene moiety at the P1-position were synthesised (Table 6 and Table 7).

All compounds with chlorothiophene at the P1-position (Table 6) showed inhibitory activity toward FXa. In contrast, only compounds which have pyridyl group at the P4-position (compounds **e11** and **e12**) showed slight inhibitory activity toward FXIIa. These results are consistent with the previous findings that demonstrated the importance of the chlorothiophene moiety for the inhibitory activity against FXa, and that the nitrogen atom at the end of the P4-position was advantageous for the activity toward FXIIa. Factor XIIa did not tolerate all other groups at the P4-position of this series of the compounds. Compound **e11** shows an improved selectivity for FXIIa compared to **e12**. However, both compounds are more selective to FXa than FXIIa (SF< 1).

Table 6*: In vitro* FXIIa and FXa inhibitory activity of compounds e10-16.

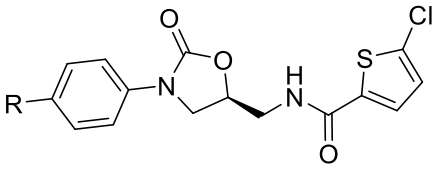

Compd	R=	IC_{50} µM ±SD		SF
		FXIIa	FXa	
e10	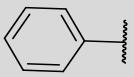	ia	3.70±2.0	na
e11	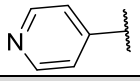	129±13	0.27±0.01	0.002
e12	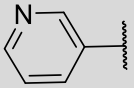	187±22	1.23±0.02	0.0065
e13	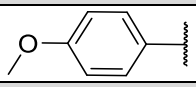	ia	96±6.0	na
e14	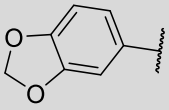	ia	118±15	na
e15	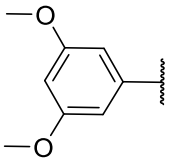	ia	128±12	na
e16	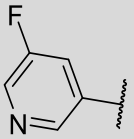	ia	0.36±0.01	na

Both FXIIa and FXa did not tolerate *tert*-butylbenzene at the P1-position (Table 7). However, compounds with nitrogen at the terminal end of the P4-position (compounds **g8** and **g11**) showed slight activity toward FXIIa. Compound **g11** with *tert*-butylbenzene at the P1-position and pyridyl group at the P4-position was less active against FXIIa than **e11** with chlorothiophene at the P1-position. Similarly, compound **g8** was less active against FXIIa than compound **e8**. This decrease in the inhibitory activity when *tert*-butylbenzene was substituted at the P1-position was consistent with the previous finding that the S1-subpocket of FXIIa cannot accommodate *tert*-butylbenzene (Figure 23). Furthermore, the slight activity exhibited by compound **g8** indicates that piperazine was superior to piperazinone (**g9**) at the P4-position. Moreover, compound **g8** was more selective to FXIIa than FXa (SF> 1). Compound **g8** was 102-fold more selective to FXIIa than **e8** (Table 5). Furthermore, the

inhibitory potency towards FXIIa decreases by 6-fold whereas it decreases by 644-fold towards FXa when chlorothiophene moiety replaced with tert-butylbenzene (**e8** vs **g8**). This confirms the idea that chlorothiophene moiety at the P1-position is essential for the inhibitory potency towards FXa. However, it is not necessary for the inhibitory activity toward FXIIa. Although triazole methylcarboxlate group appeared in one of the potential FXIIa inhibitors, compound **e18** with triazole derivative at the P4-position was neither active against FXIIa nor FXa.

Table 7: *In vitro* FXIIa and FXa inhibitory activity of compounds with the *tert*-butyl group at the P1-position.

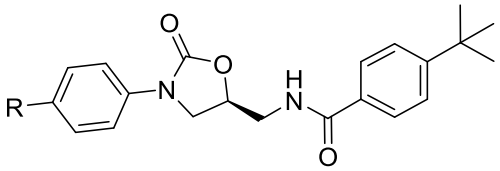

Compd	R=	IC_{50} µM ±SD		SF
		FXIIa	FXa	
g1	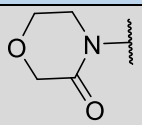	ia	122±6.0	na
g2	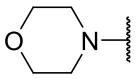	ia	ia	na
g3	Br	ia	ia	na
g4	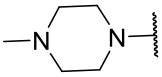	ia	ia	na
g5	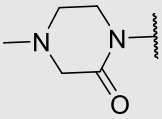	ia	ia	na
g8	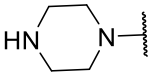	134±9.0	232±7.0	1.73
g9	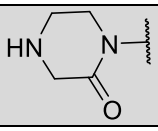	ia	115±2.0	na
g10	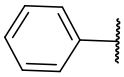	ia	ia	na
g11	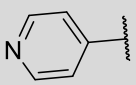	324±12	253±7.0	0.78
g12	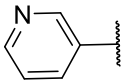	ia	ia	na
g13	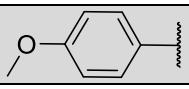	ia	ia	na

Table 7 continued:

Compd	R=	IC_{50} µM ±SD		SF
		FXIIa	FXa	
g14	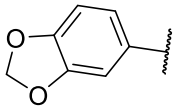	ia	ia	na
g15	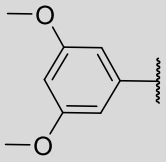	ia	ia	na
g16	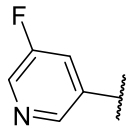	ia	ia	na
g17	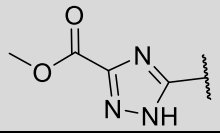	ia	ia	na

4.5. Rivaroxaban analogues with morpholine or piperazine-derivatives at the P4-position

As this project aimed to shift rivaroxaban activity from FXa to FXIIa, so it is logical to interest in changes that decrease the activity of rivaroxaban against FXa and make the compound more active against FXIIa. As mentioned earlier, minor changes in the morpholinone moiety of rivaroxaban give rise to considerable loss of activity (compound **e1** vs **e2**). Additionally, piperazine derivatives at the P4-position improve the activity and selectivity of the compounds toward FXIIa (compounds **e8** and **g8**). Therefore, to explore favourable P4-surrogates, several compounds with morpholine or piperazine-derivatives at the P4-position were synthesised (Table 8 and Table 9).

Table 8: *In vitro* FXIIa and FXa inhibitory activity of compounds with morpholine at the P4-position.

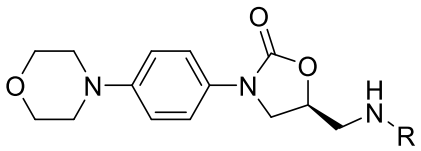

Compd	R=	IC_{50} µM ±SD		SF
		FXIIa	FXa	
f2	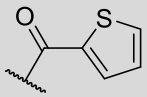	ia	0.34±0.0	na
j2	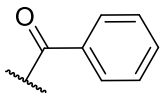	ia	56±12	na
k2	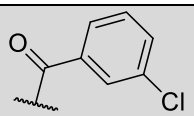	ia	32±3.0	na
l2	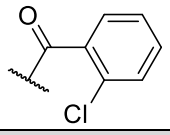	ia	76±19	na
m2	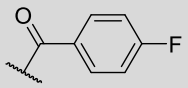	ia	2.58±1.0	na
n2	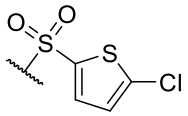	ia	27±6.0	na
p2	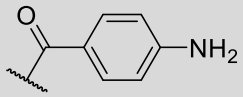	22±5.0	4.56±0.03	0.21
r2	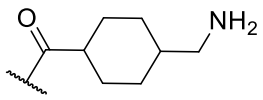	54±12	15±3.0	0.28
t2	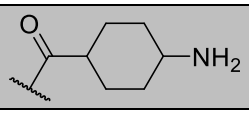	126±4.0	32±5.0	0.25
v2	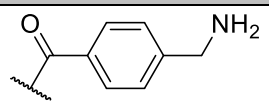	17±1.0	1.34±1.0	0.08

As expected, omitting the chlorine atom of the chlorothiophene moiety as well as the carbonyl group of the morpholinone moiety results in further decrease in the activity toward FXa. Compound **f2** (Table 8**)** was 5-fold less potent than **e2** against FXa, and it was inactive against FXIIa. Furthermore, substitution of the amide linker between the P1-moiety and the oxazolidinone core with sulfonyl group (as in compound **n2**) further decrease the activity toward FXa even in the presence of the chlorothiophene group. These findings confirmed

the idea that the orientation of the chlorothiophene moiety and the Cl-π interaction in the S1-pocket is essential for the inhibitory activity of the compounds toward FXa. Accordingly, an aromatic ring with or without chlorine substituent was attempted at the P1-position (compounds **j2**, **k2**, and **l2**). None of these compounds was active against FXIIa, and the introduction of the aromatic group at the P1-position caused a significant loss of activity against FXa. Compound with a fluorine atom at 4-position of the aromatic ring (**m2**) was also inactive against FXIIa and has only modest activity against FXa.

In this series of compounds (Table 8), only molecules with amine derivatives at the P1-position (**p2**, **r2**, **t2**, and **v2**) were active against FXIIa. The activity of compounds **p2, r2, t2, and v2** against both enzymes decrease in the following order **v2**>**p2**>**r2**>**t2**. Furthermore, compounds **p2**, **r2**, and **t2** have almost the same selectivity for FXIIa, and they were about 2-fold more selective to this enzyme than compound **v2**. Additionally, compounds **p2**, **r2**, and **v2** were more selective to FXIIa than compounds with morpholinone group at the P1-position (**p1**, **r1**, **v1**). These findings confirm the notion that was observed earlier that the S1-subpocket of both enzymes prefer groups in this order: benzylamine>aniline>cyclohexylmethylamine>cyclohexylamine. This was an interesting result at this stage of the project. Therefore, this trend was combined with another trend observed earlier by comparing compounds **e4**, **e5**, **e8**, and **e9**, that all have piperazine derivatives at the P4-position. Therefore, compounds with piperazine derivatives at the P4-position were synthesised and compared with each other and with the previous compounds (Table 9).

Compounds **f4** and **l4** (Table 9) lost the inhibitory activity completely toward both enzymes. Interestingly, compounds **p4**, **r4**, **t4**, and **v4** were more potent against FXIIa than FXa though they have modest inhibitory activity against both enzymes. Compounds **p4, r4, t4,** and **v4** were 5-, 7-, 4-, and 12-fold more active against FXIIa than FXa, respectively. Furthermore, these compounds appear to be more selective to FXIIa than FXa (SF> 1). Compound **v4** with methylpiperazine at the P4-position and benzylamine at the P1-position was the most active and selective compound amongst this series of compounds.

Compound **v4** was 3-fold and 1.7-fold more selective to FXIIa than compounds **p4** and **t4,** and **r4**, respectively.

Table 9: *In vitro* FXIIa and FXa inhibitory activity of compounds with piperazine derivatives at the P4-position

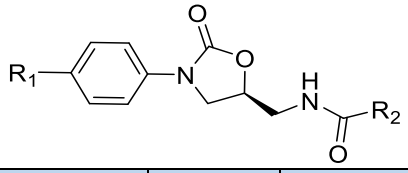

R1=	R2=	compd	IC_{50} µM ±SD		SF
			FXIIa	FXa	
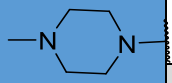	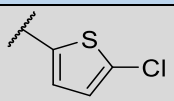	**f4**	ia	ia	na
	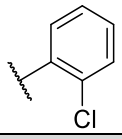	**l4**	ia	ia	na
	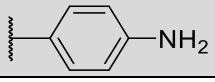	**p4**	6.90±1.0	33±5.0	4.78
	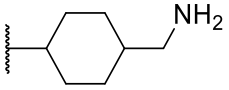	**r4**	15±0.5	110±10	7.33
	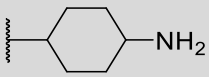	**t4**	8.74±0.0	35±2.0	4.0
	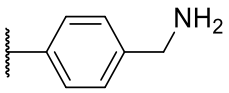	**v4**	0.98±0.0	12±2.0	12.24
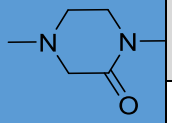	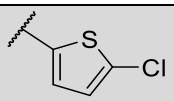	**f5**	ia	93±12	na
	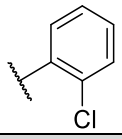	**l5**	ia	ia	na
	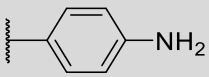	**p5**	160±16	0.97±0.6	0.006
	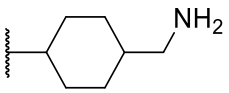	**r5**	254±3.0	14±2.0	0.055
	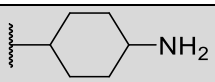	**t5**	217±3.0	21±2.0	0.096
	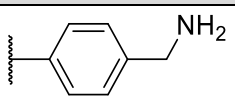	**v5**	18±0.5	1.46±2.0	0.081
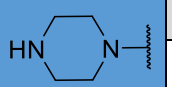	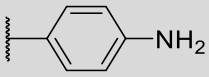	**p8**	0.89±1.0	1.66±1.0	1.86
	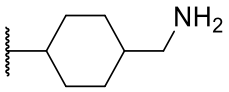	**r8**	1.47±0.0	42±12	28.57

Table 9 continued:

R1=	R2=	compd	IC_{50} µM ±SD		SF
			FXIIa	FXa	
	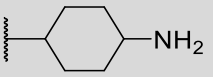	**t8**	1.35±0.0	16±0.5	11.85
	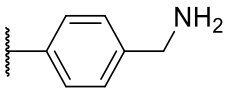	**v8**	0.18±0.1	13±3.0	72.22
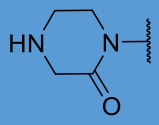	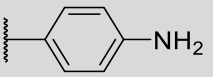	**p9**	17±1.0	0.02±0.9	0.001
	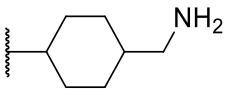	**r9**	36±2.0	1.18±0.1	0.033
	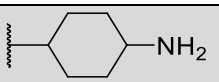	**t9**	32±6.0	1.24±2.0	0.039
	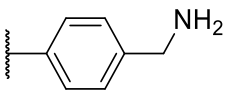	**v9**	1.56±1.0	0.04±0.4	0.026

Although the trend of activity of compounds **p4**, **r4**, **t4**, and **v4** (Table 9) against FXIIa was not the same that observed with compounds **p1, r1, t1, and v1**, it is still the benzylamine was the preferred group at the S1-position of both enzymes amongst this series of compounds. The trend of decreased in the activity toward FXIIa amongst these compounds was: benzylamine **v4**> aniline **p4**> cyclohexylamine **t4**> cyclohexylmethylamine **r4.** Compound **v4** with benzylamine group at the P1-position was 7-fold more active against FXIIa than compound **p4** with only aniline at this position. Similarly, compound **r4** is almost 2-fold more active than **t4** against FXIIa. These results confirmed the previous conclusion that the S1-position of FXIIa accommodate groups with aromatic rings at the P1-position more favourable than cyclic derivatives. Moreover, the methyl group spacer between the aromatic ring and the amine group was advantageous for the activity against FXIIa.

Although compounds with methylpiperazinone at the P4-position (Table 9) were less active against FXIIa than compounds with methylpiperazine, they have the same trend of activity when comparing their P1 groups. Compound **v5** with benzylamine group at the P1-position is more active against FXIIa than compounds with aniline **p5**, cyclohexylmethylamine **r5**, and cyclohexane **t5**. Unsurprisingly, compounds with methylpiperazinone at the P4-position are more active against FXa than the corresponding compounds with

methylpiperazine. Moreover, compounds with methylpiperazinone at the P1-position were less selective to FXIIa than FXa (SF<1), and also they were less selective to FXIIa when compared with compounds with methylpiperazine. For example, compound **v5** was 151-fold less selective to and 18-fold less potent against FXIIa than **v4.** The increase in the activity of these compound against FXa and the decrease in the selectivity for FXIIa could be attributed influence of the carbonyl group at the P4-position.

These conclusions were further confirmed by comparing compounds piperazine or piperazinone at the P4-position (Table 9). Compound **v8** that has benzylamine group at the P1-position and piperazine group at the P4-position was more active against FXIIa than **p8**, **r8**, and **t8** that have aniline, cyclohexylmethylamine, and cyclohexylamine at the P4-position, respectively. Similarly, compound **v9** was more active against FXIIa than **p9**, **r9**, and **t9**. Putting unsubstituted piperazine group at the P4-position significantly improves the inhibitory activity of the compounds against FXIIa. Similarly, the selectivity of these compounds to FXIIa was increased considerably compared to compounds with substituted piperazine group at this position. For example, compound **v8** was 72-fold more selective to FXIIa than FXa. Additionally, this compound was 5-fold, 100-fold, and 9-fold more active against FXIIa than **v4**, **v5**, and **v9**, respectively.

These findings confirmed the previously noticed idea that the substitution at the amine group of piperazine negatively impacts the inhibitory activity of the compound against FXIIa. Generally, substitution with methyl group has a similar effect on the activity and selectivity of the compounds. In contrast, substitution with carbonyl group has a significant impact on the selectivity more than the inhibitory potency of the compound. For example, compound **v5** was 5-fold less active against and 6-fold less selective to FXIIa than compound **v8**. However, compound **v9** was 9-fold less active against and 2769-fold less selective to FXIIa than compound **v8**. These results suggest that the carbonyl group at the P4-position was not preferable for the activity against FXIIa though it is essential for FXa inhibition.

Compound **v8** with piperazine group at the P4-position and benzylamine at the P1-position is the most active compound against FXIIa so far. It is 72-fold more potent against FXIIa than FXa though its inhibitory activity against FXIIa is still weak. Therefore, it requires more modification to improve its activity and selectivity toward FXIIa.

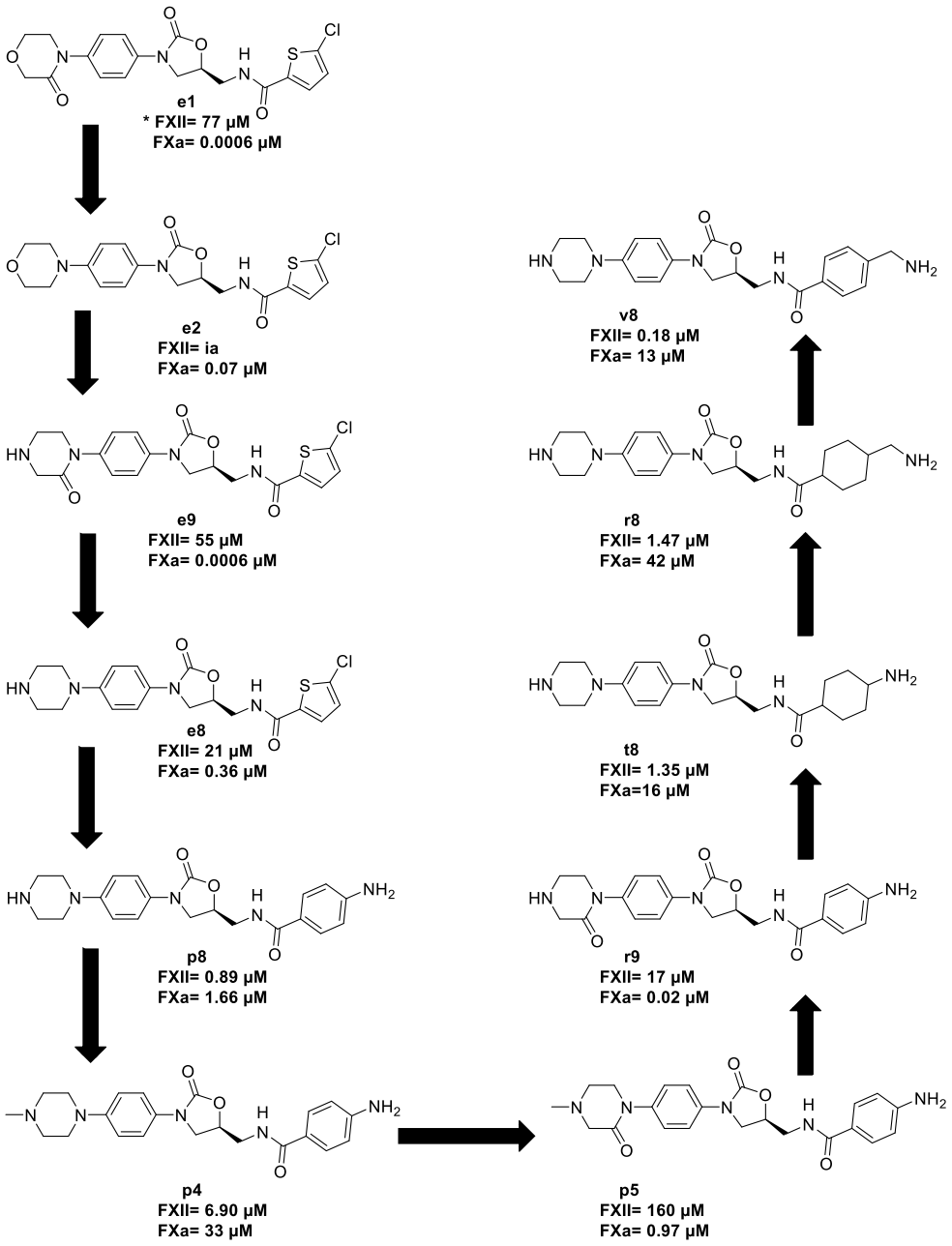

Scheme 18: Major changes that lead to the discovery of compound **v8** and the effect of these changes on the activity against FXIIa and FXa. $^{*}IC_{50}$.

Scheme 18 illustrates the major changes that lead to the discovery of compound **v8** and the effect of these changes on the activity against FXIIa and

FXa. The presence of the chlorothiophene group at the P1-position was advantageous for the activity against FXa. On the other hand, a remarkable drop in the activity against FXa was noticed by only deleting the carbonyl group of morpholinone moiety (**e1**vs **e2**). However, this change abolishes the activity toward FXIIa. Changing the morpholinone moiety at the P4-position to piperazinone caused an increase in the inhibitory activity of compound **e9** toward FXIIa though this compound is as active as rivaroxaban against FXa. Given that the importance of the carbonyl group for the inhibitory activity against FXa, it was expected that deleting this group from the P4-position will decrease the inhibitory activity toward this enzyme. This was confirmed by removing the carbonyl group of piperazinone moiety. Compound **e8** with piperazine at the P4-position was far less potent than compound **e9** against FXa. In contrast, this compound is 2-fold more potent against FXIIa than **e9**. Therefore, by comparing compounds **e1**, **e2**, **e9**, and **e8,** it was concluded that the inhibitory activity against FXIIa was negatively impacted by the presence of carbonyl group at the P4-position. Conversely, the terminal nitrogen at this position was advantageous for the inhibition of FXIIa.

As mentioned earlier the Cl-π interaction at the P1-position plays a crucial role for the inhibitory activity against FXa. Deleting only the chlorine atom from this position decreases the activity of rivaroxaban by 13-fold (compound **e1** vs **f1**). Therefore, fixing piperazine at the P4-position and doing a series of changes at the P1-position have led us to compound **p8** that has aniline group at the P1-position. This compound was almost 2-fold more potent against FXIIa than FXa. Substituting piperazine with a methyl group (compound **p4**) made the compound less active against both enzymes. Adding carbonyl group to this compound had a profound effect on the inhibitory activity against both enzymes. Compound **p5** was 28-fold less active against FXIIa, and it was 34-fold more active against FXa than compound **p4**. Deleting the methyl group from methylpiperazine moiety improves the activity towards both enzymes (compound **r9** vs **p5**). Therefore, these results confirmed the previous conclusion that piperazine at the P4-position was favourable for FXIIa. Hence, fixing piperazine at the P4-position and shifting the aniline at the P1-position to cyclohexylamine decrease the activity of the compound toward both

enzymes (compound **t8** vs **p8**). Similarly, cyclohexylmethylamine (compound **r8**) at the P1-position further decrease the activity against both enzymes compared to **t8**, though this compound still more potent to FXIIa than FXa. Interestingly, benzylamine group at the P1-position and piperazine group at the P4-position give rise compound **v8** which has an IC_{50} (FXIIa) of 0.18 µM, and it was 72-fold more active against FXIIa than FXa.

Docking studies (Figure 27) shows that compound **v8** forms hydrogen bond contacts with Trp215 and Gly219 residues in FXa. However, the absence of the carbonyl group at the P4-position caused a loss in π-π contact at the aromatic pocket of FXa enzyme as well as the loss of Cl-π interaction due to the absence of the chlorine atom at the S1-pocket. On the other hand, compound **v8** forms a hydrogen bond with Ser174 residue at the S4-position of FXIIa. Therefore, it seems that the π-π and Cl-π interactions are crucial for the activity against FXa whereas the inhibitory activity against FXIIa depends more on the electrostatic contacts at the S1- and S4-subpockets.

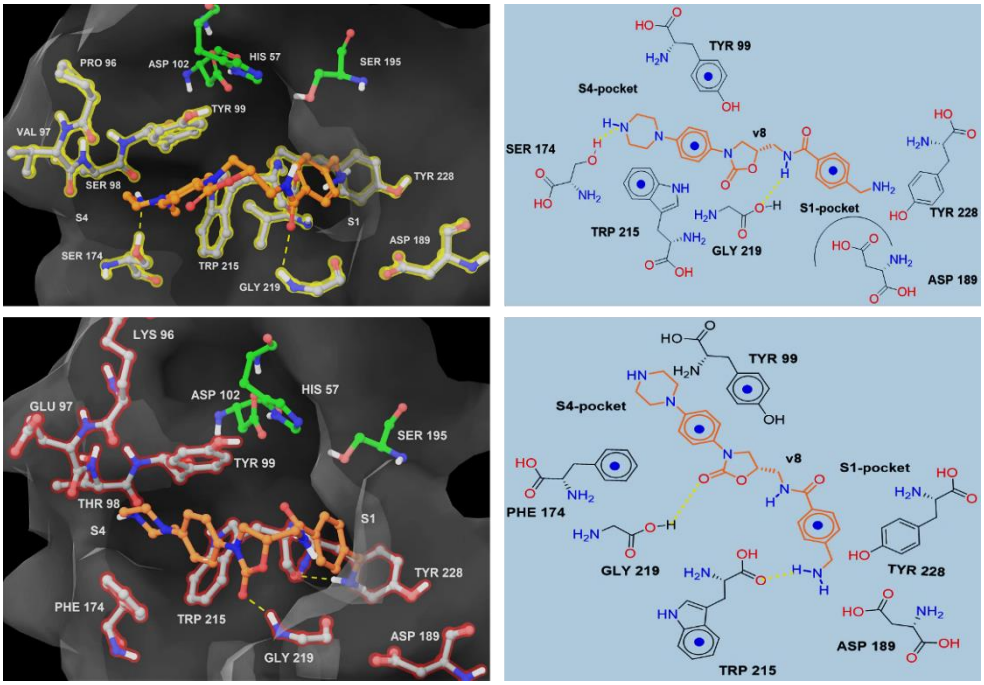

Figure 27: Comparison of binding modes of v8 docked to FXIIa-H (above) and FXa (PDB:2w26) (below). On the left side is the 2D-schematic representation of the binding modes. Only important residues at the S1- and S4- pocket were shown (FXIIa: yellow silhouetted; FXa: red silhouetted). Grey: carbon backbone of the enzyme's residues; green: carbon backbone of the catalytic triad; blue: nitrogen; red: oxygen; white: hydrogen; yellow dotted line: hydrogen bonds.

4.6. Rivaroxaban fragments

As mentioned earlier chlorothiophene moiety at the P1-position was found to be optimum for the activity against FXa. Chlorothiophene group fits into the S1-subpocket of the enzyme and contact with Tyr228 residue through Cl-π-interaction.[1] Additionally, from the previous results of this project, it was found that some compounds with chlorothiophene at the P1-position give slight activity toward FXIIa such as **e8** and **e11**. Furthermore, docking studies showed that the major structural difference between FXa and FXIIa is in the S4-subpocket. Therefore, in order to explore the effect of different fragments of rivaroxaban on the activity toward FXIIa or FXa, various rivaroxaban fragments were synthesised. In one attempt, the chlorothiophene group at the P1-position and the oxazolidinone core were preserved, and various groups were attached to the nitrogen atom of the oxazolidinone core. In another attempt, only the chlorothiophene group at the P1-position was kept unchanged and connected to the various groups through an amide linkage (Table 10).

Unfortunately, none of the compounds in this series showed any activity towards FXIIa, but three compounds were found to be slightly active toward FXa (compounds **e17**, **e18** and **e24**). Docking of compound **e24** to FXa and FXIIa showed that this compound adopts different binding modes in FXa enzyme than rivaroxaban due to the lack of the P4-part of the molecule. As mentioned earlier, the main structural difference between FXIIa and FXa, according to the docking studies using the homology model that was designed at the start of this project, lies in the S4-subpocket. Therefore, docking showed that compound **e24** forms π-π- contact through its chlorothiophene moiety with the aromatic system in the S4-pocket of FXa. On the other hand, the lack of the phenylalanine residue at the S4-pocket of FXIIa and its substitution with serine renders this pocket less hydrophobic than that of FXa. Therefore, the chlorothiophene group of compound **e24** resides in the S1-pocket of FXIIa leaving the S4-pocket unoccupied. Thus, it was concluded that, due to the hydrophobicity of the S4-pocket of FXa, FXa inhibitors adopt the conformation that permits the formation of π-π stacking whenever that possible.

Table 10: *In vitro* inhibitory activity against FXIIa and FXa of rivaroxaban fragments

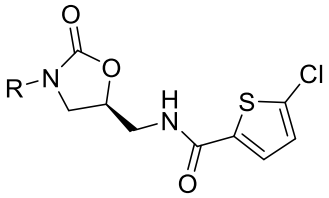

Compd	R=	IC_{50} µM±SD		SF
		FXIIa	FXa	
e17	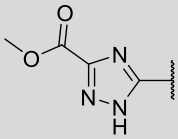	ia	17±3.0	na
e18	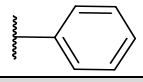	ia	93.0±18.0	na
e19	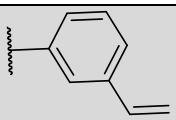	ia	ia	na
e20	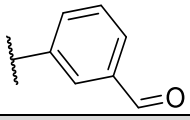	ia	ia	na
e21	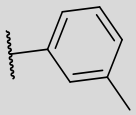	ia	ia	na
e22	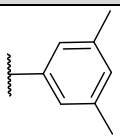	ia	ia	na
e23	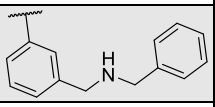	ia	ia	na
e24	H	ia	33.0±4.0	na
e25		ia	ia	na
e26	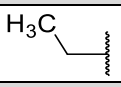	ia	ia	na
e27	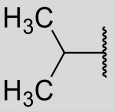	ia	ia	na
e28	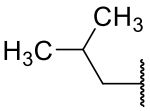	ia	ia	na
e29	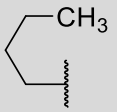	ia	ia	na
e31	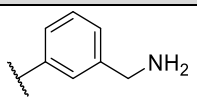	ia	ia	na

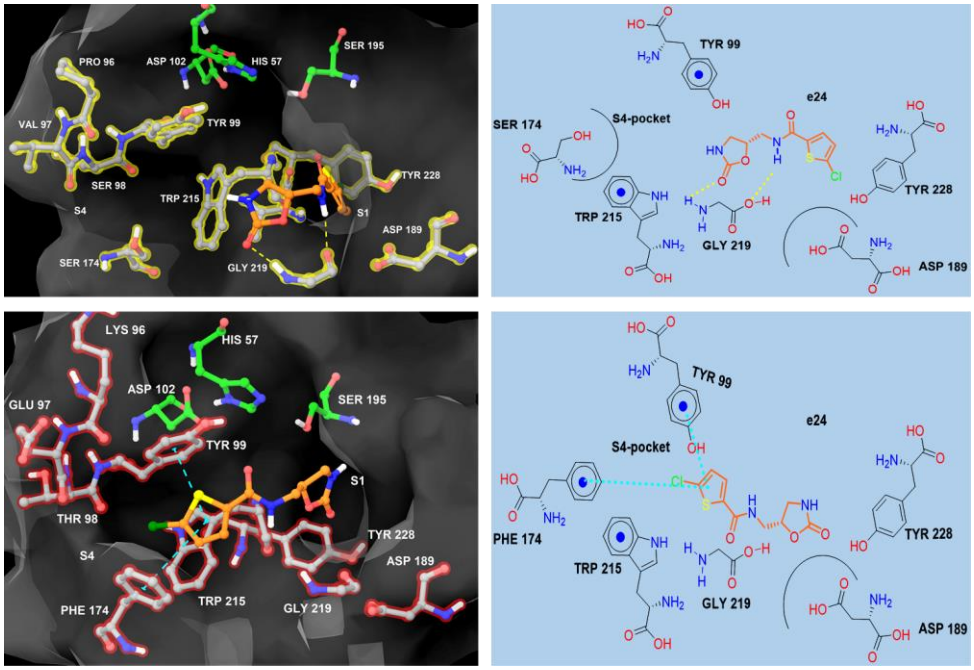

Figure 28: Comparison of binding modes of **e24** docked to FXIIa-H (above) and FXa (PDB: 2w26) (below). On the left side is the 2D-schematic representation of the binding modes. Only important residues at the S1- and S4- pocket were shown (FXIIa: yellow silhouetted; FXa: red silhouetted). Grey: carbon backbone of the enzyme's residues; light green: carbon backbone of the catalytic triad; dark green: chlorine; blue: nitrogen; red: oxygen; yellow: sulfur; white: hydrogen; yellow dotted line: hydrogen bond; blue dotted line; π-π stacking.

Docking of compounds **e17** and **e18** into FXa and FXIIa confirmed the notion that FXa prefers more aromatic moieties at the S4-subpockets than FXIIa (

Figure 29). Compound **e17** has methylcarboxytriazol group at P4- Position. This group appears in one of the potential FXIIa inhibitors worked by another member of Peter Fischer's group (unpublished data). However, compound **e17** was inactive against FXIIa and showed modest activity against FXa (17µM). Compound **e17** flip around in FXa and the triazole moiety fits in the S1-pocket instead of S4, while the chlorothiophene moiety forms π-π- contacts in the aromatic pocket of FXa. In contrast, this compound takes the conventional binding mode with FXIIa where the chlorothiophene group fit to S1-pocket and the S4-pocket accommodate the triazole. Compound **e18,** which has phenyl group at the P4-position, form a π-contact through its phenyl moiety with the S4-pocket of FXIIa and FXa while the chlorothiophene group resides in the S1-pocket (

Figure 29). These findings indicate that, when the chlorothiophene group is at the P1-position, the compound tends to be active against FXa when there is a

possibility to form π-π-interaction with its aromatic pocket. However, π-π-interaction play a minor role in the activity toward FXIIa because its S4-position is less aromatic.

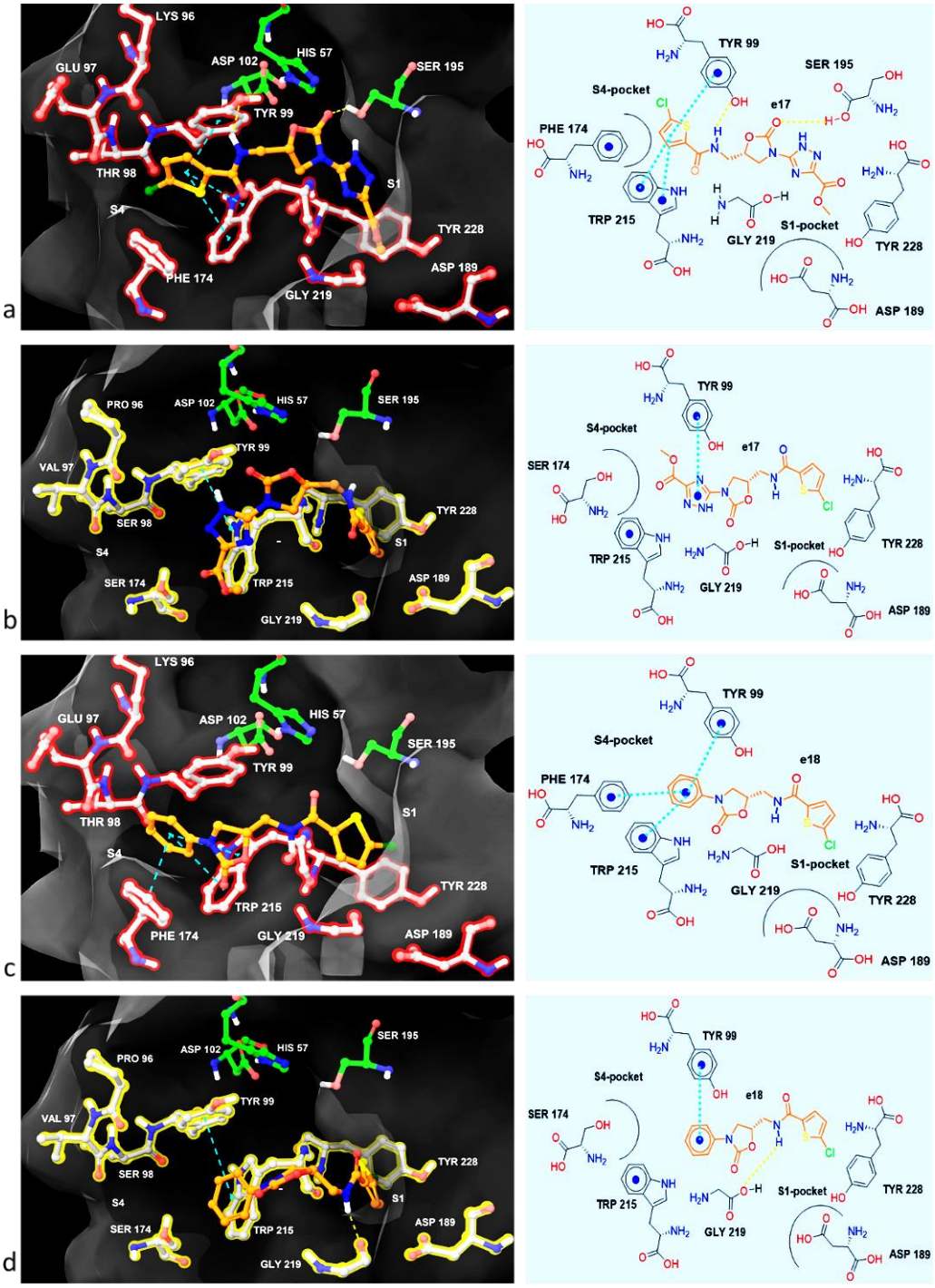

Figure 29: Comparison of binding modes of **e17** and **e18** in FXIIa and FXa.a) and c) compounds **e17** and **e18**, respectively, docked to FXa (PDB: 2w26); b) and d) compounds **e17** and **e18**, respectively, docked to FXIIa-H. On the left side is the 2D-schematic representation of the binding modes. Only important residues at the S1- and S4- pocket were shown (FXIIa: yellow silhouetted; FXa: red silhouetted). Grey: carbon backbone of the enzyme's residues; light green: carbon backbone of the catalytic triad; dark green: chlorine; blue: nitrogen; red: oxygen; yellow: sulfur; yellow dotted line: hydrogen bond; blue dotted line; π-π stacking.

The lack of the activity of the small fragments against FXIIa was expected because even the intact molecule (rivaroxaban) has only modest activity toward FXIIa. Therefore, it was concluded that the chlorothiophene moiety might be of less importance for the inhibition of FXIIa than for FXa. This may partly be due to a subtle difference in the S1-pockets of the enzymes that cannot be recognised in the docking studies. Additionally, the difference in the S4-pocket between FXIIa and FXa enzymes plays a key role in determining the inhibitory activity of the synthesised compounds.

4.7. Benzamidine derivatives

Benzamidine containing compounds are classic inhibitors of serine proteases, and the benzamidine fragment is a medium-potency inhibitor for all members of the trypsin family (Ki ∼15 nM).[283] Furthermore, early FXa inhibitors contained benzamidine, naphtylamidine or other basic groups,[336] thought to be necessary for binding in the S1-pocket, but the poor bioavailability often associated with the amidine group directed efforts to replace this functionality with less basic or nonpolar neutral groups.[288,337] The amidine moiety forms a bidentate salt bridge with Asp189 deep within the S1 pocket of FXa, which provides effective solvent shielding for a thermodynamically favoured interaction.[285] In this project, it was noticed, so far, that compounds with an amine group at the P1-position exhibited greater activity against FXIIa than compounds containing other groups such as chlorothiophene (compounds **p1**, **r1**, **v1** vs **e1**). Therefore, it was anticipated that compounds with benzamidine would be potent against FXIIa. Thus, to explore the effect of benzamidine group at P1-pocket on the activity towards FXIIa compared to that of FXa, analogues featuring a P1-benzamidine were evaluated (Table 11).

Table 11: *In vitro* inhibitory activity of benzamidine derivatives against FXIIa and FXa.

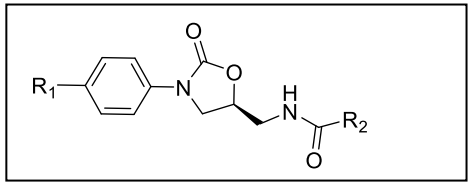

R_1=	R_2=	IC_{50} µM ±SD		SF	R_2=	IC_{50} µM ±SD		SF	R_2=	IC_{50} µM ±SD		SF
		FXIIa	FXa			FXIIa	FXa			FXIIa	FXa	
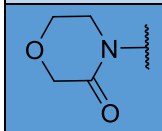	**h1**	ia	0.07±0.0	na	**y1**	195±19	101±15	0.51	**z1**	0.93±0.52	0.003±0.0	0.003
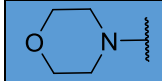	**h2**	ia	23±4	na	**y2**	149±6.0	ia	na	**z2**	1.56±0.03	0.04±0.0	0.03
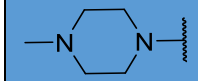	**h4**	ia	ia	na	**y4**	276±9.0	ia	na	**z4**	37.50±5.50	0.013±0.0	0.0004
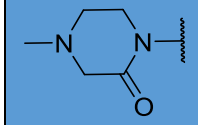	**h5**	ia	1.52±1.0	na	**y5**	ia	125±2.50	na	**z5**	2.15±0.02	0.021±0.0	0.0098
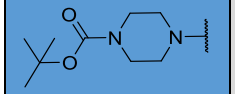	**h6**	ia	ia	na	**y6**	ia	ia	na	**z6**	ia	ia	na
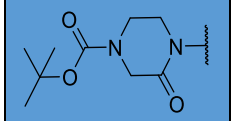	**h7**	ia	ia	na	**y7**	ia	ia	na	**z7**	ia	ia	na
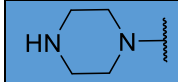	**h8**	112±7.0	149±3.50	1.33	**y8**	37±5.0	11±4.0	0.30	**z8**	0.12±0.05	1.70±0.20	14.17
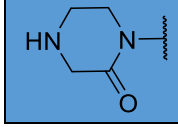	**h9**	237±6.0	0.08±0.0	0.0003	**y9**	172±7.0	3.50±0.10	0.03	**z9**	0.24±0.02	0.002±0.0	0.008

The procedure that was chosen to synthesised benzamidine derivatives involves the conversion of benzonitrile to amidoxime, and then amidoximes reduction with potassium formate. Therefore, the nitriles and amidoximes intermediates were also tested for an inhibitory activity toward FXIIa and FXa. Morpholine, morpholinone, methylpiperazine, methylpiperazinone, piperazine, and piperazinone were chosen as P4-surrogate because of the potential of the piperazine derivatives at the P4-position to give compounds that were active against FXIIa, for example, compound **v8**. In addition, compounds with Boc-piperazine and Boc-piperazinone at the P4-position were also pharmacologically tested (Table 11).

Compounds with benzonitrile at the P1-position were inactive against FXIIa whatever the group at the P4-position was, apart from compounds with piperazine and piperazinone (**h8** and **h9**). Furthermore, a compound with piperazine was more active against FXIIa than a compound with piperazinone (**h8** vs **h9**). Expectedly, compounds with morpholinone (**h1**), methylpiperazinone (**h5**), and piperazinone (**h9**) were far more active against FXa than FXIIa du to the importance of the carbonyl group at the P4-position for the activity against FXa. On the other hand, compound **h8**, which has piperazine group at this position, was more active against FXIIa than FXa. Moreover, compound **h8** was more selective to FXIIa than FXa (SF= 1.33).

Docking of compound **h8** to FXIIa-H and FXa shows that this compound has fewer electrostatic contact with FXIIa than FXa though the *in vitro* inhibitory activity assay showed that it is more active against FXIIa than FXa (Figure 30). The increased activity of compound **h8** toward FXIIa is probably attributed to the importance of Cl-π interaction at the P1-position and π-π stacking at the P4-position, which this compound deprived of, for the inhibitory activity against FXa more than FXIIa. This notion could be enforced by comparing the binding mode of compound **h1** in FXIIa and FXa (Figure 31). The aryl group of compound **h1** forms a π-π stacking with Tyr99 at the S4-subpockets of both enzymes. However, **h1** was inactive against FXIIa, but it was more than 2000-fold more active against FXa than **h8.** Nevertheless, compound **h1** was more than 100-fold less active against FXa than rivaroxaban (**e1**) because it was deprived of the important Cl- π interaction.

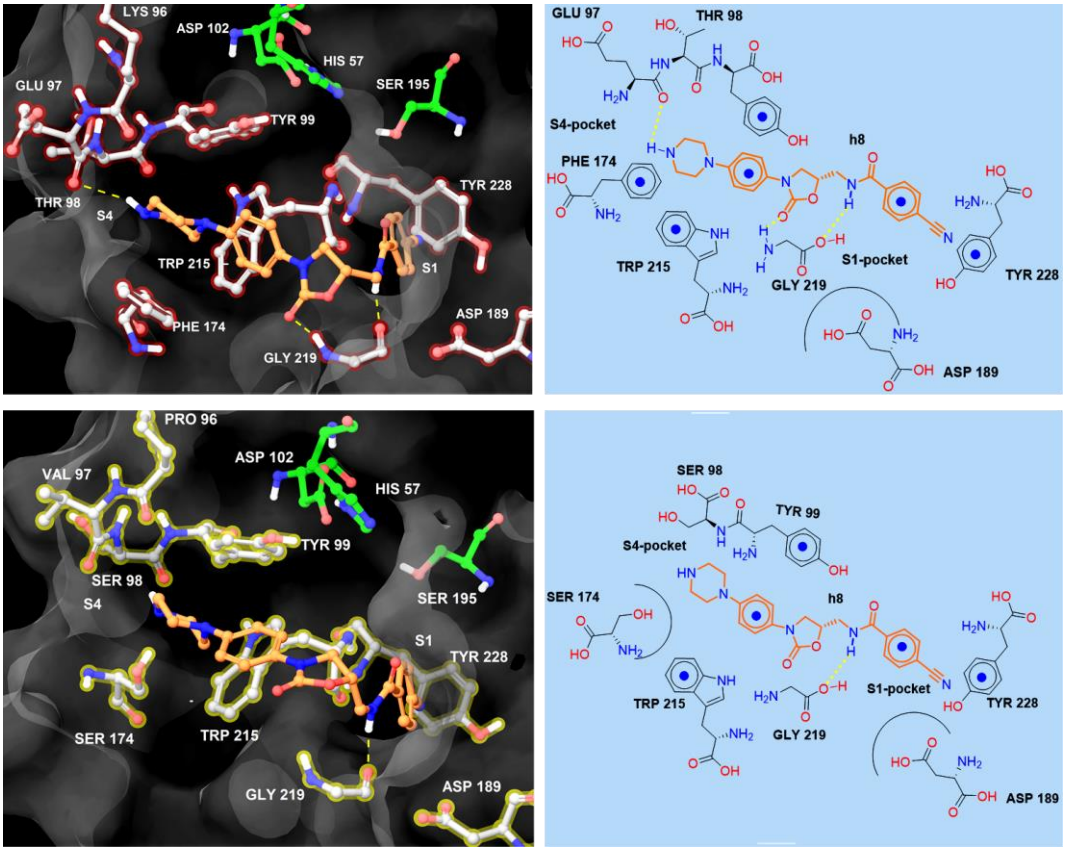

Figure 30: Compound **h8** docked to FXa (PDB: 2w26) (above); and to FXIIa-H (below). On the left side is the 2D-schematic representation of the binding modes. Only important residues at the S1- and S4- pocket were shown (yellow silhouetted: FXIIa residues; red silhouetted FXa residues). Orange: carbon backbone of the docked compound; grey: carbon backbone of the enzyme's residues; light green: carbon backbone of the catalytic triad; blue: nitrogen; red: oxygen; yellow: sulfur; white: hydrogen; yellow dotted line: hydrogen bond.

Almost the same trend was also noticed in compounds with amidoxime at the P1-position (compounds **y1**-**y9**). However, those compounds were generally more active against FXIIa and less active against FXa than compounds with nitrile except for compound with piperazine at the P4-position (**y8**), which was more active than compound **h8** against both enzymes. These compounds were also more selective to FXa than FXIIa (SF< 1). Compound **y8** was 3-fold and 13-fold more active than compound **h8** against FXIIa and FXa, respectively. This compound was also 3-fold more potent against FXa than FXIIa, and it was more selective to FXa. These results contradict the previous findings that showed compounds with piperazine moiety at the P4-position were generally more active against FXIIa than FXa. Docking studies showed that the amidoxime group at the P1-position of compound **y8** forms an important salt bridge with Asp189 residue at the S1-position of FXIIa enzyme miming the guanidine group of arginine of the natural substrate, whereas in FXa this was

not the case. However, the P4-group in these compounds takes unusual orientation and extends more toward the solvent accessible surface in FXIIa than in FXa (Figure 32).

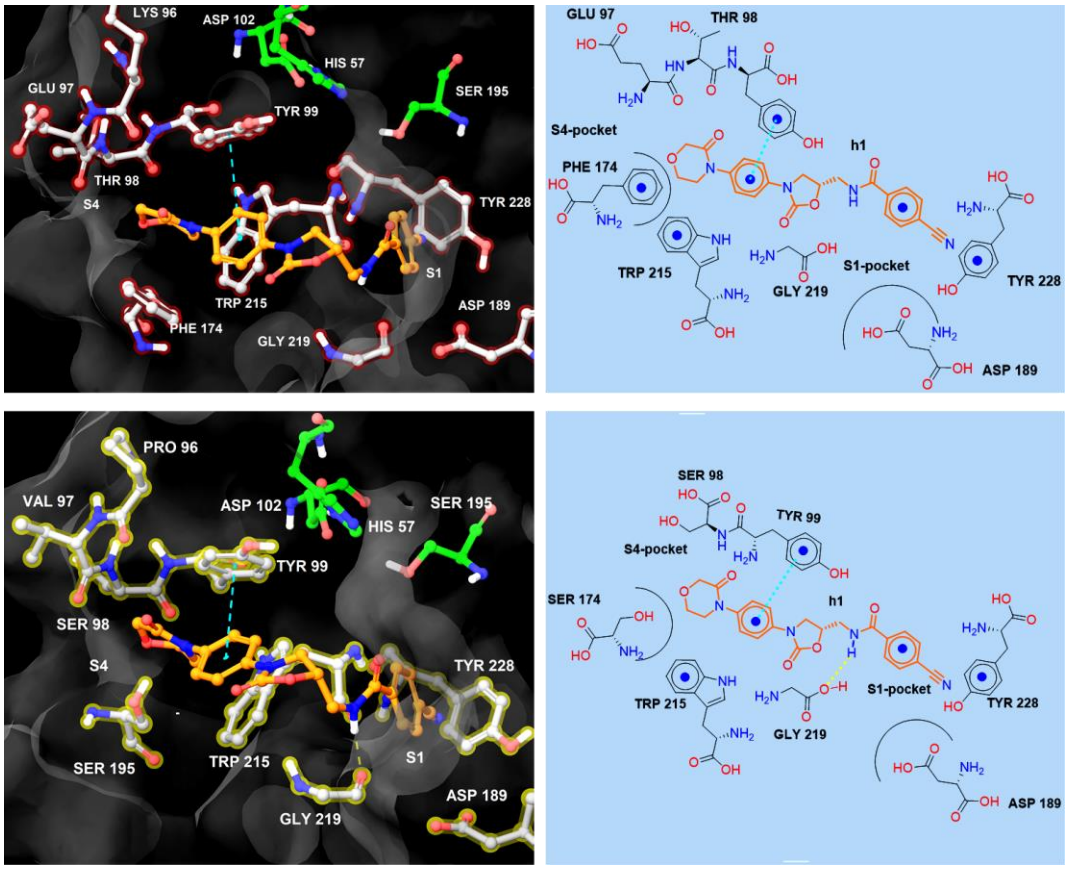

Figure 31: Compound **h1** docked to FXa (PDB: 2w26) (above); and to FXIIa-H (below). On the left side is the 2D-schematic representation of the binding modes. Only important residues at the S1- and S4- pocket were shown (yellow silhouetted: FXIIa residues; red silhouetted: FXa residues). Orange: carbon backbone of the docked compound; grey: carbon backbone of the enzyme's residues; light green: carbon backbone of the catalytic triad; blue: nitrogen; red: oxygen; yellow: sulfur; white: hydrogen; yellow dotted line: hydrogen bond; blue dotted line: π-π interaction.

The S1-pocket of FXIIa prefer amidoxime at the P1-position more than nitrile. This was noticed by comparing compounds **h1** vs **y1, h2** vs **y2,** and **h8** vs **y8**. However, the chlorothiophene moiety was more preferable than both nitrile and amidoxime (**e1** vs **h1** and **y1**). Yet, the most favourable group at this position was benzylamine (compounds **v8**). Given that the basicity of these group increases in this order nitrile<amidoxime<benzylamine<benzamidine, it was expected that the benzamidine group at the P1-position would increase the activity of the compounds against FXIIa more than FXa.

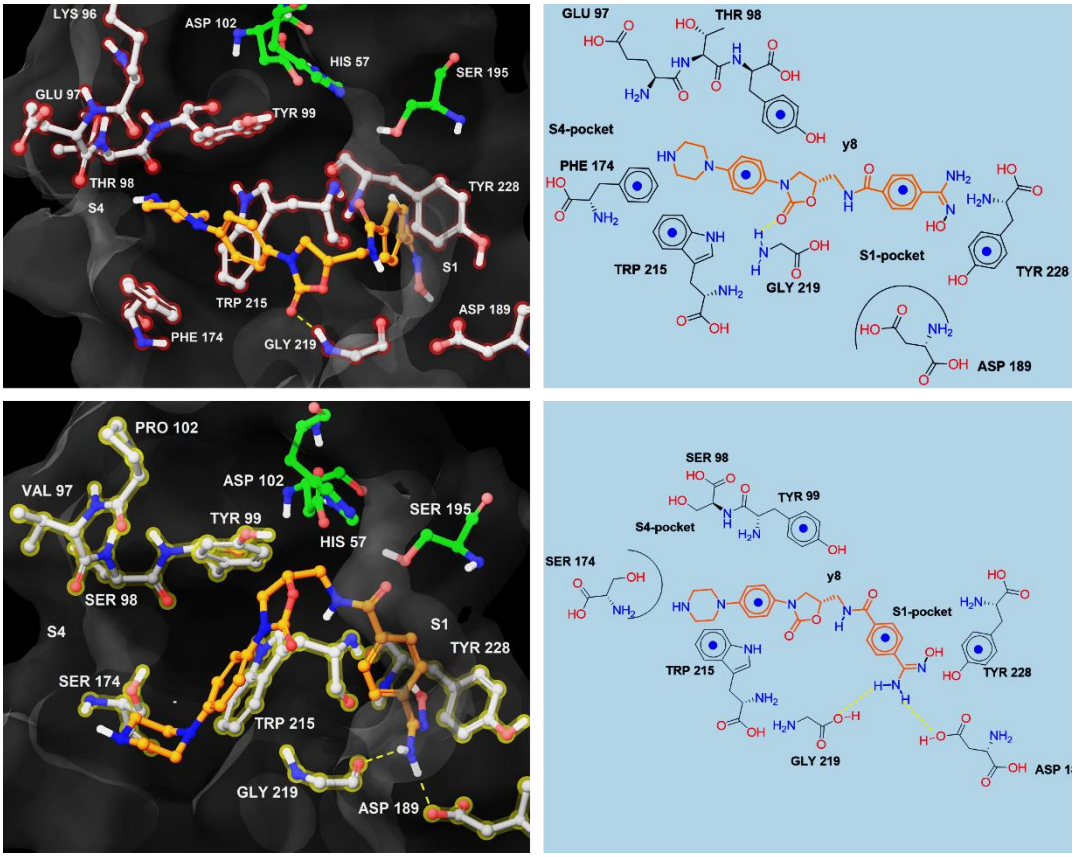

Figure 32: Compound **y8** docked to FXa (PDB: 2w26) (above); and to FXIIa-H (below). On the left side is the 2D-schematic representation of the binding modes. Only important residues at the S1- and S4- pocket were shown (yellow silhouetted: FXIIa residues; red silhouetted FXa residues). Orange: carbon backbone of the docked compound; grey: carbon backbone of the enzyme's residues; blue: nitrogen; red: oxygen; yellow: sulfur; white: hydrogen; yellow dotted line: hydrogen bond.

Compounds with benzamidine at the P1-position were generally more active against both enzymes than compounds with benzonitrile or amidoxime groups. However, the presence of benzamidine was more advantageous for the activity against FXIIa than FXa. For example, compound **z1** was 82-fold more active than rivaroxaban (**e1**) against FXIIa. In contrast, this compound was 5-fold less active against FXa than rivaroxaban. Moreover, comparing the selectivity factor (SF) of compounds **z1** (SF= 0.003) and **e1** ($7\times\ 10^{-7}$) reveals that substitution of the chlorothiophene group at the P1-position with benzamidine has led to a significant improvement in the selectivity for FXIIa. Additionally, compounds with morpholine at the P4-position were generally inactive or have modest activity against FXIIa (see Table 8), but compounds with benzamidine group at the P1-position showed increased inhibitory activity against FXIIa despite the presence of morpholine group at the P4-position. However, the selectivity for FXIIa decreased. For example, compound **e2** (see Table 5) was

inactive against FXIIa whereas compound **z2** has an IC_{50} of 1.56 µM against this enzyme. Moreover, compounds **p2**, **r2**, **t2**, and **v2** (see Table 8) were less active against FXIIa than compound **z2**, but they were more selective to this enzyme than FXa comparing to **z2**.

As it has been noticed earlier, the substitutions at piperazine group at the P4-position has a negative effect on compounds' potency against FXIIa. Compound **z8**, which has unsubstituted piperazine group at the P4-position was more active against FXIIa than compounds **z4**-**z7** and **z9**, which all have substituted piperazine. Furthermore, this compound (**z8**) was 1.5-fold more active against FXIIa than compound **v8**, which has benzylamine at the P1-position. However, compound **v8** was more selective to FXIIa than FXa (the SF of **v8** was 72.22 whereas it is 14.17 for **z8**).

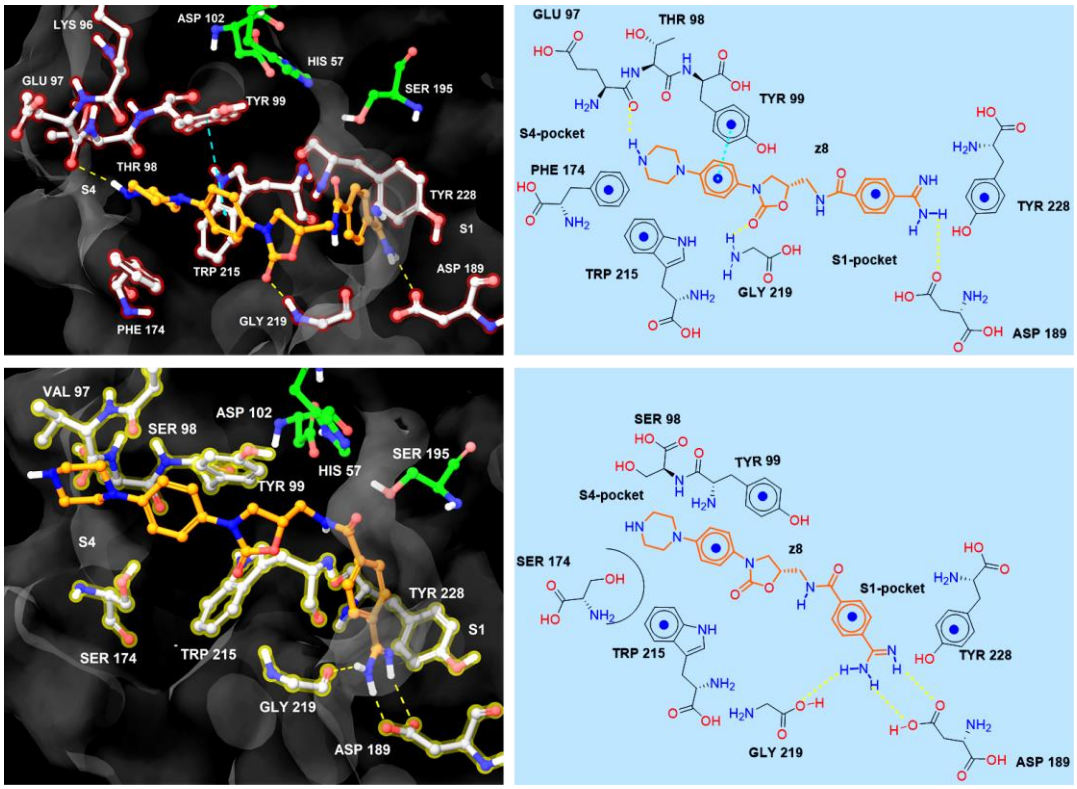

Figure 33: Compound **z8** docked to FXa (PDB: 2w26) (above); and to FXIIa-H (below). On the left side is the 2D-schematic representation of the binding modes. Only important residues at the S1- and S4- pocket were shown (yellow silhouetted: FXIIa residues; red silhouetted: FXa residues). Orange: carbon backbone of the docked compound; grey: carbon backbone of the enzyme's residues; light green: carbon backbone of the catalytic triad; blue: nitrogen; red: oxygen; yellow: sulfur; white: hydrogen yellow dotted line: hydrogen bond; blue dotted line: π-π interactions.

The amidine group of compounds with benzamidine at the P1-position mimics the guanidine or amine group of arginine or lysine, respectively, of the

common substrates of serine proteases.[286] Docking of compound **z8** to the crystal structure of FXa (PDB: 2w26) and to the homology model of FXIIa (FXIIa-H) shows that the benzamidine group fit in the S1-pocket of both enzymes (Figure 33). In FXa, Asp189 residue participates in ionic and hydrogen-bond interactions with the positively charged P1 arginine of the substrate. X-ray Crystal structure of FXa complexed with one of its inhibitor that has benzamidine group (Figure 34) shows that the cation of the benzamidine forms a bidentate salt bridge with Asp189, like that formed with the guanidine group of arginine of the natural substrate. However, compound **z8** seems to form fewer electrostatic contacts in the S1-pocket of FXa. In contrast compound **z8** docked to FXIIa-H shows that this compound forms a salt bridge with Asp-189 in addition to the hydrogen bond with Gly219. In contrast, the piperazine group at the P4-position seem to sit more comfortably in the S4-pocket of FXa than that of FXIIa. These findings probably mean that the S1-interactions are more determinant of the inhibitory activity of the compounds against both enzymes than S4-interactions. For example, the Cl-π interaction at the S1-subpocket of FXa boosted the inhibitory activity of the compounds against FXa regardless of the contacts at the S4-subpocket. Similarly, the salt bridge at the S1-pocket of FXIIa increases the activity of the compounds even if the P4-group had fewer contacts at the S4-position.

Although compound **z8** is the most potent compound against FXIIa so far, the amidine groups are highly hydrophilic and strongly basic ($pK_a \sim 12.5$). These characteristics lead to poor or insufficient oral absorption of amidine-containing compounds. Moreover, these compounds are also characterised by very short half-life due to the property of high clearance.[287] Therefore, replacement of amidine group with derivatives of low basicity have been tried.

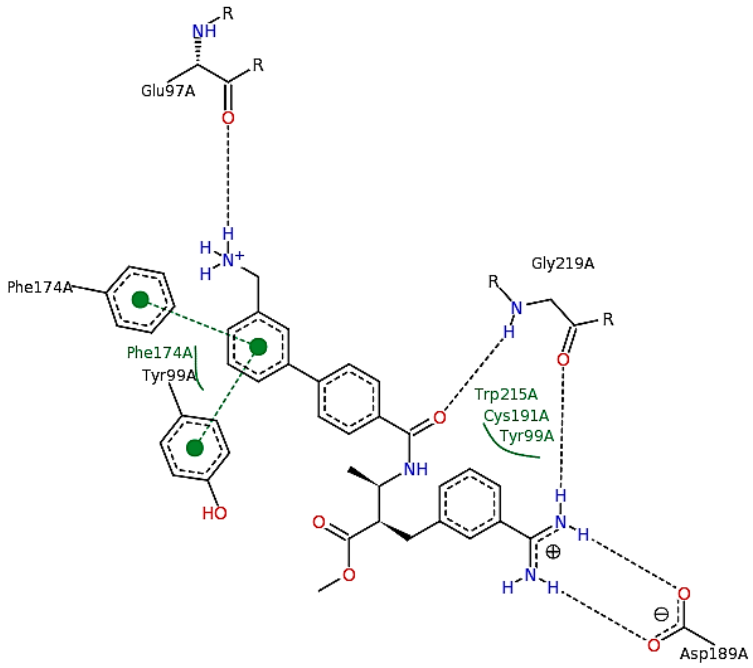

Figure 34: The binding mode of compound RPR128515 to FXa according to the X-ray crystal structure (PDB: 1EZQ). Black dashed lines indicate hydrogen bonds and salt bridges. Green dashed lines show π-π interactions. Source https://www.rcsb.org/pdb/explore/explore.do?structureId=1EZQ

4.8. Compounds with an amide or sulphonamide group at the P1-position

Compared to amines or amidines, amides are very weak bases. While the conjugate acid of an amine or an amidine has a pK_a of about 9 and 12, respectively, the conjugate acid of an amide has a pK_a around -0.5. The primary amine of the sulphonamide group, on the other hand, rendered acidic by the adjacent sulphonyl group. This makes the amide and sulphonamide containing molecules more favourable as drug candidates than those contain amine or amidine. Therefore, a series of compounds containing amide or sulphonamide group at the P1-position were synthesised and pharmacologically tested for inhibitory activity against FXIIa and FXa (Table 12).

Table 12: *In vitro* inhibitory activity of compounds containing amide or sulphonamide at the P1-position.

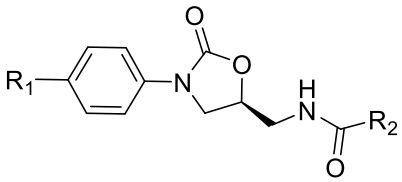

R_1=	R_2= 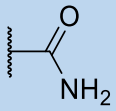	IC_{50} µM ±SD		SF	R_2= 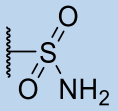	IC_{50} µM ±SD		SF
		FXIIa	FXa			FXIIa	FXa	
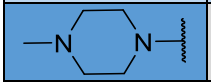	**w4**	12±4.50	118±16	9.83	**x4**	168±13	ia	na
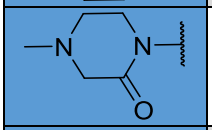	**w5**	75±0.50	86±20	1.15	**x5**	ia	113±12	na
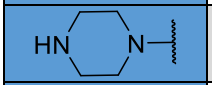	**w8**	0.16±0.05	33±3.0	206	**x8**	113±8.0	221±15	1.95
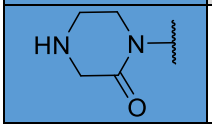	**w9**	44±6.0	0.08±0.0	0.002	**x9**	201±7.0	88±5.0	0.44

For comparison purposes, the molecules that have been chosen as P4-surrogate were methylpiperazine, methylpiperazinone, piperazine and piperazinone. The trend of inhibitory activity toward FXIIa and FXa was the same as noticed with previous compounds which have piperazine derivatives at the P4-position. The inhibitory potency of these compounds toward FXIIa was increased in this order: methylpiperazinone<methylpiperazine<piperazinone<piperazine. However, compounds with amide group at the P1-position were generally more active than compounds with any other group at this position apart from benzamidine. For example, compounds **w4, w5, w8,** and **w9**, with an amide group at the P1-position and methylpiperazine, methylpiperazinone, piperazine, and piperazinone at the P4-position, respectively, were more potent to FXIIa than their corresponding compounds **h4**, **h5**, **h8**, and **h9** with benzonitrile, and **y4**, **y5**, **y8**, and **y9** with amidoxime at the P1-position. On the other hand, Compounds with benzamidine at the P1-position were generally more active than their corresponding compounds with an amide group apart from

compound **z4** which is 3-fold less potent to FXIIa than **w4**. However, compounds with an amidine group at the P1-position were less selective to FXIIa than FXa than compounds with an amide group. For example, compound **z8,** which has an amidine group at the P1-position and piperazine moiety at the P4-position, was 14-fold less potent to FXa than FXIIa (SF= 14). On the other hand, compound **w8**, which preserve the piperazine at the P4-position and has an amide at the P1-position, was 206-fold less active against factor FXa than FXIIa (SF= 206). Therefore, compound **w8**, though its inhibitory potency toward FXIIa is still weak, it is considered to be selective to FXIIa.

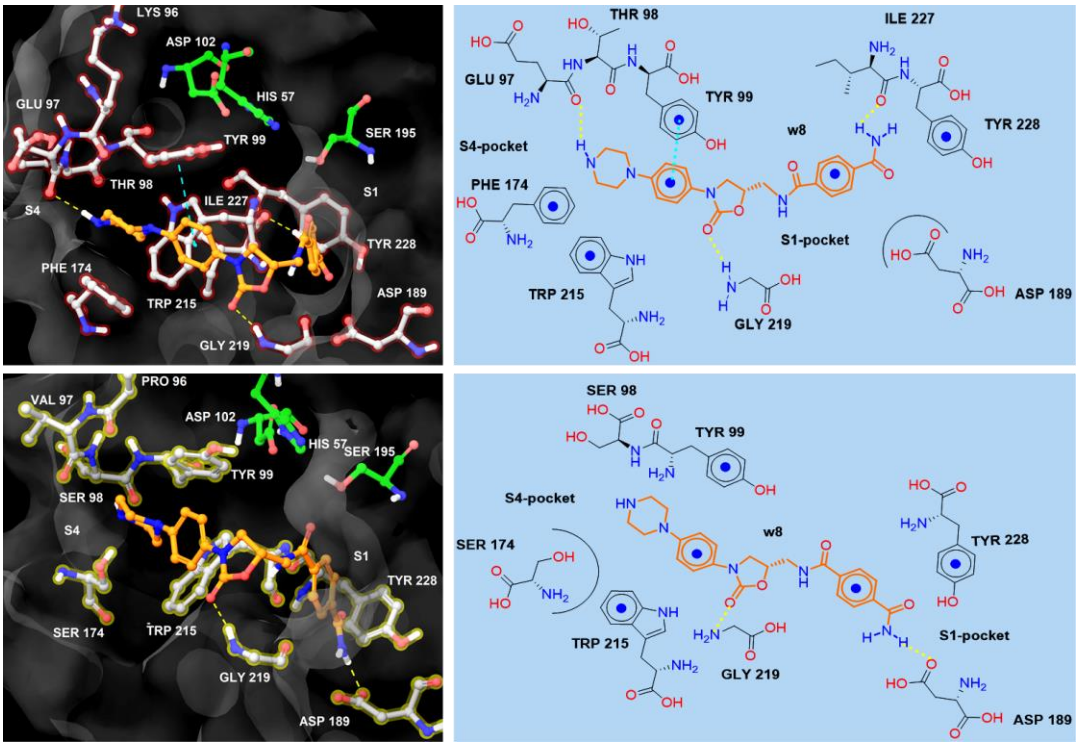

Figure 35: Compound **w8** docked to FXa (above) (PDB: 2w26); and to FXIIa (below). On the left side is the 2D-schematic representation of the binding modes. Only important residues at the S1- and S4- pocket were shown (yellow silhouetted: FXIIa residues; red silhouetted: FXa residues). Orange: carbon backbone of the docked compound; grey: carbon backbone of the enzyme's residues; light green: carbon backbone of the catalytic triad; blue: nitrogen; red: oxygen; yellow: sulfur; white: hydrogen; yellow dotted line: hydrogen bond; blue dotted line: π-π interaction.

Docking of compound **w8** to FXIIa-H and FXa showed that there were different interaction at the S1-positions of FXIIa and FXa (Figure 35). In FXIIa, the amide group forms a salt bridge with Asp189 residue. In contrast, the amide group forms hydrogen bonds with ILE-227 in the S1-pocket of FXa. At the S4-subpocket, it seems that compound **w8** has more contact in FXa than

in FXIIa. However, this compound was more active against FXIIa than FXa. In addition, it was selective to FXIIa more than FXa. This activity and selectivity can be explained in light of other results which suggest that compounds forming a salt bridge with aspartate residue at the bottom of the S1-pocket were more potent than other compounds missing such interaction (**z8** vs **h8**). Furthermore, compounds with Cl-π interaction with tyrosine residue at the bottom of the S1-pocket were much more active against FXa than FXIIa (for example **e1**). Additionally, given that the S4-pocket of FXa shaped by the aromatic rings of Tyr99, Trp215, and Phe174, compounds with more hydrophobic interaction at the S4-pocket were more potent against FXa than FXIIa, such as compounds **h1**, **y1**, and **z1**. These notions confirmed by comparing compounds **z8** and **w8**. Compound **z8** was 19-fold more potent against FXa than **w8.**

According to the docking studies, there were two main differences in the binding mode of compounds **z8** and **w8** in FXa. Compound **z8** forms a salt bridge with Asp189 at the S1-pocket through its amidine group and forms π-π stacking at the S4-pocket. On the other hand, compound **w8** deprived of such interactions. At FXIIa, both the amidine group and the amide group of the compounds **z8** and **w8**, respectively, forms hydrogen bond contact with aspartate residue at the bottom of the S1-pocket, but it seems that the P4-group of **w8** fit into the S4-pocket of FXIIa tighter than that of compound **z8**. This may explain the difference in the activity amongst compounds **z8** and **w8** against FXIIa (compound **z8** is 1.5-fold more active against FXIIa than **w8**).

As noticed earlier, inserting carbonyl group at piperazine moiety at the P4-position causes a significant drop in the activity toward FXIIa and a significant increase in the activity toward FXa. For example, compound **w9** was 275-fold less active against FXIIa, and it was 400-fold more potent to FXa than compound **w8**. On the other hand, introducing methyl group at the nitrogen atom of piperazine decrease the activity towards both enzymes (**w4** vs **w8**). Compound with methylpiperazinone (**w5**) at the P4-position was less potent against FXIIa and more potent against FXa than compound with methylpiperazine (**w4**).

Compounds with sulphonamide group at the P1-position was generally less active against both enzymes than their corresponding compounds with amide. Compound **x8** was 706-fold less potent against FXIIa than compound **w8**, and it was only 2-fold more potent against FXIIa than FXa. In addition, compounds with substituted piperazine at the P4-position show a similar trend of activity to other compounds against both enzymes.

Although the docking studies show that compound **x8** forms hydrogen bond contacts at the S1-position of FXIIa more than compound **w8**, it was anticipated that the significant drop of activity of this compound toward FXIIa was because of the lack of the salt bridge with aspartate residue at the bottom of this pocket. Moreover, this may also be true as a reason for the drop in the activity against FXa too, especially that the docking studies show no contact for this compound with S1-pocket of FXa (Figure 36).

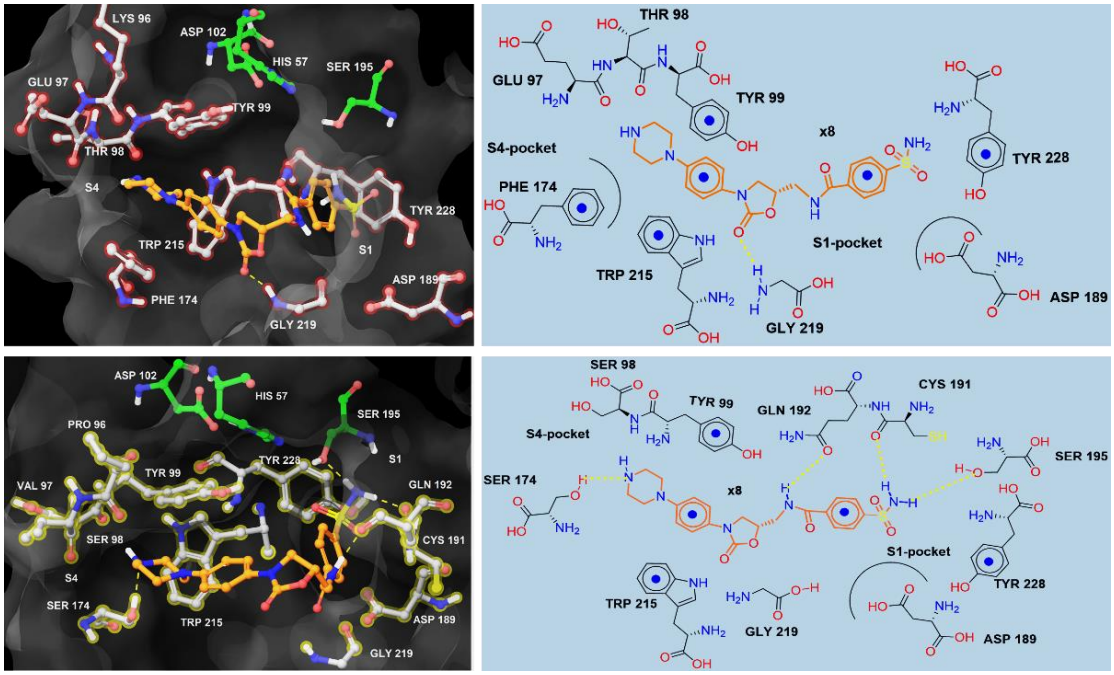

Figure 36: Compound **x8** docked to FXa (above) (PDB: 2w26); and to FXIIa (below). On the left side is the 2D-schematic representation of the binding modes. Only important residues at the S1- and S4- pocket were shown (yellow silhouetted: FXIIa residues; red silhouetted: FXa residues). Orange: carbon backbone of the docked compound; grey: carbon backbone of the enzyme's residues; light green: carbon backbone of the catalytic triad; blue: nitrogen; red: oxygen; yellow: sulfur; yellow dotted line: hydrogen bond; blue dotted line: π-π interaction.

In summary, the S1-pocket of FXIIa tolerate amide group at the P1-position more than sulphonamide. The amine of the amide group forms a salt bridge with the aspartate residue at the bottom of the S1-pocket of FXIIa. This

interaction mimics the natural substrate interaction at the S1-pocket. The inhibitory activity of the compounds against FXIIa increased significantly if the P1-position of the compound could form a salt bridge with Asp189. On the other hand, the activity of the compounds against FXa depends on two factors. Its ability to form Cl-π Interaction at the S1-pocket and to form π-π at the S4-position.

4.9. General Conclusion

The discovery and development of FXIIa inhibitors are of valuable interest for blood coagulation assays as well as for clinical applications for the treatment and prophylaxis of patients with thromboembolic diseases. However, the structural information of FXIIa that aid in the discovery of such inhibitors was scarce. Therefore, a homology model of FXIIa based on the crystal structure of its catalytic domain (PDB: 4XE4) and the crystal structure of FXa in complex with rivaroxaban (PDB: 2W26) was built at the start of this project. This homology model reveals that FXa and FXIIa share the same conformation of the binding site at the S1-subpocket. However, the S4-subpocket of both enzymes was shaped by different amino acids. Furthermore, it was found that rivaroxaban has a modest inhibitory activity against FXIIa. Therefore, rivaroxaban analogues with various groups at the P1- and P4-positions were synthesised to obtain compounds higher inhibitory activity and selectivity for FXIIa than FXa.

Although the binding sites of FXIIa and FXa were similar in most aspects, certain differences can be exploited to synthesise rivaroxaban analogue more potent and selective toward FXIIa than FXa.

As an early exploration, and to probe the effect of chirality on FXIIa inhibitory activity, rivaroxaban (**e1**) in it *S*- as well as *R*-conformation was synthesised and pharmacologically tested for inhibitory activity against FXIIa and FXa. Rivaroxaban in its *S*-conformation is selective FXa inhibitor. However, it has only modest inhibitory activity against FXIIa in vitro (IC_{50}= 77 µM). On the other hand, *R*-enantiomer of rivaroxaban was inactive against FXIIa and it is more than 3000-fold less active against FXa than the *S*-enantiomer. This confirms the initial docking studies that were done in this project. These

docking studies showed that both FXa and FXIIa binding sites are similar in most aspects especially at the S1-subpocket. It also showed that both enzymes tolerate *S*-enantiomers more than *R*-enantiomers.

Several closely related rivaroxaban analogues were then prepared and tested for pharmacological activity against FXIIa and FXa (**f1-i1)** and **(o1-v1**). Amongst these compounds only ones with an amine group at the P1-position shows an inhibitory potency against FXIIa, especially those with aniline (**p1**) and benzylamine (**v1**). Compounds with aniline (**p1**), cyclohexylmethylamine (**r1**), or benzylamine (**v1**) at the P1-position was more active against FXIIa than rivaroxaban. On the other hand, omitting the chlorine atom of a chlorothiophene moiety of rivaroxaban caused profound loss of inhibitory activity against FXa (**f1** vs **e1**) (see Scheme 19). Furthermore, compounds **p1, r1, t1** and **v1** were much less active against FXa than rivaroxaban, and this reflects the importance of the chlorothiophene moiety at the p1-position for the activity against FXa. From this set of compounds, it was learned that there was a trend of inhibitory activity against FXIIa. For instance, compound with benzylamine at the P1-position (**v1**) was more active than compound with aniline (**p1**), which in turn more potent than compound with cyclohexylmethylamine (**r1**), and at the bottom of the trend was compound with cyclohexylamine (**t1**).

The second set of compounds was prepared so that the chlorothiophene moiety was fixed at the P1-position and various groups were tried as P4-surrogate. Amongst this series of compounds, compound **e8** with piperazine group at the P4-position was 3-folds more potent than rivaroxaban against FXIIa. Also this compound was 500-fold less potent against FXa than rivaroxaban. Substitution of the piperazine moiety with methyl or carbonyl group decrease the activity against FXIIa. However, carbonyl group at position-2 of the piperazine group boosted the activity of the compound toward FXa (**e9** vs **e8**). These results were consistent with literature reported results of the importance of the carbonyl group for the activity against FXa.[273] The effect of piperazine derivatives at the P4-position on the inhibitory activity of FXa was further confirmed through the preparation of a series of compounds with *tert*-butylbenzene at the P1-position and various groups at the P4-positions

including substituted and unsubstituted piperazine group (Table 7). The only compound with unsubstituted piperazine shows activity against FXIIa though (**g8**). Furthermore, the effect of the amine group substitution at the P1-position was tested through the synthesis of compounds with morpholine at the P4-position and various groups at the P1-position including amine derivatives (Table 8). Compound **v2** with benzylamine at the P1-position was the most active compound against FXIIa amongst this series of compounds with an IC_{50} of 17 µM.

Two important structural features of FXIIa inhibitor have been extracted from the previous results, an amine derivative at the P1-position and piperazine derivative at the P4-position. Combining these two features, we obtained the compounds described in Table 9. Amongst these compounds, compound **v8** with piperazine at the P4-position and benzylamine at the P1-position was the most active compound against FXIIa with an *In vitro* IC_{50} of 0.18 µM. Interestingly, compound **v8** was 72-fold more potent against FXIIa than FXa.

To confirm the results that showed that an amine derivative at the P1-position and piperazine at the P4-position were the two structural requirements of FXIIa inhibitors, a series of compounds with nitrile, amidoxime, or amidine groups at the P1-position and piperazine derivatives at the P4-position were prepared (Table 11). Amongst this series of compounds, compound **z8,** with benzamidine group at the p1-position and piperazine at the P4-position, was the most active compound against FXIIa and it was 15-fold more potent against FXIIa than FXa. Compound **z8** was 1.5-fold more potent against FXIIa than compound **v8,** but it was less selective to FXIIa.

Compounds with amide or sulphonamide group at the P1-position were prepared in order to shift from the highly basic amidine group, which is not desirable as drug candidates, to more neutral groups at the P1-position. Sulphonamide group was not tolerated at this position by both enzymes. In addition, compounds with an amide group were less potent against both enzymes than their counterparts with an amidine group. However, the drop in the activity was more noticeable against FXa than FXIIa. Therefore, we obtain compound **w8** with an in vitro IC_{50} value of 0.16 µM against FXIIa and 33 µM

against FXa. This means that compound **w8** was 206-fold more selective to FXIIa than FXa (Scheme 19).

Docking studies showed that FXa inhibitory activity depends mainly on hydrophobic interactions at the S1- and S4-subpockets. Compounds deprived of the Cl-π interactions at the S1-pocket and/or π-π stacking at the S4-pocket were always less potent against FXa than compounds that can make such interactions. However, the S4-pocket of FXIIa shaped by less hydrophobic residues than that of FXa. The inhibitory potency against FXIIa depends mainly on electrostatic interaction with Asp189 residue at the bottom of the S1-pocket. Although compound **w8** does not meet my objective which was to synthesise FXIIa inhibitor with an IC_{50} between 1-30 nM, it can be considered as a starting point to synthesise more potent inhibitors.

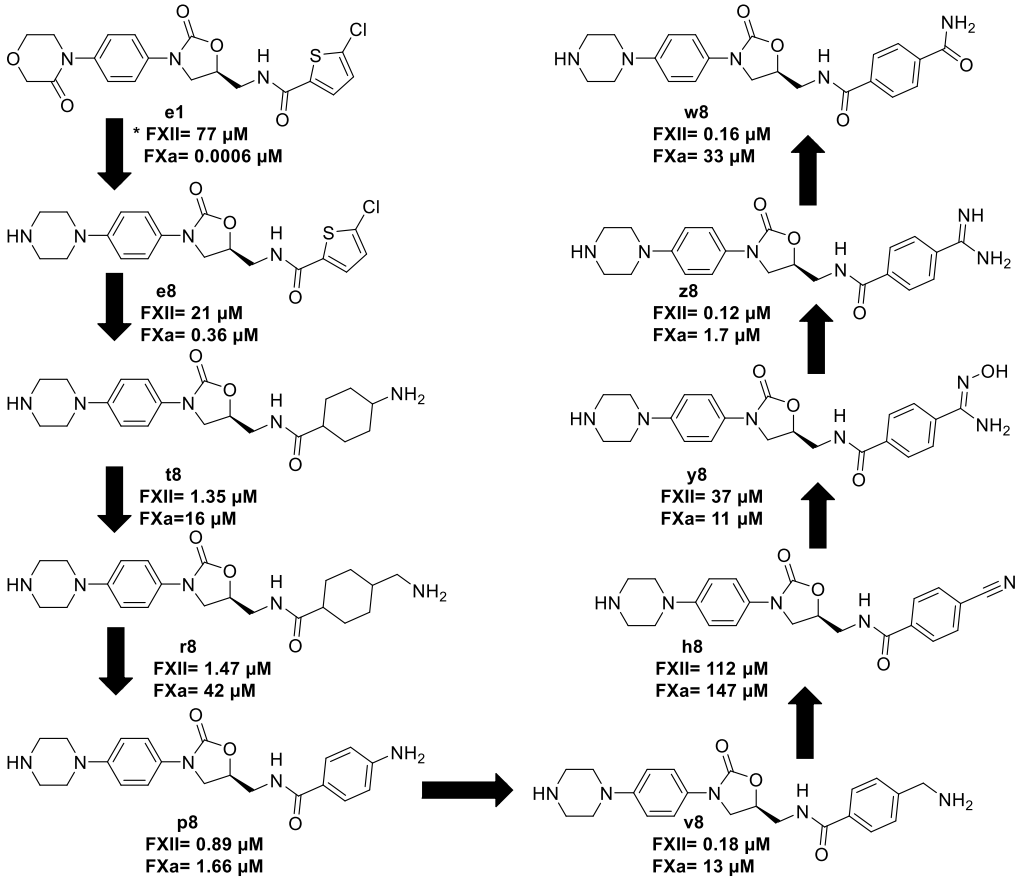

Scheme 19: Major changes that lead to the discovery of compound **w8** and the effect of these changes on the activity against FXIIa and FXa. *IC_{50}.

4.10. Future work

4.10.1. Chemistry

The main objective of this study was to design and synthesise FXIIa inhibitors with a FXIIa IC_{50} < 100 nM and have at least 100-fold selectivity for FXIIa compared to other closely related serine proteases. Compound **w8** was 206-fold more potent against FXIIa than FXa. However, it has an IC_{50} value against FXIIa of 0.16 µM in *in vitro* enzymatic assay. Therefore, compound **w8** is about one order of magnitude from where it needs to be. Hence, the chemistry part of this project could be continued through modification of compound **w8** in an attempt to increase its potency against, and selectivity for FXIIa

Figure 37 shows the potential sites for modification of compound **w8**. Ring A, which represents the P1-position of the molecule, is benzamide group in compound **w8**. By comparing compounds **h8**, **y8**, and **z8** (see Table 11), which have nitrile, amidoxime, and amidine groups at P1-position, respectively, the inhibitory activity against FXIIa appears to be increased with increasing basicity of the P1-groups. However compound **w8** which has carboxamide group at P1-position, which cannot be ionised at physiological conditions, is just 1.33-fold less potent against FXIIa than compound **z8**, which has an amidine group. Moreover, **w8** is more selective to FXIIa than **z8**. Further decrease in the basicity of the P1-group (e.g. compound **x8**, which has the sulphonamide group at P1-position) leads to a significant drop in the activity against FXIIa. Therefore, it seems that the S1-position of FXIIa tolerates groups at the P1-position of the inhibitors according to their ionisation state. Therefore, to explore the effect of varying the basicity and the ability to form H-bonds of the groups at the P1-position of the inhibitors on the inhibitory potency against FXIIa and FXa, various groups with different pK_a values can be tried at P1-position of the inhibitors, as shown in Figure 37. The synthetic starting materials containing these groups could be purchased from commercial sources as acyl chloride or carboxylic acid derivative and introduced into the compounds according to the procedure shown in Scheme 4.

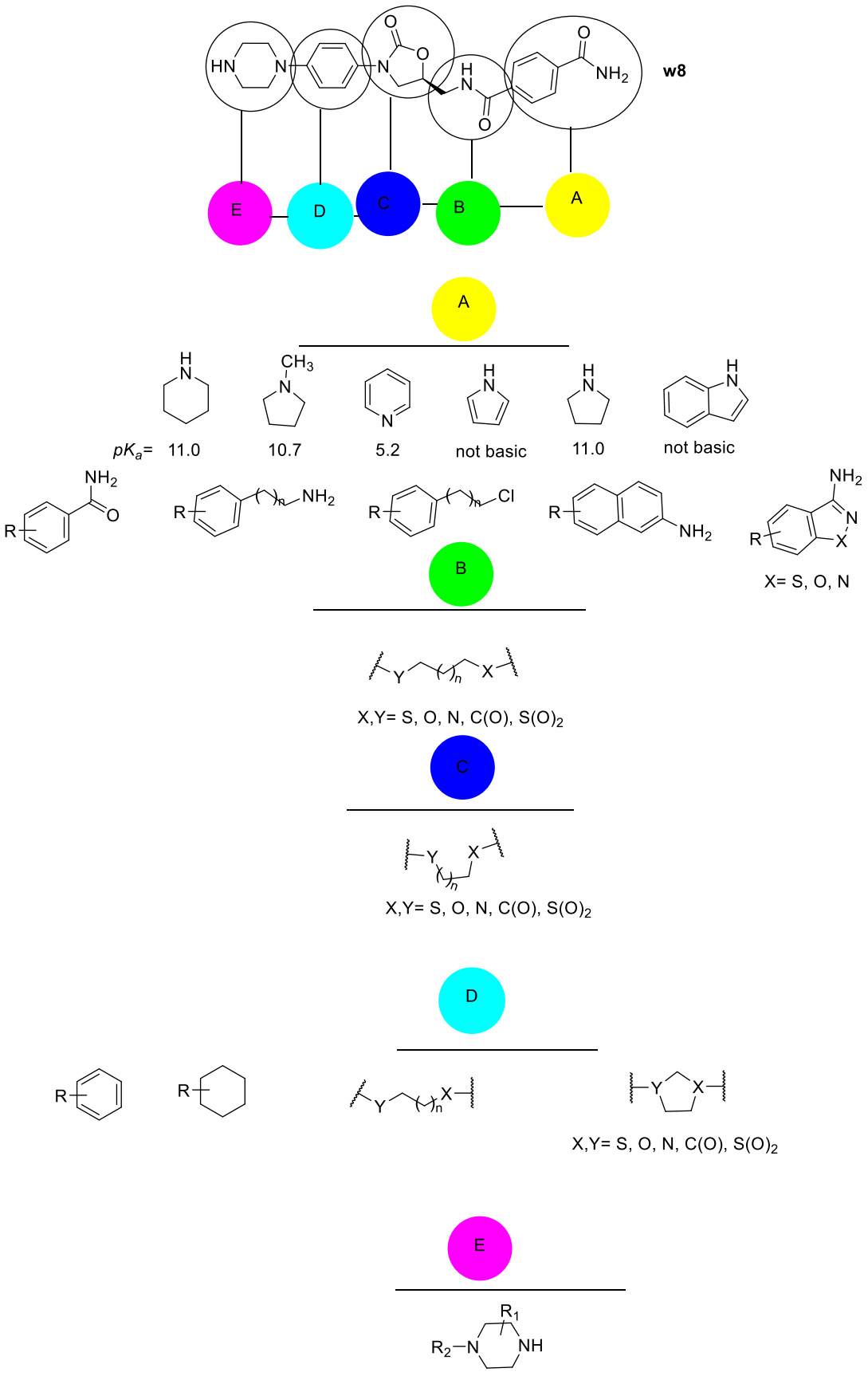

Figure 37: Future work suggestion to amend compound **w8**.

The amide group at the P1-position could be hydrolysed into carboxyl group in the body.[338] Therefore, a compound with a carboxyl group at p1-position could be synthesised and tested for any potential inhibitory activity against FXIIa. The effect of the conversion of the primary amide group at the P1-position of compound **w8** into secondary or tertiary amide should also be considered. Moreover, in an attempt to improve the inhibitory activity of compound **w8** against FXIIa, various groups at P1-position could be tried as shown in Figure 37. For example, the linker between the terminal amine and the aromatic ring can be of varying length. Additionally, the terminal amine group can be replaced with chlorine atom or other halogens. Furthermore, the effect of the substitution of the aromatic ring at the P1-position could be experimented with, too.

As shown in Figure 35, compound **w8** docked to the FXIIa-H model showed that the amide linker between the oxazolidinone core and the benzamide group at the P1-position does not participate in any polar interaction with the enzyme. Therefore, the effect of replacing of this linker (ring B in Figure 37) with various groups on the inhibitory activity against FXIIa should be tested. Additionally, the effect of opening the oxazolidinone core of the compound and substituting it with various groups should be tried as shown in Figure 37.

As explained earlier, the high binding affinity of rivaroxaban to FXa seems to be dependent on three key features. These features are the two hydrogen bonds between rivaroxaban and Gly219 residue of the enzyme, the co-planar conformation between the aryl ring and the oxazolidinone core, and the Cl-π interaction between the thiophene moiety and Tyr228 residue.[267,285] In an attempt to synthesise compounds with higher binding affinity to FXa than rivaroxaban and with an improved pharmacokinetic profile, Tao Xue *et al.* bridged the benzene ring and oxazolidinone ring by an additional linker to form a novel [6,6,5] tricyclic fused oxazolidinone scaffold to maintain this preferred conformation.[339] The result of this work was promising because the researcher obtained compound **79** (Scheme 20), a highly potent, selective, direct, and orally bioavailable FXa inhibitor with excellent in vivo antithrombotic efficacy and preferable pharmacokinetic profiles. Therefore, this work can be reproduced with compound **w8** giving that the docking

studies show that this compound takes the 'L-shape' orientation in FXIIa and that the oxazolidinone core forms a hydrogen bond with Gly219 residue of FXIIa (Figure 35).

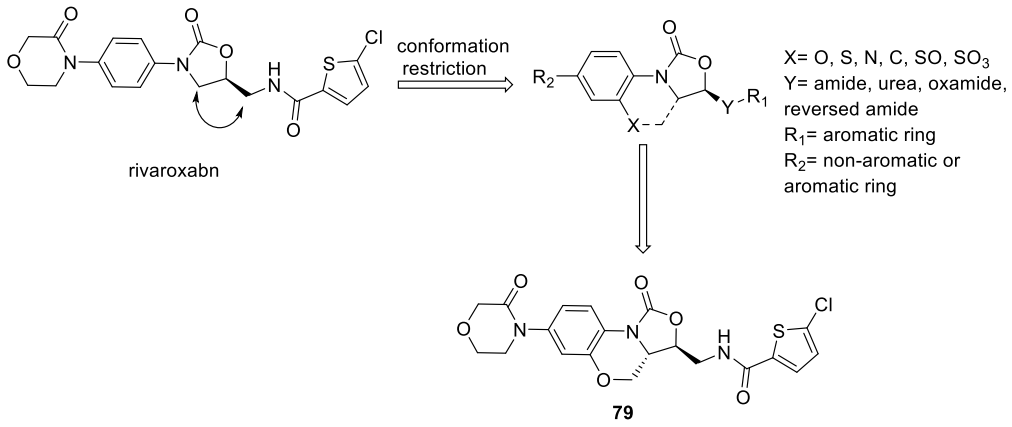

Scheme 20: Formation of [6,6,5] tricyclic fused oxazolidinone scaffold by Tao Xue et al. to obtain a compound with higher binding affinity to FXa than rivaroxaban. [339]

Compound **w8** could be amended in the same manner to obtain a series of conformationally restricted mimics containing [6,6,5] tricyclic fused oxazolidinone scaffold. The same route described for the synthesis of compound **79** can be adopted to synthesis **w8** analogues with [6,6,5] tricyclic fused oxazolidinone scaffold with minor modifications as explained in

Scheme 21, with the key intermediate **80** can be synthesised using the published procedure.[340]

The co-planar conformation between the aryl ring and oxazolidinone core of rivaroxaban has an indispensable effect on maintaining its high binding affinity to FXa. If the co-planar conformation is disturbed into an unfavourable twist arrangement by introducing a substitution at the 2-position of the aryl ring, then the activity against FXa decreases sharply.[267] However, as discussed in the previous section, the co-planarity between the aromatic ring and the group at the P4-position of FXIIa inhibitors seems to have a negative effect on the inhibitory potency of the compounds against FXIIa (e.g. comparing compounds **w8** and **w9**, Table 12). Therefore, various groups could be introduced into the aryl ring of compound **w8** (ring D in Figure 37) in an attempt to decrease its potency against FXa and hence increase the selectivity for FXIIa. One of the suggested substitutions is putting fluorine atom at

position-2 of the aryl ring. It is known from rivaroxaban discovery that compound with a fluorine atom at this position (compound **34** in Table 2) was 2-fold less active against FXa than rivaroxaban.[267] Moreover, fluorine atom can be substituted on the piperazine ring (ring E in Figure 37), so it can improve the pharmacokinetic properties of the compound through perturbation of the *pKa* of the compound.[341] In addition fluorine can contribute to the efficiency of drugs in many ways such as modulation of lipophilicity, metabolic stability, and hydrogen bonding and electrostatic interactions (for the importance of fluorine in medicinal chemistry see references 341 and 342).[341,342]

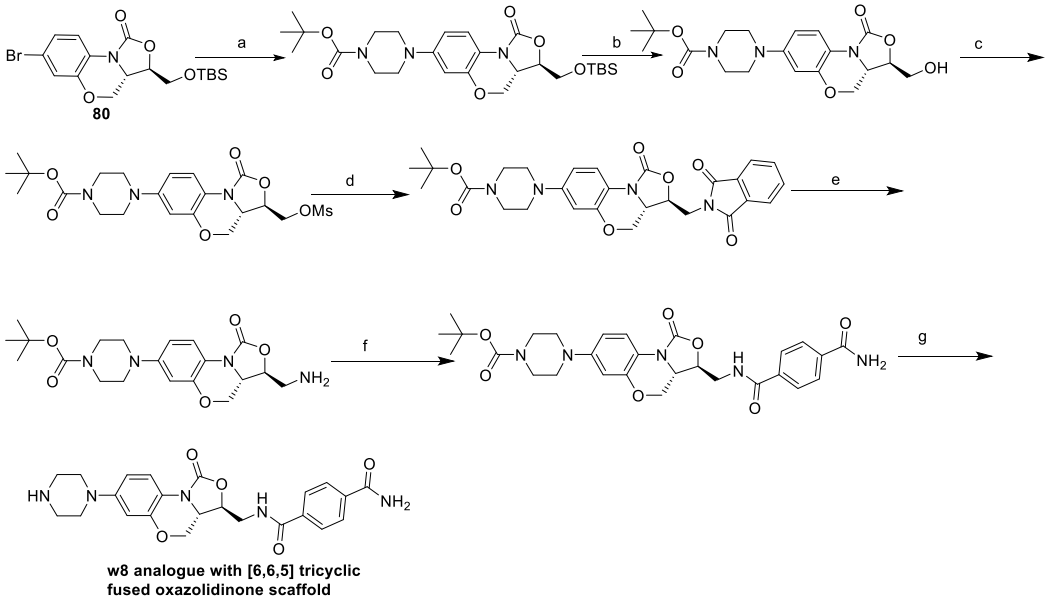

Scheme 21: synthesis of **w8** analogue with [6,6,5] tricyclic fused oxazolidinone scaffold. Reagents and conditions: (a) 1-Boc-piperazine, $Pd_2(dba)_3$, Xantphos, Cs_2CO_3, 1,4-dioxane, reflux for 20 h; (b) TBAF (Tetra-n-butylammonium fluoride), THF, 0 °C to room temp, 3 h; (c) MsCl, Et_3N, DMF, 0 °C to room temp, 2 h; (d) potassium phthalimide, DMF, 80 °C, 8 h; (e) MeNH2, EtOH, reflux, 5 h; (f) 4-carbamoylbenzoic acid, HBTU, DCM, TEA, 3-12 h; (g) concentrated HCl in dioxane, rt, 5h.

The piperazine group at the P4-position of compound **w8** is highly prone to bioactivation inside the body to electrophilic iminium ions and/or carbinolamines. These products could be decomposed via N-dealkylation and might react with nucleophilic sites within cellular macromolecules and contribute to the pharmacology or toxicology of aliphatic amines.[343,344] Therefore, to attenuate the extent for the formation of iminium species,

piperazine group can be modified by introducing steric hindrance on the aryl ring or on the piperazine group itself or installing alkyl or halogen groups on the piperazine ring. Moreover, to minimise oxidation of the piperazine nitrogen and the formation of a reactive iminium moiety, piperazine can be replaced by other heterocycles that are not prone to iminium formation (for example, lactams).

4.10.2. *In vitro* inhibitory activity toward other serine proteases:

In the current project, the synthesised compounds were tested for *in vitro* inhibitory activity toward FXIIa and FXa only. Given the structural similarities between serine protease in general and coagulation factor specifically, it is essential to test the synthesised compounds for the inhibitory activity toward other structurally related serine proteases, for example, thrombin, FVIIa, FXIa, FIXa, plasmin, kallikrein, tPA, uPA, HGFA, and trypsin. Many UV- or fluorescence-based approaches can be used to measure serine proteases activity. However, the fluorescence-based methods have been widely used in assays for proteases and other drug targets mainly because of their high sensitivity.[345]

The effect of compound **w8** on prothrombinase activity could be measured through prothrombinase-induced clotting time assay as described in the literature.[346] prothrombinase-induced clotting time assay was one of the tests performed during the preclinical development of rivaroxaban.[347] Therefore, **w8** could be substituted for rivaroxaban in this test to see whether **w8** has any inhibitory activity against FXa or thrombin. This test is sensitive to FXa and thrombin inhibitors. Therefore, the selectivity of **w8** could be confirmed by performing this test.

4.10.3. Coagulation assays

Activated partial thromboplastin time (aPTT) and prothrombin time (PT) could be evaluated for compound **w8** in human or animal plasma to determine its *in vitro* anticoagulant activity. PT measures the effect of the compound on the extrinsic pathway of coagulation, whereas aPTT represents the effect on the intrinsic pathway. These tests could be performed using commercially

available kits according to the procedure described in the literature.[339] Clotting times could be measured in a coagulometer according to the manufacturer instruction.

4.10.4. *In vivo* studies: arteriovenous shunt model

The antithrombotic effect of compound **w8** or other anticipated FXIIa inhibitors could be determined in an AV shunt in anesthetised rats as described in the literature.[348] Briefly, The right common carotid artery and the left jugular vein is cannulated with two 100 mm-long, saline-filled, polyethylene catheters. Then, The catheters are connected with a 30 mm-long polyethylene tube containing a rough nylon thread (40 mm × 0.15 mm), folded to create a 20 mm-long double string. The test compound is dissolved in polyethylene glycol/ water/glycerol (996 g/100 g/60 g) and given by intravenous bolus injection into a tail vein 10 min before thrombus induction. Alternatively, the test compound is dissolved in solutol/ethanol/water (40%/10%/50% [v/v/v]) and administered orally 90 min before thrombus induction. The shunt is opened for 15 min, and the nylon thread that covered with the thrombus is then withdrawn and weighed. Blood samples are withdrawn from the carotid artery just after thrombus removal.

Other *in vivo* tests that could be performed to evaluate the antithrombotic efficacy and bleeding risk of compound **w8** and other anticipated FXIIa inhibitors include: rat tail-bleeding model, rabbit ear-bleeding model, $FeCl_3$-induced venous thrombosis in rats, electrically induced rat carotid artery thrombosis. The detailed procedure for each of these tests was explained in the literature.[267,339]

4.10.5. Determination of the solubility, permeability and absorption of the test compounds:

Solubility is one of the important parameters to achieve the desired concentration of drug in systemic circulation for a desired pharmacological response. Low aqueous solubility is the major problem encountered with formulation development of new chemical entities as well as for the generic

development.[349] There are many experimental and computational approaches to estimate solubility and permeability of drug candidates.

In the discovery setting, 'the rule of 5' predicts that poor absorption or permeation is more likely when there are more than 5 H-bond donors, 10 H-bond acceptors, the molecular weight is greater than 500 and the calculated Log P (CLogP) is greater than 5. Compound **w8** fulfil the drug-likeness rules: 3 H-bond donors; 6 H-bond acceptors; the molecular weight is 423; and CLogP is 0.88. However, the solubility of compound **w8** and other anticipated FXIIa inhibitors should be calculated experimentally according to the methods explained in the literature.[350]

To predict the suitability of compound **w8** and other anticipated FXIIa inhibitors for oral administration, permeability coefficients across monolayers of the human colon carcinoma cell line Caco-2, cultured on permeable supports could be assessed. According to the literature, this method is used to trace the permeability of a test compound in two directions, from the apical to the basolateral side or vice versa, and both passive and active transport processes could be studied.[351]

4.10.6. Metabolism

It is an important part of the drug discovery to predict toxicities of the drug candidates and to minimise the bioactivation liabilities as early as in the stage of drug discovery and lead optimisation. Therefore, the measurement of covalent binding levels of compound **w8** or other anticipated FXIIa inhibitors to liver microsomal proteins could be experimented *in vitro* as well as *in vivo* studies using animal models.

If the radiolabelled drug required for the exact mass balance studies, the previously reported synthesis of compound **w8** (see Scheme 4) could be taken as an approach for the synthesis of carbon-14 labelled **w8** using 4-carbamoyl[^{14}C]benzoic acid, which could be purchased from commercial sources, in the final step.

The *in vitro* biotransformation of compound **w8** could be assessed by measurement of covalent binding to liver microsomal proteins in the presence

and the absence of NADPH, as well as the use of trapping agents such as glutathione or cyanide ions to provide structural information on reactive intermediates.[344,352] These in vitro experiments could be enforced with *in vivo* covalent binding studies in animal models, such as rats or rabbits.[353]

In summary, many *in vitro* and *in vivo* experiments could be performed on compound **w8** and other anticipated FXIIa inhibitors in the preclinical stage of this study. The procedures and techniques for all of these experiments are detailed in the literature. In addition to these experiments, the obtaining of a high-resolution X-ray crystal structure of FXIIa in complex with one of its inhibitors would be of a valuable asset for this project.

Chapter 5: Experimental section

5.1. Materials and instrumentation

All chemical substances were purchased from Sigma Aldrich, Alfa Aesar, VWR International, Flourochem, and Fisher Scientific. They are used in reactions without further purifications. Solvents were purchased from Fisher (England), VWR (England), Sigma-Aldrich Company Ltd (England), and Cambridge Isotope Laboratories Inc (England) and they are either analytical or HPLC grade. Thin layer chromatography (TLC) plates were supplied by Merck. Flash liquid chromatography (flash-LC) cartridges were supplied by Biotage (Cardiff, Wales).

Unless otherwise stated, reactions were carried out under inert nitrogen gas at room temperature. LC-MS and TLC on commercially available pre-coated aluminium and silica-backed plates (Merck Kieselgel 60 F254) were used to monitor the reactions. Several dyes were used for staining such as ninhydrin (solution in ethanol), $KMnO_4$ or phosphomolybdic acid (PMA). The visualisation was done by examination under UV light (254 and 366 nm). All organic extracts after aqueous workup procedures were dried over Na_2SO_4 before gravity filtering and evaporation to dryness. Organic solvents were evaporated *in vacuo* at $\leq 40°C$ (water bath temperature) using a rotary evaporator.

An Isolera, Flash master III system was used for flash chromatography. Analytical LC-MS was performed using a Shimadzu UFLCXR system coupled to an Applied Biosystems API2000 mass spectrometer. The column by default used was Phenomenex Gemini-NX 3µm-110 A C18, 50x2 mm at a flow rate of 0.5 mL/min. UV detection was recorded at 220 (channel2) and 254 nm (channel1). Short gradient: Pre-equilibration run for one min at 5% B; then: 5 to 98% solvent B in 2min, 98% B for 2 min, 98 to 10% B in 0.5min then 10% for one min. Solvent A: 0.1% formic acid in water; solvent B: 0.1% formic acid in MeCN.

Melting points (Mp) were recorded on a Reichert 7905 apparatus or Perkin Elmer Pyris 1 differential scanning calorimeter and are uncorrected. Literature

melting points obtained from research papers found using chemical structure searching computer software, such as Sci-Finder Scholar and Reaxys. Where no literature melting points are supplied, no compound data or melting point information was available for that compound synthesised. Proton nuclear magnetic resonance (^{1}H NMR) spectra were recorded on a Bruker-AV 400 instrument at 400.13 MHz, and ^{13}C NMR spectra were recorded at 101.62 MHz. Chemical shifts (δ) are in parts per million (ppm) with reference to the chemical shift of the deuterated solvent or the internal standard tetramethylsilane (TMS). Coupling constants (*J*) are in Hz and multiplicities are given by singlet (s), doublet (d), triplet (t), quartet (q), multiplet (m), doublet of doublets (dd).

High-resolution mass spectrum (HRMS) – a time of flight, electrospray (TOF ES +/-) were recorded on a Waters 2795 separation module/Micromass LCT platform and calibrated to within +/- 10 ppm with theoretical mass values provided for comparison. The specific rotation was recorded on ADP220 polarimeter, Bellingham and Stanley Limited.

5.2. Half-maximal inhibitory concentration (IC_{50}) assay

The half maximal inhibitory concentration (IC_{50}) of the synthesised compounds against FXIIa and FXa was carried out according to the following procedure (the protocol for the *in vitro* assay of FXIIa and FXa activity was set by Dr James Awford of the University of Nottingham):

Materials:

PBS tablets (oxoid BR0014G), Tween 20 (Sigma P1379), DMSO (sigma 276855. 99.9%). Human αFXIIa, Human βFXIIa, Human FXa (Enzyme Research Laboratories), Pro-Phe-Arg-7AMC (Sigma P9273), PPACK dihydrochloride (D-Phe-Pro-Arg-CMK, Calbiochem or Autogen Bioclear (Source Bioscience cat ABE4144)), Boc-Ile-Glu-Gly-Arg-7-amido-4-methylcoumarin hydrochloride **(**Boc-Ile-Glu-Gly-Arg-7AMC, B9936, Calbiochem).

Equipment:

Polypropylene centrifuge tubes (Griener 188261 and 227270), 15 mL and 50 mL), 96 well propylene plates (Greiner 651201), solid white polystyrene flat bottom 384 well plates (Griener 781075), plate reader (EnVision 2014 Multiple Reader s/n 1040131, Perkin Elmer), Pipettes (single channel Gilson and 8 channel Matrix pipettes)

Procedure:

1. Preparation of stock solutions:

1.1 Preparation of buffer

Ten tablets of BPS (5 in each 50ml propylene centrifuge tube) were dissolved in 50 mL of distilled water and shaken an automated shaker until dissolve. Once dissolved, the 100 mL of PBS was made to 1 L with distilled water. The buffer was stored at room temperature and used within a week of its preparation date.

1.2 Preparation of 1% (w/v) Tween 20 PBS

Tween 20 (0.100 g) was added to PBS (9.9 mL) in a centrifuge tube (15 mL). The tube was then rolled for approximately 20 minutes. This solution was stored at 4 °C and used within two weeks of its preparation.

2. Preparation of enzymes

2.1 Preparation of enzyme buffer (0.03% (v/v) Tween PBS)

Tween 20 PBS (1% (w/v), 1.5 mL) and the PBS buffer solution (48.5 mL) were added into centrifuge tube (50 mL). This enzyme buffer was prepared daily.

2.2 αFXIIa

Lyophilised αFXIIa (0.5 mg/vial) was dissolved in enzyme buffer (0.03%(v/v) Tween 20 PBS, 625 µL) and rolling for approximately 20 minutes to give 0.8 mg/ml. αFXIIa enzyme was then aliquoted in 24 µL volumes and stored at -80 °C. In a time of the test, an aliquot of αFXIIa (24 µL) was thawed, pulsed in a microcentrifuge, and made to 1.2 ng/µL with 16 mL 0.03% (v/v) Tween 20 PBS buffer.

2.3 βFXIIa

Lyophilised βFXIIa (0.1 mg/vial) was dissolved in enzyme buffer (0.03%(v/v) Tween 20 PBS, 250 µL) and rolling for approximately 20 minutes to give 0.4 mg/ml. βFXIIa enzyme was then aliquoted in 18 µL volumes and stored at -80 °C. In a time of the test, an aliquot of βFXIIa (18 µL) was thawed, pulsed in a microcentrifuge, and made to 0.45 ng/µL with 16 mL 0.03% (v/v) Tween 20 PBS buffer.

2.4 FXa

Lyophilised FXa (0.8 mg/vial) was dissolved in enzyme buffer (0.03%(v/v) Tween 20 PBS, 800 µL) and rolling for approximately 20 minutes to give 1 mg/ml. FXa enzyme was then aliquoted in 20 µL volumes and stored at -80 °C. In a time of the test, an aliquot of FXa (10 µL) was thawed, pulsed in a microcentrifuge, and made to 0.69 ng/µL with 14.48 mL of 0.03% (v/v) Tween 20 PBS buffer.

3. Preparation of substrates

3.1 FXIIa substrate

The substrate (25 mg, MW 575.66 g/mol) was made to 20 mM in DMSO (2.17 mL), then aliquoted to 50 µL and stored at -20 °C. AT the time of the test, one aliquot of the substrate (50 µL, 20 mM), was thawed and made to 33.324 mL with PBS buffer (33.274 ml).

3.2 FXa substrate

The substrate (2 mg, MW 730.8 g/mol) was made to 20 mM in DMSO (348 µL), then aliquoted to 20 µL and stored at -20 °C. At the time of the test, one aliquot of the substrate (20 µL, 20 mM), was thawed and made to 13.33 mL with PBS buffer (13.31 mL). The concentration of stock was 30 µM.

4. Preparation of the standard control (PPACK)

PPACK (5 mg) was made to 10 mM by dissolving it in DMSO (954 µL), then aliquoted in 20 µL volumes and stored at -20 °C. At the time of the test 10 µL of PPACK was made to 1 mM by dilution with 90 µL of DMSO.

5. Preparation of test compounds

Test compounds were prepared by first made the compound to a concentration of 10 mM by dissolving it in DMSO. Second, we made a serial dilution of the test compounds in DMSO first, then in PBS buffer.

For serial dilution in DMSO, 37 µL of the test compound (10 mM) and PPACK (1 mM) was mixed with 80 µL of DMSO; then seven serial dilutions were made with 80 µL of DMSO (dilution factor= 3.16).

A second serial dilution step was made with 6 µL of the test compound or PPACK from each concentration of the previous step and 194 µL of PBS so that the dilution factor will be 33.33. This generates curves with a top working concentration of 300 µM for the test compound and 0.0300 µM for PPACK. If any of the compounds were showed to be very active (this was noticed with rivaroxaban and some other compounds tested against FXa) and the curve did not define by any point in the first round of the test, the serial dilution of the compound continues until it was certain that more than one point will define the curve.

6. Combine of the substrate, test compounds and enzymes

The substrate (10 µl) was added first to each well of 384-well plates. Then, PPACK and the test compounds (10 µl) were added to the same wells in triplicate. Finally, the enzyme (10 µL) was added to the wells as soon as possible. After that, the 384-well plate was placed on a plate shaker for 30 seconds before the Relative Fluorescence Units (RFU) reading for initial time point (T1) at 380/460 nm with triplicate read. The plate then incubated in a dark place for 2.5 hours for FXIIa and 1 h for FXa. Finally, the reading for the final time point (T_{end}) was recorded in triplicate too.

7. IC_{50} data calculation

IC_{50} curves were plotted in excel. The mean for the triplicate RFU data reads at T1 and T_{end} calculated separately. Plate background (Bg) RFU at T1 was subtracted from both T1 RFU and T_{end} RFU, then T1 RFU was subtracted from T_{end} RFU to give RFU change per well over 2.5 hours for FXIIa and 1 hour for FXa. The T_{end} RFU background was not deducted from the T_{end} plate

reading to ensure that the background had not changed over the incubation period. The (T_{end} - T1 Bg) – (T1-T1 Bg) data was copied into the IC_{50} sheet tab in excel, and the mean of the triplicate compound wells RFU read was calculated and IC_{50} curves plotted.

This RFU data was copied into GraphPad Prism (GraphPad Prism version 7.00 for Windows, GraphPad Software, La Jolla California USA, www.graphpad.com) for IC_{50} determination. The curves were all constrained to fit through zero RFU unless this was not possible. Where precipitation, fluorescence or colour interferences were suspected, the data points were removed as necessary, and if required the Hill slope was constrained to one to allow a curve fit. In practice, this meant some IC_{50} values were only defined by one point with the Hill Slope constrained to one. A repeat test for each compound against all three enzymes (αFXIIa, βFXIIa, and FXa) was performed regardless of the IC_{50} value. If the IC_{50} was not defined by any point because the compound was so potent against the enzyme, the serial dilution was increased until it was certian that the curve will be defined by more than one point (as the case with compound **e1** against FXa). The IC_{50} data of all tested compounds was almost the same against αFXIIa and βFXIIa. Therefore, the data that had been shown here was those for the tested compounds against αFXIIa.

5.3. Modelling experiments

In this study, all computational analysis was carried out on Linux workstation on high-performance computers (HPC), Genuine Intel (R) Core (TM) i7-3820 CPU @ 3.60 Hz 83601 MHz x86-64. The operation system is CentOS release 6.5 (Final), system type: OEGstone DX79SI, serial number: P1103083575, location: CBS A32. The X-ray structure of FXa in complex with rivaroxaban (PDB ID: 2w26) and the X-ray structure of FXIIa serine protease domain (PDB ID: 4XE4) was obtained from the protein data bank. The Schrödinger suits 2014-4: Bioluminate, version 1.9, Schrödinger, LLC, New York, NY, 2015 was used for this purpose. For the docking studies, crystal structures were further prepared by protein preparation wizard which is available in Schrodinger release 2015-2, maestro, version 10.2, Schrodinger LLC, New

York, NY, 2015 and Schrödinger Release 2016-2: Maestro, Schrödinger, LLC, New York, NY, 2016. The protein preparation facility was used to add hydrogen, create zero-order bonds to metal, create disulfide bonds, and delete water molecules beyond 5 Å from hetero groups. The average root mean square deviation of the heavy atoms was minimised until 3 Å. Similarly, the ionisation, stereoisomers, and generation of low energy ring conformations of all compounds were done by using ligand preparation wizard in maestro. The Grid generation was performed using Grid-based ligand docking available in Small-molecule drug discovery suit 2015-2 Glide, version 6.7, Schrodinger LLC, New York, NY, 2015 and Schrödinger Release 2016-2: Glide, Schrödinger, LLC, New York, NY, 2016. The Van der Waals radii of the protein were scaled to 1 and the partial charge cut off for polarity at 0.25. For FXa a grid box with coordinate X= 7.899, Y= 5.104, Z= 21.501 was generated at the centroid of the active site for docking. The active site was defined with 10 Å around the ligand present in the crystal structure. The active centre for FXIIa was determined by the following residues His57, Tyr99, Asp102, Ser195, Ser174, Trp215, Gly219, and Tyr228. A grid centre was generated at the centroid of the active centre with coordinate X= 14,122, Y=8.514, Z= 21.705.

5.4. General procedures

5.4.1. General procedure A:

This procedure was used for the synthesis of compounds illustrated in Scheme 4, and it includes five steps:

Step 1:

Scenario 1: To one equivalent of the desired substituted aniline (**Ia-g**) in ethanol/water (9:1) (5 mL for each mmol of the starting material) was added one equivalent of 2-{[(2S)-oxiran-2-yl]methyl}-1H-isoindole-1,3(2H)-dione (**35**). The mixture was refluxed at 87 °C for 14 h. The product started to precipitate from the solution slowly, or it began to participate when the reaction was stopped, and DEE was added. The precipitate was filtered and washed with diethyl ether three times. Then the precipitate was dissolved in

MeOH. MeOH was added and heated until a brown solution was formed with the appearance of undissolved yellow precipitate (impurity). The precipitate was filtered and washed with MeOH. The filtrate (the desired product) was evaporated *in vacuo,* and the resulting powder was dried *in vacuo* to afford the pure target compound.

Scenario 2: To one equivalent of the desired substituted aniline (**Ia-g**) in ethanol/water (9:1) (5 mL for each mmol of the starting material) was added one equivalent of **35**. The mixture was refluxed at 87 °C for 14 h. The reaction mixture then allowed to cool to an ambient temperature and concentrated *in vacuo.* The pure product then obtained by purification through flash-LC using the gradient of MeOH/DCM solvent.

Step 2:

Scenario 1: To one equivalent of the desired product from step 1 suspended in anhydrous THF (9 mL for every 1 mmol of the starting material) under nitrogen, was added two equivalent of CDI (N,N'-carbonyldiimidazole) and a catalytic amount of 4-(dimethylamino)pyridine. The reaction mixture was stirred at 60 °C for 14 h. Then a second portion of CDI (2 eq.) was added, and the reaction mixture was stirred for another 14 h. The precipitate was filtered and washed with THF. The filtrate was evaporated *in vacuo*, and then MeOH was added with heating and continuous stirring. The mixture was left to cool, and the resulting precipitate was filtered and washed with MeOH. MeOH was also added to the precipitate from the first filtration step and heated with continuous stirring until a clear solution was formed. Then the mixture was left to cool. This leads to the formation of a yellow precipitate (the desired product). The precipitate was filtered and washed with MeOH. The precipitates then combined and dried *in vacuo* to afford the pure desired product

Scenario 2: To one equivalent of the desired product from step 1 suspended in anhydrous THF (9 mL for every 1 mmol of the starting material) under nitrogen was added two equivalent of CDI (N,N'-carbonyldiimidazole) and a catalytic amount of 4-(dimethylamino)pyridine. The reaction mixture was stirred at 60 °C for 14 h. Then a second portion of CDI (2 eq.) was added, and

the reaction mixture was stirred for another 14 h. The reaction mixture was allowed to cool to an ambient temperature and concentrated *in vacuo.* The resulting residue was purified by flash-LC using the gradient of DCM/MeOH or EtOAc/ether to afford the pure desired compound.

Step 3a:

Scenario 1: Methylamine (40% in water, 13 equivalent) was added to a suspension of the desired compound from step 2 (1equivalent) in ethanol (10 mL for every 1mmol of the starting material), and the reaction mixture was refluxed for 3h. The reaction mixture was allowed to cool to an ambient temperature and concentrated *in vacuo.* The pure desired compound was obtained by purification by flash-LC using the gradient of 1N NH_3 in MeOH/DCM.

Scenario 2: Methylamine (40% in water, 13 equivalent) was added to a suspension of the desired compound from step 2 (1equivalent) in ethanol (10 mL for every 1mmol of the starting material). The reaction mixture was refluxed for 3h and evaporated *in vacuo*. The reaction mixture was allowed to cool to an ambient temperature and concentrated *in vacuo.* The resulting residue was dissolved in DCM. Then the organic layer was washed with 5% aqueous HCl solution three times. The aqueous layer was collected and basified by the addition of NaOH solution and then washed with DCM three times. The organic layer was collected, and the solvent evaporated *in vacuo* to afford the desired product.

Step 3b: To the suspension of the desired compound from step 2 (1 equivalent) in ethanol (10 mL for every 1mmol of the starting material), hydrazine (20 equivalent) was added. The mixture was stirred for 3 h at 87 °C. The reaction was stopped, and the reaction mixture was evaporated *in vacuo*. The crude material was then purified by Flash-LC using gradients of 1N NH_3 in MeOH/DCM to afford the desired pure compound.

Step 3c: The desired product obtained from step 2 was dissolved in 2-propanol/water (6:1) solvent (9 mL for every 1mmol of the starting material), then 5-equivalent of sodium borohydride was added with continuous stirring for 12-24 h at room temperature. If TLC indicates complete consumption of

starting material, 18-equivalent of glacial acetic acid was added carefully. After that, the reaction flask stoppered, and the reaction mixture stirred at 80 °C for 2-6 h. Then 5% aqueous NaOH solution was added, and the crude mixture extracted with DCM. The organic layer was collected and purified with flash- using gradients of 1N NH_3/DCM in MeOH to afford the desired pure compound.

Step 4:

Scenario 1: a suspension of the desired product from step 3 (1 eq.) was made in dichloromethane (DCM) (10 mL for every 1mmol of the starting material) under nitrogen and at 0 °C. Then (1 eq.) of Hunig's base was added. After that, the desired acyl chloride (1.2 eq.) was added slowly. The mixture was left to warm to room temperature and then stirred for 3 h. The reaction was stopped, and 10 mL of water was added and extracted with 10 mL DCM (3 times). The organic phase was washed with brine, dried on sodium sulphate, and then concentrated *in vacuo*, and purified by flash-LC using the gradient of DCM/MeOH, DCM/1N NH_3 in MeOH, or ethyl acetate/diethyl ether to afford the desired pure compound.

Scenario 2: A desired carboxylic acid (1 eq.) was dissolved in DCM (8 mL for every 1mmol of the starting material) before adding TEA (2 eq.). Then, HBTU (1.2 eq.) was added, and the reaction mixture was stirred for 30 minutes at room temperature. One equivalent of the desired compound from step 3 was added with continuous stirring. The reaction mixture was stirred at room temperature for 14 h. The reaction was stopped, and water was added, and the crude product extracted from DCM. The organic layer was collected, washed with brine, and dried over Na_2SO_4. The solvent was evaporated *in vacuo*, and the resulting residue was further purified by flash-LC using the gradient of DCM/MeOH.

Step 5:

Scenario 1: A desired Boc-protected compound from step 5 was dissolved in dioxane and treated with access of 4M HCl in dioxane. The reaction mixture was stirred for 6-12 h. The solvent was removed *in vacuo*, and the hydrochloric acid salt of the desired compounds was then obtained by

recrystallisation from DCM. The resulting solid was then dissolved in a saturated solution of Na_2CO_3 or $NaHCO_3$. Then an organic solvent was added, and the free base then extracted into the organic layer. The organic layer then collected, washed with brine solution and dried over sodium sulphate. The solvent was removed under vacuum to obtain the desired product.

Senario2: A desired Boc-protected compound from step 5 was dissolved in dioxane and treated with access of 4M HCl in dioxane. The reaction mixture was stirred for 6-12 h. The solvent was removed *in vacuo*, and the hydrochloric acid salt of the desired compound was obtained by recrystallisation from DCM. The resulting solid was then suspended in DCM with continuous stirring at room temperature. After that Amberlyst® A21 dried by stirring with THF was added and the mixture was stirred for 3-6 h. The Amberlyst® A21 was then removed by filtration, and the filtrate was condensed under high vacuum to get the free amine compound.

5.4.2. General procedure B

This procedure was used for the synthesis of compounds **y1-y9** and **z1-z9,** and it includes 4 steps.

Step 1: hydroxylamine hydrochloride (2 eq.) was dissolved in ethanol, then TEA was added with vigorous stirring at 80 °C. After that, the desired benzonitrile compound (1 eq.) was added, and the reaction mixture was stirred at 80 °C for 14-24 h. The solution was cooled, and the solvent was removed in *vacuo*, and the residue was suspended with water and extracted with DCM. The organic layer then collected, washed with brine solution and dried over sodium sulphate. The solvent was then removed *in vacuo* and the resulting residue then purified by flash-LC using the gradient of DCM/MeOH to obtain the desired product.

Step 2: The desired Boc-protected compound from step 1 was dissolved in dioxane and treated with access of 4M HCl in dioxane. The reaction mixture was stirred for 6-12 h. The solvent was removed *in vacuo*, and the resulting residue was dissolved in ethyl acetate or DCM before adding a saturated solution of Na_2CO_3, and the free base then extracted into the organic layer. The

organic layer then collected, washed with brine solution and dried over sodium sulphate. The solvent was removed under vacuum to obtain the desired product.

Step 3: The desired amidoxime derivative from step 1 (1 equivalent) was dissolved in a mixture of glacial AcOH and potassium formate solution in MeOH (10 equivalent), followed by the addition of 10% Pd/C. The mixture was stirred at r.t. until the reaction was complete based on TLC and/or LC/MS (the reactions completed in 24-48 h). The solids were filtered, washed with MeOH, and the filtrate was evaporated. The residue was dissolved in anhydrous EtOH and 5 M HCl in anhydrous EtOH (12 eq.) was then added. The solids were filtered, washed with anhydrous EtOH and the filtrate was evaporated to yield pure amidine hydrochloride.

Step 4

Scenario 1: A desired Boc-protected compound from step 3 was dissolved in dioxane and treated with access of 4M HCl in dioxane. The reaction mixture was stirred for 6-12 h. The solvent was removed *in vacuo*, and the resulting residue was dissolved in ethyl acetate or DCM before adding a saturated solution of Na_2CO_3, and the free base then extracted into the organic layer. The organic layer was washed with brine solution and dried over sodium sulphate. The solvent was removed *in vacuo* to afford the pure desired product.

Scenario 2: A desired Boc-protected compound from step 3 was dissolved in dioxane and treated with access of 4M HCl in dioxane. The reaction mixture was stirred for 6-12 h. The solvent was removed *in vacuo*, and the resulting residue was dissolved in DCM with continuous stirring at room temperature. After that Amberlyst® A21 dried by stirring with THF was added and the mixture was stirred for 3-6 h. The Amberlyst® A21 was then removed by filtration, and the filtrate was condensed under high vacuum to get the free amine compound.

5.4.3. General procedure C

This procedure was used for the synthesis of compounds **e10-e16 and g10-g16**. Compound **e3** or **g3** (1 equivalent) was suspended in dioxane/water (10:1)

in a microwave tube. The desired boronate Pinacol esters (2 equivalent), $Pd_2(dba)_3$ (10%), and Na_2CO_3 (3 equivalent) was added to the reaction mixture. The reaction mixture was then heated in microwave at 110 °C for 2 h. After that, the crude material was filtered on celite and washed with ethyl acetate. The filtrate was then extracted with saturated sodium bicarbonate solution three times. The organic layer was washed with brine solution and dried over sodium sulphate. The crude product was then purified by flash-LC using the gradient of ethyl acetate/DEE to afford the pure desired compound.

5.4.4. General procedure D

This procedure was used for the synthesis of compounds e**17** and **g17,** and it includes 8 steps.

Step 1: The commercially available methyl 3-amino-1H-1,2,4-triazole-5-carboxylate (1.420 g, 10 mmol, 1 eq.) and 2-benzofuran-1,3-dione (phthalic anhydride) (1.480 g, 10 mmol, 1eq.) were suspended in 20 ml of dioxane and heated at 120°C for 48h. After the reaction mixture was cooled down at room temperature, the resulting precipitate was filtered, and the cake was washed with water then EtOAc to obtain the intended compound as a colourless solid.

Step 2: The product from step 1 (1 eq.) was dissolved in DMF before adding 2-(Trimethylsilyl)ethoxymethyl chloride (SEMCl) (1eq.) and NaH (1.1 equivalent). The reaction mixture was stirred at 50 °C for 12 h. The reaction was stopped, and the solvent was removed under high pressure. The pure desired compound was obtained by purification through flash-LC using DCM/MeOH gradient.

Step3: Methylamine (40% in water, 13 eq.) was added to a suspension of the desired compound from step 2 (1 eq.) in ethanol, and the reaction mixture was refluxed for 8h. The reaction mixture was allowed to cool to an ambient temperature and concentrated *in vacuo.* The pure desired compound was obtained by purification by flash-LC using the gradient of DCM/ 1M NH_3 in MeOH.

Step4: To one equivalent of the desired product of step 3 in ethanol/water (9:1) was added one equivalent of 2-{[(2S)-oxiran-2-yl]methyl}-1H-isoindole-

1,3(2H)-dione. The mixture was refluxed at 87 °C for 14 h. Then another one equivalent of 2-{[(2S)-oxiran-2-yl]methyl}-1H-isoindole-1,3(2H)-dione was added, and the reaction mixture was refluxed for another 14 h. The reaction mixture then allowed to cool to an ambient temperature and concentrated *in vacuo.* The pure product then obtained by purification through flash-LC using the gradient of DCM/MeOH solvent.

Step 5: To one equivalent of the desired product of step 1 suspended in anhydrous THF under nitrogen was added two equivalents of CDI (N,N'-carbonyldiimidazole) and a catalytic amount of 4-(dimethylamino)pyridine. The reaction mixture was stirred at 60 °C for 14 h. Then a second portion of CDI (2 eq.) was added, and the reaction mixture was stirred for another 14 h. The reaction mixture was allowed to cool to an ambient temperature and concentrated *in vacuo.* The resulting residue was purified by flash-LC using the gradient of DCM/MeOH to afford the pure desired compound.

Step 6: Methylamine (40% in water, 13 equivalent) was added to a suspension of the desired compound from step 5 (1equivalent) in ethanol, and the reaction mixture was refluxed for 8h. The reaction mixture was allowed to cool to an ambient temperature and concentrated *in vacuo.* The pure desired compound was obtained by purification by flash-LC using the gradient of DCM/ 1M NH_3 in MeOH.

Step 7: A suspension of the desired product from step 6 (1equivalent) was made in dichloromethane (DCM) under nitrogen and at 0 °C. Then (1 equivalent) of Hunig's base was added. After that, the desired acyl chloride (1.2 equivalent) was added slowly. The mixture was left to warm to room temperature and then stirred for 3 h. The reaction was stopped, and 10 ml of water was added and extracted with 10 ml DCM (3 times). The organic phase was washed with brine, dried on sodium sulphate, and then concentrated *in vacuo* and purified by flash LC using gradient using the gradient of DCM/1M NH_3 in MeOH to afford the desired pure compound.

Step 8: The desired product from step 7 was dissolved in dioxane and treated with access of 4M HCl in dioxane. The reaction mixture was stirred for 14 h. The solvent was removed *in vacuo,* and the resulting residue was dissolved in

DCM before adding a saturated solution of Na_2CO_3, and the free base then extracted into the organic layer. The organic layer then collected, washed with brine solution and dried over sodium sulphate. The solvent was removed under vacuum to obtain the desired product.

5.4.5. General procedure E

This procedure was used for the synthesis of compounds **e18-e31**, and it includes 5 steps.

Step 1: The commercially available (*R*)-epichlorohydrin (1 equivalent) was added dropwise over 30 minutes to a mixture of sodium cyanate (2 equivalent) and magnesium sulphate (0.2 eq.) in water at 60 °C. The mixture was stirred for 5 h. Then water was removed under high vacuum, and ethyl acetate was added, then the mixture was filtered, and the filter cake washed with ethyl acetate (x2). Finally, the combined ethyl acetate fractions were combined, washed with brine, dried over Na_2SO_4 and concentrated *in vacuo* to afford the desired compound.

Step 2: A solution of the product of step 1 (1equivalent) and potassium phthalimide (1.1 equivalent) in DMF was heated to 80 °C for 12 h. The reaction was cooled to ambient temperature, diluted with water and extracted with DCM (×3), the combined organic layer was washed with brine solution and then dried over Na_2SO_4. The solution was evaporated in vacuo the solvent was evaporated under vacuum and the residue extracted from ethyl acetate/petroleum ether to give the desired compound.

Step 3

Scenario 1: The desired product of step 2 was dissolved in anhydrous dioxane in Schlenk tube. Then 1 equivalent of the desired bromine derivative, 5 mmol % of CuI, 10 mol% (1*R*,2*R*)-cyclohexane-1,2-diamine, and 2 equivalents of K_2CO_3 were added under nitrogen gas. The reaction mixture was purged with nitrogen gas for 5 minutes before it was refluxed for 14 h with continuous stirring. After that, the reaction was stopped and allowed cool to ambient temperature. The solvent was removed *in vacuo,* and the targeted compound was obtained by purification by flash-LC using the gradient of DCM/MeOH.

Scenario 2: The desired product of step 2 was dissolved in DMF before adding 2 equivalents of the desired iodo compound. The resulting solution was cooled to 0 °C. Sodium hydride (2 eq.) was added followed by additional DMF solvent. The reaction then allowed to warm to room temperature, and stirred for 6-14 h. The solvent was removed under high pressure, and the resulting residue was dissolved in ethyl acetate. Water was added, and the organic layer was collected, washed with brine, dried over sodium sulphate, filtered and concentrated under reduced pressure. The resulting residue was purified by flash-LC using the gradient of DCM/MeOH.

Step 4: Methylamine (40% in water, 13 equivalent) was added to a suspension of the desired compound from step 3 (1equivalent) in ethanol, and the reaction mixture was refluxed for 3h. The reaction mixture was allowed to cool to an ambient temperature and concentrated *in vacuo.* The pure desired compound was obtained by purification by flash-LC using the gradient of DCM/ 1M NH_3 in MeOH.

Step 5: A suspension of the desired product from step 4 (1equivalent) was made in dichloromethane (DCM) under nitrogen and at 0 °C. Then (1 equivalent) of Hunig's base was added. After that, the desired acyl chloride (1.2 equivalent) was added slowly. The mixture was left to warm to room temperature and then stirred for 3 h. The reaction was stopped, and 10 ml of water was added and extracted with 10 ml DCM (3 times). The organic phase was washed with brine, dried on sodium sulphate, and then concentrated *in vacuo* and purified by flash LC using gradient using the gradient of DCM/ MeOH to afford the desired pure compound.

5.4.6. General procedure F

This procedure was used to synthesise the starting materials **a5, a6, a7**.

Step 1:

The commercially available piperazine (13 mmol, 1.110 g, 1 eq.) or piperazin-2-one (12.5 mmol, 1.25 g, 1 eq.) was suspended in anhydrous DCM (62 mL) and then di-*tert*-butyl dicarbonate (1 eq.) was added at 0 °C. The reaction mixture then stirred at room temperature for 14 h. during this time a

homogeneous solution was formed. The solvent was evaporated under vacuum to afford the compounds *tert*-butyl piperazine-1-carboxylate or *tert*-butyl-3-oxopiperazine-1-carboxylate, respectively, which has been used in the next reaction without further purification.

Step 2:

Compounds obtained from step 1 or the commercially available 4-methylpiperazin-2-one (1eq) was dissolved in anhydrous dioxane (5 mL for every 1 mmol of the starting material) in Schlenk tube. Then 1-equivalent of Iodoaniline, 5 mmol % of CuI, 10 mol% (1*R*,2*R*)-cyclohexane-1,2-diamine, and 2-equivalents of K_2CO_3 were added under nitrogen gas. The reaction was achieved in an oxygen-free environment, and the mixture was purged with nitrogen gas for 5 minutes before it was refluxed for 14 h with continuous stirring. After that, the reaction was stopped and allowed to be cooled to ambient temperature. The solvent was removed *in vacuo,* and the target compounds were obtained by purification of the crude product by flash-LC using gradients of 1N NH_3 in MeOH/DCM solvents.

5.5. Synthesis

2-{(2*R*)-2-hydroxy-3-[4-(3-oxomorpholin-4-yl)anilino]propyl}-1*H*-isoindole-1,3(2*H*)-dione (b1)

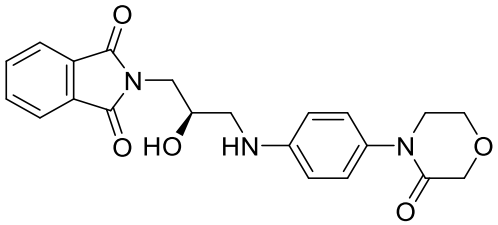

This compound was synthesised according to the general procedure A-step 1-scenario 1, by reacting the commercially available 4-(4-aminophenyl)morpholin-3-one **a1** (2.703 g, 14 mmol) with **35** (2.852 g, 14 mmol). The title compound (4.811 g, 12.24 mmol, 87% yield) was obtained as a white powder. MS: m/z calculated for $C_{21}H_{22}N_3O_4^+$ 396.1553 $[M+H]^+$, MS: found 396.1572. HPLC: t_R 2.29 (95%). Mp: 215 ˚C. $[\alpha]^{22}_D$ = 6° (c= 1, DMSO) (lit. Mp= 214 °C, $[\alpha]^{25}_D$ = 6.24° (c= 1, DMSO)).[354] ^{1}H NMR (DMSO-*d*$_6$): 7.90-7.81 (m, 4H), 7.02 (d, *J*= 8.8 Hz, 2H), 6.63 (d, *J*= 8.8 Hz, 2H), 5.66 (t, *J*= 5.9 Hz, 1H), 5.17 (d, *J*= 5.2 Hz, 1H), 4.14 (s, 2H), 4.10 (q, *J*= 5.5 Hz, 1H),3.97-4.07 (m, 1H), 3.99-3.90 (m, 2H), 3.71-3.57 (m, 4H), 3.07-2.99 (m,1H). ^{13}C NMR (DMSO-*d*$_6$): 168.55, 166.24, 147.93, 134.71, 132.28, 130.83, 126.92, 123.38, 112.49, 68.22, 66.81, 64.04, 50.08, 47.92, 42.88.

2-({(5*S*)-2-oxo-3-[4-(3-oxomorpholin-4-yl)phenyl]-1,3-oxazolidin-5-yl}methyl)-1*H*-isoindole-1,3(2*H*)-dione (c1)

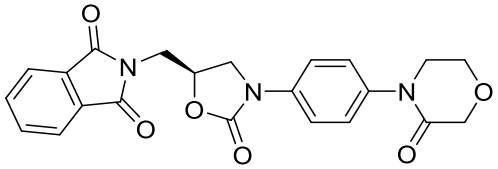

This compound was synthesised according to the general procedure A-step 2-scenario 1 starting with **b1** (3.953 g, 10 mmol). The title compound (2.989 g, 7.10 mmol, 71% yield)) was obtained as a white powder. MS: m/z calculated for $C_{22}H_{20}N_3O_6^+$ 422.1346 $[M+H]^+$, MS: found 422.1359 $[M+H]^+$. HPLC: t_R 2.39 (89%). Mp: 221 ˚C. $[\alpha]_D^{22}$= 75° (c= 1, DMSO) (lit. Mp= 223 °C, $[\alpha]^{25}_D$ = 75.26° (c= 1, DMSO)).[354] ^{1}H NMR (DMSO-*d*$_6$): 7.94-7.82 (m, 4H), 7.52 (d, *J*= 8.8 Hz, 2H), 7.40 (d, *J*= 8.8 Hz, 2H), 5.00-4.89 (m, 1H), 4.22 (t, *J*= 8.8 Hz, 1H), 4.19 (s, 2H), 4.05-3.87 (m, 5H), 3.75-3.65 (m, 2H). ^{13}C NMR (DMSO-*d*$_6$): 168.28, 166.44, 154.29, 137.62, 136.87, 135.07, 131.98, 126.42, 123.71, 118.8, 70.52, 68.20, 63.94, 49.48, 49.06, 48.28.

(*S*)-4-(4-(5-(aminomethyl)-2-oxooxazolidin-3-yl)phenyl)morpholin-3-one (d1)

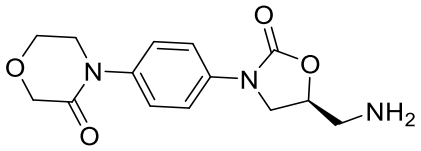

This compound was synthesised according to the general procedure A-step 3a-scenario 1sarting with **c1** (2.561 g, 6.0 mmol). The title compound (1.222 g, 4.25 mmol, 70% yield) was obtained as a white powder. MS: m/z calculated for $C_{14}H_{18}N_3O_4^+$ 292.1291 $[M+H]^+$, MS: found 292.1304 $[M+H]^+$. HPLC: t_R 0.56 min (92%). Mp: 150 °C (lit. Mp= 148.3-149.8 °C).[355] $[\alpha]^{23}_D$= - 41° (c= 1, DMSO). ^{1}H NMR (DMSO-d6): δ 7.58 (d, J= 9.1 Hz, 2H), 7.42 (d, J= 9.1 Hz, 2H), 4.69-4.61 (m, 1H), 4.20 (s, 2H), 4.09 (t, J= 8.7 Hz, 1H), 3.95 (dd, J= 5.3 Hz, 3.7 Hz, 2H), 3.88 (dd, J = 8.9 Hz, 6.4 Hz, 1H), 3.72 (dd, J = 5.3 Hz, 3.7 Hz, 2H), 3.17 (s, 1H), 2.90-2.80 (m, 2H), 2.54 (s, 1H). 13C NMR (DMSO-d6): δ 166.43, 145.85, 137.38, 137.19, 126.40, 118.67, 74.00, 68.20, 63.95, 49.50, 47.53, 44.42.

5-chloro-*N*-({(5*S*)-2-oxo-3-[4-(3-oxomorpholin-4-yl)phenyl]-1,3-oxazolidin-5-yl}methyl)thiophene-2-carboxamide (e1)

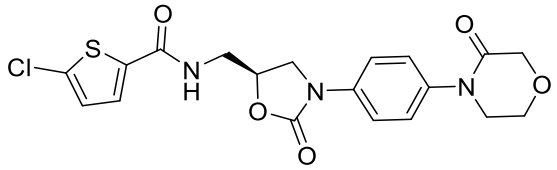

This compound was synthesised according to the general procedure A-step 4-scenario 1 by reacting **d1** (0.121 g, 0.41 mmol) with the commercially available 5-chlorothiophene-2-carbonyl chloride (0.089 g, 0.5 mmol). The title compound (0.128 g, 0.29 mmol, 72% yield) was obtained as a white powder. MS: m/z calculated for $C_{19}H_{19}ClN_3O_5S^+$ 436.0728 $[M+H]^+$, MS: found 436.0742 $[M+H]^+$. HPLC: t_R 2.45 (97%). Mp: 228 °C. $[\alpha]^{21}$D= -36° (c= 1, DMSO) (lit. Mp= 229-230 °C, $[\alpha]^{23}_D$ = -38° (c= 1, DMSO)).[356] ^{1}H NMR (DMSO-*d6*): 9.01 (t, J= 5.8 Hz, 1H), 7.73 (d, J=4.1 Hz, 1H), 7.59 (d, J=9.0 Hz, 2H), 7.46 (d, J= 9.0, 2H), 7.24 (d, J= 4.1 Hz, 1H), 4.92-4.84 (m, 1H), 4.23 (t, J= 10.3 Hz, 3H), 4.03-3.99 (m, 2H), 3.89 (dd, J= 9.2 Hz, 6.1 Hz, 1H), 3.78-373 (m, 2H), 3.65 (t, J= 5.3 Hz, 2H). ^{13}C NMR (DMSO-*d6*): δ 166.43, 161.27, 154.57, 138.92, 137.55, 136.96, 133.73, 128.92, 128.62, 126.24, 118.82, 71.79, 68.20, 63.94, 49.48, 47.91, 42.68.

_N_-({(5_S_)-2-oxo-3-[4-(3-oxomorpholin-4-yl)phenyl]-1,3-oxazolidin-5-yl}methyl)thiophene-2-carboxamide (f1)

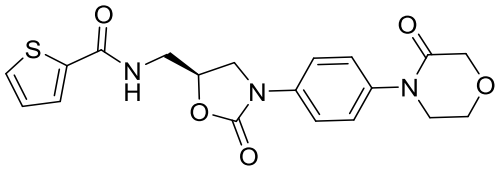

This compound was synthesised according to the general procedure A-step 4-scenario 1 by reacting **d1** (0.116 g, 0.4 mmol) with thiophene-2-carbonyl chloride (0.070 g, 0.48 mmol). The title compound (0.129 g, 0.32 mmol, 81% yield) was obtained as a white powder. MS: m/z calculated for $C_{19}H_{20}N_3O_5S^+$ 402.1118 $[M+H]^+$, MS: found 402.1134 $[M+H]^+$. HPLC: t_R 2.23 (97%). Mp: 206 ° C (lit. Mp= 202.2-205.2 °C).[357] $[\alpha]^{22}D$ = -63° (c= 1, DMSO). ^1H NMR (DMSO-*d6*): δ 8.91 (t, J= 5.8 Hz, 1H), 7.84 (d, J= 3.5 Hz, 2H), 7.81 (d, J= 5.0 Hz, 1H), 7.59 (d, J=8.9 Hz, 2H), 7.45 (d, J= 8.9 Hz, 2H), 4.90-4.81 (m, 1H), 4.23 (t, J= 8.3 Hz, 3H), 4.03-3.98 (m, 2H), 3.89 (dd, J= 9.0 Hz, 6.0 Hz, 1H), 3.75 (t, J= 5.5 Hz, 2H), 3.66 (t, J= 5.5 Hz, 2H). ^{13}C NMR (DMSO-*d6*): δ 166.43, 162.27, 154.60, 139.78, 137.54, 136. 98, 131.57, 128.97, 128.40, 126.41, 118.83, 71.83, 68.20, 63.94, 49.48, 47.94, 42.66.

4-*tert*-butyl-*N*-({(5*S*)-2-oxo-3-[4-(3-oxomorpholin-4-yl)phenyl]-1,3-oxazolidin-5-yl}methyl)benzamide (g1)

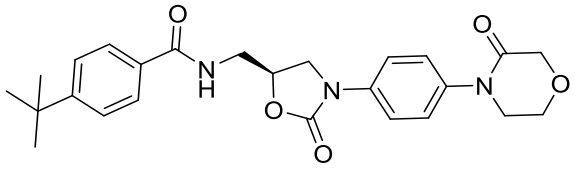

This compound was synthesised according to the general procedure A-step 4-scenario 1 by reacting **d1** (0.131 g, 0.45 mmol) with 4-*tert*-butylbenzoyl chloride (0.105 g, 0.54 mmol). The title compound (0.162 g, 0.36 mmol, 80% yield) was obtained as a white powder. MS: m/z calculated for $C_{25}H_{30}N_3O_5^+$ 452.2179 $[M+H]^+$, MS: found 452.2199 $[M+H]^+$. HPLC: t_R 2.29 (95%). Mp: 246 ° C. $[\alpha]^{23}D$= -39° (c=1, DMSO). ^1H NMR (DMSO-d_6): δ 8.08 (t, *J* = 7.8 Hz, 1H), 7.75 (d, *J*=7.5 Hz, 2H), 7.48 (d, *J*=7.5 Hz, 2H), 7.36 (d, *J*=7.5 Hz, 2H), 7.17 (d, *J*=7.5 Hz, 2H), 4.88-4.79 (m, 1H), 4.20(t, J= 8.5 Hz, 3H), 3.96-3.88 (m, 2H), 3.89 (dd, J= 9.1 Hz, 6.1 Hz, 1H), 3.61 (t, J= 5.5Hz, 2H), 3.53 (t, J= 5.5 Hz, 2H), 1.43 (s, 9H). ^{13}C NMR (DMSO-d_6): δ 171.08, 165.83, 154.35, 153.60, 139.94, 137.54, 135. 21, 131.66, 125.16, 118.83, 117.56, 71.99, 68.20, 63.94, 49.48, 47.94, 42.66, 34.68, 31.76.

4-cyano-*N*-({(5*S*)-2-oxo-3-[4-(3-oxomorpholin-4-yl)phenyl]-1,3-oxazolidin-5-yl}methyl)benzamide (h1)

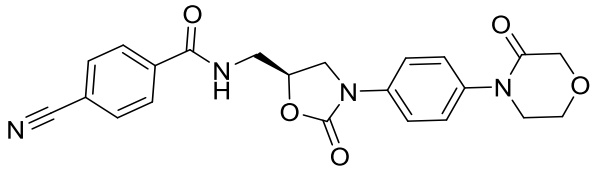

This compound was synthesised according to the general procedure A-step 4-scenario 1 by reacting **d1** (0.145 g, 0.50 mmol) with the commercially available 4-cyanobenzoyl chloride (0.099 g, 0.60 mmol). The title compound (0.159 g, 0.38 mmol, 76% yield) was obtained as a white powder. MS: m/z calculated for $C_{22}H_{21}N_4O_5^+$ 421.1506 $[M+H]^+$, MS: found 421.1517 $[M+H]^+$. HPLC: t_R 2.12 (96%). Mp: 233 ° C. $[\alpha]^{23}D$= -71° (c= 1, DMSO). ^1H NMR (DMSO-d_6): δ 8.50 (t, *J* = 7.8 Hz, 1H), 7.92 (s, 4H), 7.33 (d, *J*=7.5 Hz, 2H), 7.13 (d, *J*=7.5 Hz, 2H), 4.88-4.79 (m, 1H), 4.21(t, J= 8.5 Hz, 3H), 3.95-3.85 (m, 2H), 3.85 (dd, J= 8.9 Hz, 5.3 Hz, 1H), 3.59 (t, J= 5.5Hz, 2H), 3.51 (t, J= 5.5 Hz, 2H). ^{13}C NMR (DMSO-d_6): δ 166.81, 165.67, 154.15, 142.94, 137.54, 133. 51, 131.56, 128.16, 118.21, 118.91, 117.56, 113.25, 71.99, 68.20, 63.94, 49.48, 47.94, 42.66.

2-(4-chlorophenoxy)-*N*-({(5*S*)-2-oxo-3-[4-(3-oxomorpholin-4-yl)phenyl]-1,3-oxazolidin-5-yl}methyl)acetamide (i1)

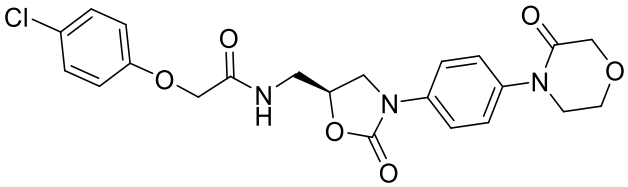

This compound was synthesised according to the general procedure A-step 4-scenario 1 by reacting **d1** (0.145 g, 0.50 mmol) with the commercially available (4-chlorophenoxy)acetyl chloride (0.123 g, 0.60 mmol). The title compound (0.166 g, 0.36 mmol, 73% yield) was obtained as a white powder. MS: m/z calculated for $C_{22}H_{23}ClN_3O_6^+$ 460.1269 $[M+H]^+$, MS: found 460.1280 $[M+H]^+$. HPLC: t_R 2.63 (94%). Mp: 276 ° C. $[\alpha]^{23}D$= 66° (c= 1, DMSO). ^1H NMR (DMSO-d_6): δ 7.36 (t, *J* = 7.8 Hz, 1H), 7.30-7.25 (m, 2H), 7.18 (d, *J*=7.5 Hz, 2H), 7.14-7.10 (m, 2H), 7.08-7.03 (d, *J*= 7.5, 2H), 4.86-4.781 (m, 1H), 4.55 (d, *J*=12.3, 1H), 4.37 (d, *J*= 12.5, 1H), 4.19(t, J= 8.5 Hz, 3H), 3.90-3.80 (m, 2H), 3.88 (dd, J= 9.2 Hz, 6.1 Hz, 1H), 3.58 (t, J= 5.5Hz, 2H), 3.57 (t, J= 5.5 Hz, 2H). ^{13}C NMR (DMSO-d_6): δ 170.81, 166.87, 158.66,

154.15, 142.89, 136.80, 129.41, 126.55, 118.90, 117.54, 115.21, 72.01, 69.10, 66.54, 65.73, 50.48, 45.94, 41.36.

tert-butyl {4-[({(5*S*)-2-oxo-3-[4-(3-oxomorpholin-4-yl)phenyl]-1,3-oxazolidin-5-yl}methyl)carbamoyl]phenyl}carbamate (o1)

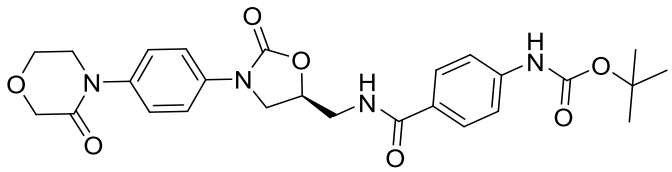

This compound was synthesised according to the general procedure A-step 4-scenario 2 by reacting **d1** (0.218 g, 0.75 mmol) with the commercially available 4-[(*tert*-butoxycarbonyl)amino]benzoic acid (0.177 g, 0.75 mmol). The title compound (0.275 g, 0.54 mmol, 72% yield) was obtained as a white powder. MS: m/z calculated for $C_{26}H_{31}N_4O_7^+$ 511.2187 $[M+H]^+$, MS: found 511.2202 $[M+H]^+$. HPLC: t_R 2.87 (95%). Mp: 296 ° C. ^{1}H NMR (DMSO-d_6): δ 7.92-7.85 (m, *J* =, 3H), 7.81 (d, *J*=7.8 Hz, 1H), 7.42-7.36(m, 2H), 7.16 (d, *J*=7.5 Hz, 2H), 7.11 (d, *J*=7.5 Hz, 2H), 4.86-4.77(m, 1H), 4.24 (t, J= 8.6 Hz, 3H), 3.99-3.92 (m, 2H), 3.85 (dd, J= 8.8 Hz, 6.2 Hz, 1H), 3.55 (t, J= 5.8 Hz, 2H), 3.42 (t, J= 6.5 Hz, 2H), 2.21 (s, 9H). ^{13}C NMR (DMSO-d_6): δ 167.71, 166.83, 156.13, 153.77, 145.94, 138.23, 135.15, 128. 51, 126.24, 117.36, 115.99, 111.46, 81.78, 71.90, 68.20, 66.94, 47.50, 43.14, 40.12, 26.16.

tert-butyl ({4-[({(5*S*)-2-oxo-3-[4-(3-oxomorpholin-4-yl)phenyl]-1,3-oxazolidin-5-yl}methyl)carbamoyl]cyclohexyl}methyl)carbamate (q1)

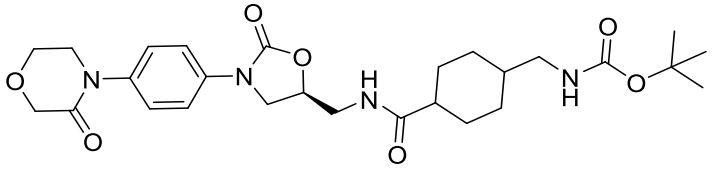

This compound was synthesised according to the general procedure A-step 4-scenario 2 by reacting **d1** (0.261 g, 0.90 mmol) with the commercially available 4-{[(*tert*-butoxycarbonyl)amino]methyl}cyclohexane-1-carboxylic acid (0.231 g, 0.90 mmol) . The title compound (0.318 g, 0.60 mmol, 67% yield) was obtained as a white powder. MS: m/z calculated for $C_{27}H_{39}N_4O_7^+$ 531.2813 $[M+H]^+$, MS: found 531.2831$[M+H]^+$. HPLC: t_R 2.98 (95%). Mp: 301 ° C. ^{1}H NMR (DMSO-d_6) δ 8.1 (t, *J*= 7.0 Hz, 1H), 7.36 (d, *J*= 8.6 Hz, 2H), 7.18 (d, *J*= 8.6 Hz, 2H), 6.76 (t, *J*= 7.0 Hz, 1H), 4.89-4.80 (m, 1H), 4.31(s, 2H), 4.14-4.04 (m, 1H), 4.00-3.90 (m, 2H), 3.89-3.80 (m, 2H), 3.79 (dd, J= 9.3 Hz, 6.3 Hz, 1H), 3.60-3.40 (m, 2H), 3.34-3.25 (m, 2H), 3.20, (dt,

J=12.4, 7.2 Hz, 1H), 2.33 (p, *J*= 7.0, 1H), 2. 28-2.25 (m, 4H), 2.18-210 (m, 4H), 2.06 (s, 9H). ^{13}C NMR (DMSO-d_6): δ 168.16, 166.83, 156.13, 154.76, 142.88, 136.48, 118.35, 117.05, 79.55, 72.91, 68.20, 65.14, 47.50, 46.15, 45.76, 43.13, 40.12, 36.11, 28.95, 27.17, 24.35.

tert-butyl {4-[({(5*S*)-2-oxo-3-[4-(3-oxomorpholin-4-yl)phenyl]-1,3-oxazolidin-5-yl}methyl)carbamoyl]cyclohexyl}carbamate (s1)

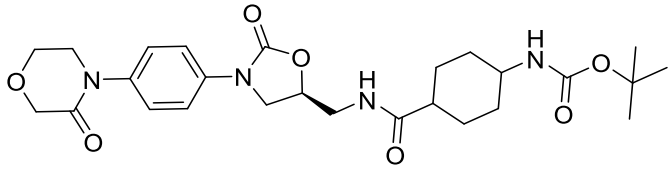

This compound was synthesised according to the general procedure A-step 4-scenario 2 by reacting **d1** (0.247 g, 0.85 mmol) with the commercially available 4-[(*tert*-butoxycarbonyl)amino]cyclohexane-1-carboxylic acid (0.206 g, 0.85 mmol). The title compound (0.267 g, 0.53 mmol, 61% yield) was obtained as a white powder. MS: m/z calculated for $C_{26}H_{37}N_4O_7^+$ 517.2656 $[M+H]^+$, MS: found 517.2679 $[M+H]^+$. HPLC: t_R 2.50 (95%). Mp: 287 ° C. ^{1}H NMR (DMSO-d_6) δ 8.0 (t, *J*= 7.0 Hz, 1H), 7.35 (d, *J*= 8.6 Hz, 2H), 7.19 (d, *J*= 8.6 Hz, 2H), 4.88-4.80 (m, 1H), 4.30 (d, *J*= 9 Hz, 3H), 3.99 (dd, J= 9.1 Hz, 6.1 Hz, 1H), 3.96-3.89 (m, 2H), 3.82-3.75 (m, 2H), 3.77-3.69 (m, 1H), 3.63-3.49 (m, 2H), 3.36 (m, 1H), 3.20-3.10, (m, 1H), 2.28-2.25 (m, 4H), 2.18-2.10 (m, 4H), 2.05 (s, 9H). ^{13}C NMR (DMSO-d_6): δ 168.15, 165.99, 155.18, 154.75, 142.83, 135.50, 118.35, 118.05, 80.33, 71.29, 70.44, 66.50, 53.44, 47.50, 46.13, 45.76, 41.13, 31.13, 28.95, 25.88.

tert-butyl ({4-[({(5*S*)-2-oxo-3-[4-(3-oxomorpholin-4-yl)phenyl]-1,3-oxazolidin-5-yl}methyl)carbamoyl]phenyl}methyl)carbamate (u1)

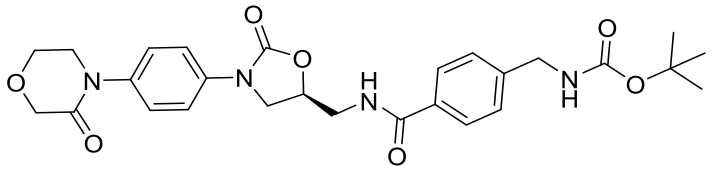

This compound was synthesised according to the general procedure A-step 4-scenario 2 by reacting **d1** (0.291 g, 1 mmol) with the commercially available 4-{[(*tert*-butoxycarbonyl)amino]methyl}benzoic acid (0.251 g, 1 mmol). The title compound (0.387 g, 0.73 mmol, 74% yield) was obtained as a white powder. MS: m/z calculated for $C_{27}H_{33}N_4O_7^+$ 525.2343 $[M+H]^+$, MS: found 525.2361 $[M+H]^+$. HPLC: t_R 2.67 (97%). Mp: 236 ° C. ^{1}H NMR (DMSO-d_6): δ 8.01 (t, *J*= 7.8 Hz, 1H), 7.88-7.81 (m, 2H), 7.41- 7.35 (m, 4H), 7.17 (d, *J*=

7.8 Hz, 2H), 5.19 (t, *J*= 8.7 Hz, 1H), 4.88-4.80 (m, 1H), 4.43 (m, 1H), 4.36-4.26 (m, 1H), 4.21(S, 3H), 4.00 (dd, J= 8.9 Hz, 5.9 Hz, 1H), 3.96-3.89 (m, 2H), 3.87-3.78 (m, 2H), 3.66-3.49 (m, 2H), 1.89 (s, 9H). ^{13}C NMR (DMSO-d_6): δ 166.79, 165.87, 156.33, 154.74, 142.83, 139.51, 136.14, 131.17, 128.63, 127.98, 118.35, 117.85, 79.66, 71.30, 70.37, 66.50, 47.68, 46.12, 44.76, 41.10, 28.95.

4-amino-*N*-({(5*S*)-2-oxo-3-[4-(3-oxomorpholin-4-yl)phenyl]-1,3-oxazolidin-5-yl}methyl)benzamide (p1)

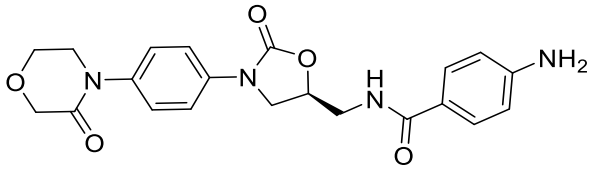

This compound was synthesised according to the general procedure A-step 5-scenario 1 starting with compound **o1** (0.204 g, 0.40 mmol). The title compound (0.118 g, 0.28 mmol, 72% yield) was obtained as a white powder. MS: m/z calculated for $C_{21}H_{23}N_4O_5^+$ 411.1664 $[M+H]^+$, MS: found 411.1670 $[M+H]^+$. HPLC: t_R 1.89 (96%). Mp: 216 ° C. $[\alpha]^{23}D$= -43° (c= 1, DMSO). ^{1}H NMR (DMSO-d_6): δ 8.12 (t, J= 7.8 Hz, 1H), 7.57-7.52 (m, 2H), 7.36 (m, 2H), 7.17 (d, *J*= 8.6 Hz, 2H), 7.15-7.07 (m, 2H), 5.84 (s, 2H), 4.89-4.80 (m, 1H), 4.31 (s, 2H), 4.18-4.05 (m, 1H), 4.00 (td, J= 7.0, 0.6 Hz, 2H), 3.88 (dd, J= 9.0 Hz, 6.0 Hz, 1H), 3.86-3.78 (m, 2H), 3.66-3.49 (m, 2H). ^{13}C NMR (DMSO-d_6): δ 168.88, 166.93, 154.33, 152.87, 143.54, 138.23, 135.15, 128. 50, 126.24, 118.97, 112.16, 71.90, 69.21, 67.01, 47.50, 46.64, 41.22.

4-(aminomethyl)-*N*-({(5*S*)-2-oxo-3-[4-(3-oxomorpholin-4-yl)phenyl]-1,3-oxazolidin-5-yl}methyl)cyclohexane-1-carboxamide (r1)

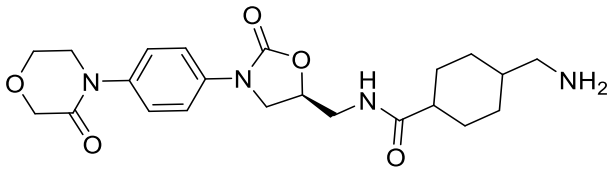

This compound was synthesised according to the general procedure A-step 5-scenario 1 starting with compound **q1** (0.265 g, 0.50 mmol). The title compound (0.145g, 0.33 mmol, 53% yield) was obtained as a white powder. MS: m/z calculated for $C_{22}H_{31}N_4O_5^+$ 431.2288 $[M+H]^+$, MS: found 431.2301$[M+H]^+$. HPLC: t_R 2.21 (96%). Mp: 222 ° C. $[\alpha]^{23}D$= 70° (c= 1, DMSO). ^{1}H NMR (DMSO-d_6): δ 7.96 (t, *J*= 7.0 Hz, 1H), 7.63 (d, *J*= 8.9 Hz,

2H), 7.48 (d, *J*= 8.9 Hz, 2H), 4.91-4.81 (m, 1H), 4.61(s, 2H), 4.44-4.35 (m, 1H), 4.16-4.09 (m, 2H), 4.00 (dd, J= 9.1 Hz, 6.1 Hz, 1H), 3.87-3.82 (m, 1H), 3.61-3.60 (m, 1H), 3.59-3.55 (m, 2H), 3.32-3.27 (m, 2H), 3.22-3.16, (m, 1H), 2.33-2.27 (m, 1H), 2.24-2.20 (m, 4H), 2.17-2.11 (m, 4H), 1.82 (t, *J*= 7.0, 2H). ^{13}C NMR (DMSO-d_6): δ 178.18, 166.81, 154.33, 143.90, 136.51, 119.46, 117.05, 71.56, 67.91, 66.26, 49.52, 47.67, 46.73, 43.18, 41.52, 36.14, 28.95, 26.36.

4-amino-*N*-({(5*S*)-2-oxo-3-[4-(3-oxomorpholin-4-yl)phenyl]-1,3-oxazolidin-5-yl}methyl)cyclohexane-1-carboxamide (t1)

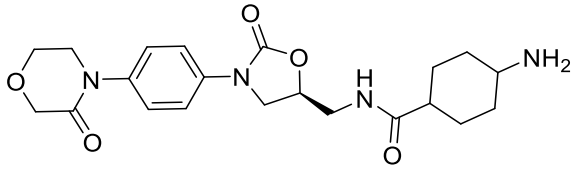

This compound was synthesised according to the general procedure A-step 5-scenario 1 starting with compound **s1** (0.206 g, 0.40 mmol). The title compound (0.091 g, 0.20 mmol, 55% yield) was obtained as a white powder. MS: m/z calculated for $C_{21}H_{29}N_4O_5^+$ 417.2132 $[M+H]^+$, MS: found 417.2147 $[M+H]^+$. HPLC: t_R 1.95 (96%). Mp: 231 ° C. $[\alpha]^{23}D$= 31° (c= 1, DMSO). ^{1}H NMR (DMSO-d_6): δ 8.0 (t, *J*= 7.1 Hz, 1H), 7.36 (d, *J*= 8.6 Hz, 2H), 7.21 (d, *J*= 8.6 Hz, 2H), 4.91-4.82 (m, 1H), 4.31 (s, 2H), 4.14-4.04 (m, 1H), 4.00 (m, 2H), 3.88 (dd, J= 8.6 Hz, 5.8 Hz, 1H), 3.85-3.78 (m, 1H), 3.77-3.69 (m, 1H), 3.60-3.40 (m, 2H), 3.08 (d, *J*=7.08 Hz, 2H), 2.84-2.69 (m, 1H), 2.32-2.26 (m, 1H), 1.78-166 (m, 4H), 1.62 (m, 2H), 1.49 (m, 2H). ^{13}C NMR (DMSO-d_6): δ 177.66, 168.26, 155.18, 142.82, 136.56, 119.45, 117.01, 71.33, 69.41, 66.54, 51.20, 47.50, 47.06, 45.75, 41.18, 33.95, 25.15.

4-(aminomethyl)-*N*-({(5*S*)-2-oxo-3-[4-(3-oxomorpholin-4-yl)phenyl]-1,3-oxazolidin-5-yl}methyl)benzamide (v1)

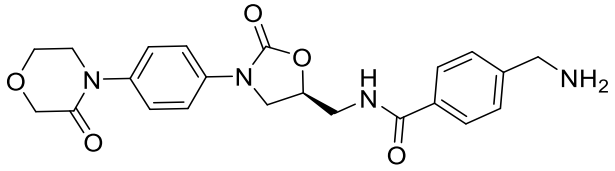

This compound was synthesised according to the general procedure A-step 5-scenario 1 starting with compound **u1** (0.314 g, 0.60 mmol). The title compound (0.142 g, 0.33 mmol, 56% yield) was obtained as a white powder. MS: m/z calculated for $C_{22}H_{25}N_4O_5^+$ 425.1819 $[M+H]^+$, MS: found 425.1831 $[M+H]^+$. HPLC: t_R 1.45 (96%). Mp: 211 ° C. $[\alpha]^{22}D$= 22° (c= 1, DMSO). ^{1}H

NMR (DMSO-d_6): δ 8.01 (t, *J*= 7.8 Hz, 1H), 7.90-7.81 (m, 2H), 7.36- 7.25 (m, 4H), 7.19-7.09 (m, 2H), 4.89-4.81 (m, 1H), 4.31 (s, 2H), 4.14-4.03 (m, 1H), 4.07-3.96 (m, 2H), 3.91 (dd, J= 8.6 Hz, 6.0 Hz, 1H), 3.88-3.78 (m, 4H), 3.66-3.49 (m, 2H), 1.74 (t, *J*= 6.7 Hz, 2H). ^{13}C NMR (DMSO-d_6): δ 166.80, 166.12, 154.74, 143.13, 142.55, 136.14, 131.18, 128.61, 127.88, 118.33, 117.80, 71.56, 69.31, 66.51, 47.67, 46.15, 45.12, 41.13.

2-{(2*R*)-2-hydroxy-3-[4-(morpholin-4-yl)anilino]propyl}-1*H*-isoindole-1,3(2*H*)-dione (b2)

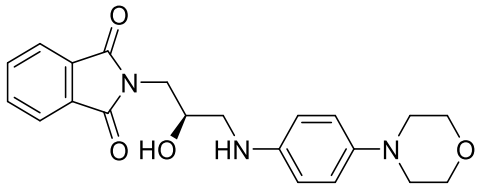

This compound was synthesised according to the general procedure A-step 1-scenario 1 by reacting the commercially available 4-(morpholin-4-yl)aniline **a2** (1.780 g, 10 mmol) with **35** (2.030 g, 10 mmol) . The title compound (3.162 g, 8.3 mmol, 83 % yield) was obtained as a white powder. MS: m/z calculated for $C_{21}H_{24}N_3O_4^+$ 382.1761 $[M+H]^+$, MS: found 382.1781 $[M+H]^+$. HPLC: t_R 2.42 min (95%). Mp: 172.6 °C. $[\alpha]^{22}_D$= 3° (c= 1, DMSO). ^{1}H NMR (DMSO-d_6): δ 7.88-7.78 (m, 4H), 6.74 (d, *J*= 8.8 Hz, 2H), 6.55 (d, *J*=8.8 Hz, 2H), 5.11 (d, *J*= 5.4, 1H), 4.94-5.09 (broad s,1H), 4.03-3.93 (m, 1H), 3.73-3.67 (m, 4H), 3.66-3.56 (m, 2H), 3.19-3.01 (m, 1H), 3.00- 2.92 (m, 1H), 2.91-2.83 (m, 4H). ^{13}C NMR (DMSO-d_6): δ 168.54, 143.43, 142.97, 134.71, 132.28, 123.37, 118.02, 113.65, 66.89, 66.78, 51.00, 48.64, 42.95.

2-({(5*S*)-3-[4-(morpholin-4-yl)phenyl]-2-oxo-1,3-oxazolidin-5-yl}methyl)-1*H*-isoindole-1,3(2*H*)-dione (c2)

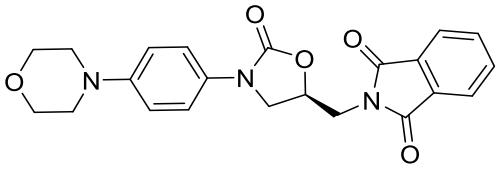

This compound was synthesised according to the general procedure A-step 2-scenario 1, starting with **b2** (3.048 g, 8 mmol). The title compound (2.805 g, 6.88 mmol, 86% yield) was obtained as yellow solid. MS: m/z calculated for $C_{22}H_{22}N_3O_5^+$ 408.1555 $[M+H]^+$, MS: found 408.1565 $[M+H]^+$. HPLC: t_R 2.56 min (91 %). Mp: 223 °C. $[\alpha]_D^{22}$= 62° (c= 1, DMSO). ^{1}H NMR ($CDCl_3$): δ 7.96-7.84 (m, 4H), 7.43 (d, *J*= 8.8 Hz, 2H), 6.97 (d, *J*= 8.8Hz, 2H), 4.95-4.86 (m, 1H), 4.15 (t, *J*= 8.8, 1H), 3.99 (q, *J*= 7.6 Hz, 1H),3.94 (dd, *J*= 13.1 Hz, 7.0

Hz, 1H), 3.90-3.83 (m, 1H), 3.77-3.70 (m, 4H), 3.09-3.03 (m, 4H). ^{13}C NMR ($CDCl_3$): δ 167.99, 154.24, 147.36, 134.39, 131.47, 130.54, 123.66, 119.15, 115.26, 69.55, 66.84, 49.56, 48.85, 40.85.

(5*S*)-5-(aminomethyl)-3-[4-(morpholin-4-yl)phenyl]-1,3-oxazolidin-2-one (d2).

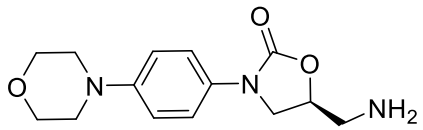

This compound was synthesised according to the general procedure A-step 3a-scenario 2 starting with **c2** (2.645 g, 6.5 mmol). The title compound (1.440 g, 5.2 mmol, 80% yield)**.** MS: m/z calculated for $C_{14}H_{20}N_3O_3^+$ 278.1499 $[M+H]^+$, MS: found 278.1503 $[M+H]^+$. HPLC: t_R 0.66 min (94 %). Mp: 98 °C. ^{1}H NMR (DMSO-*d*$_6$): δ 7.41 (d, *J*= 9.1 Hz, 2H), 6.95 (d, *J*=9.1 Hz, 2H), 4.60-4.52 (m, 1H), 4.00 (t, *J*= 8.8 Hz, 1H), 3.96 (dd, J= 5.2 Hz, 3.8 Hz, 1H), 3.87 (dd, J = 9.0 Hz, 6.5 Hz, 1H), 3.71 (dd, J = 5.2 Hz, 3.6 Hz, 2H), 3.70-3.65 (m, 1H), 3.54 (d, 1H) 3.08-3.02 (m, 4H), 2.81-2.77 (m, 1H), 2.32 (s, 2H).^{13}C NMR (DMSO-*d*$_6$): δ 154.75 , 148.27, 134.52, 120.12, 116.23, 71.49, 66.83, 49.50, 48.23, 42.45.

5-chloro-*N*-({(5*S*)-3-[4-(morpholin-4-yl)phenyl]-2-oxo-1,3-oxazolidin-5-yl}methyl)thiophene-2-carboxamide (e2)

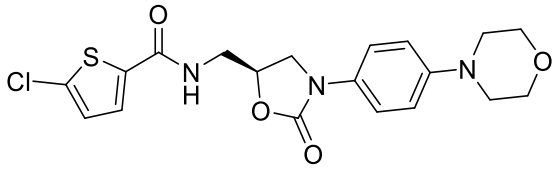

This compound was synthesised according to the general procedure A-step 4-scenario1 by reacting compound **d2** (0.138 g, 0.50 mmol) and 5-chlorothiophene-2-carbonyl chloride (0.108 g, 0.60 mmol). The title compound (0.137 g, 0.33 mmol, 66%) was obtained as a white solid. MS: m/z calculated for $C_{19}H_{21}ClN_3O_4S^+$ 422.0935 $[M+H]^+$, MS: found 422.0931 $[M+H]^+$. HPLC: t_R 2.59 min (99 %). Mp: 201 °C (lit. Mp.= 198 °C).[267] $[\alpha]_D^{21}$= -39° (c= 1, DMSO).^{1}H NMR (DMSO-*d*$_6$): δ 8.97 (t, *J*= 5.4 Hz, 1H), 7.69 (d, *J*=4.1 Hz, 1H), 7.39 (d, *J*= 9.0 Hz, 2H), 7.20 (d, *J*= 4.1 Hz, 1H), 6.97 (d, *J*= 9.0 Hz, 2H), 4.84-4.75 (m, 1H), 4.12 (t, *J*= 9.0 Hz, 1H), 3.77 (dd, J = 9.1 Hz, 6.2 Hz, 1H), (m, 1H), 3.76-3.70 (m, 4H), 3.59 (t, *J*= 5.3 Hz, 2H), 3.09-3.03 (m, 4H).^{13}C NMR (DMSO-*d*$_6$): δ 161.25, 154.69, 148.14, 138.96, 133.71, 130.93, 128.89, 128.61, 120.06, 115.95, 71.60, 66.52, 49.24, 48.20, 42.74.

_N_-({(5_S_)-3-[4-(morpholin-4-yl)phenyl]-2-oxo-1,3-oxazolidin-5-yl}methyl)thiophene-2-carboxamide (f2)

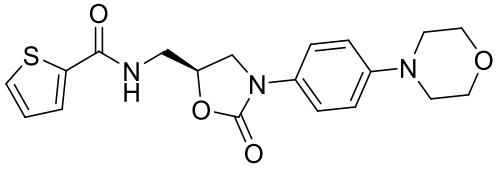

This compound was synthesised according to the general procedure A-step 4-scenario1 by reacting compound **d2** (0.110 g, 0.40 mmol) and thiophene-2-carbonyl chloride (0.070 g, 0.48 mmol). The title compound (0.109 g, 0.28 mmol, 71%) was obtained as a white solid. MS: m/z calculated for $C_{19}H_{22}N_3O_4S^+$ 388.1325 $[M+H]^+$, MS: found 388.1337 $[M+H]^+$. HPLC: t_R 2.40 min (95%). Mp: 181 ˚C. $[\alpha]_D^{22}$= -36° (c= 1, DMSO).^{1}H NMR ($CDCl_3$): δ 7.55-7.59 (m, 2H), 7.39 (d, *J*= 9.1, 2H), 7.08 (t, *J*= 4.2, 1H), 6.89 (d, *J*= 9.1, 2H), 6.54 (t, *J*= 5.8, 1H), 4.89-4.81 (m, 1H), 4.08 (t, *J*=8.8, 1H), 3.97-3.89 (m, 1H), 3.88-3.81 (m, 4H), 3.79 (dd, J = 9.2 Hz, 6.2 Hz, 1H), 3.16-3.07 (m, 5H).^{13}C NMR ($CDCl_3$): δ 162.23, 155.62, 148.41, 140.66, 137.66, 130.76, 128.68, 127.88, 120.15, 116.27, 70.83, 68.36, 52.10, 46.88, 40.33.

4-*tert*-butyl-*N*-({(5*S*)-3-[4-(morpholin-4-yl)phenyl]-2-oxo-1,3-oxazolidin-5-yl}methyl)benzamide (g2)

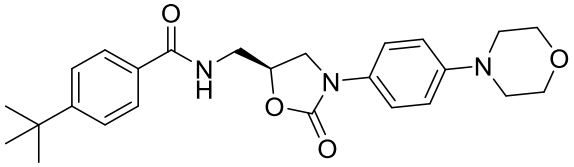

This compound was synthesised according to the general procedure A-step 4-scenario1 by reacting compound **d2** (0.152 g, 0.55 mmol) and 4-(*tert*-butyl)benzoyl chloride (0.129 g, 0.66 mmol). The title compound (0.93 g, 0.44 mmol, 81%) was obtained as a white solid. MS: m/z calculated for $C_{25}H_{31}N_3O_4^+$ 437.2309 $[M+H]^+$, MS: found 437.2330 $[M+H]^+$. HPLC: t_R 2.76 (96%). Mp: 279˚C. $[\alpha]_D^{21}$= 53° (c= 1, DMSO).^{1}H NMR (DMSO-d_6): δ 8.41 (t, J= 6.1 Hz, 1H), 8.06-7.98 (m, 2H), 7.43 (d, J= 9.3Hz, 2H), 7.31-7.29 (m, 2H), 7.10 (d, J= 9.3 Hz, 2H), 4.93-4.80 (m, 1H), 3.96 (t, J= 8.7 Hz, 1H), 3.80 (dd, J = 9.3 Hz, 6.2 Hz, 1H), 3.75-3.71 (m, 4H), 3.70-3.56 (m, 2H), 3.11-3.03 (m, 4H), 2.16 (s, 9H).^{13}C NMR (DMSO-d_6): δ 168.89, 167.26, 145.66, 147.91, 131.03, 130.22, 120.15, 116.08, 115.91, 115.78, 71.54, 66.51, 49.23, 48.22, 42.81, 34.71, 31.10.

4-cyano-*N*-({(5*S*)-3-[4-(morpholin-4-yl)phenyl]-2-oxo-1,3-oxazolidin-5-yl}methyl)benzamide (h2)

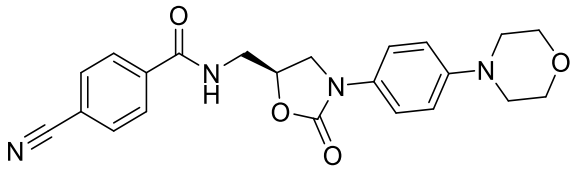

This compound was synthesised according to the general procedure A-step 4-scenario1 by reacting compound **d2** (0.138 g, 0.50 mmol) and 4-cyanobenzoyl chloride (0.099 g, 0.60 mmol). The title compound (0.153 g, 0.37 mmol, 76%) was obtained as a white solid. MS: m/z calculated for $C_{22}H_{23}N_4O_4^+$ 407.1714 $[M+H]^+$, MS: found 407.1724 $[M+H]^+$. HPLC: t_R 2.36 min (96%). Mp: 213 ˚C. $[\alpha]_D^{22}$= -41° (c= 1, DMSO).^{1}H NMR ($CDCl_3$): δ 8.36 (d, J=8.5 2H), 8.16 (d, J=8.5 2H), 7.12 (d, *J*= 9.1, 2H), 6.89 (d, *J*= 9.1, 2H), 6.51 (t, *J*= 5.8, 1H), 4.90-4.82 (m, 1H), 4.01 (t, *J*=8.8, 1H), 3.97-3.90 (m, 1H), 3.87-3.83 (m, 4H), 3.78 (dd, J = 9.1 Hz, 6.2 Hz, 1H), 3.16-3.07 (m, 5H).^{13}C NMR ($CDCl_3$): δ 166.30, 154.15, 144.30, 136.80, 132.75, 130.76, 128.58, 127.88, 118.15, 117.05, 70.88, 68.46, 51.10, 46.44, 41.13.

***N*-({(5*S*)-3-[4-(morpholin-4-yl)phenyl]-2-oxo-1,3-oxazolidin-5-yl}methyl)benzamide (j2)**

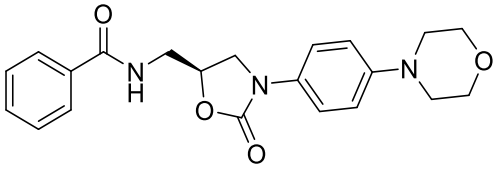

This compound was synthesised according to the general procedure A-step 4-scenario1 by reacting compound **d2** (0.138 g, 0.50 mmol) and benzoyl chloride (0.084 g, 0.60 mmol). The title compound (0.153 g, 0.40 mmol, 81%) was obtained as a white solid. MS: m/z calculated for $C_{21}H_{24}N_3O_4^+$ 382.1761$[M+H]^+$, MS: found 382.1779 $[M+H]^+$. HPLC: t_R 2.40 min (96 %). Mp: 231 °C. $[\alpha]_D^{22}$= -58° (c= 1, DMSO). ^{1}H NMR (DMSO-*d*$_6$): δ 8.83 (t, *J*= 6.1, 1H), 7.84 (d, *J*= 7.1, 2H), 7.54 (t, *J*=7.4, 1H), 7.47 (t, *J*=7.7, 2H), 7.40 (d, *J*=7.8, 2H), 6.97 (d, *J*=7.8, 2H), 4.78-4.88 (m, 1H), 4.13 (t, *J*=8.8, 1H), 3.79 (dd, J = 9.3 Hz, 6.1 Hz, 1H), 3.77-3.70 (m, 4H), 3.68-3.55 (m, 2H), 3.09-3.03 (m, 4H).^{13}C NMR (DMSO-*d*$_6$): δ 167.47, 154.77, 148.08, 134.52, 131.85, 130.99, 128.77, 127.74, 120.05, 115.96, 71.56, 66.52, 49.25 , 48.28, 42.28.

3-chloro-*N*-({(5*S*)-3-[4-(morpholin-4-yl)phenyl]-2-oxo-1,3-oxazolidin-5-yl}methyl)benzamide (k2)

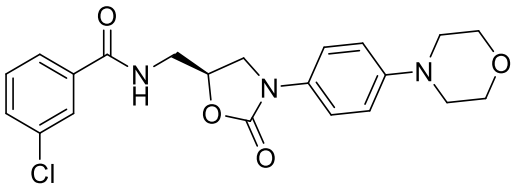

This compound was synthesised according to the general procedure A-step 4-scenario1 by reacting compound **d2** (0.138 g, 0.50 mmol) and 3-chlorobenzoyl chloride (0.105 g, 0.60 mmol). The title compound (0.135 g, 0.33 mmol, 66%) was obtained as a white solid. MS: m/z calculated for $C_{21}H_{23}ClN_3O_4^+$ 416.1371 $[M+H]^+$, MS: found 416.1390 $[M+H]^+$. HPLC: t_R 2.56 (97%). Mp: 233 °C. $[\alpha]_D^{21}$= -29° (c= 1, DMSO).^{1}H NMR ($CDCl_3$): 7.82 (t, *J*= 1.7, 1H), 7.69 (d, *J*=7.7 Hz, 1H), 7.49-7.45 (m, 1H), 7.38 (d, *J*= 9.1 Hz, 2H), 7.34 (d, *J*= 7.7 Hz, 1H), 7.28 (d, *J*= 8.8 Hz, 1H), 6.9 (d, *J*= 9.1, 2H), 4.84-4.92 (m, 1H), 4.10 (t, *J*= 8.8, 1H), 3.97-3.89 (m,1H), 3.89-3.84 (m, 5H), 3.80 (dd, J = 9.1 Hz, 6.1 Hz, 1H), 3.15-3.08 (m, 4H). ^{13}C NMR ($CDCl_3$): 167.1, 155.01, 148.42, 135.41 (C23), 134.77, 131.87, 130.30, 129.90, 127.66, 125.24, 120.21, 116.25, 71.97, 66.80, 49.51, 48.24, 42.82.

2-chloro-*N*-({(5*S*)-3-[4-(morpholin-4-yl)phenyl]-2-oxo-1,3-oxazolidin-5-yl}methyl)benzamide (l2)

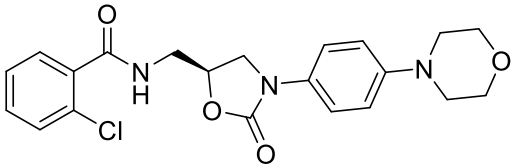

This compound was synthesised according to the general procedure A-step 4-scenario1 by reacting compound **d2** (0.138 g, 0.50 mmol) and 2-chlorobenzoyl chloride (0.105 g, 0.60 mmol). The title compound (0.113, 0.27 mmol, 55%) was obtained as a white solid. MS: m/z calculated for $C_{21}H_{23}ClN_3O_4^+$ 416.1371 $[M+H]^+$, MS: found 416.1369 $[M+H]^+$. HPLC: t_R 2.41 (94%). Mp: 174 ˚C. $[\alpha]_D^{21}$= -34° (c= 1, DMSO). ^{1}H NMR (DMSO-d_6): 8.85 (t, *J*= 6.4, 1H), 7.50-7.46 (m, 1H), 7.46-7.43 (m, 1H), 7.42-7.39 (d, *J*= 9.0 Hz, 2H), 7.39-7.36 (m, 2H), 6.99 (d, *J*= 9.0, 2H), 4.79-4.87 (m, 1H), 4.14 (t, *J*= 9.2, 1H), 3.78 (dd, J = 9.1 Hz, 6.1 Hz, 1H), 3.76-3.71 (m, 4H), 3.69-3.55 (m, 2H), 3.09-3.04 (m, 4H). ^{13}C NMR (DMSO-d_6): 167.63, 154.74, 147.99, 137.16, 131.30,

131.06, 130.24, 129.99, 129.23, 127.50, 119.87, 115.95, 71.54, 66.53, 49.24, 47.89, 42.02.

4-fluoro-*N*-({(5*S*)-3-[4-(morpholin-4-yl)phenyl]-2-oxo-1,3-oxazolidin-5-yl}methyl)benzamide (m2)

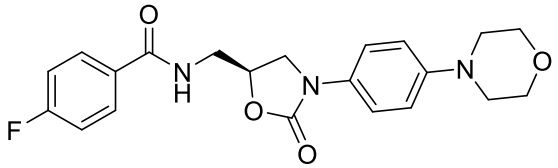

This compound was synthesised according to the general procedure A-step 4-scenario1 by reacting compound **d2** (0.166 g, 0.60 mmol) and 4-fluorobenzoyl chloride (0.112 g, 0.72 mmol). The title compound (0.133 g, 0.33 mmol, 56%) was obtained as a white solid. MS: m/z calculated for $C_{21}H_{23}FN_3O_4^+$ 400.1667 $[M+H]^+$, MS: found 400.1656 $[M+H]^+$. HPLC: t_R 2.46 (94%). Mp: 234 ˚C. $[\alpha]_D^{21}$= 61° (c= 1, DMSO).^{1}H NMR (DMSO-*d*$_6$): 8.89 (t, *J*= 6.1 Hz, 1H), 7.97-7.91 (m, 2H), 7.39 (d, *J*= 9.3Hz, 2H), 7.35-7.29 (m, 2H), 6.97 (d, *J*= 9.3 Hz, 2H), 4.78-4.87 (m, 1H), 4.13 (t, *J*= 8.7 Hz, 1H), 3.79 (dd, J = 9.4 Hz, 6.0 Hz, 1H), 3.76-3.70 (m, 4H), 3.70-3.55 (m, 2H), 3.09-3.03 (m, 4H).^{13}C NMR (DMSO-*d*$_6$): 168.99, 166.38, 145.76, 148.08, 130.98, 130.39, 120.05, 115.95, 115.81, 115.60, 71.54, 66.52, 49.24, 48.28, 42.86.

5-chloro-*N*-({(5*R*)-3-[4-(morpholin-4-yl)phenyl]-2-oxo-1,3-oxazolidin-5-yl}methyl)thiophene-2-sulfonamide (n2)

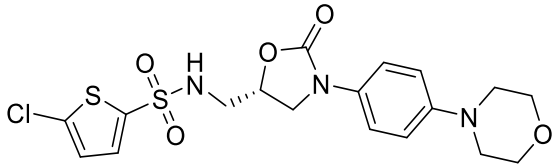

This compound was synthesised according to the general procedure A-step 4-scenario1 by reacting compound **d2** (0.166 g, 0.60 mmol) and (5-chlorothiophen-2-yl) (oxo)methanesulfonyl chloride (0.156 g, 0.72 mmol) . The title compound (0.205 g, 0.45 mmol, 75%) was obtained as a white solid. MS: m/z calculated for $C_{18}H_{21}ClN_3O_5S_2^+$ 458.0605 $[M+H]^+$, MS: found 458.0609 $[M+H]^+$. HPLC: t_R 1.83min (96%). Mp: 258˚C. $[\alpha]_D^{22}$= -33° (c= 1, DMSO). ^{1}H NMR (DMSO-*d*$_6$): δ 7.38 (d, *J* = 7.6 Hz, 1H), 7.34-7.27 (m, 2H), 7.03-6.96 (m, 2H), 6.91 (d, *J* = 7.5 Hz, 1H), 6.76 (t, *J* = 10.1 Hz, 1H), 4.63 (p, *J* = 7.0 Hz, 1H), 4.07-3.97 (m, 1H), 3.85 (t, *J* = 7.1 Hz, 4H), 3.79 (dd, J = 9.2 Hz, 6.2 Hz, 1H), 3.26–3.15 (m, 5H), 3.10 (m, 1H). ^{13}C NMR (DMSO-*d*$_6$) δ

154.30, 146.80, 144.93, 133.02, 131.39, 128.96, 122.08, 116.29, 72.05, 66.74, 48.53, 47.73, 46.13.

tert-butyl {4-[({(5*S*)-3-[4-(morpholin-4-yl)phenyl]-2-oxo-1,3-oxazolidin-5-yl}methyl)carbamoyl]phenyl}carbamate (o2)

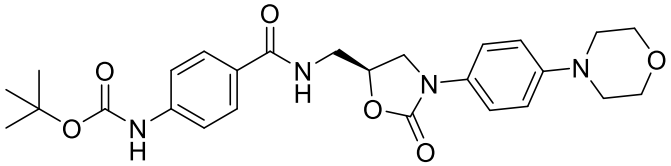

This compound was synthesised according to the general procedure A-step 4-scenario 2 by reacting compound **d2** (0.277 g, 1 mmol) with 4-((*tert* butoxycarbonyl) amino) benzoic acid (0.237 g, 1 mmol). The title compound (0.426 g, 0.86 mmol, 86%) was obtained as a white solid. MS: m/z calculated for $C_{26}H_{33}N_4O_6^+$ 497.2394 $[M+H]^+$, MS: found 497.2405 $[M+H]^+$. HPLC: t_R 2.89 (96%). Mp: 301˚C. $[\alpha]_D^{21}$= 35° (c= 1, DMSO).^{1}H NMR (DMSO-*d6*): 8.98 (t, J= 6.1 Hz, 1H), 8.12-8.01 (m, 2H), 7.55 (d, J= 9.3Hz, 2H), 7.30-7.27 (m, 2H), 7.17 (d, J= 9.3 Hz, 2H), 6.85 (s, 1H), 4.67-4.55 (m, 1H), 3.97 (t, J= 8.7 Hz, 1H), 3.77 (dd, J = 9.1 Hz, 6.1 Hz, 1H), 3.65-3.60 (m, 4H), 3.70-3.56 (m, 2H), 3.12-3.04 (m, 4H), 1.76 (s, 9H).^{13}C NMR (DMSO-*d6*): 168.89, 167.25, 154.33, 144.98, 148.01, 132.98, 130.33, 121.13, 116.19, 116.06, 115.88, 81.60, 66.53, 49.23, 48.02, 42.91, 33.37, 28.12.

tert-butyl ({4-[({(5*S*)-3-[4-(morpholin-4-yl)phenyl]-2-oxo-1,3-oxazolidin-5-yl}methyl)carbamoyl]cyclohexyl}methyl)carbamate (q2)

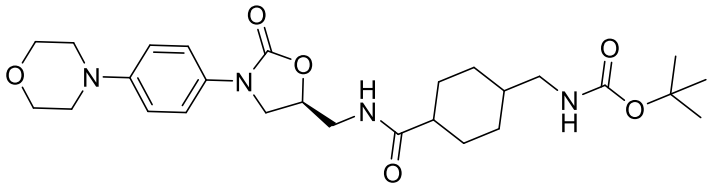

This compound was synthesised according to the general procedure A-step 4-scenario2 by reacting compound **d2** (0.277 g, 1 mmol) with the commercially available 4-{[(*tert*-butoxycarbonyl)amino]methyl}cyclohexane-1-carboxylic acid (0.257 g, 1 mmol). The title compound (0.361 g, 0.70 mmol, 81%) was obtained as a white solid. MS: m/z calculated for $C_{27}H_{41}N_4O_6^+$ 517.3020 $[M+H]^+$, MS: found 517.3035 $[M+H]^+$. HPLC: t_R 2.36 (93%). Mp: 310˚C. ^{1}H NMR (DMSO-d_6): δ 8.06 (t, *J*=6.5, 1H), 7.36-7.27 (m, 2H), 7.03-6.96 (m, 2H), 5.25 (t, *J* = 7.2 Hz, 1H), 4.89-4.81 (m, 1H), 4.14-4.04 (m, 2H), 3.85 (t, *J* = 7.1 Hz, 4H), 3.78 (dd, J = 9.1 Hz, 6.2 Hz, 1H), 3.60 – 3.40 (m, 2H), 3.38-3.30 (m, 1H), 3.26-3.15 (m, 4H), 2.45-2.35 (m, 1H), 2.11-201 (m, 1H), 1.86-1.73 (m,

4H), 1.68-1.47 (m, 4H), 1.41 (s, 9H).^{13}C NMR (DMSO-d_6): 168.89, 157.33, 144.40, 131.34, 121.13, 115.89, 81.64, 75.10, 66.14, 57.13, 50.43, 46.42, 45.11, 44.37, 36.80, 33.59, 28.30, 26.13.

***tert*-butyl {4-[({(5*S*)-3-[4-(morpholin-4-yl)phenyl]-2-oxo-1,3-oxazolidin-5-yl}methyl)carbamoyl]cyclohexyl}carbamate (s2)**

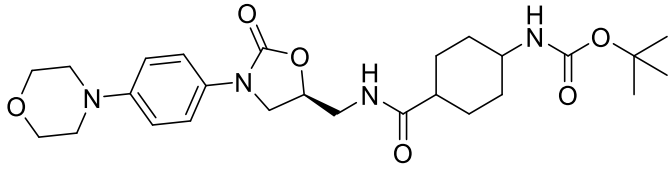

This compound was synthesised according to the general procedure A-step 4-scenario2 by reacting compound **d2** (0.277 g, 1 mmol) with 4-[(tert-butoxycarbonyl)amino] cyclohexane-1-carboxylic acid (0.243 g, 1 mmol). The title compound (0.291 g, 0.57 mmol, 58%) was obtained as a white solid. MS: m/z calculated for $C_{26}H_{39}N_4O_6^+$ 503.2864 $[M+H]^+$, MS: found 503.2881 $[M+H]^+$. HPLC: t_R 2.33 (95%). Mp: 312˚C. ^{1}H NMR (DMSO-d_6): δ 7.35 (d, J= 7.5 Hz, 2H), 7.03 (d, J= 7.5 Hz, 2H), 5.62 (t, J= 5.5Hz, 1H), 4.69-4.64 (m, 1H), 4.91-480 (m, 1H), 4.30 (d, *J* = 9.5 Hz, 1H), 4.03 (dd, *J* = 12.2, 7.0 Hz, 1H), 3.85 (t , J= 7.5 Hz, 4H), 3.76 (t, *J* = 7.1 Hz, 1H), 3.71 (dd, *J* = 12.3, 7.1 Hz, 1H), 3.59-3.50 (m, 2H), 3.46-39 (m, 1H), 3.22 (t, *J* = 7.1 Hz, 4H), 2.34 (p, *J* = 6.9 Hz, 1H), 1.83-1.73 (m, 4H), 1.76-1.66 (m, 2H), 1.48 (s, 9H). ^{13}C NMR (DMSO-d_6): δ 176.27, 156.35, 154.30, 146.82, 132.93, 118.30, 116.28, 78.74, 72.01, 66.75, 50.01, 48.99, 47.30, 42.70, 41.19, 29.59, 28.31, 25.63.

***tert*-butyl ({4-[({(5*S*)-3-[4-(morpholin-4-yl)phenyl]-2-oxo-1,3-oxazolidin-5-yl}methyl)carbamoyl]phenyl}methyl)carbamate (u2)**

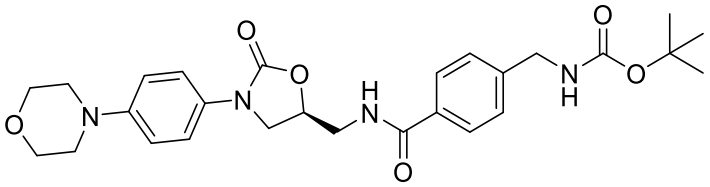

This compound was synthesised according to the general procedure A-step 4-scenario2 by reacting compound **d2** (0.277 g, 1 mmol) with 4-{[(tert-butoxycarbonyl)amino] methyl}benzoic acid (0.251 g, 1 mmol). The title compound (0.316g, 0.62 mmol, 62%) was obtained as a white solid. MS: m/z calculated for $C_{27}H_{35}N_4O_6^+$ 511.2551 $[M+H]^+$, MS: found 511.2563 $[M+H]^+$. HPLC: t_R 2.56 (94%). Mp: 331˚C. ^{1}H NMR (DMSO-d_6): δ 8.01 (t, *J* = 7.8 Hz, 1H), 7.88-7.81 (m, 2H), 7.37-7.27 (m, 4H), 7.03-6.96 (m, 2H), 5.19 (t, *J* = 8.7

Hz, 1H), 4.96-4.86 (m, 1H), 4.43-439 (m, 1H), 4.31-4.27 (m, 1H), 4.08-3.98 (m, 1H), 3.85 (t, *J* = 7.1 Hz, 4H), 3.79 (dd, J = 9.6 Hz, 6.3 Hz, 1H), 3.66-3.49 (m, 2H), 3.22 (t, *J* = 7.1 Hz, 4H), 1.40 (s, 9H). ^{13}C NMR (DMSO-d_6): δ 168.01, 155.53, 154.30, 146.80, 142.49, 133.88, 132.92, 127.68, 122.09, 116.29, 78.83, 71.99, 71.98, 66.74, 48.53, 47.27, 44.01, 43.99, 28.30.

4-amino-*N*-({(5*S*)-3-[4-(morpholin-4-yl)phenyl]-2-oxo-1,3-oxazolidin-5-yl}methyl)benzamide (p2)

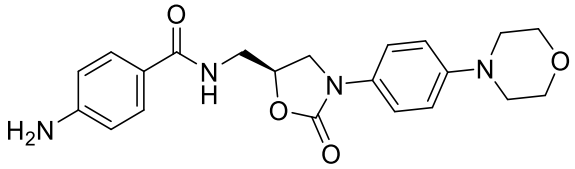

This compound was synthesised according to the general procedure A-step 5-scenario 2 starting with compound **o2** (0.372 g, 0.75 mmol). The title compound (0.157 g, 0.40 mmol, 57%) was obtained as an off-white solid. MS: m/z calculated for $C_{21}H_{25}N_4O_4^+$ 397.1870 $[M+H]^+$, MS: found 397.1883 $[M+H]^+$. HPLC: t_R 2.01 (96%). Mp: 298˚C. $[\alpha]_D^{22}$= 41° (c= 1, DMSO). ^{1}H NMR (DMSO-d_6): δ 8.88 (t, J= 6.1 Hz, 1H), 7.95-7.99 (m, 2H), 7.43 (d, J= 9.3Hz, 2H), 7.30-7.35 (m, 2H), 7.12 (d, J= 9.3 Hz, 2H), 4.89-4.81 (m, 1H), 4.15 (s, 2H), 4.03 (t, J= 8.7 Hz, 1H), 3.77 (dd, J = 9.4 Hz, 6.2 Hz, 1H) , 3.74-3.72 (m, 4H), 3.66-3.50 (m, 2H), 3.15-3.10 (m, 4H).^{13}C NMR (DMSO-d_6): δ 167.90, 166.43, 145.56, 147.89, 136.80, 128.16, 126.15, 117.88, 116.05, 113.90, 71.30, 66.65, 52.11, 47.43, 41.51.

4-(aminomethyl)-*N*-({(5*S*)-3-[4-(morpholin-4-yl)phenyl]-2-oxo-1,3-oxazolidin-5-yl}methyl)cyclohexane-1-carboxamide (r2)

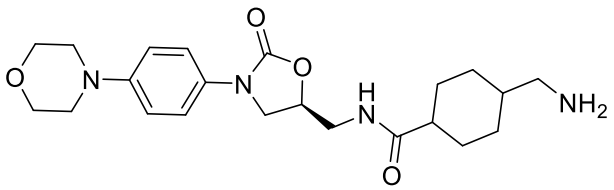

This compound was synthesised according to the general procedure A-step 5-scenario 2 starting with compound **q2** (0.309 g, 0.60 mmol). The title compound (0.137 g, 0.33 mmol, 55%) was obtained as a white solid. MS: m/z calculated for $C_{22}H_{33}N_4O_4^+$ 417.2496 $[M+H]^+$, MS: found 417.2505 $[M+H]^+$. HPLC: t_R 2.05 (95%). Mp: 293˚C. $[\alpha]_D^{22}$= 31° (c= 1, DMSO). ^{1}H NMR (DMSO-d_6): δ 8.02 (t, *J*=7.5 Hz, 1H), 7.71 (d, *J*= 8.5 Hz, 2H), 7.54 (d, *J*= 8.5 Hz, 2H), 4.93-481 (m, 1H), 4.14-4.04 (m, 1H), 3.85 (t, *J* = 7.1 Hz, 4H), 3.78

(dd, J = 9.3 Hz, 6.2 Hz, 1H), 3.60-3.40 (m, 2H), 3.22 (t, *J* = 7.1 Hz, 4H), 2.78-2.66 (m, 1H), 2.56-241 (m, 1H), 2.33 (p, *J* = 7.0 Hz, 1H), 1.82-172 (t, *J* = 6.9 Hz, 2H), 1.74-169 (m, 4H), 1.68-1.41 (m, 5H). ^{13}C NMR (DMSO-*d*$_6$): δ 172.79, 167.33, 155.41, 141.30, 122.15, 117.69, 82.74, 67.11, 49.63, 47.48, 41.11, 33.37, 40.80, 39.96, 28.98, 26.12.

4-amino-N-({(5*S*)-3-[4-(morpholin-4-yl)phenyl]-2-oxo-1,3-oxazolidin-5-yl}methyl)cyclohexane-1-carboxamide (t2)

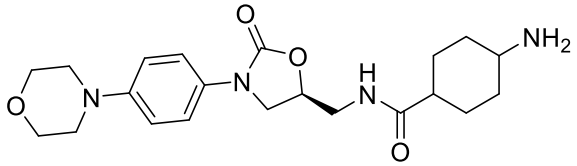

This compound was synthesised according to the general procedure A-step 5-scenario 1 starting with compound **s2** (0.251 g, 0.5 mmol). The title compound (0.112 g, 0.27 mmol, 56%) was obtained as a white solid. MS: m/z calculated for $C_{21}H_{31}N_4O_4^+$ 403.2339 $[M+H]^+$, MS: found 403.2361 $[M+H]^+$. HPLC: t_R 2.05 (95%). Mp: 293˚C. $[\alpha]_D^{21}$= 41° (c= 1, DMSO). ^{1}H NMR (DMSO-*d*$_6$): δ 8.01 (t, J= 7.5 Hz, 1H), 7.35-7.28 (m, 2H), 7.03-6.97 (m, 2H), 4.89-4.81 (m, 1H), 4.03 (dd, *J* = 12.2, 7.0 Hz, 1H), 3.85 (t, *J* = 7.1 Hz, 4H), 3.71 (dd, *J* = 12.4, 7.1 Hz, 1H), 3.54-349 (m, 1H), 3.46-3.39 (m, 1H), 3.22 (t, *J* = 7.1 Hz, 4H), 3.08 (d, *J* = 7.3 Hz, 2H), 2.78-2.73 (m,1H), 2.32 (p, *J* = 7.0 Hz, 1H), 1.83-1.73 (m, 4H), 1.67-1.57 (m, 2H), 1.46-1.39 (m, 2H). ^{13}C NMR (DMSO-*d*$_6$): δ 176.27, 154.30, 146.82, 146.75, 132.93, 132.91, 122.12, 116.29, 72.01, 71.97, 66.73, 50.23, 48.53, 48.52, 47.22, 42.69, 41.41, 31.90, 27.70.

4-(aminomethyl)-*N*-({(5*S*)-3-[4-(morpholin-4-yl)phenyl]-2-oxo-1,3-oxazolidin-5-yl}methyl)benzamide (v2)

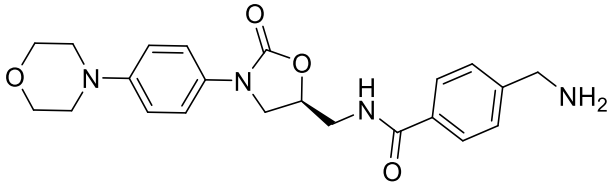

This compound was synthesised according to the general procedure A-step 5-scenario 2 starting with compound **u2** (0.280 g, 0.55 mmol). The title compound (0.135 g, 0.32 mmol, 60%) was obtained as a white solid. MS: m/z calculated for $C_{22}H_{27}N_4O_4^+$ 411.2026 $[M+H]^+$, MS: found 411.2031 $[M+H]^+$. HPLC: t_R 1.95 (95%). Mp: 245˚C. $[\alpha]_D^{22}$= -61° (c= 1, DMSO). ^{1}H NMR (DMSO-*d*$_6$): δ 8.60 (t, *J*= 6.7 Hz, 2H), 8.04 (t, *J* = 7.8 Hz, 1H), 7.90-7.82 (m, 2H), 7.34-7.25 (m, 2H), 7.20-7.10 (d, J= 8.6 Hz, 2H), 7.06-6.96 (d, J= 8.6 Hz,

2H), 4.89-4.81 (m, 1H), 4.08-3.96 (m, 2H), 3.92-3.80 (m, 5H), 3.76 (dd, J = 10.3 Hz, 7.2 Hz, 1H), 3.66-3.49 (m, 2H), 3.22 (t, *J* = 7.1 Hz, 2H), 1.74 (t, *J* = 6.7 Hz, 2H). ^{13}C NMR (DMSO-d_6): δ 168.01, 154.30, 146.80, 133.84, 132.92, 127.84, 127.43, 122.07, 116.29, 71.97, 66.74, 66.74, 48.53, 47.27, 45.59, 42.82.

2-[(2*R*)-3-(4-bromoanilino)-2-hydroxypropyl]-1*H*-isoindole-1,3(2*H*)-dione (b3)

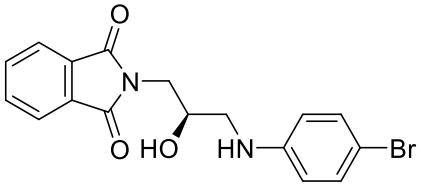

This compound was synthesised according to the general procedure A-step 1-scenario 2 by reacting the commercially available 4-bromoaniline **a3** (1.720 g, 10 mmol) with **35** (2.030 g, 10 mmol). The title compound (3.029 g, 8.1 mmol, 81% yield) was obtained as a white powder. MS: m/z calculated for $C_{17}H_{16}BrN_2O_3^+$ 375.0388 $[M+H]^+$, MS: found 375.0402. HPLC: t_R 2.67 (95%). Mp: 115˚C. ^{1}H NMR (DMSO-d_6): δ 7.85-7.78 (m, 2H), 7.76 (d, *J*= 6.8 Hz, 2H), 7.24 (d, *J*= 6.8, 2H), 6.57-6.50 (m, 2H), 6.19 (t, *J*= 6.7 Hz, 1H), 4.29 (m, 1H), 4.00 (dd, *J*= 12.4, 6.9 Hz, 1H), 3.92 (d, *J*= 6.7, 1H), 3.84 (m, 1H), 3.38 (dt, *J*= 12.3, 6.7, 1H), 3.28 (dt, *J*= 12.4, 6.8, 1H). ^{13}C NMR (DMSO-d_6): δ 168.54, 148.46, 134.13, 131.87, 130.99, 123.39, 114.20, 106.98, 69.57, 47.17, 43.17.

2-{[(5*S*)-3-(4-bromophenyl)-2-oxo-1,3-oxazolidin-5-yl]methyl}-1*H*-isoindole-1,3(2*H*)-dione (c3)

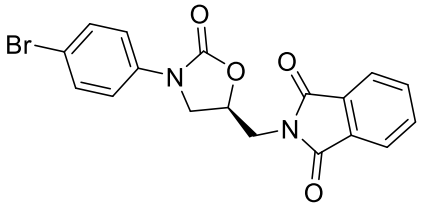

This compound was synthesised according to the general procedure A-step 2-scenario 2 starting with **b3** (2.917 g, 7.8 mmol). The title compound (2.495 g, 6.23 mmol, 80% yield)) was obtained as a white powder. MS: m/z calculated for $C_{18}H_{14}BrN_2O_4^+$ 401.0131 $[M+H]^+$, MS: found 401.0149 $[M+H]^+$. HPLC: t_R 2.51 (97%). Mp: 156 ˚C. ^{1}H NMR (DMSO-d_6): δ 8.14-8.07 (m, 2H), 7.86 (d, *J*= 8.9 Hz, 2H), 7.79-7.69 (m 4H), 4.89-4.80 (m, 1H), 4.45-4.36 (m, 1H), 4.18-

4.06 (m, 2H), 3.76-3.66 (m, 1H). ^{13}C NMR (DMSO-d_6): δ 168.29, 154.15, 136.80, 134.16, 132.01, 131.77, 124.22, 123.81, 116.83, 74.57, 47.56, 42.29.

(5*S*)-5-(aminomethyl)-3-(4-bromophenyl)-1,3-oxazolidin-2-one (d3)

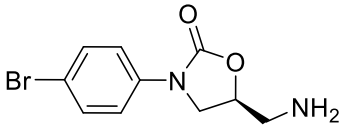

This compound was synthesised according to the general procedure A-step 3c-scenario 2 starting with **c3** (2.400 g, 6 mmol). The title compound (1.154 g, 4.26 mmol, 71% yield) was obtained as a white powder. MS: m/z calculated for $C_{10}H_{12}BrN_2O_2^+$ 272.0076 $[M+H]^+$, MS: found 272.0091 $[M+H]^+$. HPLC: t_R 0.86 min (96%). Mp: 143 °C. ^{1}H NMR (DMSO-d_6): δ 8.14-8.07 (m, 2H), 7.80-7.72 (m, 2H), 4.59 (m, 1H), 3.96 (dd, J= 5.4 Hz, 3.8 Hz, 1H), 3.85 (dd, J = 9.1 Hz, 6.3 Hz, 1H), 3.71 (dd, J = 5.5 Hz, 3.5 Hz, 2H), 2.44 (t, *J* = 7.5 Hz, 2H). ^{13}C NMR (DMSO-d_6): δ 154.15, 136.87, 132.08, 122.99, 116.23, 75.27, 48.59, 47.53.

***N*-{[(5*S*)-3-(4-bromophenyl)-2-oxo-1,3-oxazolidin-5-yl]methyl}-5-chlorothiophene-2-carboxamide (e3)**

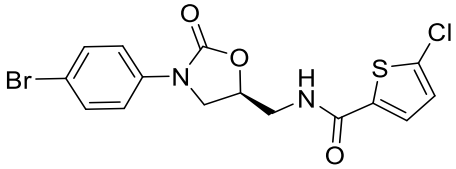

This compound was synthesised according to the general procedure A-step 4-scenario 1 by reacting **d3** (0.542 g, 2 mmol) with the commercially available 5-chlorothiophene-2-carbonyl chloride (0.434 g, 2.4 mmol). The title compound (0.594 g, 1.44 mmol, 72% yield) was obtained as a white powder. MS: m/z calculated for $C_{15}H_{13}BrClN_2O_3S^+$ 414.9513 $[M+H]^+$, MS: found 414.9523 $[M+H]^+$. HPLC: t_R 1.76 (98%). Mp: 199 °C. $[\alpha]^{22}_D$= -96° (c= 1, DMSO). ^{1}H NMR (DMSO-d_6): δ 8.14-8.07 (m, 2H), 7.80-7.72 (m, 2H), 7.42 (t, *J* = 7.5 Hz, 1H), 7.34 (d, *J* = 7.5 Hz, 1H), 7.03 (d, *J* = 7.5 Hz, 1H), 4.89-4.81 (m, 1H), 4.14-4.05 (m, 1H), 3.90 (dd, J= 9.3 Hz, 6.2 Hz, 1H), 3.62-3.45 (m, 2H). ^{13}C NMR (DMSO-d_6): δ 160.73, 154.15, 140.12, 136.80, 134.48, 132.08, 130.97, 127.49, 124.15, 117.92, 71.30, 47.88, 41.76.

_N_-{[(5_S_)-3-(4-bromophenyl)-2-oxo-1,3-oxazolidin-5-yl]methyl}-4-tert-butylbenzamide (g3)

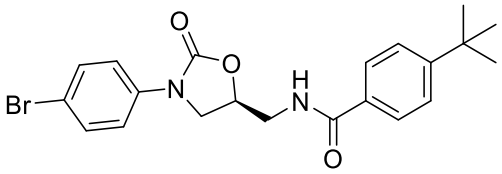

This compound was synthesised according to the general procedure A-step 4-scenario 1 by reacting **d3** (0.542 g, 2 mmol) with 4-*tert*-butylbenzoyl chloride (0.470 g, 2.4 mmol). The title compound (0.739 g, 1.7 mmol, 86% yield) was obtained as a white powder. MS: m/z calculated for $C_{21}H_{24}BrN_2O_3^+$ 431.0964 $[M+H]^+$, MS: found 431.0971 $[M+H]^+$. HPLC: t_R 2.18 (95%). Mp: 233 ° C. $[\alpha]^{23}_D$= 98° (c= 1, DMSO). ^{1}H NMR (DMSO-d_6): δ 8.14-8.03 (m, 3H), 7.80-7.68 (m, 4H), 7.48-7.41 (m, 2H), 4.89-481 (m, 1H), 4.14-4.05 (m, 1H), 3.89 (dd, J= 9.1 Hz, 6.1 Hz, 1H), 3.66-3.49 (m, 1H), 2.04 (s, 9H). ^{13}C NMR (DMSO-d_6): δ 166.18, 154.25, 153.26, 136.80, 132.05, 131.00, 128.58, 125.57, 124.36, 116.38, 71.30, 47.54, 41.63, 34.70, 32.05.

4-(4-methylpiperazin-1-yl)aniline (a4)

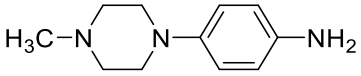

a. 1-chloro-4-nitrobenzene (4.89 g, 31 mmol) was added to 1-methylpiperazine (6.87 ml, 62 mmol) and the reaction mixture was stirred overnight at 140 °C. The reaction was stopped and evaporated *in vacuo*. The product was recrystallised from ethyl acetate to afford 1-methyl-4-(4-nitrophenyl)piperazine as a yellow powder (6.508 g, 29.45 mmol, 95% yield). MS: m/z calculated for $C_{11}H_{16}N_3O_2^+$ 222.1237 $[M+H]^+$, MS: found 222.1255 $[M+H]^+$. HPLC: t_R 0.47 (93%). Mp: 105 °C (lit. Mp= 108-110).[358] ^{1}H NMR (DMSO-d_6): δ 8.03 (d, J=9.2, 2H), 7.02 (d, J= 9.2, 2H), 3.43-3.48 (m, 4H), 2.41-2.49 (m, 4H), 2.20 (s, 3H). ^{13}C NMR (DMSO-d_6): δ 154.71, 136.60, 125.78, 112.63, 54.10, 46.22, 45.61

b. 1-methyl-4-(4-nitrophenyl)piperazine (2.21 g, 10 mmol) was suspended in 40 ml THF and stirred at room temperature until all the material dissolved, then, 0.22g (10% mol) of Pd/C was added. The reaction stirred under hydrogen gas for 48 h. The reaction mixture was filtered over celite and washed with THF. The filtrate was dried under vacuum to afford the product 4-(4-methylpiperazin-1-yl)aniline **1d** as a pink solid (1.890 g, 9.9 mmol, 99%

yield). MS: m/z calculated for $C_{11}H_{18}N_3^+$ 192.1495 $[M+H]^+$, MS: found 192.1506 $[M+H]^+$. HPLC: t_R 0.45 (90%). Mp: 90 °C (lit. Mp= 85-87).[358] ^{1}H NMR (DMSO-d_6): δ 6.67 (d, J= 8.8, 2H), 6.48 (d, J= 8.8, 2H), 4.53 (broad singlet, 2H), 2.88 (t, J= 4.8, 4H), 2.41 (t, J= 4.8, 4H), 2.19 (S, 3H). ^{13}C NMR (DMSO-d_6): δ 142.91, 142.50, 118.30, 115.22, 55.42, 50.68, 46.27.

2-{(2*R*)-2-hydroxy-3-[4-(4-methylpiperazin-1-yl)anilino]propyl} -1*H*-isoindole-1,3(2*H*)-dione (b4)

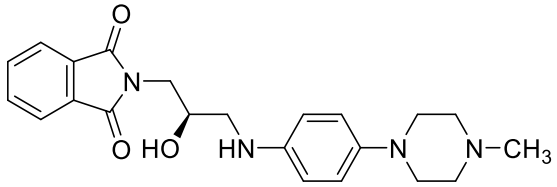

This compound was synthesised according to the general procedure A-step 1-scenario 1 by reacting **a4** (1.881 g, 9.85 mmol) with **35** (1.999 g, 9.85 mmol). The title compound (2.761 g, 7 mmol, 71% yield) was obtained as a white powder. MS: m/z calculated for $C_{22}H_{27}N_4O_3^+$ 395.2077 $[M+H]^+$, MS: found 395.2097. HPLC: t_R 2.41 (95%). Mp: 193 ˚C. ^{1}H NMR (DMSO-d_6): δ 7.85-7.79 (m, 4H), 6.89 (d, *J*= 6.8 Hz, 2H), 6.55 (d, *J*=6.8 Hz, 2H), 6.09 (t, *J*= 6.7, 1H), 4.96-5.06 (broad s,1H), 4.29-3.20 (m, 1H), 3.65-3.51 (m, 2H), 3.39-3.19 (m, 1H), 3.00- 2.91 (m, 1H), 3.45-3.36 (m, 4H), 2.30-2.18 (m, 4H), 2.17 (s, 3H). ^{13}C NMR (DMSO-d_6): δ 168.78, 154.24, 148.44, 133.17, 132.01, 123.55, 115.12, 114.80, 69.67, 56.81, 49.93, 46.23, 45.90, 42.89.

2-({(5*S*)-3-[4-(4-methylpiperazin-1-yl)phenyl]-2-oxo-1,3-oxazolidin-5-yl} methyl)-1*H*-isoindole-1,3(2*H*)-dione (c4)

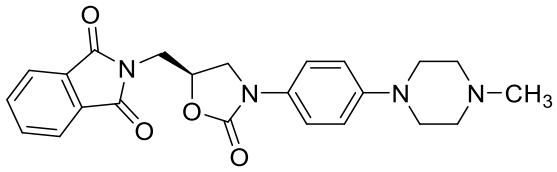

This compound was synthesised according to the general procedure A-step 2-scenario 1, starting with **b4** (2.679 g, 6.8 mmol). The title compound (2.456 g, 5.84 mmol, 86% yield) was obtained as yellow solid. MS: m/z calculated for $C_{23}H_{25}N_4O_4^+$ 421.1870 $[M+H]^+$, MS: found 421.1889 $[M+H]^+$. HPLC: t_R 2.57 min (93 %). Mp: 229 °C. $[\alpha]_D^{22}$= - 7° (c= 1, DMSO). ^{1}H NMR ($CDCl_3$): δ 7.85-7.78 (m, 2H), 7.76-7.69 (m, 2H), 7.34 (d, *J*= 8.8 Hz, 2H), 7.03 (d, *J*= 8.8 Hz, 2H), 4.90-4.81 (m, 1H), 4.45 (*J*= 6.7, 1H), 4.18-4.06 (m, 2H), 3.91 (dd, J= 10.2 Hz, 6.3 Hz, 1H), 3.58-3.44 (m, 2H), 3.40-3.26 (m, 4H), 3.18-3.11 (m,

2H), 3.01 (s, 3H). ^{13}C NMR ($CDCl_3$): δ 169.08, 155.37 ,154.33, 136.12, 134.39, 131.45, 124.18, 118.25, 117.16, 74.88, 56.80, 49.56, 47.85, 45.18, 42.96.

(5*S*)-5-(aminomethyl)-3-[4-(4-methylpiperazin-1-yl)phenyl]-1,3-oxazolidin-2-one (d4)

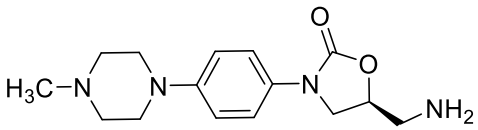

This compound was synthesised according to the general procedure A-step 3c starting with **c4** (2.394 g, 5.7 mmol). The title compound (1.338 g, 4.61 mmol, 81% yield). MS: m/z calculated for $C_{15}H_{23}N_4O_2^+$ 291.1815 $[M+H]^+$, MS: found 291.1830 $[M+H]^+$. HPLC: t_R 0.55 min (96 %). Mp: 106 °C. ^{1}H NMR (DMSO-d_6): δ 7.34 (d, J= 8.9 Hz, 2H), 7.01 (d, J= 8.9 Hz, 2H), 4.65-4.54 (m, 1H), 3.97 (dd, J= 5.3 Hz, 3.9 Hz, 1H), 3.89 (dd, J = 9.1 Hz, 6.5 Hz, 1H), 3.77 (dd, J = 5.2 Hz, 3.8 Hz, 2H), 3.75-3.54 (m, 3H), 3.18-3.12 (m, 4H), 2.81-2.77 (m, 3H), 2.44 (s, 3H).13C NMR (DMSO-d_6): δ 154.65 , 154.33, 136.50, 118.22, 116.21, 71.57, 56.93, 49.51, 48.22, 47.15, 45.35.

5-chloro-*N*-({(5*S*)-3-[4-(4-methylpiperazin-1-yl)phenyl]-2-oxo-1,3-oxazolidin-5-yl}methyl)thiophene-2-carboxamide (e4)

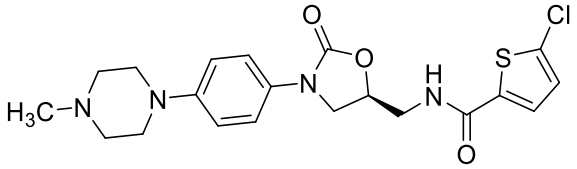

This compound was synthesised according to the general procedure A-step 4-scenario1 by reacting compound **d4** (0.145 g, 0.50 mmol) and 5-chlorothiophene-2-carbonyl chloride (0.108 g, 0.60 mmol). The title compound (0.119 g, 0.27 mmol, 55%) was obtained as a white solid. MS: m/z calculated for $C_{20}H_{24}ClN_4O_3S^+$ 435.1252 $[M+H]^+$, MS: found 435.1267 $[M+H]^+$. HPLC: t_R 2.66 min (96 %). Mp: 204 °C. $[\alpha]_D^{21}$= -77° (c= 1, DMSO). ^{1}H NMR (DMSO-d_6): δ 8.43 (t, *J*= 5.6 Hz, 1H), 8.08 (d, *J*=4.5 Hz, 1H), 7.15 (d, *J*= 8.9 Hz, 2H), 7.00 (d, *J*= 4.5 Hz, 1H), 6.91 (d, *J*= 8.9 Hz, 2H), 4.81-4.71 (m, 1H), 3.89 (dd, J= 9.2 Hz, 6.1 Hz, 1H), 3.81-3.75 (m, 1H), 3.70-3.64 (m, 2H), 3.60-3.54 (m, 2H), 3.49 (t, *J*= 5.3 Hz, 2H), 3.08-2.96 (m, 4H), 2.43 (s, 3H).^{13}C NMR (DMSO-d_6): δ 160.35, 154.69, 154.06, 141.18, 136.91, 134.56, 130.90, 127.99, 119.36, 116.77, 71.60, 56.58, 49.88, 47.29, 45.18, 41.75.

***N*-({(5*S*)-3-[4-(4-methylpiperazin-1-yl)phenyl]-2-oxo-1,3-oxazolidin-5-yl}methyl)thiophene-2-carboxamide (f4)**

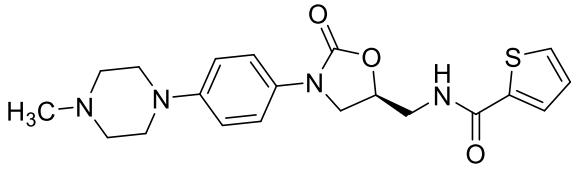

This compound was synthesised according to the general procedure A-step 4-scenario1 by reacting compound **d4** (0.145 g, 0.50 mmol) and thiophene-2-carbonyl chloride (0.087 g, 0.60 mmol). The title compound (0.114 g, 0.28 mmol, 57%) was obtained as a grey solid. MS: m/z calculated for $C_{20}H_{25}N_4O_3S^+$ 401.1642 $[M+H]^+$, MS: found 401.1653 $[M+H]^+$. HPLC: t_R 2.12 min (95%). Mp: 196 ˚C. $[\alpha]_D^{22}$= -91° (c= 1, DMSO).^{1}H NMR ($CDCl_3$): δ 7.86-7.75 (m, 2H), 7.61 (d, *J*= 8.9, 2H), 7.12 (t, *J*= 4.0 Hz, 1H), 6.91 (d, *J*= 8.9, 2H), 6.44 (t, *J*= 7.5, 1H), 4.86-4.75 (m, 1H), 4.18-4.03 (m, 1H), 3.91 (dd, J= 9.4 Hz, 6.5 Hz, 1H), 3.89-3.80 (m, 5H), 3.11-3.05 (m, 5H), 2.41 (s, 3H).^{13}C NMR ($CDCl_3$): δ 166.36, 160.52, 155.54, 150.18, 136.41, 133.46, 130.98, 128.13, 123.25, 117.13, 71.45, 56.80, 49.45, 47.18, 45.93, 41.12.

4-*tert*-butyl-*N*-({(5*S*)-3-[4-(4-methylpiperazin-1-yl)phenyl]-2-oxo-1,3-oxazolidin-5-yl}methyl)benzamide (g4)

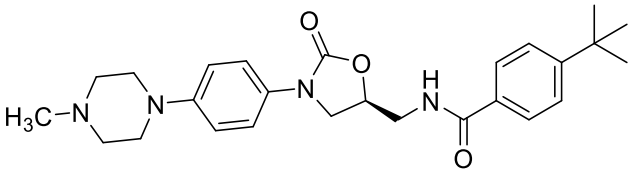

This compound was synthesised according to the general procedure A-step 4-scenario1 by reacting compound **d4** (0.159 g, 0.55 mmol) and 4-(*tert*-butyl)benzoyl chloride (0.129 g, 0.66 mmol). The title compound (0.172 g, 38 mmol, 70%) was obtained as a white solid. MS: m/z calculated for $C_{26}H_{35}N_4O_3^+$ 451.2704 $[M+H]^+$, MS: found 451.2716 $[M+H]^+$. HPLC: t_R 2.45 min (94%). Mp: 281˚C. $[\alpha]_D^{21}$= 44° (c= 1, DMSO).^{1}H NMR (DMSO-d_6): δ 8.08 (t, J = 7.8 Hz, 1H), 7.75-7.68 (m, 2H), 7.48-7.41 (m, 2H), 7.34 (d, *J*= 7.6, 2H), 7.00 (d, *J*= 7.6, 2H), 4.89-7.81 (m, 1H), 4.14–4.05 (m, 1H), 3.88 (dd, J=

9.2 Hz, 6.1 Hz, 1H), 3.66-3.44 (m, 4H), 3.40-3.27 (m, 5H), 3.01 (s, 3H), 1.34 (s, 9H).^{13}C NMR (DMSO-*d*$_6$): δ 169.61, 168.12, 158.61, 154.25, 136.80, 131.00, 128.15, 122.55, 118.89, 117.05, 71.31, 56.80, 49.90, 47.43, 45.90, 41.45, 34.72, 31.09.

4-cyano-*N*-({(5*S*)-3-[4-(4-methylpiperazin-1-yl)phenyl]-2-oxo-1,3-oxazolidin-5-yl}methyl)benzamide (h4)

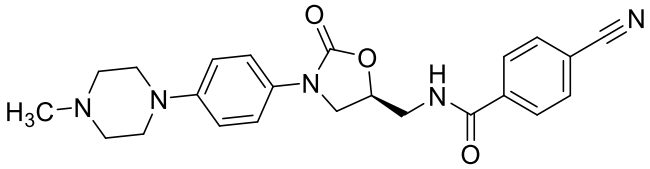

This compound was synthesised according to the general procedure A-step 4-scenario1 by reacting compound **d4** (0.116 g, 0.40 mmol) and 4-cyanobenzoyl chloride (0.079 g, 0.48 mmol). The title compound (0.118 g, 28 mmol, 71%) was obtained as a white solid. MS: m/z calculated for $C_{23}H_{26}N_5O_3^+$ 420.2030 $[M+H]^+$, MS: found 420.2049 $[M+H]^+$. HPLC: t_R 2.0 min (95%). Mp: 215 ˚C. $[\alpha]_D^{22}$= 44° (c= 1, DMSO).^{1}H NMR ($CDCl_3$): δ 8.50 (t, *J* = 7.8 Hz, 1H), 7.92 (s, 4H), 7.36 (d, *J*= 9.6, 2H), 7.03 (d, *J*= 9.6, 2H), 4.91-4.81 (m, 1H), 4.16-4.07 (m, 1H), 3.92 (dd, J= 10.6 Hz, 6.1 Hz, 1H), 3.60-3.52 (m, 4H), 3.35-3.25 (m, 5H), 3.01 (s, 3H).^{13}C NMR ($CDCl_3$): δ 166.30, 154.30, 154.15, 136.80, 132.75, 131.00, 128.58, 118.85, 118.65, 117.05, 113.95, 71.30, 56.80, 49.90, 47.43, 45.90, 41.45.

2-chloro-*N*-({(5*S*)-3-[4-(4-methylpiperazin-1-yl)phenyl]-2-oxo-1,3-oxazolidin-5-yl}methyl)benzamide (l4)

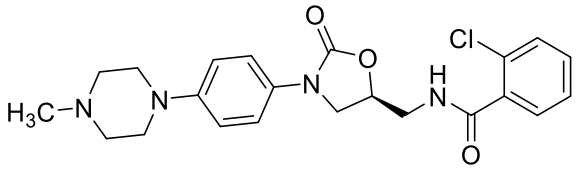

This compound was synthesised according to the general procedure A-step 4-scenario1 by reacting compound **d4** (0.145 g, 0.50 mmol) and 2-chlorobenzoyl chloride (0.105 g, 0.60 mmol). The title compound (0.130 g, 0.30 mmol, 61%) was obtained as a white solid. MS: m/z calculated for $C_{22}H_{26}ClN_4O_3^+$ 429.9245 $[M+H]^+$, MS: found 429.9261 $[M+H]^+$. HPLC: t_R 1.98 min (97%). Mp: 181 ˚C. $[\alpha]_D^{21}$= -49° (c= 1, DMSO). ^{1}H NMR (DMSO-*d*$_6$): δ 8.09 (t, *J*=6.5, 1H), 7.53-7.46 (m, 1H), 7.46-7.36 (m, 3H), 7.35-7.25 (m, 3H), 7.03-6.96 (m, 1H), 4.89-4.81 (m, 1H), 4.15 (m, 1H), 4.09 (dd, *J* = 12.5, 7.0 Hz, 1H), 3.90-3.81 (m, 2H), 3.68-3.44 (m, 4H), 3.10-3.05 (m, 4H), 2.49 (s, 3H). ^{13}C

NMR (DMSO-d_6): δ 168.66, 154.75, 154.78, 135.18, 134.34, 131.98, 131.36, 130.06, 129.23, 127.51, 118.88, 117.67, 71.34, 56.53, 49.24, 47.89, 45.67, 41.22.

tert-butyl {4-[({(5*S*)-3-[4-(4-methylpiperazin-1-yl)phenyl]-2-oxo-1,3-oxazolidin-5-yl}methyl)carbamoyl]phenyl}carbamate (o4)

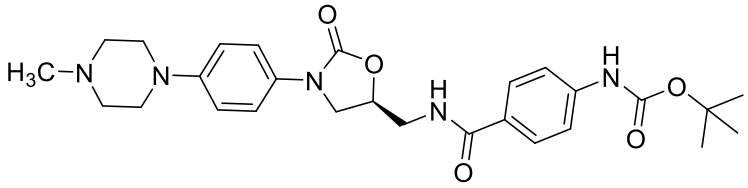

This compound was synthesised according to the general procedure A-step 4-scenario2 by reacting compound **d4** (0.145 g, 0.50 mmol) with 4-((*tert* butoxycarbonyl) amino) benzoic acid (0.118 g, 0.50 mmol). The title compound (0.216 g, 0.28 mmol, 85%) was obtained as a white solid. MS: m/z calculated for $C_{27}H_{36}N_5O_5^+$ 510.2711 $[M+H]^+$, MS: found 510.2716 $[M+H]^+$. HPLC: t_R 3.01 min (95%). Mp: 292˚C. ^{1}H NMR (DMSO-d_6): δ 8.68 (t, J= 6.0, 1H), 7.92-7.85 (m, 2H), 7.51 (d, *J*= 9.6, 2H), 7.43-7.35 (m, 2H), 7.27 (d, *J*= 9.6, 2H), 6.96 (m, 1H), 4.83-4.71 (m, 1H), 4.14-4.05 (m, 1H), 3.89 (dd, J= 9.6 Hz, 6.5 Hz, 1H), 3.73-3.64 (m, 2H), 3.62-3.54 (m, 4H), 3.40-3.27 (m, 4H), 3.01 (s, 3H), 1.42 (s, 9H). ^{13}C NMR (DMSO-d_6): δ 168.89, 166.35, 154.31, 145.01, 140.06, 136.99, 130.33, 126.18, 118.19, 117.56, 115.88, 81.61, 71.67, 56.78, 49.23, 48.10, 45.21, 41.01, 28.33.

tert-butyl ({4-[({(5*S*)-3-[4-(4-methylpiperazin-1-yl)phenyl]-2-oxo-1,3-oxazolidin-5-yl}methyl)carbamoyl]cyclohexyl}methyl)carbamate (q4)

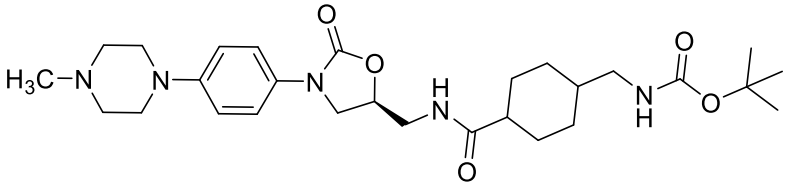

This compound was synthesised according to the general procedure A-step 4-scenario2 by reacting compound **d4** (0.145 g, 0.50 mmol) with the commercially available 4-{[(*tert*-butoxycarbonyl)amino]methyl}cyclohexane-1-carboxylic acid (0.128 g, 0.50 mmol). The title compound (0.227 g, 0.43 mmol, 86%) was obtained as an off-white solid. MS: m/z calculated for $C_{28}H_{44}N_5O_5^+$ 530.3337 $[M+H]^+$, MS: found 530.3355 $[M+H]^+$. HPLC: t_R 2.07 min (95%). Mp: 296˚C. ^{1}H NMR (DMSO-d_6) δ 8.02 (t, *J*=6.5, 1H) 7.33-7.22 (m, 2H), 7.13-7.04 (m, 2H), 6.75 (t, *J* = 7.2 Hz, 1H), 4.91-4.80 (m, 1H), 4.18-

4.09 (m, 1H), 3.93 (dd, J= 9.4 Hz, 6.3 Hz, 1H), 3.84-3.75 (m, 4H), 3.66-3.60 (m, 3H), 3.44-3.26 (m, 5H), 2.54-2.44 (m, 1H), 2.21 (s, 3H), 2.11-201 (m, 1H), 1.85-1.72 (m, 4H), 1.68-1.45 (m, 4H), 1.42 (s, 9H).^{13}C NMR (DMSO-*d*$_6$): 177.56, 157.33, 155.10, 154.54 131.33, 120.11, 117.79, 81.63, 74.95, 59.16, 52.33, 50.41, 45.95, 45.01, 44.37, 41.35, 36.81, 28.98, 28.01, 26.12.

tert-butyl {4-[({(5*S*)-3-[4-(4-methylpiperazin-1-yl)phenyl]-2-oxo-1,3-oxazolidin-5-yl}methyl)carbamoyl]cyclohexyl}carbamate (s4)

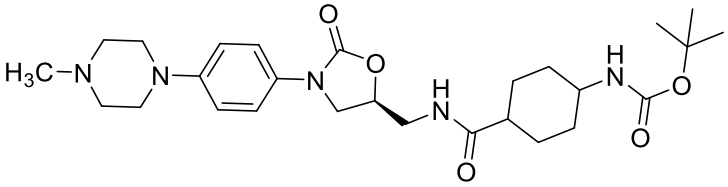

This compound was synthesised according to the general procedure A-step 4-scenario2 by reacting compound **d4** (0.145 g, 0.50 mmol) with 4-[(*tert*-butoxycarbonyl)amino] cyclohexane-1-carboxylic acid (0.121 g, 0.50 mmol). The title compound (0.206 g, 0.40 mmol, 80%) was obtained as a white solid. MS: m/z calculated for $C_{27}H_{42}N_5O_5^+$ 516.3180 $[M+H]^+$, MS: found 516.3189 $[M+H]^+$. HPLC: t_R 2.01 min (96%). Mp: 296˚C. ^{1}H NMR (DMSO-*d*$_6$): δ 8.03 (t, J= 6.5, 1H), 7.36-7.27 (m, 2H), 7.03-6.96 (m, 2H), 4.89-4.80 (m, 1H), 4.30 (d, *J* = 9.5 Hz, 1H), 4.14-4.04 (m, 1H), 3.89 (dd, J=8.9 Hz, 6.1 Hz, 1H), 3.61-3.40 (m, 5H), 3.40-3.26 (m, 6H), 3.01 (s, 3H), 2.34 (p, *J* = 6.9 Hz, 1H), 1.84-1.73 (m, 4H), 1.77-1.70 (m, 1H), 1.73-1.65 (m, 1H), 1.50-1.37 (m, 2H), 1.40 (s, 9H). ^{13}C NMR (DMSO-*d*$_6$): δ 178.84, 155.58, 154.30, 154.15, 136.80, 118.85, 117.05, 80.35, 71.30, 56.80, 51.95, 49.90, 47.43, 45.90, 45.80, 41.45, 31.73, 28.31, 25.88.

tert-butyl ({4-[({(5*S*)-3-[4-(4-methylpiperazin-1-yl)phenyl]-2-oxo-1,3-oxazolidin-5-yl}methyl)carbamoyl]phenyl}methyl)carbamate (u4)

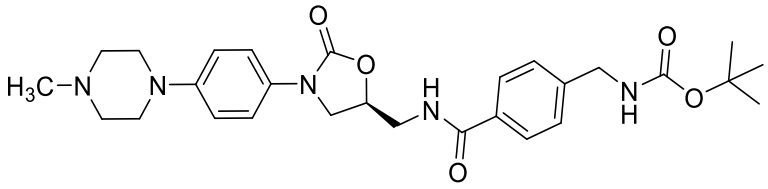

This compound was synthesised according to the general procedure A-step 4-scenario2 by reacting compound **d4** (0.145 g, 0.50 mmol) with 4-{[(*tert*-butoxycarbonyl)amino] methyl}benzoic acid (0.125 g, 0.50 mmol). The title compound (0.217 g, 0.41 mmol, 83%) was obtained as a white solid. MS: m/z calculated for $C_{28}H_{38}N_5O_5^+$ 524.2867 $[M+H]^+$, MS: found 524.2877 $[M+H]^+$.

HPLC: t_R 2.32 min (96%). Mp: 301˚C. ^{1}H NMR (DMSO-d_6) δ: ^{1}H NMR (DMSO-d_6) δ 8.03 (t, *J* = 7.8 Hz, 1H), 7.87-7.80 (m, 2H), 7.36-7.26 (m, 4H), 7.04-6.95(m, 2H), 5.22 (t, *J* = 8.5 Hz, 1H), 4.89-4.81 (m, 1H), 4.40-4.31 (m, 1H), 4.30-4.21 (m, 1H), 4.14-4.05 (m, 1H), 3.95 (dd, J= 9.0 Hz, 6.1 Hz, 1H), 3.66-3.44 (m, 4H), 3.40-3.26 (m, 6H), 2.96 (s, 3H), 1.40 (s, 9H). ^{13}C NMR (DMSO-d_6): δ 168.01, 166.95, 155.34, 154.06, 139.88, 136.19, 131.11, 127.68, 126.40, 118.29, 117.33, 79.91, 71.99, 56.71, 48.50, 46.25, 44.06, 43.96, 41.17, 28.30.

N^1-({(5*S*)-3-[4-(4-methylpiperazin-1-yl)phenyl]-2-oxo-1,3-oxazolidin-5-yl}methyl)benzene-1,4-dicarboxamide (w4)

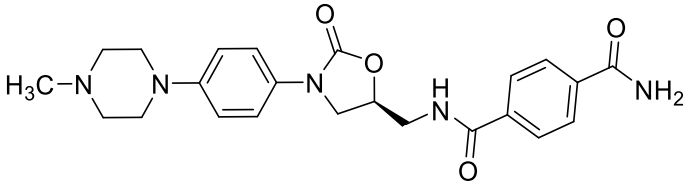

This compound was synthesised according to the general procedure A-step 4-scenario 2 by reacting compound **d4** (0.145 g, 0.50 mmol) with 4-carbamoylbenzoic acid (0.078 g, 0.50 mmol). The title compound (0.111 g, 0.25 mmol, 51%) was obtained as a white solid. MS: m/z calculated for $C_{23}H_{28}N_5O_4^+$ 438.2136 $[M+H]^+$, MS: found 438.2148 $[M+H]^+$. HPLC: t_R 2.43 min (96%). Mp: 281˚C. $[\alpha]_D^{22}$= 61° (c= 1, DMSO). ^{1}H NMR (DMSO-d_6): δ 8.46 (t, *J*= 7.8 Hz, 1H), 8.18-8.12 (m, 2H), 7.79-7.72 (m, 2H), 7.34 (d, *J*=8.5 Hz, 2H), 7.03 (d, *J*=8.5 Hz, 2H), 6.87 (s, 2H), 4.92-4.81 (m, 1H), 4.14-4.05 (m, 1H), 3.93 (dd, J= 9.2 Hz, 6.1 Hz, 1H), 3.66-3.44 (m, 4H), 3.40-3.27 (m, 6H), 3.01 (s, 3H). ^{13}C NMR (DMSO-d_6): δ 167.11, 165.01, 156.33, 154.17, 139.81, 136.23, 130.16, 127.76, 126.46, 118.34, 117.40, 71.30, 56.74, 49.92, 47.43, 45.90, 41.45.

***N*-({(5*S*)-3-[4-(4-methylpiperazin-1-yl)phenyl]-2-oxo-1,3-oxazolidin-5-yl}methyl)-4-sulfamoylbenzamide (x4)**

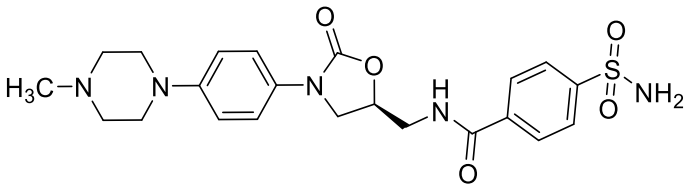

This compound was synthesised according to the general procedure A-step 4-scenario 2 by reacting compound **d4** (0.145 g, 0.50 mmol) with 4-

sulfamoylbenzoic acid (0.101 g, 0.50 mmol). The title compound (0.129 g, 0.29 mmol, 50%) was obtained as a white solid. MS: m/z calculated for $C_{22}H_{28}N_5O_5S^+$ 447.1806 $[M+H]^+$, MS: found 474.1825 $[M+H]^+$. HPLC: t_R 2.78 min (96%). Mp: 268˚C. $[\alpha]_D^{22}$= 63° (c= 1, DMSO) ^{1}H NMR (DMSO-d_6): δ 8.70 (t, *J* = 7.8 Hz, 1H), 8.25-8.17 (m, 2H), 7.93-7.86 (m, 2H), 7.34-7.27 (m, 2H), 7.24 (s, 2H), 7.03-6.96 (m, 2H), 4.89-4.81 (m, 1H), 4.16-4.07(m, 1H), 3.88 (dd, J= 8.6 Hz, 6.2 Hz, 1H), 3.66-3.44 (m, 4H), 3.40-3.27 (m, 6H), 3.03 (s, 3H). ^{13}C NMR (DMSO-d_6): δ 169.21, 167.13, 156.18, 154.17, 146.92, 136.25, 133.17, 129.18 127.76, 118.33, 117.47, 71.33, 57.94, 49.92, 47.43, 45.90, 41.45.

4-amino-*N*-({(5*S*)-3-[4-(4-methylpiperazin-1-yl)phenyl]-2-oxo-1,3-oxazolidin-5-yl}methyl)benzamide (p4)

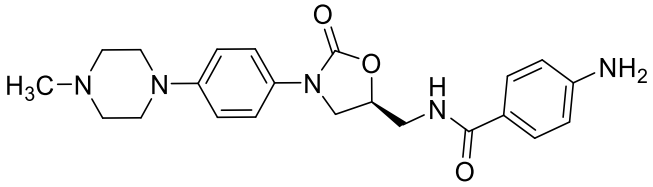

This compound was synthesised according to the general procedure A-step 5-scenario 1 starting with compound **o4** (0.166 g, 0.32 mmol). The title compound (0.116 g, 0.28 mmol, 87%) was obtained as a white solid. MS: m/z calculated for $C_{22}H_{28}N_5O_3^+$ 410.2187 $[M+H]^+$, MS: found 410.2191 $[M+H]^+$. HPLC: t_R 1.68 min (96%). Mp: 240˚C. $[\alpha]_D^{22}$= 86° (c= 1, DMSO). ^{1}H NMR (DMSO-d_6): δ 8.12 (t, *J* = 7.8 Hz, 1H), 7.57-7.49 (m, 2H), 7.34-7.27 (m, 2H), 7.23 (d, *J*= 9.1 Hz, 2H), 7.03 (d, *J*= 9.1, 2H), 4.93-4.82 (m, 1H), 4.18 (s, 2H), 4.14-4.05 (m, 1H), 3.91 (dd, J= 9.3 Hz, 6.1 Hz, 1H), 3.66-3.44 (m, 4H), 3.40-3.27 (m, 6H), 3.01 (s, 3H). ^{13}C NMR (DMSO-d_6): δ 168.91, 154.16, 153. 22, 152.45, 136.81, 128.26, 126.28, 118.35, 117.98, 112.25, 71.31, 56.55, 50.31, 47.33, 45.13, 41.45.

4-(aminomethyl)-*N*-({(5*S*)-3-[4-(4-methylpiperazin-1-yl)phenyl]-2-oxo-1,3-oxazolidin-5-yl}methyl)cyclohexane-1-carboxamide (r4)

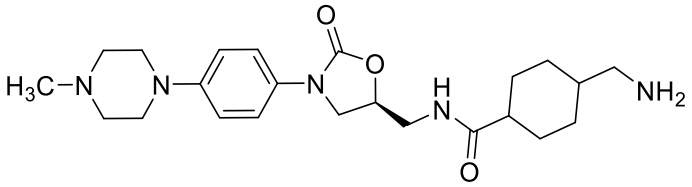

This compound was synthesised according to the general procedure A-step 5-scenario 1 starting with compound **q4** (0.167 g, 0.31 mmol). The title

compound (0.091 g, 0.21 mmol, 67%) was obtained as a white solid. MS: m/z calculated for $C_{23}H_{36}N_5O_3^+$ 430.2813 $[M+H]^+$, MS: found 430.2830 $[M+H]^+$. HPLC: t_R 2.05 min (96%). Mp: 269˚C. $[\alpha]_D^{22}$= 61° (c= 1, DMSO). ^{1}H NMR (DMSO-d_6): δ 8.01 (t, *J*= 7.5 Hz, 1H), 7.71 (d, J= 8.5 Hz , 2H), 7.50 (d, *J*= 8.5 Hz, 2H), 4.89-4.81 (m, 1H), 4.14-4.04 (m, 1H), 3.86 (dd, J= 9.5 Hz, 6.5 Hz, 1H), 3.60-3.51 (m, 1H), 3.55-3.47 (m, 2H), 3.50-3.40 (m, 1H), 3.40-3.26 (m, 6H), 3.01 (s,3), 2.78 (m, 1H), 2.56 (m, 1H), 2.38-730 (m, 1H), 1.82 (t, *J* = 6.9 Hz, 2H), 1.74 (m, 4H), 1.68-1.41 (m, 5H).^{13}C NMR (DMSO-d_6): δ 178.77, 155.41, 154.57, 136.15, 118.16, 117.68, 71.84, 56.31, 50.22, 49.61, 47.63, 45.18, 44.22, 42.63, 41.86, 28.88, 26.15.

4-amino-*N*-({(5*S*)-3-[4-(4-methylpiperazin-1-yl)phenyl]-2-oxo-1,3-oxazolidin-5-yl}methyl)cyclohexane-1-carboxamide (t4)

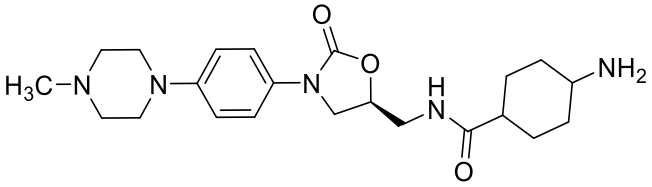

This compound was synthesised according to the general procedure A-step 5-scenario 1 starting with compound **s4** (0.151 g, 0.29 mmol). The title compound (0.088 g, 0.21 mmol, 73%) was obtained as a white solid. MS: m/z calculated for $C_{22}H_{34}N_5O_3^+$ 416.2656 $[M+H]^+$, MS: found 416.2676 $[M+H]^+$. HPLC: t_R 1.98 min (96%). Mp: 254˚C. $[\alpha]_D^{21}$= 89° (c= 1, DMSO). ^{1}H NMR (DMSO-d_6) δ 8.03 (t, J= 7.6 Hz, 1H), 7.36-7.27 (m, 2H), 7.08-6.91 (m, 2H), 4.96-4.85 (m, 1H), 4.14-4.04 (m, 1H), 3.87 (dd, J= 9.4 Hz, 6.1 Hz, 1H), 3.60-3.50 (m, 2H), 3.54-3.47 (m, 1H), 3.50-3.40 (m, 1H), 3.40-3.26 (m, 6H), 3.08 (d, *J* = 7.3 Hz, 2H), 3.01 (s, 3H), 2.84-2.69 (m, 1H), 2.32 (m, 1H), 1.80-176 (m, 4H), 1.66-159 (m, 2H), 1.55-146 (m, 2H). ^{13}C NMR (DMSO-d_6): δ 178.28, 156.31, 156.06, 136.75, 118.18, 117.39, 71.01, 56.73, 51.29, 49.63, 47.62, 45.96, 45.12, 41.56, 33.96, 25.26.

4-(aminomethyl)-*N*-({(5*S*)-3-[4-(4-methylpiperazin-1-yl)phenyl]-2-oxo-1,3-oxazolidin-5-yl}methyl)benzamide (v4)

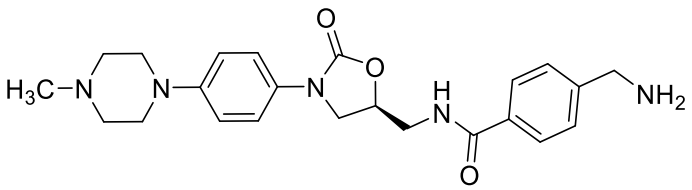

This compound was synthesised according to the general procedure A-step 5-scenario 1 starting with compound **u4** (0.157 g, 0.30 mmol). The title compound (0.101 g, 0.24 mmol, 80%) was obtained as a white solid. MS: m/z calculated for $C_{23}H_{30}N_5O_4^+$ 424.2343 $[M+H]^+$, MS: found 424.2355 $[M+H]^+$. HPLC: t_R 1.88 min (95%). Mp: 233˚C. $[\alpha]_D^{22}$= -41° (c= 1, DMSO). ^{1}H NMR (DMSO-d_6): δ 8.61 (t, *J*= 6.7, 2H), 8.01 (t, *J* = 7.8 Hz, 1H), 7.93-7.85 (m, 2H), 7.36-7.27 (m, 2H), 7.20 (d, J= 8.5 Hz, 2H), 7.10 (d, J= 8.5 Hz, 2H), 4.89-4.81 (m, 1H), 4.14-4.05 (m, 1H), 3.87 (dd, J= 9.3 Hz, 5.9 Hz, 1H), 3.92-3.80 (m, 2H), 3.66-3.44 (m, 4H), 3.40-3.26 (m, 6H), 3.04 (s, 3H). ^{13}C NMR (DMSO-d_6): δ 169.11, 156.30, 154.12, 143.56, 136.17, 131.93, 128.98, 127.44, 118.87, 117.47, 71.97, 56.56, 49.52, 47.18, 46.45, 45.60, 41.80.

1-(4-aminophenyl)-4-methylpiperazin-2-one (a5)

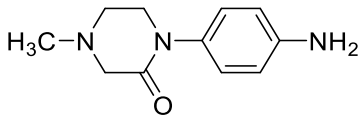

This compound was synthesised according to the general procedure F-step 2 starting with the commercially available 4-methylpiperazin-2-one (1.71 g, 15 mmol). The titled compound (1.721 g, 8.40 mmol, 56%) was obtained as a yellow solid. MS: m/z calculated for $C_{11}H_{16}N_3O^+$ 206.1288 $[M+H]^+$, MS: found 206.1304 $[M+H]^+$. HPLC: t_R 0.43 min (96%). Mp: 155 °C (lit. Mp= 158-160).[359] ^{1}H NMR (DMSO-d_6): δ 6.97 (d, *J*= 8.6 Hz, 2H), 6.74 (d, *J*= 8.6 Hz, 2H), 3.62 (t, *J* = 7.1 Hz, 4H), 3.42 (s, 2H), 2.83 (t, *J* = 7.1 Hz, 2H), 2.25 (s, 3H). ^{13}C NMR (DMSO-d_6): δ 166.19, 142.20, 141.09, 118.23, 117.10, 57.16, 54.33, 47.56, 44.38.

2-{(2*R*)-2-hydroxy-3-[4-(4-methyl-2-oxopiperazin-1-yl)anilino]propyl}-1*H*-isoindole-1,3(2*H*)-dione (b5)

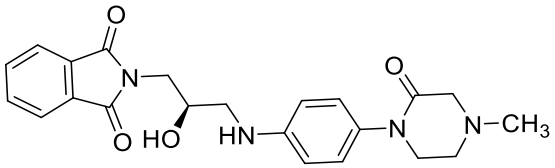

This compound was synthesised according to the general procedure A-step 1-scenario 1 by reacting **a5** (1.642 g, 8 mmol) with **35** (1.624 g, 8 mmol). The title compound (2.679 g, 6.50 mmol, 82% yield) was obtained as a white powder. MS: m/z calculated for $C_{22}H_{25}N_4O_4^+$ 409.1870 $[M+H]^+$, MS: found

409.1886. HPLC: t_R 1.83 min (96%). Mp: 196 ˚C. ^{1}H NMR (DMSO-d_6): δ 7.85-7.78 (m, 2H), 7.76-7.69 (m, 2H), 7.08 (d, *J*= 6.8 Hz, 2H), 6.56 (d, *J*=6.8 Hz, 2H), 6.09 (t, *J* = 6.7 Hz, 1H), 5.07-4.97 (broad s, 1H), 4.29-4.22 (m, 1H), 4.00 (dd, *J* = 12.4, 6.9 Hz, 1H), 3.92 (d, *J* = 6.7 Hz, 1H), 3.90-3.79 (m, 2H), 3.44-3.33 (m, 3H), 3.28 (dt, *J* = 12.4, 6.9 Hz, 1H), 2.90-2.75 (m, 2H), 2.25 (s, 3H). ^{13}C NMR (DMSO-d_6): δ 168.89, 166.18, 148.44, 142.68, 134.27, 131.61, 123.53, 117.23, 115.12, 70.61, 57.93, 54.77, 48.91, 47.21, 44.91, 42.90.

2-({(5*S*)-3-[4-(4-methyl-2-oxopiperazin-1-yl)phenyl]-2-oxo-1,3-oxazolidin-5-yl}methyl)-1*H*-isoindole-1,3(2*H*)-dione (c5)

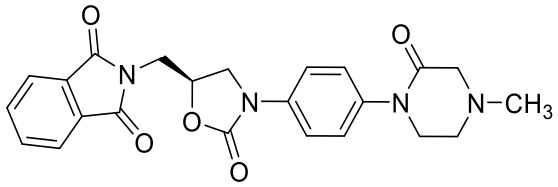

This compound was synthesised according to the general procedure A-step 2-scenario 1, starting with **b5** (2.570 g, 6.30 mmol). The title compound (2.242 g, 5.1 mmol, 82% yield) was obtained as yellow solid. MS: m/z calculated for $C_{23}H_{23}N_4O_5^+$ 435.4595 $[M+H]^+$, MS: found 435.4611 $[M+H]^+$. HPLC: t_R 1.96 min (96 %). Mp: 198 °C. ^{1}H NMR (DMSO-d_6): δ 7.87-7.77 (m, 2H), 7.77-7.70 (m, 2H), 7.36 (d, *J*= 8.5 Hz, 2H), 7.17 (d, *J*= 8.5 Hz, 2H), 4.92-4.82 (m, 1H), 4.45-4.36 (m, 1H), 4.18-4.08 (m, 2H), 3.91-3.78 (m, 3H), 3.42 (s, 2H), 2.94-2.74 (m, 2H), 2.25 (s, 3H). ^{13}C NMR ($CDCl_3$): δ 168.18, 166.45, 154.15, 142.29, 136.14, 134.41, 131.46, 123.27, 118.25, 117.18, 74.25, 57.12, 54.26, 49.51, 47.84, 44.18, 42.87.

1-{4-[(5*S*)-5-(aminomethyl)-2-oxo-1,3-oxazolidin-3-yl]phenyl}-4-methylpiperazin-2-one (d5)

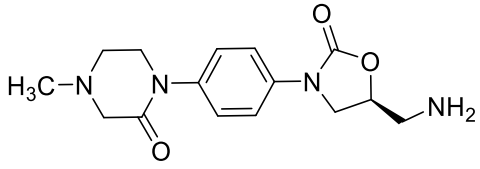

This compound was synthesised according to the general procedure A-step 3b starting with **c5** (2.126 g, 4.9 mmol). The title compound (0.834 g, 2.74 mmol, 56% yield). MS: m/z calculated for $C_{15}H_{21}N_4O_3^+$ 305.1608 $[M+H]^+$, MS: found 305.1627 $[M+H]^+$. HPLC: t_R 0.34 min (97 %). Mp: 108 °C. ^{1}H NMR (DMSO-d_6): δ 7.40 (d, J= 8.6 Hz, 2H), 7.07 (d, J= 8.6 Hz, 2H), 4.88-4.79 (m, 1H), 3.96 (dd, J= 5.2 Hz, 3.5 Hz, 1H), 3.87 (dd, J = 8.8 Hz, 6.3 Hz, 1H), 3.71` (dd, J = 5.2 Hz, 3.3 Hz, 2H), 3.42 (s, 2H), 3.01-2.65 (m, 4H), 2.36 (t, *J* = 7.5

Hz, 2H), 2.25 (s, 3H). ^{13}C NMR (DMSO-d_6): δ 169.85, 166.62, 155.21, 143.00, 137.86, 134.21, 131.95, 124.40, 119.85, 118.06, 74.21, 57.83, 55.77, 48.43, 47.41, 44.28, 42.71.

5-chloro-*N*-({(5*S*)-3-[4-(4-methyl-2-oxopiperazin-1-yl)phenyl]-2-oxo-1,3-oxazolidin-5-yl}methyl)thiophene-2-carboxamide (e5)

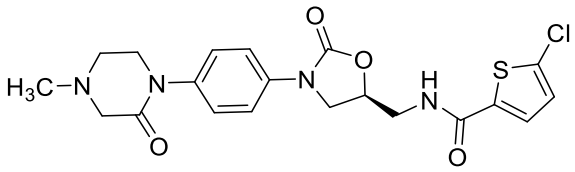

This compound was synthesised according to the general procedure A-step 4-scenario1 by reacting compound **d5** (0.106 g, 0.35 mmol) and 5-chlorothiophene-2-carbonyl chloride (0.076 g, 0.42 mmol). The title compound (0.087 g, 0.19 mmol, 56%) was obtained as a white solid. MS: m/z calculated for $C_{20}H_{22}ClN_4O_4S^+$ 449.1045 $[M+H]^+$, MS: found 494.1065 $[M+H]^+$. HPLC: t_R 2.41 min (95 %). Mp: 194 °C. $[\alpha]_D^{21}$= -89° (c= 1, DMSO). ^{1}H NMR (DMSO-d_6): δ 8.36 (t, *J*= 5.6 Hz, 1H), 8.04 (d, *J*=4.5 Hz, 1H), 7.09 (d, *J*= 8.8 Hz, 2H), 6.94 (d, *J*= 4.5 Hz, 1H), 6.86 (d, *J*= 8.8 Hz, 2H), 4.81-4.71 (m, 1H), 3.89 (dd, J= 9.1 Hz, 6.1 Hz, 1H), 3.87 (t, *J* = 7.1 Hz, 2H), 3.83-3.74 (m, 1H), 3.55 (t, *J* = 7.1 Hz, 2H), 3.42 (s, 2H), 2.94-2.74 (m, 2H), 2.25 (s, 3H). ^{13}C NMR (DMSO-d_6): δ 168.63, 161.73, 156.20, 143.91, 142.83, 135.81, 133.25, 128.11, 127.50, 118.90, 117.15, 71.36, 56.80, 54.78, 48.41, 47.52, 43.28, 41.50.

***N*-({(5*S*)-3-[4-(4-methyl-2-oxopiperazin-1-yl)phenyl]-2-oxo-1,3-oxazolidin-5-yl}methyl)thiophene-2-carboxamide (f5)**

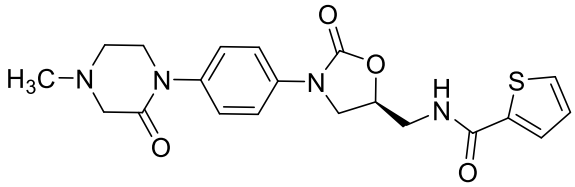

This compound was synthesised according to the general procedure A-step 4-scenario1 by reacting compound **d5** (0.091 g, 0.30 mmol) and thiophene-2-carbonyl chloride (0.052 g, 36 mmol). The title compound (0.090 g, 0.21 mmol, 73%) was obtained as a grey solid. MS: m/z calculated for $C_{20}H_{23}N_4O_4S^+$ 415.1435 $[M+H]^+$, MS: found 415.11540 $[M+H]^+$. HPLC: t_R 2.10 min (96%). Mp: 190 ˚C. $[\alpha]_D^{22}$= -63° (c= 1, DMSO).^{1}H NMR ($CDCl_3$): δ 8.13-8.01 (m, 2H), 7.96 (d, *J*= 8.8, 2H), 7.43 (t, *J*= 4.1 Hz, 1H), 7.06 (d, *J*=

8.8, 2H), 6.64 (t, *J*= 7.5, 1H), 4.89-4.81 (m, 1H), 3.88 (dd, J= 9.2 Hz, 6.3 Hz, 1H),, 3.84 (t, *J* = 7.0 Hz, 2H), 3.82-3.72(m, 1H), 3.56 (t, *J* = 7.0 Hz, 2H), 3.45 (s, 2H), 2.90-2.70 (m, 2H), 2.26 (s, 3H). ^{13}C NMR ($CDCl_3$): δ 167.61, 161.56, 156.14, 142.93, 138.51, 131.83, 131.98, 129.51, 128.21, 118.90, 117.06, 71.31, 57.83, 54.78, 48.53, 47.42, 44.27, 41.55.

4-*tert*-butyl-*N*-({(5*S*)-3-[4-(4-methyl-2-oxopiperazin-1-yl)phenyl]-2-oxo-1,3-oxazolidin-5-yl}methyl)benzamide (g5)

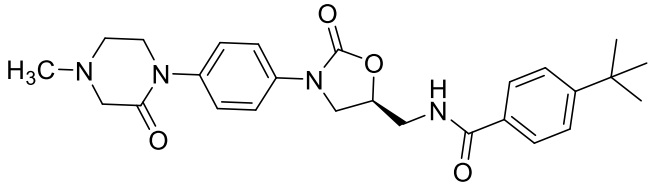

This compound was synthesised according to the general procedure A-step 4-scenario1 by reacting compound **d5** (0.091 g, 0.30 mmol) and 4-(*tert*-butyl)benzoyl chloride (0.070 g, 36 mmol) . The title compound (0.111g, 0.24 mmol, 81%) was obtained as a white solid. MS: m/z calculated for $C_{26}H_{33}N_4O_4^+$ 465.2496 $[M+H]^+$, MS: found 465.2506 $[M+H]^+$. HPLC: t_R 2.22 min (98%). Mp: 241˚C. $[\alpha]_D^{21}$= 96° (c= 1, DMSO). ^{1}H NMR (DMSO-*d*$_6$): δ 8.12 (t, J = 7.5 Hz, 1H), 7.79-7.65 (m, 2H), 7.50-7.40 (m, 2H), 7.36 (d, *J*= 7.5 Hz, 2H), 7.00 (d, *J*= 7.5 Hz, 2H), 4.91-4.82 (m, 1H), 3.86 (dd, J= 9.1 Hz, 6.1 Hz, 1H), 3.88 (t, *J* = 7.1 Hz, 2H), 3.86-3.76 (m, 1H), 3.61-3.56 (m, 2H), 3.43 (s, 2H), 2.95-2.75(m, 2H), 2.26 (s, 3H), 1.36 (s, 9H). ^{13}C NMR (DMSO-*d*$_6$): δ 168.15, 167.31, 156.33, 152.27, 142.94, 136.81, 133.15, 128.60, 125.53, 118.85, 117.35, 71.30, 57.14, 55.73, 48.51, 47.41, 45.28, 42.46, 35.73, 33.10

4-cyano-*N*-({(5*S*)-3-[4-(4-methyl-2-oxopiperazin-1-yl)phenyl]-2-oxo-1,3-oxazolidin-5-yl}methyl)benzamide (h5)

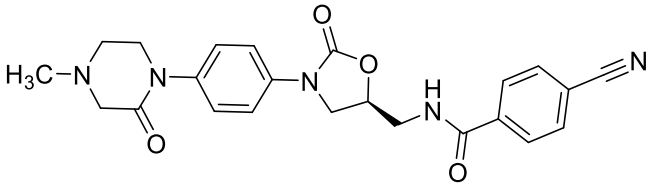

This compound was synthesised according to the general procedure A-step 4-scenario 1 by reacting compound **d5** (0.182 g, 0.60 mmol) and 4-cyanobenzoyl chloride (0.118 g, 0.72 mmol). The title compound (0.207 g, 0.47 mmol, 80%) was obtained as a white solid. MS: m/z calculated for $C_{23}H_{24}N_5O_4^+$ 434.1823 $[M+H]^+$, MS: found 434.1833 $[M+H]^+$. HPLC: t_R 1.98 min (95%). Mp: 214 ˚C. $[\alpha]_D^{22}$= 41° (c= 1, DMSO).^{1}H NMR ($CDCl_3$): δ 8.53 (t, *J* = 7.8 Hz, 1H),

8.09-8.1 (m, 2H), 7.93-7.86 (m, 2H), 7.43(d, *J*= 9.5, 2H), 7.13 (d, *J*= 9.5, 2H), 4.91-4.81 (m, 1H), 3.87 (dd, J= 9.4 Hz, 6.0 Hz, 1H),, 3.86 (t, *J* = 7.0 Hz, 2H), 3.82-3.71 (m, 1H), 3.65-3.57 (m, 2H), 3.46 (s, 2H), 2.90-2.70 (m, 2H), 2.23 (s, 3H).^{13}C NMR ($CDCl_3$): δ 168.66, 156.31, 154.15, 142.94, 136.80, 132.75, 131.00, 128.56, 119.98, 118.01, 117.25, 115.92, 71.30, 57.75, 56.89, 47.41, 45.66, 43.26, 42.46.

2-chloro-*N*-({(5*S*)-3-[4-(4-methyl-2-oxopiperazin-1-yl)phenyl]-2-oxo-1,3-oxazolidin-5-yl}methyl)benzamide (l5)

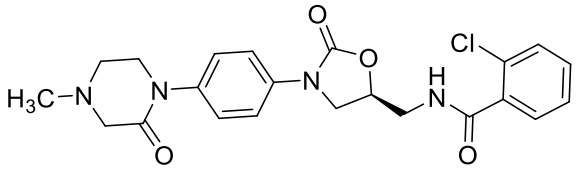

This compound was synthesised according to the general procedure A-step 4-scenario1 by reacting compound **d5** (0.090 g, 0.30 mmol) and 2-chlorobenzoyl chloride (0.063 g, 0.36 mmol). The title compound (0.081, 0.18 mmol, 62%) was obtained as a white solid. MS: m/z calculated for $C_{22}H_{24}ClN_4O_4^+$ 443.1481 $[M+H]^+$, MS: found 443.1499 $[M+H]^+$. HPLC: t_R 1.76 min (97%). Mp: 183 ˚C. $[\alpha]_D^{21}$= -51° (c= 1, DMSO). ^{1}H NMR (DMSO-d_6): δ 8.04 (t, *J*= 6.6, 1H), 7.63-7.56 (m, 1H), 7.43-7.32 (m, 3H), 7.36-7.24 (m, 3H), 7.08-6.99 (m, 1H), 4.94-4.85 (m, 1H), 4.22-4.13 (m, 1H), 3.96-3.90 (m, 2H), 3.87 (dd, J= 9.1 Hz, 6.1 Hz, 1H), 3.78-3.57 (m, 2H), 3.42 (s, 2H), 2.94-2.74 (m, 2H), 2.25 (s, 3H).^{13}C NMR (DMSO-d_6): δ 176.33, 168.71, 156.35, 141.94, 139.81, 138.22, 133.43, 129.89, 128.16, 127.98, 127.07, 118.98, 117.09, 74.61, 57.68, 54.77, 50.72, 49.75, 47.42, 44.27.

***tert*-butyl {4-[({(5*S*)-3-[4-(4-methylpiperazin-1-yl)phenyl]-2-oxo-1,3-oxazolidin-5-yl}methyl)carbamoyl]phenyl}carbamate (o5)**

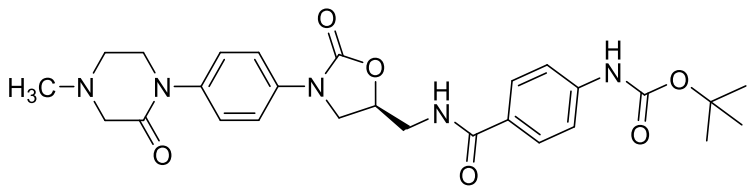

This compound was synthesised according to the general procedure A-step 4-scenario 2 by reacting compound **d5** (0.152 g, 0.50 mmol) with 4-((*tert* butoxycarbonyl) amino) benzoic acid (0.118 g, 0.50 mmol). The title compound (0.219 g, 0.42 mmol, 84%) was obtained as a white solid. MS: m/z calculated for $C_{27}H_{34}N_5O_6^+$ 524.2504 $[M+H]^+$, MS: found 524.2514 $[M+H]^+$.

HPLC: t_R 2.96 min (96%). Mp: 281˚C. ^{1}H NMR (DMSO-d_6): δ 8.45 (t, J= 6.5 Hz, 1H), 7.93-7.84 (m, 2H), 7.56 (d, *J*= 9.0 Hz, 2H), 7.45-7.33 (m, 2H), 7.30 (d, *J*= 9.0 Hz, 2H), 7.00 (m, 1H), 4.89-4.81 (m, 1H), 3.89 (dd, J= 9.2 Hz, 6.1 Hz, 1H), 3.87 (t, *J* = 7.1 Hz, 2H), 3.83-3.74 (m, 1H), 3.64-3.56 (m, 2H), 3.40 (s, 2H), 2.93–2.72 (m, 2H), 2.21 (s, 3H), 1.41 (s, 9H). ^{13}C NMR (DMSO-*d6*): δ 168.63, 166.31, 156.25, 151.31, 143.93, 137.81, 137.08, 128.71, 127.66, 119.07, 117.22, 116.15, 82.61, 71.37, 57.66, 54.77, 48.43, 47.47, 44.98, 41.40, 27.89.

tert-butyl ({4-[({(5*S*)-3-[4-(4-methyl-2-oxopiperazin-1-yl)phenyl]-2-oxo-1,3-oxazolidin-5-yl}methyl)carbamoyl]cyclohexyl}methyl)carbamate (q5)

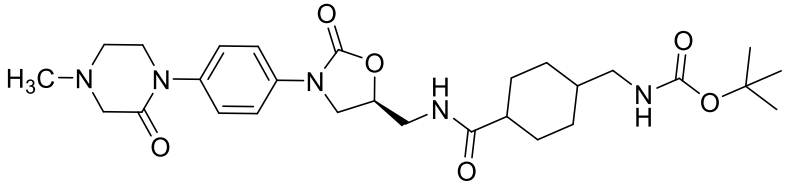

This compound was synthesised according to the general procedure A-step 4-scenario 2 by reacting compound **d5** (0.152 g, 0.50 mmol) with the commercially available 4-{[(*tert*-butoxycarbonyl)amino]methyl}cyclohexane-1-carboxylic acid (0.128 g, 0.50 mmol). The title compound (0.214 g, 0.39 mmol, 79%) was obtained as an off-white solid. MS: m/z calculated for $C_{28}H_{42}N_5O_6^+$ 544.3130 $[M+H]^+$, MS: found 544.3147 $[M+H]^+$. HPLC: t_R 2.00 min (96%). Mp: 250˚C. ^{1}H NMR (DMSO-d_6): δ 8.01 (t, *J*=6.5 Hz, 1H), 7.33-7.23 (m, 2H), 7.14-7.05 (m, 2H), 6.76 (t, *J* = 7.2 Hz, 1H), 4.90-4.81 (m, 1H), 4.14-4.04 (m, 1H), 3.89 (dd, J= 9.4 Hz, 6.2 Hz, 1H), 3.77-3.68 (m, 1H), 3.60-3.40 (m, 2H), 3.42 (s, 2H), 3.26-3.20 (m, 1H), 3.17-3.08 (m, 1H), 2.94-2.74 (m, 2H), 2.44-2.35 (m, 1H), 2.25 (s, 3H), 2.15-2.05 (m, 1H), 1.83–1.71 (m, 2H), 1.71-1.54 (m, 4H), 1.54-1.41 (m, 2H), 1.39 (s, 9H). ^{13}C NMR (DMSO-d_6): δ 178.81, 165.61, 156.15, 154.15, 145.33, 135.81, 118.85, 117.06, 79.81, 71.31, 57.20, 54.71, 48.43, 47.41, 45.80, 44.33, 43.40, 41.4`, 35.37, 28.19, 26.31, 25.99.

tert-butyl {4-[({(5*S*)-3-[4-(4-methyl-2-oxopiperazin-1-yl)phenyl]-2-oxo-1,3-oxazolidin-5-yl}methyl)carbamoyl]cyclohexyl}carbamate (s5)

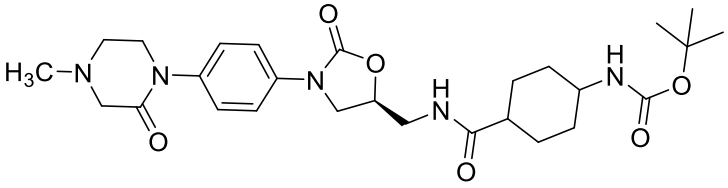

This compound was synthesised according to the general procedure A-step 4-scenario2 by reacting compound **d4** (0.152 g, 0.50 mmol) with 4-[(tert-butoxycarbonyl)amino] cyclohexane-1-carboxylic acid (0.121 g, 0.50 mmol) . The title compound (0.203 g, 0.38 mmol, 77%) was obtained as a white solid. MS: m/z calculated for $C_{27}H_{40}N_5O_6^+$ 530.2973 $[M+H]^+$, MS: found 530.2977 $[M+H]^+$. HPLC: t_R 2.01 min (96%). Mp: 245˚C. ^{1}H NMR (DMSO-d_6): δ 8.01 (t, J= 6.5 Hz, 1H), 7.35-7.26(m, 2H), 7.05-6.93 (m, 2H), 4.91-4.81 (m, 1H), 4.48 (d, *J* = 9.7 Hz, 1H), 3.92 (dd, J= 9.3 Hz, 6.2 Hz, 1H), 3.87 (t, *J* = 7.1 Hz, 2H), 3.77-3.68 (m, 1H), 3.61-3.52 (m, 1H), 3.56-3.49 (m, 1H), 3.47-3.40 (m, 1H), 3.38 (s, 2H), 2.94-2.74 (m, 2H), 2.44-2.33 (m, 1H), 2.25 (s, 3H), 1.86-1.58 (m, 6H), 1.52-1.36 (m, 2H), 1.42 (s, 9H). ^{13}C NMR (DMSO-d_6): δ 178.82, 167.66, 156.60, 154.14, 141.93, 137.8`, 119.90, 118.01, 81.56, 70.31, 58.35, 56.78, 51.98, 47.44, 47.41, 46.81, 44.33, 41.41, 33.78, 28.32, 25.70.

***tert*-butyl ({4-[({(5*S*)-3-[4-(4-methyl-2-oxopiperazin-1-yl)phenyl]-2-oxo-1,3-oxazolidin-5-yl}methyl)carbamoyl]phenyl}methyl)carbamate (u5)**

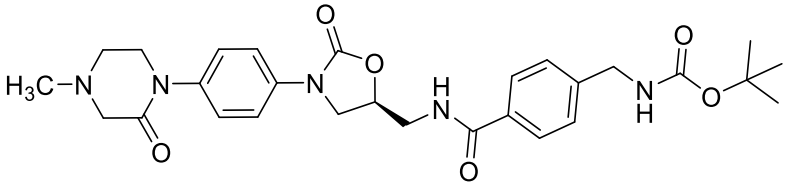

This compound was synthesised according to the general procedure A-step 4-scenario2 by reacting compound **d4** (0.152 g, 0.50 mmol) with 4-{[(tert-butoxycarbonyl)amino] methyl}benzoic acid (0.125 g, 0.50 mmol). The title compound (204 g, 0.38 mmol, 78%) was obtained as a white solid. MS: m/z calculated for $C_{28}H_{36}N_5O_6^+$ 538.2660 $[M+H]^+$, MS: found 538.2675 $[M+H]^+$. HPLC: t_R 2.22 min (96%). Mp: 270˚C. ^{1}H NMR (DMSO-d_6) δ: ^{1}H NMR (DMSO-d_6): δ 8.06 (t, *J* = 7.7 Hz, 1H), 7.87–7.80 (m, 2H), 7.35–7.25 (m, 4H), 7.05–6.96(m, 2H), 5.21 (t, *J* = 8.5 Hz, 1H), 4.89-4.81 (m, 1H), 4.48-4.41 (m, 1H), 4.38-4.31 (m, 1H), 3.93 (dd, J= 9.1 Hz, 6.5Hz, 1H), 3.87 (t, *J* = 7.1 Hz, 2H), 3.83-3.74 (m, 1H), 3.63-3.56 (m, 2H), 3.41 (s, 2H), 2.93-2.73 (m, 2H), 2.23 (s, 3H), 1.39 (s, 9H). ^{13}C NMR (DMSO-d_6): δ 166.61, 166.34, 156.12, 155.55, 141.95, 140.92, 135.81, 131.00, 129.51, 128.61, 118.84, 117.06, 80.09, 71.36, 57.01, 55.75, 48.47, 47.40, 44.30, 43.99, 41.43, 28.36.

N^1-({(5*S*)-3-[4-(4-methyl-2-oxopiperazin-1-yl)phenyl]-2-oxo-1,3-oxazolidin-5-yl}methyl)benzene-1,4-dicarboxamide (w5)

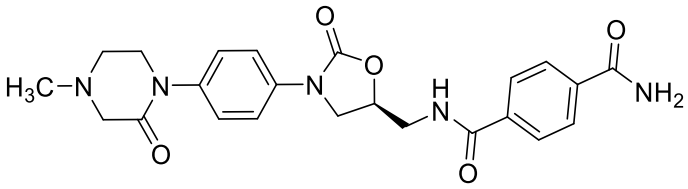

This compound was synthesised according to the general procedure A-step 4-scenario2 by reacting compound **d4** (0.152 g, 0.50 mmol) with 4-carbamoylbenzoic acid (0.082 g, 0.50 mmol). The title compound (0.112 g, 0.24 mmol, 50%) was obtained as a white solid. MS: m/z calculated for $C_{23}H_{26}N_5O_5^+$ 452.1928 $[M+H]^+$, MS: found 452.1947 $[M+H]^+$. HPLC: t_R 2.12 min (96%). Mp: 245˚C. $[\alpha]_D^{22}$= 56° (c= 1, DMSO) ^{1}H NMR (DMSO-d_6): δ 8.45 (t, *J*= 7.8 Hz, 1H), 8.20-8.11 (m, 2H), 7.80-7.73 (m, 2H), 7.35 (d, *J*=8.5 Hz, 2H), 7.05 (d, *J*=8.5 Hz, 2H), 6.88 (s, 2H), 4.92-4.81 (m, 1H), 3.91 (dd, J= 9.1 Hz, 6.1 Hz, 1H), 3.85 (t, *J* = 7.1 Hz, 2H), 3.82-3.73 (m, 1H), 3.63-3.55 (m, 2H), 3.42 (s, 2H), 2.94-2.75 (m, 2H), 2.26 (s, 3H). ^{13}C NMR (DMSO-d_6): δ 168.81, 167.64, 166.31, 154.19, 141.92, 136.85 ,136.13, 131.12, 128.59, 127.99, 118.83, 117.07, 71.33, 57.64 ,54.72, 48.13, 47.45, 44.22, 41.44.

***N*-({(5*S*)-3-[4-(4-methyl-2-oxopiperazin-1-yl)phenyl]-2-oxo-1,3-oxazolidin-5-yl}methyl)-4-sulfamoylbenzamide (x5)**

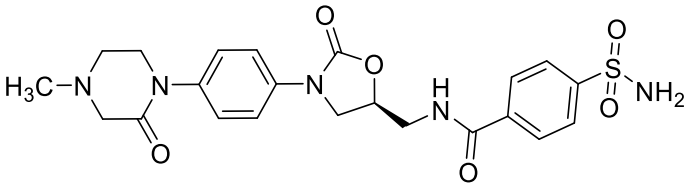

This compound was synthesised according to the general procedure A-step 4-scenario2 by reacting compound **d5** (0.152 g, 0.50 mmol) with 4-sulfamoylbenzoic acid (0.101 g, 0.50 mmol). The title compound (0.126 g, 0.26, 52%) was obtained as a white solid. MS: m/z calculated for $C_{22}H_{26}N_5O_6S^+$ 488.1598 $[M+H]^+$, MS: found 488.1614 $[M+H]^+$. HPLC: t_R 2.50 min (95%). Mp: 267˚C. $[\alpha]_D^{22}$= 54° (c= 1, DMSO). ^{1}H NMR (DMSO-d_6): δ 8.73 (t, *J* = 7.8 Hz, 1H), 8.26-8.19 (m, 2H), 7.92-7.87 (m, 2H), 7.37-7.26 (m, 2H), 7.28 (s, 2H), 7.05-6.98 (m, 2H), 4.97-4.87 (m, 1H), 3.85 (dd, J= 9.3 Hz, 6.1 Hz, 1H), 3.83 (t, *J* = 7.1 Hz, 2H), 3.81-3.72 (m, 1H), 3.63-3.55 (m, 2H), 3.44 (s, 2H), 2.96-2.76 (m, 2H), 2.23 (s, 3H). ^{13}C NMR (DMSO-d_6): δ 168.81, 166.31, 155.16, 145.19, 142.92, 136.81, 133.89, 129.99, 128.00, 118.86, 117.25, 72.88, 57.63, 54.71, 48.41, 47.46, 44.98, 41.42.

4-amino-*N*-({(5*S*)-3-[4-(4-methyl-2-oxopiperazin-1-yl)phenyl]-2-oxo-1,3-oxazolidin-5-yl}methyl)benzamide (p5)

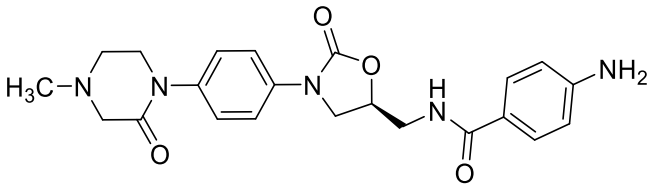

This compound was synthesised according to the general procedure A-step 5-scenario 1 starting with compound **o5** (0.169 g, 0.32 mmol). The title compound (0.075 g, 0.17 mmol, 55%) was obtained as a white solid. MS: m/z calculated for $C_{22}H_{26}N_5O_4^+$ 424.1979 $[M+H]^+$, MS: found 424.1987 $[M+H]^+$. HPLC: t_R 1.48 min (97%). Mp: 222˚C. $[\alpha]_D^{22}$= 31° (c= 1, DMSO). ^{1}H NMR (DMSO-d_6): δ 8.10 (t, *J* = 7.8 Hz, 1H), 7.56-7.50 (m, 2H), 7.36-7.28 (m, 2H), 7.25 (d, *J*= 9.1 Hz, 2H), 7.05 (d, *J*= 9.1, 2H), 4.93-4.82 (m, 1H), 4.18 (s, 2H), 4.14-4.05 (m, 1H), 3.99 (dd, J= 9.2 Hz, 6.4 Hz, 1H), 3.66-3.44 (m, 4H), 3.40-3.27 (m, 4H), 3.01 (s, 3H). ^{13}C NMR (DMSO-d_6): δ 167.61, 166.31, 154.18, 153.26, 141.93, 137.81, 129.80, 126.61, 118.88, 117.07, 112.91, 71.45, 57.67, 55.78, 48.99, 47.34, 43.98, 41.42.

4-(aminomethyl)-*N*-({(5*S*)-3-[4-(4-methyl-2-oxopiperazin-1-yl)phenyl]-2-oxo-1,3-oxazolidin-5-yl}methyl)cyclohexane-1-carboxamide (r5)

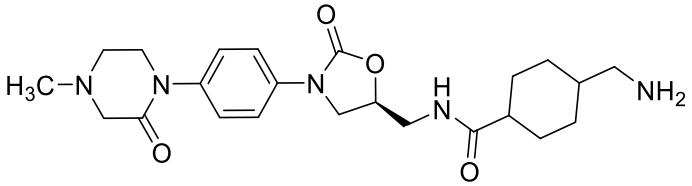

This compound was synthesised according to the general procedure A-step 5-scenario 1 starting with compound **q5** (0.164 g, 0.30 mmol). The title compound (0.068 g, 0.15 mmol, 51%) was obtained as a white solid. MS: m/z calculated for $C_{23}H_{34}N_5O_4^+$ 444.2605 $[M+H]^+$, MS: found 444.2608 $[M+H]^+$. HPLC: t_R 198 min (95%). Mp: 233˚C. $[\alpha]_D^{22}$= 66° (c=1, DMSO). ^{1}H NMR (DMSO-d_6): δ 8.01 (t, *J*= 7.5 Hz, 1H), 7.73 (d, J= 8.5 Hz , 2H), 7.52 (d, *J*= 8.5 Hz, 2H), 4.89-4.81 (m, 1H), 3.88 (dd, J= 9.1 Hz, 6.1 Hz, 1H), 3.81 (t, *J* = 7.1 Hz, 2H), 3.77–3.68 (m, 1H), 3.59-351 (m, 1H), 3.55-3.42 (m, 1H), 3.42 (s, 2H), 2.95–2.76 (m, 2H), 2.51-2.44 (m, 1H), 2.35-2.29 (m, 1H), 2.25 (s, 3H), 1.82-1.41 (m, 12H).^{13}C NMR (DMSO-d_6): δ 178.82, 166.62, 154.15, 142.94, 136.80, 118.85, 117.05, 71.30, 57.75, 54.77, 49.00, 47.43, 47.42, 45.80, 44.27, 41.45, 41.40, 28.95, 26.40.

4-amino-*N*-({(5*S*)-3-[4-(4-methyl-2-oxopiperazin-1-yl)phenyl]-2-oxo-1,3-oxazolidin-5-yl}methyl)cyclohexane-1-carboxamide (t5)

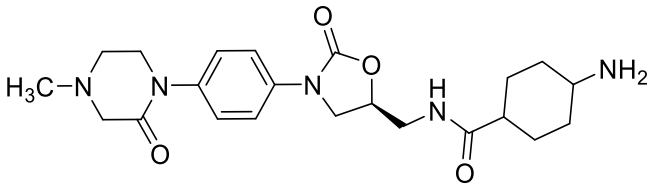

This compound was synthesised according to the general procedure A-step 5-scenario 1 starting with compound **s5** (0.163 g, 0.30 mmol). The title compound (0.076, 0.17 mmol, 58%) was obtained as a white solid. MS: m/z calculated for $C_{22}H_{32}N_5O_4^+$ 430.2449 $[M+H]^+$, MS: found 430.2466 $[M+H]^+$. HPLC: t_R 1.89 min (92%). Mp: 221˚C. $[\alpha]_D^{21}$= 96° (c= 1, DMSO). ^{1}H NMR (DMSO-d_6): δ 8.05 (t, J= 7.6 Hz, 1H), 7.38-7.25 (m, 2H), 7.09-6.92 (m, 2H), 4.96-4.84 (m, 1H), 3.89 (dd, J= 8.8 Hz, 5.8 Hz, 1H), 3.87 (t, *J* = 7.1 Hz, 2H), 3.78-3.66 (m, 1H), 3.54 (m, 1H), 3.58-3.45 (m, 1H), 3.43 (s, 2H), 2.84-279 (m, 1H), 2.86-2.69 (m, 2H), 2.41-234 (m, 1H), 2.25 (s, 2H), 2.05 (d, *J* = 7.3 Hz, 2H), 1.84-1.70 (m, 2H), 1.75-1.58 (m, 4H), 1.55-1.45 (m, 4H). ^{13}C NMR (DMSO-d_6): δ 178.80, 167.61, 152.30, 143.97, 135.82, 119.09, 117.06, 72.36, 57.83, 55.89, 51.22, 48.43, 47.40, 45.81, 43.35, 41.40, 33.26, 25.16.

4-(aminomethyl)-*N*-({(5*S*)-3-[4-(4-methyl-2-oxopiperazin-1-yl)phenyl]-2-oxo-1,3-oxazolidin-5-yl}methyl)benzamide (v5)

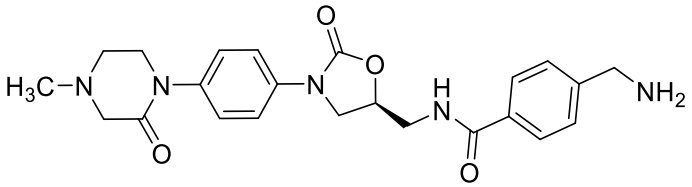

This compound was synthesised according to the general procedure A-step 5-scenario 1 starting with compound **u5** (0.169 g, 0.31 mmol). The title compound (0.090 g, 0.20 mmol, 66%) was obtained as a white solid. MS: m/z calculated for $C_{23}H_{28}N_5O_4^+$ 438.2136 $[M+H]^+$, MS: found 438.2141 $[M+H]^+$. HPLC: t_R 1.76 min (95%). Mp: 213˚C. $[\alpha]_D^{22}$= -61° (c= 1, DMSO). ^{1}H NMR (DMSO-d_6): δ 8.66 (t, *J*= 6.6, 2H), 8.08 (t, *J* = 7.8 Hz, 1H), 7.93-7.85 (m, 2H), 7.36-7.27 (m, 2H), 7.26 (d, J= 8.5 Hz, 2H), 7.11 (d, J= 8.5 Hz, 2H), 4.89-4.81 (m, 1H), 3.89 (dd, J= 9.3 Hz, 6.1 Hz, 1H), 3.92-3.76 (m, 4H), 3.80-3.71 (m, 1H), 3.64-3.56 (m, 2H), 3.42 (s, 2H), 2.95-2.76 (m, 2H), 2.25 (s, 3H). ^{13}C NMR (DMSO-d_6): δ 168.63, 166.32, 156.16, 143.98, 141.91, 137.81, 131.09, 128.59, 127.67, 118.82, 117.04, 71.33, 57.54, 56.71, 48.45, 47.41, 46.05, 44.33, 41.51.

***tert*-butyl 4-(4-aminophenyl)piperazine-1-carboxylate (a6)**

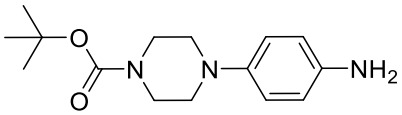

This compound was synthesised according to the general procedure F-step 2 starting with Boc-piperazine (1.860 g, 10 mmol), which was synthesised according to general step G-step 1. The titled compound (1.556 g, 5.62 mmol, 56%) was obtained as a yellow solid. MS: m/z calculated for $C_{15}H_{24}N_3O_2^+$ 278.1863 $[M+H]^+$, MS: found 278.1883 $[M+H]^+$. HPLC: t_R 0.54 min (96%). Mp: 145 °C (lit. Mp= 145).[360] ^{1}H NMR (DMSO-d_6) δ 6.96 (d, *J*= 8.6 Hz, 2H), 6.73 (d, *J*= 8.6 Hz, 2H), 4.52 (t, *J* = 7.1 Hz, 2H), 3.32 (m, 4H), 2.29 (m, 4H), 1.42 (s, 9H). ^{13}C NMR (DMSO-d_6): δ 156.19, 154.33, 140.22, 118.25, 116.18, 79.66, 49.78, 43.55, 28.18.

***tert*-butyl 4-(4-{[(2*R*)-3-(1,3-dioxo-1,3-dihydro-2H-isoindol-2-yl)-2-hydroxypropyl]amino}phenyl)piperazine-1-carboxylate (b6)**

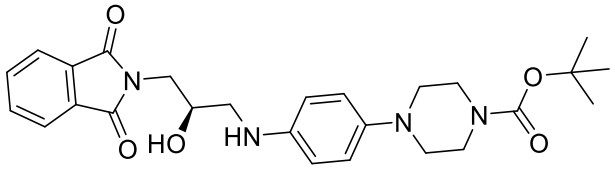

This compound was synthesised according to the general procedure A-step 1-scenario 2 by reacting **a6** (1.498 g, 5.4 mmol) with **35** (1.096 g, 5.4 mmol). The title compound (1.998 g, 4.16 mmol, 77% yield) was obtained as a white powder. MS: m/z calculated for $C_{26}H_{33}N_4O_5^+$ 481.2445 $[M+H]^+$, MS: found 481.2456. HPLC: t_R 2.87 min (93%). Mp: 198 ˚C. ^{1}H NMR (DMSO-d_6): δ 7.86-7.80 (m, 4H), 6.91 (d, *J*= 6.8 Hz, 2H), 6.56 (d, *J*= 6.8 Hz, 2H), 6.11 (t, *J*= 6.7, 1H), 4.88 -5.01 (broad s,1H), 4.08 (d, *J* = 6.7 Hz, 1H), 4.00 (dd, *J* = 12.4, 7.0 Hz, 1H), 3.84 (dd, *J* = 12.4, 7.0 Hz, 1H), 3.75-3.66 (m, 4H), 3.59-3.47 (m, 4H), 3.45-3.33 (m, 1H), 3.33-3.22 (m, 1H), 1.45 (s, 9H). ^{13}C NMR (DMSO-d_6): δ 169.98, 156.86, 154.34, 148.41, 134.15, 131.99, 123.46, 115.11, 114.81, 79.76, 71.09, 49.91, 47.56, 43.66, 42.72, 28.41.

***tert*-butyl 4-(4-{(5*S*)-5-[(1,3-dioxo-1,3-dihydro-2*H*-isoindol-2-yl)methyl]-2-oxo-1,3-oxazolidin-3-yl}phenyl)piperazine-1-carboxylate (c6)**

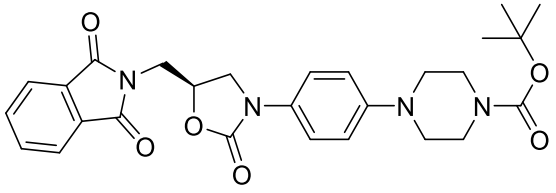

This compound was synthesised according to the general procedure A-step 2-scenario 2 (the solvent used for purification was gradient of EtOAc/ether), starting with **b6** (1.948 g, 4 mmol). The title compound (1.769 g, 3.5 mmol 86% yield) was obtained as yellow solid. MS: m/z calculated for $C_{27}H_{31}N_4O_6^+$ 507.2238 $[M+H]^+$, MS: found 507.2246 $[M+H]^+$. HPLC: t_R 2.91 min (93 %). Mp: 230 °C. ^{1}H NMR ($CDCl_3$): δ 7.84-7.76 (m, 2H), 7.74-7.66 (m, 2H), 7.36 (d, *J*= 8.8 Hz, 2H), 7.06 (d, *J*= 8.8Hz, 2H), 4.90-4.81 (m, 1H), 4.45-4.36 (m, 1H), 4.18-4.08 (m, 2H), 3.87-3.78 (m, 1H), 3.75-3.66 (m, 4H), 3.59-3.47 (m, 4H), 1.47 (s, 9H).^{13}C NMR ($CDCl_3$): δ 167.76, 154.81, 154.33, 154.17, 136.88, 134.13, 132.06, 123.44, 118.87, 117.09, 79.71, 76.22, 49.99, 47.45, 43.66, 42.61, 27.46.

tert-butyl 4-{4-[(5*S*)-5-(aminomethyl)-2-oxo-1,3-oxazolidin-3-yl]phenyl}piperazine-1-carboxylate (d6)

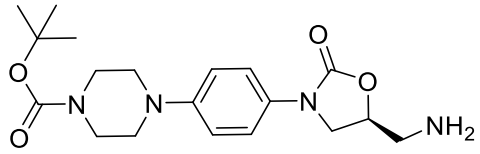

This compound was synthesised according to the general procedure A-step 3a-scenario 2 starting with **c6** (1.718 g, 3.4 mmol). The title compound (1.059 g, 2.81 mmol, 83% yield). MS: m/z calculated for $C_{19}H_{29}N_4O_4^+$ 377.2183 $[M+H]^+$, MS: found 377.2204 $[M+H]^+$. HPLC: t_R 0.99 min (96 %). Mp: 123 °C. ^{1}H NMR (DMSO-d_6): δ 7.38 (d, J= 8.9 Hz, 2H), 7.12 (d, J= 8.9 Hz, 2H), 4.75-4.61 (m, 1H), 3.96 (dd, J= 5.2 Hz, 3.5 Hz, 1H), 3.89 (dd, J = 8.8 Hz, 6.5 Hz, 1H), 3.71 (dd, J = 5.2 Hz, 3.8 Hz, 2H), 3.77-3.68 (m, 2H), 3.61-3.49 (m, 4H), 3.09-2.99 (m, 1H), 2.84-2.75 (m, 1H), 2.36 (t, *J* = 7.5 Hz, 2H), 1.49 (s, 9H).^{13}C NMR (DMSO-d_6): δ 158.81, 156.33, 154.17, 137.86, 119.86, 117.09, 79.71, 75.79, 49.91, 47.50, 47.33, 43.68, 28.40.

tert-butyl 4-{4-[(5*S*)-5-{[(5-chlorothiophene-2-carbonyl)amino]methyl}-2-oxo-1,3-oxazolidin-3-yl]phenyl}piperazine-1-carboxylate (e6)

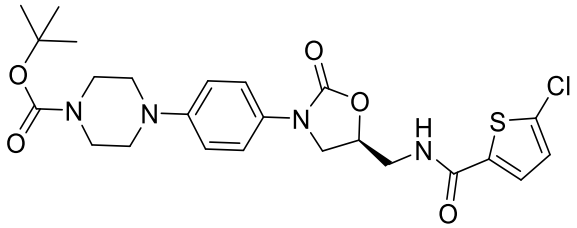

This compound was synthesised according to the general procedure A-step 4-scenario1 by reacting compound **d6** (0.225 g, 0.60 mmol) and 5-chlorothiophene-2-carbonyl chloride (0.130 g, 0.72 mmol). The title compound (0.205 g, 0.39 mmol, 66%) was obtained as a white solid. MS: m/z calculated for: $C_{24}H_{30}ClN_4O_5S^+$ 521.1620 $[M+H]^+$, MS: found 521.1636 $[M+H]^+$. HPLC: t_R 2.43 min (96 %). Mp: 210°C. $[\alpha]_D^{21}$= -87° (c= DMSO). ^{1}H NMR (DMSO-*d*$_6$): δ 8.42 (t, *J*= 5.7 Hz, 1H), 8.06 (d, *J*=4.6 Hz, 1H), 7.18 (d, *J*= 8.8 Hz, 2H), 7.06 (d, *J*= 4.5 Hz, 1H), 6.99 (d, *J*= 8.8 Hz, 2H), 4.89-4.81 (m, 1H), 3.89 (dd, J= 9.2 Hz, 6.1 Hz, 1H), 3.86-3.77 (m, 1H), 3.75-3.64 (m, 4H), 3.63-3.52 (m, 4H), 3.13-3.02 (m, 1H), 2.86-2.77 (m, 1H), 1.45 (s, 9H). ^{13}C NMR (DMSO-*d*$_6$): δ 163.71, 156.81, 155.31, 154.15, 141.40, 136.86, 134.33, 128.41, 127.50, 118.91, 117.06, 79.71, 71.36, 49.93, 47.42, 43.66, 41.46, 28.45.

tert-butyl 4-(4-{(5*S*)-5-[(4-tert-butylbenzamido)methyl]-2-oxo-1,3-oxazolidin-3-yl}phenyl)piperazine-1-carboxylate (g6)

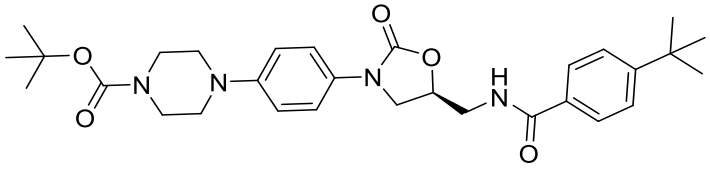

This compound was synthesised according to the general procedure A-step 4-scenario1 by reacting compound **d6** (0.188 g, 0.50 mmol) and 4-(*tert*-butyl)benzoyl chloride (0.117 g, 0.60 mmol). The title compound (0.217 g, 0.40 mmol, 81%) was obtained as a white solid. MS: m/z calculated for $C_{30}H_{41}N_4O_5^+$ 537.3071 $[M+H]^+$, MS: found 537.3089 $[M+H]^+$. HPLC: t_R 2.45 min (94%). Mp: 287 ˚C. $[\alpha]_D^{21}$= 63° (c= 1, DMSO). ^{1}H NMR (DMSO-*d*$_6$): δ 8.02 (t, J = 7.8 Hz, 1H), 7.73-7.65 (m, 2H), 7.45-7.38 (m, 2H), 7.33 (d, *J*= 7.6, 2H), 6.96 (d, *J*= 7.6, 2H), 4.86-7.77 (m, 1H), 3.88 (dd, J= 10.2 Hz, 6.3 Hz, 1H), 3.83-3.74 (m, 1H), 3.72-3.61 (m, 4H), 3.60-3.49 (m, 4H), 3.09-2.99 (m, 1H), 2.81-2.73 (m, 1H), 1.42 (s, 9H), 1.35 (s, 9H) .^{13}C NMR (DMSO-*d*$_6$): δ 168.31, 156.84, 154.33, 154.18, 153.29, 136.81, 131.17, 128.51, 125.67, 118.86, 117.15, 79.71, 71.33, 49.98, 46.43, 45.61, 43.44, 35.73, 33.08, 29.11.

tert-butyl 4-(4-{(5*S*)-5-[(4-cyanobenzamido)methyl]-2-oxo-1,3-oxazolidin-3-yl}phenyl)piperazine-1-carboxylate (h6)

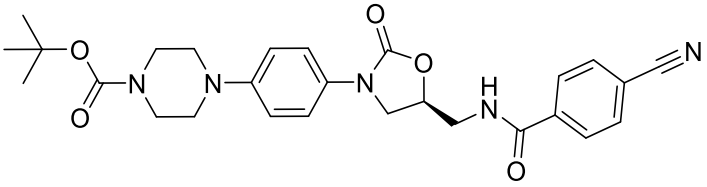

This compound was synthesised according to the general procedure A-step 4-scenario1 by reacting compound **d6** (0.752 g, 2 mmol) and 4-cyanobenzoyl chloride (0.396 g, 2.4 mmol). The title compound (0.756 g, 1.5 mmol 75%) was obtained as a white solid. MS: m/z calculated for $C_{27}H_{32}N_5O_5^+$ 506.2398 $[M+H]^+$, MS: found 506.2412 $[M+H]^+$. HPLC: t_R 1.98 min (96%). Mp: 233 ˚C. $[\alpha]_D^{22}$= 54° (c= 1, DMSO). ^{1}H NMR ($CDCl_3$): δ 8.46 (t, *J* = 7.8 Hz, 1H), 7.93 (s, 4H), 7.34 (d, *J*= 9.5, 2H), 7.02 (d, *J*= 9.5, 2H), 4.93-4.82 (m, 1H), 3.89 (dd, J= 9.2 Hz, 6.1 Hz, 1H), 3.81-3.75 (m, 1H), 3.70-3.60 (m, 4H), 3.59-3.48 (m, 4H), 3.08-3.01 (m, 1H), 2.83-2.72 (m, 1H), 1.45 (s, 9H). ^{13}C NMR ($CDCl_3$): δ 168.31, 156.86, 155.33, 154.18, 138.81, 133.76, 132.16, 128.58, 119.86, 118.65, 117.15, 114.98, 79.72, 71.33, 49.91, 47.47, 43.62, 41.47, 28.45.

5-chloro-*N*-({(5*S*)-2-oxo-3-[4-(piperazin-1-yl)phenyl]-1,3-oxazolidin-5-yl}methyl)thiophene-2-carboxamide (e8)

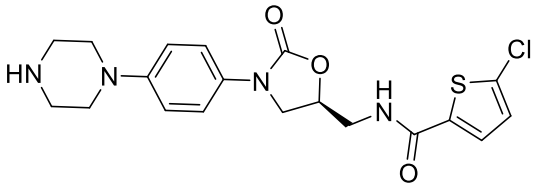

This compound was synthesised according to the general procedure A-step 5-scenario 1 starting with compound **e6** (0.155 g, 0.30 mmol). The title compound (0.063g, 0.15 mmol, 51%) was obtained as a white solid. MS: m/z calculated for $C_{19}H_{22}ClN_4O_3S^+$ 421.1096 $[M+H]^+$, MS: found 421.1106 $[M+H]^+$. HPLC: t_R 2.33 min (99 %). Mp: 189 °C. $[\alpha]_D^{21}$= 49° (c=1, DMSO).^{1}H NMR (DMSO-d_6): δ 8.83 (t, *J*= 5.5 Hz, 1H), 7.59 (d, *J*=4.0 Hz, 1H), 7.28 (d, *J*= 9.0 Hz, 2H), 7.19 (d, *J*= 4.0 Hz, 1H), 6.93 (d, *J*= 9.0 Hz, 2H), 4.83-4.73 (m, 1H), 3.87 (dd, J= 8.9 Hz, 6.3 Hz, 1H), 3.84-3.74 (m, 1H), 3.59 (t, *J* = 7.0 Hz, 2H), 3.38 (t, *J* = 7.0 Hz, 4H), 3.17 (m, 1H), 3.14-3.05 (m, 4H).^{13}C NMR (DMSO-d_6): δ 163.72, 156.31, 155.13, 141.81, 135.81, 135.27, 131.30, 127.50, 118.84, 117.09, 71.31, 48.98, 47.44, 45.45, 41.49.

4-*tert*-butyl-*N*-({(5*S*)-2-oxo-3-[4-(piperazin-1-yl)phenyl]-1,3-oxazolidin-5-yl}methyl)benzamide (g8)

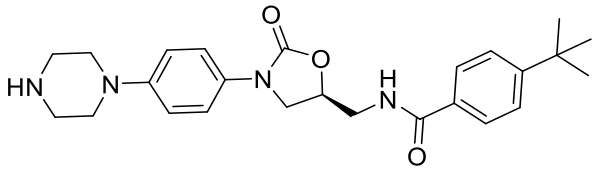

This compound was synthesised according to the general procedure A-step 5-scenario 1 starting with compound **g6** (0.166 g, 0.30 mmol). The title compound (0.114 g, 0.26 mmol, 85%) was obtained as a white solid. MS: m/z calculated for $C_{25}H_{33}N_4O_3^+$ 437.2547 $[M+H]^+$, MS: found 437.2565 $[M+H]^+$. HPLC: t_R 2.33 min (96%). Mp: 277˚C. $[\alpha]_D^{21}$= 87° (c=1, DMSO).^{1}H NMR (DMSO-d_6): δ 8.41 (t, J= 6.0 Hz, 1H), 8.15-8.01 (m, 2H), 7.45 (d, J= 9.0 Hz, 2H), 7.35-7.30 (m, 2H), 7.15 (d, J= 9.0 Hz, 2H), 4.89-4.81 (m, 1H), 4.33-4.21 (m, 1H), 3.91 (dd, J= 8.6 Hz, 6.1 Hz, 1H), 3.63-3.56 (m, 2H), 3.39 (t, *J* = 7.0 Hz, 4H), 3.19 (m, 1H), 3.14-3.05 (m, 4H), 1.34 (s, 9H). ^{13}C NMR (DMSO-d_6): δ 169.31, 156.31, 154.18, 153.29, 136.89, 133.18, 129.55, 124.19, 119.35, 118.15, 73.31, 48.89, 47.45, 44.73, 42.46, 34.71, 31.15.

4-cyano-*N*-({(5S)-2-oxo-3-[4-(piperazin-1-yl)phenyl]-1,3-oxazolidin-5-yl}methyl)benzamide (h8)

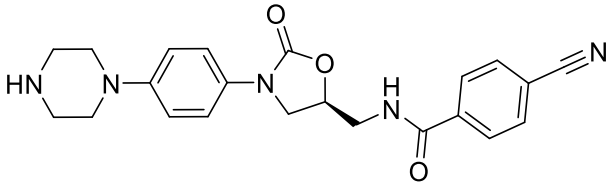

This compound was synthesised according to the general procedure A-step 5-scenario 1 starting with compound **h6** (0.328 g, 0.65 mmol). The title compound (0.199 g, 0.49 mmol, 76%) was obtained as a white solid. MS: m/z calculated for $C_{22}H_{24}N_5O_3^+$ 406.1874 $[M+H]^+$, MS: found 406.1885 $[M+H]^+$. HPLC: t_R 2.22 min (98%). Mp: 200 ˚C. $[\alpha]_D^{22}$= -44° (c=1, DMSO). ^{1}H NMR ($CDCl_3$): δ 8.37 (d, J=8.5 2H), 8.18 (d, J=8.5 2H), 7.12 (d, *J*= 9.0, 2H), 6.91 (d, *J*= 9.0, 2H), 6.56 (t, *J*= 5.5, 1H), 4.90-4.82 (m, 1H), 4.24-4.18 (m, 1H), 3.89 (dd, J= 9.3 Hz, 6.2Hz, 1H), 3.63-3.55 (m, 2H), 3.39 (t, *J* = 7.0 Hz, 4H), 3.17 (m, 1H), 3.16-3.07 (m, 4H). ^{13}C NMR ($CDCl_3$): δ 169.33, 159.31, 154.16, 137.77, 131.76, 130.78, 128.61, 118.95, 118.85, 117.65, 114.00, 71.33, 49.33, 48.15, 45.77, 41.43.

***tert*-butyl 4-{4-[(5*S*)-5-({4-[(*tert*-butoxycarbonyl) amino]benzamido} methyl)-2-oxo-1,3-oxazolidin-3-yl]phenyl}piperazine-1-carboxylate (o6)**

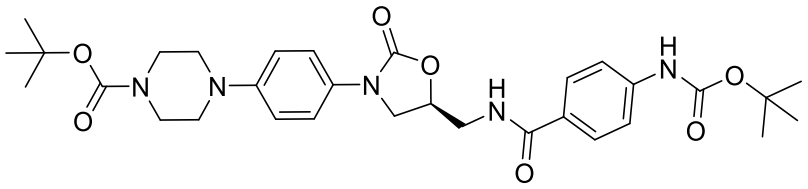

This compound was synthesised according to the general procedure A-step 4-scenario2 by reacting compound **d6** (0.376 g, 1 mmol) with 4-((*tert* butoxycarbonyl) amino) benzoic acid (0.237 g, 1 mmol). The title compound (0.493 g, 0.83 mmol, 83%) was obtained as a white solid. MS: m/z calculated for $C_{31}H_{42}N_5O_7^+$ 596.3079 $[M+H]^+$, MS: found 596.3099 $[M+H]^+$. HPLC: t_R 3.45 min (96%). Mp: 306˚C. ^{1}H NMR (DMSO-d_6): δ 8.48 (t, J= 6.0, 1H), 8.03 (t, *J*= 7.0, 1H) 7.88-7.80 (m, 2H), 7.51 (d, *J*= 9.5, 2H), 7.45-7.34 (m, 2H), 7.28 (d, *J*= 9.5, 2H), 4.89-4.81 (m, 1H), 3.94 (dd, J= 9.3 Hz, 6.2 Hz, 1H), 3.84-3.74 (m, 1H), 3.73-3.63 (m, 2H), 3.60-3.54 (m, 4H), 3.43-3.39 (m, 4H), 1.49 (s, 9H), 1.40 (s, 9H). ^{13}C NMR (DMSO-d_6): δ 169.48, 156.83, 155.31, 154.17, 153.38, 139.91, 137.82, 128.76, 127.69, 119.33, 118.45, 117.26, 83.61, 80.76, 72.32, 50.99, 48.44, 44.61, 42.47, 29.18, 28.33.

***tert*-butyl 4-{4-[(5*S*)-5-{[(4-{[(*tert*-butoxycarbonyl)amino]methyl} cyclohexane-1-carbonyl)amino]methyl}-2-oxo-1,3-oxazolidin-3-yl]phenyl}piperazine-1-carboxylate (q6)**

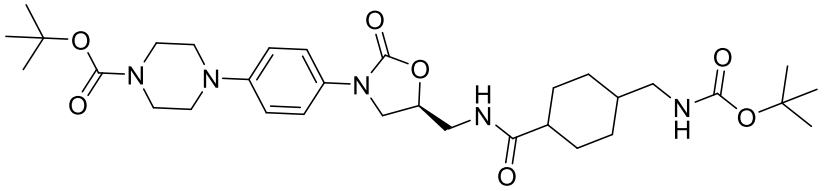

This compound was synthesised according to the general procedure A-step 4-scenario2 by reacting compound **d6** (0.376 g, 1 mmol) with the commercially available 4-{[(*tert*-butoxycarbonyl)amino]methyl}cyclohexane-1-carboxylic acid (0.257 g, 1 mmol). The title compound (0.387 g, 0.63 mmol, 63%) was obtained as an off-white solid. MS: m/z calculated for $C_{32}H_{50}N_5O_7^+$ 616.3705 $[M+H]^+$, MS: found 616.3724 $[M+H]^+$. HPLC: t_R 3.5 min (94%). Mp: 312 ˚C. ^{1}H NMR (DMSO-d_6): δ 8.01 (t, *J*= 6.4, 1H) 7.35-7.25 (m, 2H), 7.15-7.06 (m, 2H), 6.74 (t, *J* = 7.0 Hz, 1H), 4.91-4.80 (m, 1H), 4.18-4.09 (m, 2H), 3.86-3.77 (m, 4H), 3.65-3.59 (m, 3H), 3.44-3.26 (m, 5H), 2.54-2.44 (m, 1H), 2.11-201 (m, 1H), 1.84-1.71 (m, 4H), 1.69-1.54 (m, 4H), 1.47 (s, 9H), 1.40 (s, 9H).^{13}C NMR (DMSO-d_6): δ178.97, 159.13, 158.88, 156.36, 154.18, 138.81, 118.95,

117.06, 79.81, 79.76, 73.31, 53.96, 45.41, 43.81, 41.56, 39.86, 38.41, 35.56, 29.15, 28.41, 27.16, 26.08.

tert-butyl 4-(4-{(5*S*)-5-[({4-[(_tert_-butoxycarbonyl)amino]cyclohexane-1-carbonyl}amino)methyl]-2-oxo-1,3-oxazolidin-3-yl}phenyl)piperazine-1-carboxylate (s6)

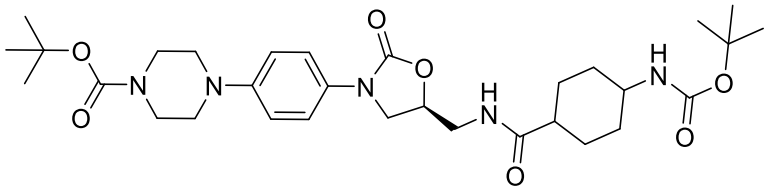

This compound was synthesised according to the general procedure A-step 4-scenario2 by reacting compound **d6** (0.376 g, 1 mmol) with the commercially available 4-[(tert-butoxycarbonyl)amino] cyclohexane-1-carboxylic acid (0.243 g, 1 mmol). The title compound (0.456 g, 0.76 mmol, 76%) was obtained as a white solid. MS: m/z calculated for $C_{31}H_{48}N_5O_7^+$ 602.3548 $[M+H]^+$, MS: found 602.3566 $[M+H]^+$. HPLC: t_R 2.32 min (95%). Mp: 290˚C. ^{1}H NMR (DMSO-d_6) δ 8.02 (t, J= 6.5, 1H), 7.67 (m, 1H), 7.41-7.29 (m, 2H), 7.05-6.99 (m, 2H), 4.89-4.80 (m, 1H), 4.16-4.11 (m, 2H), 3.88-3.79 (m, 4H), 3.64-3.59 (m, 3H), 3.45-3.28 (m, 5H), 1.86-1.71 (m, 4H), 1.69-1.53 (m, 4H), 1.49 (s, 9H), 1.43(s, 9H). ^{13}C NMR (DMSO-d_6): δ 177.81, 156.59, 155.81, 154.36, 153.22, 135.81, 118.86, 117.15, 80.33, 78.98, 71.32, 51.69, 50.06, 47.45, 45.81, 43.65, 42.46, 33.72, 28.41, 27.31, 25.71.

tert-butyl 4-(4-{(5*S*)-5-[(4-{[(_tert_-butoxycarbonyl)amino]methyl} benzamido)methyl]-2-oxo-1,3-oxazolidin-3-yl}phenyl)piperazine-1-carboxylate (u6)

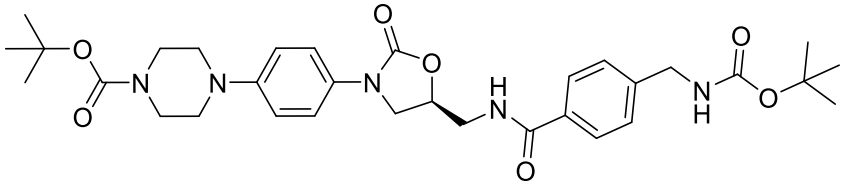

This compound was synthesised according to the general procedure A-step 4-scenario2 by reacting compound **d6** (0.376 g, 1 mmol) with the commercially available 4-{[(tert-butoxycarbonyl)amino] methyl}benzoic acid (0.251 g, 1 mmol). The title compound (0.420 g, 0.69 mmol, 69%) was obtained as a white solid. MS: m/z calculated for $C_{32}H_{44}N_5O_7^+$ 610.3235 $[M+H]^+$, MS: found 610.3253 $[M+H]^+$. HPLC: t_R 2.56 min (95%). Mp: 296˚C. ^{1}H NMR (DMSO-d_6) δ: ^{1}H NMR (DMSO-d_6) δ 8.04 (t, *J* = 7.5 Hz, 1H), 7.89-7.81 (m, 2H), 7.35-7.24 (m, 4H), 7.12-7.00(m, 2H), 5.26 (t, *J* = 8.5 Hz, 1H), 4.89-4.81

(m, 1H), 4.46-4.35 (m, 1H), 4.35-4.26 (m, 1H), 4.18 – 4.08 (m, 1H), 3.88 (dd, J= 9.1 Hz, 6.1 Hz, 1H),, 3.68 – 3.47 (m, 4H), 3.45– 3.34 (m, 3H), 3.33-3.26 (m, 3H), 1.51 (s, 9H), 1.39 (s, 9H). ^{13}C NMR (DMSO-d_6): δ 169.31, 156.51, 154.86, 153.32, 152.19, 139.25, 137.86, 135.15, 129.99, 127.69, 118.81, 117.55, 79.86, 77.73, 71.39, 49.98, 45.44, 44.14, 43.66, 41.47, 29.45, 28.36.

***tert*-butyl 4-(4-{(5*S*)-5-[(4-carbamoylbenzamido)methyl]-2-oxo-1,3-oxazolidin-3-yl}phenyl)-3-oxopiperazine-1-carboxylate (w6)**

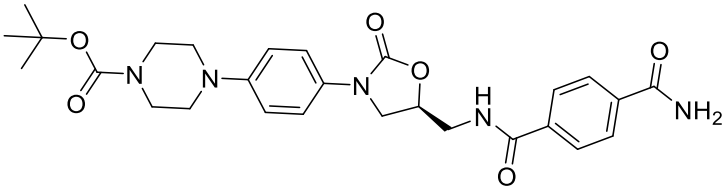

This compound was synthesised according to the general procedure A-step 4-scenario 1 by reacting compound **d6** (0.376 g, 1 mmol) with 4-carbamoylbenzoic acid (0.165 g, 1 mmol). The title compound (0.277 g, 0.53 mmol, 53%) was obtained as a white solid. MS: m/z calculated for $C_{27}H_{34}N_5O_6^+$ 524.2504 $[M+H]^+$, MS: found 524.25017 $[M+H]^+$. HPLC: t_R 2.13 min (96%). Mp: 246˚C. ^{1}H NMR (DMSO-d_6): δ 8.40 (t, *J*= 7.5 Hz, 1H), 8.21-8.10 (m, 2H), 7.89-7.76 (m, 2H), 7.42 (d, *J*= 8.5 Hz, 2H), 7.12 (d, *J*= 8.5 Hz, 2H), 6.91 (s, 2H), 4.94-4.83 (m, 1H), 4.18-4.07 (m, 1H), 3.91 (dd, J= 9.1 Hz, 6.3 Hz, 1H), 3.76-3.54 (m, 4H), 3.41-3.33 (m, 3H), 3.31-3.27 (m, 3H), 2.13 (s, 9H). ^{13}C NMR (DMSO-d_6): δ 167.35, 158.13, 156.86, 155.31, 154.18, 139.23, 138.82, 130.00, 129.53, 127.45, 118.84, 117.25, 79.83, 79.72, 71.35, 48.12, 46.49, 45.05, 43.95, 41.43, 28.41, 28.36.

***tert*-butyl 3-oxo-4-(4-{(5*S*)-2-oxo-5-[(4-sulfamoylbenzamido)methyl]-1,3-oxazolidin-3-yl}phenyl)piperazine-1-carboxylatem (x6)**

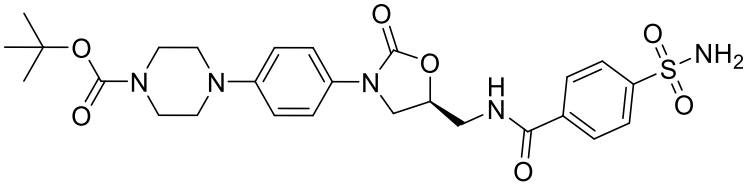

This compound was synthesised according to the general procedure A-step 4-scenario 1 by reacting compound **d6** (0.376 g, 1 mmol) with 4-sulfamoylbenzoic acid (0.201 g, 1 mmol). The title compound (0.324 g, 0.58 mmol, 58%) was obtained as a yellow solid. MS: m/z calculated for $C_{26}H_{34}N_5O_7S^+$ 560.2173 $[M+H]^+$, MS: found 560.2185 $[M+H]^+$. HPLC: t_R 2.43 min (96%). Mp: 234˚C. ^{1}H NMR (DMSO-d_6): δ 8.76 (t, *J* = 7.5 Hz, 1H),

8.23-8.17 (m, 2H), 7.96-7.90 (m, 2H), 7.45-7.33 (m, 2H), 7.30 (s, 2H), 7.13-7.02 (m, 2H), 4.96-4.84 (m, 1H), 4.23-4.17 (m, 1H), 3.92 (dd, J= 9.3 Hz, 6.2 Hz, 1H), 3.86-3.64 (m, 4H), 3.51-3.43 (m, 3H), 3.36-3.30 (m, 3H), 1.42 (s, 9H). ^{13}C NMR (DMSO-d_6): δ 170.36, 156.81, 155.31, 154.14, 145.68, 137.86, 134.41, 130.01, 127.56, 118.81, 117.75, 79.73, 71.36, 50.06, 47.42, 43.61, 41.46, 28.59.

N^1-({(5*S*)-2-oxo-3-[4-(piperazin-1-yl)phenyl]-1,3-oxazolidin-5-yl}methyl)benzene-1,4-dicarboxamide (w8)

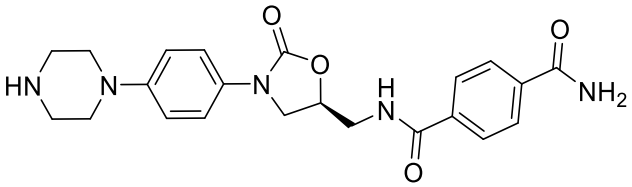

This compound was synthesised according to the general procedure A-step 5-scenario 1 starting with compound **w6** (0.221 g, 0.43 mmol). The title compound (0.091 g, 0.21 mmol, 51%) was obtained as a white solid. MS: m/z calculated for $C_{22}H_{26}N_5O_4^+$ 424.1979 $[M+H]^+$, MS: found 424.1999 $[M+H]^+$. HPLC: t_R 2.02 min (97%). Mp: 221˚C. $[\alpha]_D^{22}$= -43° (c= 1, DMSO). ^{1}H NMR (DMSO-d_6): δ 8.26 (t, *J*= 7.8 Hz, 1H), 8.19-8.13 (m, 2H), 7.81-7.74 (m, 2H), 7.52 (d, *J*= 8.6 Hz, 2H), 7.23 (d, *J*= 8.6 Hz, 2H), 6.81 (s, 2H), 4.89-4.80 (m, 1H), 4.17-4.08 (m, 1H), 3.89 (dd, J= 9.1 Hz, 6.0 Hz, 1H), 3.63-3.55 (m, 2H), 3.39 (t, *J* = 7.0 Hz, 4H), 3.21-3.15 (m, 1H), 3.14-3.05 (m, 4H). ^{13}C NMR (DMSO-d_6): δ 168.93, 167.31, 156.31, 154.13, 136.86, 136.11, 131.13, 128.68, 128.56, 119.43, 118.99, 71.36, 47.03, 47.53, 45.86, 41.44.

***N*-({(5*S*)-2-oxo-3-[4-(piperazin-1-yl)phenyl]-1,3-oxazolidin-5-yl}methyl)-4-sulfamoylbenzamide (x8)**

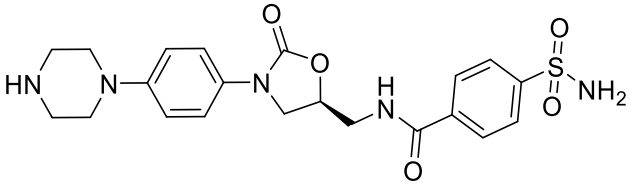

This compound was synthesised according to the general procedure A-step 5-scenario1 starting with compound **x6** (0.264 g, 47 mmol). The title compound (0.087 g, 0.19 mmol, 43%) was obtained as a yellow solid. MS: m/z calculated for $C_{21}H_{26}N_5O_5S^+$ 460.1649 $[M+H]^+$, MS: found 460.1659$[M+H]^+$. HPLC: t_R 2.11 min (97%). Mp: 200 ˚C. $[\alpha]_D^{22}$ = 33° (c= 1, DMSO). ^{1}H NMR (DMSO-d_6): δ 8.80 (t, *J* = 7.6 Hz, 1H), 8.25-8.18 (m, 2H), 7.92-7.80 (m, 2H), 7.35-7.27

(m, 2H), 7.26 (s, 2H), 7.13-7.02 (m, 2H), 4.90-4.80 (m, 1H), 4.28-4.06 (m, 1H), 3.91 (dd, J= 10.2 Hz, 6.8 Hz, 1H), 3.71-3.60 (m, 2H), 3.44 (t, *J* = 7.1 Hz, 4H), 3.25-3.17 (m, 1H), 3.23-3.11 (m, 4H). ^{13}C NMR (DMSO-d_6): δ 170.36, 156.81, 155.31, 154.14, 145.68, 137.86, 134.41, 130.01, 127.56, 118.81, 117.75, 79.73, 71.36, 50.06, 47.42, 43.61, 41.46, 28.59.

4-amino-*N*-({(5*S*)-2-oxo-3-[4-(piperazin-1-yl)phenyl]-1,3-oxazolidin-5-yl}methyl)benzamide (p8)

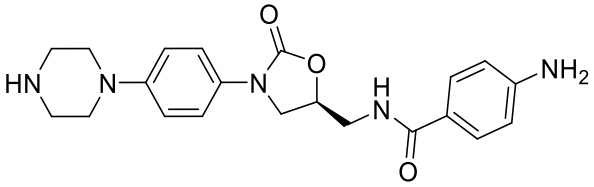

This compound was synthesised according to the general procedure A-step 5-scenario 1 starting with compound **o6** (0.403 g, 0.68 mmol). The title compound (0.152 g, 0.38 mmol, 57%) was obtained as an off-white solid. MS: m/z calculated for $C_{21}H_{26}N_5O_3^+$ 396.2030 $[M+H]^+$, MS: found 396.2046 $[M+H]^+$. HPLC: t_R 1.63 min (96%). Mp: 265˚C. $[\alpha]_D^{22}$= 31° (c= 1, DMSO). ^{1}H NMR (DMSO-d_6): δ 8.30 (t, J= 7.8 Hz, 1H), 7.63-7.54 (m, 2H), 7.36 (d, J= 9.5 Hz, 2H), 7.36-7.25 (m, 2H), 7.18 (d, J= 9.5 Hz, 2H), 5.48 (s, 2H), 4.91-4.81 (m, 1H), 4.27-4.18 (m, 1H), 3.87 (dd, J= 9.1Hz, 6.2 Hz, 1H), 3.53-3.49 (m, 2H), 3.33 (t, *J* = 7.0 Hz, 4H), 3.27-3.15 (m, 1H), 3.14-3.05 (m, 4H). ^{13}C NMR (DMSO-d_6): δ 168.30, 156.31, 154.19, 152.26, 137.77, 128.86, 127.61, 118.81, 117.05, 112.99, 71.36, 48.81, 47.42, 45.75, 41.46.

4-(aminomethyl)-*N*-({(5S)-2-oxo-3-[4-(piperazin-1-yl)phenyl]-1,3-oxazolidin-5-yl}methyl)cyclohexane-1-carboxamide (r8)

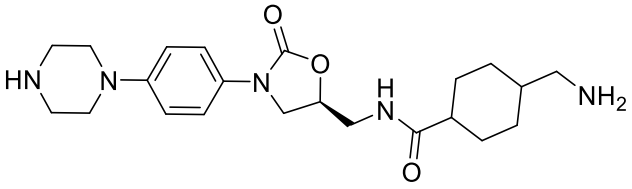

This compound was synthesised according to the general procedure A-step 5-scenario 1 starting with compound **q6** (0.297 g, 0.48 mmol). The title compound (0.106 g, 0.25 mmol, 53%) was obtained as a white solid. MS: m/z calculated for $C_{22}H_{34}N_5O_3^+$ 416.2656 $[M+H]^+$, MS: found 416.2667 $[M+H]^+$. HPLC: t_R 1.99 min (94%). Mp: 257˚C. $[\alpha]_D^{22}$= 70° (c= 1, DMSO). ^{1}H NMR (DMSO-d_6): δ 8.01 (t, *J*=7.5 Hz, 1H), 7.76 (d, *J*= 8.5 Hz, 2H), 7.59 (d, *J*= 8.5 Hz, 2H), 4.97-4.87 (m, 1H), 4.24-4.18 (m, 1H), 3.87 (t, *J*= 7.0, 4H), 3.91 (dd,

J= 9.3 Hz, 6.2 Hz, 1H), 3.60-3.42 (m, 2H), 3.39 (t, *J* = 7.0 Hz, 4H), 3.21-3.15 (m, 1H), 3.14-3.05 (m, 4H), 2.76-2.60 (m, 1H), 2.53-2.44 (m, 1H), 2.41-2.30 (m, 1H), 1.74-1.68 (m, 2H), 1.82-1.41 (m, 5H). ^{13}C NMR (DMSO-*d*$_6$): δ 178.83, 156.36, 154.19, 137.81, 118.86, 117.17, 71.36, 49.89, 48.71, 46.44, 45.99, 45.07, 41.46, 41.44, 28.96, 26.57.

4-amino-*N*-({(5S)-2-oxo-3-[4-(piperazin-1-yl)phenyl]-1,3-oxazolidin-5-yl}methyl)cyclohexane-1-carboxamide (t8)

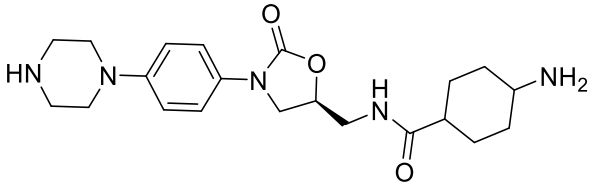

This compound was synthesised according to the general procedure A-step 5-scenario 1 starting with compound **s6** (0.366 g, 0.60 mmol). The title compound (0.136 g, 0.34 mmol, 56%) was obtained as a white solid. MS: m/z calculated for $C_{21}H_{32}N_5O_3^+$ 402.2500 $[M+H]^+$, MS: found 402.2516 $[M+H]^+$. HPLC: t_R 1.99 min (96%). Mp: 221˚C. $[\alpha]_D^{21}$= 103° (c= 1, DMSO). ^{1}H NMR (DMSO-*d*$_6$): δ 8.01 (t, J= 7.5 Hz, 1H), 7.35-7.28 (m, 2H), 7.03-6.97 (m, 2H), 4.89-4.81 (m, 1H), 4.14-4.04 (m, 1H), 3.88 (dd, J= 9.1 Hz, 6.1 Hz, 1H), 3.60-3.42 (m, 2H), 3.39 (t, *J* = 7.0 Hz, 4H), 3.20-3.12 (m, 1H), 3.14-3.05 (m, 4H), 2.88-2.79 (m, 1H), 2.47-2.33 (m, 1H), 2.02 (d, *J* = 7.3 Hz, 2H), 1.84-1.70 (m, 2H), 1.72-1.56 (m, 4H), 1.53-1.40 (m, 2H). ^{13}C NMR (DMSO-*d*$_6$): δ 178.87, 156.30, 154.25, 136.87, 119.81, 117.15, 71.34, 51.29, 49.91, 47.43, 46.80, 45.78, 41.44, 33.23, 25.26.

4-(aminomethyl)-*N*-({(5S)-2-oxo-3-[4-(piperazin-1-yl)phenyl]-1,3-oxazolidin-5-yl}methyl)benzamide (v8)

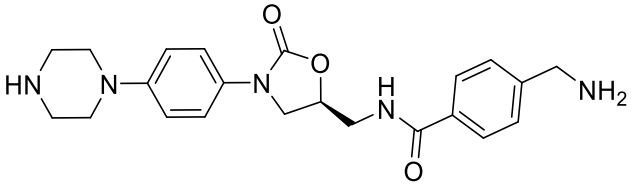

This compound was synthesised according to the general procedure A-step 5-scenario 1 starting with compound **u6** (0.330 g, 0.54mmol). The title compound (0.113 g, 0.27 mmol, 51%) was obtained as a white solid. MS: m/z calculated for $C_{22}H_{28}N_5O_3^+$ 410.2187 $[M+H]^+$, MS: found 410.2201 $[M+H]^+$. HPLC: t_R 1.78 min (95%). Mp: 201˚C. $[\alpha]_D^{22}$= -101° (c= 1, DMSO). ^{1}H NMR (DMSO-*d*$_6$): δ 8.43 (t, *J*= 6.5 Hz, 2H), 7.96 (t, *J* = 7.8 Hz, 1H), 7.86-7.80 (m,

2H), 7.27-7.19 (m, 2H), 7.17-7.06 (d, J= 8.6 Hz, 2H), 7.03-6.95 (d, J= 8.6 Hz, 2H), 4.88-4.79 (m, 1H), 4.17-4.08 (m, 1H), 3.86 (dd, J= 9.1 Hz, 6.3 Hz, 1H), 3.79-3.64 (m, 1H), 3.63-3.55 (m, 2H), 3.39 (t, *J* = 7.0 Hz, 4H), 3.24-3.15 (m, 1H), 3.14-3.05 (m, 4H). ^{13}C NMR (DMSO-d_6): δ 166.36, 156.39, 154.18, 144.91, 136.88, 131.61, 128.56, 127.62, 118.81, 117.15, 71.38, 48.92, 47.46, 46.17, 45.75, 41.44.

tert-butyl 4-(4-aminophenyl)-3-oxopiperazine-1-carboxylate (a7)

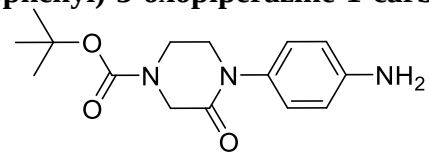

This compound was synthesised according to the general procedure F-step 2 starting with Boc-3-oxopiperazine (2.024 g, 10 mmol) which was synthesised according to the general procedure G-step 1. The titled compound (1.619 g, 5.56 mmol, 55%) was obtained as a yellow solid. MS: m/z calculated for $C_{15}H_{22}N_3O_3^+$ 292.1656 $[M+H]^+$, MS: found 292.1666 $[M+H]^+$. HPLC: t_R 0.54 min (96%). Mp: 163 °C. ^{1}H NMR (DMSO-d_6): δ 7.01 (d, *J*= 8.5 Hz, 2H), 6.81 (d, *J*= 8.5 Hz, 2H), 3.82 (t, *J* = 7.0Hz, 4H), 3.46 (s, 2H), 2.85 (t, *J* = 7.0 Hz, 2H), 1.49 (s, 9H). ^{13}C NMR (DMSO-d_6): δ167.66, 156.24, 141.95, 141.28, 117.15, 117.35, 81.57, 47.52, 45.93, 43.66, 28.27.

tert-butyl 4-(4-{[(2*R*)-3-(1,3-dioxo-1,3-dihydro-2*H*-isoindol-2-yl)-2-hydroxypropyl]amino}phenyl)-3-oxopiperazine-1-carboxylate (b7)

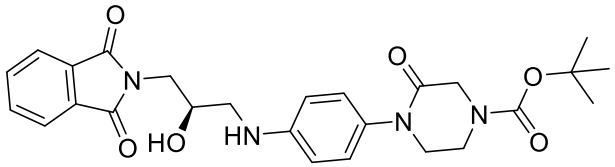

This compound was synthesised according to the general procedure A-step 1-scenario 2 by reacting compound **a7** (1.455 g, 5 mmol) with **35** (1.015 g, 5 mmol). The title compound (2.124 g, 4.3 mmol, 86% yield) was obtained as a white powder. MS: m/z calculated for $C_{26}H_{31}N_4O_6^+$ 495.2238 $[M+H]^+$, MS: found 495.2249. HPLC: t_R 2.89 min (96%). Mp: 206 ˚C. ^{1}H NMR (DMSO-d_6): δ 7.88-7.79 (m, 2H), 7.78-7.66 (m, 2H), 7.15 (d, *J*= 6.5 Hz, 2H), 6.69 (d, *J*= 6.5 Hz, 2H), 6.15 (t, *J* = 6.7 Hz, 1H), 5.09-4.97 (broad s, 1H), 4.33-4.21 (m, 1H), 4.36-4.14 (m, 1H), 3.96 (d, *J* = 6.7 Hz, 1H), 3.96-3.81 (m, 2H), 3.45-3.38 (m, 3H), 3.32-3.26 (m, 1H), 2.91-2.75 (m, 2H), 1.49 (s, 9H). ^{13}C NMR

(DMSO-d_6): δ 168.75, 166.66, 156.82, 148.45, 141.94, 135.12, 130.95, 122.38, 117.07, 115.16, 81.56, 69.98, 48.54, 47.43, 45.48, 43.67, 42.88, 28.26.

tert-butyl 4-(4-{(5*S*)-5-[(1,3-dioxo-1,3-dihydro-2*H*-isoindol-2-yl)methyl]-2-oxo-1,3-oxazolidin-3-yl}phenyl)-3-oxopiperazine-1-carboxylate (c7)

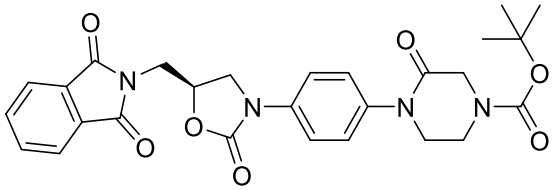

This compound was synthesised according to the general procedure A-step 2-scenario 2 starting with **b7** (1.976 g, 4 mmol)**.** The title compound (1.726 g, 3.32 mmol, 83% yield) was obtained as a white solid. MS: m/z calculated for $C_{27}H_{29}N_4O_7^+$ 521.2031 $[M+H]^+$, MS: found 421.2048 $[M+H]^+$. HPLC: t_R 3.06 min (96 %). Mp: 201 °C. ^{1}H NMR (DMSO-d_6): δ 7.86-7.75 (m, 2H), 7.78-7.71 (m, 2H), 7.36 (d, *J*= 8.6 Hz, 2H), 7.19 (d, *J*= 8.6 Hz, 2H), 4.92-4.81 (m, 1H), 4.47-4.35 (m, 1H), 4.19-4.09 (m, 2H), 3.92-3.80 (m, 3H), 3.46 (s, 2H), 2.96-2.75 (m, 2H), 1.51 (s, 9H). ^{13}C NMR ($CDCl_3$): δ 168.77, 166.65, 156.76, 154.19, 143.95, 136.81, 134.19, 131.95, 123.39, 118.89, 117.15, 81.57, 75.18, 47.55, 47.56, 44.48, 43.61, 42.59, 28.26.

tert-butyl 4-{4-[(5*S*)-5-(aminomethyl)-2-oxo-1,3-oxazolidin-3-yl]phenyl}-3-oxopiperazine-1-carboxylate (d7)

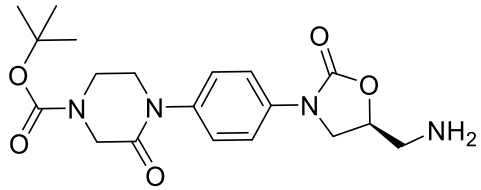

This compound was synthesised according to the general procedure A-step 3a-scenario 2 starting with **c7** (1.560 g, 3 mmol). The title compound (0.912 g, 2.33 mmol, 78 % yield). MS: m/z calculated for $C_{19}H_{27}N_4O_5^+$ 391.1976.1608 $[M+H]^+$, MS: found 391.1991 $[M+H]^+$. HPLC: t_R 1.18 min (96 %). Mp: 113 °C. ^{1}H NMR (DMSO-d_6): δ 7.46 (d, J= 8.0 Hz, 2H), 7.17 (d, J= 8.0 Hz, 2H), 4.87-4.77 (m, 1H), 4.06-3.98 (m, 4H), 3.95 (dd, J= 5.2 Hz, 3.5Hz, 1H), 3.87 (dd, J = 8.8 Hz, 6.5 Hz, 1H), 3.71 (dd, J = 5.3 Hz, 3.6 Hz, 2H), 2.98-2.75 (m, 1H), 2.78-2.65 (m, 1H), 2.34 (t, *J* = 7.0 Hz, 2H), 1.49 (s, 9H). ^{13}C NMR (DMSO-d_6): δ 166.62, 155.18, 154.18, 142.93, 136.86, 118.81, 117.06, 80.58, 75.71, 47.45, 47.40, 47.32, 44.54, 43.66, 28.21.

***tert*-butyl 4-{4-[(5*S*)-5-{[(5-chlorothiophene-2-carbonyl)amino]methyl}-2-oxo-1,3-oxazolidin-3-yl]phenyl}-3-oxopiperazine-1-carboxylate (e7)**

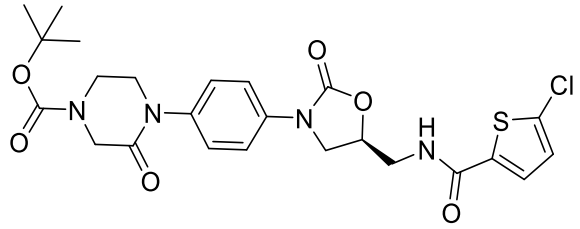

This compound was synthesised according to the general procedure A-step 4-scenario1 by reacting compound **d7** (0.195 g, 0.5 mmol) and 5-chlorothiophene-2-carbonyl chloride (0.108 g, 0.6 mmol). The title compound (0.162 g, 0.30 mmol, 61%) was obtained as a white solid. MS: m/z calculated for $C_{24}H_{28}ClN_4O_6S^+$ 535.1413 $[M+H]^+$, MS: found 535.1419 $[M+H]^+$. HPLC: t_R 2.21 min (95 %). Mp: 201 °C. $[\alpha]_D^{21}$= 41° (c= 1, DMSO). ^{1}H NMR (DMSO-*d*$_6$): δ 8.34 (t, *J*= 6.0 Hz, 1H), 8.08 (d, *J*= 4.6 Hz, 1H), 7.09 (d, *J*= 8.8 Hz, 2H), 6.94 (d, *J*= 4.6 Hz, 1H), 6.87 (d, *J*= 8.8 Hz, 2H), 4.80-4.72 (m, 1H), 4.15-4.06 (m, 1H), 4.06-3.98 (m, 4H), 3.88 (dd, J= 9.1 Hz, 6.1 Hz, 1H), 3.60 – 3.45 (m, 4H), 1.45 (s, 9H). ^{13}C NMR (DMSO-*d*$_6$): δ 167.63, 161.73, 155.96, 154.18, 142.96, 140.28, 136.88, 135.27, 128.50, 127.31, 118.86, 117.15, 80.56, 71.31, 48.47, 47.41, 44.50, 43.61, 41.46, 28.26.

***tert*-butyl 4-(4-{(5*S*)-5-[(4-*tert*-butylbenzamido)methyl]-2-oxo-1,3-oxazolidin-3-yl}phenyl)-3-oxopiperazine-1-carboxylate (g7)**

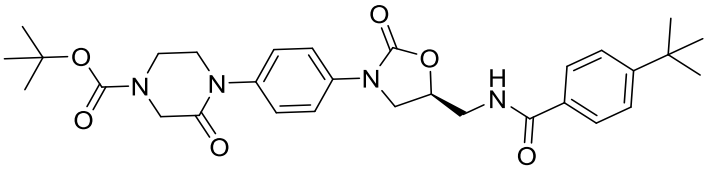

This compound was synthesised according to the general procedure A-step 4-scenario1 by reacting compound **d7** (0.195 g, 0.5 mmol) and 4-(*tert*-butyl)benzoyl chloride (0.117 g, 0.6 mmol). The title compound (0.228 g, 0.41 mmol, 83%) was obtained as a white solid. MS: m/z calculated for $C_{30}H_{39}N_4O_6^+$ 551.2864 $[M+H]^+$, MS: found 551.2881 $[M+H]^+$. HPLC: t_R 2.20 min (97%). Mp: 210˚C. $[\alpha]_D^{21}$= 54° (c= 1, DMSO). ^{1}H NMR (DMSO-*d*$_6$): δ 8.26 (t, J = 7.8 Hz, 1H), 7.75-7.68 (m, 2H), 7.48-7.41 (m, 2H), 7.34 (d, *J*= 7.5 Hz, 2H), 7.17 (d, *J*= 7.5 Hz, 2H), 4.92-7.81 (m, 1H), 4.17-4.08 (m, 1H), 4.06 – 3.98 (m, 4H), 3.87 (dd, J= 9.5 Hz, 6.3 Hz, 1H), 3.63-3.45 (m, 4H), 1.45 (s, 9H), 1.34 (s, 9H). ^{13}C NMR (DMSO-*d*$_6$): δ 167.69, 166.31, 156.88, 154.15,

153.26, 142.94, 136.80, 131.16, 128.58, 125.57, 118.86, 117.06, 80.57, 71.36, 48.08, 47.41, 44.24, 42.67, 41.47, 34.81, 31.07, 28.26.

tert-butyl 4-(4-{(5*S*)-5-[(4-cyanobenzamido)methyl]-2-oxo-1,3-oxazolidin-3-yl}phenyl)-3-oxopiperazine-1-carboxylate (h7)

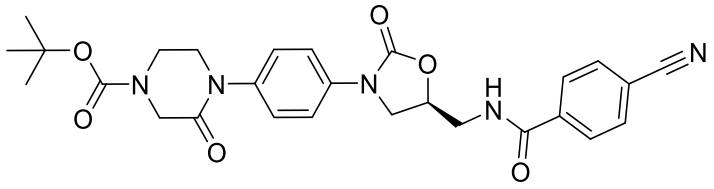

This compound was synthesised according to the general procedure A-step 4-scenario1 by reacting compound **d7** (0.585 g, 1.5 mmol) and 4-cyanobenzoyl chloride (0.297 g, 1.8 mmol). The title compound (0.546 g, 1.05 mmol, 71%) was obtained as a white solid. MS: m/z calculated for $C_{27}H_{30}N_5O_6^+$ 520.2191 $[M+H]^+$, MS: found 520.2198 $[M+H]^+$. HPLC: t_R 1.88 min (95%). Mp: 211 ˚C. $[\alpha]_D^{22}$= -77° (c= 1, DMSO). ^{1}H NMR (DMSO-*d*$_6$): δ 8.47 (t, *J* = 7.0 Hz, 1H), 8.08-8.0 (m, 2H), 7.92-7.85(m, 2H), 7.43 (d, *J*= 9.6, 2H), 7.14 (d, *J*= 9.6, 2H), 4.92-4.80 (m, 1H), 4.17-4.08 (m, 1H), 4.06-3.98 (m, 4H), 3.86 (dd, J= 9.2 Hz, 6.2 Hz, 1H), 3.63-3.45 (m, 4H), 1.45 (s, 9H).^{13}C NMR (DMSO-*d*$_6$): δ 167.64, 166.36, 156.87, 154.18, 142.95, 136.86, 132.77, 131.13, 128.58, 118.86, 118.71, 117.04, 113.85, 80.59, 71.36, 48.44, 47.43, 44.46, 43.65, 41.15, 28.35.

5-chloro-*N*-({(5*S*)-2-oxo-3-[4-(2-oxopiperazin-1-yl)phenyl]-1,3-oxazolidin-5-yl}methyl)thiophene-2-carboxamide (e9)

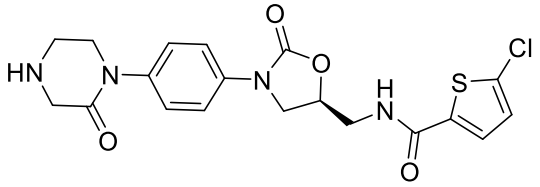

This compound was synthesised according to the general procedure A-step 5-scenario1 starting with compound **e7** (0.106 g, 0.20 mmol). The title compound (0.071 g, 0.16 mmol, 83%) was obtained as a white solid. MS: m/z calculated for $C_{19}H_{20}ClN_4O_4S^+$ 435.0888 $[M+H]^+$, MS: found 435.0901 $[M+H]^+$. HPLC: t_R 2.16 min (96 %). Mp: 193 °C. $[\alpha]_D^{21}$= -45° (c= 1, DMSO). ^{1}H NMR (DMSO-*d*$_6$): δ 8.38 (t, *J*= 5.5 Hz, 1H), 8.04 (d, *J*=4.5 Hz, 1H), 7.08 (d, *J*= 8.8 Hz, 2H), 6.94 (d, *J*= 4.5 Hz, 1H), 6.83 (d, *J*= 8.8 Hz, 2H), 4.83-4.72(m, 1H), 4.16-4.07 (m, 1H), 3.92 (t, *J* = 7.0 Hz, 2H), 3.89 (dd, J= 9.3 Hz, 6.2 Hz, 1H), 3.62 – 3.51 (m, 4H), 3.16-2.98 (m, 2H), 1.58 (m, 1H). ^{13}C NMR

(DMSO-d_6): δ 165.93, 160.73, 154.16, 142.83, 140.81, 136.76, 134.25, 129.31, 127.52, 118.81, 117.17, 71.31, 48.42, 47.86, 46.62, 45.67, 41.41.

4-*tert*-butyl-*N*-({(5*S*)-2-oxo-3-[4-(2-oxopiperazin-1-yl)phenyl]-1,3-oxazolidin-5-yl}methyl)benzamide (g9)

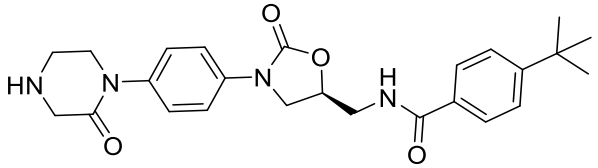

This compound was synthesised according to the general procedure A-step 5-scenario 1 starting with compound **g7** (0.192 g, 0.35 mmol). The title compound (0.127 g, 0.28 mmol, 81%) was obtained as a white solid. MS: m/z calculated for $C_{25}H_{31}N_4O_4^+$ 451.2340 $[M+H]^+$, MS: found 451.2358 $[M+H]^+$. HPLC: t_R 2.05 min (98%). Mp: 215˚C. $[\alpha]_D^{21}$= 77° (c= 1, DMSO). ^{1}H NMR (DMSO-d_6): δ 8.10 (t, J = 7.5 Hz, 1H), 7.78-7.64 (m, 2H), 7.51-7.42 (m, 2H), 7.35 (d, *J*= 7.5 Hz, 2H), 7.04 (d, *J*= 7.5 Hz, 2H), 4.93-7.81 (m, 1H), 4.18-4.05 (m, 1H), 3.96 (t, *J* = 7.0 Hz, 2H), 3.91 (dd, J= 9.2 Hz, 6.4 Hz, 1H), 3.64-3.52 (m, 4H), 3.18-2.96 (m, 2H), 1.57 (m, 1H), 1.36 (s, 9H). ^{13}C NMR (DMSO-d_6): δ 166.30, 165.52, 154.15, 153.26, 142.94, 136.80, 131.00, 128.58, 125.57, 118.85, 117.05, 71.30, 47.43, 46.17, 46.04, 45.63, 41.45, 34.72, 31.09.

4-cyano-*N*-({(5*S*)-2-oxo-3-[4-(2-oxopiperazin-1-yl)phenyl]-1,3-oxazolidin-5-yl}methyl)benzamide (h9)

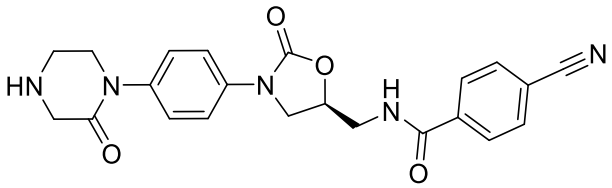

This compound was synthesised according to the general procedure A-step 5-scenario 1 starting with compound **h7** (0.311 g, 0.6 mmol). The title compound (0.188 g, 0.45 mmol, 75%) was obtained as a white solid. MS: m/z calculated for $C_{22}H_{22}N_5O_4^+$ 420.1666 $[M+H]^+$, MS: found 420.1678 $[M+H]^+$. HPLC: t_R 1.87 min (95%). Mp: 200 ˚C. $[\alpha]_D^{22}$= 56° (c= 1, DMSO).^{1}H NMR ($CDCl_3$): δ 8.49 (t, *J* = 7.5 Hz, 1H), 8.17-8.11 (m, 2H), 8.10-7.0 (m, 2H), 7.23 (d, *J*= 8.9, 2H), 6.87 (d, *J*= 8.9, 2H), 4.93-4.82 (m, 1H), 4.17-4.05 (m, 1H), 3.97 (t, *J* = 7.0 Hz, 2H), 3.87 (dd, J= 9.2 Hz, 6.2 Hz, 1H), 3.66-3.51 (m, 4H), 3.18-2.95 (m, 2H), 1.56 (m, 1H). ^{13}C NMR ($CDCl_3$): δ 166.36, 165.75,

155.16, 142.91, 136.86, 132.79, 131.16, 128.59, 118.81, 118.65 117.03, 113.96, 71.35, 48.49, 47.64, 46.47, 45.61, 41.46.

tert-butyl 4-{4-[(5*S*)-5-({4-[(*tert*-butoxycarbonyl)amino]benzamido} methyl)-2-oxo-1,3-oxazolidin-3-yl]phenyl}-3-oxopiperazine-1-carboxylate (o7)

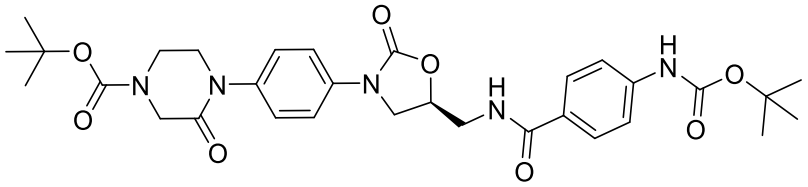

This compound was synthesised according to the general procedure A-step 4-scenario2 by reacting compound **d7** (0.390 g, 1 mmol) with 4-(*(tert* butoxycarbonyl) amino) benzoic acid (0.237 g, 1 mmol). The title compound (0.395 g, 0.65 mmol, 65%) was obtained as a white solid. MS: m/z calculated for $C_{31}H_{40}N_5O_8^+$ 610.2871 $[M+H]^+$, MS: found 610.2889 $[M+H]^+$. HPLC: t_R 2.54 min (96%). Mp: 271˚C. ^{1}H NMR (DMSO-d_6): δ 8.43 (t, J= 7.0 Hz, 1H), 7.89-7.81 (m, 2H), 7.79-7.75 (m, 2H), 7.23 (d, *J*= 9.0, 2H), 6.87 (d, *J*= 9.0, 2H), 7.04 (m, 1H), 4.94-4.82 (m, 1H), 4.18-4.08 (m, 1H), 3.86 (t, *J* = 7.0 Hz, 2H), 3.88 (dd, J= 9.1 Hz, 6.1 Hz, 1H), 3.67-3.57 (m, 2H), 3.41 (s, 2H), 2.93-2.72 (m, 2H), 1.49 (s, 9H), 1.40 (s, 9H). ^{13}C NMR (DMSO-*d6*): δ 168.63, 166.39, 156.82, 154.17, 153.36, 142.92, 138.86, 136.80, 128.71, 126.69, 118.65, 117.93, 117.03, 81.61, 80.57, 71.39, 47.43, 47.42, 44.27, 43.65, 41.49, 29.25, 28.22.

tert-butyl 4-{4-[(5*S*)-5-{[(4-{[(*tert*-butoxycarbonyl)amino]methyl} cyclohexane-1-carbonyl)amino]methyl}-2-oxo-1,3-oxazolidin-3-yl]phenyl}-3-oxopiperazine-1-carboxylate (q7)

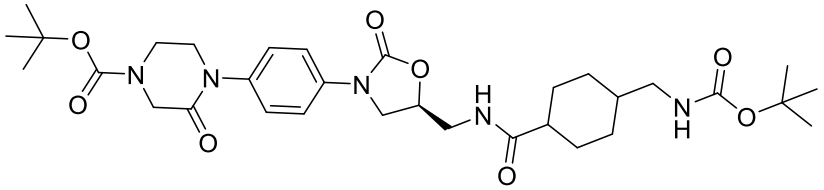

This compound was synthesised according to the general procedure A-step 4-scenario2 by reacting compound **d7** (0.390 g, 1 mmol) with the commercially available 4-{[(*tert*-butoxycarbonyl)amino]methyl}cyclohexane-1-carboxylic acid (0.257 g, 1 mmol). The title compound (0.389 g, 0.62 mmol, 62%) was obtained as a white solid. MS: m/z calculated for $C_{32}H_{48}N_5O_8^+$ 630.3497

[M+H]$^+$, MS: found 630.3508 [M+H]$^+$. HPLC: t_R 2.46 min (94 %). Mp: 234˚C. ^{1}H NMR (DMSO-d_6): δ 8.13 (t, *J*= 6.6 Hz, 1H), 7.36-7.24 (m, 2H), 7.18-7.06 (m, 2H), 6.78 (t, *J* = 7.0 Hz, 1H), 4.90-4.81 (m, 1H), 4.24-4.18 (m, 1H), 3.91 (t, *J* = 7.0 Hz, 2H), 3.87 (dd, J= 9.3 Hz, 6.2 Hz, 1H), 3.66-3.45 (m, 2H), 3.48 (s, 2H), 3.38-3.31 (m, 1H), 3.27-317 (m, 1H), 2.98-2.86 (m, 2H), 2.56-2.45 (m, 1H), 2.25-2.15 (m, 1H), 1.86–1.77 (m, 2H), 1.73-1.64 (m, 4H), 1.62-1.53 (m, 2H), 1.49 (s, 9H), 1.42(s, 9H). ^{13}C NMR (DMSO-d_6): δ 178.96, 168.52, 166.21, 156.48, 154.75, 142.91,136.87, 118.89, 117.03, 80.77, 78.84, 71.39, 48.42, 47.46, 45.81, 44.08, 43.68, 43.11, 41.46, 35.63, 30.95, 29.16, 28.23, 25.81.

tert-butyl 4-(4-{(5*S*)-5-[({4-[(_tert_-butoxycarbonyl)amino]cyclohexane-1-carbonyl}amino)methyl]-2-oxo-1,3-oxazolidin-3-yl}phenyl)-3-oxopiperazine-1-carboxylate (s7)

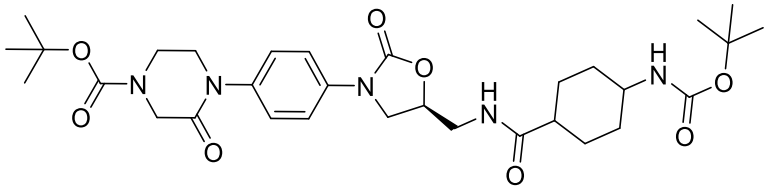

This compound was synthesised according to the general procedure A-step 4-scenario2 by reacting compound **d7** (0.390 g, 1 mmol) with 4-[(tert-butoxycarbonyl)amino] cyclohexane-1-carboxylic acid (0.343 g, 1 mmol). The title compound (0.319 g, 0.52 mmol, 52%) was obtained as a white solid. MS: m/z calculated for $C_{31}H_{46}N_5O_8^+$ 616.3341 [M+H]$^+$, MS: found 616.3358 [M+H]$^+$. HPLC: t_R 2.10 min (96%). Mp: 234˚C. ^{1}H NMR (DMSO-d_6): δ 8.04 (t, J= 6.0 Hz, 1H), 7.36-7.27 (m, 2H), 7.08-6.96 (m, 2H), 4.91-4.81 (m, 1H), 4.49 (d, *J* = 9.5 Hz, 1H), 4.16–4.06 (m, 1H), 3.88 (t, *J* = 7.0 Hz, 2H), 3.86 (dd, J= 8.9 Hz, 5.8 Hz, 1H), 3.61-3.53 (m, 1H), 3.55-3.49 (m, 1H), 3.48-3.42 (m, 1H), 3.39 (s, 2H), 2.94-2.74 (m, 2H), 2.44-2.36 (m, 1H), 1.86-1.68 (m, 6H), 1.58-1.51 (m, 2H), 149 (s, 9H), 1.40 (s, 9H). ^{13}C NMR (DMSO-d_6): δ 178.87, 168.63, 159.58, 156.56, 154.18, 142.67, 136.83, 118.88, 117.15, 80.67, 80.395,71.31 ,51.68, 47.43, 47.44, 45.86, 44.14, 43.66, 41.47, 31.75, 28.32, 28.26, 25.60.

***tert*-butyl 4-(4-{(5*S*)-5-[(4-{[(*tert*-butoxycarbonyl)amino]methyl} benzamido)methyl]-2-oxo-1,3-oxazolidin-3-yl}phenyl)-3-oxopiperazine-1-carboxylate (u7)**

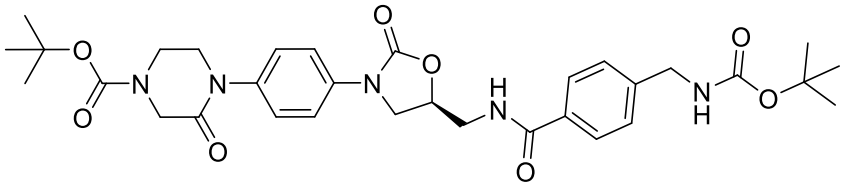

This compound was synthesised according to the general procedure A-step 4-scenario2 by reacting compound **d7** (0.390 g, 1 mmol) with 4-{[(tert-butoxycarbonyl)amino] methyl}benzoic acid (0.251 g, 1 mmol). The title compound (0.361 g, 0.58 mmol, 58%) was obtained as a white solid. MS: m/z calculated for $C_{32}H_{42}N_5O_8^+$ 624.3028 $[M+H]^+$, MS: found 624.3054 $[M+H]^+$. HPLC: t_R 2.26 min (96%). Mp: 256˚C. ^{1}H NMR (DMSO-d_6) δ: ^{1}H NMR (DMSO-d_6): δ 8.03 (t, *J* = 7.5 Hz, 1H), 7.77–7.68 (m, 2H), 7.25–7.16 (m, 4H), 6.99–6.92(m, 2H), 5.11 (t, *J* = 8.5 Hz, 1H), 4.87-4.78 (m, 1H), 4.39-4.31 (m, 1H), 4.28-4.20 (m, 1H), 4.11-3.99 (m, 1H), 3.92 (t, *J* = 7.1 Hz, 2H), 3.89 (dd, J= 9.2 Hz, 6.1 Hz, 1H), 3.52-3.48 (m, 2H), 3.34 (s, 2H), 2.84-2.70 (m, 2H), 1.47 (m, 9H), 1.39 (s, 9H). ^{13}C NMR (DMSO-d_6): δ 167.63, 166.37, 156.21, 154.67, 154.21, 142.97, 139.21, 136.86, 131.44, 128.56, 127.73, 118.86, 117.16, 80.58, 79.85, 71.35, 47.45, 47.41, 44.20, 44.08, 43.68, 41.51, 28.37, 28.26.

***tert*-butyl 4-(4-{(5*S*)-5-[(4-carbamoylbenzamido)methyl]-2-oxo-1,3-oxazolidin-3-yl}phenyl)-3-oxopiperazine-1-carboxylate (w7)**

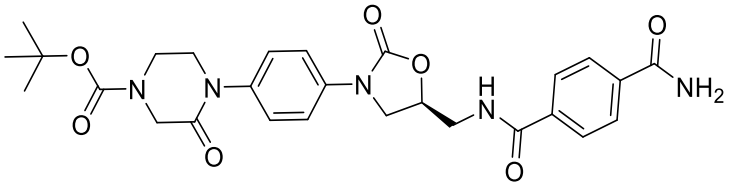

This compound was synthesised according to the general procedure A-step 4-scenario 2 by reacting compound **d7** (0.195 g, 0.5 mmol) with 4-carbamoylbenzoic acid (0.082 g, 0.5 mmol). The title compound (0.150 g, 0.28 mmol, 56%) was obtained as a white solid. MS: m/z calculated for $C_{27}H_{32}N_5O_7^+$ 538.2296 $[M+H]^+$, MS: found 538.2307 $[M+H]^+$. HPLC: t_R 2.34 min (95%). Mp: 296˚C. $[\alpha]_D^{22}$= 53° (c= 1, DMSO). ^{1}H NMR (DMSO-d_6): δ 8.51 (t, *J*= 7.5 Hz, 1H), 8.31-8.20 (m, 2H), 7.96-7.85 (m, 2H), 7.39 (d, *J*=8.5 Hz, 2H), 7.18 (d, *J*=8.5 Hz, 2H), 6.91 (s, 2H), 4.95-4.84 (m, 1H), 4.23-4.17 (m, 1H), 3.94 (t, *J* = 7.0 Hz, 2H), 3.89 (dd, J= 9.2 Hz, 6.3 Hz, 1H), 3.63-3.56

(m, 2H), 3.42 (s, 2H), 2.94-2.86 (m, 2H), 1.42 (s, 9H). ^{13}C NMR (DMSO-d_6): δ 168.86, 167.65, 166.31, 156.76, 154.15, 143.06, 137.83, 136.31, 131.25, 128.56, 128.13 ,118.86, 117.15, 80.56, 71.31, 47.45, 47.45, 44.46, 43.63, 41.58, 28.15.

tert-butyl 3-oxo-4-(4-{(5*S*)-2-oxo-5-[(4-sulfamoylbenzamido)methyl]-1,3-oxazolidin-3-yl}phenyl)piperazine-1-carboxylate (x7)

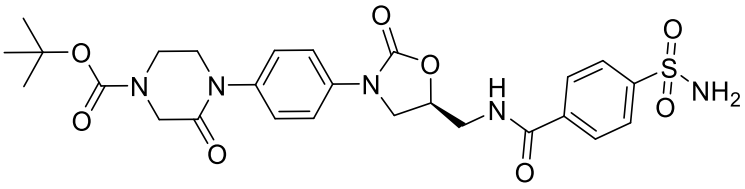

This compound was synthesised according to the general procedure A-step 4-scenario 2 by reacting compound **d7** (0.195 g, 0.5 mmol) with 4-sulfamoylbenzoic acid (0.101 g, 0.5 mmol). The title compound (0.151 g, 0.26 mmol, 53%) was obtained as a white solid. MS: m/z calculated for $C_{26}H_{32}N_5O_8S^+$ 574.1966 $[M+H]^+$, MS: found 574.1960 $[M+H]^+$. HPLC: t_R 2.53 min (95%). Mp: 266˚C. $[\alpha]_D^{22}$= 60° (c= 1, DMSO). ^{1}H NMR (DMSO-d_6): δ 8.84 (t, *J* = 7.8 Hz, 1H), 8.31-8.24 (m, 2H), 8.05-7.93 (m, 2H), 7.41-7.29 (m, 2H), 7.36 (s, 2H), 7.15-7.03 (m, 2H), 4.95-4.84 (m, 1H), 4.26-4.15 (m, 1H), 3.96 (t, *J* = 7.1 Hz, 2H), 3.88 (dd, J= 9.6 Hz, 6.1 Hz, 1H), 3.71-3.64 (m, 2H), 3.48 (s, 2H), 2.98-2.85 (m, 2H), 1.41 (s, 9H). ^{13}C NMR (DMSO-d_6): δ 167.82, 166.35, 156.85, 154.15, 145.61, 142.98, 136.81, 133.26, 130.17, 127.56, 118.86, 117.04, 80.58, 71.31, 47.44, 47.43, 44.46, 43.64, 41.46, 28.26.

N^1-({(5*S*)-2-oxo-3-[4-(2-oxopiperazin-1-yl)phenyl]-1,3-oxazolidin-5-yl}methyl)benzene-1,4-dicarboxamide (w9)

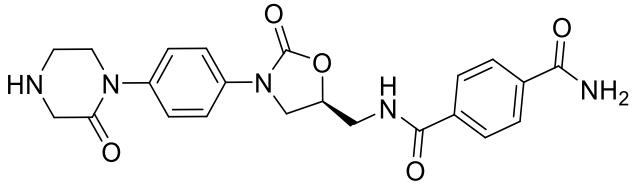

This compound was synthesised according to the general procedure A-step 5-scenario 1 starting with compound **w7** (0.107 g, 0.2 mmol). The title compound (0.075 g, 0.17 mmol, 87%) was obtained as a white solid. MS: m/z calculated for $C_{22}H_{24}N_5O_5^+$ 438.1772 $[M+H]^+$, MS: found 438.1786 $[M+H]^+$. HPLC: t_R 1.76 min (96%). Mp: 221˚C. $[\alpha]_D^{22}$= 45° (c= 1, DMSO). ^{1}H NMR (DMSO-d_6): δ 8.36 (t, *J*= 7.5 Hz, 1H), 8.15-8.06 (m, 2H), 7.77-7.63 (m, 2H), 7.41 (d, *J*= 8.5 Hz, 2H), 7.16 (d, *J*= 8.5 Hz, 2H), 6.56 (s, 2H), 4.93-4.82 (m,

1H), 4.13-4.04 (m, 1H), 3.93 (t, *J* = 7.0 Hz, 2H), 3.87 (dd, J= 9.2 Hz, 6.2 Hz, 1H), 3.59 (d, *J* = 6.6 Hz, 2H), 3.21-3.05 (m, 2H), 3.07 (td, *J* = 7.0, 5.6 Hz, 2H), 1.58 (tt, *J* = 6.6, 5.6 Hz, 1H). ^{13}C NMR (DMSO-d_6): δ 167.93, 166.36, 165.61, 154.17, 142.98, 136.88, 136.13, 131.32, 129.21, 128.13, 118.86, 117.15, 71.31, 47.45, 46.51, 46.26, 45.66, 41.47.

_N_-({(5_S_)-2-oxo-3-[4-(2-oxopiperazin-1-yl)phenyl]-1,3-oxazolidin-5-yl}methyl)-4-sulfamoylbenzamide (x9)

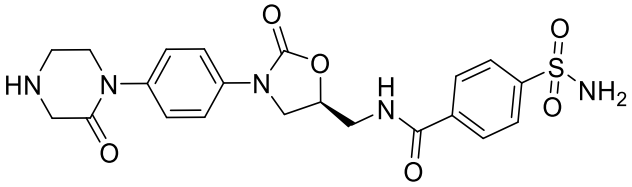

This compound was synthesised according to the general procedure A-step 5-scenario 1 starting with compound **x7** (0.114 g, 0.2 mmol). The title compound (0.076 g, 0.16 mmol, 81 %) was obtained as a yellow solid. MS: m/z calculated for $C_{21}H_{24}N_5O_6S^+$ 474.1442 $[M+H]^+$, MS: found 474.1456 $[M+H]^+$. HPLC: t_R 1.99 min (96%). Mp: 196 ˚C. $[\alpha]_D^{22}$ = 53° (c= 1, DMSO). ^{1}H NMR (DMSO-d_6): δ 8.82 (t, *J* = 7.5 Hz, 1H), 8.28-8.19 (m, 2H), 7.93-7.81 (m, 2H), 7.36-7.25 (m, 2H), 7.36 (s, 2H), 7.15-7.03 (m, 2H), 4.93-4.81 (m, 1H), 4.17-4.08 (m, 1H), 3.96 (t, *J* = 7.0 Hz, 2H), 3.88 (dd, J= 9.2 Hz, 6.1 Hz, 1H), 3.45 (d, *J* = 6.5 Hz, 2H), 3.33-3.15 (m, 2H), 3.13 (td, *J* = 7.0, 5.5 Hz, 2H), 1.59 (tt, *J* = 6.5, 5.5 Hz, 1H). ^{13}C NMR (DMSO-d_6): δ 167.42, 166.22, 155.25, 145.63, 143.07, 136.77, 133.21, 129.95, 127.56, 118.46, 117.15, 71.36, 48.56, 46.55, 46.28, 45.66, 41.47.

4-amino-_N_-({(5_S_)-2-oxo-3-[4-(2-oxopiperazin-1-yl)phenyl]-1,3-oxazolidin-5-yl}methyl)benzamide (p9)

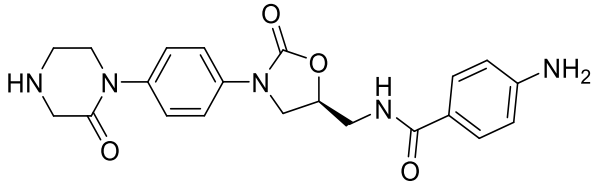

This compound was synthesised according to the general procedure A-step 5-scenario 1 starting with compound **o7** (0.334 g, 0.55 mmol). The title compound (0.116 g, 0.28 mmol, 52%) was obtained as an off-white solid. MS: m/z calculated for $C_{21}H_{24}N_5O_4^+$ 410.1823 $[M+H]^+$, MS: found 410.1846 $[M+H]^+$. HPLC: t_R 1.66 min (96%). Mp: 223˚C. $[\alpha]_D^{22}$= 90° (c= 1, DMSO). ^{1}H NMR (DMSO-d_6): δ 8.31 (t, J= 7.8 Hz, 1H), 7.64-7.56 (m, 2H), 7.38 (d, J= 9.5

Hz, 2H), 7.36-7.23(m, 2H), 7.19 (d, J= 9.5 Hz, 2H), 5.46 (s, 2H), 4.93-4.80 (m, 1H), 4.28-4.20 (m, 1H), 3.91 (t, *J* = 7.1 Hz, 2H), 3.89 (dd, J= 9.2 Hz, 6.1 Hz, 1H), 3.60 (d, *J* = 6.8 Hz, 2H), 3.33-3.14 (m, 2H), 3.15 (td, *J* = 7.1, 5.5 Hz, 2H), 1.60 (tt, *J* = 6.8, 5.5 Hz, 1H). ^{13}C NMR (DMSO-*d*$_6$): δ 167.33, 165.83, 155.17, 152.27, 142.86, 136.98, 128.81, 126.68, 118.66, 117.13, 112.93, 71.39, 48.51, 47.50, 46.67, 45.62, 41.35.

4-(aminomethyl)-*N*-({(5*S*)-2-oxo-3-[4-(2-oxopiperazin-1-yl)phenyl]-1,3-oxazolidin-5-yl}methyl)cyclohexane-1-carboxamide (r9)

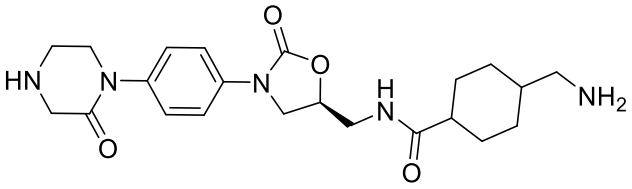

This compound was synthesised according to the general procedure A-step 5-scenario 1 starting with compound **q7** (0.345 g, 0.55 mmol). The title compound (0.122 g, 0.28 mmol, 52%) was obtained as a white solid. MS: m/z calculated for $C_{22}H_{32}N_5O_4^+$ 430.2449 $[M+H]^+$, MS: found 430.2457 $[M+H]^+$. HPLC: t_R 1.85 min (96%). Mp: 203˚C. $[\alpha]_D^{22}$= 99° (c= 1, DMSO). ^{1}H NMR (DMSO-*d*$_6$): δ 8.03(t, *J*=7.5 Hz, 1H), 7.78 (d, *J*= 8.5 Hz, 2H), 7.61 (d, *J*= 8.5 Hz, 2H), 4.94-4.83 (m, 1H), 4.14-4.04 (m, 1H), 3.93 (t, *J*= 7.1 Hz, 2H), 3.86 (dd, J= 8.6 Hz, 5.6 Hz, 1H),, 3.59 (d, *J*= 6.6 Hz, 2H), 3.58-3.49 (m, 1H), 3.52-3.40 (m, 1H), 3.16-2.98 (m, 2H), 2.77-2.69 (m, 1H), 2.56-2.44 (m, 1H), 2.41-3.33 (m, 2H), 1.77-1.71 (m, 2H), 1.69-160 (m, 2H), 1.58-147 (m, 4H), 1.41-1.35 (m, 3H).^{13}C NMR (DMSO-*d*$_6$): δ 178.88, 166.16, 154.25, 142.96, 136.81, 119.86, 117.17, 71.30, 49.22, 48.41, 47.44, 46.07, 45.99, 45.03, 41.34, 41.48, 28.96, 26.39.

4-amino-N-({(5*S*)-2-oxo-3-[4-(2-oxopiperazin-1-yl)phenyl]-1,3-oxazolidin-5-yl}methyl)cyclohexane-1-carboxamide (t9)

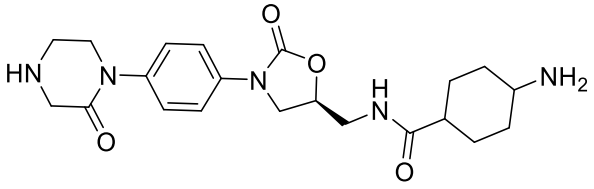

This compound was synthesised according to the general procedure A-step 5-scenario 1 starting with compound **s7** (0.276 g, 0.45 mmol). The title compound (0.113 g, 0.27 mmol, 61%) was obtained as a white solid. MS: m/z calculated for $C_{21}H_{30}N_5O_4^+$ 416.2292 $[M+H]^+$, MS: found 416.2308 $[M+H]^+$.

HPLC: t_R 1.87 min (96%). Mp: 213˚C. $[\alpha]_D^{21}$= 56° (c= 1, DMSO). ^{1}H NMR (DMSO-d_6): δ 8.06 (t, J= 7.6 Hz, 1H), 7.36-7.29(m, 2H), 7.04-6.97 (m, 2H), 4.90-4.80 (m, 1H), 4.14-4.04 (m, 1H), 3.93 (t, *J* = 7.1 Hz, 2H), 3.85 (dd, J= 9.1 Hz, 6.0 Hz, 1H), 3.59 (d, *J* = 6.6 Hz, 2H), 3.58-3.49 (m, 1H), 3.52-3.40 (m, 1H), 3.16-2.98 (m, 2H), 2.88-2.75 (m, 1H), 2.41-2.33 (m, 1H), 2.02 (d, *J*= 7.3 Hz, 2H), 1.84-1.70 (m, 2H), 1.72-1.53 (m, 5H), 1.53-1.40 (m, 2H).^{13}C NMR (DMSO-d_6): δ 178.76, 166.18, 154.25, 142.46, 136.88, 118.89, 117.35, 71.30, 51.28, 47.43, 47.44, 46.19, 45.81, 45.17, 41.77, 33.23, 25.87.

4-(aminomethyl)-*N*-({(5*S*)-2-oxo-3-[4-(2-oxopiperazin-1-yl)phenyl]-1,3-oxazolidin-5-yl}methyl)benzamide (v9)

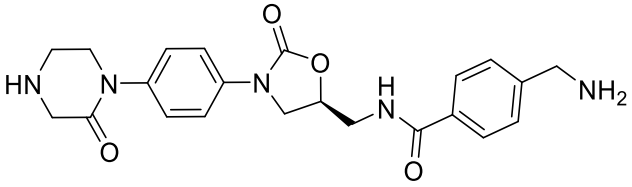

This compound was synthesised according to the general procedure A-step 5-scenario 1 starting with compound **u7** (0.311g, 0.5 mmol). The title compound (0.116 g, 0.27 mmol, 55%) was obtained as a white solid. MS: m/z calculated for $C_{22}H_{26}N_5O_4^+$ 424.1979 $[M+H]^+$, MS: found 424.1997 $[M+H]^+$. HPLC: t_R 1.70 min (95%). Mp: 199˚C. $[\alpha]_D^{22}$= -57° (c= 1, DMSO). ^{1}H NMR (DMSO-d_6): δ 8.41 (t, *J*= 6.6 Hz, 2H), 7.98 (t, *J* = 7.5 Hz, 1H), 7.89-7.81 (m, 2H), 7.30-7.21 (m, 2H), 7.18-7.08 (d, J= 8.6 Hz, 2H), 7.05-6.99 (d, J= 8.6 Hz, 2H), 4.89-4.80 (m, 1H), 4.18- 4.09 (m, 1H), 3.92 (t, *J* = 7.1 Hz, 2H), 3.88 (dd, J= 8.9 Hz, 6.1 Hz, 1H), 3.73-3.61 (m, 1H), 3.61-3.55 (m, 4H), 3.16-2.98 (m, 2H), 1.61-1.55 (m, 1H). ^{13}C NMR (DMSO-d_6): δ 167.36, 165.93, 154.17, 143.98, 142.98, 136.83, 131.44, 128.56, 127.17, 118.86, 117.15, 71.36, 47.47, 46.38, 46.23, 46.09, 45.66, 41.44.

4-(*N*-hydroxycarbamimidoyl)-*N*-({(5*S*)-2-oxo-3-[4-(3-oxomorpholin-4-yl)phenyl]-1,3-oxazolidin-5-yl}methyl)benzamide (y1)

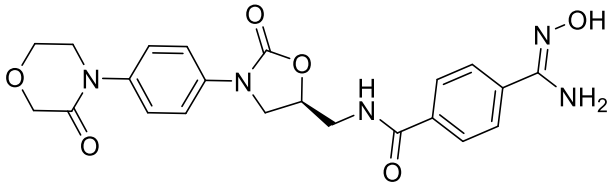

This compound was synthesised according to the general procedure B-step 1 starting with compound **h1** (0.420 g, 1 mmol). The title compound (0.235 g, 0.52 mmol, 52%) was obtained as a white solid. MS: m/z calculated for

$C_{22}H_{24}N_5O_6^+$ 454.1721 $[M+H]^+$, MS: found 454.1739 $[M+H]^+$. HPLC: t_R 1.30 min (95%). Mp: 188 ˚C. $[\alpha]_D^{22}$= -45° (c= 1, DMSO). ^{1}H NMR (DMSO-d_6): δ 9.46 (s, 1H), 8.13 (t, J = 7.8 Hz, 1H), 7.69-7.58 (m, 4H), 7.34-7.27 (m, 2H), 7.15-7.07 (m, 2H), 5.24 (s, 2H), 4.87-4.79 (m, 1H), 4.31 (s, 2H), 4.14-4.05 (m, 1H), 4.00-3.91 (m, 2H), 3.88 (dd, J= 9.0 Hz, 6.1 Hz, 1H), 3.86-3.74 (m, 2H), 3.60-3.53 (m, 2H). ^{13}C NMR (DMSO-d_6): δ 167.38, 166.15, 154.08, 150.23, 142.45, 136.18, 134.06, 130.36, 128.34, 126.24, 118.86, 117.19, 71.39, 69.87, 66.12, 47.28, 46.45, 41.29.

4-(*N*-hydroxycarbamimidoyl)-*N*-({(5*S*)-3-[4-(morpholin-4-yl)phenyl]-2-oxo-1,3-oxazolidin-5-yl}methyl)benzamide (y2)

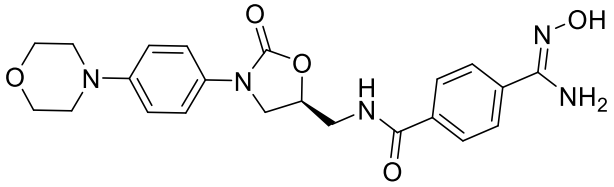

This compound was synthesised according to the general procedure B-step 1 starting with compound **h2** (0.406 g, 1 mmol)**.** The title compound (0.188 g, 0.43 mmol, 43%) was obtained as a white solid. MS: m/z calculated for $C_{22}H_{26}N_5O_5^+$ 440.1928 $[M+H]^+$, MS: found 440.1937 $[M+H]^+$. HPLC: t_R 1.34 min (96%). Mp: 190 ˚C. $[\alpha]_D^{22}$= 36° (c= 1, DMSO). ^{1}H NMR (DMSO-d_6): δ 9.71 (s, 1H), 8.14 (t, *J* = 7.8 Hz, 1H), 7.70-7.61 (m, 4H), 7.34-7.27 (m, 2H), 7.03-6.96 (m, 2H), 5.31 (s, 2H), 4.89-4.79 (m, 1H), 4.17-4.08 (m, 1H), 4.02-3.94 (m, 2H), 3.88 (dd, J= 9.1 Hz, 6.1 Hz, 1H), 3.74 (d, *J* = 7.1 Hz, 2H), 3.63-3.55 (m, 2H), 3.21 (t, *J* = 7.1 Hz, 4H). ^{13}C NMR (DMSO-d_6): δ 168.39, 156.16, 151.25, 144.36, 136.73, 133.95, 131.34, 128.59, 125.55, 118.87, 117.17, 71.32, 66.67, 52.17, 47.44, 41.46.

4-(*N*-hydroxycarbamimidoyl)-*N*-({(5*S*)-3-[4-(4-methylpiperazin-1-yl)phenyl]-2-oxo-1,3-oxazolidin-5-yl}methyl)benzamide (y4)

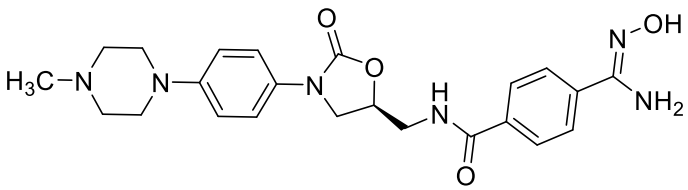

This compound was synthesised according to the general procedure B-step 1 starting with compound **h4** (0.419 g, 1 mmol). The title compound (0.149 g, 0.33 mmol, 33%) was obtained as a white solid. MS: m/z calculated for

$C_{23}H_{29}N_6O_4^+$ 453.2245 $[M+H]^+$, MS: found 453.2261 $[M+H]^+$. HPLC: t_R 1.36 min (95%). Mp: 191 ˚C. $[\alpha]_D^{22}$= 53° (c= 1, DMSO). ^{1}H NMR (DMSO-d_6): δ 9.36 (s, 1H), 8.23 (t, *J* = 7.8 Hz, 1H), 7.71-7.62 (m, 4H), 7.33-7.27 (m, 2H), 7.04-6.95 (m, 2H), 5.33 (s, 2H), 4.89-4.79 (m, 1H), 4.16-4.09 (m, 1H), 3.89 (dd, J= 8.9 Hz, 6.1 Hz, 1H), 3.63-3.56 (m, 2H), 3.55-3.45 (m, 2H), 3.38-3.27 (m, 2H), 3.26-3.18 (m, 2H), 2.86-2.73 (m, 2H), 2.45 (s, 3H). ^{13}C NMR (DMSO-d_6): δ 168.35, 156.31, 154.28, 151.16, 136.82, 133.94, 131.16, 128.59, 126.64, 118.87, 117.12, 71.31, 56.66, 50.91, 47.46, 45.89, 41.48.

4-(*N*-hydroxycarbamimidoyl)-*N*-({(5*S*)-3-[4-(4-methyl-2-oxopiperazin-1-yl)phenyl]-2-oxo-1,3-oxazolidin-5-yl}methyl)benzamide (y5)

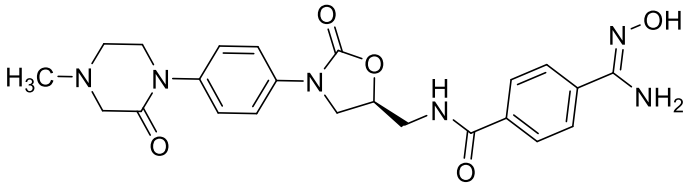

This compound was synthesised according to the general procedure B-step 1 starting with compound **h5** (0.433 g, 1 mmol). The title compound (0.116 g, 0.25 mmol, 25%) was obtained as a white solid. MS: m/z calculated for $C_{23}H_{27}N_6O_5^+$ 467.2037 $[M+H]^+$, MS: found 467.2057 $[M+H]^+$. HPLC: t_R 1.30 min (95%). Mp: 173 ˚C. $[\alpha]_D^{22}$= 61° (c= 1, DMSO). ^{1}H NMR (DMSO-d_6): δ 9.51 (s, 1H), 8.12 (t, *J* = 7.6 Hz, 1H), 7.96-7.88 (m, 2H), 7.87-7.75 (m, 2H), 7.36-7.29 (m, 2H), 7.17-7.09 (m, 2H), 5.27 (s, 2H), 4.88-4.80 (m, 1H), 4.17-4.09 (m, 1H), 3.89 (dd, J= 9.0 Hz, 6.3 Hz, 1H), 3.83-3.74 (m, 2H), 3.63-3.55 (m, 2H), 3.42 (s, 2H), 2.94-2.74 (m, 2H), 2.25 (s, 3H). ^{13}C NMR (DMSO-d_6): δ 167.68, 166.31, 155.17, 151.18, 142.96, 138.85, 133.95, 131.23, 128.57, 125.62, 118.89, 117.11, 72.32, 56.51, 54.87, 48.45, 47.41, 44.31, 41.47.

***tert*-butyl 4-{4-[(5*S*)-5-{[4-(*N*-hydroxycarbamimidoyl)benzamido]methyl}-2-oxo-1,3-oxazolidin-3-yl]phenyl}piperazine-1-carboxylate (y6)**

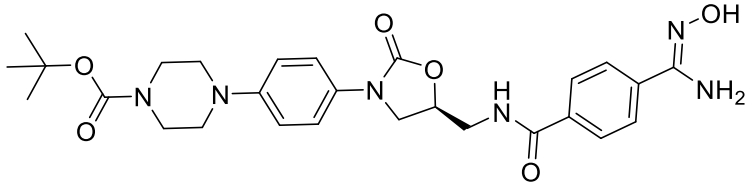

This compound was synthesised according to the general procedure B-step 1 starting with compound **h6** (0.505 g, 1 mmol)**.** The title compound (0.306 g, 0.57 mmol, 57%) was obtained as a white solid. MS: m/z calculated for $C_{27}H_{35}N_6O_6^+$ 539.2613 $[M+H]^+$, MS: found 539.2625 $[M+H]^+$. HPLC: t_R 1.67

min (95%). Mp: 190 ˚C. $[\alpha]_D^{22}$= -73° (c= 1, DMSO). ^{1}H NMR (DMSO-d_6): δ 9.41 (s, 1H), 8.10 (t, *J* = 7.7 Hz, 1H), 7.70-7.61 (m, 4H), 7.36-7.23 (m, 2H), 7.05-6.92(m, 2H), 5.36 (s, 2H), 4.85-4.71 (m, 1H), 4.17-4.08 (m, 1H), 3.87 (dd, J= 9.0 Hz, 5.9 Hz, 1H), 3.77-3.56 (m, 4H), 3.46-3.33 (m, 3H), 3.32-3.28(m, 3H), 1.51 (s, 9H). ^{13}C NMR (DMSO-d_6): δ 168.31, 157.81, 154.41, 154.18, 151.25, 136.81, 134.92, 131.34, 128.56, 125.76, 118.91, 117.12, 79.764, 71.34, 49.98, 47.45, 43.74, 41.43, 28.47.

tert-butyl 4-{4-[(5*S*)-5-{[4-(*N*-hydroxycarbamimidoyl)benzamido]methyl}-2-oxo-1,3-oxazolidin-3-yl]phenyl}-3-oxopiperazine-1-carboxylate (y7)

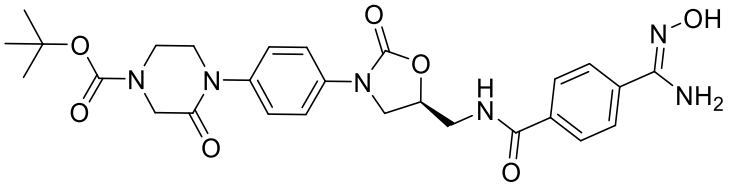

This compound was synthesised according to the general procedure B-step 1 starting with compound **h7** (0.519 g, 1 mmol). The title compound (0.226 g, 0.41 mmol, 41%) was obtained as a white solid. MS: m/z calculated for $C_{27}H_{33}N_6O_7^+$ 553.2405 $[M+H]^+$, MS: found 553.2419 $[M+H]^+$. HPLC: t_R 1.68 min (97%). Mp: 188 ˚C. $[\alpha]_D^{22}$= 31° (c= 1, DMSO). ^{1}H NMR (DMSO-d_6): δ 9.46 (s, 1H), 8.08 (m, 1H), 7.89-7.80 (m, 2H), 7.79-7.68 (m, 2H), 7.46-7.39 (m, 2H), 7.24-7.13 (m, 2H), 5.25 (s, 2H), 4.84-4.82 (m, 1H), 4.26-4.15 (m, 1H), 4.01-3.93 (m, 2H), 3.86 (dd, J= 9.0 Hz, 6.1 Hz, 1H), 3.73-3.65 (m, 2H), 3.51 (s, 2H), 3.00-2.86 (m, 2H), 1.49 (s, 9H). ^{13}C NMR (DMSO-d_6): δ 168.63, 167.31, 156.73, 154.18, 150.25, 143.96, 136.88, 133.88, 131.34, 128.59, 125.69, 118.76, 117.15, 80.58, 71.38, 47.44, 47.43, 44.49, 43.61, 41.46, 28.28.

4-(*N*-hydroxycarbamimidoyl)-*N*-({(5*S*)-2-oxo-3-[4-(piperazin-1-yl)phenyl]-1,3-oxazolidin-5-yl}methyl)benzamide (y8)

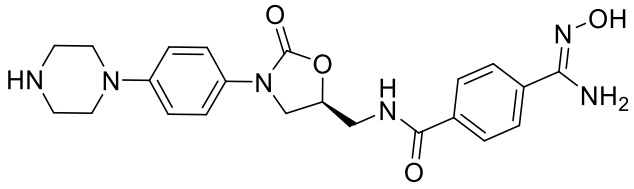

This compound was synthesised according to the general procedure B-step 2 starting with compound **y6** (0.269, 0.50 mmol) or in another batch this compound was synthesised according to the general procedure B-step1 starting with compound **h8** (0.405 g, 1 mmol). The title compound (0.065 g, 0.15 mmol, 30%, or 0.087 g, 0.2 mmol, 20%, respectively) was obtained as a white

solid. MS: m/z calculated for $C_{22}H_{27}N_6O_4^+$ 439.2088 $[M+H]^+$, MS: found 439.2102 $[M+H]^+$. HPLC: t_R 1.50 min (94%). Mp: 193 ˚C. $[\alpha]_D^{22}$= 66° (c= 1, DMSO). ^{1}H NMR (DMSO-d_6): δ 9.36 (s, 1H), 8.18-8.14 (m, 1H), 7.88-7.63 (m, 4H), 7.37-7.26 (m, 2H), 7.06-6.97 (m, 2H), 5.36 (s, 2H), 4.89-4.81 (m, 1H), 4.26-4.17 (m, 1H), 3.88 (dd, J= 9.3 Hz, 6.2 Hz, 1H), 3.55-3.46 (m, 2H), 3.36-3.21 (m, 4H), 3.25-3.14 (m, 1H), 3.15-3.03 (m, 4H). ^{13}C NMR (DMSO-d_6): δ 172.13, 156.33, 154.26, 151.14, 136.81, 133.96, 132.91, 129.59, 125.65, 118.86, 117.15, 74.75, 50.65, 49.58, 48.85, 45.77.

4-(*N*-hydroxycarbamimidoyl)-*N*-({(5*S*)-2-oxo-3-[4-(2-oxopiperazin-1-yl)phenyl]-1,3-oxazolidin-5-yl}methyl)benzamide (y9)

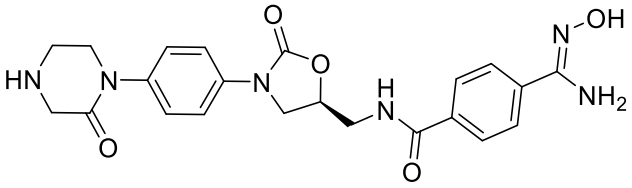

This compound was synthesised according to the general procedure B-step 2 starting with compound **y7** (0.193 g, 0.35 mmol) or in another batch this compound was synthesised according to the general procedure B-step1 starting with compound **h9** (0.419 g, 1 mmol). The title compound (0.034 g, 0.077 mmol, 22% or 0.113 g, 0.25 mmol, 25%) was obtained as a white solid. MS: m/z calculated for $C_{22}H_{25}N_6O_5^+$ 453.1881 $[M+H]^+$, MS: found 453.1896 $[M+H]^+$. HPLC: t_R 1.43 min (95%). Mp: 201 ˚C. $[\alpha]_D^{22}$= -78° (c= 1, DMSO). ^{1}H NMR (DMSO-d_6) δ 9.39 (s, 1H), 8.17 (t, *J* = 7.8 Hz, 1H), 7.73-7.62 (m, 4H), 7.34-7.30 (m, 2H), 7.18-7.10 (m, 2H), 5.24 (s, 2H), 4.89-4.80 (m, 1H), 4.19- 4.08 (m, 1H), 3.87 (dd, J= 9.2 Hz, 6.2 Hz, 1H), 3.88-3.75 (m, 2H), 3.61-3.56 (m, 4H), 3.16-2.96 (m, 2H), 1.61-1.54 (m, 1H). ^{13}C NMR (DMSO-d_6): δ 168.36, 167.01, 155.14, 151.15, 142.96, 136.82, 133.83, 131.34, 128.69, 125.62, 118.86, 117.15, 71.33, 47.45, 46.48, 46.28, 45.66, 41.41.

4-carbamimidoyl-*N*-({(5*S*)-2-oxo-3-[4-(3-oxomorpholin-4-yl)phenyl]-1,3-oxazolidin-5-yl}methyl)benzamide (z1)

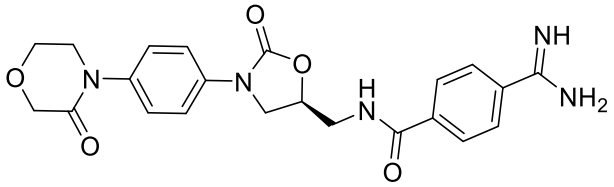

This compound was synthesised according to the general procedure B-step 3 starting with compound **y1** (0.181 g, 0.4 mmol). The title compound (0.096 g,

0.22 mmol, 55%) was obtained as a white solid. MS: m/z calculated for $C_{22}H_{24}N_5O_5^+$ 438.1772 $[M+H]^+$, MS: found 438.1791 $[M+H]^+$. HPLC: t_R 1.15 min (95%). Mp: 201 ˚C. $[\alpha]_D^{22}$= -96° (c= 1, DMSO). ^{1}H NMR (DMSO-d_6): δ ^{1}H NMR (DMSO-d_6) δ 8.34 (s, 1H), 8.23 (t, *J* = 7.7 Hz, 1H), 7.83-7.78 (m, 2H), 7.76-7.68 (m, 2H), 7.37-7.30 (m, 2H), 7.18-7.10 (m, 2H), 6.23 (s, 2H), 4.89-4.81 (m, 1H), 4.33 (s, 2H), 4.14-4.06 (m, 1H), 4.05-3.99 (m, 2H), 3.89 (dd, J= 9.4 Hz, 6.2 Hz, 1H), 3.85-3.72 (m, 2H), 3.60-3.51 (m, 2H). ^{13}C NMR (DMSO-d_6): δ 167.31, 166.22, 165.15, 154.25, 142.99, 136.81, 131.13, 128.59, 127.42, 125.67, 118.88, 117.15, 71.33, 69.76, 66.51, 47.48, 46.31, 41.46.

4-carbamimidoyl-*N*-({(5*S*)-3-[4-(morpholin-4-yl)phenyl]-2-oxo-1,3-oxazolidin-5-yl}methyl)benzamide (z2)

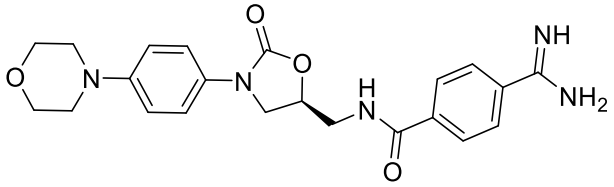

This compound was synthesised according to the general procedure B-step 3 starting with compound **y2** (0.131 g, 0.3 mmol). The title compound (0.076 g, 0.18 mmol, 60%) was obtained as a white solid. MS: m/z calculated for $C_{22}H_{26}N_5O_4^+$ 424.1979 $[M+H]^+$, MS: found 424.1989 $[M+H]^+$. HPLC: t_R 1.10 min (95%). Mp: 171 ˚C. $[\alpha]_D^{22}$= -56° (c= 1, DMSO). ^{1}H NMR (DMSO-d_6): δ 8.36 (s, 1H), 8.26 (t, *J* = 7.8 Hz, 1H), 7.82-7.75 (m, 2H), 7.74-7.66 (m, 2H), 7.34-7.27 (m, 2H), 7.03-6.96 (m, 2H), 6.23 (s, 2H), 4.89-4.78 (m, 1H), 4.18-4.09 (m, 1H), 3.90 (dd, J= 8.9 Hz, 6.2 Hz, 1H), 3.84-3.79 (m, 2H), 3.75 (d, *J* = 7.0 Hz, 2H), 3.62-3.56 (m, 2H), 3.23 (t, *J* = 7.1 Hz, 4H). ^{13}C NMR (DMSO-d_6): δ 168.35, 165.15, 155.14, 144.36, 136.88, 131.45, 128.56, 127.43, 125.61, 118.89, 117.15, 71.31, 66.68, 51.15, 47.44, 41.46.

4-carbamimidoyl-*N*-({(5*S*)-3-[4-(4-methylpiperazin-1-yl)phenyl]-2-oxo-1,3-oxazolidin-5-yl}methyl)benzamide (z4)

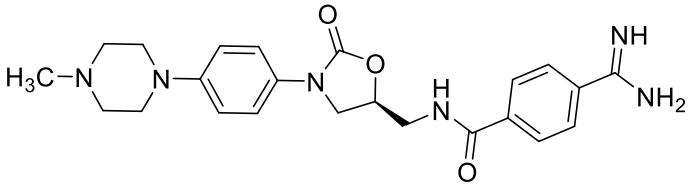

This compound was synthesised according to the general procedure B-step 3 starting with compound **y4** (0.113 g, 0.25 mmol). The title compound (0.039g,

0.09 mmol, 36%) was obtained as a white solid. MS: m/z calculated for $C_{23}H_{29}N_6O_3^+$ 437.2296 $[M+H]^+$, MS: found 437.2305 $[M+H]^+$. HPLC: t_R 1.16 min (96%). Mp: 206 ˚C. $[\alpha]_D^{22}$= -98° (c= 1, DMSO). ^{1}H NMR (DMSO-d_6): δ 8.38 (s, 1H), 8.25 (t, *J* = 7.8 Hz, 1H), 7.837.756 (m, 2H), 7.78-7.63 (m, 2H), 7.35-7.28 (m, 2H), 7.06 – 6.99 (m, 2H), 6.25 (s, 2H), 4.93-4.83 (m, 1H), 4.17-4.11 (m, 1H), 3.89 (dd, J= 9.3 Hz, 6.2 Hz, 1H), 3.65-3.58 (m, 2H), 3.57-3.46 (m, 2H), 3.39-3.27 (m, 2H), 3.28-3.19 (m, 2H), 2.85-2.73 (m, 2H), 2.46 (s, 3H). ^{13}C NMR (DMSO-d_6): δ 166.35, 165.12, 154.36, 156.17, 136.81, 131.33, 128.59, 127.43, 125.64, 118.86, 117.15, 71.36, 56.82, 49.91, 47.43, 45.92, 41.46.

4-carbamimidoyl-*N*-({(5*S*)-3-[4-(4-methyl-2-oxopiperazin-1-yl)phenyl]-2-oxo-1,3-oxazolidin-5-yl}methyl)benzamide (z5)

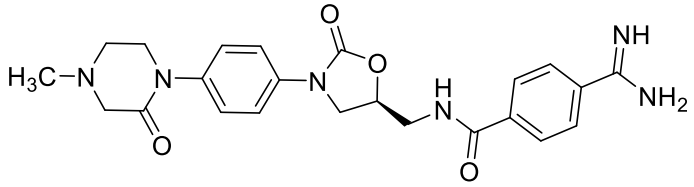

This compound was synthesised according to the general procedure B-step 3 starting with compound **y5** (0.139 g, 0.30 mmol)**.** The title compound (0.033, 0.075 g, 25%) was obtained as a white solid. MS: m/z calculated for $C_{23}H_{27}N_6O_4^+$ 451.2088 $[M+H]^+$, MS: found 451.2105 $[M+H]^+$. HPLC: t_R 1.33 min (95%). Mp: 213 ˚C. $[\alpha]_D^{22}$= 66° (c= 1, DMSO). ^{1}H NMR (DMSO-d_6): δ 8.35 (s, 1H), 8.22 (t, *J* = 7.8 Hz, 1H), 7.82-7.76 (m, 2H), 7.74-7.65 (m, 2H), 7.35-7.28 (m, 2H), 7.18-7.08 (m, 2H), 6.24 (s, 2H), 4.89-4.82 (m, 1H), 4.19-4.11 (m, 1H), 3.91 (dd, J= 9.2 Hz, 5.9 Hz, 1H), 3.84-3.72 (m, 2H), 3.64-3.56 (m, 2H), 3.43 (s, 2H), 2.94-2.72 (m, 2H), 2.26 (s, 3H). ^{13}C NMR (DMSO-d_6): δ 168.62, 166.35, 165.15, 154.20, 142.95, 136.83, 131.13, 128.56, 127.42, 125.64, 118.86, 117.15, 71.31, 57.56, 54.78, 47.44, 47.43, 44.28, 41.46.

***tert*-butyl 4-(4-{(5*S*)-5-[(4-carbamimidoylbenzamido)methyl]-2-oxo-1,3-oxazolidin-3-yl}phenyl)piperazine-1-carboxylate (z6)**

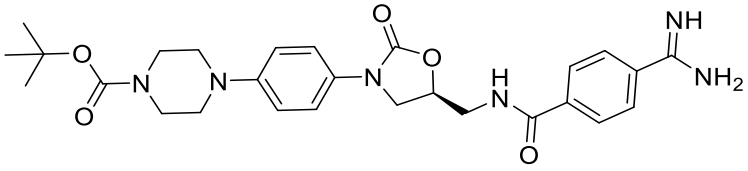

This compound was synthesised according to the general procedure B-step 3 starting with compound **y6** (0.484 g, 0.90 mmol). The title compound (0.196 g,

0.38 mmol, 42%) was obtained as a white solid. MS: m/z calculated for $C_{27}H_{35}N_6O_5^+$ 523.2663 $[M+H]^+$, MS: found 523.2673 $[M+H]^+$. HPLC: t_R 1.50 min (95%). Mp: 199 ˚C. $[\alpha]_D^{22}$= -65° (c= 1, DMSO). ^{1}H NMR (DMSO-d_6): δ 8.37 (s, 1H), 8.23 (t, *J* = 7.6 Hz, 1H), 7.85-7.74 (m, 2H), 7.73-7.62 (m, 2H), 7.38-7.26 (m, 2H), 7.05-6.95 (m, 2H), 6.24 (s, 2H), 4.91-8.79 (m, 1H), 4.18-4.09 (m, 1H), 3.89 (dd, J= 8.9 Hz, 6.2 Hz, 1H), 3.78-3.57 (m, 4H), 3.46-3.35 (m, 3H), 3.32-3.29(m, 3H), 1.49 (s, 9H). ^{13}C NMR (DMSO-d_6): δ 167.31, 166.15, 154.81, 154.34, 154.16, 136.81, 131.32, 128.56, 127.43, 125.62, 118.81, 117.15, 79.77, 71.87, 49.96, 47.44, 43.67, 41.46, 28.44.

tert-butyl 4-(4-{(5*S*)-5-[(4-carbamimidoylbenzamido)methyl]-2-oxo-1,3-oxazolidin-3-yl}phenyl)-3-oxopiperazine-1-carboxylate (z7)

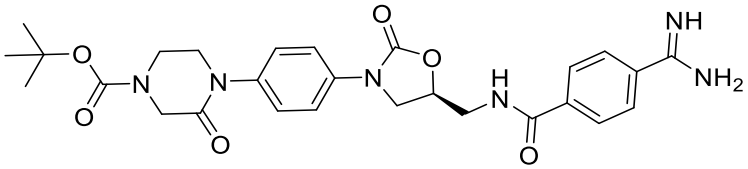

This compound was synthesised according to the general procedure B-step 3 starting with compound **y7** (0.386 g, 0.70 mmol). The title compound (0.165 g, 0.30 mmol, 44%) was obtained as a white solid. MS: m/z calculated for $C_{27}H_{33}N_6O_6^+$ 537.2456 $[M+H]^+$, MS: found 537.2458 $[M+H]^+$. HPLC: t_R 1.66 min (98%). Mp: 184 ˚C. $[\alpha]_D^{22}$= 38° (c= 1, DMSO). ^{1}H NMR (DMSO-d_6): δ 8.36 (s, 1H), 8.29 (t, *J* = 7.8 Hz, 1H), 7.82-7.76 (m, 2H), 7.75-7.65 (m, 2H), 7.36-7.28 (m, 2H), 7.18-7.10 (m, 2H), 6.25 (s, 2H), 4.85-477 (m, 1H), 4.27-4.18 (m, 1H), 3.97 (t, *J* = 7.1 Hz, 2H), 3.85 (dd, J= 9.2 Hz, 6.1 Hz, 1H), 3.73-3.67 (m, 2H), 3.53 (s, 2H), 3.01-2.86 (m, 2H), 1.48 (s, 9H). ^{13}C NMR (DMSO-d_6): δ 168.63, 167.31, 165.15, 156.73, 154.15, 142.95, 136.81, 131.15, 128.59, 127.43, 125.64, 118.86, 117.15, 80.58, 71.31, 47.45, 47.43, 44.39, 43.66, 41.46, 28.26.

4-carbamimidoyl-*N*-({(5*S*)-2-oxo-3-[4-(piperazin-1-yl)phenyl]-1,3-oxazolidin-5-yl}methyl)benzamide (z8)

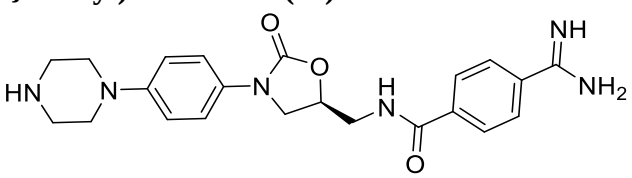

This compound was synthesised according to the general procedure B-step 4 scenario 2 starting with compound **z6** (0.130 g, 0.25 mmol) or in another batch this compound was synthesised according to the general procedure B-step 3

starting with compound **y8** (0.109 g, 0.25 mmol). The title compound (0.029 g, 0.07 mmol, 28% or 0.034, 0.08, 33%, respectively) was obtained as a white solid. MS: m/z calculated for $C_{22}H_{27}N_6O_3^+$ 423.2139 $[M+H]^+$, MS: found 423.2150 $[M+H]^+$. HPLC: t_R 1.22 min (96%). Mp: 203 ˚C. $[\alpha]_D^{22}$= 81° (c= 1, DMSO). ^{1}H NMR (DMSO-d_6): δ 8.38 (s, 1H), 8.27 (t, *J* = 7.8 Hz, 1H), 7.83-7.76 (m, 2H), 7.76-7.66 (m, 2H), 7.36-7.28 (m, 2H), 7.03-6.96 (m, 2H), 6.24 (s, 2H), 4.89-4.80 (m, 1H), 4.27-4.18 (m, 1H), 3.87 (dd, J= 8.9 Hz, 6.1 Hz, 1H), 3.75-3.65 (m, 2H), 3.55-3.47 (m, 2H), 3.36-3.22(m, 4H), 3.25-3.15 (m, 1H), 3.17-3.05 (m, 4H). ^{13}C NMR (DMSO-d_6): δ 166.33, 165.12, 156.36, 154.17, 136.81, 131.33, 128.56, 127.43, 125.65, 118.86, 117.15, 71.35, 48.92, 47.44, 46.76, 41.40.

4-carbamimidoyl-*N*-({(5*S*)-2-oxo-3-[4-(2-oxopiperazin-1-yl)phenyl]-1,3-oxazolidin-5-yl}methyl)benzamide (z9)

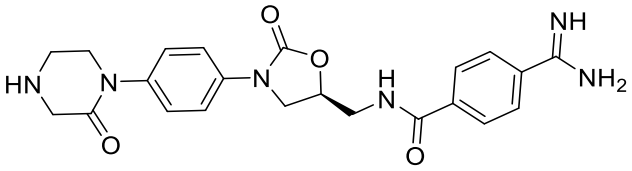

This compound was synthesised according to the general procedure B-step 4-scenario 1 starting with compound **z7** (0.107 g, 0.2 mmol) or in another batch this compound was synthesised according to the general procedure B-step3 starting with compound **y9** (0.113 g, 0.25 mmol). The title compound (0.031 g, 0.07 mmol, 36% or 0.038 g, 0.08 mmol, 35%) was obtained as a white solid. MS: m/z calculated for $C_{22}H_{25}N_6O_4^+$ 437.1932 $[M+H]^+$, MS: found 437.1951 $[M+H]^+$. HPLC: t_R 1.40 min (95%). Mp: 212 ˚C. $[\alpha]_D^{22}$= 76° (c= 1, DMSO). ^{1}H NMR (DMSO-d_6) δ ^{1}H NMR (DMSO-d_6) δ 8.39(s, 1H), 8.28 (t, *J* = 7.8 Hz, 1H), 7.85-7.73 (m, 2H), 7.75-7.64 (m, 2H), 7.37-7.30 (m, 2H), 7.18-7.08 (m, 2H), 6.25(s, 2H), 4.89-4.80 (m, 1H), 4.20- 4.09 (m, 1H), 3.96 (t, *J* = 7.0 Hz, 2H), 3.89 (dd, J= 9.2 Hz, 6.3 Hz, 1H), 3.62-3.57 (m, 4H), 3.17-2.97 (m, 2H), 1.61-1.55 (m, 1H). ^{13}C NMR (DMSO-d_6): δ 166.36, 166.06, 165.12, 154.17, 142.93, 136.96, 131.31, 128.56, 127.47, 125.61, 118.85, 117.15, 71.31, 47.48, 46.45, 46.26, 45.62, 41.46.

_N_-{[(5_S_)-3-([1,1'-biphenyl]-4-yl)-2-oxo-1,3-oxazolidin-5-yl]methyl}-5-chlorothiophene-2-carboxamide (e10)

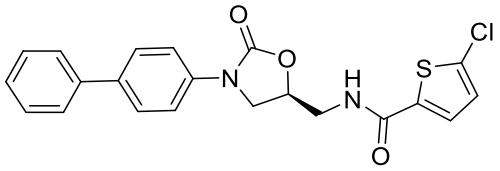

This compound was synthesised according to the general procedure C by reacting compound **e3** (0.124 g, 0.3 mmol) with the commercially available 4,4,5,5-tetramethyl-2-phenyl-1,3,2-dioxaborolane (0.122 g, 0.6 mmol). The title compound (0.095 g, 0.23 mmol, 77%) was obtained as a white solid. MS: m/z calculated for $C_{21}H_{18}ClN_2O_3S^+$ 413.0721 $[M+H]^+$. MS: found 413.0734 $[M+H]^+$. HPLC: t_R 2.54 min (96%). Mp: 235 °C. $[\alpha]^{17}_D$= 73° (c= 1, DMSO). ^{1}H NMR (DMSO-d_6): δ 8.38 (t, J= 7.0 Hz, 1H), 7.66 (m, 3H), 7.64-7.60 (m, 2H), 7.60 (t, *J* = 7.5 Hz, 1H), 7.52-7.46 (m, 2H), 7.43-7.37 (m, 1H), 7.34 (d, *J* = 7.5 Hz, 1H), 7.03 (d, *J* = 7.5 Hz, 1H), 4.91-4.84 (m, 1H), 4.16-4.10 (m, 1H), 3.86 (dd, J= 9.2 Hz, 6.0 Hz, 1H), 3.55 (t, *J* = 7.2 Hz, 2H). ^{13}C NMR (DMSO-d_6): δ 168.23, 155.46, 148.92, 137.85, 135.42, 132.82, 129.30, 128.39, 127.36, 125.54. 121.25, 119.98, 118.56, 117.06, 76.73, 47.67, 41.00, 40.00.

5-chloro-_N_-({(5_S_)-2-oxo-3-[4-(pyridin-4-yl)phenyl]-1,3-oxazolidin-5-yl}methyl)thiophene-2-carboxamide (e11)

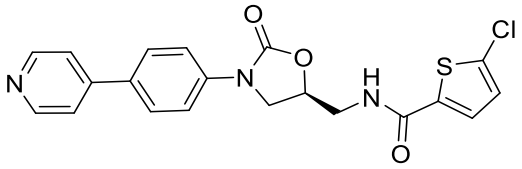

This compound was synthesised according to the general procedure C by reacting compound **e3** (0.124 g, 0.3 mmol) with the commercially available 4-(4,4,5,5-tetramethyl-1,3,2-dioxaborolan-2-yl)pyridine (0.123 g, 0.6 mmol). The title compound (0.068 g, 0.16 mmol, 56%) was obtained as a white solid. MS: m/z calculated for $C_{20}H_{17}ClN_3O_3S^+$ 411.0674 $[M+H]^+$. MS: found 414.0687 $[M+H]^+$. HPLC: t_R 2.34 min (96%). Mp: 223 °C. $[\alpha]^{17}_D$= -56° (c= 1, DMSO). ^{1}H NMR (DMSO-d_6): δ 8.81-8.77 (m, 2H), 7.78-7.74 (m, 2H), 7.70-7.64 (m, 4H), 7.60 (t, *J* = 7.5 Hz, 1H), 7.34 (d, *J* = 7.5 Hz, 1H), 7.03 (d, *J* = 7.5 Hz, 1H), 4.89-4.81 (m, 1H), 4.16-4.10 (m, 1H), 3.85 (dd, J= 8.3 Hz, 7.1 Hz, 1H), 3.55 (t, *J* = 7.2 Hz, 2H). ^{13}C NMR (DMSO-d_6): δ 162.74, 155.17, 151.65, 148.46, 141.36, 139.38, 136.86, 134.34, 130.58, 128.50, 127.15, 124.71, 112.96, 71.32, 47.44, 41.46.

5-chloro-*N*-({(5*S*)-2-oxo-3-[4-(pyridin-3-yl)phenyl]-1,3-oxazolidin-5-yl}methyl)thiophene-2-carboxamide (e12)

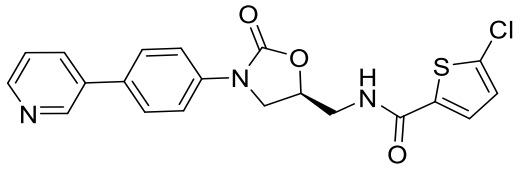

This compound was synthesised according to the general procedure C by reacting compound **e3** (0.124 g, 0.3 mmol) with the commercially available 3-(4,4,5,5-tetramethyl-1,3,2-dioxaborolan-2-yl)pyridine (0.123 g, 0.6 mmol). The title compound (0.071 g, 0.17 mmol, 58%) was obtained as a white solid. MS: m/z calculated for $C_{20}H_{17}ClN_3O_3S^+$ 411.0674 $[M+H]^+$. MS: found 414.0689 $[M+H]^+$. HPLC: t_R 2.33 min (96%). Mp: 267 °C. $[\alpha]^{17}_D$= -43° (c= 1, DMSO). ^{1}H NMR (DMSO-d_6): δ 8.84 (d, *J* = 1.5 Hz, 1H), 8.65 (dd, *J* = 7.5, 1.5 Hz, 1H), 7.92 (dt, *J* = 7.7, 1.5 Hz, 1H), 7.71-7.63 (m, 4H), 7.60 (t, *J* = 7.5 Hz, 1H), 7.48 (t, *J* = 7.5 Hz, 1H), 7.34 (d, *J* = 7.5 Hz, 1H), 7.03 (d, *J* = 7.5 Hz, 1H), 4.89-4.81 (m, 1H), 4.16-4.10 (m, 1H), 3.84 (dd, J= 8.8 Hz, 7.1 Hz, 1H), 3.55 (t, *J* = 7.2 Hz, 2H). ^{13}C NMR (DMSO-d_6): δ 160.73, 154.15, 148.42, 148.27, 140.35, 136.93, 136.80, 136.49, 134.26, 134.14, 130.57, 127.49, 126.06, 123.43, 112.98, 71.30, 47.43, 41.45.

5-chloro-*N*-{[(5*S*)-3-(4'-methoxy[1,1'-biphenyl]-4-yl)-2-oxo-1,3-oxazolidin-5-yl]methyl}thiophene-2-carboxamide (e13)

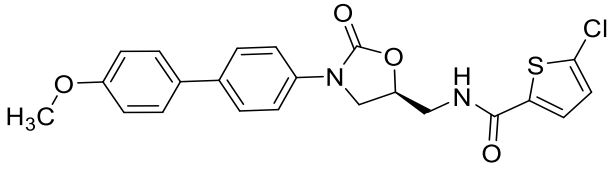

This compound was synthesised according to the general procedure C by reacting compound **e3** (0.248 g, 0.6 mmol) with the commercially available 2-(4-methoxyphenyl)-4,4,5,5-tetramethyl-1,3,2-dioxaborolane(0.280 g, 1.2 mmol). The title compound (0.118 g, 0.26 mmol, 45%) was obtained as a white solid. MS: m/z calculated for $C_{22}H_{20}ClN_2O_4S^+$ 443.0827 $[M+H]^+$. MS: found 443.0833 $[M+H]^+$. HPLC: t_R 2.50 min (96%). Mp: 206 °C. $[\alpha]^{17}_D$= -76° (c= 1, DMSO). ^{1}H NMR (DMSO-d_6): δ 8.36 (t, *J*=7.5, 1H) 7.69-7.64 (m, 2H), 7.63-7.57 (m, 4H), 7.34 (d, *J* = 7.5 Hz, 1H), 7.03 (d, *J* = 7.5 Hz, 1H), 7.03-6.98 (m, 2H), 4.90-4.83 (m, 1H), 4.14-4.06 (m, 1H), 3.83 (dd, J= 9.4 Hz, 7.1 Hz, 1H),3.78 (s, 3H), 3.56 (t, *J* = 7.2 Hz, 2H). ^{13}C NMR (DMSO-d_6): δ 160.73,

159.83, 154.17, 140.58, 136.83, 134.31, 132.86, 132.09, 130.56, 128.36, 127.51, 127.18, 114.36, 113.03, 71.30, 55.26, 47.46, 41.44.

5-chloro-*N*-{[(5*S*)-3-(3',5'-dimethoxy[1,1'-biphenyl]-4-yl)-2-oxo-1,3-oxazolidin-5-yl]methyl}thiophene-2-carboxamide (e14)

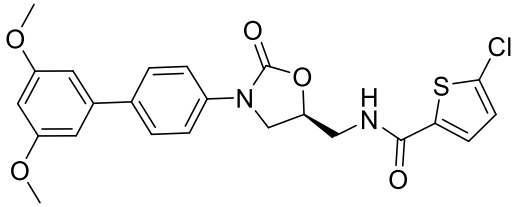

This compound was synthesised according to the general procedure C by reacting compound **e3** (0.248 g, 0.6 mmol) with the commercially 2-(3,5-dimethoxyphenyl)-4,4,5,5-tetramethyl-1,3,2-dioxaborolane (0.316 g, 1.2 mmol). The title compound (0.116 g, 0.24 mmol, 41%) was obtained as a white solid. MS: m/z calculated for $C_{23}H_{22}ClN_2O_5S^+$ 473.0932 $[M+H]^+$. MS: found 473.0950 $[M+H]^+$. HPLC: t_R 2.06 min (96%). Mp: 214 °C. $[\alpha]^{17}_D$= 90° (c= 1, DMSO). ^{1}H NMR (DMSO-d_6): δ 8.34 (t, *J*=7.5, 1H), 7.66-7.57 (m, 4H), 7.32 (d, *J* = 7.5 Hz, 1H), 7.06 (d, *J* = 7.5 Hz, 1H), 6.78 (d, *J* = 1.5 Hz, 2H), 6.45 (t, *J* = 1.5 Hz, 1H), 4.89-4.81 (m, 1H), 4.16-4.11 (m, 1H), 3.86 (s, 6H), 3.83 (dd, J= 8.9 Hz, 6.8 Hz, 1H), 3.50 (t, *J* = 7.2 Hz, 2H). ^{13}C NMR (DMSO-d_6): δ 161.76, 160.73, 154.16, 142.66, 140.17, 139.27, 136.81, 134.27, 130.15, 128.50, 127.16, 112.99, 105.61, 101.27, 71.31, 55.63, 47.45, 41.47.

***N*-({(5*S*)-3-[4-(2*H*-1,3-benzodioxol-5-yl)phenyl]-2-oxo-1,3-oxazolidin-5-yl}methyl)-5-chlorothiophene-2-carboxamide (e15)**

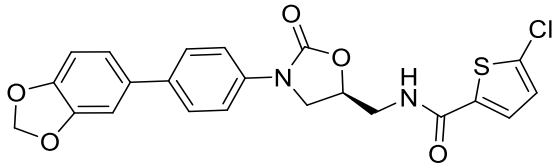

This compound was synthesised according to the general procedure C by reacting compound **e3** (0.248 g, 0.6 mmol) with the commercially available 2-(benzo[d][1,3]dioxol-5-yl)-4,4,5,5-tetramethyl-1,3,2-dioxaborolane (0.297 g, 1.2 mmol). The title compound (0.109 g, 0.24 mmol, 40%) was obtained as a white solid. MS: m/z calculated for $C22H_{18}ClN_2O_5S^+$ 457.0619 $[M+H]^+$. MS: found 457.0539 $[M+H]^+$. HPLC: t_R 2.12 min (96%). Mp: 267 °C. $[\alpha]^{17}_D$= 56° (c= 1, DMSO). ^{1}H NMR (DMSO-d_6): δ 8.38 (d, *J* = 7.0 Hz, 1H), 7.69-7.64 (m, 2H), 7.62-7.57 (m, 2H), 7.34 (d, *J* = 7.5 Hz, 1H), 7.29 (dd, *J* = 7.5, 1.5 Hz, 1H), 7.05-7.01 (m, 2H), 6.95 (d, *J* = 7.4 Hz, 1H), 6.05 (s, 2H), 4.91-4.81 (m ,

1H), 4.16-4.11 (m, 1H), 3.85 (dd, J= 9.2 Hz, 6.5 Hz, 1H), 3.52 (t, *J* = 7.2 Hz, 2H). ^{13}C NMR (DMSO-d_6): δ 160.73, 154.17, 147.74, 147.73, 140.50, 138.56, 137.03, 136.84, 134.27, 130.55, 129.35, 128.91, 127.5, 113.98, 112.06, 108.90, 101.17, 71.30, 47.43, 41.48.

5-chloro-*N*-({(5*S*)-3-[4-(5-fluoropyridin-3-yl)phenyl]-2-oxo-1,3-oxazolidin-5-yl}methyl)thiophene-2-carboxamide (e16)

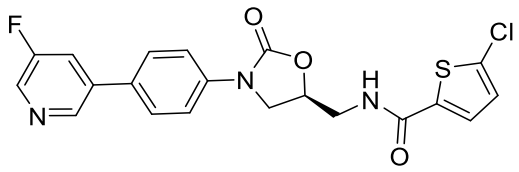

This compound was synthesised according to the general procedure C by reacting compound **e3** (0.248 g, 0.6 mmol) with the commercially available 3-fluoro-5-(4,4,5,5-tetramethyl-1,3,2-dioxaborolan-2-yl)pyridine (0.267 g, 1.2 mmol). The title compound (0.103 g, 0.24 mmol, 40%) was obtained as a white solid. MS: m/z calculated for $C_{20}H_{16}ClFN_3O_3S^+$ 432.0579 $[M+H]^+$. MS: found 432.0596 $[M+H]^+$. HPLC: t_R 2.41 min (97%). Mp: 215 °C. $[\alpha]^{16}_D$ -87° (c= 1, DMSO). ^{1}H NMR (DMSO-d_6): δ 8.57 (d, *J* = 1.5 Hz, 1H), 8.37 (dd, *J* = 8.1, 1.5 Hz, 1H), 7.76 (dt, *J* = 8.1, 1.5 Hz, 1H), 7.71-7.63 (m, 4H), 7.60 (t, *J* = 7.5 Hz, 1H), 7.34 (d, *J* = 7.5 Hz, 1H), 7.03 (d, *J* = 7.5 Hz, 1H), 4.90-4.83 (m, 1H), 4.16-4.10 (m, 1H), 3.84 (dd, J= 9.2 Hz, 6.3 Hz, 1H), 3.50 (t, *J* = 7.2 Hz, 2H).^{13}C NMR (DMSO-d_6): δ 161.18, 160.94, 154.56, 149.85, 140.54, 137.00, 136.76, 135.44, 134.45, 130.32. 127.55, 126.34, 117.45, 112.33, 76.73, 41.00, 40.03.

***N*-{[(5*S*)-3-([1,1'-biphenyl]-4-yl)-2-oxo-1,3-oxazolidin-5-yl]methyl}-4-*tert*-butylbenzamide (g10)**

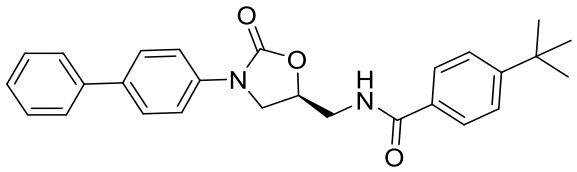

This compound was synthesised according to the general procedure C by reacting compound **g3** (0.124 g, 0.3 mmol) with the commercially available 4,4,5,5-tetramethyl-2-phenyl-1,3,2-dioxaborolane (0.122 g, 0.6 mmol). The title compound (0.059 g, 0.14 mmol, 46%) was obtained as a white solid. MS: m/z calculated for $C_{27}H_{29}N_2O_3^+$ 429.2173 $[M+H]^+$. MS: found 429.2188 $[M+H]^+$. HPLC: t_R 3.66 min (94%). Mp: 270 °C. $[\alpha]^{13}_D$ 51° (c= 1, DMSO). ^{1}H NMR (DMSO-d_6): δ 8.26 (t, *J* = 7.8 Hz, 1H), 7.79-7.71 (m, 2H), 7.69-7.65 (m,

4H), 7.64-7.60 (m, 2H), 7.52-7.46 (m, 2H), 7.49-7.43 (m, 2H), 7.43-7.37 (m, 1H), 4.95-4.86 (m, 1H), 4.16-4.12 (m, 1H), 3.83 (dd, J= 9.3 Hz, 5.8 Hz, 1H), 3.59 (t, *J* = 7.3 Hz, 2H), 1.34 (s, 9H). ^{13}C NMR (DMSO-d_6): δ 168.23, 154.26, 151.63, 147.54, 145.43, 141.02, 139.43, 137.24, 131.16, 129.88, 128.46, 126.32, 120.21, 117.32, 71.15, 53.56, 43.45, 34.11, 33.66.

4-*tert*-butyl-*N*-({(5*S*)-2-oxo-3-[4-(pyridin-4-yl)phenyl]-1,3-oxazolidin-5-yl}methyl)benzamide (g11)

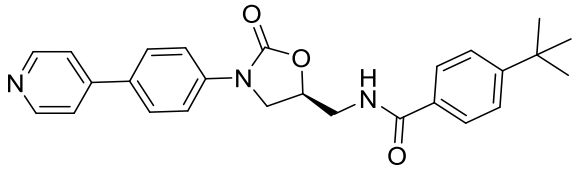

This compound was synthesised according to the general procedure C by reacting compound **g3** (0.248 g, 0.6 mmol) with the commercially available 4-(4,4,5,5-tetramethyl-1,3,2-dioxaborolan-2-yl)pyridine (0.246 g, 1.2 mmol). The title compound (0.102 g, 0.24 mmol, 40%) was obtained as a white solid. MS: m/z calculated for $C_{26}H_{28}N_3O_3^+$ 430.2125 $[M+H]^+$. MS: found 430.2144 $[M+H]^+$. HPLC: t_R 2.68 min (94%). Mp: 241 °C. $[\alpha]^{16}_D$= 88° (c= 1, DMSO). ^{1}H NMR (DMSO-d_6): δ 8.81-8.77 (m, 2H), 8.26 (t, *J* = 7.8 Hz, 1H), 7.83 -7.76 (m, 2H), 7.75-7.72 (m, 2H), 7.70-7.64 (m, 4H), 7.47-7.42 (m, 2H), 4.89-4.80 (m, 1H), 4.17-4.11 (m, 1H), 3.85 (dd, J= 8.9 Hz, 6.1 Hz, 1H), 3.61 (t, *J* = 7.3 Hz, 2H), 1.34 (s, 8H).^{13}C NMR (DMSO-d6):168.50, 152.11, 149.33, 146.56, 144.82, 138.69, 138.41, 138.15, 130.96, 128.17, 128.00, 121.35, 120.96, 77.36, 46.51, 44.32, 41.15, 30.56.

4-*tert*-butyl-*N*-({(5*S*)-2-oxo-3-[4-(pyridin-3-yl)phenyl]-1,3-oxazolidin-5-yl}methyl)benzamide (g12)

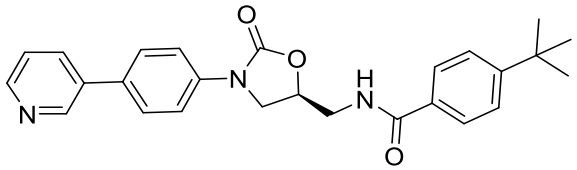

This compound was synthesised according to the general procedure C by reacting compound **g3** (0.248 g, 0.6 mmol) with the commercially available 3-(4,4,5,5-tetramethyl-1,3,2-dioxaborolan-2-yl)pyridine (0.246 g, 1.2 mmol) The title compound (0.131 g, 0.30 mmol, 51%) was obtained as a white solid. MS: m/z calculated for $C_{26}H_{28}N_3O_3^+$ 430.2125 $[M+H]^+$. MS: found 430.2148 $[M+H]^+$. HPLC: t_R 2.66 min (95%). Mp: 244 °C. $[\alpha]^{16}_D$= 88° (c 1, DMSO). ^{1}H NMR (DMSO-d_6): δ 8.84 (d, *J* = 1.5 Hz, 1H), 8.65 (dd, *J* = 7.5, 1.5 Hz, 1H),

8.26 (t, *J* = 7.8 Hz, 1H), 7.96-7.90 (m, 1H), 7.74-7.69 (m, 2H), 7.71-7.63 (m, 4H), 7.48 (t, *J* = 7.5 Hz, 1H), 7.47-7.42 (m, 2H), 4.89-4.81 (m, 1H), 4.16-4.10 (m, 1H), 3.86 (dd, J= 9.4 Hz, 6.2 Hz, 1H), 3.59 (t, *J* = 7.3 Hz, 2H), 1.36 (s, 9H). ^{13}C NMR (DMSO-d_6):168.50, 152.11, 149.33, 146.56, 144.82, 140.07, 138.41, 138.15, 130.96, 129.17, 128.00, 125.23, 121.35, 120.96, 112.32, 77.36, 46.51, 44.32, 41.15, 30.56.

4-*tert*-butyl-*N*-{[(5*S*)-3-(4'-methoxy[1,1'-biphenyl]-4-yl)-2-oxo-1,3-oxazolidin-5-yl]methyl}benzamide (g13)

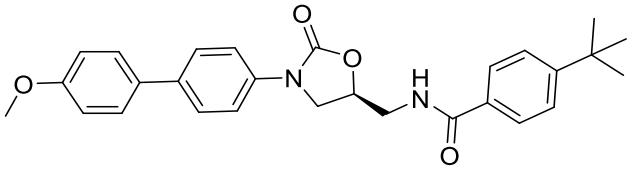

This compound was synthesised according to the general procedure C by reacting compound **g3** (0.248 g, 0.6 mmol) with the commercially available 2-(4-methoxyphenyl)-4,4,5,5-tetramethyl-1,3,2-dioxaborolane (0.80 g, 1.2 mmol). The title compound (0.131 g, 0.28 mmol, 48%) was obtained as a white solid. MS: m/z calculated for $C_{28}H_{31}N_2O_4^+$ 459.2278 $[M+H]^+$. MS: found 459.2297 $[M+H]^+$. HPLC: t_R 2.44 min (96%). Mp: 221 °C. $[\alpha]^{16}_D$= 36° (c= 1, DMSO). ^{1}H NMR (DMSO-d_6): δ 8.25 (t, *J* = 7.8 Hz, 1H), 7.74-7.64 (m, 4H), 7.63-7.57 (m, 4H), 7.47-7.42 (m, 2H), 7.03-6.98 (m, 2H), 4.890-4.80 (m, 1H), 4.17.12 (m, 1H), 3.84 (dd, J= 9.3 Hz, 6.0 Hz, 1H), 3.79 (s, 3H), 3.57 (t, *J* = 7.3 Hz, 2H), 1.36 (s, 9H). ^{13}C NMR (DMSO-d_6): 166.33, 158.88, 151.13, 150.91, 144.36, 131.18, 130.96, 128.15, 127.71, 126.15, 121.32, 119.25, 110.11, 112.93, 65.15, 61.33, 57.24, 51.42, 33.15, 30.25.

4-*tert*-butyl-*N*-{[(5*S*)-3-(3',5'-dimethoxy[1,1'-biphenyl]-4-yl)-2-oxo-1,3-oxazolidin-5-yl]methyl}benzamide (g14)

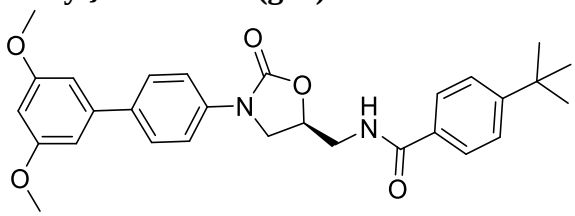

This compound was synthesised according to the general procedure C by reacting compound **g3** (0.248 g, 0.6 mmol) with the commercially 2-(3,5-dimethoxyphenyl)-4,4,5,5-tetramethyl-1,3,2-dioxaborolane (0.316 g, 1.2 mmol). The title compound (0.149 g, 0.30 mmol, 51%) was obtained as a white solid. MS: m/z calculated for $C_{29}H_{33}N_2O_5^+$ 489.2384 $[M+H]^+$. MS:

found 489.2401 $[M+H]^+$. HPLC: t_R 2.20 min (96%). Mp: 197 °C. $[\alpha]^{16}_D$ = 99° (c= 1, DMSO).^{1}H NMR (DMSO-d_6): δ 8.28 (t, *J* = 7.8 Hz, 1H), 7.74-7.66 (m, 4H), 7.62-7.57 (m, 2H), 7.47-7.42 (m, 2H), 6.79 (d, *J* = 1.5 Hz, 2H), 6.45 (t, *J* = 1.5 Hz, 1H), 4.88-4.79 (m, 1H), 4.16-4.12 (m, 1H), 3.86 (s, 6H), 3.82 (dd, J= 8.9 Hz, 6.1 Hz, 1H),3.55 (t, *J* = 7.3 Hz, 2H), 1.36 (s, 9H). ^{13}C NMR (DMSO-d_6): 165.30, 161.37, 151.22, 145.56, 140.16, 138.61, 133.72, 126.13, 125.90, 121.33, 112.00, 110.95, 108.31, 102.25, 71.13, 55.33, 48.95, 41.43, 34.15, 30.22.

_N_-({(5_S_)-3-[4-(2_H_-1,3-benzodioxol-5-yl)phenyl]-2-oxo-1,3-oxazolidin-5-yl}methyl)-4-_tert_-butylbenzamide (g15)

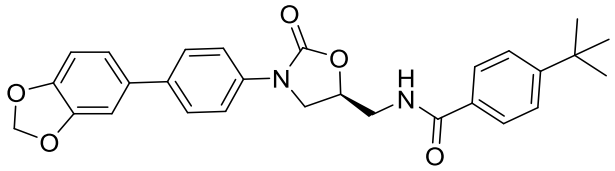

This compound was synthesised according to the general procedure C by reacting compound **g3** (0.248 g, 0.6 mmol) with the commercially available 2-(benzo[d][1,3]dioxol-5-yl)-4,4,5,5-tetramethyl-1,3,2-dioxaborolane (0.297 g, 1.2 mmol). The title compound (0.116 g, 0.24, 41%) was obtained as a white solid. MS: m/z calculated for $C_{28}H_{29}N_2O_5^+$ 473.2071 $[M+H]^+$. MS: found 473.2076 $[M+H]^+$. HPLC: t_R 2.01 min (94%). Mp: 212 °C. $[\alpha]^{16}_D$ = 96° (c= 1, DMSO). ^{1}H NMR (DMSO-d_6): δ 8.29 (t, *J* = 7.8 Hz, 1H), 7.77-7.64 (m, 4H), 7.63-7.56 (m, 2H), 7.47-7.43 (m, 2H), 7.26 (dd, *J* = 7.5, 1.5 Hz, 1H), 7.03 (d, *J* = 1.5 Hz, 1H), 6.98 (d, *J* = 7.4 Hz, 1H), 6.05 (s, 2H), 4.89-4.80 (m, 1H), 4.18-4.14 (m, 1H), 3.81 (dd, J= 9.1 Hz, 6.1 Hz, 1H), 3.58 (t, *J* = 7.3 Hz, 2H), 1.36 (s, 9H). ^{13}C NMR (DMSO-d_6): 164.31, 155.69, 151.32, 148.64, 147.71, 138.34, 137.91, 135.62, 130.61, 128.96, 127.93, 127.61, 121.32, 118.03, 111.22, 105.42, 101.15, 81.13, 57.23, 41.93, 34.25, 30.13.

4-_tert_-butyl-_N_-({(5_S_)-3-[4-(5-fluoropyridin-3-yl)phenyl]-2-oxo-1,3-oxazolidin-5-yl}methyl)benzamide (g16)

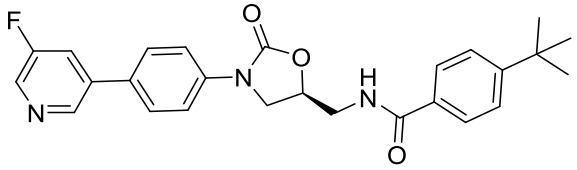

This compound was synthesised according to the general procedure C by reacting compound **g3** (0.316 g, 0.6 mmol) with the commercially available 3-

fluoro-5-(4,4,5,5-tetramethyl-1,3,2-dioxaborolan-2-yl)pyridine (0.267 g, 1.2 mmol). The title compound (0.150 g, 0.33 mmol, 56%) was obtained as a white solid. MS: m/z calculated for $C_{26}H_{27}FN_3O_3^+$ 448.2031 $[M+H]^+$. MS: found 448.2045 $[M+H]^+$. HPLC: t_R 2.67 min (97%). Mp: 261 °C. $[\alpha]^{16}_D$ = 94° (c= 1, DMSO). ^{1}H NMR (DMSO-d_6): δ 8.52 (d, *J* = 1.5 Hz, 1H), 8.33 (dd, *J* = 8.1, 1.5 Hz, 1H), 8.27 (t, *J* = 7.8 Hz, 1H), 7.75 (dt, *J* = 8.1, 1.5 Hz, 1H), 7.75-7.63 (m, 4H), 7.45-7.40 (m, 2H), 4.89-4.80 (m, 1H), 4.17-4.09(m, 1H), 3.85 (dd, J= 9.3 Hz, 6.1 Hz, 1H),3.62 (t, *J* = 7.3 Hz, 2H), 1.36 (s, 9H). ^{13}C NMR (DMSO-d6): δ 166.30, 160.10, 154.56, 153.26, 149.33, 137.00, 136.93, 136.80, 135.16, 131.00. 128.06, 125.57, 116.45, 112.98, 71.30, 47.43, 41.45, 34.72, 31.09.

methyl 3-(1,3-dioxo-1,3-dihydro-2*H*-isoindol-2-yl)-1*H*-1,2,4-triazole-5-carboxylate (46)

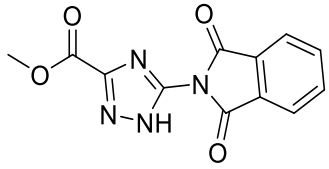

This compound was synthesised according to the general procedure D-step 1 by reacting methyl 3-amino-1*H*-1,2,4-triazole-5-carboxylate (1.42 g, 10 mmol) and 2-benzofuran-1,3-dione (phthalic anhydride) (1.48 g, 10 mmol). The title compound (1.911 g, 7 mmol, 70 %) was obtained as a white solid. MS: m/z calculated for $C_{12}H_9N_4O_4^+$ 273.0618 $[M+H]^+$. MS: found 273.0633 $[M+H]^+$. HPLC: t_R 0.96 min (97%). Mp: 98 °C. ^{1}H NMR (DMSO-d_6): δ 9.42 (s, 1H), 7.97-7.86 (m, 4H), 4.03 (s, 3H). ^{13}C NMR (DMSO-d_6): δ 165.67, 158.46, 140.11, 136.17, 134.33, 131.86, 123.52, 52.25.

methyl 5-(1,3-dioxo-1,3-dihydro-2*H*-isoindol-2-yl)-1-{[2-(trimethylsilyl)ethoxy]methyl}-1*H*-1,2,4-triazole-3-carboxylate (47)

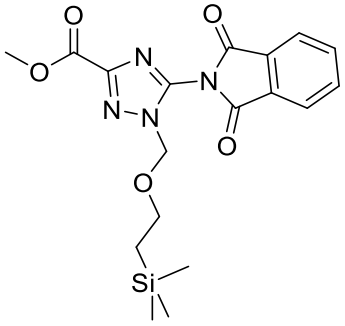

This compound was synthesised according to the general procedure D-step 2 starting with compound **46** (1.768 g, 6.5 mmol)**.** The title compound (1.985 g,

4.94 mmol, 76%) was obtained as a white solid. MS: m/z calculated for $C_{18}H_{23}N_4O_5Si^+$ 403.1432 $[M+H]^+$. MS: found 403.1450 $[M+H]^+$. HPLC: t_R 1.20 min (96%). Mp: 150 °C. ^{1}H NMR (DMSO-d_6): δ 7.96-7.91 (m, 4H), 5.42 (s, 2H), 3.96 (s, 3H), 3.54 (t, *J* = 7.1 Hz, 2H), 0.93 (t, *J* = 7.1 Hz, 2H), 0.05 (s, 9H). ^{13}C NMR (DMSO-d_6): δ 165.23, 160.13, 158.87, 138.95, 134.33, 131.76, 123.51, 74.13, 64.36, 52.25, 18.10, -1.43.

methyl 5-amino-1-{[2-(trimethylsilyl)ethoxy]methyl}-1*H*-1,2,4-triazole-3-carboxylate (48)

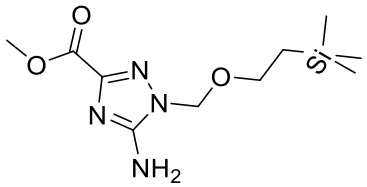

This compound was synthesised according to the general procedure D-step 3 starting with compound **47** (1.809 g, 4.5 mmol). The title compound (0.979 g, 3.6 mmol, 80%) was obtained as a white solid. MS: m/z calculated for $C_{10}H_{21}N_4O_3Si^+$ 273.1377 $[M+H]^+$. MS: found 273.1395 $[M+H]^+$. HPLC: t_R 1.33 min (96%). Mp: 143 °C. ^{1}H NMR (DMSO-d_6): δ 7.91 (s, 2H), 5.32 (s, 2H), 4.01 (s, 3H), 3.53 (t, *J* = 7.1 Hz, 2H), 0.92 (t, *J* = 7.1 Hz, 2H), 0.05 (s, 9H). ^{13}C NMR (DMSO-d_6): δ 160.14, 159.55, 152.96, 74.88, 64.49, 52.24, 18.08, -1.42.

methyl 5-{[(2*R*)-3-(1,3-dioxo-1,3-dihydro-2*H*-isoindol-2-yl)-2-hydroxypropyl]amino}-1-{[2-(trimethylsilyl)ethoxy]methyl}-1*H*-1,2,4-triazole-3-carboxylate (49)

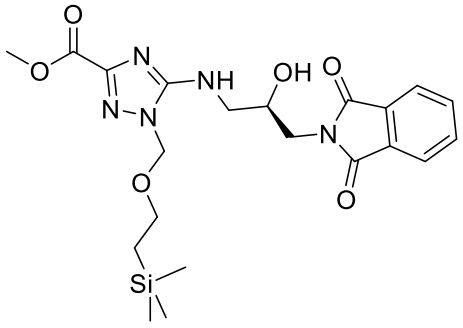

This compound was synthesised according to the general procedure D-step 4 by reacting compound **48** (0.924 g, 3.4 mmol) with **35** (0.690 g, 3.4 mmol). The title compound (1.187 g, 2.5 mmol, 74%) was obtained as a white solid. MS: m/z calculated for $C_{21}H_{30}N_5O_6Si^+$ 476.1960 $[M+H]^+$. MS: found 476.1977 $[M+H]^+$. HPLC: t_R 1.43 min (96%). Mp: 165 °C. ^{1}H NMR (DMSO-d_6): 8.86 (t, *J* = 7.5 Hz, 1H), 7.86-7.79 (m, 4H), 5.46 (d, *J* = 12.5 Hz, 1H), 5.27

(d, *J* = 12.3 Hz, 1H), 4.45-4.39 (m, 1H), 4.27 (dd, *J* = 12.4, 6.9 Hz, 1H), 4.08 (d, *J* = 6.7 Hz, 1H),4.02 (s, 3H), 3.98 (dd, *J* = 12.4, 6.9 Hz, 1H), 3.61-3.52 (m, 2H), 3.55-3.48 (m, 1H), 3.45-3.39 (m, 1H), 0.96-0.84 (m, 2H), 0.05 (s, 9H). ^{13}C NMR (DMSO-d_6): δ 168.79, 160.16, 159.25, 155.15, 134.12, 131.97, 123.42, 74.05, 70.57, 64.58, 52.26, 45.72, 44.50, 18.09, -1.44.

methyl 5-{(5*S*)-5-[(1,3-dioxo-1,3-dihydro-2*H*-isoindol-2-yl)methyl]-2-oxo-1,3-oxazolidin-3-yl}-1-{[2-(trimethylsilyl)ethoxy]methyl}-1*H*-1,2,4-triazole-3-carboxylate (50)

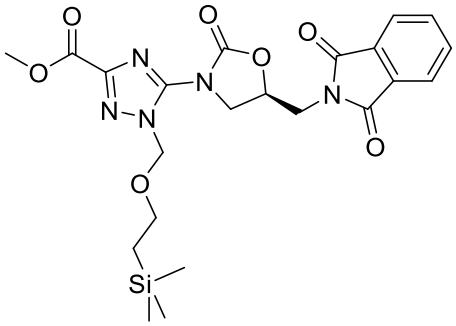

This compound was synthesised according to the general procedure D-step 5 starting with compound **49** (1.140 g, 2.4 mmol). The title compound (1.002 g, 2 mmol, 86%) was obtained as a white solid. MS: m/z calculated for $C_{22}H_{28}N_5O_7Si^+$ 502.1753 $[M+H]^+$. MS: found 502.1771 $[M+H]^+$. HPLC: t_R 1.44 min (96%). Mp: 168 °C. ^{1}H NMR (DMSO-d_6): δ 7.88-7.80 (m, 4H), 5.49 (d, *J* = 12.5 Hz, 1H), 5.26 (d, *J* = 12.3 Hz, 1H), 4.98-4.87 (m, 1H), 4.46-4.39 (m, 1H), 4.30-4.25 (m, 1H), 4.19-4.12 (m, 1H), 4.02-3.93 (m, 4H), 3.61-3.46 (m, 2H), 0.96-0.84 (m, 2H), 0.05 (s, 9H). ^{13}C NMR (DMSO-d_6): δ 168.76, 161.13, 158.87, 155.55, 146.76, 134.12, 131.95, 123.46, 75.75, 74.25, 64.49, 52.26, 48.29, 44.25, 18.10, -1.44.

(methyl 5-[(5*S*)-5-(aminomethyl)-2-oxo-1,3-oxazolidin-3-yl]-1-{[2-(trimethylsilyl)ethoxy]methyl}-1*H*-1,2,4-triazole-3-carboxylate

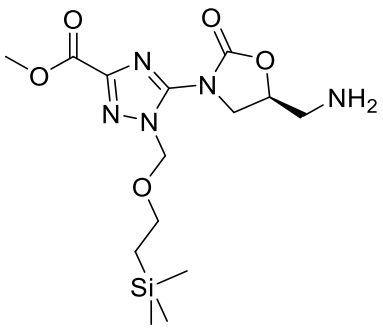

This compound was synthesised according to the general procedure D-step 6 starting with compound **50** (0.901 g, 1.8 mmol). The title compound (0.586 g,

1.58 mmol, 88%) was obtained as a white solid. MS: m/z calculated for $C_{14}H_{26}N_5O_5Si^+$ 372.1698 $[M+H]^+$. MS: found 372.1712 $[M+H]^+$. HPLC: t_R 1.00 min (96%). Mp: 163 °C. ^{1}H NMR (DMSO-d_6): 5.46 (d, *J* = 12.5 Hz, 1H), 5.27 (d, *J* = 12.3 Hz, 1H), 4.68 (p, *J* = 7.0 Hz, 1H), 4.26-4.20 (m, 1H), 4.00 (s, 3H), 3.96 (dd, *J* = 12.2, 7.1 Hz, 1H), 3.87 (dd, J = 8.9 Hz, 6.5 Hz, 1H), 3.75 (dd, J = 5.2 Hz, 3.5 Hz, 2H), 2.78-2.70 (m, 1H), 2.36 (t, *J* = 7.5 Hz, 2H), 0.96-0.84 (m, 2H), 0.05 (s, 9H). ^{13}C NMR (DMSO-d_6): δ 161.15, 160.11, 158.92, 155.79, 141.83, 76.29, 75.05, 64.49, 52.26, 48.24, 47.65, 18.12, -1.46.

methyl 5-[(5*S*)-5-{[(5-chlorothiophene-2-carbonyl)amino]methyl}-2-oxo-1,3-oxazolidin-3-yl]-1-{[2-(trimethylsilyl)ethoxy]methyl}-1*H*-1,2,4-triazole-3-carboxylate (52)

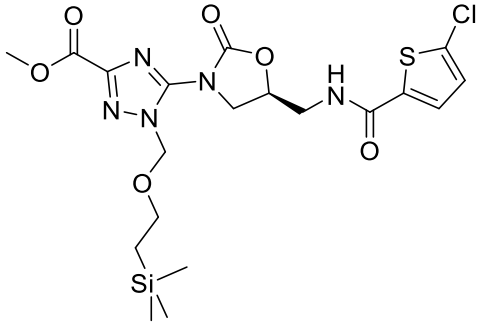

This compound was synthesised according to the general procedure D-step 7 by reacting compound **51** (0.185 g, 0.5 mmol) and 5-chlorothiophene-2-carbonyl chloride (0.108 g, 0.6 mmol). The title compound (0.201 g, 0.39 mmol, 78%) was obtained as a white solid. MS: m/z calculated for $C_{19}H_{27}ClN_5O_6SSi^+$ 516.1134 $[M+H]^+$. MS: found 516.1147 $[M+H]^+$. HPLC: t_R 2.20 min (96%). Mp: 210 °C. ^{1}H NMR (DMSO-d_6): δ 7.63 (t, *J* = 7.5 Hz, 1H), 7.38 (d, *J* = 7.5 Hz, 1H), 7.09 (d, *J* = 7.5 Hz, 1H), 5.49 (d, *J* = 12.5 Hz, 1H), 5.29 (d, *J* = 12.3 Hz, 1H), 4.92-4.82 (m, 1H), 4.27-4.19 (m, 1H), 4.04 (s, 3H) 3.87 (dd, J= 9.3 Hz, 6.1 Hz, 1H), 3.61-3.55 (m, 3H), 3.53-3.46 (m, 1H), 0.98-0.85 (m, 2H), 0.05 (s, 9H). ^{13}C NMR (DMSO-d_6): δ 161.26, 160.17, 158.89, 155.64, 145.85, 141.17, 134.28, 127.51, 126.75, 75.12, 71.31, 64.47, 52.26, 48.38, 41.46, 18.10, -1.41.

methyl 5-{(5*S*)-5-[(4-*tert*-butylbenzamido)methyl]-2-oxo-1,3-oxazolidin-3-yl}-1-{[2-(trimethylsilyl)ethoxy]methyl}-1*H*-1,2,4-triazole-3-carboxylate (53)

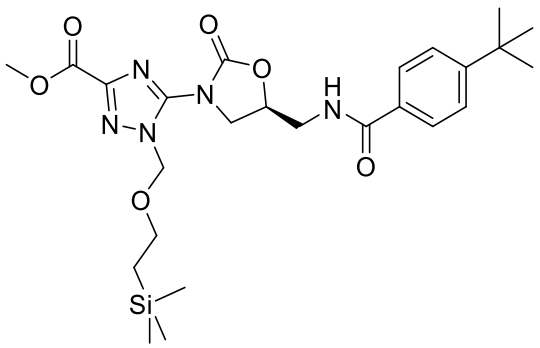

This compound was synthesised according to the general procedure D-step 7 by reacting compound **51** (0.185 g, 0.5 mmol) and 4-(*tert*-butyl)benzoyl chloride (0.117 g, 0.6 mmol). The title compound (0.223 g, 0.42 mmol, 85%) was obtained as a white solid. MS: m/z calculated for $C_{25}H_{38}N_5O_6Si^+$ 532.2586 $[M+H]^+$. MS: found 532.2601 $[M+H]^+$. HPLC: t_R 2.56 min (96%). Mp: 256 °C. ^{1}H NMR (DMSO-d_6): δ 8.25 (t, *J* = 7.8 Hz, 1H), 7.74-7.69 (m, 2H), 7.47-7.43 (m, 2H), 5.48 (d, *J* = 12.5 Hz, 1H), 5.29 (d, *J* = 12.3 Hz, 1H), 4.90-4.80 (m, 1H), 4.28-4.22 (m, 1H), 4.01 (s, 3H), 3.85 (dd, J= 9.3 Hz, 6.2 Hz, 1H), 3.62-3.48 (m, 4H), 1.34 (s, 9H), 0.96-0.84 (m, 2H), 0.05 (s, 9H). ^{13}C NMR (DMSO-d_6): δ 166.34, 160.18, 158.97, 155.66, 153.34, 139.91, 131.07, 128.61, 125.56, 74.18, 71.30, 65.09, 52.25, 48.15, 41.45, 34.74, 31.08, 18.08, -1.42.

methyl 3-[(5*S*)-5-{[(5-chlorothiophene-2-carbonyl)amino]methyl}-2-oxo-1,3-oxazolidin-3-yl]-1*H*-1,2,4-triazole-5-carboxylate (e17)

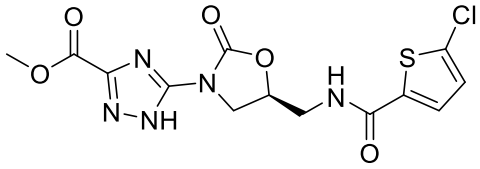

This compound was synthesised according to the general procedure D-step 8 starting with compound **52** (0.154 g, 0.3 mmol). The title compound (0.084 g, 0.22 mmol, 75%) was obtained as a white solid. MS: m/z calculated for $C_{13}H_{13}ClN_5O_5S^+$ 386.0320 $[M+H]^+$. MS: found 386.0337 $[M+H]^+$. HPLC: t_R 2.01 min (96%). Mp: 206 °C. ^{1}H NMR (DMSO-d_6): δ 9.61 (s, 1H), 7.60 (t, *J* = 7.5 Hz, 1H), 7.35 (d, *J* = 7.5 Hz, 1H), 7.04 (d, *J* = 7.5 Hz, 1H), 4.98-4.88 (m, 1H), 4.28 (dd, *J* = 12.2, 7.0 Hz, 1H), 4.01 (m, 3H), 3.89 (dd, J= 8.9 Hz, 6.2 Hz,

1H), 3.55 (t, *J* = 7.2 Hz, 2H). ^{13}C NMR (DMSO-d_6): δ 161.65, 160.18, 158.02, 155.60, 146.03, 140.20, 134.26, 127.87, 127.49, 71.30, 52.24, 46.62, 41.45.

methyl 3-{(5*S*)-5-[(4-*tert*-butylbenzamido)methyl]-2-oxo-1,3-oxazolidin-3-yl}-1*H*-1,2,4-triazole-5-carboxylate (g17)

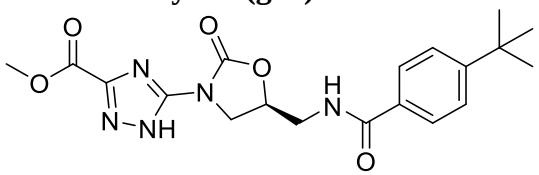

This compound was synthesised according to the general procedure D-step 8 starting with compound **53** (0.186 g, 0.35 mmol). The title compound (0.096 g, 0.24 mmol, 70%) was obtained as a white solid. MS: m/z calculated for $C_{19}H_{24}N_5O_5^+$ 402.1772 $[M+H]^+$. MS: found 402.1789 $[M+H]^+$. HPLC: t_R 2.56 min (96%). Mp: 23 °C. ^{1}H NMR (DMSO-d_6): δ 9.54 (s, 1H), 8.26 (t, *J* = 7.8 Hz, 1H), 7.74-7.69 (m, 2H), 7.47-7.42 (m, 2H), 4.97-4.84 (m, 1H), 4.31-4.24 (m, 1H), 4.02 (m, 3H), 3.87 (dd, J= 9.0 Hz, 6.1 Hz, 1H), 3.55 (t, *J* = 7.3 Hz, 2H), 1.32 (s, 9H). ^{13}C NMR (DMSO-d_6): δ 166.36, 159.94, 155.55, 153.28, 141.09, 131.03, 128.60, 125.58, 71.32, 52.26, 46.38, 41.47, 34.74, 31.11.

(5*R*)-5-(chloromethyl)-1,3-oxazolidin-2-one (43)

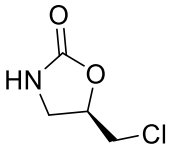

This compound was synthesised according to the general procedure E-step 1 by reacting (*R*)-epichlorohydrin (4.6 g, 50 mmol), sodium cyanate (6.5 g, 100 mmol) and magnesium sulphate (1.2 g, 10 mmol). The title compound (6.023 g, 44.5 mmol, 89%) was obtained as a white solid. MS: m/z calculated for $C_4H_7ClNO_2^+$ 136.0160 $[M+H]^+$. MS: found 136.0173 $[M+H]^+$. HPLC: t_R 0.56 min (96%). Mp: 68 °C (Lit. Mp = 67-68).[361] ^{1}H NMR (DMSO-d_6): δ 7.57 (t, *J* = 6.3 Hz, 1H), 4.97-4.86 (m, 1H), 3.90-3.84 (m, 1H), 3.84-3.78 (m, 1H), 3.47-3.39 (m, 1H), 3.29-3.21 (m, 1H). ^{13}C NMR (DMSO-d_6): δ 158.19, 73.83, 46.17, 42.48.

2-{[(5*R*)-2-oxo-1,3-oxazolidin-5-yl]methyl}-1*H*-isoindole-1,3(2*H*)-dione (44)

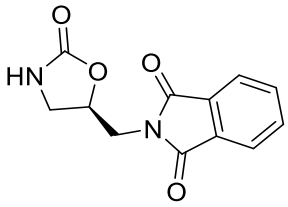

This compound was synthesised according to the general procedure E-step 2 by reacting **43** (2.295 g, 17 mmol) with potassium phthalimide (3.459 g, 18.7 mmol). The title compound (3.721 g, 15 mmol, 89%) was obtained as a white solid. MS: m/z calculated for $C_{12}H_{11}N_2O_4^+$ 247.0713 $[M+H]^+$. MS: found 247.0724 $[M+H]^+$. HPLC: t_R 1.10 min (96%). Mp: 196 °C (Lit. Mp = 195-197).[361] ^{1}H NMR (DMSO-d_6): δ 7.85-7.79 (m, 4H), 6.88 (t, *J* = 5.9 Hz, 1H), 4.93-4.82 (m, 1H), 4.42-4.36 (m, 1H), 4.15-4.09 (m, 1H), 3.45-3,40 (m, 1H), 3.29-3.22 (m, 1H) . ^{13}C NMR (DMSO-d_6): δ 168.79, 159.66, 134.15, 131.88, 123.38, 74.97, 45.56, 42.61.

2-{[(5*S*)-2-oxo-3-phenyl-1,3-oxazolidin-5-yl]methyl}-1*H*-isoindole-1,3(2*H*)-dione (54)

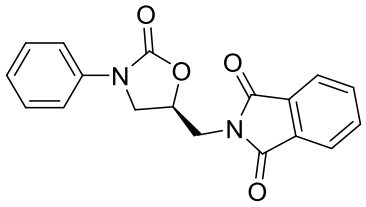

This compound was synthesised according to the general procedure E-step 3-scenario 1 by reacting compound **44** (0.494 g, 2 mmol) with bromobenzene (0.314 g, 2 mmol). The title compound (0.360 g, 1.12 mmol, 56%) was obtained as a white solid. MS: m/z calculated for $C_{18}H_{15}N_2O_4^+$ 323.1026 $[M+H]^+$. MS: found 323.1040 $[M+H]^+$. HPLC: t_R 1.68 min (96%). Mp: 210 °C. ^{1}H NMR (DMSO-d_6): δ 7.85-7.79 (m, 4H), 7.36-7.30 (m, 2H), 7.23-7.18 (m, 2H), 7.13-7.09 (m, 1H), 4.92-4.81 (m, 1H), 4.44-4.37 (m, 1H), 4.18-4.09 (m, 2H), 3.89 (dd, J= 9.0 Hz, 6.0 Hz, 1H). ^{13}C NMR (DMSO-d_6): δ 168.81, 154.19, 136.79, 134.14, 132.05, 129.19, 123.43, 123.36, 120.51, 74.66, 47.45, 42.93.

2-{[(5*S*)-3-(3-ethenylphenyl)-2-oxo-1,3-oxazolidin-5-yl]methyl}-1*H*-isoindole-1,3(2*H*)-dione (55)

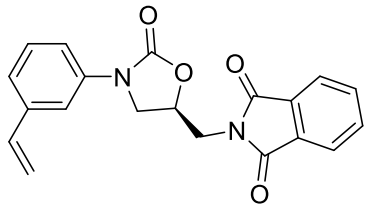

This compound was synthesised according to the general procedure E-step 3-scenario 1 by reacting compound **44** (0.494 g, 2 mmol) with 1-bromo-3-vinylbenzene (0.366 g, 2 mmol). The title compound (0.285 g, 0.82 mmol, 41%) was obtained as a white solid. MS: m/z calculated for $C_{20}H_{17}N_2O_4^+$ 349.1183 $[M+H]^+$. MS: found 349.1201 $[M+H]^+$. HPLC: t_R 1.32 min (96%). Mp: 193 °C. ^{1}H NMR (DMSO-d_6): δ 7.86-7.78 (m, 4H), 7.53 (t, *J* = 1.5 Hz, 1H), 7.39-7.30 (m, 1H), 7.26 (t, *J* = 7.4 Hz, 1H), 7.24-7.13 (m, 1H), 6.68-6.62 (m, 1H), 5.77 (dd, *J* = 16.8, 2.7 Hz, 1H), 5.47 (dd, *J* = 10.1, 2.6 Hz, 1H), 4.91-4.81 (m, 1H), 4.41 (dd, *J* = 12.4, 6.9 Hz, 1H), 4.18-4.07 (m, 2H), 3.85 (dd, J= 8.9 Hz, 5.8 Hz, 1H). ^{13}C NMR (DMSO-d_6): δ 168.78, 154.15, 142.08, 135.38, 134.11, 133.11, 131.94, 129.80, 127.67, 123.39, 120.44, 115.11, 113.56, 74.51, 47.43, 42.86.

3-{(5*S*)-5-[(1,3-dioxo-1,3-dihydro-2*H*-isoindol-2-yl)methyl]-2-oxo-1,3-oxazolidin-3-yl}benzaldehyde (56)

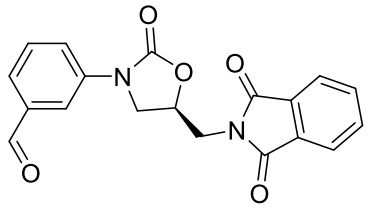

This compound was synthesised according to the general procedure E-step 3-scenario 1 by reacting compound **44** (0.494 g, 2 mmol) with 3-bromobenzaldehyde (0.370 g, 2 mmol). The title compound (0.281 g, 0.80 mmol, 40%) was obtained as a white solid. MS: m/z calculated for $C_{19}H_{15}N_2O_5^+$ 351.0975 $[M+H]^+$. MS: found 351.0986 $[M+H]^+$. HPLC: t_R 1.18 min (96%). Mp: 186 °C. ^{1}H NMR (DMSO-d_6): δ 9.69 (d, *J* = 0.8 Hz, 1H), 8.05 (t, *J* = 1.5 Hz, 1H), 7.86-7.77 (m, 4H), 7.75-7.70 (m, 1H), 7.69-7.51 (m, 1H), 7.46 (t, *J* = 7.5 Hz, 1H), 4.93-4.81 (m, 1H), 4.45 (dd, *J* = 12.5, 6.9 Hz, 1H), 4.16-4.08 (m, 2H), 3.88 (dd, J= 9.3 Hz, 6.2 Hz, 1H). ^{13}C NMR (DMSO-d_6): δ 192.42, 168.79, 154.16, 143.43, 137.06, 134.12, 131.96, 129.67, 123.59, 123.38, 120.45, 119.04, 74.68, 47.44, 42.91.

2-{[(5*S*)-3-(3-methylphenyl)-2-oxo-1,3-oxazolidin-5-yl]methyl}-1*H*-isoindole-1,3(2*H*)-dione (57)

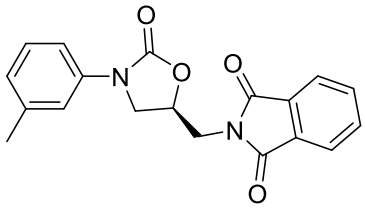

This compound was synthesised according to the general procedure E-step 3-scenario 1 by reacting compound **44** (0.494 g, 2 mmol) with 1-bromo-3-methylbenzene (0.342 g, 2 mmol). The title compound (0.409 g, 1.22 mmol, 61%) was obtained as a white solid. MS: m/z calculated for $C_{19}H_{17}N_2O_4^+$ 337.1183 $[M+H]^+$. MS: found 337.1199 $[M+H]^+$. HPLC: t_R 1.19 min (96%). Mp: 188 °C. ^{1}H NMR (DMSO-d_6): δ 7.86-7.78 (m, 4H), 7.41-7.35 (m, 1H), 7.32 (t, *J* = 1.6 Hz, 1H), 7.24 (t, *J* = 7.5 Hz, 1H), 6.92-6.86 (m, 1H), 4.91-4.81 (m, 1H), 4.42 (dd, *J* = 12.5, 6.9 Hz, 1H), 4.18-4.12 (m, 2H), 3.87 (dd, J= 9.2 Hz, 6.0 Hz, 1H), 2.29 (d, *J* = 0.9 Hz, 3H). ^{13}C NMR (DMSO-d_6): δ 168.79, 154.14, 142.19, 138.83, 134.10, 131.92, 129.12, 123.38, 120.42, 118.05, 112.70, 74.86, 47.43, 42.85, 21.83.

2-{[(5*S*)-3-(3,5-dimethylphenyl)-2-oxo-1,3-oxazolidin-5-yl]methyl}-1*H*-isoindole-1,3(2*H*)-dione (58)

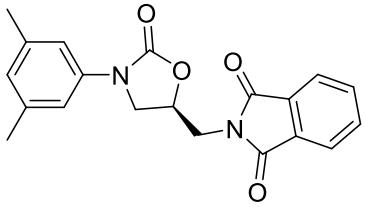

This compound was synthesised according to the general procedure E-step 3-scenario 1 by reacting compound **44** (0.494 g, 2 mmol) with 1-bromo-3,5-dimethylbenzene (0.370 g, 2 mmol). The title compound (0.441 g, 1.26 mmol, 63%) was obtained as a white solid. MS: m/z calculated for $C_{20}H_{19}N_2O_4^+$ 351.1339 $[M+H]^+$. MS: found 351.1349 $[M+H]^+$. HPLC: t_R 1.34 min (96%). Mp: 199 °C. ^{1}H NMR (DMSO-d_6): δ. 7.86-7.80 (m, 4H), 7.20 (d, *J* = 1.4 Hz, 2H), 6.80 (t, *J* = 1.2 Hz, 1H), 4.91-4.81 (m, 1H), 4.44-4.37 (m, 1H), 4.17-4.09 (m, 2H), 3.89 (dd, J= 9.4 Hz, 6.5 Hz, 1H), 2.26 (s, 6H).^{13}C NMR (DMSO-d_6): δ 169.06, 154.16, 141.55, 138.49, 134.12, 132.96, 123.40, 118.89, 112.72, 75.12, 47.44, 42.82, 21.74.

***tert*-butyl [(3-{(5*S*)-5-[(1,3-dioxo-1,3-dihydro-2*H*-isoindol-2-yl)methyl]-2-oxo-1,3-oxazolidin-3-yl}phenyl)methyl]carbamate (59)**

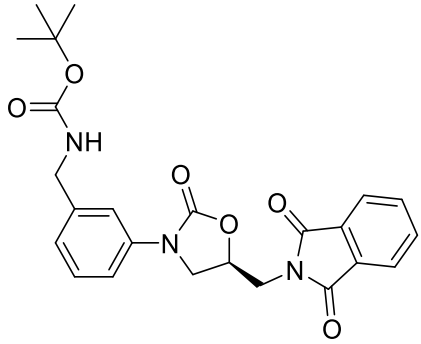

This compound was synthesised according to the general procedure E-step 3-scenario 1 by reacting compound **44** (0.988 g, 4 mmol) with tert-butyl (3-bromobenzyl) carbamate (1.144 g, 4 mmol). The title compound (0.648 g, 1.44 mmol, 36%) was obtained as a white solid. MS: m/z calculated for $C_{24}H_{26}N_3O_6^+$ 452.1816 $[M+H]^+$. MS: found 452.1831 $[M+H]^+$. HPLC: t_R 1.65 min (96%). Mp: 216 °C. ^{1}H NMR (DMSO-d_6): δ 7.86-7.78 (m, 4H), 7.49 (p, *J* = 1.3 Hz, 1H), 7.45-7.39 (m, 1H), 7.30 (t, *J* = 7.5 Hz, 1H), 7.19-7.11 (m, 1H), 6.13 (t, *J* = 8.9 Hz, 1H), 4.89-4.80 (m, 1H), 4.41 (dd, *J* = 12.4, 6.9 Hz, 1H), 4.39-3.30 (m, 1H), 4.28-4.22 (m, 1H), 4.18-4.10 (m, 2H), 3.87 (dd, J= 9.1 Hz, 6.1 Hz, 1H), 1.39 (s, 9H). ^{13}C NMR (DMSO-d_6): δ 168.78, 156.11, 154.15, 142.15, 136.25, 134.11, 131.94, 127.96, 127.67, 123.39, 120.44, 117.73, 79.84, 75.50, 47.43, 46.27, 42.67, 28.30.

2-{[(5*S*)-3-{3-[(benzylamino)methyl]phenyl}-2-oxo-1,3-oxazolidin-5-yl]methyl}-1*H*-isoindole-1,3(2*H*)-dione (60)

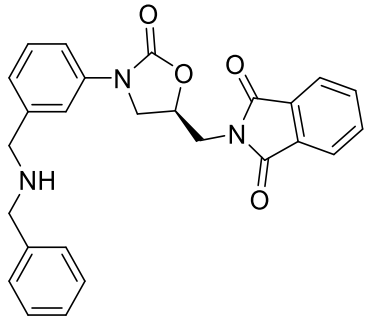

This compound was synthesised according to the general procedure E-step 3-scenario 1 by reacting compound **44** (0.494 g, 2 mmol) with *N*-benzyl-1-(3-bromophenyl)methanamine **(**0.552 g, 2 mmol). The title compound (0.291 g, 0.66 mmol, 33%) was obtained as a white solid. MS: m/z calculated for $C_{26}H_{24}N_3O_4^+$ 442.1761 $[M+H]^+$. MS: found 442.1777 $[M+H]^+$. HPLC: t_R 1.90 min (96%). Mp: 289 °C. ^{1}H NMR (DMSO-d_6): δ 7.86-7.79 (m, 4H), 7.47 (p, *J*

= 1.4 Hz, 1H), 7.44-7.38 (m, 1H), 7.37-7.24 (m, 6H), 7.18-7.10 (m, 1H), 4.90-4.81 (m, 1H), 4.40 (dd, *J* = 12.5, 6.9 Hz, 1H), 4.18-4.10 (m, 2H), 3.89 (dd, J= 8.9 Hz, 6.0 Hz, 1H), 3.87-3.80 (m, 4H), 3.11 (m, 1H). ^{13}C NMR (DMSO-d_6): δ 168.78, 154.14, 141.55, 140.41, 136.38, 134.12, 131.95, 128.25, 128.15, 127.96, 127.67, 127.18, 123.38, 120.44, 118.05, 74.87, 53.12, 50.05, 47.46, 42.68.

2-{[(5*S*)-3-methyl-2-oxo-1,3-oxazolidin-5-yl]methyl}-1*H*-isoindole-1,3(2*H*)-dione (61)

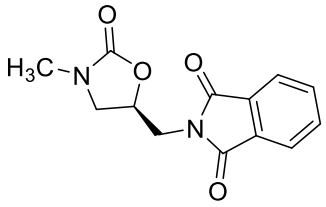

This compound was synthesised according to the general procedure E-step 3-scenario 2 by reacting compound **44** (0.988 g, 4 mmol) with iodomethane **(**1.128 g, 8 mmol). The title compound (0.572 g, 2.2 mmol, 55 %) was obtained as a white solid. MS: m/z calculated for $C_{13}H_{13}N_2O_4^+$ 261.0870 $[M+H]^+$. MS: found 261.0877 $[M+H]^+$. HPLC: t_R 1.32 min (96%). Mp: 188 °C. ^{1}H NMR (DMSO-d_6): δ 7.85-7.79 (m, 4H), 4.89-4.79 (m, 1H), 4.43-4.37 (m, 1H), 3.81 (dd, J= 8.6 Hz, 5.9 Hz, 1H), 3.43-3.37 (m, 1H), 3.25-3.18 (m, 1H), 2.95 (s, 3H). ^{13}C NMR (DMSO-d_6): δ 168.78, 157.94, 134.11, 131.94, 123.39, 74.01, 51.48, 43.85, 30.07.

2-{[(5*S*)-3-ethyl-2-oxo-1,3-oxazolidin-5-yl]methyl}-1*H*-isoindole-1,3(2*H*)-dione (62)

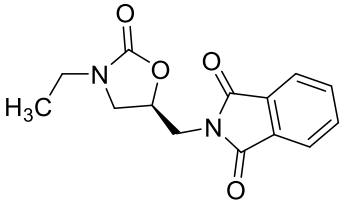

This compound was synthesised according to the general procedure E-step 3-scenario 2 by reacting compound **44** (0.988 g, 4 mmol) with iodoethane (1.242 g, 8 mmol). The title compound (0.548 g, 2 mmol, 51 %) was obtained as a white solid. MS: m/z calculated for $C_{14}H_{15}N_2O_4^+$ 275.1026 $[M+H]^+$. MS: found 275.1038 $[M+H]^+$. HPLC: t_R 1.67 min (96%). Mp: 196 °C. ^{1}H NMR (DMSO-d_6): δ 7.86-7.79 (m, 4H), 4.90-4.81 (m, 1H), 4.40 (dd, *J* = 12.2, 6.9 Hz, 1H), 3.89 (dd, J= 9.0 Hz, 5.9 Hz, 1H), 3.43 (d, *J* = 7.9 Hz, 1H), 3.42 (d, *J* = 7.9 Hz, 1H), 3.40-3.33 (m, 1H), 3.21-3.15 (m, 1H), 1.24 (t, *J* = 7.9 Hz, 3H).

^{13}C NMR (DMSO-d_6): δ 168.79, 157.60, 134.12, 131.95, 123.40, 74.51, 48.83, 43.43, 40.07, 12.79.

2-{[(5*S*)-2-oxo-3-(propan-2-yl)-1,3-oxazolidin-5-yl]methyl}-1*H*-isoindole-1,3(2*H*)-dione (63)

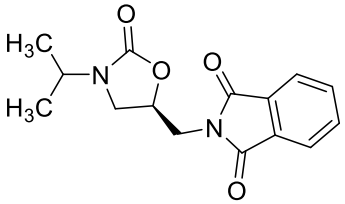

This compound was synthesised according to the general procedure E-step 3-scenario 2 by reacting compound **44** (0.988 g, 4 mmol) with 2-iodopropane (1.352 g, 8 mmol). The title compound (0.528 g, 1.84 mmol, 46 %) was obtained as a white solid. MS: m/z calculated for $C_{15}H_{17}N_2O_4^+$ 289.1183 $[M+H]^+$. MS: found 289.1196 $[M+H]^+$. HPLC: t_R 1.77 min (94%). Mp: 200 °C. ^{1}H NMR (DMSO-d_6): δ 7.86-7.79 (m, 4H), 6.18-6.10 (m, 1H), 4.88-4.77 (m, 1H), 4.43-4.37 (m, 1H), 3.87 (dd, J= 9.5 Hz, 6.5 Hz, 1H), 3.45-3.39 (m, 1H), 3.23 (dd, *J* = 12.2, 6.9 Hz, 1H), 2.76 (d, *J* = 6.8 Hz, 3H), 2.71 (d, *J* = 6.8 Hz, 3H). ^{13}C NMR (DMSO-d_6): δ 168.78, 156.91, 134.12, 131.98, 123.36, 73.95, 50.21, 49.88, 43.04, 20.73.

2-{[(5*S*)-3-(2-methylpropyl)-2-oxo-1,3-oxazolidin-5-yl]methyl}-1*H*-isoindole-1,3(2*H*)-dione (64)

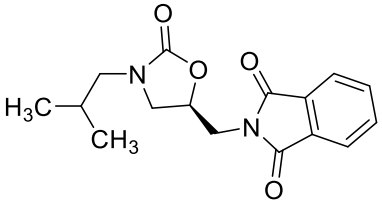

This compound was synthesised according to the general procedure E-step 3-scenario 2 by reacting compound **44** (0.988 g, 4 mmol) with 1-iodo-2-methylpropane (1.472 g, 8 mmol). The title compound (0.398 g, 1.32 mmol, 33 %) was obtained as a white solid. MS: m/z calculated for $C_{16}H_{19}N_2O_4^+$ 303.1339 $[M+H]^+$. MS: found 303.1345 $[M+H]^+$. HPLC: t_R 2.04 min (94%). Mp: 219 °C. ^{1}H NMR (DMSO-d_6): δ 7.85-7.79 (m, 4H), 4.90-4.81 (m, 1H), 4.43-4.37 (m, 1H), 3.88 (dd, J= 10.6 Hz, 6.5 Hz, 1H), 3.39-3.33 (m, 1H), 3.21-3.14 (m, 1H), 2.95 (dd, *J* = 12.3, 7.0 Hz, 1H), 2.78 (dd, *J* = 12.3, 7.0 Hz, 1H), 2.07-2.02 (m, 1H), 0.91 (d, *J* = 6.6 Hz, 3H), 0.86 (d, *J* = 6.6 Hz, 3H). ^{13}C NMR (DMSO-d_6): δ 168.79, 157.96, 134.13, 131.95, 123.41, 75.31, 57.20, 50.33, 42.29, 26.54, 20.59.

2-{[(5S)-3-butyl-2-oxo-1,3-oxazolidin-5-yl]methyl}-1H-isoindole-1,3(2H)-dione (65)

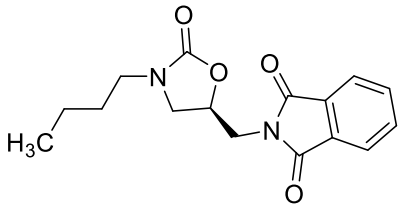

This compound was synthesised according to the general procedure E-step 3-scenario 2 by reacting compound **44** (0.988 g, 4 mmol) with 1-iodobutane (1.472 g, 8 mmol). The title compound (0.362 g, 1.2 mmol, 30%) was obtained as a white solid. MS: m/z calculated for $C_{16}H_{19}N_2O_4^+$ 303.1339 $[M+H]^+$. MS: found 303.1356 $[M+H]^+$. HPLC: t_R 2.15 min (94%). Mp: 233 °C. ^{1}H NMR (DMSO-d_6): δ 7.84-7.78 (m, 4H), 4.88-4.80 (m, 1H), 4.43-4.37 (m, 1H), 3.93 (dd, J= 10.1 Hz, 5.1 Hz, 1H), 3.40-3.28 (m, 2H), 3.22-3.14 (m, 2H), 1.59-1.51 (m, 2H), 1.39-1.23 (m, 2H), 0.95 (t, *J* = 7.9 Hz, 3H). ^{13}C NMR (DMSO-d_6): δ 168.78, 157.78, 134.11, 131.94, 123.39, 74.46, 49.81, 47.49, 43.30, 29.92, 20.27, 13.95.

(5*S*)-5-(aminomethyl)-3-phenyl-1,3-oxazolidin-2-one (66)

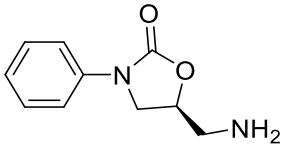

This compound was synthesised according to the general procedure E-step 4 starting with compound **54** (0.322 g, 1 mmol). The title compound (0.153 g, 0.8 mmol, 80%) was obtained as a white solid. MS: m/z calculated for $C_{10}H_{13}N_2O_2^+$ 193.0972 $[M+H]^+$. MS: found 193.0988 $[M+H]^+$. HPLC: t_R 0.69 min (94%). Mp: 135 °C. ^{1}H NMR (DMSO-d_6): δ 7.36-7.30 (m, 2H), 7.23-7.18 (m, 2H), 7.09-7.03 (m, 1H), 4.68-4.60 (m, 1H), 3.96 (dd, J= 5.3 Hz, 3.4 Hz, 1H), 3.86 (dd, J = 8.9 Hz, 6.6 Hz, 1H), 3.72 (dd, J = 5.3 Hz, 3.7 Hz, 2H), 2.36 (t, *J* = 7.5 Hz, 2H). ^{13}C NMR (DMSO-d_6): δ 154.16, 136.82, 129.17, 123.31, 120.45, 75.18, 48.79, 47.45.

(5*S*)-5-(aminomethyl)-3-(3-ethenylphenyl)-1,3-oxazolidin-2-one (67)

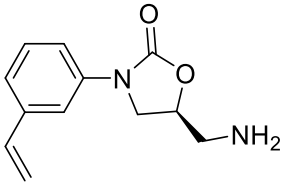

This compound was synthesised according to the general procedure E-step 4 starting with compound **55** (0.243 g, 0.7 mmol). The title compound (0.104 g, 0.48 mmol, 69%) was obtained as a white solid. MS: m/z calculated for $C_{12}H_{15}N_2O_2^+$ 219.1128 $[M+H]^+$. MS: found 219.1141 $[M+H]^+$. HPLC: t_R 0.72 min (96%). Mp: 140 °C. ^{1}H NMR (DMSO-d_6): δ 7.54 (t, *J* = 1.5 Hz, 1H), 7.39-7.33 (m, 1H), 7.25 (t, *J* = 7.4 Hz, 1H), 7.22-7.15 (m, 1H), 6.64 (dd, *J* = 16.8, 10.0 Hz, 1H), 5.76 (dd, *J* = 16.8, 2.7 Hz, 1H), 5.45 (dd, *J* = 10.0, 2.6 Hz, 1H), 4.64-4.53 (m, 1H), 3.97 (dd, J= 5.4 Hz, 3.4 Hz, 1H), 3.89 (dd, J = 8.7 Hz, 6.6 Hz, 1H), 3.71 (dd, J = 5.3 Hz, 3.7 Hz, 2H), 2.36 (t, *J*= 7.5 Hz, 2H). ^{13}C NMR (DMSO-d_6): δ 154.16, 141.96, 135.36, 134.33, 129.81, 127.68, 120.45, 115.12, 111.80, 75.06, 48.68, 47.44.

3-[(5*S*)-5-(aminomethyl)-2-oxo-1,3-oxazolidin-3-yl]benzaldehyde (68)

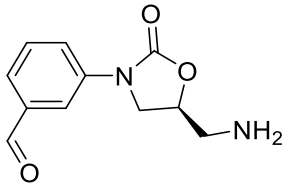

This compound was synthesised according to the general procedure E-step 4 starting with compound **56** (0.227 g, 0.65 mmol). The title compound (0.088 g, 0.40 mmol, 61%) was obtained as a white solid. MS: m/z calculated for $C_{11}H_{13}N_2O_3^+$ 221.0921 $[M+H]^+$. MS: found 221.0934 $[M+H]^+$. HPLC: t_R 0.68 min (96%). Mp: 151 °C. ^{1}H NMR (DMSO-d_6): δ 9.69 (d, *J* = 1.1 Hz, 1H), 8.05 (t, *J* = 1.5 Hz, 1H), 7.75-7.70 (m, 1H), 7.69-7.64 (m, 1H), 7.45 (t, *J* = 7.5 Hz, 1H), 4.64-4.56 (m, 1H), 3.93 (dd, J= 5.2 Hz, 3.4 Hz, 1H), 3.82 (dd, J = 8.8 Hz, 6.6 Hz, 1H), 3.75 (dd, J = 5.4 Hz, 3.7 Hz, 2H), 2.38 (t, *J* = 7.5 Hz, 2H). ^{13}C NMR (DMSO-d_6): δ 192.40, 154.15, 143.28, 137.08, 129.65, 123.56, 120.443, 119.01, 75.23, 48.72, 47.43.

(5*S*)-5-(aminomethyl)-3-(3-methylphenyl)-1,3-oxazolidin-2-one (69)

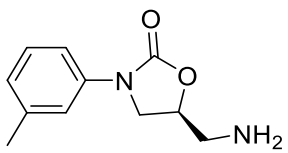

This compound was synthesised according to the general procedure E-step 4-staring with compound **57** (0.336 g, 1 mmol). The title compound (0.125 g, 0.61 mmol, 61%) was obtained as a white solid. MS: m/z calculated for $C_{11}H_{15}N_2O_2^+$ 207.1128 $[M+H]^+$. MS: found 207.1144 $[M+H]^+$. HPLC: t_R 0.71

min (94%). Mp: 96 °C. ^{1}H NMR (DMSO-d_6): δ 7.39-7.34 (m, 1H), 7.33 (t, *J* = 1.5 Hz, 1H), 7.22 (t, *J* = 7.5 Hz, 1H), 6.90-6.85 (m, 1H), 4.67-4.56 (m, 1H), 3.96 (dd, J= 6.3 Hz, 5.4 Hz, 1H), 3.86 (dd, J = 9.9 Hz, 6.5 Hz, 1H), 3.72 (dd, J = 5.4 Hz, 3.9 Hz, 2H), 2.36 (t, *J* = 7.4 Hz, 2H), 2.29 (d, *J* = 0.9 Hz, 3H). ^{13}C NMR (DMSO-d_6): δ 154.16, 142.09, 138.86, 129.15, 120.46, 118.06, 112.72, 75.43, 48.73, 47.435, 21.86.

(5*S*)-5-(aminomethyl)-3-(3,5-dimethylphenyl)-1,3-oxazolidin-2-one (70)

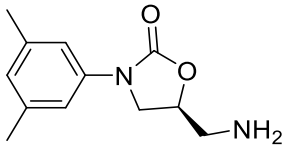

This compound was synthesised according to the general procedure E-step 4 starting with compound **58** (0.350 g, 1 mmol). The title compound (0.145 g, 0.66 mmol, 66%) was obtained as a white solid. MS: m/z calculated for $C_{12}H_{17}N_2O_2^+$ 221.1285 $[M+H]^+$. MS: found 221.1302 $[M+H]^+$. HPLC: t_R 0.98 min (96%). Mp: 151°C. ^{1}H NMR (DMSO-d_6): δ 7.19 (d, *J* = 1.4 Hz, 2H), 6.79 (t, *J* = 1.2 Hz, 1H), 4.63-4.59 (m, 1H), 3.96 (dd, J= 8.3 Hz, 5.2 Hz, 1H), 3.86 (dd, J = 10.9 Hz, 7.6 Hz, 1H), 3.74 (dd, J = 5.5 Hz, 3.7 Hz, 2H), 2.37 (t, *J* = 7.5 Hz, 2H), 2.26 (s, 6H).^{13}C NMR (DMSO-d_6): δ 154.16, 141.41, 138.49, 118.85, 112.72, 75.66, 48.62, 47.44, 21.74.

***tert*-butyl ({3-[(5*S*)-5-(aminomethyl)-2-oxo-1,3-oxazolidin-3-yl]phenyl}methyl)carbamate (71)**

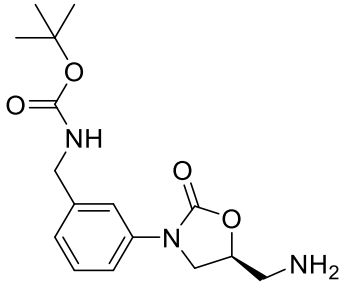

This compound was synthesised according to the general procedure E-step 4 starting with compound **59** (0.542 g, 1.2 mmol). The title compound (0.231 g, 0.72 mmol, 61%) was obtained as a white solid. MS: m/z calculated for $C_{16}H_{24}N_3O_4^+$ 322.1761 $[M+H]^+$. MS: found 322.1779 $[M+H]^+$. HPLC: t_R 1.10 min (96%). Mp: 212 °C. ^{1}H NMR (DMSO-d_6): δ 7.56-7.47 (m, 1H), 7.47-7.40 (m, 1H), 7.30 (t, *J* = 7.5 Hz, 1H), 7.20-7.18 (m, 1H), 6.13 (t, *J* = 8.9 Hz, 1H), 4.66-4.58 (m, 1H), 4.35-4.29 (m, 1H), 4.28-4.19 (m, 1H), 3.94 (dd, J= 7.3 Hz, 3.4 Hz, 1H), 3.83 (dd, J = 8.3 Hz, 6.1 Hz, 1H), 3.70 (dd, J = 5.6 Hz, 3.9 Hz,

2H), 2.36 (t, *J* = 7.5 Hz, 2H), 1.39 (s, 9H). ^{13}C NMR (DMSO-d_6): δ 156.11, 154.15, 142.02, 137.44, 127.96, 127.67, 120.44, 115.96, 79.84, 76.04, 48.71, 47.43, 46.33, 28.30.

(5*S*)-5-(aminomethyl)-3-{3-[(benzylamino)methyl]phenyl}-1,3-oxazolidin-2-one (72)

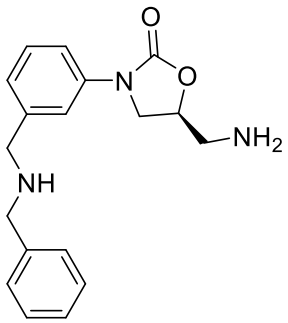

This compound was synthesised according to the general procedure E-step 4 starting with compound **60** (0.264 g, 0.6 mmol). The title compound (0.139 g, 0.45 mmol, 75 %) was obtained as a white solid. MS: m/z calculated for $C_{18}H_{22}N_3O_2^+$ 312.1707 $[M+H]^+$. MS: found 312.1707 $[M+H]^+$. HPLC: t_R 1.27 min (96%). Mp: 241 °C. ^{1}H NMR (DMSO-d_6): 7.49-7-43 (m, 1H), 7.45-7.40 (m, 1H), 7.37-7.24 (m, 7H), 7.18-7.12 (m, 1H), 4.65-4.57 (m, 1H), 3.91 (dd, J= 8.3 Hz, 5.4 Hz, 1H), 3.80 (dd, J = 8.1 Hz, 6.1 Hz, 1H), 3.69 (dd, J = 5.5 Hz, 3.6 Hz, 2H), 3.72-3.66 (m, 2H), 3.11 (p, *J* = 8.6 Hz, 1H), 2.96-2.91 (m, 1H), 2.75-2.68 (m, 1H), 2.36 (t, *J* = 7.5 Hz, 2H). ^{13}C NMR (DMSO-d_6): δ 154.15, 141.39, 140.40, 137.57, 128.23, 128.00, 127.96, 127.67, 127.17, 120.44, 116.29, 75.39, 53.10, 49.81, 48.40, 47.43.

(5S)-5-(aminomethyl)-1,3-oxazolidin-2-one (73)

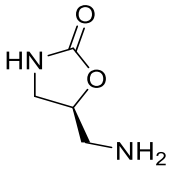

This compound was synthesised according to the general procedure E-step 4 starting with compound **44** (0.492 g, 2 mmol). The title compound (0.078 g, 0.68 mmol, 34%) was obtained as a yellow oil. MS: m/z calculated for $C_4H_9N_2O_2^+$ 117.0659 $[M+H]^+$. MS: found 117.0670 $[M+H]^+$. HPLC: t_R 0.21 min (95%). ^{1}H NMR ($CDCl_3$): δ 6.89 (t, *J* = 6.3 Hz, 1H), 4.56-4.48 (m, 1H), 3.42–3.35 (m, 1H), 3.25-319 (m, 1H), 3.02-2.97 (m, 1H), 2.85-2.79 (m, 1H), 2.46 (t, *J* = 7.3 Hz, 2H). ^{13}C NMR ($CDCl_3$): δ 159.64, 75.44, 48.49, 44.81.

(5*S*)-5-(aminomethyl)-3-methyl-1,3-oxazolidin-2-one (74)

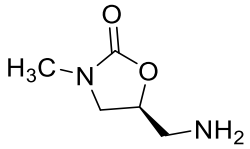

This compound was synthesised according to the general procedure E-step 4 starting with compound **61** (0.468 g, 1.8 mmol). The title compound (0.101 g, 0.77 mmol, 43%) was obtained as a yellow solid. MS: m/z calculated for $C_5H_{11}N_2O_2^+$ 131.0815 $[M+H]^+$. MS: found 131.0827 $[M+H]^+$. HPLC: t_R 0.32 min (95%). Mp: 87 °C. ^{1}H NMR (DMSO-d_6): δ 4.39 (m, 1H), 3.40-3.33 (m, 1H), 3.21-3.14 (m, 1H), 3.02-2.95 (m, 1H), 2.95 (s, 3H), 2.86-2.79 (m, 1H), 2.38 (t, *J* = 7.5 Hz, 2H). ^{13}C NMR (DMSO-d_6): δ 158.17, 74.56, 54.42, 48.64, 30.08.

(5*S*)-5-(aminomethyl)-3-ethyl-1,3-oxazolidin-2-one (75)

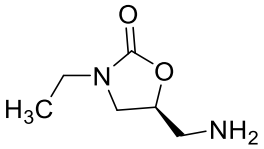

This compound was synthesised according to the general procedure E-step 4 starting with compound **62** (0.438 g, 1.8 mmol). The title compound (0.112 g, 0.77, 41%) was obtained as a yellow solid. MS: m/z calculated for $C_6H_{13}N_2O_2^+$ 145.0972 $[M+H]^+$. MS: found 145.0988 $[M+H]^+$. HPLC: t_R 0.41 min (95%). Mp: 106 °C. ^{1}H NMR (DMSO-d_6): δ 4.40 (m, 1H), 3.42 (q, *J* = 7.9 Hz, 2H), 3.37-3.30 (m, 1H), 3.17-3.11 (m, 1H), 2.98-2.88 (m, 1H), 2.81-2.76 (m, 1H), 2.36 (t, *J* = 7.5 Hz, 2H), 1.24 (t, *J* = 7.9 Hz, 3H). ^{13}C NMR (DMSO-d_6): δ 157.81, 75.04, 51.75, 46.84, 39.94, 12.79.

(5*S*)-5-(aminomethyl)-3-(propan-2-yl)-1,3-oxazolidin-2-one (76)

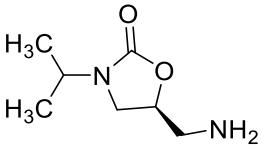

This compound was synthesised according to the general procedure E-step 4 starting with compound **63** (0.460 g, 1.6 mmol). The title compound (0.102 g, 0.64 mmol, 40%) was obtained as a yellow solid. MS: m/z calculated for $C_7H_{15}N_2O_2^+$ 159.1128 $[M+H]^+$. MS: found 159.1128 $[M+H]^+$. HPLC: t_R 0.61 min (95%). Mp: 118 °C. ^{1}H NMR (DMSO-d_6): δ 6.15-6.10 (m, 1H), 4.41 (m, 1H), 3.41-3.35 (m, 1H), 3.23-3.16 (m, 1H), 3.04-2.98 (m, 1H), 2.86-2.79 (m,

1H), 2.76 (d, *J* = 6.8 Hz, 3H), 2.71 (d, *J* = 6.8 Hz, 3H), 2.35 (t, *J* = 7.5 Hz, 2H). ^{13}C NMR (DMSO-d_6): δ 157.12, 74.48, 49.51, 48.44, 46.23, 20.72.

(5S)-5-(aminomethyl)-3-(2-methylpropyl)-1,3-oxazolidin-2-one (77)

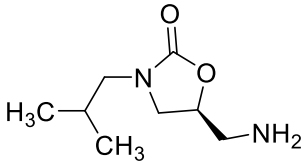

This compound was synthesised according to the general procedure E-step 4 starting with compound **64** (0.302 g, 1 mmol). The title compound (0.096 g, 0.56 mmol, 56 %) was obtained as a yellow solid. MS: m/z calculated for $C_8H_{17}N_2O_2^+$ 173.1285 $[M+H]^+$. MS: found 173.1294 $[M+H]^+$. HPLC: t_R 0.82 min (95%). Mp: 131 °C. ^{1}H NMR (DMSO-d_6): δ 4.40 (m, 1H), 3.98 (dd, J= 5.3 Hz, 3.4 Hz, 1H), 3.85 (dd, J = 8.8 Hz, 6.6 Hz, 1H), 3.71 (dd, J = 5.3 Hz, 3.7 Hz, 2H), 2.86-2.75 (m, 2H), 2.37 (t, *J* = 7.5 Hz, 2H), 2.02-1.95 (m, 1H), 0.91 (d, *J* = 6.6 Hz, 3H), 0.86 (d, *J* = 6.8 Hz, 3H). ^{13}C NMR (DMSO-d_6): δ 158.17, 75.84, 56.25, 53.23, 47.84, 26.53, 20.58.

(5*S*)-5-(aminomethyl)-3-butyl-1,3-oxazolidin-2-one (78)

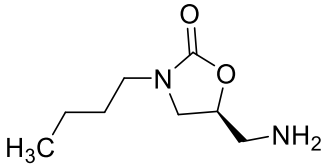

This compound was synthesised according to the general procedure E-step 4 starting with compound **65** (0.302 g, 1 mmol). The title compound (0.104 g, 0.61 mmol, 61%) was obtained as a yellow solid. MS: m/z calculated for $C_8H_{17}N_2O_2^+$ 173.1285 $[M+H]^+$. MS: found 173.1282 $[M+H]^+$. HPLC: t_R 0.86 min (95%). Mp: 133 °C. ^{1}H NMR (DMSO-d_6): δ 4.39 (m, 1H), 3.36-3.28 (m, 2H), 3.22-3.11 (m, 2H), 2.03-2.97 (m, 1H), 2.86-2.75 (m, 1H), 2.36 (t, *J* = 7.5 Hz, 2H), 1.59-1.51 (m, 2H), 1.39-1.23 (m, 2H), 0.95 (t, *J* = 7.9 Hz, 3H). ^{13}C NMR (DMSO-d_6): δ 158.23, 75.09, 52.72, 47.46, 46.55, 29.92, 20.27, 13.95.

5-chloro-*N*-{[(5*S*)-2-oxo-3-phenyl-1,3-oxazolidin-5-yl]methyl}thiophene-2-carboxamide (e18)

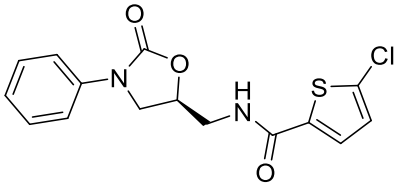

This compound was synthesised according to the general procedure E-step 5- by reacting compound **66** (0.096 g, 0.5mmol). with 5-chlorothiophene-2-carbonyl chloride (0.108 g, 0.6 mmol). The title compound (0.124 g, 0.37 mmol, 75 %) was obtained as a white solid. MS: m/z calculated for $C_{15}H_{14}ClN_2O_3S^+$ 337.0408 $[M+H]^+$. MS: found 337.0422 $[M+H]^+$. HPLC: t_R 1.98 min (96%). Mp: 224 °C. $[\alpha]^{22}_D$ = 26° (c= 1, DMSO). ^{1}H NMR (DMSO-d_6): δ 7.60 (t, *J* = 7.5 Hz, 1H), 7.36-7.30 (m, 3H), 7.23-7.18 (m, 2H), 7.11-7.06 (m, 1H), 7.03 (d, *J* = 7.5 Hz, 1H), 4.90-4.81 (m, 1H), 4.16-4.10 (m, 1H), 3.88 (dd, J= 9.1 Hz, 6.1 Hz, 1H), 3.55 (t, *J* = 7.2 Hz, 2H).^{13}C NMR (DMSO-d_6): δ 160.74, 154.15, 140.18, 136.81, 134.26, 129.92, 129.18, 127.49, 123.33, 120.45, 71.31, 47.44, 41.46.

5-chloro-*N*-{[(5*S*)-3-(3-ethenylphenyl)-2-oxo-1,3-oxazolidin-5-yl]methyl}thiophene-2-carboxamide (e19)

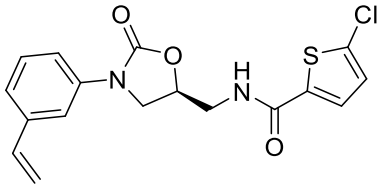

This compound was synthesised according to the general procedure E-step 5- by reacting compound **67** (0.076 g, 0.35 mmol). with 5-chlorothiophene-2-carbonyl chloride (0.076 g, 0.42 mmol). The title compound (0.090 g, 0.25 mmol, 71 %) was obtained as a white solid. MS: m/z calculated for $C_{17}H_{16}ClN_2O_3S^+$ 363.0565 $[M+H]^+$. MS: found 363.0582 $[M+H]^+$. HPLC: t_R 2.10 min (96%). Mp: 231 °C. $[\alpha]^{22}_D$ = -55° (c= 1, DMSO). ^{1}H NMR (DMSO-d_6): δ 7.61 (t, *J* = 7.5 Hz, 1H), 7.54 (t, *J* = 1.5 Hz, 1H), 7.38-7.33 (m, 2H), 7.27 (t, *J* = 7.4 Hz, 1H), 7.25-7.20 (m, 1H), 7.05 (d, *J* = 7.5 Hz, 1H), 6.66 (dd, *J* = 16.8, 10.0 Hz, 1H), 5.78 (dd, *J* = 16.8, 2.7 Hz, 1H), 5.48 (dd, *J* = 10.1, 2.6 Hz, 1H), 4.89-4.79 (p, *J* = 7.0 Hz, 1H), 4.16-4.12(m, 1H), 3.89 (dd, J= 10.6 Hz, 6.3 Hz, 1H), 3.56 (t, *J* = 7.2 Hz, 2H).^{13}C NMR (DMSO-d_6): δ 160.74, 154.18, 141.82, 140.28, 135.41, 134.28, 133.54, 130.81, 129.77, 128.15, 127.50, 120.45, 115.12, 112.86, 71.32, 47.46, 41.46.

5-chloro-*N*-{[(5*S*)-3-(3-formylphenyl)-2-oxo-1,3-oxazolidin-5-yl]methyl}thiophene-2-carboxamide (e20)

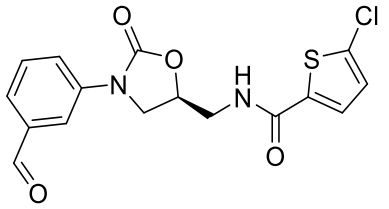

This compound was synthesised according to the general procedure E-step 5- by reacting compound **68** (0.066 g, 0.30 mmol) with 5-chlorothiophene-2-carbonyl chloride (0.065 g, 0.36 mmol). The title compound (0.072 g, 0.20 mmol, 68 %) was obtained as a white solid. MS: m/z calculated for $C_{16}H_{14}ClN_2O_4S^+$ 365.0357 $[M+H]^+$. MS: found 365.0376 $[M+H]^+$. HPLC: t_R 2.06 min (96%). Mp: 220 °C. $[\alpha]^{22}_D$ = 21° (c= 1, DMSO). ^{1}H NMR (DMSO-d_6): δ 9.68 (d, *J* = 1.1 Hz, 1H), 8.04 (t, *J* = 1.5 Hz, 1H), 7.74-7.64 (m, 2H), 7.59 (t, *J* = 7.5 Hz, 1H), 7.44 (t, *J* = 7.5 Hz, 1H), 7.32 (d, *J* = 7.5 Hz, 1H), 7.01 (d, *J* = 7.5 Hz, 1H), 4.88-4.77 (pm, 1H), 4.14-4.08 (m, 1H), 3.87 (dd, J= 9.0 Hz, 6.3 Hz, 1H), 3.53 (t, *J* = 7.2 Hz, 2H).^{13}C NMR (DMSO-d_6): δ 192.43, 160.74, 154.17, 143.16, 140.18, 137.03, 134.28, 129.67, 128.72, 127.51, 123.58, 120.46, 119.04, 71.33, 47.47, 41.46.

5-chloro-*N*-{[(5*S*)-3-(3-methylphenyl)-2-oxo-1,3-oxazolidin-5-yl]methyl}thiophene-2-carboxamide (e21)

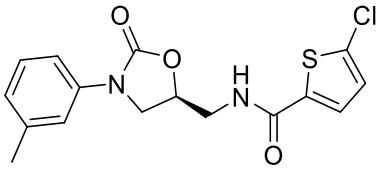

This compound was synthesised according to the general procedure E-step 5- by reacting compound **69** (0.103 g, 0.5 mmol) with 5-chlorothiophene-2-carbonyl chloride (0.108 g, 0.6 mmol). The title compound (0.131 g, 0.37, 75%) was obtained as a white solid. MS: m/z calculated for $C_{16}H_{16}ClN_2O_3S^+$ 351.0565 $[M+H]^+$. MS: found 351.0580 $[M+H]^+$. HPLC: t_R 2.00 min (96%). Mp: 240 °C. $[\alpha]^{22}_D$ = -37° (c= 1, DMSO). ^{1}H NMR (DMSO-d_6): δ 7.60 (t, *J* = 7.5 Hz, 1H), 7.39-7.30 (m, 3H), 7.24 (t, *J* = 7.5 Hz, 1H), 7.03 (d, *J* = 7.5 Hz, 1H), 6.91-6.85 (m, 1H), 4.89-4.80 (m, 1H), 4.16-4.11(m, 1H), 3.89 (dd, J= 9.3 Hz, 6.2 Hz, 1H), 3.56 (t, *J* = 7.2 Hz, 2H), 2.29 (d, *J* = 0.9 Hz, 3H). ^{13}C NMR (DMSO-d_6): δ 160.77, 154.16, 141.95, 139.30, 138.85, 134.26, 129.76, 129.14, 127.47, 120.48, 118.13, 112.74, 71.36, 47.48, 41.46, 21.88.

5-chloro-*N*-{[(5*S*)-3-(3,5-dimethylphenyl)-2-oxo-1,3-oxazolidin-5-yl]methyl}thiophene-2-carboxamide (e22)

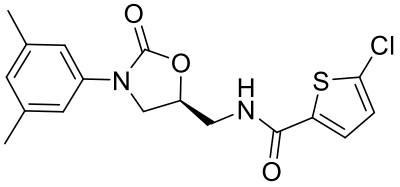

This compound was synthesised according to the general procedure E-step 5- by reacting compound **70** (0.111 g, 0.5 mmol) with 5-chlorothiophene-2-carbonyl chloride (0.180 g, 6 mmol). The title compound (0.112 g, 0.31 mmol, 62%) was obtained as a white solid. MS: m/z calculated for $C_{17}H_{18}ClN_2O_3S^+$ 365.0721 $[M+H]^+$. MS: found 365.0734 $[M+H]^+$. HPLC: t_R 2.23 min (96%). Mp: 251 °C. $[\alpha]^{22}_D$ = 46° (c= 1, DMSO). ^{1}H NMR (DMSO-d_6): δ 7.62 (t, *J* = 7.5 Hz, 1H), 7.36 (d, *J* = 7.5 Hz, 1H), 7.17 (d, *J* = 1.4 Hz, 2H), 7.05 (d, *J* = 7.5 Hz, 1H), 6.79 (q, *J* = 1.2 Hz, 1H), 4.91-4.82 (m, 1H), 4.17-4.11 (m, 1H), 3.82 (dd, *J* = 12.3, 6.9 Hz, 1H), 3.56 (t, *J* = 7.2 Hz, 2H), 2.26 (s, 6H). ^{13}C NMR (DMSO-d_6): δ 160.74, 154.16, 141.27, 140.42, 138.49, 134.27, 129.58, 127.51, 118.85, 112.72, 71.31, 47.45, 41.46, 21.74.

***tert*-butyl ({3-[(5*S*)-5-{[(5-chlorothiophene-2-carbonyl)amino]methyl}-2-oxo-1,3-oxazolidin-3-yl]phenyl}methyl)carbamate (e30)**

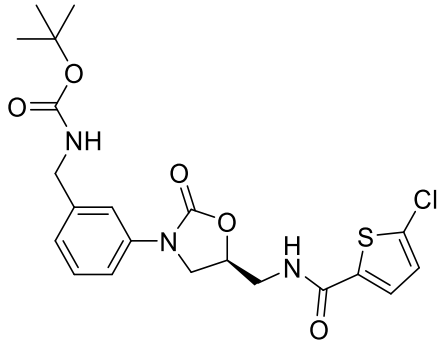

This compound was synthesised according to the general procedure E-step 5- by reacting compound **71** (0.192 g, 0.6 mmol) with 5-chlorothiophene-2-carbonyl chloride (0.130 g, 0.72 mmol). The title compound (0.209 g, 0.45 mmol, 76%) was obtained as a white solid. MS: m/z calculated for $C_{21}H_{25}ClN_3O_5S^+$ 466.1198 $[M+H]^+$. MS: found 466.1210 $[M+H]^+$. HPLC: t_R 2.68 min (96%). Mp: 287 °C. $[\alpha]^{22}_D$ = -59° (c= 1, DMSO). ^{1}H NMR (DMSO-d_6): δ 7.60 (t, *J* = 7.5 Hz, 1H), 7.55-7.47 (m, 1H), 7.44-7.38 (m, 1H), 7.34 (d, *J* = 7.5 Hz, 1H), 7.31 (t, *J* = 7.5 Hz, 1H), 7.19-7.14 (m, 1H), 7.03 (d, *J* = 7.5 Hz, 1H), 6.13 (t, *J* = 8.9 Hz, 1H), 4.89-4.80 (m, 1H), 4.36-4.29 (m, 1H), 4.28-4.22 (m, 1H), 4.18-4.12 (m, 1H), 3.89 (dd, J= 11.1 Hz, 6.0 Hz, 1H), 3.54 (t, *J* = 7.2

Hz, 2H), 1.39 (s, 9H). ^{13}C NMR (DMSO-d_6): δ 160.72, 156.11, 154.15, 141.88, 140.89, 136.66, 134.26, 127.96, 127.78, 127.67, 127.49, 120.44, 116.99, 79.84, 71.30, 47.43, 46.29, 41.45, 28.30.

_N_-{[(5_S_)-3-{3-[(benzylamino)methyl]phenyl}-2-oxo-1,3-oxazolidin-5-yl]methyl}-5-chlorothiophene-2-carboxamide (e23)

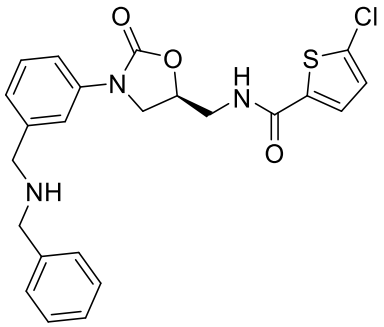

This compound was synthesised according to the general procedure E-step 5- by reacting compound **72** (0.108 g, 0.35 mmol) with 5-chlorothiophene-2-carbonyl chloride (0.076 g, 0.42 mmol). The title compound (0.064 g, 0.14 mmol, 42%) was obtained as a white solid. MS: m/z calculated for $C_{23}H_{23}ClN_3O_3S^+$ 456.1143 $[M+H]^+$. MS: found 456.1160 $[M+H]^+$. HPLC: t_R 3.10 min (96%). Mp: 296 °C. $[\alpha]^{22}_D$ = -77° (c= 1, DMSO). ^{1}H NMR (DMSO-d_6): δ 7.60 (t, *J* = 7.5 Hz, 1H), 7.49-7.48 (m, 2H), 7.36-7.24 (m, 7H), 7.18-7.12 (m, 1H), 7.03 (d, *J* = 7.5 Hz, 1H), 4.92-7.83 (m, 1H), 4.16-4.10 (m, 1H), 3.89 (dd, J= 10.1 Hz, 6.3Hz, 1H), 3.87-3.77 (m, 4H), 3.56 (t, *J* = 7.2 Hz, 2H), 3.12 (p, *J* = 8.6 Hz, 1H). ^{13}C NMR (DMSO-d_6): δ 160.73, 154.16, 141.28, 140.75, 140.41, 136.78, 134.27, 130.12, 128.24, 128.114, 127.97, 127.65, 127.51, 127.18, 120.46, 117.34, 71.31, 53.12, 49.94, 47.46, 41.46.

5-chloro-_N_-{[(5_S_)-2-oxo-1,3-oxazolidin-5-yl]methyl}thiophene-2-carboxamide (e24)

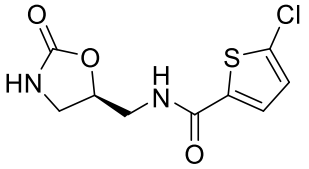

This compound was synthesised according to the general procedure E-step 5- by reacting compound **73** (0.058 g, 0.5 mmol) with 5-chlorothiophene-2-carbonyl chloride (0.108 g, 0.6 mmol). The title compound (0.091 g, 0.35 mmol, 71%) was obtained as a white solid. MS: m/z calculated for $C_9H_{10}ClN_2O_3S^+$ 261.0095 $[M+H]^+$. MS: found 261.0109 $[M+H]^+$. HPLC: t_R 1.21 min (96%). Mp: 136 °C. $[\alpha]^{22}_D$ = -19° (c= 1, DMSO). ^{1}H NMR (DMSO-

d_6): δ 7.68 (t, *J* = 7.6 Hz, 1H), 7.34 (d, *J* = 7.5 Hz, 1H), 7.12 (t, *J* = 6.6 Hz, 1H), 7.03 (d, *J* = 7.5 Hz, 1H), 4.92-4.82 (m, 1H), 3.50 (t, *J* = 7.3 Hz, 2H), 3.40-3.35 (m, 1H), 3.29-3.21 (m, 1H). ^{13}C NMR (DMSO-d_6): δ 160.33, 159.68, 140.09, 134.29, 129.18, 127.56, 74.62, 45.66, 41.47.

5-chloro-*N*-{[(5*S*)-3-methyl-2-oxo-1,3-oxazolidin-5-yl]methyl}thiophene-2-carboxamide (e25)

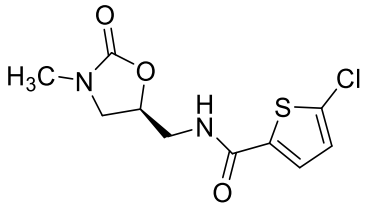

This compound was synthesised according to the general procedure E-step 5- by reacting compound **74** (0.078 g, 0.6 mmol) with 5-chlorothiophene-2-carbonyl chloride (0.130 g, 0.72 mmol). The title compound (0.115 g, 0.42 mmol, 71%) was obtained as a white solid. MS: m/z calculated for $C_{10}H_{12}ClN_2O_3S^+$ 275.0252 $[M+H]^+$. MS: found 275.0252 $[M+H]^+$. HPLC: t_R 1.76 min (96%). Mp: 188 °C. $[\alpha]^{22}_D$ = 22° (c= 1, DMSO). ^{1}H NMR (DMSO-d_6): δ 7.60 (t, *J* = 7.5 Hz, 1H), 7.34 (d, *J* = 7.5 Hz, 1H), 7.03 (d, *J* = 7.5 Hz, 1H), 4.89-4.90 (m, 1H), 3.52 (t, *J* = 7.2 Hz, 2H), 3.40-3.33 (m, 1H), 3.21-3.14 (m, 1H), 2.95 (s, 3H). ^{13}C NMR (DMSO-d_6): δ 161.74, 158.05, 140.08, 134.27, 129.16, 127.50, 71.31, 52.45, 41.46, 30.09.

5-chloro-*N*-{[(5*S*)-3-ethyl-2-oxo-1,3-oxazolidin-5-yl]methyl}thiophene-2-carboxamide (e26)

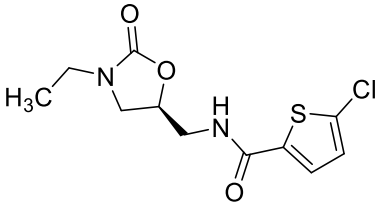

This compound was synthesised according to the general procedure E-step 5- by reacting compound **75** (0.086 g, 0.6 mmol) with 5-chlorothiophene-2-carbonyl chloride (0.130 g, 72 mmol). The title compound (0.120 g, 0.42 mmol, 70%) was obtained as a white solid. MS: m/z calculated for $C_{11}H_{14}ClN_2O_3S^+$ 289.0408 $[M+H]^+$. MS: found 289.0419 $[M+H]^+$. HPLC: t_R 1.82 min (96%). Mp: 192°C. $[\alpha]^{22}_D$ = 44° (c= 1, DMSO). ^{1}H NMR (DMSO-d_6): δ 7.63 (t, *J* = 7.5 Hz, 1H), 7.36 (d, *J* = 7.5 Hz, 1H), 7.03 (d, *J* = 7.5 Hz, 1H), 4.92-4.80 (m, 1H), 3.54 (t, *J* = 7.2 Hz, 2H), 3.44 (q, *J* = 7.9 Hz, 2H),

3.37-3.30 (m, 1H), 3.17-3.11 (m, 1H), 1.25 (t, *J* = 7.9 Hz, 3H).^{13}C NMR (DMSO-d_6): δ 161.72, 156.55, 140.26, 134.28, 129.10, 127.48, 74.22, 49.83, 41.45, 40.55, 12.89.

5-chloro-*N*-{[(5*S*)-2-oxo-3-(propan-2-yl)-1,3-oxazolidin-5-yl]methyl}thiophene-2-carboxamide (e27)

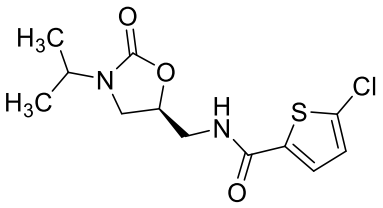

This compound was synthesised according to the general procedure E-step 5- by reacting compound **76** (0.079 g, 0.5 mmol) with 5-chlorothiophene-2-carbonyl chloride (0.108 g, 0.6 mmol). The title compound (0.099 g, 0.33 mmol, 66%) was obtained as a white solid. MS: m/z calculated for $C_{12}H_{16}ClN_2O_3S^+$ 303.0565 $[M+H]^+$. MS: found 303.0581 $[M+H]^+$. HPLC: t_R 1.80 min (96%). Mp: 190 °C. $[\alpha]^{22}_D$ = -67° (c= 1, DMSO). ^{1}H NMR (DMSO-d_6): δ 7.63 (t, *J* = 7.5 Hz, 1H), 7.37 (d, *J* = 7.5 Hz, 1H), 7.03 (d, *J* = 7.5 Hz, 1H), 6.14-6.08 (m, 1H), 4.88-4.77 (m, 1H), 3.54 (t, *J* = 7.2 Hz, 2H), 3.41-3.35 (m, 1H), 3.23-3.16 (m, 1H), 2.77 (d, *J* = 6.8 Hz, 3H), 2.72 (d, *J* = 6.8 Hz, 3H).^{13}C NMR (DMSO-d_6): δ 160.74, 157.22, 140.30, 134.27, 128.84, 127.51, 73.66, 50.32, 49.69, 41.46, 20.73.

5-chloro-N-{[(5S)-3-(2-methylpropyl)-2-oxo-1,3-oxazolidin-5-yl]methyl}thiophene-2-carboxamide (e28)

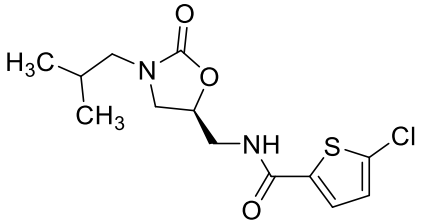

This compound was synthesised according to the general procedure E-step 5- by reacting compound **77** (0.077 g, 0.45 mmol) with 5-chlorothiophene-2-carbonyl chloride (0.097 g, 0.54 mmol). The title compound (0.091 g, 0.29 mmol, 65%) was obtained as a white solid. MS: m/z calculated for $C_{13}H_{18}ClN_2O_3S^+$ 317.0721 $[M+H]^+$. MS: found 317.0736 $[M+H]^+$. HPLC: t_R 1.88 min (96%). Mp: 201 °C. $[\alpha]^{22}_D$ = 66° (c= 1, DMSO). ^{1}H NMR (DMSO-d_6): δ 7.62 (t, *J* = 7.5 Hz, 1H), 7.364 (d, *J* = 7.5 Hz, 1H), 7.03 (d, *J* = 7.5 Hz, 1H), 4.89-4.80 (m, 1H), 3.53 (t, *J* = 7.2 Hz, 2H), 3.34 (dd, *J* = 12.3, 7.1 Hz,

1H), 3.15 (dd, *J* = 12.3, 6.9 Hz, 1H), 2.96 (dd, *J* = 12.3, 7.0 Hz, 1H), 2.78 (dd, *J* = 12.3, 7.0 Hz, 1H), 2.06-2.01 (m, 1H), 0.91 (d, *J* = 6.6 Hz, 3H), 0.86 (d, *J* = 6.8 Hz, 3H). ^{13}C NMR (DMSO-d_6): δ 160.74, 158.05, 140.45, 134.26, 128.67, 127.49, 75.00, 56.77, 51.27, 41.45, 26.53, 20.58.

_N_-{[(5_S_)-3-butyl-2-oxo-1,3-oxazolidin-5-yl]methyl}-5-chlorothiophene-2-carboxamide (e29)

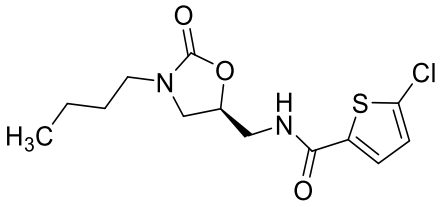

This compound was synthesised according to the general procedure E-step 5- by reacting compound **78** (0.077 g, 0.45 mmol) with 5-chlorothiophene-2-carbonyl chloride (0.097 g, 0.54 mmol). The title compound (0.086 g, 0.27 mmol, 61%) was obtained as a white solid. MS: m/z calculated for $C_{13}H_{18}ClN_2O_3S^+$ 317.0721 $[M+H]^+$. MS: found 317.0734 $[M+H]^+$. HPLC: t_R 1.91 min (96%). Mp: 222 °C. $[\alpha]^{22}_D$ = -35° (c= 1, DMSO). ^{1}H NMR (DMSO-d_6): δ 7.59 (t, *J* = 7.5 Hz, 1H), 7.31 (d, *J* = 7.5 Hz, 1H), 7.03 (d, *J* = 7.5 Hz, 1H), 4.85-4.75 (m, 1H), 3.52 (t, *J* = 7.2 Hz, 2H), 3.36-3.28 (m, 2H), 3.22-3.11 (m, 2H), 1.59-1.55 (m, 2H), 1.39-1.23 (m, 2H), 0.95 (t, *J* = 7.9 Hz, 3H). ^{13}C NMR (DMSO-d_6): δ 163.73, 157.86, 140.56, 134.27, 128.72, 127.50, 74.23, 50.76, 47.07, 41.45, 29.92, 20.27, 13.96.

_N_-({(5_S_)-3-[3-(aminomethyl)phenyl]-2-oxo-1,3-oxazolidin-5-yl}methyl)-5-chlorothiophene-2-carboxamide (e31)

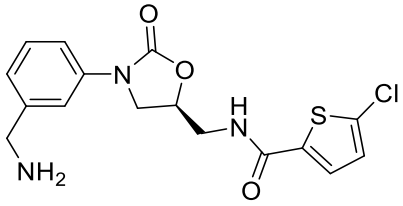

This compound was synthesised according to the general procedure E-step 6- starting with compound **e30** (0.162 g, 0.35 mmol). The title compound (0.076 g, 0.21 mmol, 60%) was obtained as a white solid. MS: m/z calculated for $C_{16}H_{17}ClN_3O_3S^+$ 366.0674 $[M+H]^+$. MS: found 366.0688 $[M+H]^+$. HPLC: t_R 1.67 min (96%). Mp: 243 °C. $[\alpha]^{22}_D$ = -59° (c= 1, DMSO). ^{1}H NMR (DMSO-d_6): δ 7.61 (t, *J* = 7.5 Hz, 1H), 7.54 (t, *J* = 6.7 Hz, 2H), 7.47-7.40 (m, 2H), 7.36-7.30 (m, 2H), 7.18-7.10 (m, 1H), 7.03 (d, *J* = 7.5 Hz, 1H), 4.88-4.78 (m, 1H), 4.18-4.14 (m, 1H), 3.88 (dd, J= 9.1 Hz, 6.1 Hz, 1H), 3.66-3.58 (m, 2H),

3.61-3.53 (m, 2H). ^{13}C NMR (DMSO-d_6): δ 160.76, 154.16, 144.53, 142.45, 140.39, 134.29, 129.73, 127.97, 127.51, 120.45, 117.05, 115.456, 71.35, 47.44, 46.43, 41.46.

References

(1) Straub, A.; Roehrig, S.; Hillisch, A. Oral, Direct Thrombin and Factor Xa Inhibitors: The Replacement for Warfarin, Leeches, and Pig Intestines? *Angewandte Chemie, International Edition* **2011,** *50* (20), 4574.

(2) Ratnoff, O. D.; Colopy, J. E. A familial hemorrhagic trait associated with a deficiency of a clot-promoting fraction of plasma. *The Journal of clinical investigation* **1955,** *34* (4), 602.

(3) Ratnoff, O. D.; Rosenblum, J. M. Role of Hageman factor in the initiation of clotting by glass; evidence that glass frees Hageman factor from inhibition. *The American journal of medicine* **1958,** *25* (2), 160.

(4) Bowie, E. W.; Owen, C. The clinical and laboratory diagnosis of hemorrhagic disorders. *Disorders of Hemostasis. Orlando, FL: Grune & Stratton* **1984**, 43.

(5) Hardisty, R. M.; Margolis, J. The role of Hageman factor in the initiation of blood coagulation. *British journal of haematology* **1959,** *5* (2), 203.

(6) Lynch, J.; Shariat-Madar, Z. Physiological effects of the plasma Kallikrein-Kinin System: roles of the blood coagulation factor XII (Hageman factor). *Journal of Clinical Toxicology* **2012,** *2* (3), e105.

(7) Pham, M.; Kleinschnitz, C.; Helluy, X.; Bartsch, A. J.; Austinat, M.; Behr, V. C.; Renné, T.; Nieswandt, B.; Stoll, G.; Bendszus, M. Enhanced cortical reperfusion protects coagulation factor XII-deficient mice from ischemic stroke as revealed by high-field MRI. *Neuroimage* **2010,** *49* (4), 2907.

(8) Renne, T.; Nieswandt, B.; Gailani, D. The intrinsic pathway of coagulation is essential for thrombus stability in mice. *Blood Cells, Molecules, & Diseases* **2006,** *36* (2), 148.

(9) Renné, T.; Pozgajová, M.; Grüner, S.; Schuh, K.; Pauer, H. U.; Burfeind, P.; Gailani, D.; Nieswandt, B. Defective thrombus formation in mice lacking coagulation factor XII. *Journal of Experimental Medicine* **2005,** *202* (2), 271.

(10) Revenko, A. S.; Gao, D.; Crosby, J. R.; Bhattacharjee, G.; Zhao, C.; May, C.; Gailani, D.; Monia, B. P.; MacLeod, A. R. Selective depletion of plasma prekallikrein or coagulation factor XII inhibits thrombosis in mice without increased risk of bleeding. *Blood* **2011,** *118* (19), 5302.

(11) Schousboe, I. Pharmacological regulation of factor XII activation may be a new target to control pathological coagulation. *Biochemical Pharmacology* **2008,** *75* (5), 1007.

(12) Kleinschnitz, C.; Stoll, G.; Bendszus, M.; Schuh, K.; Pauer, H. U.; Burfeind, P.; Renné, C.; Gailani, D.; Nieswandt, B.; Renné, T. Targeting coagulation factor XII provides protection from pathological thrombosis in cerebral ischemia without interfering with hemostasis. *Journal of Experimental Medicine* **2006,** *203* (3), 513.

(13) Robert W. Colman; Alexander W. Claws; James N. George; Samuel Z. Goldhaber; Marder, V. J. In *Hemostasis and thrombosis: Basic principles and clinicl practice*; Robert W. Colman;Victor J. Marder;Alexander W. Claws;James N. George;Goldhaber, S. Z., Eds.; PA: Lippincott Williams & Wilkins: Philadelphia, 2006.

(14) Colman, R. W.; Claws, A. W.; George, J. N.; Goldhaber, S. Z.; Marder, V. J. In *Hemostasis and thrombosis: Basic principles and clinicl practice*; Robert, W. C.; Victor, J. M.; Alexander, W. C.; James, N. G.; Goldhaber, S. Z., Eds.; PA: Lippincott Williams & Wilkins: Philadelphia, 2006.

(15) Packham, M. A. Role of platelets in thrombosis and hemostasis. *Canadian journal of physiology and pharmacology* **1994,** *72* (3), 278.

(16) Monroe, D. M. In *Practical Hemostasis and Thrombosis*; Second edtion ed.; Nigel Key, M. M., Denise O'Shaughnessy, David Lillicrap, , Ed.; WILEY-BLACKWELL: USA, 2009.

(17) Ruggeri, Z. M.; Ware, J. von Willebrand factor. *The Federation of American Societies for Experimental Biology Journal* **1993,** *7* (2), 308.

(18) Roth, G. J. Developing relationships: arterial platelet adhesion, glycoprotein Ib, and leucine-rich glycoproteins. *Blood* **1991,** *77* (1), 5.

(19) Groot, P. G.; Sixma, J. J. Platelet adhesion. *British journal of haematology* **1990,** *75* (3), 308.

(20) Lopez, J. A.; Chen, J. Pathophysiology of venous thrombosis. *Thrombosis Research* **2009,** *123* (Suppl. 4), S30.

(21) Mandal, S. K.; Pendurthi, U. R.; Rao, L. V. M. Cellular localization and trafficking of tissue factor. *Blood* **2006,** *107* (12), 4746.

(22) Huang, X.; Ding, W.-Q.; Vaught, J. L.; Wolf, R. F.; Morrissey, J. H.; Harrison, R. G.; Lind, S. E. A soluble tissue factor-annexin V chimeric protein has both procoagulant and anticoagulant properties. *Blood* **2006,** *107* (3), 980.

(23) Butenas, S.; Orfeo, T.; Mann, K. G. Tissue factor in coagulation: Which? Where? When? *Arteriosclerosis, thrombosis, and vascular biology* **2009,** *29* (12), 1989.

(24) Crawley, J. T. B.; Lane, D. A. The Haemostatic Role of Tissue Factor Pathway Inhibitor. *Arteriosclerosis, Thrombosis, and Vascular Biology* **2008,** *28* (2), 233.

(25) Esmon, C. T.; Lollar, P. Involvement of thrombin anion-binding exosites 1 and 2 in the activation of factor V and factor VIII. *Journal of Biological Chemistry* **1996,** *271* (23), 13882.

(26) Davie, E. W. A Brief Historical Review of the Waterfall/Cascade of Blood Coagulation. *Journal of Biological Chemistry* **2003,** *278* (51), 50819.

(27) Davie, E. W.; Fujikawa, K.; Kisiel, W. The coagulation cascade: initiation, maintenance, and regulation. *Biochemistry* **1991,** *30* (43), 10363.

(28) Crawley, J. T. B.; Zanardelli, S.; Chion, C. K. N. K.; Lane, D. A. The central role of thrombin in hemostasis. *Journal of Thrombosis and Haemostasis* **2007,** *5* (Suppl. 1), 95.

(29) Mosesson, M. W. Fibrinogen and fibrin structure and functions. *Journal of Thrombosis and Haemostasis* **2005,** *3* (8), 1894.

(30) Renne, T. The procoagulant and proinflammatory plasma contact system. *Seminars in Immunopathology* **2012,** *34* (1), 31.

(31) Kato, H.; Shimada, T.; Ohno, Y.; Sugo, T.; Kodama, K. Activation mechanism of bovine factor XII on foreign surfaces--activation by polysaccharide sulfate and sulfatide and inhibition by platelet components. *Rinsho byori. The Japanese journal of clinical pathology* **1982,** *Suppl 50*, 102.

(32) Kato, H. Initiation mechanism of intrinsic blood coagulation: activation of factor XII and roles of high-molecular-weight kininogen (author's transl). *Seikagaku* **1980,** *52* (11), 1173.

(33) van der Meijden, P. E.; Munnix, I. C.; Auger, J. M.; Govers-Riemslag, J. W.; Cosemans, J. M.; Kuijpers, M. J.; Spronk, H. M.; Watson, S. P.; Renne, T.; Heemskerk, J. W. Dual role of collagen in factor XII-dependent thrombus formation. *Blood* **2009,** *114* (4), 881.

(34) de Maat, S.; van Dooremalen, S.; de Groot, P. G.; Maas, C. A nanobody-based method for tracking factor XII activation in plasma. *Journal of Thrombosis and Haemostasis* **2013,** *110* (3), 458.

(35) Leung, P. Y.; Hurst, S.; Berny-Lang, M. A.; Verbout, N. G.; Gailani, D.; Tucker, E. I.; Wang, R. K.; McCarty, O. J.; Gruber, A. Inhibition of Factor XII-Mediated Activation of Factor XI Provides Protection Against Experimental Acute Ischemic Stroke in Mice. *Translational Stroke Research* **2012,** *3* (3), 381.

(36) Geng, Y.; Verhamme, I. M.; Messer, A.; Sun, M.-f.; Smith, S. B.; Bajaj, S. P.; Gailani, D. A Sequential Mechanism for Exosite-mediated Factor IX Activation by Factor XIa. *Journal of Biological Chemistry* **2012,** *287* (45), 38200.

(37) Stoilova-McPhie, S.; Lynch, G. C.; Ludtke, S.; Pettitt, B. M. Domain organization of membrane-bound factor VIII. *Biopolymers* **2013,** *99* (7), 448.

(38) Woodward, M.; Rumley, A.; Welsh, P.; MacMahon, S.; Lowe, G. A comparison of the associations between seven hemostatic or inflammatory variables and coronary heart disease. *Journal of Thrombosis and Haemostasis* **2007,** *5* (9), 1795.

(39) Rasche, H. Haemostasis and thrombosis: an overview. *European Heart Journal Supplements* **2001,** *3* (suppl_Q), Q3.

(40) Colman, R. W. Are hemostasis and thrombosis two sides of the same coin? *Journal of Experimental Medicine* **2006,** *203* (3), 493.

(41) Renne, T.; Pozgajova, M.; Gruener, S.; Schuh, K.; Pauer, H.-U.; Burfeind, P.; Gailani, D.; Nieswandt, B. Defective thrombus formation in mice lacking coagulation factor XII. *Journal of Experimental Medicine* **2005,** *202* (2), 271.

(42) Wang, X.; Cheng, Q.; Xu, L.; Feuerstein, G.; HSU, M. Y.; Smith, P.; Seiffert, D.; Schumacher, W.; Ogletree, M.; Gailani, D. Effects of factor IX or factor XI deficiency on ferric chloride-induced carotid artery occlusion in mice. *Journal of Thrombosis and Haemostasis* **2005,** *3* (4), 695.

(43) Elizabeth Roman, P. J. L., Catherine S. Mano In *Haematology: Basic principles and practice*; Sixth Edition ed.; Ronald Hoffman, E. J. B. J., Leslie E. Silberstien, Helen Hislop, Jeffery weitz, John Anastazi, Ed.; Saunders: NewYork, 2013.

(44) Salomon, O.; Steinberg, D.; Seligshon, U. Variable bleeding manifestations characterize different types of surgery in patients with severe factor XI

deficiency enabling parsimonious use of replacement therapy. *Haemophilia* **2006,** *12* (5), 490.

(45) Lämmle, B.; Wuillemin, W. A.; Huber, I.; Krauskopf, M.; Zürcher, C.; Pflugshaupt, R.; Furlan, M. Thromboembolism and bleeding tendency in congenital factor XII deficiency--a study on 74 subjects from 14 Swiss families. *Journal of Thrombosis and Haemostasis* **1991,** *65* (2), 117.

(46) Kaplan, A. P. Intrinsic coagulation, thrombosis, and bleeding [letter]. *Blood* **1996,** *87* (5), 2090.

(47) Gailani, D.; Renne, T. Intrinsic pathway of coagulation and arterial thrombosis. *Arteriosclerosis, Thrombosis, and Vascular Biology* **2007,** *27* (12), 2507.

(48) Mackman, N. Role of Tissue Factor in Hemostasis, Thrombosis, and Vascular Development. *Arteriosclerosis, Thrombosis, and Vascular Biology* **2004,** *24* (6), 1015.

(49) Morrissey, J. H. Tissue factor: a key molecule in hemostatic and nonhemostatic systems. *International journal of hematology* **2004,** *79* (2), 103.

(50) Gailani, D.; Broze Jr, G. J. Factor XI activation in a revised model of blood coagulation. *Science* **1991,** *253* (5022), 909.

(51) Ponczek, M. B.; Gailani, D.; Doolittle, R. F. Evolution of the contact phase of vertebrate blood coagulation. *Journal of Thrombosis and Haemostasis* **2008,** *6* (11), 1876.

(52) Renne, T.; Schmaier, A. H.; Nickel, K. F.; Blomback, M.; Maas, C. In vivo roles of factor XII. *Blood* **2012,** *120* (22), 4296.

(53) Citarella, F.; Tripodi, M.; Fantoni, A.; Bernardi, F.; Romeo, G.; Rocchi, M. Assignment of human coagulation factor XII (fXII) to chromosome 5 by cDNA hybridization to DNA from somatic cell hybrids. *Human Genetics* **1988,** *80* (4), 397.

(54) Cool, D. E.; MacGillivray, R. T. Characterization of the human blood coagulation factor XII gene. Intron/exon gene organization and analysis of the 5'-flanking region. *Journal of Biological Chemistry* **1987,** *262* (28), 13662.

(55) Saito, H.; Ratnoff, O. D.; Pensky, J. Radioimmunoassay of human Hageman factor (factor XII). *Journal of Laboratory and Clinical Medicine* **1976,** *88* (3), 506.

(56) Pixley, R. A.; Colman, R. W. Factor XII: Hageman factor. *Methods in Enzymology* **1993,** *222*, 51.

(57) Griffin, J. H.; Cochrane, C. G. Human factor XII (Hageman factor). *Methods in Enzymology* **1976,** *45*, 56.

(58) Silverberg, M.; Kaplan, A. P. Human Hageman factor and its fragments. *Methods in enzymology* **1988,** *163*, 68.

(59) Pankov, R.; Yamada, K. M. Fibronectin at a glance. *Journal of Cell Science* **2002,** *115* (20), 3861.

(60) Plow, E. F.; Haas, T. A.; Zhang, L.; Loftus, J.; Smith, J. W. Ligand binding to integrins. *Journal of Biological Chemistry* **2000,** *275* (29), 21785.

(61) Mosher, D. F. Physiology of fibronectin. *Annual review of medicine* **1984,** *35*, 561.

(62) Ginsberg, M. H.; Painter, R. G.; Forsyth, J.; Birdwell, C.; Plow, E. F. Thrombin increases expression of fibronectin antigen on the platelet surface. *Proceedings of the National Academy of Sciences of the United States of America* **1980,** *77* (2), 1049.

(63) Ginsberg, M. H.; Plow, E. F. Fibronectin expression on the platelet surface occurs in concert with secretion. *Journal of Supramolecular Structure and Cellular Biochemistry* **1981,** *17* (1), 91.

(64) Mosher, D. F. Organization of the provisional fibronectin matrix: control by products of blood coagulation. *Journal of Thrombosis and Haemostasis* **1995,** *74* (1), 529.

(65) McKeown-Longo, P. J.; Mosher, D. F. Interaction of the 70,000-mol-wt amino-terminal fragment of fibronectin with the matrix-assembly receptor of fibroblasts. *The Journal of Cell Biology* **1985,** *100* (2), 364.

(66) Kamykowski, G. W.; Mosher, D. F.; Lorand, L.; Ferry, J. D. Modification of shear modulus and creep compliance of fibrin clots by fibronectin. *Biophysical Chemistry* **1981,** *13* (1), 25.

(67) Stavrou, E.; Schmaier, A. H. Factor XII: what does it contribute to our understanding of the physiology and pathophysiology of hemostasis & thrombosis. *Thrombosis Research* **2010,** *125* (3), 210.

(68) Pixley, R. A.; Stumpo, L. G.; Birkmeyer, K.; Silver, L.; Colman, R. W. A monoclonal antibody recognizing an icosapeptide sequence in the heavy

chain of human factor XII inhibits surface-catalyzed activation. *Journal of Biological Chemistry* **1987,** *262* (21), 10140.

(69) Clarke, B. J.; Côté, H. C.; Cool, D. E.; Clark-Lewis, I.; Saito, H.; Pixley, R. A.; Colman, R. W.; MacGillivray, R. T. Mapping of a putative surface-binding site of human coagulation factor XII. *Journal of Biological Chemistry* **1989,** *264* (19), 11497.

(70) Samuel, M.; Samuel, E.; Villanueva, G. B. Histidine residues are essential for the surface binding and autoactivation of human coagulation factor XII. *Biochemical and Biophysical Research Communications* **1993,** *191* (1), 110.

(71) Citarella, F.; Ravon, D. M.; Pascucci, B.; Felici, A.; Fantoni, A.; Hack, C. E. Structure/function analysis of human factor XII using recombinant deletion mutants. Evidence for an additional region involved in the binding to negatively charged surfaces. *European Journal Biochemistry* **1996,** *238* (1), 240.

(72) Citarella, F.; Fedele, G.; Roem, D.; Fantoni, A.; Hack, C. E. The second exon-encoded factor XII region is involved in the interaction of factor XII with factor XI and does not contribute to the binding site for negatively charged surfaces. *Blood* **1998,** *92* (11), 4198.

(73) La Rusch, G. A.; Mahdi, F.; Shariat-Madar, Z.; Adams, G.; Sitrin, R. G.; Zhang, W. M.; McCrae, K. R.; Schmaier, A. H. Factor XII stimulates ERK1/2 and Akt through uPAR, integrins, and the EGFR to initiate angiogenesis. *Blood* **2010,** *115* (24), 5111.

(74) Maas, C.; Schiks, B.; Strangi, R. D.; Hackeng, T. M.; Bouma, B. N.; Gebbink, M. F. B. G.; Bouma, B. Identification of fibronectin type I domains as amyloid-binding modules on tissue-type plasminogen activator and three homologs. *Amyloid* **2008,** *15* (3), 166.

(75) Chen, Z.-L.; Singh, P.; Norris, E. H.; Strickland, S.; Revenko, A. S.; MacLeod, A. R. Depletion of coagulation factor XII ameliorates brain pathology and cognitive impairment in Alzheimer disease mice. *Blood* **2017,** *129* (18), 2547.

(76) Selkoe, D. J.; Hardy, J. The amyloid hypothesis of Alzheimer's disease at 25 years. *European Molecular Biology Organization molecular medicine* **2016,** *8* (6), 595.

(77) Musiek, E. S.; Holtzman, D. M. Three dimensions of the amyloid hypothesis: time, space and'wingmen'. *Nature neuroscience* **2015**, 800.

(78) Konings, J.; Govers-Riemslag, J. W.; Philippou, H.; Mutch, N. J.; Borissoff, J. I.; Allan, P.; Mohan, S.; Tans, G.; Ten Cate, H.; Ariens, R. A. Factor XIIa regulates the structure of the fibrin clot independently of thrombin generation through direct interaction with fibrin. *Blood* **2011,** *118* (14), 3942.

(79) Johne, J.; Blume, C.; Benz, P. M.; Pozgajová, M.; Ullrich, M.; Schuh, K.; Nieswandt, B.; Walter, U.; Renné, T. Platelets promote coagulation factor XII-mediated proteolytic cascade systems in plasma. journal of *Biolological Chemistry* **2006,** *387* (2), 173.

(80) Mahdi, F.; Madar, Z. S.; Figueroa, C. D.; Schmaier, A. H. Factor XII interacts with the multiprotein assembly of urokinase plasminogen activator receptor, gC1qR, and cytokeratin 1 on endothelial cell membranes. *Blood* **2002,** *99* (10), 3585.

(81) Henderson, L. M.; Figueroa, C. D.; Muller-Esterl, W.; Bhoola, K. D. Assembly of contact-phase factors on the surface of the human neutrophil membrane. *Blood* **1994,** *84* (2), 474.

(82) Bernardo, M. M.; Day, D. E.; Olson, S. T.; Shore, J. D. Surface-independent acceleration of factor XII activation by zinc ions. I. Kinetic characterization of the metal ion rate enhancement. *Journal of Biolological Chemistry* **1993,** *268* (17), 12468.

(83) Rojkaer, R.; Schousboe, I. Partial identification of the Zn2+-binding sites in factor XII and its activation derivatives. *European journal of biochemistry/ Federation of European Biochemical Societies* **1997,** *247* (2), 491.

(84) Cochrane, C. G.; Revak, S. D.; Wuepper, K. D. Activation of Hageman factor in solid and fluid phases. A critical role of kallikrein. *Journal of Experimental Medicine* **1973,** *138* (6), 1564.

(85) Cohen, S. Epidermal growth factor. *In vitro cellular & developmental biology : journal of the Tissue Culture Association* **1987,** *23* (4), 239.

(86) Guntinas-Lichius, O.; Wittekindt, C. The role of growth factors for disease and therapy in diseases of the head and neck. *DNA and Cell Biolology* **2003,** *22* (9), 593.

(87) Carpenter, G.; Cohen, S. Epidermal growth factor. *Journal of Biolological Chemistry* **1990,** *265* (14), 7709.

(88) Harris, R. C.; Chung, E.; Coffey, R. J. EGF receptor ligands. *Experimental Cell Research* **2003,** *284* (1), 2.

(89) Campbell, I. D.; Bork, P. Epidermal growth factor-like modules. *Current Opinion in Structural Biology* **1993,** *3* (3), 385.

(90) Stenflo, J. Structure-function relationships of epidermal growth factor modules in vitamin K-dependent clotting factors. *Blood* **1991,** *78* (7), 1637.

(91) Ploug, M.; Roenne, E.; Behrendt, N.; Jensen, A. L.; Blasi, F.; Danoe, K. Cellular receptor for urokinase plasminogen activator. Carboxyl-terminal processing and membrane anchoring by glycosyl-phosphatidylinositol. *Journal of Biological Chemistry* **1991,** *266* (3), 1926.

(92) Thielens, N. M.; Aude, C. A.; Lacroix, M. B.; Gagnon, J.; Arlaud, G. J. Ca2+ binding properties and Ca2(+)-dependent interactions of the isolated NH2-terminal alpha fragments of human complement proteases C1-r and C1-s. *Journal of Biological Chemistry* **1990,** *265* (24), 14469.

(93) Hertzberg, M. S.; Ben-Tal, O.; Furie, B.; Furie, B. C. Construction, expression, and characterization of a chimera of Factor IX and Factor X. The role of the second epidermal growth factor domain and serine protease domain in Factor Va binding. *Journal of Biological Chemistry* **1992,** *267* (21), 14759.

(94) Skogen, W. F.; Esmon, C. T.; Cox, A. C. Comparison of coagulation factor Xa and des-(1-44)factor Xa in the assembly of prothrombinase. *Journal of Biological Chemistry* **1984,** *259* (4), 2306.

(95) Wong, M. Y.; Gurr, J. A.; Walsh, P. N. The second epidermal growth factor-like domain of human factor IXa mediates factor IXa binding to platelets and assembly of the factor X activating complex. *Biochemistry* **1999,** *38* (28), 8948.

(96) LaRusch, G. A.; Mahdi, F.; Shariat-Madar, Z.; Adams, G.; Sitrin, R. G.; Zhang, W. M.; McCrae, K. R.; Schmaier, A. H. Factor XII stimulates ERK1/2 and Akt through uPAR, integrins, and the EGFR to initiate angiogenesis. *Blood* **2010,** *115* (24), 5111.

(97) Schmeidler-Sapiro, K. T.; Ratnoff, O. D.; Gordon, E. M. Mitogenic effects of coagulation factor XII and factor XIIa on HepG2 cells. *Proceedings of the National Academy of Sciences of the United States of America* **1991,** *88* (10), 4382.

(98) Gordon, E. M.; Venkatesan, N.; Salazar, R.; Tang, H.; Schmeidler-Sapiro, K.; Buckley, S.; Warburton, D.; Hall, F. L. Factor XII-induced mitogenesis is mediated via a distinct signal transduction pathway that activates a mitogen-

activated protein kinase. *Proceedings of the National Academy of Sciences of the United States of America* **1996,** *93* (5), 2174.

(99) Beringer, D. X.; Kroon-Batenburg, L. M. The structure of the FnI-EGF-like tandem domain of coagulation factor XII solved using SIRAS. *Acta Crystallographica Section F: Structural Biology Communications* **2013,** *69* (Pt 2), 94.

(100) Schousboe, I.; Halkier, T. Zinc ions promote the binding of factor XII/factor XIIA to acidic phospholipids but have no effect on the binding of high-Mr kininogen. *European Journal of Biochemistry* **1991,** *197* (2), 309.

(101) Shore, J. D.; Day, D. E.; Bock, P. E.; Olson, S. T. Acceleration of surface-dependent autocatalytic activation of blood coagulation factor XII by divalent metal ions. *Biochemistry* **1987,** *26* (8), 2250.

(102) Castellino, F. J.; Beals, J. M. The genetic relationships between the kringle domains of human plasminogen, prothrombin, tissue plasminogen activator, urokinase, and coagulation factor XII. Journal of Molecular Evolution **1987,** *26* (4), 358.

(103) Ikeo, K.; Takahashi, K.; Gojobori, T. Different evolutionary histories of kringle and protease domains in serine proteases: a typical example of domain evolution. *Journal of Molecular Evolution* **1995,** *40* (3), 331.

(104) Magnusson, S.; Sottrup-Jensen L.; PetersenT. E.; Dudek-Wojciechowska, G.; Claeys, H. In *Proteolysis and physiological regulation*; Robbins, D. W.; Brew, K., Eds.; Academic Press: New York, 1976.

(105) Shim, B.-S.; Kang, B.-H.; Hong, Y.-K.; Kim, H.-K.; Lee, I.-H.; Lee, S.-Y.; Lee, Y.-J.; Lee, S.-K.; Joe, Y. A. The kringle domain of tissue-type plasminogen activator inhibits in vivo tumor growth. *Biochemical and Biophysical Research Communications* **2005,** *327* (4), 1155.

(106) Pennica, D.; Holmes, W. E.; Kohr, W. J.; Harkins, R. N.; Vehar, G. A.; Ward, C. A.; Bennett, W. F.; Yelverton, E.; Seeburg, P. H.; et al. Cloning and expression of human tissue-type plasminogen activator cDNA in E. coli. *Nature (London)* **1983,** *301* (5897), 214.

(107) Guenzler, W. A.; Steffens, G. J.; Oetting, F.; Kim, S. M. A.; Frankus, E.; Flohe, L. The primary structure of high molecular mass urokinase from human urine. The complete amino acid sequence of the A chain. *Hoppe-Seyler's Zeitschrift Fur Physiologische Chemie* **1982,** *363* (10), 1155.

(108) Pozzi, N.; Chen, Z.; Gohara, D. W.; Niu, W.; Heyduk, T.; Di Cera, E. Crystal Structure of Prothrombin Reveals Conformational Flexibility and Mechanism of Activation. *Journal of Biological Chemistry* **2013,** *288* (31), 22734.

(109) Cao, Y.; Cao, R.; Veitonmaki, N. Kringle structures and antiangiogenesis. *Current Medicinal Chemistry - Anti-Cancer Agents* **2002,** *2* (6), 667.

(110) Lucas, M. A.; Fretto, L. J.; McKee, P. A. The binding of human plasminogen to fibrin and fibrinogen. *Journal of Biological Chemistry* **1983,** *258* (7), 4249.

(111) Slaughter, T. F.; Greenberg, C. S. Antifibrinolytic drugs and perioperative hemostasis. *American journal of hematology* **1997,** *56* (1), 32.

(112) Stephens, R. W.; Bokman, A. M.; Myohanen, H. T.; Reisberg, T.; Tapiovaara, H.; Pedersen, N.; Grondahl-Hansen, J.; Llinas, M.; Vaheri, A. Heparin binding to the urokinase kringle domain. *Biochemistry* **1992,** *31* (33), 7572.

(113) Ravon, D. M.; Citarella, F.; Lubbers, Y. T.; Pascucci, B.; Hack, C. E. Monoclonal antibody F1 binds to the kringle domain of factor XII and induces enhanced susceptibility for cleavage by kallikrein. *Blood* **1995,** *86* (11), 4134.

(114) Cool, D. E.; Edgell, C. J. S.; Louie, G. V.; Zolle, M. J.; Brayer, G. D.; MacGillivray, R. T. A. Characterization of human blood coagulation factor XII cDNA. Prediction of the primary structure of factor XII and the tertiary structure of β-factor XIIa. *Journal of Biological Chemistry* **1985,** *260* (25), 13666.

(115) Williamson, M. P. The structure and function of proline-rich regions in proteins. *Biochemistry* **1994,** *297* (2), 249.

(116) Jackson, C. M.; Nemerson, Y. Blood coagulation. *Annual Review of Biochemistry* **1980,** *49*, 765.

(117) Cool, D. E.; Edgell, C. J.; Louie, G. V.; Zoller, M. J.; Brayer, G. D.; MacGillivray, R. T. Characterization of human blood coagulation factor XII cDNA. Prediction of the primary structure of factor XII and the tertiary structure of beta-factor XIIa. Journal of Biological Chemistry **1985,** *260* (25), 13666.

(118) McMullen, B. A.; Fujikawa, K. Amino acid sequence of the heavy chain of human alpha-factor XIIa (activated Hageman factor). *Journal of Biological Chemistry* **1985,** *260* (9), 5328.

(119) Fujikawa, K.; McMullen, B. A. Amino acid sequence of human β-factor XIIa. *Journal of Biological Chemistry* **1983,** *258* (18), 10924.

(120) Key, N. S. Epidemiologic and clinical data linking factors XI and XII to thrombosis. *ASH Education Program Book* **2014,** *2014* (1), 66.

(121) van Montfoort, M. L.; Meijers, J. C. Recent insights into the role of the contact pathway in thrombo-inflammatory disorders. *ASH Education Program Book* **2014,** *2014* (1), 60.

(122) Gailani, D.; Bane, C. E.; Gruber, A. Factor XI and contact activation as targets for antithrombotic therapy. *Journal of Thrombosis and Haemostasis* **2015,** *13* (8), 1383.

(123) Wendel, H. P.; Jones, D. W.; Gallimore, M. J. FXII levels, FXIIa-like activities and kallikrein activities in normal subjects and patients undergoing cardiac surgery. *Immunopharmacology* **1999,** *45* (1), 141.

(124) Plötz, F.; Van Oeveren, W.; Bartlett, R.; Wildevuur, C. Blood activation during neonatal extracorporeal life support. *The Journal of thoracic and cardiovascular surgery* **1993,** *105* (5), 823.

(125) Larsson, M.; Rayzman, V.; Nolte, M. W.; Nickel, K. F.; Bjorkqvist, J.; Jamsa, A.; Hardy, M. P.; Fries, M.; Schmidbauer, S.; Hedenqvist, P.et al. A factor XIIa inhibitory antibody provides thromboprotection in extracorporeal circulation without increasing bleeding risk. *Science Translational Medicine* **2014,** *6* (222), 222ra17.

(126) Yau, J. W.; Liao, P.; Fredenburgh, J. C.; Stafford, A. R.; Revenko, A. S.; Monia, B. P.; Weitz, J. I. Selective depletion of factor XI or factor XII with antisense oligonucleotides attenuates catheter thrombosis in rabbits. *Blood* **2014,** *123* (13), 2102.

(127) Jaffer, I.; Fredenburgh, J.; Hirsh, J.; Weitz, J. Medical device-induced thrombosis: what causes it and how can we prevent it?. *Journal of Thrombosis and Haemostasis* **2015,** *13* (S1), S72.

(128) Cheng, Q.; Tucker, E. I.; Pine, M. S.; Sisler, I.; Matafonov, A.; Sun, M. F.; White-Adams, T. C.; Smith, S. A.; Hanson, S. R.; McCarty, O. J.et al. A role for factor XIIa-mediated factor XI activation in thrombus formation in vivo. *Blood* **2010,** *116* (19), 3981.

(129) Matafonov, A.; Leung, P. Y.; Gailani, A. E.; Grach, S. L.; Puy, C.; Cheng, Q.; Sun, M. F.; McCarty, O. J.; Tucker, E. I.; Kataoka, H.et al. Factor XII inhibition reduces thrombus formation in a primate thrombosis model. *Blood* **2014**, 123 (11), 1739.

(130) Samuel, M.; Pixley, R. A.; Villanueva, M. A.; Colman, R. W.; Villanueva, G. B. Human factor XII (Hageman factor) autoactivation by dextran sulfate. Circular dichroism, fluorescence, and ultraviolet difference spectroscopic studies. *Journal of Biological Chemistry* **1992,** *267* (27), 19691.

(131) Long, A. T.; Kenne, E.; Jung, R.; Fuchs, T. A.; Renné, T. Contact system revisited: an interface between inflammation, coagulation, and innate immunity. *Journal of Thrombosis and Haemostasis* **2016**.

(132) Griffin, J. H. Role of surface in surface-dependent activation of Hageman factor (blood coagulation factor XII). *Proceedings of the National Academy of Sciences of the United States of America* **1978,** *75* (4), 1998.

(133) Maas, C.; Oschatz, C.; Renne, T. The plasma contact system 2.0. *Seminars in Thrombosis and Hemostasis* **2011,** *37* (4), 375.

(134) Müller, F.; Renné, T. Novel roles for factor XII-driven plasma contact activation system. *Current Opinion in Hematology* **2008,** *15* (5), 516.

(135) Bjoerkqvist, J.; Sala-Cunill, A.; Renne, T. Hereditary angioedema: a bradykinin-mediated swelling disorder. *Thrombosis and Haemostasis* **2013,** *109* (3), 368.

(136) Dunn, J. T.; Silverberg, M.; Kaplan, A. P. The cleavage and formation of activated human Hageman factor by autodigestion and by kallikrein. *The Journal of biological chemistry* **1982,** *257* (4), 1779.

(137) Ogiwara, K.; Nogami, K.; Nishiya, K.; Shima, M. Plasmin-induced procoagulant effects in the blood coagulation: a crucial role of coagulation factors V and VIII. *Blood Coagulation Fibrinolysis* **2010,** *21* (6), 568.

(138) Revak, S. D.; Cochrane, C. G.; Griffin, J. H. The binding and cleavage characteristics of human Hageman factor during contact activation. A comparison of normal plasma with plasmas deficient in factor XI, prekallikrein, or high molecular weight kininogen. *The Journal of clinical investigation* **1977,** *59* (6), 1167.

(139) Fujikawa, K.; McMullen, B. A. Amino acid sequence of human beta-factor XIIa. *The Journal of biological chemistry* **1983,** *258* (18), 10924.

(140) Kirby, E. P.; McDevitt, P. J. The binding of bovine factor XII to kaolin. *Blood* **1983,** *61* (4), 652.

(141) Bock, P. E.; Srinivasan, K. R.; Shore, J. D. Activation of intrinsic blood coagulation by ellagic acid: insoluble ellagic acid-metal ion complexes are the activating species. *Biochemistry* **1981,** *20* (25), 7258.

(142) Tans, G.; Griffin, J. H. Properties of sulfatides in factor-XII-dependent contact activation. *Blood* **1982,** *59* (1), 69.

(143) Morrison, D. C.; Cochrane, C. G. Direct evidence for Hageman factor (factor XII) activation by bacterial lipopolysaccharides (endotoxins). *Journal of Experimental Medicine* **1974,** *140* (3), 797.

(144) Fujikawa, K.; Heimark, R. L.; Kurachi, K.; Davie, E. W. Activation of bovine factor XII (Hageman factor) by plasma kallikrein. *Biochemistry* **1980,** *19* (7), 1322.

(145) Wiggins, R. C.; Cochrane, C. G. Hageman factor and the contact activation system. *Handbook of Inflammation* **1979,** *1* (Chem. Messengers Inflammatory Process), 179.

(146) Josh Yeh, C. H.; Dimachkie, Z. O.; Golas, A.; Cheng, A.; Parhi, P.; Vogler, E. A. Contact activation of blood plasma and factor XII by ion-exchange resins. *Biomaterials* **2012,** *33* (1), 9.

(147) Walsh, P. N.; Griffin, J. H. Contributions of human platelets to the proteolytic activation of blood coagulation factors XII and XI. *Blood* **1980,** *57* (1), 106.

(148) Muller, F.; Mutch, N. J.; Schenk, W. A.; Smith, S. A.; Esterl, L.; Spronk, H. M.; Schmidbauer, S.; Gahl, W. A.; Morrissey, J. H.; Renne, T. Platelet polyphosphates are proinflammatory and procoagulant mediators in vivo. *Cell* **2009,** *139* (6), 1143.

(149) van der Meijden, P. E. J.; Heemskerk, J. W. M. Polyphosphates: a link between platelet activation, intrinsic coagulation and inflammation? *Expert Review of Hematology* **2010,** *3* (3), 269.

(150) Smith, S. A.; Choi, S. H.; Davis-Harrison, R.; Huyck, J.; Boettcher, J.; Rienstra, C. M.; Morrissey, J. H. Polyphosphate exerts differential effects on blood clotting, depending on polymer size. *Blood* **2010,** *116* (20), 4353.

(151) Walsh, P.; Griffin, J. Contributions of human platelets to the proteolytic activation of blood. *Blood* **1981,** *57* (1).

(152) Ruiz, F. A.; Lea, C. R.; Oldfield, E.; Docampo, R. Human platelet dense granules contain polyphosphate and are similar to acidocalcisomes of

bacteria and unicellular eukaryotes. *Journal of Biological Chemistry* **2004,** *279* (43), 44250.

(153) Mackman, N.; Gruber, A. Platelet polyphosphate: an endogenous activator of coagulation factor XII. *Journal of Thrombosis and Haemostasis* **2010,** *8* (5), 865.

(154) Smith, S. A.; Morrissey, J. H. Polyphosphate enhances fibrin clot structure. *Blood* **2008,** *112* (7), 2810.

(155) Smith, S. A.; Mutch, N. J.; Baskar, D.; Rohloff, P.; Docampo, R.; Morrissey, J. H. Polyphosphate modulates blood coagulation and fibrinolysis. *Proceedings of the National Academy of Sciences of the United States of America* **2006,** *103* (4), 903.

(156) Faxälv, L.; Boknäs, N.; Ström, J. O.; Tengvall, P.; Theodorsson, E.; Ramström, S.; Lindahl, T. L. Putting polyphosphates to the test: evidence against platelet-induced activation of factor XII. *Blood* **2013,** *122* (23), 3818.

(157) Labberton, L.; Kenne, E.; Long, A. T.; Nickel, K. F.; Di Gennaro, A.; Rigg, R. A.; Hernandez, J. S.; Butler, L.; Maas, C.; Stavrou, E. X. Neutralizing blood-borne polyphosphate in vivo provides safe thromboprotection. *Nature Communications* **2016,** *7*.

(158) Maas, C.; Govers-Riemslag, J. W.; Bouma, B.; Schiks, B.; Hazenberg, B. P.; Lokhorst, H. M.; Hammarström, P.; ten Cate, H.; de Groot, P. G.; Bouma, B. N.et al. Misfolded proteins activate factor XII in humans, leading to kallikrein formation without initiating coagulation. *Journal of Clinical Investigation* **2008,** *118* (9), 3208.

(159) von Bruehl, M.-L.; Stark, K.; Steinhart, A.; Chandraratne, S.; Konrad, I.; Lorenz, M.; Khandoga, A.; Tirniceriu, A.; Coletti, R.; Koellnberger, M.et al. Monocytes, neutrophils, and platelets cooperate to initiate and propagate venous thrombosis in mice in vivo. *Journal of Experimental Medicine* **2012,** *209* (4), 819.

(160) Fuchs, T. A.; Brill, A.; Duerschmied, D.; Schatzberg, D.; Monestier, M.; Myers, D. D.; Wrobleski, S. K.; Wakefield, T. W.; Hartwig, J. H.; Wagner, D. D. Extracellular DNA traps promote thrombosis. *Proceedings of the National Academy of Sciences* **2010,** *107* (36), 15880.

(161) Sanchez, J.; Elgue, G.; Larsson, R.; Nilsson, B.; Olsson, P. Surface-adsorbed fibrinogen and fibrin may activate the contact activation system. *Thrombosis Research* **2008,** *122* (2), 257.

(162) Mann, K. G.; Butenas, S.; Brummel, K. The Dynamics of Thrombin Formation. *Arteriosclerosis, Thrombosis, and Vascular Biology* **2003,** *23* (1), 17.

(163) Pauer, H. U.; Renné, T.; Hemmerlein, B.; Legler, T.; Fritzlar, S.; Adham, I.; Müller-Esterl, W.; Emons, G.; Sancken, U.; Engel, W.et al. Targeted deletion of murine coagulation factor XII gene-a model for contact phase activation in vivo. *Thrombosis and Haemostasis* **2004,** *92* (3), 503.

(164) Renne, T.; Pozgajova, M.; Gruner, S.; Schuh, K.; Pauer, H. U.; Burfeind, P.; Gailani, D.; Nieswandt, B. Defective thrombus formation in mice lacking coag andulation factor XII. *Journal of Experimental Medicine* **2005,** *202* (2), 271.

(165) Cheng, Q.; Tucker, E. I.; Pine, M. S.; Matafonov, A.; Sun, M.-f.; White-Adams, T. C.; Smith, S. A.; Hanson, S. R.; McCarty, O. J.; Renné, T. A role for factor XIIa–mediated factor XI activation in thrombus formation in vivo. *Blood* **2010,** *116* (19), 3981.

(166) Decrem, Y.; Rath, G.; Blasioli, V.; Cauchie, P.; Robert, S.; Beaufays, J.; Frere, J. M.; Feron, O.; Dogne, J. M.; Dessy, C.et al. Ir-CPI, a coagulation contact phase inhibitor from the tick Ixodes ricinus, inhibits thrombus formation without impairing hemostasis. *Journal of Experimental Medicine* **2009,** *206* (11), 2381.

(167) Andrews, R. K.; Berndt, M. C. Platelet physiology and thrombosis. *Thrombosis Research* **2004,** *114* (5-6), 447.

(168) Berndt, M. C.; Shen, Y.; Dopheide, S. M.; Gardiner, E. E.; Andrews, R. K. The vascular biology of the glycoprotein Ib-IX-V complex. *Thrombosis and Haemostasis* **2001,** *86* (1), 178.

(169) Kleinschnitz, C.; Pozgajova, M.; Pham, M.; Bendszus, M.; Nieswandt, B.; Stoll, G. Targeting platelets in acute experimental stroke: impact of glycoprotein Ib, VI, and IIb/IIIa blockade on infarct size, functional outcome, and intracranial bleeding. *Circulation* **2007,** *115* (17), 2323.

(170) Yamane, T.; Mitsumata, M.; Yamaguchi, N.; Nakazawa, T.; Mochizuki, K.; Kondo, T.; Kawasaki, T.; Murata, S.-i.; Yoshida, Y.; Katoh, R. Laminar high shear stress up-regulates type IV collagen synthesis and down-regulates

MMP-2 secretion in endothelium. A quantitative analysis. *Cell Tissue Research.* **2010,** *340* (3), 471.

(171) Siljander, P. R. M.; Munnix, I. C. A.; Smethurst, P. A.; Deckmyn, H.; Lindhout, T.; Ouwehand, W. H.; Farndale, R. W.; Heemskerk, J. W. M. Platelet receptor interplay regulates collagen-induced thrombus formation in flowing human blood. *Blood* **2004,** *103* (4), 1333.

(172) Furie, B.; Furie, B. C. Mechanisms of thrombus formation. *New England Journal of Medicine* **2008,** *359* (9), 938.

(173) Turpie, A. G. G. Advances in oral anticoagulation treatment: the safety and efficacy of rivaroxaban in the prevention and treatment of thromboembolism. *Therapeutic Advances in Hematology* **2012,** *3* (5), 309.

(174) World health orginisation In *Fact sheets*; fact sheet N 310 ed.; World Health Orginisation: www.who.int/mediacentre/factsheets/fs310/en/, July 2013; Vol. 2014.

(175) Cohen, A. T.; Agnelli, G.; Anderson, F. A.; Arcelus, J. I.; Bergqvist, D.; Brecht, J. G.; Greer, I. A.; Heit, J. A.; Hutchinson, J. L.; Kakkar, A. K.et al. Venous thromboembolism (VTE) in Europe The number of VTE events and associated morbidity and mortality. *Thrombosis and Haemostasis* **2007,** *98* (4), 756.

(176) Halbmayer, W. M.; Mannhalter, C.; Feichtinger, C.; Rubi, K.; Fischer, M. Factor XII (Hageman factor) deficiency: a risk factor for development of thromboembolism. Incidence of factor XII deficiency in patients after recurrent venous or arterial thromboembolism and myocardial infarction. *Wiener Medizinische Wochenschrift* **1993,** *143* (2), 43.

(177) Goodnough, L. T.; Saito, H.; Ratnoff, O. D. Thrombosis or myocardial infarction in congenital clotting factor abnormalities and chronic thrombocytopenias: a report of 21 patients and a review of 50 previously reported cases. *Medicine (Baltimore)* **1983,** *62* (4), 248.

(178) Girolami, A.; De Marco, L.; Dal Bo Zanon, R.; Patrassi, G.; Cappellato, M. G. Rarer quantitative and qualitative abnormalities of coagulation. *Clinical Haematology* **1985,** *14* (2), 385.

(179) Lammle, B.; Wuillemin, W. A.; Huber, I.; Krauskopf, M.; Zurcher, C.; Pflugshaupt, R.; Furlan, M. “Thromboembolism and bleeding tendency in congenital factor XII deficiency--a study on 74 subjects from 14 Swiss

families," Central Hematology Laboratory, Inselspital, University of Bern, Switzerland, **1991**.

(180) Ratnoff O. D.; Busse R. J.; Shean R. P. The demise of John Hageman. The New England Journal of Medicine **1968**; 279, 760.

(181) Girolami, A.; Randi, M. L.; Gavasso, S.; Lombardi, A. M.; Spiezia, F. The Occasional Venous Thromboses Seen in Patients with Severe (Homozygous) FXII Deficiency are Probably Due to Associated Risk Factors: A Study of Prevalence in 21 Patients and Review of the Literature. *Journal of Thrombosis and Thrombolysis* **2004,** *17* (2), 139.

(182) Girolami, A.; Morello, M.; Girolami, B.; Lombardi, A. M.; Bertolo, C. Myocardial infarction and arterial thrombosis in severe (homozygous) FXII deficiency: no apparent causative relation. *Clinical and Applied Thrombosis/Hemostasis* **2005,** *11* (1), 49.

(183) Koster, T.; Rosendaal, F. R.; Briet, E.; Vandenbroucke, J. P. John Hageman's factor and deep-vein thrombosis: Leiden thrombophilia Study. *British journal of haematology* **1994,** *87* (2), 422.

(184) von Känel, R.; Wuillemin, W. A.; Furlan, M.; Lämmle, B. Factor XII clotting activity and antigen levels in patients with thromboembolic disease. *Blood Coagulation & Fibrinolysis* **1992,** *3* (5), 555.

(185) Gordon, E. M.; Donaldson, V. H.; Saito, H.; Su, E.; Ratnoff, O. D. Reduced titers of Hageman factor (factor XII) in Orientals. *Annals of Internal Medicine* **1981,** *95* (6), 697.

(186) Heit John, A. The epidemiology of venous thromboembolism in the community. *Arteriosclerosis, Thrombosis, and Vascular Biology* **2008,** *28* (3), 370.

(187) Doggen, C. J.; Rosendaal, F. R.; Meijers, J. C. Levels of intrinsic coagulation factors and the risk of myocardial infarction among men: Opposite and synergistic effects of factors XI and XII. *Blood* **2006,** *108* (13), 4045.

(188) Endler, G.; Marsik, C.; Jilma, B.; Schickbauer, T.; Quehenberger, P.; Mannhalter, C. Evidence of a U-shaped association between factor XII activity and overall survival. *Journal of Thrombosis and Haemostasis* **2007,** *5* (6), 1143.

(189) Zito, F.; Drummond, F.; Bujac, S. R.; Esnouf, M. P.; Morrissey, J. H.; Humphries, S. E.; Miller, G. J. Epidemiological and genetic associations of

activated factor XII concentration with factor VII activity, fibrinopeptide A concentration, and risk of coronary heart disease in men. *Circulation* **2000,** *102* (17), 2058.

(190) Grundt, H.; Nilsen, D. W. T.; Hetland, O.; Valente, E.; Fagertun, H. E. Activated factor 12 (FXIIa) predicts recurrent coronary events after an acute myocardial infarction. American Heart Journal **2004,** *147* (2), 260.

(191) Ferrero-Miliani, L.; Nielsen, O.; Andersen, P.; Girardin, S. Chronic inflammation: importance of NOD2 and NALP3 in interleukin-1β generation. *Clinical & Experimental Immunology* **2007,** *147* (2), 227.

(192) Libby, P.; Ridker, P. M.; Maseri, A. Inflammation and atherosclerosis. *Circulation* **2002,** *105* (9), 1135.

(193) Coussens, L. M.; Werb, Z. Inflammation and cancer. *Nature* **2002,** *420* (6917), 860.

(194) Hotamisligil, G. S. Inflammation and metabolic disorders. *Nature* **2006,** *444* (7121), 860.

(195) Wellen, K. E.; Hotamisligil, G. S. Inflammation, stress, and diabetes. *The Journal of clinical investigation* **2005,** *115* (5), 1111.

(196) Golias, C.; Charalabopoulos, A.; Stagikas, D.; Charalabopoulos, K.; Batistatou, A. The kinin system—bradykinin: biological effects and clinical implications. Multiple role of the kinin system—bradykinin. *Hippokratia* **2007,** *11* (3), 124.

(197) Kaplan, A. P.; Joseph, K.; Silverberg, M. Pathways for bradykinin formation and inflammatory disease. *Journal of Allergy and Clinical Immunology* **2002,** *109* (2), 195.

(198) Nickel, K. F.; Long, A. T.; Fuchs, T. A.; Butler, L. M.; Renne, T. Factor XII as a Therapeutic Target in Thromboembolic and Inflammatory Diseases. *Arteriosclerosis, Thrombosis, and Vascular Biology* **2017,** *37* (1), 13.

(199) Zamolodchikov, D.; Chen, Z.-L.; Conti, B. A.; Renné, T.; Strickland, S. Activation of the factor XII-driven contact system in Alzheimer's disease patient and mouse model plasma. *Proceedings of the National Academy of Sciences* **2015,** *112* (13), 4068.

(200) Chan, A. K.; Paredes, N. The coagulation system in humans. *Haemostasis: Methods and Protocols* **2013**, 3.

(201) Mackman, N. Triggers, targets and treatments for thrombosis. *Nature* **2008,** *451* (7181), 914.

(202) Whitaker, I. S.; Rao, J.; Izadi, D.; Butler, P. Historical Article: Hirudo medicinalis: ancient origins of, and trends in the use of medicinal leeches throughout history. *British Journal of Oral and Maxillofacial Surgery* **2004,** *42* (2), 133.

(203) Gomez-Outes, A.; Luisa Suarez-Gea, M.; Calvo-Rojas, G.; Lecumberri, R.; Rocha, E.; Pozo-Hernández, C.; Isabel Terleira-Fernandez, A.; Vargas-Castrillón, E. Discovery of anticoagulant drugs: a historical perspective. *Current drug discovery technologies* **2012,** *9* (2), 83.

(204) Wardrop, D.; Keeling, D. The story of the discovery of heparin and warfarin. *British journal of haematology* **2008,** *141* (6), 757.

(205) Hommes, D. W.; Bura, A.; Mazzolai, L.; Büller, H. R.; Jan, W. Subcutaneous heparin compared with continuous intravenous heparin administration in the initial treatment of deep vein thrombosis: a meta-analysis. *Annals of internal medicine* **1992,** *116* (4), 279.

(206) Capila, I.; Linhardt, R. J. Heparin–protein interactions. *Angewandte Chemie International Edition* **2002,** *41* (3), 390.

(207) Lever, R.; Page, C. P. Novel drug development opportunities for heparin. *Nature Reviews Drug Discovery* **2002,** *1* (2), 140.

(208) Hirsh, J. Heparin. *New England Journal of Medicine* **1991,** *324* (22), 1565.

(209) Kumar, R.; Beguin, S.; Hemker, H. C. The effect of fibrin clots and clot-bound thrombin on the development of platelet procoagulant activity. *Thrombosis and haemostasis* **1995,** *74* (3), 962.

(210) Teitel, J. M.; Rosenberg, R. D. Protection of factor Xa from neutralization by the heparin-antithrombin complex. *Journal of Clinical Investigation* **1983,** *71* (5), 1383.

(211) Pieters, J.; Willems, G.; Hemker, H. C.; Lindhout, T. Inhibition of factor IXa and factor Xa by antithrombin III/heparin during factor X activation. *Journal of biological chemistry* **1988,** *263* (30), 15313.

(212) Weitz, J. I.; Crowther, M. Direct thrombin inhibitors. *Thrombosis research* **2002,** *106* (3), V275.

(213) Bates, S. M.; Weitz, J. I. Direct thrombin inhibitors for treatment of arterial thrombosis: potential differences between bivalirudin and hirudin. *The American journal of cardiology* **1998,** *82* (8), 12P.

(214) Ramacciotti, E.; Clark, M.; Sadeghi, N.; Hoppensteadt, D.; Thethi, I.; Gomes, M.; Fareed, J. Contaminants in heparin: review of the literature, molecular profiling, and clinical implications. *Clinical and Applied Thrombosis/ Hemostasis* **2011,** *17* (2), 126.

(215) Greinacher, A.; Pötzsch, B.; Amiral, J.; Dummel, V.; Eichner, A.; Mueller-Eckhardt, C. Heparin-associated thrombocytopenia: isolation of the antibody and characterization of a multimolecular PF4-heparin complex as the major antigen. *Thrombosis and haemostasis* **1994,** *71* (2), 247.

(216) O'Brien, P. J.; Mureebe, L. Direct thrombin inhibitors. *Journal of cardiovascular pharmacology and therapeutics* **2012,** *17* (1), 5.

(217) Ansell, J.; Hirsh, J.; Poller, L.; Bussey, H.; Jacobson, A.; Hylek, E. The pharmacology and management of the vitamin K antagonists: the seventh ACCP conference on antithrombotic and thrombolytic therapy. *Chest* **2004,** *126* (3, Suppl.), 204S.

(218) Becker, R. C.; Meade, T. W.; Berger, P. B.; Ezekowitz, M.; O'Connor, C. M.; Vorchheimer, D. A.; Guyatt, G. H.; Mark, D. B.; Harrington, R. A. The primary and secondary prevention of coronary artery disease: American College of Chest Physicians evidence-based clinical practice guidelines (8th edition). *Chest* **2008,** *133* (6, Suppl.), 776S.

(219) Ansell, J.; Hirsh, J.; Hylek, E.; Jacobson, A.; Crowther, M.; Palareti, G. Pharmacology and management of the vitamin K antagonists: American College of Chest Physicians evidence-based clinical practice guidelines. *Chest Journal* **2008,** *133* (6_suppl), 160S.

(220) Mehta, A. Y.; Jin, Y.; Desai, U. R. An update on recent patents on thrombin inhibitors (2010–2013). *Expert opinion on therapeutic patents* **2014,** *24* (1), 47.

(221) Kola, I.; Landis, J. Can the pharmaceutical industry reduce attrition rates?. *Nature reviews Drug discovery* **2004,** *3* (8), 711.

(222) Pope, A. J. In *Chemical Biology: Approaches to drug discovery and development to targeting disease.*; Civjan, N., Ed.; John Wiley & Sons, Inc.: New Jersey, **2012**.

(223) Walker, B.; Lynas, J. Strategies for the inhibition of serine proteases. *Cellular and Molecular Life Sciences* **2001,** *58* (4), 596.

(224) Ansell, J. Factor Xa or thrombin: is factor Xa a better target?. *Journal of Thrombosis and Haemostasis* **2007,** *5* (s1), 60.

(225) Maraganore, J.; Bourdon, P.; Jablonski, J.; Ramachandran, K.; Fenton, J. d. Design and characterization of hirulogs: a novel class of bivalent peptide inhibitors of thrombin. *Biochemistry* **1990,** *29* (30), 7095.

(226) Stürzebecher, J.; Markwardt, F.; Voigt, B.; Wagner, G.; Walsmann, P. Cyclic amides of Nα-arylsulfonylaminoacylated 4-amidinophenylalanine-tight binding inhibitors of thrombin. *Thrombosis research* **1983,** *29* (6), 635.

(227) Kikumoto, R.; Tamao, Y.; Tezuka, T.; Tonomura, S.; Hara, H.; Ninomiya, K.; Hijikata, A.; Okamoto, S. Selective inhibition of thrombin by (2R, 4R)-4-methyl-1-[N2-[1, 2, 3, 4-tetrahydro-8-quinolinyl) sulfonyl]-L-arginyl]-2-piperidinecarboxylic acid. *Biochemistry* **1984,** *23* (1), 85.

(228) Lee, W. M.; Larrey, D.; Olsson, R.; Lewis, J. H.; Keisu, M.; Auclert, L.; Sheth, S. Hepatic findings in long-term clinical trials of ximelagatran. *Drug Safety* **2005,** *28* (4), 351.

(229) Wei, Y.-y.; Tang, R.-b. Progress in anticoagulant therapy with dabigatran for atrial fibrillation. *Shiyong Yixue Zazhi* **2013,** *29* (5), 683.

(230) Harenberg, J.; Marx, S.; Krejczy, M.; Wehling, M. New anticoagulants, promising and failed developments. *British Journal of Pharmacology* **2012,** *165* (2), 363.

(231) Lee, C. J.; Ansell, J. E. Direct thrombin inhibitors. *British Journal of Clinical Pharmacology* **2011,** *72* (4), 581.

(232) Eikelboom, J. E.; Weitz, J. I. Dabigatran etexilate for prevention of venous thromboembolism. *Thrombosis and Haemostasis* **2009,** *101* (1), 2.

(233) Morell, J.; Sullivan, B.; Khalabuda, M.; McBride, B. F. Role of orally available antagonists of factor Xa in the treatment and prevention of thromboembolic disease: focus on rivaroxaban. *Journal of Clinical Pharmacology* **2010,** *50* (9), 986.

(234) Giebl, A.; Gurtler, K. New oral anticoagulants in perioperative medicine. *Anaesthesist* **2014,** *63* (4), 347.

(235) Cohen, A. T.; Imfeld, S.; Rider, T. Phase III Trials of New Oral Anticoagulants in the Acute Treatment and Secondary Prevention of VTE: Comparison and Critique of Study Methodology and Results. *Advances In Therapy.* **2014,** *31* (5), 473.

(236) Quinlan, D. J.; Eriksson, B. I. Novel oral anticoagulants for thromboprophylaxis after orthopaedic surgery. *Best Practice & Research Clinical Haematology* **2013,** *26* (2), 171.

(237) Broussalis, E.; Anna, W.; Trinka, E.; Mutzenbach, S.; Killer, M. Latest developments in anticoagulant drug discovery. *Drug Discovery Today* **2014**, 19 (7), 921.

(238) Chang, P. New anticoagulants for venous thromboembolic disease. *IDrugs journal* **2004,** *7* (1), 50.

(239) Acanfora, D.; Acanfora, C.; Scicchitano, P.; Longobardi, M.; Furgi, G.; Casucci, G.; Lanzillo, B.; Dentamaro, I.; Zito, A.; Incalzi, R. A. Safety and Feasibility of Treatment with Rivaroxaban for Non-Canonical Indications: A Case Series Analysis. *Clinical drug investigation* **2016,** *36* (10), 857.

(240) Lip, G. Y.; Pan, X.; Kamble, S.; Kawabata, H.; Mardekian, J.; Masseria, C.; Bruno, A.; Phatak, H. Major bleeding risk among non-valvular atrial fibrillation patients initiated on apixaban, dabigatran, rivaroxaban or warfarin: a “real-world” observational study in the United States. *International journal of clinical practice* **2016,** *70* (9), 752.

(241) Vene, N.; Mavri, A.; Gubenšek, M.; Tratar, G.; Cuderman, T. V.; Perme, M. P.; Blinc, A. Risk of Thromboembolic Events in Patients with Non-Valvular Atrial Fibrillation After Dabigatran or Rivaroxaban Discontinuation–Data from the Ljubljana Registry. *PloS one* **2016,** *11* (6), e0156943.

(242) Lu, G.; DeGuzman, F. R.; Hollenbach, S. J.; Karbarz, M. J.; Abe, K.; Lee, G.; Luan, P.; Hutchaleelaha, A.; Inagaki, M.; Conley, P. B. A specific antidote for reversal of anticoagulation by direct and indirect inhibitors of coagulation factor Xa. *Nature Medicine* **2013,** *19* (4), 446.

(243) Ansell, J. E.; Bakhru, S. H.; Laulicht, B. E.; Steiner, S. S.; Grosso, M.; Brown, K.; Dishy, V.; Noveck, R. J.; Costin, J. C. Use of PER977 to reverse the anticoagulant effect of edoxaban. *New England Journal of Medicine* **2014,** *371* (22), 2141.

(244) Pollack Jr, C. V.; Reilly, P. A.; Eikelboom, J.; Glund, S.; Verhamme, P.; Bernstein, R. A.; Dubiel, R.; Huisman, M. V.; Hylek, E. M.; Kamphuisen, P. W. Idarucizumab for dabigatran reversal. *New England Journal of Medicine* **2015,** *373* (6), 511.

(245) Burnett, A.; Siegal, D.; Crowther, M. Specific antidotes for bleeding associated with direct oral anticoagulants. *British Medical Journal (online)* **2017,** *357*.

(246) Xu, Y.; Cai, T.-Q.; Castriota, G.; Zhou, Y.; Hoos, L.; Jochnowitz, N.; Loewrigkeit, C.; Cook, J. A.; Wickham, A.; Metzger, J. M.et al. Factor XIIa inhibition by Infestin-4: in vitro mode of action and in vivo antithrombotic benefit. *Thrombosis and Haemostasis* **2014,** *111* (4), 694.

(247) Hagedorn, I.; Schmidbauer, S.; Pleines, I.; Kleinschnitz, C.; Kronthaler, U.; Stoll, G.; Dickneite, G.; Nieswandt, B. Factor XIIa inhibitor recombinant human albumin Infestin-4 abolishes occlusive arterial thrombus formation without affecting bleeding. *Circulation* **2010,** *121* (13), 1510.

(248) Woodruff, R. S.; Xu, Y.; Layzer, J.; Wu, W.; Ogletree, M. L.; Sullenger, B. A. Inhibiting the intrinsic pathway of coagulation with a factor XII-targeting RNA aptamer. *Thrombosis and Haemostasis* **2013,** *11* (7), 1364.

(249) Kleinschnitz, C.; Stoll, G.; Bendszus, M.; Schuh, K.; Pauer, H. U.; Burfeind, P.; Renne, C.; Gailani, D.; Nieswandt, B.; Renne, T. Targeting coagulation factor XII provides protection from pathological thrombosis in cerebral ischemia without interfering with hemostasis. *Journal of Experimental Medicine* **2006,** *203* (3), 513.

(250) Baeriswyl, V.; Calzavarini, S.; Chen, S.; Zorzi, A.; Bologna, L.; Angelillo-Scherrer, A.; Heinis, C. A synthetic factor XIIa inhibitor blocks selectively intrinsic coagulation initiation. *American Chemical Society chemical biology* **2015,** *10* (8), 1861.

(251) Robert, S.; Bertolla, C.; Masereel, B.; Dogne, J.-M.; Pochet, L. Novel 3-Carboxamide-coumarins as Potent and Selective FXIIa Inhibitors. *Journal of Medicinal Chemistry* **2008,** *51* (11), 3077.

(252) Bouckaert, C.; Serra, S.; Rondelet, G.; Dolušić, E.; Wouters, J.; Dogné, J.-M.; Frédérick, R.; Pochet, L. Synthesis, evaluation and structure-activity relationship of new 3-carboxamide coumarins as FXIIa inhibitors. *European journal of medicinal chemistry* **2016,** *110*, 181.

(253) Björkqvist, J.; de Maat, S.; Lewandrowski, U.; Di Gennaro, A.; Oschatz, C.; Schönig, K.; Nöthen, M. M.; Drouet, C.; Braley, H.; Nolte, M. W. Defective glycosylation of coagulation factor XII underlies hereditary angioedema type III. *The Journal of clinical investigation* **2015,** *125* (8), 3132.

(254) Frenzel, A.; Hust, M.; Schirrmann, T. Expression of recombinant antibodies. *Frontiers in immunology* **2013,** *4*, 217.

(255) Chames, P.; Van Regenmortel, M.; Weiss, E.; Baty, D. Therapeutic antibodies: successes, limitations and hopes for the future. *British journal of pharmacology* **2009,** *157* (2), 220.

(256) Campos, I. T.; Tanaka-Azevedo, A. M.; Tanaka, A. S. Identification and characterization of a novel factor XIIa inhibitor in the hematophagous insect, Triatoma infestans (Hemiptera: Reduviidae). *Federation of European Biochemical Societies letters* **2004,** *577* (3), 512.

(257) TANS, G.; JANSSEN-CLAESSEN, T.; ROSING, J.; GRIFFIN, J. H. Studies on the effect of serine protease inhibitors on activated contact factors. *European Journal of Biochemistry* **1987,** *164* (3), 637.

(258) Müller, F.; Mutch, N. J.; Schenk, W. A.; Smith, S. A.; Esterl, L.; Spronk, H. M.; Schmidbauer, S.; Gahl, W. A.; Morrissey, J. H.; Renné, T. Platelet polyphosphates are proinflammatory and procoagulant mediators in vivo. *Cell* **2009,** *139* (6), 1143.

(259) Sala-Cunill, A.; Björkqvist, J.; Senter, R.; Guilarte, M.; Cardona, V.; Labrador, M.; Nickel, K. F.; Butler, L.; Luengo, O.; Kumar, P. Plasma contact system activation drives anaphylaxis in severe mast cell–mediated allergic reactions. *Journal of Allergy and Clinical Immunology* **2015,** *135* (4), 1031.

(260) Baeriswyl, V.; Calzavarini, S.; Gerschheimer, C.; Diderich, P.; Angelillo-Scherrer, A.; Heinis, C. Development of a selective peptide macrocycle inhibitor of coagulation factor XII toward the generation of a safe antithrombotic therapy. *Journal of Medicinal Chemistry* **2013,** *56* (9), 3742.

(261) Hojima, Y.; Pierce, J. V.; Pisano, J. J. Hageman factor fragment inhibitor in corn seeds: purification and characterization. *Thrombosis Research* **1980,** *20* (2), 149.

(262) Rand, M. D.; Lock, J.; Van't Veer, C.; Gaffney, D.; Mann, K. Blood clotting in minimally altered whole blood. *Blood* **1996,** *88* (9), 3432.

(263) Krishnamoorthi, R.; Gong, Y. X.; Richardson, M. A new protein inhibitor of trypsin and activated Hageman factor from pumpkin (Cucurbita maxima) seeds. *Federation of European Biochemical Societies Letters* **1990,** *273* (1-2), 163.

(264) Frédérick, R.; Robert, S.; Charlier, C.; de Ruyck, J.; Wouters, J.; Pirotte, B.; Masereel, B.; Pochet, L. 3, 6-Disubstituted coumarins as mechanism-based inhibitors of thrombin and factor Xa. *Journal of medicinal chemistry* **2005,** *48* (24), 7592.

(265) Kraft, P.; Schwarz, T.; Pochet, L.; Stoll, G.; Kleinschnitz, C. COU254, a specific 3-carboxamide-coumarin inhibitor of coagulation factor XII, does not protect mice from acute ischemic stroke. *Experimental & Translational Stroke Medicine* **2010,** *2* (1), 5.

(266) Pathak, M.; Wilmann, P.; Awford, J.; Li, C.; Hamad, B. K.; Fischer, P. M.; Dreveny, I.; Dekker, L. V.; Emsley, J. Coagulation factor XII protease domain crystal structure. *Thrombosis and Haemostasis* **2015,** *13* (4), 580.

(267) Roehrig, S.; Straub, A.; Pohlmann, J.; Lampe, T.; Pernerstorfer, J.; Schlemmer, K.-H.; Reinemer, P.; Perzborn, E. Discovery of the Novel Antithrombotic Agent 5-Chloro-N-({(5S)-2-oxo-3- [4-(3-oxomorpholin-4-yl)phenyl]-1,3-oxazolidin-5-yl}methyl)thiophene-2-carboxamide (BAY 59-7939): An Oral, Direct Factor Xa Inhibitor. *Journal of Medicinal Chemistry* **2005,** *48* (19), 5900.

(268) Levine, M. N.; Raskob, G.; Beyth, R. J.; Kearon, C.; Schulman, S. Hemorrhagic complications of anticoagulant treatment: the seventh ACCP conference on antithrombotic and thrombolytic therapy. *Chest* **2004,** *126* (3, Suppl.), 287S.

(269) Symons, G.; Pulm, C. Anticoagulation: where have we come from and where are we going? the evidence for and against novel anticoagulants. *South African Medical Journal* **2014,** *104* (2), 143.

(270) Siegal, D. M.; Garcia, D. A.; Crowther, M. A. How I treat target-specific oral anticoagulant-associated bleeding. *Blood* **2014,** *123* (8), 1152.

(271) Siguret, V.; Gouin-Thibault, I.; Gaussem, P.; Pautas, E. Optimizing the Use of Anticoagulants (Heparins and Oral Anticoagulants) in the Elderly. *Drugs and Aging* **2013,** *30* (9), 687.

(272) Kearon, C.; Akl, E. A. Duration of anticoagulant therapy for deep vein thrombosis and pulmonary embolism. *Blood* **2014,** *123* (12), 1794.

(273) Colman, R. W.; Schmaier, A. H. Contact system: a vascular biology modulator with anticoagulant, profibrinolytic, antiadhesive, and proinflammatory attributes. *Blood* **1997,** *90* (10), 3819.

(274) Fischer, P. M. Computational chemistry approaches to drug discovery in signal transduction. *Biotechnology journal* **2008,** *3* (4), 452.

(275) Cozzini, P.; Kellogg, G. E.; Spyrakis, F.; Abraham, D. J.; Costantino, G.; Emerson, A.; Fanelli, F.; Gohlke, H.; Kuhn, L. A.; Morris, G. M. Target flexibility: an emerging consideration in drug discovery and design. *Journal of medicinal chemistry* **2008,** *51* (20), 6237.

(276) Herbert Nar, M. B., Angela Schmid,; Jean-Marie Stassen, W. W.; Henning W.M. Priepke, I. K. K.; Uwe J. Ries; Hauel, N. H. Structural Basis for Inhibition Promiscuity of Dual Specific Thrombin and Factor Xa Blood Coagulation Inhibitors. *Structure* **2001,** *9*, 8.

(277) Middendorp, S. J.; Wilbs, J.; Quarroz, C.; Calzavarini, S.; Angelillo-Scherrer, A.; Heinis, C. Peptide Macrocycle Inhibitor of Coagulation Factor XII with Subnanomolar Affinity and High Target Selectivity. *Journal of medicinal chemistry* **2017,** *60* (3), 1151.

(278) Kolyadko, V. N.; Lushchekina, S. V.; Vuimo, T. A.; Surov, S. S.; Ovsepyan, R. A.; Korneeva, V. A.; Vorobiev, I. I.; Orlova, N. A.; Minakhin, L.; Kuznedelov, K. New infestin-4 mutants with increased selectivity against factor XIIa. *PloS one* **2015,** *10* (12), e0144940.

(279) Schechter, I.; Berger, A. On the size of the active site in proteases. I. Papain. 1967. *Biochemical and Biophysical Research Communications* **2012,** *425* (3), 497.

(280) Bouma, B. N.; Griffin, J. H. Human blood coagulation factor XI. Purification, properties, and mechanism of activation by activated factor XII. *Journal Biological Chemistry* **1977,** *252* (18), 6432.

(281) Ageno, W.; Gallus, A. S.; Wittkowsky, A.; Crowther, M.; Hylek, E. M.; Palareti, G. Oral anticoagulant therapy: antithrombotic therapy and prevention of thrombosis: American College of Chest Physicians evidence-based clinical practice guidelines. *Chest Journal* **2012,** *141* (2_suppl), e44S.

(282) Garcia, D. A.; Baglin, T. P.; Weitz, J. I.; Samama, M. M. Parenteral anticoagulants: antithrombotic therapy and prevention of thrombosis: American College of Chest Physicians evidence-based clinical practice guidelines. *Chest Journal* **2012,** *141* (2_suppl), e24S.

(283) Straub, A.; Lampe, T.; Pohlmann, J.; Roehrig, S.; Perzborn, E.; Schlemmer, K.-H. Substituted oxazolidinones and their use in the field of blood coagulation . **2006**, U.S. Patent 7,034,017.

(284) Straub, A.; Lampe, T.; Pohlmann, J.; Röhrig, S.; Perzborn, E.; Schlemmer, K.-H.; Pernerstorfer, J. Substituted oxazolidinones and their use in the field of blood coagulation. **2007**, U.S. Patent 7,157,456..

(285) Nar, H. The role of structural information in the discovery of direct thrombin and factor Xa inhibitors. *Trends in Pharmacological Sciences* **2012,** *33* (2), 10.

(286) Kotthaus, J.; Steinmetzer, T.; van de Locht, A.; Clement, B. Analysis of highly potent amidine containing inhibitors of serine proteases and their N-hydroxylated prodrugs (amidoximes). *Journal of enzyme inhibition and medicinal chemistry* **2011,** *26* (1), 115.

(287) Ewing, W. R.; Pauls, H. W.; Spada, A. P. Progress in the design of inhibitors of coagulation factor Xa. *Drugs Future* **1999,** *24* (7), 771.

(288) Lam, P. Y.; Clark, C. G.; Li, R.; Pinto, D. J.; Orwat, M. J.; Galemmo, R. A.; Fevig, J. M.; Teleha, C. A.; Alexander, R. S.; Smallwood, A. M. Structure-based design of novel guanidine/benzamidine mimics: potent and orally bioavailable factor Xa inhibitors as novel anticoagulants. *Journal of medicinal chemistry* **2003,** *46* (21), 4405.

(289) Bissantz, C.; Kuhn, B.; Stahl, M. A medicinal chemist's guide to molecular interactions. *Journal of medicinal chemistry* **2010,** *53* (14), 5061.

(290) Lagos, C. F.; Segovia, G. F.; Nuñez-Navarro, N.; Faúndez, M. A.; Zacconi, F. C. Novel FXa Inhibitor Identification through Integration of Ligand-and Structure-Based Approaches. *Molecules* **2017,** *22* (10), 1588.

(291) Diekema, D. J.; Jones, R. N. Oxazolidinones: A review. *Drugs* **2000,** *59* (1), 7.

(292) Prasad, J. V. N. V. New oxazolidinones. *Current Opinion in Microbiology* **2007,** *10* (5), 454.

(293) Duggan, M. E.; Furuya, T.; Edwards, D. S.; Purohit, A., Scifluor Life Sciences Inc, **2017**. Fluorinated 2-amino-4-(benzylamino) phenylcarbamate derivatives. U.S. Patent 9,556,114.

(294) Xue, T.; Ding, S.; Guo, B.; Zhou, Y.; Sun, P.; Wang, H.; Chu, W.; Gong, G.; Wang, Y.; Chen, X.et al. Design, Synthesis, and Structure-Activity and Structure-Pharmacokinetic Relationship Studies of Novel [6,6,5] Tricyclic Fused Oxazolidinones Leading to the Discovery of a Potent, Selective, and

Orally Bioavailable FXa Inhibitor. *Journal of Medicinal Chemistry* **2014,** *57* (18), 7770.

(295) Cho, Y. R.; Song, H. Y.; Lee, D. Y.; Baek, S. Y.; Chae, S. E.; Cho, S. H.; Kim, Y. O.; Lee, H. S.; Park, J. H.; Park, T. G.; Woo, S. H.; Kim, Y. Z. FXa inhibitors with cyclic amidines as P4 subunit, processes for their preparations, and pharmaceutical compositions and derivatives thereof. Regochem Bioscience Co., Ltd., S. Korea . **2008**, U.S. Patent 8,288,423.

(296) Jayaraman, V.; Tomer, S.; Kanzariya, K.; Patel, N.; Dolia, M. Improved process for preparation of rivaroxaban. Alembic Pharmaceuticals Limited, India . **2014,** WO2014020458A1.

(297) Hashmi, M. S.; Sachdeva, Y. P. Process for the preparation of rivaroxaban and intermediates thereof. Ranbaxy Laboratories Limited, India . **2015**, U.S. Patent Application 14/394,547.

(298) Hashmi, M. S.; Sachdeva, Y. P. *Process for the preparation of rivaroxaban*. Ranbaxy Laboratories Limited, India . **2014**, U.S. Patent Application 14/430,279

(299) Halama, A.; Krulis, R.; Dammer, O.; Kalasek, S. Process for the preparation of rivaroxaban based on the use of (S)-epichlorohydrin . Zentiva, K.S., Czech Rep. **2013,** CZ15 2013120465 .

(300) Rao, D. M.; Reddy, P. K.; Reddy, A. A.; Reddy, B. V. A novel process for the preparation of linezolid and related compounds. Symed Labs Limited, India . 2005, WO2005099353A2.

(301) Urbasek, M.; Hradil, P.; Grepl, M.; Fialova, P.; Oremus, V.; Slezar, P.; Farmak, A.S. Process for the preparation of rivaroxaban. Zentiva, K.S., Czech Rep. **2012**.

(302) Yuan, J.; Liu, K.; Li, L.; Yuan, Y.; Liu, X.; Li, Y. A novel synthesis of the oxazolidinone antithrombotic agent rivaroxaban. *Molecules* **2014,** *19* (9), 14999.

(303) de Figueiredo, R. M.; Fröhlich, R.; Christmann, M. N, N ‘-Carbonyldiimidazole-mediated cyclization of amino alcohols to substituted azetidines and other N-heterocycles. *The Journal of organic chemistry* **2006,** *71* (11), 4147.

(304) Montalbetti, C. A.; Falque, V. Amide bond formation and peptide coupling. *Tetrahedron* **2005,** *61* (46), 10827.

(305) Ing, H. R.; Manske, R. H. F. Modification of the Gabriel synthesis of amines. *Journal of the Chemical Society* **1926**, 2348.

(306) Wolfe, S.; Hasan, S. Five-membered rings. II. Inter and intramolecular reactions of simple amines with N-substituted phthalimides. Methylamine as a reagent for removal of a phthaloyl group from nitrogen. *Canadian Journal of chemistry* **1970,** *48* (22), 3572.

(307) Osby, J. O.; Martin, M. G.; Ganem, B. An exceptionally mild deprotection of phthalimides. *Tetrahedron letters* **1984,** *25* (20), 2093.

(308) Parker, R.-E.; Isaacs, N. Mechanisms of epoxide reactions. *Chemical reviews* **1959,** *59* (4), 737.

(309) Bergmeier, S. C.; Lapinsky, D. J. Three-membered Ring Systems. *Progress in Heterocyclic Chemistry* **2012,** *24*, 89.

(310) Faraji, M.; Farajtabar, A.; Gharib, F. Determination of water-ethanol mixtures autoprotolysis constants and solvent effect. *Journal of Applied Chemical Research* **2009,** *9* (1), 7.

(311) Hoffman, R. V. *Organic Chemistry: an intermediate text*; 2nd ed.; John Wiley and Sons: New Jersy, USA, 2004.

(312) Rao, D. M.; Reddy, P. K. Novel process for the preparation of linezolid and related compounds. Symed Labs Limited, India . **2008,** U.S. Patent Application 11/868,613.

(313) Montalbetti, C. A. G. N.; Falque, V. Amide bond formation and peptide coupling. *Tetrahedron* **2005,** *61* (46), 10827.

(314) Campbell, D.; Duron, S. G. Preparation of 8-ethyl-6-(aryl)pyrido[2,3-d]pyrimidin-7(8H)-one compds. as PAK inhibitors useful in treatment of nervous system disorders and cancer. Afraxis, Inc., USA . **2013**, WO2013043232A2.

(315) Beletskaya, I. P.; Cheprakov, A. V. Copper in cross-coupling reactions: the post-Ullmann chemistry. *Coordination chemistry reviews* **2004,** *248* (21), 2337.

(316) Andrews, M. J. I.; Edwards, P.; Chambers, M. S.; Schmidt, W.; Clase, J. A.; Bar, G.; Hirst, K. L.; Macleod, A. Triazolopyrazine compounds useful for the treatment of degenerative and inflammatory diseases and their preparation. Galapagos N.V., Belg. . **2007**, WO2007138072A2.

(317) Boyd, G. V. Reactions and synthetic uses of amidines. *Amidines and Imidates* **1991**, 2, 367.

(318) Roger, R.; Neilson, D. G. The Chemistry of Imidates. *Chemical Reviews* **1961,** *61* (2), 179.

(319) Lange, U. E.; Schäfer, B.; Baucke, D.; Buschmann, E.; Mack, H. A new mild method for the synthesis of amidines. *Tetrahedron letters* **1999,** *40* (39), 7067.

(320) Adler, M.; Kochanny, M. J.; Ye, B.; Rumennik, G.; Light, D. R.; Biancalana, S.; Whitlow, M. Crystal Structures of Two Potent Nonamidine Inhibitors Bound to Factor Xa. *Biochemistry* **2002,** *41* (52), 15514.

(321) Nadrah, K.; Dolenc, M. S. Preparation of amidines by amidoxime reduction with potassium formate. *Synlett* **2007,** *2007* (08), 1257.

(322) Eloy, F. L., R., . The Chemistry of Amidoximes and Related Compounds. *Chemical Reviews* **1962,** *2*, 155.

(323) Miyaura, N.; Suzuki, A. Palladium-catalyzed cross-coupling reactions of organoboron compounds. *Chemical reviews* **1995,** *95* (7), 2457.

(324) Garg, N. K.; Caspi, D. D.; Stoltz, B. M. The total synthesis of (+)-dragmacidin F. *Journal of the American Chemical Society* **2004,** *126* (31), 9552.

(325) Ghosh, S.; Kumar, A. S.; Mehta, G. Convenient synthesis of Valsartan via a Suzuki reaction. *Journal of Chemical Research* **2010,** *34* (4), 191.

(326) Dey, R.; Sreedhar, B.; Ranu, B. C. Molecular sieves-supported palladium (II) catalyst: Suzuki coupling of chloroarenes and an easy access to useful intermediates for the synthesis of irbesartan, losartan and boscalid. *Tetrahedron* **2010,** *66* (13), 2301.

(327) Miyaura, N.; Yamada, K.; Suzuki, A. A new stereospecific cross-coupling by the palladium-catalyzed reaction of 1-alkenylboranes with 1-alkenyl or 1-alkynyl halides. *Tetrahedron Letters* **1979,** *20* (36), 3437.

(328) Lennox, A. J.; Lloyd-Jones, G. C. Selection of boron reagents for Suzuki–Miyaura coupling. *Chemical Society Reviews* **2014,** *43* (1), 412.

(329) Onak, T. *Organoborane chemistry*; Elsevier, 2012.

(330) Barder, T. E.; Walker, S. D.; Martinelli, J. R.; Buchwald, S. L. Catalysts for Suzuki-Miyaura coupling processes: scope and studies of the effect of ligand structure. *Journal of the American Chemical Society* **2005,** *127* (13), 4685.

(331) Vedejs, E.; Chapman, R.; Fields, S.; Lin, S.; Schrimpf, M. Conversion of arylboronic acids into potassium aryltrifluoroborates: Convenient precursors of arylboron difluoride lewis acids. *The Journal of Organic Chemistry* **1995,** *60* (10), 3020.

(332) Yamakawa, T.; Jona, H.; Niiyama, K.; Yamada, K.; Iino, T.; Ohkubo, M.; Imamura, H.; Shibata, J.; Kusunoki, J.; Yang, L. Spirochromanone derivatives, their use as acetyl coenzyme A carboxylase (ACC) inhibitors, processes for preparing them, and pharmaceutical compositions containing them. Merck & Co., Inc., USA; Banyu Pharmaceutical Co., Ltd. . **2007**, WO2007011809A1.

(333) Zeng, Z.; Zimmerman, S. C. Convenient synthesis of 9-alkyl and 9-arylacridines from [2-(trimethylsilyl) ethoxy] methyl (sem) protected acridone. *Tetrahedron letters* **1988,** *29* (40), 5123.

(334) MacHacek, M. R.; Altman, M. D.; Romeo, E. T.; Vitharana, D.; Cash, B.; Siu, T.; Zhou, H.; Christopher, M.; Kattar, S. D.; Haidle, A. M. *et al*. Pyrazolyl derivatives as SYK inhibitors and their preparation. Merck Sharp & Dohme Corp., USA; Merck Canada Inc. . **2013**, WO2013192125A1.

(335) Straub, A.; Lampe, T.; Pohlmann, J.; Roehrig, S.; Perzborn, E.; Schlemmer, K.-H.; Pernerstorfer, J. Preparation of substituted oxazolidinones for use in treatment of disorders associated with blood coagulation. Bayer Healthcare AG, Germany . **2007**, 2002-181051 7157456.

(336) Al-Obeidi, F.; Ostrem, J. A. Factor Xa inhibitors. *Expert Opinion on Therapeutic Patents.* **1999,** *9* (7), 931.

(337) Casimiro-Garcia, A.; Dudley, D. A.; Heemstra, R. J.; Filipski, K. J.; Bigge, C. F.; Edmunds, J. J. Progress in the discovery of Factor Xa inhibitors. *Expert Opinion on Therapeutic Patents* **2006,** *16* (2), 119.

(338) SNAPE, T. J.; ASTLES, A. M.; DAVIES, J. Understanding the chemical basis of drug stability and degradation. *Pharmaceutical journal* **2010,** *285* (7622), 416.

(339) Xue, T.; Ding, S.; Guo, B.; Zhou, Y.; Sun, P.; Wang, H.; Chu, W.; Gong, G.; Wang, Y.; Chen, X. Design, Synthesis, and Structure–Activity and Structure–Pharmacokinetic Relationship Studies of Novel [6, 6, 5] Tricyclic Fused Oxazolidinones Leading to the Discovery of a Potent, Selective, and Orally Bioavailable FXa Inhibitor. *Journal of medicinal chemistry* **2014,** *57* (18), 7770.

(340) Cui, Y.; Dang, Y.; Yang, Y.; Ji, R. Stereocontrolled synthesis of tricyclic fused oxazolidinone as antibacterial agent. *Journal of heterocyclic chemistry* **2006,** *43* (4), 1071.

(341) Purser, S.; Moore, P. R.; Swallow, S.; Gouverneur, V. Fluorine in medicinal chemistry. *Chemical Society Reviews* **2008,** *37* (2), 320.

(342) Kirk, K. L. Fluorine in medicinal chemistry: recent therapeutic applications of fluorinated small molecules. *Journal of Fluorine Chemistry* **2006,** *127* (8), 1013.

(343) Castagnoli, N.; Rimoldi, J. M.; Bloomquist, J.; Castagnoli, K. P. Potential metabolic bioactivation pathways involving cyclic tertiary amines and azaarenes. *Chemical research in toxicology* **1997,** *10* (9), 924.

(344) Shu, Y.-Z.; Johnson, B. M.; Yang, T. J. Role of biotransformation studies in minimizing metabolism-related liabilities in drug discovery. *The American Association of Pharmaceutical Scientists journal* **2008,** *10* (1), 178.

(345) Zhang, G. In *Assay Guidance Manual [Internet]*; Sittampalam, G. S.;Coussens, N. P.;Brimacombe, K.;Grossman, A.;Arkin, M.;Auld, D.;Austin, C.;Baell, J.;Bejcek, B.;Chung, T. D. Y.et al., Eds.; Eli Lilly & Company and the National Center for Advancing Translational Sciences Bethesda (MD): USA, 2004.

(346) Calatzis, A.; Peetz, D.; Haas, S.; Spannagl, M.; Rudin, K.; Wilmer, M. Prothrombinase-induced clotting time assay for determination of the anticoagulant effects of unfractionated and low-molecular-weight heparins, fondaparinux, and thrombin inhibitors. *American journal of clinical pathology* **2008,** *130* (3), 446.

(347) Perzborn, E.; Strassburger, J.; Wilmen, A.; Pohlmann, J.; Roehrig, S.; SCHLEMMER, K. H.; Straub, A. In vitro and in vivo studies of the novel antithrombotic agent BAY 59-7939—an oral, direct Factor Xa inhibitor. *Journal of Thrombosis and Haemostasis* **2005,** *3* (3), 514.

(348) Berry, C. N.; Girard, D.; Lochot, S.; Lecoffre, C. Antithrombotic actions of argatroban in rat models of venous,'mixed'and arterial thrombosis, and its effects on the tail transection bleeding time. *British journal of pharmacology* **1994,** *113* (4), 1209.

(349) Savjani, K. T.; Gajjar, A. K.; Savjani, J. K. Drug solubility: importance and enhancement techniques. *International Scholarly Research Network pharmaceutics* **2012,** *2012*.

(350) Alsenz, J.; Kansy, M. High throughput solubility measurement in drug discovery and development. *Advanced drug delivery reviews* **2007,** *59* (7), 546.

(351) Hubatsch, I.; Ragnarsson, E. G.; Artursson, P. Determination of drug permeability and prediction of drug absorption in Caco-2 monolayers. *Nature protocols* **2007,** *2* (9), 2111.

(352) Doss, G. A.; Baillie, T. A. Addressing metabolic activation as an integral component of drug design. *Drug metabolism reviews* **2006,** *38* (4), 641.

(353) Weinz, C.; Schwarz, T.; Kubitza, D.; Mueck, W.; Lang, D. Metabolism and excretion of rivaroxaban, an oral, direct factor Xa inhibitor, in rats, dogs, and humans. *Drug Metabolism and Disposition* **2009,** *37* (5), 1056.

(354) Vishnu Newadkar, R.; Changdeo Gaikwad, A.; Madhukar Harad, A.; Dalmases Barjoan, P. Process for the preparation of rivaroxaban through acid addition salts of its intermediate. Laboratorios Lesvi, S. L., Spain . **2013**, WO2013053739A1.

(355) Li, C.; Liu, Y.; Zhang, Y.; Zhang, X. An approach to the anticoagulant agent rivaroxaban via an isocyanate-oxirane cycloaddition promoted by MgI2.etherate. *Journal of Chemical Research* **2011,** *35* (7), 400.

(356) McCarthy, J. R. Processes for preparing rivaroxaban. Indiana University Research & Technology Corporation, USA . **2015**, US20150175590A1.

(357) Tian, S.; Tang, B.; Zhang, M.; Gao, Q.; Chen, B.; Zhang, Q.; Xu, G. An Improved Synthesis of Rivaroxaban. *Organic Preparations and Procedures International* **2017,** *49* (2), 169.

(358) Kumari, S.; Mishra, C. B.; Tiwari, M. Design, synthesis and pharmacological evaluation of N-[4-(4-(alkyl/aryl/heteroaryl)-piperazin-1-yl)-phenyl]-carbamic acid ethyl ester derivatives as novel anticonvulsant agents. *Bioorganic & Medicinal Chemistry Letters* **2015,** *25* (5), 1092.

(359) Inoue, H.; Murafuji, H.; Hayashi, Y. Preparation of thienopyrazole derivatives as PDE7 inhibitors. Daiichi Asubio Pharma Co., Ltd., Japan. **2006**, WO2006004040A1.

(360) Harnett, J.; Auguet, M. Preparation and use of novel lipoic acid heterocyclic or benzene derivatives as medicines. Societe de Conseils de Recherches et d'Applications Scientifiques S.C.R.A.S. , Fr. **2001**, WO2001068643A2.

(361) Rajesh, T.; Reddy, P. S.; Manidhar, M.; Lakshmi, M. V.; Madhusudhan, G. Design and Enantiopure Synthesis of (R)-2-((2-Oxooxazolidin-5-yl) methyl) isoindoline-1, 3-dione: A Key Precursor to Build 2-Oxazolidinone Class of Antibacterial Agents. *Journal of Chemistry* **2011,** *8* (3), 1417.